Universidad de Oviedo

PROGRAMA DE DOCTORADO EN INGENIERÍA QUÍMICA, AMBIENTAL Y BIOALIMENTARIA

Biofilms mixtos: eficacia de derivados fágicos para su eliminación y estudio de su respuesta adaptativa

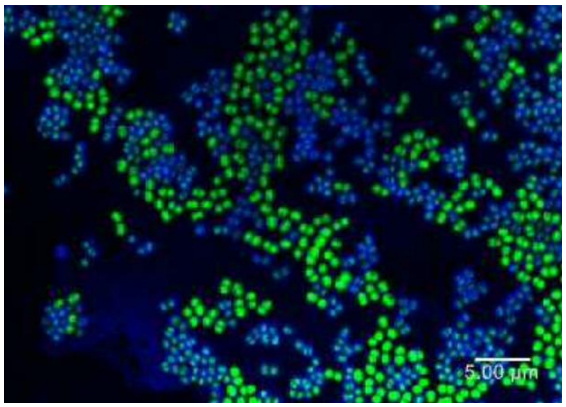

Silvia González Menéndez

IPLA-CSIC

Oviedo, 2020

Esta Tesis Doctoral ha sido realizada en el

Instituto de Productos Lácteos de Asturias (IPLA-CSIC)

Universidad de Oviedo
Universidá d'Uviéu
University of Oviedo

RESUMEN DEL CONTENIDO DE TESIS DOCTORAL

1.- Título de la Tesis	
Español/Otro Idioma: Biofilms mixtos: eficacia de derivados fágicos para su eliminación y estudio de su respuesta adaptativa.	Inglés: Mixed-species biofilms: efficacy of phage-derived products for their removal and study of their adaptive responses.

2.- Autor	
Nombre: Silvia González Menéndez	DNI/Pasaporte/NIE. [redacted]
Programa de Doctorado: Ingeniería Química, Ambiental y Bioalimentaria.	
Órgano responsable: Departamento de Ingeniería Química y Tecnología del Medio Ambiente	

RESUMEN (en español)

Los biofilms representan una fuente importante de contaminación en entornos industriales y hospitalarios. Por tanto, el desarrollo de estrategias eficientes para combatirlos es de suma importancia tanto desde el punto de vista sanitario, como económico. En este contexto, los bacteriófagos y algunas proteínas fágicas han demostrado potencial como nuevos agentes antibiofilm. Esta tesis pretende contribuir a lograr una mejor comprensión de las interacciones entre los fagos y las bacterias que forman parte del biofilm, así como el impacto potencial de los fagos y las proteínas líticas sobre la formación de estas estructuras. Para ello, se utilizó como microorganismo modelo *Staphylococcus aureus*, un patógeno oportunista de gran importancia en el ámbito hospitalario y en la industria alimentaria.

En primer lugar, se estudió el efecto del tratamiento con el fago vB_SauM_phiIPLA-RODI (phiIPLA-RODI) sobre biofilms mixtos de *S. aureus* en combinación con distintos microorganismos (*Lactobacillus plantarum*, *Enterococcus faecium*, o *Lactobacillus pentosus*). Los resultados obtenidos sugieren que el impacto del bacteriófago varía en función de las especies acompañantes y las condiciones de la infección. Además, la propagación del fago dentro de los biofilms mixtos también depende en gran medida de la especie acompañante. Por otro lado, la microscopía electrónica de barrido (SEM) y la microscopía confocal de barrido láser (CLSM) mostraron cambios en la estructura tridimensional de los biofilms mixtos después del tratamiento con fagos. Complementariamente, también se analizó la capacidad de los fagos phiIPLA-RODI y vB_SepM_phiIPLA-C1C (phiIPLAC1C) para difundir, propagarse y permanecer viables dentro de la estructura del biofilm. Para ello, se desarrolló un nuevo método basado en la formación de los biofilms sobre una membrana de policarbonato que separa una cámara superior, donde se añade el tratamiento, y una cámara inferior, en la que se recoge el eluído tras dicho tratamiento. Nuestros resultados confirmaron que ambos fagos podían penetrar a través de biofilms formados por varias cepas bacterianas. Sin embargo, el grado de penetración del fago dependía de la cepa o cepas presentes, de su susceptibilidad a los fagos y su capacidad para formar un biofilm más o menos denso.

Otro aspecto estudiado en este trabajo fue el impacto de los bacteriófagos sobre la formación de biofilms en *S. aureus*. Por un lado, se demostró que la presencia del fago virulento phiIPLA-RODI, a dosis bajas, daba lugar a una mayor acumulación de biomasa. Este fenómeno se debía a un incremento en el contenido de ADN extracelular de la matriz del biofilm. Además, los biofilms infectados con el fago

mostraron diferencias transcripcionales importantes en comparación con un control no tratado. Por ejemplo, los datos de RNA-seq revelaron una posible activación de la respuesta estricta. Por otra parte, también se examinó el efecto de la lisogenia sobre el desarrollo de biofilms en este microorganismo. Los datos obtenidos mostraron que la lisogenización con dos fagos atemperados, ϕ11 y ϕ80α, aumentaba la capacidad de la cepa *S. aureus* RN450 para generar biofilm y la producción del pigmento carotenoide estafiloxantina. Este fenotipo podría explicarse en parte por las diferencias en la expresión génica mostradas por las cepas que albergan el profago, es decir, la activación del regulón del factor sigma alternativo (SigB) y la inhibición de genes controlados por el sistema de "quorum-sensing" Agr.

Además de los bacteriófagos, se sabe que las proteínas líticas derivadas de estos son una alternativa prometedora a los antimicrobianos convencionales. Una de sus propiedades más interesantes es que no seleccionan cepas resistentes. Por otro lado, la ingeniería genética permite el diseño de nuevas proteínas "a medida" que pueden exhibir propiedades antibacterianas mejoradas. Un ejemplo de esto es la proteína quimérica CHAPSH3b. En este estudio se demostró que esta proteína lítica tiene potencial para el control de las células de *S. aureus* embebidas en biofilms. Otro aspecto interesante es que dosis subinhibitorias de CHAPSH3b inhiben la formación de biofilms en este patógeno. El análisis transcripcional reveló que este fenómeno podría estar relacionado con la inhibición de la expresión de genes que codifican autolisinas tras la exposición de las células de *S. aureus* a CHAPSH3b.

En conjunto, todos estos datos aportan información valiosa acerca de la aplicación de los bacteriófagos y sus proteínas líticas para la prevención y eliminación de biofilms de *S. aureus*.

RESUMEN (en Inglés)

Biofilms represent a major source of contamination in industrial and hospital environments. The development of efficient strategies to combat them is of the utmost importance both from the health and the economic points of view. In this context, bacteriophages and some phage proteins have shown potential as new antibiofilm agents. This thesis aims to contribute to a better understanding of the interactions between the phages and bacteria that are part of the biofilm, as well as the potential impact of phages and lytic proteins on the formation of these structures. To do that, *Staphylococcus aureus*, an opportunistic pathogen of great importance in hospital settings and the food industry, was used as a model microorganism.

Firstly, the effect of treatment with phage vB_SauM_phiIPLA-RODI (phiIPLA-RODI) on mixed biofilms formed by *S. aureus* in combination with different microorganisms (*Lactobacillus plantarum, Enterococcus faecium,* or *Lactobacillus pentosus*) was studied. The results obtained suggest that the impact of the bacteriophage varies depending on the accompanying species and the infection conditions. Furthermore, the ability of the phage to spread within mixed biofilms is also highly dependent on the accompanying species. On the other hand, scanning electron microscopy (SEM) and confocal laser scanning microscopy (CLSM) also showed changes in the three-dimensional structure of mixed-species biofilms after phage treatment. The ability of phages phiIPLA-RODI and vB_SepM_phiIPLA-C1C (phiIPLAC1C) to diffuse, spread and remain viable within the biofilm structure was also analyzed. To this purpose, a

new method was developed based on the formation of biofilms on a polycarbonate membrane that separates an upper chamber, where the treatment is added, and a lower chamber, in which the flow-through is collected after treatment. Our results confirmed that both phages could penetrate through biofilms formed by various bacterial strains. However, the degree of phage penetration depended on the strain or strains present in the biofilm according to their phage susceptibility and biofilm-forming capacity.

Another aspect studied in this work was the impact of bacteriophages on biofilm formation in *S. aureus*. On the one hand, it was demonstrated that the presence of the virulent phage phiIPLA-RODI at low doses gave rise to a greater accumulation of biomass. This phenomenon was due to an increase in the extracellular DNA content of the biofilm matrix. Furthermore, the phage-infected biofilms showed significant transcriptional differences compared to an untreated control. For instance, RNA-seq data revealed a possible activation of the stringent response. The effect of lysogeny on biofilm development in this microorganism was also examined. The data obtained showed that lysogenization with two temperate phages, ϕ11 and ϕ80α, increased biofilm formation and production of the carotenoid pigment staphyloxanthin in strain *S. aureus* RN450. These phenotypes could be partly explained by the differences in gene expression shown by the prophage-harboring strains, namely the activation of the alternative sigma factor (SigB) regulon and the inhibition of genes controlled by the Agr “quorum-sensing” system.

In addition to bacteriophages, their derived lytic proteins are also a promising alternative to conventional antimicrobials. One of their most interesting properties is that they do not select resistant strains. On the other hand, genetic engineering allows the design of new "custom" proteins that can exhibit improved antibacterial properties. An example of this is the chimeric protein CHAPSH3b. In this study, this lytic protein was shown to have potential for the control of *S. aureus* cells embedded in biofilms. Another interesting aspect is that subinhibitory doses of CHAPSH3b inhibit biofilm formation in this pathogen. Transcriptional analysis revealed that this phenomenon could be related to the inhibition of the expression of autolysin-encoding genes after exposure of *S. aureus* cells to CHAPSH3b.

Taken together, all these data provide valuable information regarding the application of bacteriophages and their lytic proteins for the prevention and elimination of *S. aureus* biofilms.

SR. PRESIDENTE DE LA COMISIÓN ACADÉMICA DEL PROGRAMA DE DOCTORADO EN _____

Agradecimientos

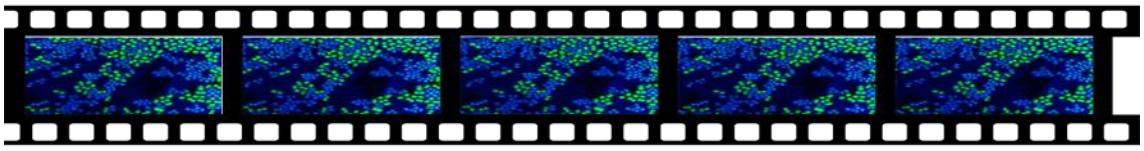

Una tesis doctoral es un trabajo que no sólo es fruto del esfuerzo personal del doctorando, sino que necesita de la ayuda de muchas personas, tanto en lo profesional como en lo personal. Con estas líneas quisiera mostrar mi agradecimiento a todas ellas.

En primer lugar, quiero agradecer a las directoras que han pasado por ese cargo, durante mi estancia en el Instituto de Productos Lácteos de Asturias (IPLA-CSIC); Dra. Clara González de Reyes Gavilán, y la Dra. María Fernández García, por permitir el desarrollo de la Tesis en el centro.

Al grupo de investigación DairySafe liderado por la Dra. Ana Rodríguez González, por acogerme.

A Pilar García Suarez, mi Directora de Tesis, que ha permitido que este proyecto se materialice.

A Lucia Fernández, que además de ser mi Directora, y la "maquinista" de este tren, es un amiga y compañera con mayúsculas.

A todos los miembros del Grupo (Ana R, Pili, Bea, Susana, Lucia, Diana, Ana B, Roxana, etc.), y también a todo el personal del IPLA, con los que he compartido durante los últimos años mis ilusiones, trabajo y esfuerzo. Gracias por enseñarme y hacer que me divirtiera mientras descubría las alegrías y también los sinsabores de investigar.

A todos mis compañer@s de laboratorio, pero en especial a Lucia, Ana B, Jorge y Susana que consiguieron darme el afecto necesario para disfrutar del día a día, y sobre todo del café.

A mis amigas, especialmente a María Jesús y a mi hermana Eva González, por escucharme, aguantarme y animarme a seguir adelante. Gracias por estar no sólo en los buenos momentos.

A mis padres, a mis hermanas y a toda la familia, por su sacrificio y apoyo incondicional durante todos estos años. Gracias, con vuestro cariño y ayuda, todo ha sido mucho más fácil.

A mi compañero Borja y a mi hijo Leo, por su paciencia, comprensión y solidaridad con este proyecto, por el tiempo que me han concedido. Sin su apoyo este trabajo nunca se habría escrito y, por eso, este trabajo es también el suyo.

A todos, muchas gracias.

Índice

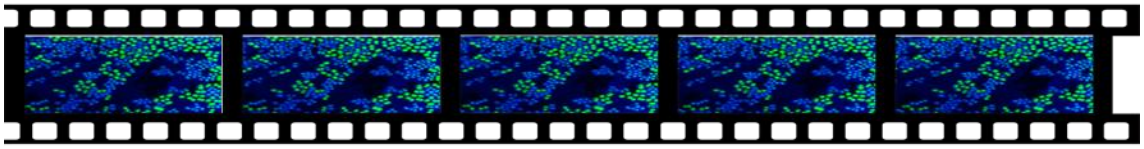

Resumen

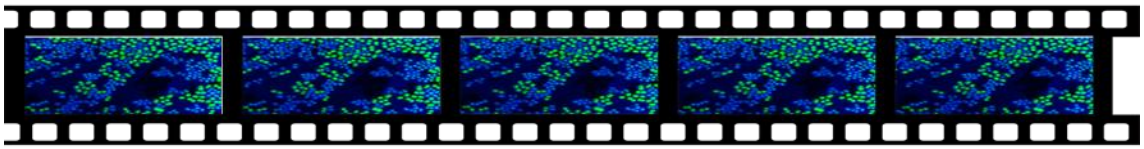

RESUMEN

Los biofilms bacterianos representan una fuente importante de contaminación en entornos industriales y hospitalarios. Por lo tanto, el desarrollo de estrategias eficientes para combatirlos es muy relevante, tanto desde el punto de vista médico como económico. En este contexto, los fagos y algunas proteínas fágicas han demostrado tener gran potencial como nuevos agentes antibiofilm que podrían complementar la acción de los antibióticos y desinfectantes. Sin embargo, el desarrollo de una estrategia exitosa basada en fagos requiere un mayor conocimiento acerca de la seguridad, eficacia y posibles efectos no deseados de este tipo de antimicrobianos. Esta Tesis pretende contribuir a lograr una mejor comprensión de las interacciones entre los fagos y las bacterias que forman parte del biofilm, así como del impacto potencial de los fagos y las proteínas líticas sobre la formación de estas estructuras.

En este trabajo se utilizó *Staphylococcus aureus* como microorganismo modelo, ya que se trata de un patógeno oportunista de gran importancia en el ámbito hospitalario y en la industria alimentaria. En primer lugar, se estudió el efecto del bacteriófago de *Staphylococcus* phiIPLA-RODI como tratamiento frente a biofilms mixtos de *S. aureus* en combinación con distintos microorganismos (*Lactobacillus plantarum*, *Enterococcus faecium* o *Lactobacillus pentosus*). Los resultados obtenidos sugieren que el impacto del tratamiento fágico en los biofilms mixtos es mucho más complejo que en aquellos formados por una sola especie bacteriana, y que varía según la especie acompañante y las condiciones específicas de la infección. Así, los tratamientos cortos (4 h) con una suspensión de fagos en condiciones de limitación de nutrientes redujeron ligeramente el número de células de *S. aureus* en biofilms no maduros (5 h), pero sin liberar las células de las especies acompañantes, que no son susceptibles al fago. En contraste, los períodos más largos de tratamiento (18 h) y sin limitación de nutrientes, fueron más eficaces para eliminar las células de *S. aureus,* ya que se produjo una disminución de hasta 2.9 unidades logarítmicas. Sin embargo, en algunos casos, estas condiciones promovieron el crecimiento de las especies acompañantes, como fue el caso de *L. plantarum*, que registró un aumento de hasta 2.3 unidades logarítmicas más que en el control no tratado. Por otra parte, también se determinó que la propagación de los fagos dentro de los biofilms mixtos dependía en gran medida de las especies que estaban

presentes, obteniéndose el título más alto en los biofilms formados por *S. aureus* y *L. pentosus*. Para completar el análisis, se recurrió a dos técnicas de microscopía, microscopía electrónica de barrido (SEM) y microscopía de barrido láser confocal (CLSM), que confirmaron los datos obtenidos mediante el recuento de bacterias viables. Por un lado, las imágenes de los biofilms de doble especie no tratados mostraron células bien organizadas pertenecientes a ambas especies. Por el contrario, los cuatro biofilms mixtos tratados con el fago phiIPLA-RODI contenían menor cantidad de células de *S. aureus* que sus respectivas muestras control. En cuanto a la especie acompañante, no se observaron cambios apreciables cuando el tratamiento se llevó a cabo en condiciones que no permitían el crecimiento bacteriano. Sin embargo, cuando se realizó el tratamiento en medio de cultivo, es decir sin limitación de nutrientes, la población de *L. plantarum* mostró un aumento como consecuencia de la eliminación de su competidor *S. aureus*. En el caso de las especies *E. faecium* y *L. pentosus* el número de células disminuía, probablemente debido a la disgregación de la estructura del biofilm y, por tanto, a la liberación de las mismas al sobrenadante.

Para entender los resultados anteriores resultó muy importante el estudio de la capacidad que tienen los bacteriófagos para difundir, propagarse y permanecer viables dentro de la estructura compleja del biofilm. Por ello, se examinaron estas propiedades para los bacteriófagos phiIPLA-RODI y phiIPLA-C1C en biofilms formados por varias cepas bacterianas con diverso grado de susceptibilidad a dichos fagos, así como diferentes capacidades de formación de biofilms. Para ello, fue preciso poner a punto un nuevo método basado en la formación de los biofilms sobre una membrana de policarbonato que separa una cámara superior, donde se añade la suspensión de fagos, y una cámara inferior, en la que se recoge el líquido eluido tras el tratamiento con fagos. Nuestros resultados confirmaron que ambos fagos podían penetrar a través de los biofilms, pero su tasa de difusión difería según la combinación de bacterias que formaban parte de la estructura. Así, los datos presentados aquí sugieren que los factores que determinan la difusión de los fagos en los biofilms están relacionados con la cantidad de biomasa total del biofilm, la susceptibilidad de la cepa al fago, el título inicial del fago que interacciona con la comunidad bacteriana, la posible retención del

fago por la matriz extracelular y la tasa de inactivación del fago en el curso de dicha interacción.

Una parte esencial de la interacción fago-bacteria que se produce en el interior de un biofilm es la respuesta de la población bacteriana a la presencia de los bacteriófagos. En esta Tesis se demuestra que los biofilms formados por algunas cepas de *S. aureus* en presencia de dosis bajas del fago phiIPLA-RODI tienen más biomasa total y su matriz extracelular está compuesta mayoritariamente por ADN. Además, las células que formaban parte del biofilm infectado mostraron diferencias transcripcionales importantes en comparación con las de un biofilm control no infectado. Significativamente, los datos del análisis realizado mediante la técnica RNA-seq revelaron la posible activación de la respuesta estricta en los biofilms infectados. Esta respuesta, coordinada por la alarmona (p)ppGpp, se activa en distintas condiciones de estrés celular y conlleva, entre otras cosas, una menor expresión de genes implicados en varias rutas biosintéticas. Además, se sabe que la respuesta estricta participa en el proceso de formación de biofilms de varios microorganismos, por lo que podría participar en el incremento en biomasa observado en presencia de phiIPLA-RODI.

Una vez establecida la influencia que los bacteriófagos virulentos pueden ejercer sobre la estructura y composición de los biofilms, nos planteamos conocer si ese efecto se producía también cuando se trata de bacteriófagos atemperados que se encuentran en el estado lisogénico. Esto sería muy interesante desde el punto de vista de la ecología microbiana, dado que la mayoría de los aislados de *S. aureus* llevan profagos en sus genomas. Por otra parte, un mejor conocimiento del impacto de los profagos sobre la fisiología de las bacterias en los biofilms sería útil para desarrollar estrategias que permitan eliminar patógenos más eficientemente. Este estudio se abordó mediante el análisis fenotípico y transcriptómico de células que formaban parte de biofilms. Las cepas utilizadas fueron *S. aureus* RN450, carente de profagos, y dos cepas derivadas de la misma, que portaban los profagos φ11 y φ80α. Tal y como se sospechaba, la presencia de profagos daba lugar a cambios fenotípicos. Así, las cepas lisogénicas mostraron una mejor capacidad para formar biofilms y, además, resultó llamativa su mayor producción del pigmento carotenoide estafiloxantina. Estos fenotipos podían explicarse, al menos en parte, por las diferencias en la expresión génica mostradas por las cepas lisogénicas.

Por un lado, la presencia del profago provocaba una activación del regulón del factor sigma alternativo (SigB), en el que se incluyen los genes de biosíntesis de la estafiloxantina. Además, se observó una inhibición de los genes controlados por el sistema de quórum sensing Agr, siendo especialmente interesantes los genes que codifican factores de dispersión como las proteasas. Una menor producción de proteínas de dispersión podría explicar la mayor acumulación de biomasa en las cepas lisogénicas.

Complementariamente al trabajo realizado con fagos, se inició un estudio sobre el efecto que ciertas proteínas fágicas podrían tener sobre los biofilms bacterianos. Se sabe que las proteínas líticas derivadas de fagos (endolisinas y peptidoglicano hidrolasas asociadas a virión) son una alternativa prometedora a los antimicrobianos convencionales. Una de sus propiedades más interesantes es que no seleccionan cepas resistentes, y además su estructura modular permite, mediante ingeniería genética, el diseño de nuevas proteínas quimera con propiedades antibacterianas mejoradas. Un ejemplo es la proteína CHAPSH3b que consta de un dominio catalítico CHAP, procedente de la peptidoglicano hidrolasa asociada al virión HydH5 del fago phiIPLA88, y de un dominio de unión a la pared celular procedente de la lisostafina. CHAPSH3b había demostrado previamente gran capacidad lítica frente a *S. aureus*. En esta Tesis se demuestra que esta proteína lítica también tiene potencial para la eliminación de células de *S. aureus* que forman parte de biofilms. Sin embargo, el hallazgo más novedoso fue encontrar que dosis subinhibitorias de CHAPSH3b pueden inhibir la formación de biofilms en algunas cepas de *S. aureus*. De hecho, el análisis transcripcional reveló que la exposición de las células de *S. aureus* a este enzima inhibe la expresión de varios genes que codifican autolisinas bacterianas. Se sabe que algunas de estas proteínas, las autolisinas AtlA y Sle1, participan en el desarrollo de biofilms estafilocócicos. Por ello, una menor expresión de las mismas podría explicar la menor formación de biofilms en presencia de CHAPSH3b. También se observó esta tendencia en la expresión génica en células expuestas a la endolisina LysH5, la cual también es efectiva frente a biofilms de *S. aureus*. Esta proteína está codificada por el fago phiIPLA88 y consta de dos dominios catalíticos (CHAP y amidasa-2) y un dominio de unión a pared (SH3b). Además, esta respuesta transcripcional podría disminuir de modo transitorio la susceptibilidad de la

cepa a la proteína. Así, una cepa mutante en el gen *atlA* mostró un ligero aumento en su capacidad para crecer en presencia de las proteínas líticas CHAPSH3b y LysH5.

En conjunto, todos estos datos aportan información valiosa acerca de la aplicación de los bacteriófagos y sus proteínas líticas para la prevención y eliminación de biofilms de *S. aureus*, poniendo de manifiesto tanto sus propiedades positivas como posibles efectos no deseados. Esto último es imprescindible para poder diseñar estrategias inteligentes de utilización de los mismos, que saquen el máximo partido posible a las ventajas de estos compuestos y, al mismo tiempo, minimicen o impidan la aparición de los posibles efectos negativos de los mismos.

Lista de figuras y tablas

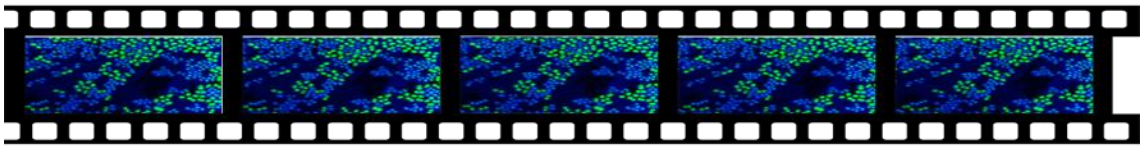

LISTA DE FIGURAS Y TABLAS

Abreviaturas

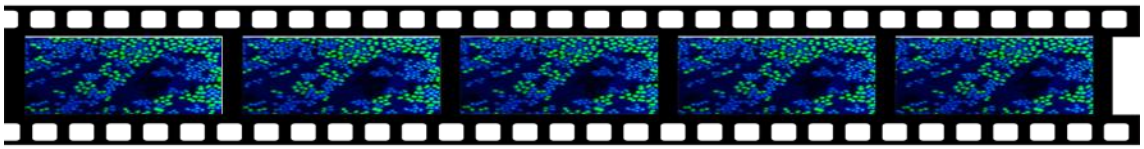

ABREVIATURAS

AIP: **A**uto**i**nducing **p**eptide (péptido autoinductor)

Agr: **a**ccessory **g**ene **r**egulator

CoNS: **C**oagulase-**N**egative **S**taphylococci (Estafilococos coagulasa negativos)

ECDC: **E**uropean **C**entre for **D**isease Prevention and **C**ontrol

eADN: ADN extracelular

GLASS: **Gl**obal **A**ntimicrobial Resistance **S**urveillance **S**ystem

ICTV: **I**nternational **C**ommittee on **T**axonomy of **V**iruses

LPSN: **L**ist of **P**rokaryotic **N**ames with **S**tanding in Nomenclature

MSCRAMMs: **M**icrobial **s**urface **c**omponents **r**ecognizing **a**dhesive **m**atrix **m**olecule**s**

OMS: **O**rganización **M**undial de la **S**alud

PIA/PNAG: **P**olisacárido de **a**dhesión **i**ntercelular / **p**oli-**N**-**a**cetil**g**lucosamina

PSMs: **P**henol-**s**oluble **m**odulins (modulinas solubles en fenol)

PVL: **L**eucocidina de **P**anton-**V**alentine

QS: **Q**uorum **s**ensing

SAgs: **S**uperantígenos

SARM: ***S****taphylococcus* ***a****ureus* **r**esistente a la **m**eticilina

SARM-AC: ***S****taphylococcus* ***a****ureus* **r**esistente a la **m**eticilina **a**sociado a la **c**omunidad

SARM-AG: ***S****taphylococcus* ***a****ureus* **r**esistente a la **m**eticilina **a**sociado a la **g**anadería.

SARM-AH: ***S****taphylococcus* ***a****ureus* **r**esistente a la **m**eticilina **a**sociado al **h**ospital o sistema sanitario.

SARV: **S**taphylococcus **a**ureus **r**esistentes a la **v**ancomicina

SASM: **S**taphylococcus **a**ureus **s**ensible a la **m**eticilina

SEs: **S**taphylococcal **E**nterotoxins (Enterotoxinas estafilocócicas)

SEls: **S**taphylococcal **e**nterotoxin-**l**ike

TSST-1: **T**oxina 1 del **s**índrome del **s**hock **t**óxico

VAPGH: **V**irion-**a**ssociated **p**eptido**g**lycan **h**ydrolases (Peptidoglicano hidrolasas asociadas a virión)

Introducción

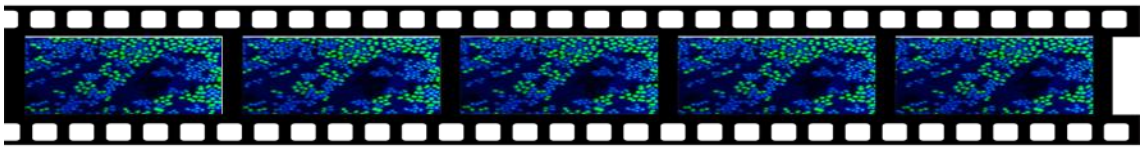

INTRODUCCIÓN

1 *STAPHYLOCOCCUS AUREUS*: UN PATÓGENO OPORTUNISTA

1.1 El género *Staphylococcus*

En 1882, el cirujano escocés Sir Alexander Ogston observó la presencia de células bacterianas cocoides agrupadas en racimos en muestras clínicas procedentes de abscesos (Ogston, 1882). Por su aspecto morfológico los denominó *Staphylococcus*, palabra latinizada procedente del griego σταφυλή (staphylḗ) 'racimo de uvas' y κόκκος (kókkos) 'grano' (http://dle.rae.es/?id=GkIperY). Dos años más tarde, el médico alemán Friedrich Julius Rosenbach distinguió dos especies de estafilococos, *S. aureus* y *Staphylococcus albus* (actualmente conocido como *Staphylococcus epidermidis*) debido al color amarillo y blanco de sus colonias, respectivamente (Parisi, 1885). Tras años de debate sobre la inclusión de los estafilococos dentro del género *Micrococcus*, en la familia Micrococcaceae, Evans y col. (1955) propusieron que *Staphylococcus* debía constituir un género aparte, dada la capacidad de estos microorganismos de crecer en ausencia de oxígeno. Finalmente, Breed introdujo el género *Staphylococcus* en la séptima edición del Manual de Bergey en 1957, clasificación posteriormente confirmada por Baird-Parker (Baird-Parker, 1965).

Actualmente, las bacterias pertenecientes al género *Staphylococcus* se incluyen dentro del filo Firmicutes, clase Bacilli, orden Bacillales y familia *Staphylococcaceae* (Manual de Bergey de Bacteriología Sistemática, 2009). De acuerdo con datos recientes de la base de datos “List of Prokaryotic Names with Standing in Nomenclature” (LPSN), el género *Staphylococcus* incluye 53 especies y 28 subespecies (Parte, 2018). La mayoría de estas especies pueden clasificarse en seis grupos en función de los resultados de análisis y comparación de la secuencia del gen del ARNr 16S, así como de fragmentos de los genes *dnaJ*, *rpoB* y *tufK*. Las especies representantes de dichos grupos son 1) *Staphylococcus auricularis*, 2) *Staphylococcus hyicus*/*Staphylococcus intermedius*, 3) *S. epidermidis*/*S. aureus*, 4) *Staphylococcus saprophyticus*, 5) *Staphylococcus simulans* y 6) *Staphylococcus sciuri* (Lamers y col., 2012). Más recientemente, gracias al desarrollo de las técnicas de secuenciación masiva se han secuenciado los genomas completos de múltiples aislados de *Staphylococcus* pertenecientes a distintas especies. Para facilitar

la realización de estudios comparativos acerca de la biología, filogenia, virulencia y taxonomía de este género se ha recogido toda esta información genómica en la base de datos StaphyloBase (Heydari y col., 2014).

El género *Staphylococcus* está formado por cocos Gram-positivos, con un diámetro de 0,5 a 1,5 µm, que pueden aparecer como células únicas o agrupados en parejas, tétradas, cadenas cortas o formando los característicos racimos de uvas (Prescott y col., 2004). Son bacterias no móviles y no esporuladas. La mayoría de los estafilococos producen catalasa, característica que se utiliza para diferenciar el género *Staphylococcus* de los géneros *Streptococcus* y *Enterococcus* que son catalasa negativos. Son microorganismos poco exigentes en cuanto a sus requerimientos nutricionales, y pueden crecer en condiciones ambientales muy diversas, aunque lo hacen mejor entre 30˚C y 37˚C, y a un pH próximo a la neutralidad. Son resistentes a la desecación y a los desinfectantes químicos, y toleran concentraciones de NaCl de hasta el 12% (Kloos y col., 1999). Algunas especies producen el enzima coagulasa (estafilococos coagulasa positivos), entre las que se incluyen *S. aureus*, *S. intermedius* y *S. hyicus*, entre otras. Por el contrario, otras especies son coagulasa negativas (CoNS), como por ejemplo *S. epidermidis* (Kania y col., 2004). En cuanto a su hábitat, varias especies del género *Staphylococcus* viven en las superficies corporales de humanos u otros animales formando parte de su microbiota habitual (Harris y Richards, 2006). Sin embargo, en ocasiones se pueden comportar como patógenos oportunistas dando lugar a infecciones de importancia veterinaria o clínica, tales como la mastitis en ganado vacuno, dermatitis en cerdos o diversas infecciones en humanos (Foster, 2012).

1.2 *Staphylococcus aureus*

1.2.1 Características generales

S. aureus (también denominado estafilococo áureo o estafilococo dorado) es el miembro más conocido dentro del género *Staphylococcus*. Como se mencionó anteriormente, su nombre se debe al color amarillo de sus colonias, que es consecuencia de la producción del pigmento carotenoide estafiloxantina (Pelz y col., 2005). Al igual que el resto de miembros de este género, se trata de una bacteria Gram positiva, anaerobia facultativa, capaz de producir catalasa, cuyas células presentan morfología cocoide y están típicamente agrupadas en racimos (Figura 1).

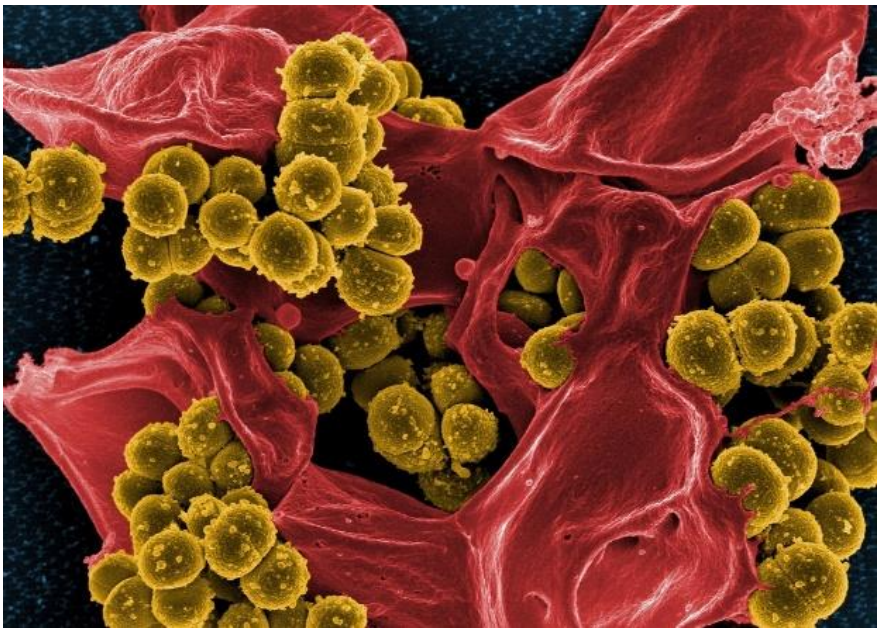

Figura 1: *Staphylococcus aureus* formando parte de un biofilm. Fotografía tomada de https://pixabay.com

La pared celular de *S. aureus* está compuesta por una capa gruesa de peptidoglicano o mureína, un polímero polisacáridico compuesto por cadenas con uniones de tipo β-(1,4) no ramificadas, que contienen subunidades alternantes de ácido N-acetilmurámico y N-acetilglucosamina. La principal función del peptidoglicano es mantener la rigidez y la resistencia osmótica de la pared bacteriana. Otro componente mayoritario de la pared celular de las bacterias Gram positivas son los ácidos teicoicos, que constituyen alrededor del 40% del peso de la pared. Estos ácidos son polímeros de glicerol o ribitol fosfato, azúcares y, algunas veces, D-alanina y están unidos de forma covalente al peptidoglicano. Cuando están unidos a los fosfolípidos de la membrana citoplasmática se les llama ácidos lipoteicoicos.

Además, la mayoría de las cepas de *S. aureus* se caracterizan por la producción de coagulasa, un enzima que permite la conversión del fibrinógeno en fibrina, criterio que se ha utilizado tradicionalmente para diferenciar esta especie de otros estafilococos, principalmente de *S. epidermidis* (Cervantes-García y col., 2014). Por otra parte, también es relevante indicar que algunas cepas de *S. aureus* producen cápsula, característica que se ha relacionado con un incremento en la virulencia.

En el cuerpo humano, este microorganismo se encuentra ampliamente distribuido sobre la piel, en las fosas nasales, vías respiratorias superiores, perineo y axilas. De hecho, se considera que aproximadamente el 30% de la población es portadora nasal asintomática de *S. aureus* (Wertheim y col., 2005). Sin embargo, este microorganismo es capaz de aprovechar situaciones en las que el hospedador presenta un sistema inmune deprimido y/o hay una rotura en la barrera de protección de las mucosas para invadir los tejidos y dar lugar a infecciones. Así, *S. aureus* es posiblemente uno de los patógenos oportunistas más importantes, tanto en el ámbito veterinario como en el clínico, y puede ocasionar infecciones de la piel, del tracto respiratorio, endocarditis, osteomielitis, septicemias e incluso la muerte (Lowy, 1998). Además, *S. aureus* se caracteriza por su versatilidad y por ser muy difícil de erradicar. La versatilidad de este microorganismo se debe a que posee un amplio arsenal de factores de virulencia, entre los que destacan su capacidad para producir toxinas (Otto, 2014) y enzimas hidrolíticos, así como a su habilidad para formar biofilms o biopelículas sobre distintas superficies (Otto, 2013a). Por otra parte, esta bacteria es muy resistente a condiciones ambientales adversas, así como a muchos agentes antimicrobianos, incluyendo múltiples antibióticos de uso clínico (Figueiredo y Ferreira, 2014).

1.2.2 Factores de virulencia

Como ya se mencionó anteriormente, *S. aureus* se caracteriza por presentar múltiples factores de virulencia que le permiten adherirse y/o invadir las superficies corporales, evitar la eliminación por el sistema inmune y causar efectos tóxicos en el hospedador.

Así, algunos **componentes estructurales de la célula bacteriana** participan también en la virulencia. Por ejemplo, el peptidoglicano puede estimular la liberación de citoquinas por los macrófagos, la activación de la vía del complemento y la agregación plaquetaria. Existen diferencias en la estructura del peptidoglicano entre las cepas de estafilococos que podrían explicar su variación en virulencia como por ejemplo, su capacidad de producir el síndrome de coagulación intravascular diseminada (Lowy, 1998). También se ha encontrado que la cápsula y los ácidos teicoicos son factores de virulencia en *S. aureus* (Harris y col, 2002*)*. Además, este patógeno presenta una serie de proteínas superficiales, ancladas a la pared celular bacteriana, que participan en la

adherencia a los tejidos del hospedador. En conjunto, estas proteínas se denominan MSCRAMMs (del inglés "microbial surface components recognizing adhesive matrix molecules") e incluyen a las proteínas de unión al colágeno (Cna), a la fibronectina (FnBPA y FnBPB) y al fibrinógeno (ClfA y ClfB), así como a la proteína A (Foster y Höök, 1998).

La mayoría de las cepas de estafilococos son productoras de **enzimas extracelulares** (nucleasas, proteasas, lipasas, hialuronidasas y colagenasas). Estos productos bacterianos pueden destruir los tejidos del hospedador y así facilitar la diseminación de la infección a los tejidos adyacentes. Por otro lado, el enzima coagulasa activa la protrombina, proteína del plasma sanguíneo que convierte el fibrinógeno en fibrina. La fibrina resultante se deposita entonces sobre las células de *S. aureus*, haciendo que estas sean menos inmunogénicas (Thammavongsa y col, 2015).

Además, *S. aureus* puede producir un gran número de **toxinas**, entre las que se incluyen las citotoxinas, que dañan la membrana de las células del hospedador desencadenando su lisis y posterior liberación de su contenido intracelular (Kaneko y Kamio, 2004). Así, aquellas toxinas que provocan la lisis de los glóbulos rojos son las hemolisinas α, β, δ y γ, mientras que las que ocasionan la lisis de los glóbulos blancos son la leucocidina de Panton-Valentine (PVL) y las leucocidinas LukD y LukE (Otto, 2014). En 2007 se descubrió que la hemolisina δ (o PSMγ) pertenece a una familia de péptidos secretados denominados modulinas solubles en fenol o PSMs, de acuerdo a sus siglas en inglés "phenol-soluble modulins" (Wang y col., 2007). Las PSMs tienen gran importancia en la patogénesis y el mantenimiento de la bacteria en el hospedador, ya que pueden provocar la lisis de eritrocitos y leucocitos, así como activar el sistema inmune, estando implicadas además en la dispersión de los biofilms (Cheung y col., 2013). Además de los ejemplos ya mencionados, *S. aureus* posee todo un arsenal de toxinas entre las que cabe señalar las exfoliatinas que están directamente asociadas con infecciones de la piel como el impétigo y el síndrome de la piel escaldada. Se han descrito tres isoformas de exfoliatinas en *S. aureus*: ETA, ETB y ETD (Prevost y col., 2003). Por otro lado, la secreción de enterotoxinas (SEs) termoestables es uno de los factores de virulencia más importantes de *S. aureus*, ya que pueden causar lo que se conoce como intoxicación alimentaria estafilocócica. Estas enterotoxinas resisten altas temperaturas,

valores de pH bajos y la acción de enzimas proteolíticos, por lo que mantienen su actividad dentro del tracto digestivo tras su ingestión. Las enterotoxinas pertenecen a la familia de las toxinas pirogénicas o superantígenos (SAgs). La clasificación de los SAgs se basa en su capacidad para producir el vómito, de manera que las que tienen capacidad emética, se designan como SEs ("staphylococcal enterotoxins"), y las que no provocan el vómito se denominan SEls ("staphylococcal enterotoxin-like") (Lina y col., 2004). Especial mención merece la toxina 1 del síndrome del shock tóxico (TSST-1), la cual no posee actividad emética (Reiser y col., 1983). Se cree que la actividad superantigénica de las SEs, además de producir una respuesta inflamatoria intestinal localizada, facilita la transcitosis que permite la entrada de la bacteria al torrente sanguíneo. Esto favorecería la interacción con los linfocitos T que proliferan y liberan una gran cantidad de quimiocinas y citocinas, desencadenando el síndrome del shock tóxico (Hu y Nakane, 2014). En *S. aureus*, los genes que codifican las SEs se encuentran en elementos genéticos móviles tales como plásmidos, profagos e islas de patogenicidad (SaPI) (Cervera-Alamar y col., 2018).

La expresión de los genes que codifican los factores de virulencia de *S. aureus* está controlada por una red compleja de factores de regulación transcripcional que incluye los sistemas Agr, SaeRS, SrrAB y ArlSR, entre otros (Novick, 2003). El más estudiado hasta el momento es el sistema Agr, que regula la producción de adhesinas de superficie (proteína A, proteína fijadora de fibronectina, etc.), así como la producción de toxinas y enzimas extracelulares (Laverty y col., 2013). El sistema regulador Agr responde a la densidad bacteriana, por lo que se trata de un sistema de percepción de cuórum o"quorum sensing". Así, los productos de los genes *agrD* y *agrB* permiten la síntesis, modificación y secreción de un péptido autoinductor (AIP) que se acumula a lo largo del crecimiento bacteriano. Al llegar a la fase postexponencial de crecimiento, cuando hay un gran número de células bacterianas, se alcanza una elevada concentración de AIP en el medio extracelular, este se une al sensor AgrC, que se autofosforila y activa al regulador de respuesta AgrA, lo que da lugar a un incremento de la transcripción del propio operón *agr*, así como de los distintos genes que forman parte del regulón controlado por este sistema y que incluyen diversas toxinas y exoenzimas (Yarwood y Schlievert, 2003; Cheung y col, 2004).

1.2.3 Resistencia a antibióticos

La introducción de los antibióticos supuso una revolución en el campo de la medicina, ya que permitió reducir drásticamente la mortalidad asociada a infecciones bacterianas. Sin embargo, su utilización masiva y/o inadecuada en los ámbitos clínico y veterinario ha llevado a la selección y propagación de cepas resistentes a estos compuestos. Como consecuencia de esto, la eficacia de los tratamientos de enfermedades infecciosas, tanto en los animales como en el ser humano, ha disminuido considerablemente (Smith, 2015). Hoy en día, se considera que la resistencia a los antimicrobianos es una de las principales amenazas a las que se enfrenta la medicina moderna (OMS, 2019). De hecho, estimaciones recientes indican que las muertes atribuibles a infecciones causadas por microorganismos resistentes a los antibióticos superarán a las causadas por el cáncer en el año 2050 (https://amr-review.org/Publicaciones). La Organización Mundial de la Salud (OMS) ha publicado en 2017 la primera lista de «patógenos prioritarios» resistentes a los antibióticos para promover el conocimiento y la investigación sobre los mismos En dicha liste se incluye a las cepas de *S. aureus* resistentes a la meticilina (SARM) y resistentes a la vancomicina (SARV) como patógenos de prioridad alta,. Los primeros datos publicados en 2018 por la OMS, gracias al Sistema Mundial de Vigilancia de la Resistencia a los Antimicrobianos, denominado GLASS por sus siglas en inglés (Global Antimicrobial Resistance Surveillance System), indican que los niveles de resistencia en algunas infecciones bacterianas graves son elevados, y que las cepas bacterianas resistentes más frecuentes pertenecen a las especies *Escherichia coli*, *Klebsiella pneumoniae, S. aureus* y *Streptococcus pneumoniae*, seguidas *de Salmonella spp*. De hecho, *S. aureus* está considerado uno de los patógenos del grupo ESKAPE (*Enterococcus faecium*, *S. aureus*, *K. pneumoniae*, *Acinetobacter baumannii*, *Pseudomonas aeruginosa* y *Enterobacter* spp.) que incluye los principales microorganismos causantes de infecciones resistentes a los antibióticos que ocurren en los hospitales de todo el mundo, debido a que “escapan” de la acción de la mayoría de las opciones terapéuticas disponibles (Peterson, 2009).

En el caso de *S. aureus*, hay datos que muestran la adquisición progresiva de resistencia a distintos grupos de compuestos antimicrobianos a lo largo de la era antibiótica. Así, la resistencia a penicilina mediada por β-lactamasas en cepas de este

patógeno fue detectada ya en 1946, y la resistencia a macrólidos y tetraciclinas se observó durante los años 50. Más adelante, se detectaron las cepas de *S. aureus* resistentes a la meticilina (SARM), que están frecuentemente asociadas a la aparición de enfermedades graves (Gordon y Lowy, 2008). La resistencia a la meticilina en este microorganismo es mediada habitualmente por el producto del gen *mecA*, que está generalmente situado en el elemento móvil SCC*mec*. Este gen codifica una proteína de unión a la penicilina denominada PBP2a, que se caracteriza por su baja afinidad por los antibióticos β-lactámicos. Como consecuencia de esto, el antibiótico no puede inhibir la actividad transpeptidasa de esta proteína, la cual es esencial para la correcta síntesis del peptidoglicano que constituye la pared celular bacteriana. El primer caso de SARM asociado al ámbito hospitalario (SARM-AH) fue observado por primera vez en un hospital de Inglaterra en 1961. Desde entonces, las cepas resistentes a la meticilina se han diseminado rápidamente por los hospitales de todo el mundo, alcanzando en la actualidad proporciones epidémicas en algunos países. Esta diseminación de los aislados SARM-AH, junto a la reciente aparición de clones de SARM adquiridos en la comunidad (SARM-AC) y asociados al ganado (SARM-AG), ha tenido un impacto importante en los sistemas de salud (Arias y col., 2008). La primera descripción de aislados SARM-AC se produjo en 1993, detectándose cepas SARM en individuos que no habían tenido ninguna interacción con ambientes hospitalarios ya que se trataba de poblaciones aborígenes de Australia (Grundmann y col., 2016; DeLEO y col., 2010). Por su parte, las cepas SARM-AG se aislaron por primera vez en 1972 en una muestra procedente de una vaca belga (Devriese y Casas, 1975), pero no se les prestó atención hasta 2005, tras la publicación de un informe sobre infecciones y altas tasas de colonización por SARM en los cerdos holandeses (Armand-Lefevre y col., 2005). Los aislados SARM-AG son genéticamente distintos de los aislados humanos, perteneciendo en su mayoría al complejo clonal CC398, y representan el reservorio más grande de SARM fuera de los hospitales (van Loo y col., 2007). Estas cepas pueden transmitirse desde los animales a personas que se encuentren en contacto estrecho con los mismos, tales como granjeros, personal de mataderos, transportistas de ganado y veterinarios. La posibilidad de que los animales actúen como una fuente o reservorio de infecciones zoonóticas por *S. aureus* se ha ejemplificado en algunos informes recientes de infecciones en humanos causadas por cepas de SARM asociadas a cerdos. Actualmente la distribuión de los diferentes clones

SARM a lo largo del mundo, junto con la adquisición de nuevo y variado material genético comienza a difuminar los límites entre estas líneas genéticas (Stefani y col., 2012).

Tabla 1: Principales diferencias entre SARM-AH, SARM-AC y SARM-AG.

Características	SARM-AH	SARM-AC	SARM-AG
Lineas genéticas más prevalentes	CC5, CC8, CC2, CC30, CC45	CC1, CC8, CC30, CC59, CC80, CC88, CC93	CC1, CC9, CC97, CC130, CC133, CC398
Virulencia	No LPV	LPV	No LPV
Fenotipo de Resistencia	A menudo multirresistentes	Habitualmente resistentes a β-lactámicos	Multirresistentes. Resistente a tetraciclina (CC398).

LPV: Leucocidina de Panton-Valentine

A pesar de la gravedad de la situación creada por la resistencia a la meticilina en este patógeno, los datos más recientes del Centro Europeo para la Prevención y el Control de Enfermedades (European Centre for Disease Prevention and Control (ECDC)) sobre la incidencia de SARM (2014-2017) han mostrado una disminución en la prevalencia de SARM en Europa, que varía entre el 1.0% y el 44.4%, si bien las tasas de mortalidad siguen siendo muy altas. Sin embargo, es necesario mencionar que los porcentajes más altos se encuentran en países mediterráneos como España, donde la prevalencia de la resistencia a la meticilina ha aumentado, alcanzando valores del 25.8% (ECDC, 2018).

El aumento progresivo de infecciones causadas por cepas SARM ha conducido a un mayor uso de la vancomicina, un glucopéptido que inhibe la síntesis de la pared celular por medio de la unión a la terminación D-Ala-D-Ala del peptidoglicano. La vancomicina ha sido el antibiótico de primera línea en el tratamiento de infecciones graves causadas por SARM durante más de cuatro décadas (van Hal y Fowler, 2013). Sin embargo, esto ha dado lugar a la aparición de cepas con susceptibilidad intermedia a dicho compuesto (SAIV) y cepas resistentes a la vancomicina (SARV). Estas cepas se

inhiben a concentraciones de 4 a 8 µg/ml (SAIV) y a concentraciones iguales o superiores a 16 µg/ml (SARV) (Lakhundi y Zhang, 2018). La disminución en la sensibilidad a la vancomicina se debe generalmente a un engrosamiento de la pared celular bacteriana por incremento de la síntesis del peptidoglicano, lo que hace que el antibiótico quede atrapado en las capas más superficiales de la pared. Por otro lado, los altos niveles de resistencia a la vancomicina (cepas SARV) suelen deberse a la adquisición del gen *vanA*, cuyo producto participa en la producción de precursores del peptidoglicano terminados en D-alanina-D-lactato que presentan una afinidad reducida por el antibiótico.

2 BIOFILMS: ESTRATEGIA DE PERSISTENCIA Y RESISTENCIA

Las condiciones de crecimiento microbiano utilizadas habitualmente en el laboratorio, donde las bacterias a menudo se cultivan de forma planctónica, difieren bastante de la realidad, ya que de forma natural los microorganismos frecuentemente crecen formando agregaciones multicelulares, y a menudo multiespecie, llamadas biofilms (Costerton et al., 1987; Hall-Stoodley et al., 2004). Para formar biofilms, las bacterias tienen que primero adherirse a una superficie biótica (tejidos vivos) o abiótica (superficies alimentarias, implantes, válvulas, etc.), y generar una matriz extracelular compuesta principalmente de proteínas, carbohidratos y/o ADN extracelular (eADN) (Dolan, 2002; Flemming y Wingender, 2010). Esta matriz adhesiva rodea a las células bacterianas y facilita su supervivencia en ambientes hostiles o extremos. Además, varios estudios han demostrado que las células que forman parte de biofilms pueden llegar a ser entre 10 y 1.000 veces más resistentes a un gran número de antibióticos y otros agentes antimicrobianos que las células de la misma cepa que se encuentran en estado planctónico (Stewart, 2015). En la actualidad se sabe que la resistencia mostrada por los biofilms tiene un carácter multifactorial (Figura 2). Entre los factores mejor conocidos se encuentran los siguientes:

• **Degradación de agentes antimicrobianos y penetración restringida de los mismos**. La matriz extracelular puede limitar la entrada de compuestos antimicrobianos al interior del biofilm, ejerciendo así una acción protectora sobre las células bacterianas que lo forman (Stewart, 1996). Este efecto puede deberse a la unión o la reacción del agente antibacteriano y las moléculas que forman la matriz. Además, hay estudios que

muestran que la matriz extracelular también favorece la acumulación de enzimas capaces de inactivar compuestos antimicrobianos. Por ejemplo, Anderl y col. (2000) mostraron que la ampicilina no podía penetrar en biofilms formados por una cepa parental de *K. pneumoniae*, pero sí en los formados por una cepa mutante no productora de β-lactamasas. Además, en muchos casos, se ha observado una correlación lineal entre el espesor de los biofilms y su resistencia a los antibióticos (Amorena y col., 1999; Monzón y col., 2001; Monzón y col., 2002).

• **Baja tasa de crecimiento dentro del biofilm**. La estructura del biofilm da lugar a la formación de gradientes en la concentración de nutrientes y oxígeno, lo que hace que las células situadas en distintas zonas del biofilm presenten estados metabólicos diferentes. Así, las células situadas en las capas más superficiales muestran un metabolismo más activo y una mayor tasa de crecimiento, mientras que las células situadas en las capas más profundas presentan un metabolismo muy bajo. La mayoría de los antibióticos son más efectivos contra células en crecimiento activo. Por ejemplo, en el caso de las penicilinas y las cefalosporinas, la tasa de destrucción bacteriana es proporcional a la tasa de crecimiento. Por este motivo, las células situadas en el interior del biofilm muestran una mayor tolerancia a la acción de muchos compuestos antimicrobianos.

• **Cambios en la producción de determinantes de resistencia**. Las condiciones ambientales específicas que se dan en el interior de los biofilms pueden dar lugar a cambios a nivel de transcriptoma o proteoma que se traduzcan en una mayor resistencia a compuestos antimicrobianos. Por ejemplo, en algunos casos se ha detectado un aumento en la expresión de bombas de eflujo en los biofilms formados por algunos microorganismos, lo que da lugar a una mayor resistencia a compuestos antimicrobianos que son así más eficientemente expulsados al exterior celular (Baugh y col., 2012; Mah y col., 2003).

• **Persistencia bacteriana**. Se sabe que los biofilms y los cultivos planctónicos en fase estacionaria presentan una mayor proporción de células persistentes, aproximadamente un 1%, que los cultivos planctónicos en fase de crecimiento activo (Spoering y Lewis, 2001). A día de hoy, la teoría más aceptada es que estas células se encuentran en un estado "durmiente" que les confiere tolerancia a la mayoría de

antibióticos y desinfectantes, siendo responsables de gran parte de las infecciones recalcitrantes (Lewis, 2008; Wood y col., 2013). En el caso de *S. epidermidis*, por ejemplo, se considera que las células persistentes constituyen el principal mecanismo de resistencia de los biofilms (Qu y col., 2010).

• **Incremento en la tasa de aparición de resistencia adquirida**. La proximidad entre las células bacterianas que forman un biofilm favorece el intercambio de material genético entre las mismas. Así, algunos autores han observado una mayor tasa de transferencia horizontal en biofilms que en cultivos planctónicos (Cook y col., 2011; Savage y col., 2013). Además, algunos estudios han encontrado una mayor frecuencia de mutación en células que están formando biofilms comparada con células planctónicas de la misma especie, lo que también puede dar lugar a una mayor frecuencia de mutaciones que confieran resistencia a antibióticos (Driffield y col., 2008; Ryder y col., 2012).

• **Resistencia al sistema inmunitario del hospedador**. Los exopolímeros que forman el biofilm protegen a las células bacterianas de los componentes del sistema inmunitario del hospedador. Por ejemplo, Barrio y col. (2000) observaron una disminución en la actividad bactericida de los neutrófilos frente a cepas de *S. aureus* productoras de exopolisacárido.

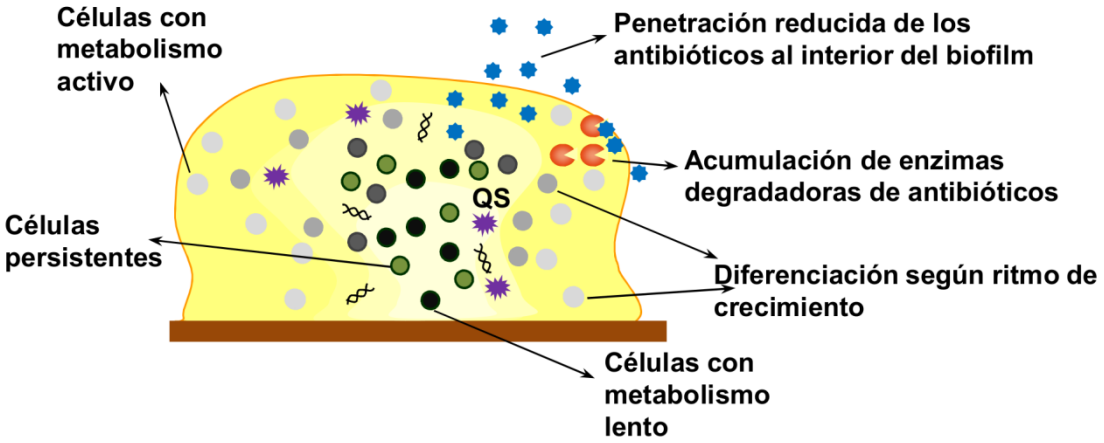

Figura 2: Mecanismos de resistencia de un biofilm. QS: quorum sensing. La intensidad del color amarillo indica la cantidad de nutrientes y oxígeno en una zona del biofilm (a mayor intensidad, mayor concentración).

2.1 Biofilms mixtos

En la mayor parte de trabajos de investigación se estudian los biofilms formados por una única especie bacteriana de interés. Sin embargo, en condiciones reales, los biofilms monoespecie solo se formarían en condiciones muy específicas en las que un microorganismo presenta un sobrecrecimiento que acaba desplazando a las otras especies del ambiente. Por el contrario, la mayor parte de las comunidades microbianas sésiles están constituidas por células pertenecientes a dos o más especies bacterianas, en ocasiones acompañadas por levaduras, algas o protozoos. Además, la complejidad estructural de estas formaciones multicelulares, en las que se distinguen microambientes de características bien diferenciadas, permite la coexistencia de organismos con necesidades fisiológicas muy diversas. Por ejemplo, en un mismo biofilm pueden convivir especies anaerobias, aerobias y microaerobias. De hecho, un estudio bastante reciente mostró que la presencia de *P. aeruginosa* facilitaba la persistencia de *Campylobacter jejuni* en biofilms formados en condiciones óxicas, ya que favorece el desarrollo de zonas microaerófilas (Culotti y Packman, 2015).

Las interacciones entre las distintas especies que forman un biofilm mixto pueden ser muy complejas, existiendo frecuentemente fenoménos de antagonismo y sinergia (Elias y Banin, 2012; Rendueles y Ghigo, 2012). Así, hay casos en que la presencia de un microorganismo determinado tiene un efecto negativo sobre el desarrollo de otro, llevando a una inhibición del crecimiento de este. Esto puede deberse, por ejemplo, a una mayor eficiencia en la competencia por los nutrientes disponibles o a la producción de una molécula con actividad antimicrobiana sobre la especie bacteriana desplazada. En otras ocasiones, sin embargo, se pueden observar fenómenos de sinergia, en los que la convivencia entre dos especies bacterianas favorece el desarrollo de ambas. De hecho, se han descrito muchos ejemplos de cooperación metabólica, que consiste en la utilización de un metabolito producido por una especie vecina. También se sabe que existen casos de coagregación, un proceso en el que bacterias distintas genéticamente se unen entre sí por medio de interacciones moleculares específicas (Rickard y col., 2003). Además, los biofilms mixtos exhiben frecuentemente una mayor resistencia a los antibióticos, los biocidas y las respuestas inmunitarias del hospedador que los biofilms monoespecie (Fux y col., 2005). Esto hace que las infecciones causadas por biofilms

multiespecie sean aún más difíciles de eliminar. Además, se han descrito casos en los que un microorganismo potencia la producción de los factores de virulencia de otro, como ocurre con *P. aeruginosa* y *S. aureus* en biofilms formados sobre heridas (Pastar y col., 2013).

Hoy en día se sabe que los sistemas de comunicación intercelular de tipo "quorum sensing" juegan un papel fundamental en el desarrollo de los biofilms mixtos, siendo en gran parte responsables de las interacciones sinérgicas y antagónicas entre las especies que los componen (Elias y Banin, 2012). Por un lado, la modulación del crecimiento poblacional de las especies vecinas, ya tenga un carácter positivo o negativo, afectará a la producción de las moléculas de señalización que median la percepción de cuórum. Esto, a su vez, controlará la producción de moléculas que participan en la adherencia a superficies, compuestos de la matriz extracelular o enzimas que promueven la dispersión del biofilm. Sin embargo, en otros casos, la comunicación interespecífica es más directa. Un ejemplo claro de este fenómeno es el sistema "universal" AI-2 que se ha identificado en múltiples especies bacterianas, tanto Gram-positivas como Gram-negativas (Waters y Bassler, 2005; Federle, 2009). Sin embargo, aún queda mucho camino por recorrer para entender en profundidad la complejidad de la comunicación entre células de distintas especies en el contexto de los biofilms.

2.2 Biofilms de *S. aureus*

Al igual que otros microorganismos, *S. aureus* puede formar biofilms sobre superficies diversas. El principal componente de la matriz extracelular en esta especie bacteriana es el polisacárido de adhesión intercelular (PIA) o poli-N-acetilglucosamina (PNAG), un polímero parcialmente desacetilado de β-1,6-N-acetilglucosamina (Götz 2002, Mack 1996; Sadovskaya, 2006). Este compuesto forma parte de la matriz extracelular en la que están embebidas las bacterias. La producción de exopolisacárido está mediada por el gen regulador *icaR* y por el operón *ica*, compuesto de los genes de biosíntesis *icaADBC* (Otto, 2009). Las bacterias no productoras de este exopolímero son, por lo general, menos adherentes que las que sí lo producen y, por ello, son menos patogénicas, mientras que las cepas de *S. aureus* productoras de PNAG son más virulentas (Kropec y col., 2005). Además del exopolisacárido, los biofilms de *S. aureus* también pueden contener ADN extracelular, ácidos teicoicos y/o proteínas. Entre las

proteínas cabe destacar la proteína Bap, que se encuentra anclada en la pared celular (Latasa y col, 2006), y es producida por algunas cepas (Archer y col, 2011).

Según Moormeier y Bayles (2017), el desarrollo de un biofilm de *S. aureus* consta de cinco etapas (Figura 3):

A. **Fijación:** Las células de *S. aureus* se adhieren a superficies abióticas o bióticas a través de interacciones hidrofóbicas o mediadas por adhesinas como las MSCRAMMs. Entre las MSCRAMMs se encuentran, por ejemplo, la proteína A y las proteínas de unión a colágeno (Cna) o a fibronectina (FnbpA), que facilitan la adhesión a biomateriales y a proteínas de la matriz del hospedador (Foster y Höök, 1998). Otra molécula relacionada con la adhesión inicial es la autolisina asociada a superficie (AtlA), la cual, además de ser capaz de unirse a la fibronectina, da lugar a la liberación de ADN extracelular a través de una lisis parcial de la población bacteriana favoreciendo la adherencia al sustrato (Heilmann y col, 1997). Además, *S. aureus* puede unirse a superficies abióticas a través de interacciones electrostáticas e hidrofóbicas, debido a que los ácidos teicoicos, polímeros de pared celular con una elevada carga negativa, juegan un papel clave en el primer paso de la formación de biofilms (Gross y col, 2001).

B. **Multiplicación:** Una vez que las células se unen a la superficie, comienza el desarrollo del biofilm gracias a la multiplicación de las células bacterianas y a la producción de la matriz extracelular. Durante esta fase, los biofilms son sensibles a la presencia de proteasas lo que indica la participación de componentes de naturaleza proteica. De hecho, algunos estudios muestran que *S. aureus* utiliza proteínas citoplásmicas como componentes de la matriz (Foulston y col., 2014). Estas proteínas se asocian a la superficie de las células bacterianas en condiciones de pH ligeramente ácido (alrededor de 5) favoreciendo la posterior unión de ADN extracelular mediante interacciones electrostáticas (Dengler y col., 2015).

C. **Éxodo:** En las dos primeras fases, el biofilm de *S. aureus* se desarrolla como una estructura más o menos plana y homogénea asociada a la superficie. Por ello, antes de entrar en la fase de maduración, que consiste en la formación de microcolonias tridimensionales, las células de *S. aureus* deben reorganizarse. Este proceso de reorganización estructural, denominado éxodo, consiste en la liberación de una subpoblación de células del biofilm a través de la actividad de una nucleasa extracelular

(Nuc) regulada por SaeRS, un sistema regulador de dos componentes que participa en el control del desarrollo de biofilms en este microorganismo (Liu y col, 2016). Este enzima lleva a cabo la degradación de parte del ADN extracelular de la matriz y desencadena una dispersión celular temprana (distinta a la mediada por el sistema Agr) que da como resultado la reestructuración del biofilm.

D. **Maduración:** En esta etapa se forman las microcolonias a partir de distintos grupos de células que han permanecido unidas durante la etapa de éxodo. La maduración del biofilm se caracteriza por una rápida división celular que forma agregaciones sólidas compuestas de células rodeadas de proteínas, incluyendo las modulinas solubles en fenol (PSMs), y de ADN extracelular. Como consecuencia de este proceso, la población bacteriana que forma el biofilm se diferencia en subpoblaciones que presentan estados metabólicos diversos.

E. **Dispersión:** Esta etapa está controlada principalmente por el sistema regulador Agr, del que ya se habló anteriormente. Así, la acumulación del péptido AIP a lo largo de la formación del biofilm induce la expresión de los genes de este regulón que codifican, entre otras, las proteínas implicadas en la dispersión del biofilm, por ejemplo proteasas extracelulares o la PSM codificada por el gen *hld* (δ-toxina).

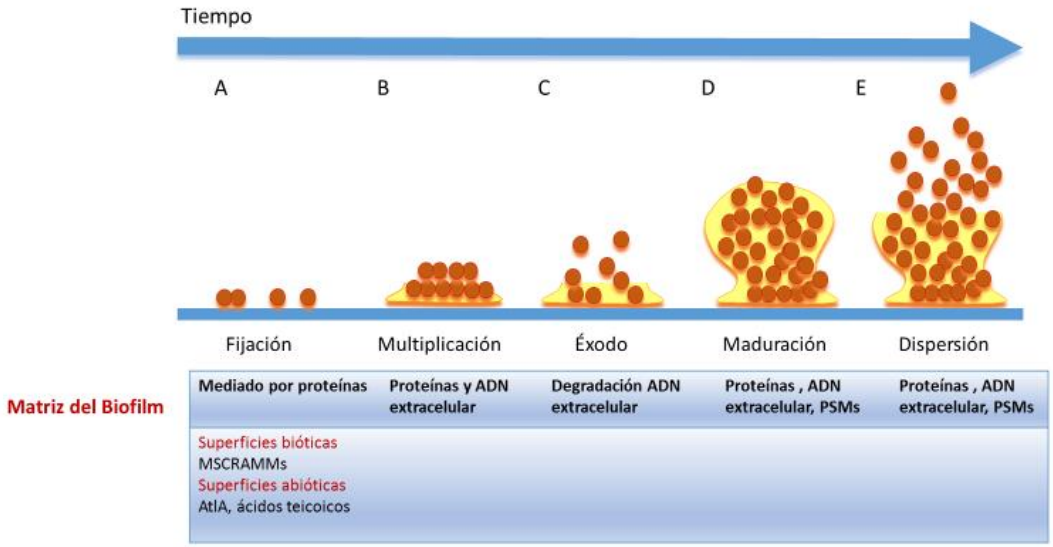

Figura 3: Distintas etapas en la formación de un biofilm de *S. aureus*. [Adaptación de Moormeier y Bayles (2017)].

2.2.1 Biofilms de *S. aureus* en el ambiente hospitalario

En entornos clínicos, las bacterias están expuestas a diversas fuentes de estrés (los antibióticos, la limitación de nutrientes y/o de oxígeno, el choque térmico, etc.) que desencadenan respuestas adaptativas en las células bacterianas. La combinación de este y otros mecanismos de defensa da como resultado la formación de estructuras multicelulares altamente resistentes que son recalcitrantes a los mecanismos de eliminación por el sistema inmune del hospedador y muy difíciles de erradicar con los agentes antimicrobianos disponibles en la actualidad, los cuales generalmente se desarrollan para la erradicación de bacterias planctónicas (de la Fuente-Núñez y col., 2013).

La formación de biofilms sobre superficies del ámbito clínico por cepas de *S. aureus* juega un papel importante en el problema de las infecciones nosocomiales. Como mencionamos anteriormente, esto se debe sobre todo a que las células bacterianas que forman el biofilm muestran una mayor resistencia al tratamiento con antimicrobianos convencionales y a la respuesta inmune del hospedador (Gordon y Lowy, 2008). Además, es importante mencionar que algunas de las cepas que se han aislado de superficies hospitalarias, incluidos estetoscopios, catéteres e incluso dispensadores de jabón desinfectante, son resistentes a la meticilina (Brooks y col., 2002; Guinto y col., 2002; Stickler, 2002). Evidentemente, esto dificulta aún más su eliminación.

Con el avance de las técnicas médicas, se ha impulsado el uso de dispositivos médicos permanentes como parte del tratamiento para diferentes enfermedades. En muchas ocasiones, se produce la formación de biofilms sobre estos dispositivos, lo que aumenta el riesgo de aparición de infecciones bacterianas, incluidas las estafilocócicas (Manandhar y col., 2018). Así, este patógeno puede adherirse a estructuras no orgánicas como catéteres, prótesis articulares, válvulas cardíacas protésicas, lentes de contacto, válvulas de derivación del líquido cefalorraquídeo y marcapasos cardíacos (McCarthy y col., 2015; Jaśkiewicz y col., 2019). En algunos casos, como en los catéteres venosos centrales, este proceso se ve favorecido por el recubrimiento de los dispositivos médicos con proteínas del hospedador después de su implantación en el cuerpo, como pueden ser las proteínas del plasma y otras proteínas de los tejidos como fibronectina, fibrinógeno, laminina, etc. (Lister y col., 2014). Dichas proteínas facilitan la unión de

aquellas células bacterianas que posean adhesinas para las mismas. Una vez que la bacteria se ha adherido a la superficie del implante y ha formado el biofilm, este actúa como una fuente de reinfección, sobre todo en pacientes inmunocomprometidos.

Además de la adhesión a superficies inertes, se sabe que *S. aureus* puede formar biofilms sobre los tejidos corporales del hospedador, lo que da lugar a diversas enfermedades como endocarditis, osteomielitis, infecciones de la piel y partes blandas, infecciones del tracto urinario, y complicaciones de la fibrosis quística, entre otras. Como es de suponer, esto contribuye al carácter crónico de estas infecciones ya que las hace menos susceptibles a la acción del sistema inmune y a los tratamientos antimicrobianos.

2.2.2 Biofilms de *S. aureus* en el sector agroalimentario

En la industria alimentaria, es muy común detectar la presencia de biofilms en conducciones, equipos y materiales diversos, ya que pueden formarse prácticamente en cualquier tipo de superficie, incluyendo plástico, cristal, madera, metal e incluso sobre los propios alimentos (Chmielewski y Frank, 2003).

Indudablemente, la persistencia de bacterias patógenas en entornos alimentarios presenta un gran riesgo para la salud pública, ya que puede conducir a brotes toxiinfecciosos. En el año 2017, por ejemplo, se registraron 5.079 brotes asociados a alimentos solo en la Unión Europea, que afectaron a 43.400 personas, con 4.541 hospitalizaciones y 33 muertes (EFSA y ECDC, 2018). Los alimentos más frecuentemente implicados en toxiinfecciones por *S. aureus* son los de origen animal, especialmente la leche y la carne (Figura 4).

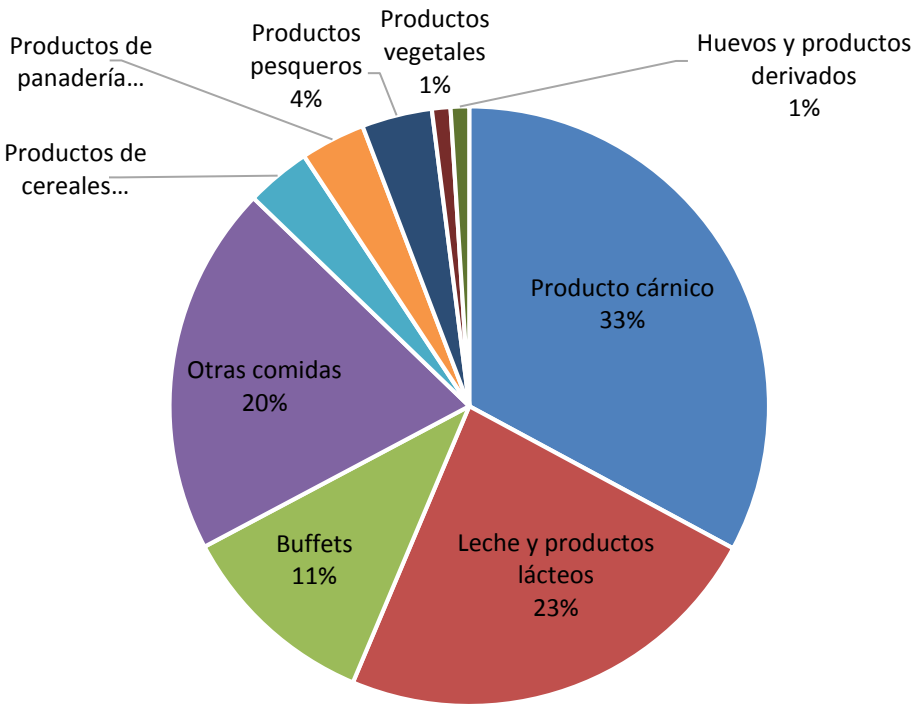

Figura 4: Alimentos implicados en brotes causados por toxinas estafilocócicas (EFSA 2006-2010).

Este microorganismo puede incorporarse a la cadena alimentaria en diferentes puntos de la misma. Por ejemplo, *S. aureus* puede proceder del ganado, lo que constituye un problema sanitario a nivel de la producción primaria. Así, *S. aureus* causa infecciones de importancia veterinaria como la mastitis en el ganado productor de leche (Silva y col., 2014) o la dermatitis en el ganado porcino (Chen y col., 2007). Estas infecciones pueden dar lugar a considerables pérdidas económicas (Crossley y col., 2009) y, en general, hacen necesaria la utilización de antibióticos, lo que a su vez contribuye a la selección de cepas bacterianas resistentes (Chang y col., 2015). Por ello, si no hay unas medidas de desinfección y manipulación adecuadas de los animales y la maquinaria, S. *aureus* puede contaminar la leche o la carne y, finalmente, causar intoxicaciones alimentarias.

Otro punto crítico de contaminación es la manipulación de los alimentos durante su producción, distribución o consumo. En este caso, el patógeno frecuentemente proviene de los manipuladores de alimentos que son ocasionalmente portadores asintomáticos de *S. aureus* (Figueroa y col., 2002). De hecho, se estima que la mitad de la población adulta está colonizada, y aproximadamente el 15% de la población es

portadora de *S. aureus* en las narinas anteriores (Taylor y Unakal, 2020). Además, las plantas de sacrificio y procesamiento de animales son entornos propicios para el intercambio de bacterias entre los animales y los manipuladores (Hatcher y col., 2017).

3 LOS BACTERIÓFAGOS

3.1 Características generales

Los bacteriófagos o fagos son virus que infectan a bacterias. Al igual que el resto de los virus, los fagos reconocen específicamente a sus células hospedadoras, les transfieren su material genético (ADN o ARN) y redirigen la maquinaria de la célula para producir nuevas partículas virales.

Los bacteriófagos fueron descubiertos hace más de un siglo, en 1915, por el bacteriólogo británico Frederick Twort, quien observó su actividad bacteriolítica y la atribuyó a la posible presencia de un virus, si bien su naturaleza era aún desconocida. Poco después, en 1917, el microbiólogo canadiense Félix d'Hérelle propuso la utilización de la palabra bacteriófago, que proviene de "bacteria" y "fagein" (del griego comer o devorar), y que es una descripción del impacto macroscópico que tienen estos virus en los cultivos bacterianos (Abedon y col, 2017; d'Hérelle, 2007).

3.1.1 Morfología y estructura

Los bacteriófagos varían en tamaño de 24 a 400 nm (Ivanovska y col., 2004). Están compuestos fundamentalmente de ácido nucléico (material genético) y proteínas. Su genoma puede componerse de ADN o de ARN el cual puede ser de cadena doble o de cadena sencilla, circular o lineal. La estructura de los fagos está determinada por las proteínas de la cápside (o proteínas estructurales) cuya función principal es la de proteger al material genético fágico (Vispo y Puchades, 2001). Así, la forma en la que se organizan las proteínas alrededor del material genético del fago define la complejidad estructural y la forma del mismo. En cuanto a la simetría de la cápside, los fagos pueden ser icosaédricos o helicoidales y en base a la estructura de la partículoa fágica, se clasifican en filamentosos y complejos (cabeza-cola) (Figura 5) (Clark y March, 2006).

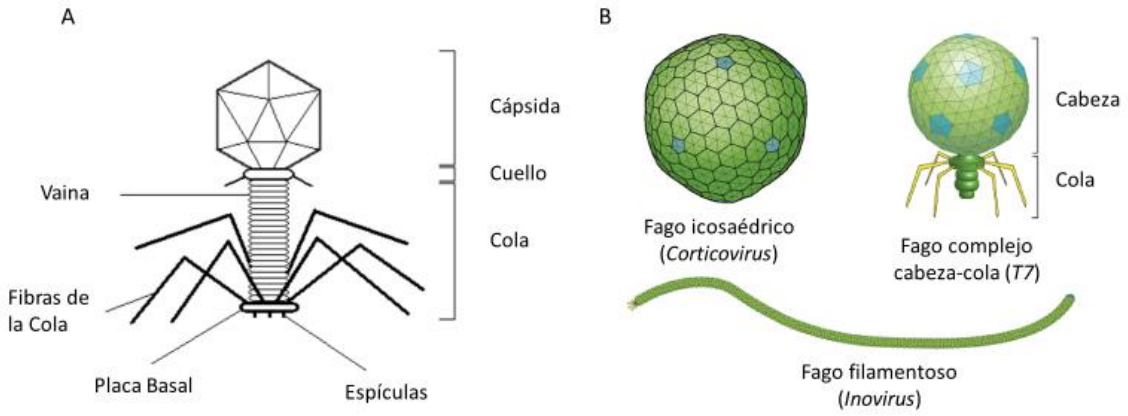

***Figura 5**:* (A) Representación esquemática de la estructura de un bacteriófago. (B) Ejemplos representativos de la simetría de los bacteriófagos. [Adaptación de Khan Academy, s.f.]

3.1.2 Taxonomía

Si bien la taxonomía es una clasificación artificial basada en criterios arbitrarios, es innegable su importancia en el campo de la biología. Así, establecer una clasificación de las distintas entidades biológicas es de gran ayuda para su estudio. En el caso de los fagos, las primeras clasificaciones se realizaron en base a la morfología de la partícula viral y la naturaleza de su ácido nucleico (Bradley, 1967), lo que finalmente se tradujo en la aceptación por parte del Comité Internacional de Taxonomía de Virus (ICTV, International Committee on Taxonomy of Viruses) de las familias *Myoviridae* (fagos de cola contráctil) y *Podoviridae* (fagos de cola corta no contráctil) en 1981, y de la familia *Siphoviridae* (fagos de cola larga no contráctil) en 1984. Posteriormente, Ackerman propuso que estas tres familias se incluyeran en el orden *Caudovirales* (1998) que incluye los fagos más abundantes compuestos por una cabeza icosaédrica y una cola, y cuyo material genético es ADN de cadena doble (Figura 6). Los fagos de la familia *Siphoviridae* son los más abundantes (61.7%), seguidos de los pertenecientes a las familias *Myoviridae* (24.5%) y *Podoviridae* (13.9%) (Ackermann, 2007). Recientemente, el ICTV ha incluido dos nuevas familias, *Ackermanviridae* y *Herelleviridae* (Barylski y col., 2019).

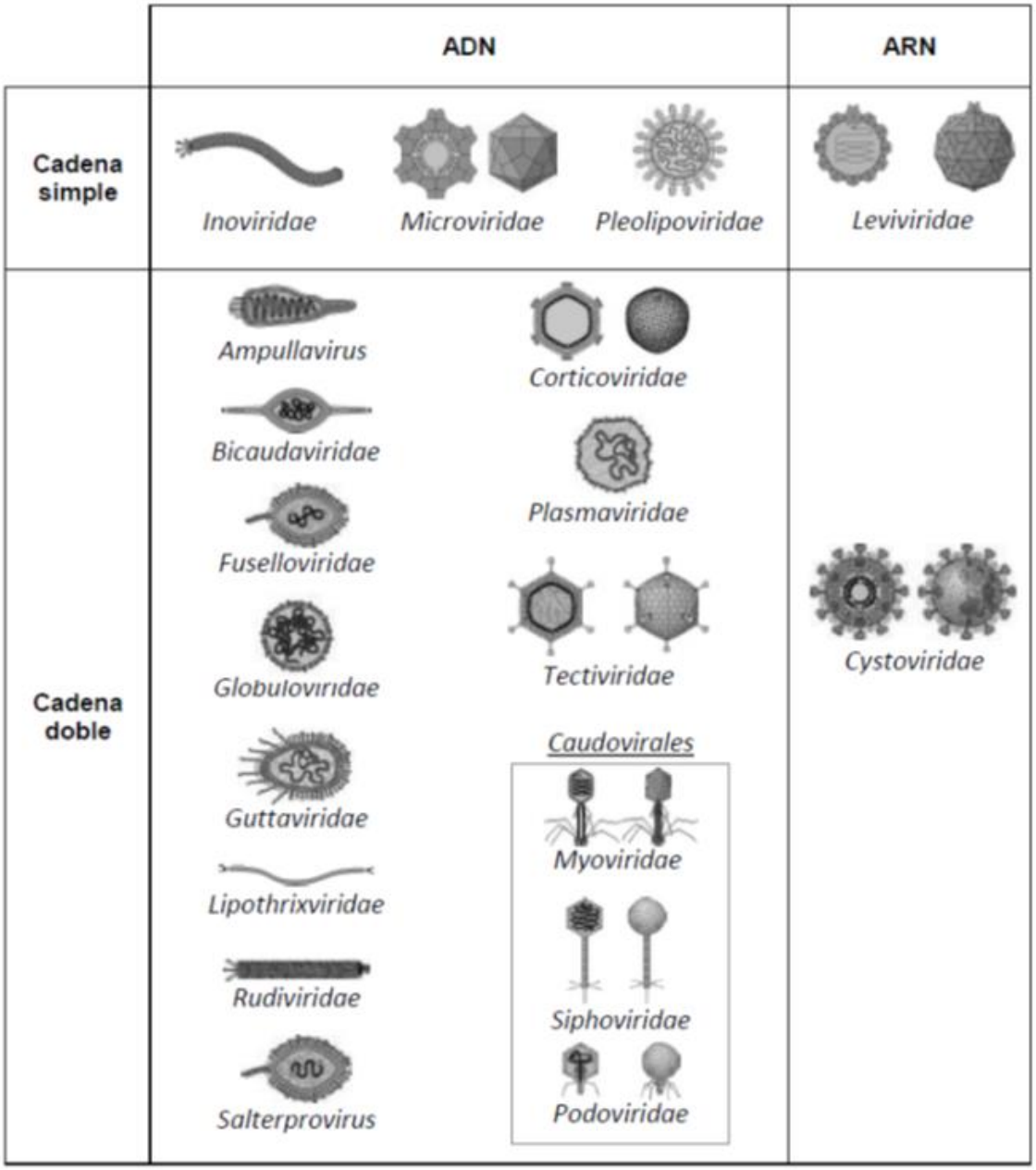

Figura 6: Clasificación taxonómica de virus que infectan microorganismos según la ICTV (King y col., 2012).

El renovado interés por los virus bacterianos junto con la llegada de las técnicas ómicas han llevado a muchos investigadores del campo de los fagos a plantear la necesidad de revisar esta clasificación (Nelson, 2004). Sin embargo, mientras que hay un consenso en la importancia de reexaminar la taxonomía de los fagos, no parece que exista un acuerdo sobre los criterios que deben utilizarse. No obstante, la gran cantidad de información recogida en las bases de datos, incluyendo las más de 9000 secuencias

de genomas completos de fagos depositadas en Genbank, será muy valiosa a la hora de llevar a cabo dicha reclasificación.

3.2 Ciclos de desarrollo

Los fagos necesitan utilizar la maquinaria de una célula hospedadora para poder multiplicarse o propagarse. Sin embargo, pueden valerse de distintas estrategias para desarrollarse dentro de dicha célula. En términos generales, los fagos se clasifican en dos tipos atendiendo a su ciclo de vida. Los fagos virulentos, que llevan a cabo el denominado ciclo lítico, y los fagos atemperados, que pueden desarrollarse siguiendo un ciclo lisogénico o un ciclo lítico (Figura 7).

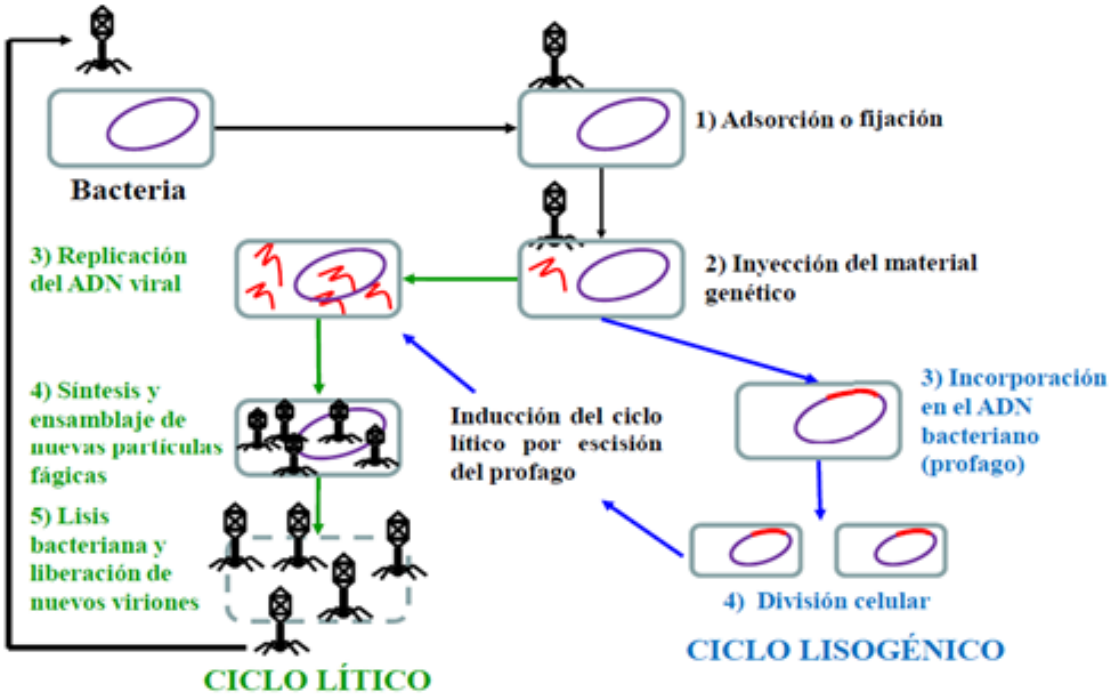

***Figura 7**:* Representación esquemática de las diferentes etapas de los ciclos de vida de un bacteriófago (Gutiérrez y col., 2010).

3.2.1 Ciclo de desarrollo lítico

La propagación de un fago virulento se realiza mediante un ciclo de multiplicación fágica denominado lítico o vegetativo, que tiene como resultado la liberación de una nueva progenie de partículas fágicas infectivas. Las etapas de este ciclo son:

Adsorción: El ciclo lítico se inicia a través de la adsorción de un fago a los receptores presentes en la superficie celular de una bacteria sensible. Este evento es altamente específico, ya que depende de la presencia de receptores adecuados

ubicados en la superficie celular bacteriana; por tanto, un fago solo puede infectar aquellas bacterias que tengan los receptores a los cuales el fago puede unirse (Hughes y col., 1998; Azeredo & Sutherland 2008).

Inyección del ADN fágico: Una vez lograda la unión irreversible de la partícula viral, el material genético del fago entra en la célula bacteriana. Este proceso se produce mediante la inyección del ADN fágico desde la cabeza hacia el interior del citoplasma a través de la cola, mientras que la partícula fágica vacía se queda en la superficie externa de la bacteria (Neve, 1996). Debido a que la adsorción y la inyección del ADN viral son eventos que ocurren casi simultáneamente, en algunos casos es complicado establecer dónde termina una etapa y comienza la siguiente.

Replicación: Una vez inyectado el material genético, comienza la transcripción de los genes tempranos del fago que, en general, tienen como función la inhibición de los mecanismos de defensa de la célula bacteriana y la utilización de la maquinaria celular para la propagación del virus. A continuación, se expresan los genes intermedios y tiene lugar la replicación del genoma fágico. Finalmente, se expresan los genes tardíos y tiene lugar la síntesis de las proteínas que formarán las partículas fágicas maduras.

Ensamblaje: Durante esta etapa, las proteínas estructurales se ensamblan y las nuevas moléculas de ADN fágico son empaquetadas en el interior de la cápside. Al final de este proceso se obtienen las partículas virales completas (Neve, 1996). En los fagos que poseen ADN de cadena doble, la maquinaria de translocación dependiente de ATP empaqueta el genoma viral en las cápsides ya formadas. Los componentes clave de esta maquinaria son el complejo terminasa, encargado de reconocer y cortar el ADN para ser empaquetado, y la proteína portal que constituye la única vía de entrada hacia el interior de la cápside (Feiss y Rao, 2012).

Lisis de la célula hospedadora: El ciclo lítico se completa cuando se produce la ruptura de la pared o lisis celular por medio de enzimas llamadas endolisinas, que están codificadas en el genoma fágico. En muchos casos, este proceso requiere la participación de una proteína transmembrana, la holina, que forma poros en la membrana celular, permitiendo así el acceso de las endolisinas al espacio periplásmico. Como resultado de la lisis, las nuevas partículas fágicas ya ensambladas son liberadas al medio externo (Brüssow, 2001; Roach y Donovan, 2015).

La duración y productividad del ciclo de vida lítico se define por varios parámetros (Figura 8). El período de latencia es el tiempo transcurrido desde la infección hasta la liberación de la progenie viral; el período de eclipse es menor que el anterior y es el tiempo que transcurre desde la infección hasta la formación de las partículas fágicas en el interior de la bacteria; por último, el tamaño de explosión es el número de fagos que se libera tras la infección de una bacteria por un único fago. Estos valores son característicos de cada pareja bacteria sensible-fago lítico (Séchaud y col., 1992).

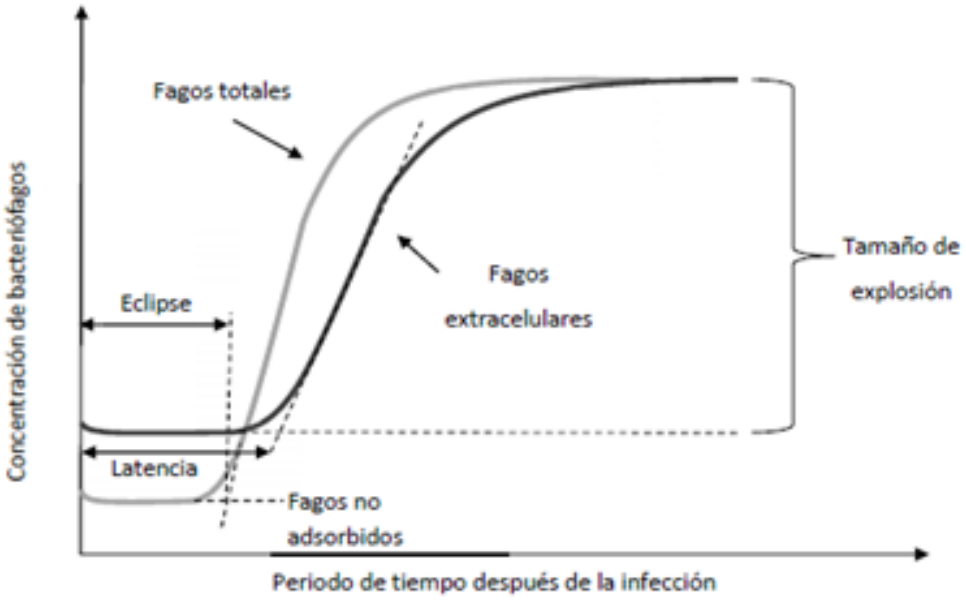

Figura 8: Fases del ciclo lítico de los bacteriófagos (Augusto, 2011).

La propagación se ve afectada por la concentración inicial de fagos, factores ambientales (pH, temperatura, etc.), la concentración bacteriana inicial y por las condiciones fisiológicas de la célula hospedadora. Con respecto a la influencia de la temperatura de incubación sobre la propagación de los fagos, se ha demostrado que la óptima suele ser cercana a la temperatura óptima de desarrollo de la célula hospedadora (González-Menéndez y col., 2018).

3.2.2 Ciclo de desarrollo lisogénico

El ciclo lisogénico es una vía alternativa a la replicación fágica. Los pasos involucrados en la adsorción del fago a la célula sensible y la inyección del ADN son idénticos a los que se producen durante el ciclo lítico pero, en este caso, el ADN fágico se inserta en el cromosoma bacteriano. Esto ocurre por medio de una recombinación

homóloga única que se produce en una región específica de homología entre el ADN viral y el ADN de la célula hospedadora, la cual es conocida como sitio de unión attP (phage attachment site) en el genoma fágico, y como attB (bacterial attachment site) en el genoma de la célula bacteriana. Como consecuencia de esto, no se produce la lisis celular y el ADN del fago se comporta como un fragmento más del cromosoma bacteriano, replicándose de forma sincronizada con este, y dando origen a una progenie de células lisogénicas. Estos fagos en estado de latencia se conocen como "profagos" y las células bacterianas que los llevan se conocen como "lisógenos". En algunos casos, una célula bacteriana es portadora de más de un profago, fenómeno que se denomina multilisogenia. La escisión del profago del cromosoma bacteriano, con la subsiguiente liberación del fago atemperado puede ocurrir espontáneamente, o mediante inducción por factores ambientales que desencadenan la respuesta SOS (luz UV, agentes mutagénicos como la mitomicina C, calor, etc) (García y col., 1999). Tras la activación de la respuesta SOS, la proteína RecA del hospedador se expresa degradando específicamente al represor Cl (responsable de mantener el estado de lisogenia), lo que induce la expresión de la proteína reguladora Cro, permitiendo de esa manera la expresión de todos los genes implicados en el ciclo lítico (Galkin y col., 2009; Oppenheim y col., 2005).

La lisogenia establece una relación simbiótica entre el fago y su hospedador, conocida como conversión lisogénica, que puede proporcionar ventajas evolutivas a la bacteria lisogénica. La más común es la protección contra la infección por fagos semejantes, fenómeno conocido como inmunidad a la superinfección. También se sabe que la conversión lisogénica permite la expresión de proteínas codificadas por el fago en la bacteria hospedadora, confiriéndole nuevas capacidades (Feiner y col., 2015).

La inducción del ciclo lítico del fago no es un proceso perfecto; a veces, los profagos pueden dejar parte de su ADN en el cromosoma bacteriano o llevarse un fragmento del ADN de la bacteria cuando tiene lugar el proceso de escisión. Cuando estos fagos infectan una nueva célula hospedadora, le transfieren los genes de la bacteria infectada anteriormente. Este fenómeno se denomina transducción, proceso mediado por fagos por el cual los genes de resistencia a los antibióticos, los genes que codifican toxinas y otros factores de virulencia pueden propagarse a través de una

población bacteriana (Brown-Jaque y col., 2015; Fortier y Sekulovic, 2013). Un ejemplo destacable es la diversidad de las cepas de *S. aureus*, la cual está determinada principalmente por la presencia de elementos genéticos móviles, muchos de los cuales son profagos o islas genómicas, como las islas de patogenicidad de *S. aureus* (SaPI), también relacionadas con los fagos (Xia y Wolz, 2014; Novick y col., 2010).

3.3 Interacciones fago-bacteria

Actualmente se considera que los fagos son las entidades biológicas más diversas y abundantes del planeta. De hecho, se les puede detectar en cualquier ecosistema, y se ha calculado que son capaces de infectar a más de 140 géneros bacterianos distintos (Reina y Reina, 2018). Teniendo en cuenta todas estas circunstancias, es evidente que estos virus juegan un papel fundamental en el mantenimiento de los ciclos biológicos y geoquímicos de la naturaleza como consecuencia de su efecto regulador sobre las poblaciones de sus respectivas bacterias hospedadoras.

Dentro de este contexto, uno de los aspectos más estudiados hasta el momento es la importancia de los virus bacterianos, tanto atemperados como virulentos, en la evolución de las comunidades microbianas (Fernández y col., 2018). De hecho, algunos estudios genómicos han revelado que el material genético procedente de fagos puede llegar a representar hasta el 20% de algunos genomas bacterianos (Casjens, 2003). Además, los fagos participan en la transferencia horizontal de material genético, contribuyendo así a la diseminación de genes, incluidos los que participan en la resistencia a antibióticos y la virulencia. Este es, sobre todo, un fenómeno asociado a los fagos atemperados (Haaber y col., 2016; Modi y col., 2013), aunque un trabajo reciente demuestra que algunos fagos virulentos también pueden participar en la transferencia horizontal (Keen y col., 2017). Así, los fagos virulentos denominados “superspreaders” (palabra inglesa que significa superdiseminadores) no poseen endonucleasas que degraden el cromosoma de la célula hospedadora durante la replicación del virus. Por ello, cuando tiene lugar la lisis de la célula infectada, se libera al exterior el material genético de la misma que puede ser entonces adquirido por otras células bacterianas mediante transformación natural, pudiendo contribuir de este modo a la dispersión de genes de resistencia a antibióticos.

Además de seleccionar cepas mutantes y favorecer la transferencia genética, la presencia de fagos puede dar lugar a cambios transcripcionales y/o fenotípicos con carácter transitorio en la población bacteriana (Fernández y col., 2018). Hasta el momento, este fenómeno se ha estudiado en mayor detalle en el caso de los fagos atemperados. Así, se sabe que algunas cepas lisógenas de distintas especies bacterianas muestran una mayor virulencia (Davies y col., 2016; Rice y col., 2009; Rossman y col., 2015), resistencia a antibióticos (Schuch y Fischetti, 2006; Wang y col., 2010), capacidad de supervivencia en condiciones adversas (Veses-García y col., 2015) o un incremento en la formación de biofilms (Schuch y Fischetti, 2006; Rice y col., 2009; Gödeke y col., 2011; Carrolo y col., 2010) en comparación con cepas isogénicas libres de profagos. En el caso de los fagos virulentos, los datos disponibles son más escasos, pero apuntan a la posibilidad de que estos también podrían tener efectos fenotípicos sobre la población hospedadora mediante mecanismos no evolutivos, es decir, no asociados a mutación o transferencia de material genético. Por ejemplo, Hosseinidoust y col. (2013a) mostraron que la infección de *P. aeruginosa*, *S. aureus* y *Salmonella* con dosis subinhibitorias de fagos daba lugar a una mayor formación de biofilms. Sin embargo, solo en el primer caso se observó que dicho cambio fenotípico se debía a la selección de mutantes resistentes al fago que eran mejores formadores de biofilms que la cepa parental. En *S. aureus* y *Salmonella* el cambio no parecía deberse a la selección de mutantes, si bien los autores no llegaron a estudiar en profundidad el mecanismo implicado en el aumento de biomasa.

Otro aspecto interesante en relación a la interacción entre las poblaciones del fago y de la bacteria hospedadora es la regulación de la misma a través de los sistemas de "quorum sensing" (Fernández y col., 2018). En concreto, varios estudios recientes han demostrado que la producción de algunos mecanismos que afectan a la susceptibilidad de la población bacteriana a fagos está coordinada con la activación de la cascada de "quorum sensing". Así, por ejemplo, en algunos casos la acumulación de estas señales lleva a una menor expresión de genes que codifican receptores de fagos, lo que da lugar a una menor tasa de adsorción y, por tanto, a una menor susceptibilidad de la célula bacteriana (Høyland-Kroghsbo y col., 2013; Hoque y col., 2016; Tan y col., 2015). También se ha encontrado evidencia de que determinadas señales modulan la expresión

de genes que participan en los sistemas de inmunidad bacterianos CRISPR-Cas de varios microorganismos (Høyland-Kroghsbo y col., 2017; Gao y col., 2015; Patterson y col., 2016). Un caso interesante es el descrito por Hargreaves y col. (2014), quienes encontraron un profago de *Clostridium difficile* que lleva los genes necesarios para la producción de una señal de "quorum sensing". Esto permitiría hipotéticamente al fago controlar el desarrollo de la población de la bacteria hospedadora. Más recientemente, Erez y col. (2017) describieron un sistema de "comunicación" entre partículas fágicas basado en la producción de un péptido (arbitrium) cuya acumulación favorece el proceso de lisogenia, evitando así la extinción de la población bacteriana.

3.4 Proteínas líticas

Entre los avances más esperanzadores en la terapia con fagos se encuentran las proteínas líticas de origen fágico (endolisinas y peptidoglicano hidrolasas asociadas a virión) ya que son capaces de lisar bacterias cuando se añaden exógenamente. Las endolisinas son proteínas codificadas por los bacteriófagos con la función de lisar o destruir la bacteria hospedadora para permitir la liberación de la progenie viral, una vez que ha terminado su ciclo de multiplicación. Estas proteínas presentan dominios específicos que les permiten anclarse selectivamente sobre la pared bacteriana, al tiempo que poseen un módulo catalítico capaz de hidrolizar el peptidoglicano bacteriano. Investigaciones recientes han revelado no solo la sorprendente diversidad catalítica de estos enzimas, sino que han proporcionado también avances en el conocimiento de su organización modular, su estructura tridimensional y su mecanismo de reconocimiento de la pared bacteriana. Todos estos resultados permiten considerar a las endolisinas como bactericidas eficaces con importantes aplicaciones en medicina y biotecnología (Fischetti, 2008).

Ciertos fagos codifican tambien peptidoglicano hidrolasas asociadas al virión (VAPGH) que son componentes estructurales de las partículas fágicas y que median la hidrólisis local del peptidoglicano poco después de su adsorción a la célula bacteriana. A diferencia de las endolisinas, que causan la lisis celular al final del ciclo de infección, la degradación localizada de peptidoglicano permite que el tubo de la cola del fago acceda al citoplasma para transferir el ADN fágico. La capacidad de estas proteínas como antimicrobianos está aún poco explotada (Rodríguez-Rubio y col., 2013).

3.5 Los bacteriófagos y las endolisinas como antimicrobianos

La mayoría de las investigaciones con fagos realizadas entre los años 1920-1930 se centraron en su utilización para el tratamiento de infecciones bacterianas (Summers, 2001). Sin embargo, la denominada terapia fágica pronto se vio mermada por la introducción de los antibióticos, que eran más fáciles de usar y exhibían un espectro de acción más amplio. Hoy en día, el uso inadecuado y el abuso de los antibióticos han provocado un aumento preocupante en la prevalencia de bacterias resistentes a los mismos. Este fenómeno ha conducido a la búsqueda de estrategias antimicrobianas alternativas, incluyendo un interés renovado en la terapia con fagos.

Sin embargo, para que se pueda llegar a un uso más generalizado de los fagos con fines terapéuticos, es primero necesario que se lleven a cabo estudios que confirmen su seguridad y eficacia. Por ejemplo, hasta el año 2005 no se había realizado ningún estudio sobre la seguridad de la administración de preparaciones de fagos en humanos. Entonces, Bruttin y col. (2005) administraron una concentración de 10^5 pfu/ml del fago T4 por vía oral a un grupo de sujetos voluntarios, y no se detectaron efectos adversos asociados a dicha ingesta. Este dato favoreció el inicio en Europa occidental de los primeros ensayos para el tratamiento de las otitis causadas por *P. aeruginosa*. Los resultados mostraron un 50% de disminución de los síntomas en pacientes tratados comparado con el 20% en los no tratados. Del mismo modo los pacientes tratados con fagos mostraron una reducción de un 80% en la carga bacteriana, mientras que en los no tratados permanecía idéntica a las 3 semanas de la administración del tratamiento (Górski y col, 2016).

También los estudios realizados en modelos animales han mostrado unos resultados muy esperanzadores. Por ejemplo, se ha utilizado con éxito un tratamiento con fagos para eliminar *E. coli* multirresistentes del intestino murino (Cisek y col., 2017) y también incrementar el porcentaje de supervivencia al 100% en ensayos de sepsis por *P. aeruginosa* resistente a imipenem (Brüssow, 2017). De forma global, estos estudios demuestran la eficacia de los fagos, siempre y cuando se tenga en cuenta el momento, es decir, la fase en la que se encuentra la infección y la vía de administración de los mismos (Viertel y col., 2014).

Por otra parte, se han realizado varios ensayos clínicos con fagos y otros están en marcha. Por ejemplo, se evaluó (fase I) un cóctel de ocho fagos frente a *S. aureus*, *P. aeruginosa* y *E. coli* para tratar pacientes con úlceras venosas infectadas. Los resultados mostraron que la preparación de fagos era segura y no hubo efectos secundarios tras su administración (Rhoads y col., 2009). La compañía británica Biocontrol Limited realizó un ensayo clínico I/II de tipo doble ciego controlado frente a la otitis crónica causada por *P. aeruginosa*. A diferencia del tratamiento con antibióticos, que requiere la administración de varias dosis en el curso del tratamiento, la terapia con fagos requirió solamente una dosis de 6×10^5 fagos. El resultado fue positivo, puesto que se redujo la concentración de *P. aeruginosa* en los oídos y se observó mejoría de la sintomatología (Wright y col., 2009). También se realizó un ensayo controlado de fase II en un grupo de 27 pacientes con infección confirmada por *P. aeruginosa* en heridas por quemadura, a los cuales se les administró un cóctel de 12 fagos virulentos. Los resultados mostraron que los casos de tratamientos fallidos se debían a la aparición de resistencia seleccionada por la utilización de dosis bajas de fagos (Jault y col., 2019). Actualmente existen varios ensayos de terapia con fagos que han finalizado las fases I y II y que no muestran problemas de seguridad, algo prometedor para llegar a su futuro ensayo clínico en fase III (Vandenheuvel et al., 2015).

Además, en algunos países como Bélgica y Francia se está aplicando la terapia fágica como terapia compasiva al amparo del artículo 37 de la Declaración de Helsinki (World Medical Association, 2013), el cual permite el uso de tratamientos experimentales para aquellos pacientes que han agotado las opciones terapéuticas convencionales. Un ejemplo es la aplicación de fagos en una paciente diabética con osteomielitis de la falange distal ocasionada por *S. aureus* resistente a penicilina (Fish y col., 2018). Otro ejemplo de éxito reciente ha sido la inyección local de una mezcla de bacteriófagos frente a *P. aeruginosa* y *S. aureus* en la cavidad articular para tratar una infección protésica crónica y recurrente (Ferry y col., 2018). Desde el año 2000 se han descrito hasta 29 casos con éxito clínico de aplicación de fagos como terapia compasiva (McCallin y col., 2019).

Los bacteriófagos también se están utilizando en algunos países como una herramienta novedosa de biocontrol en la industria alimentaria para reducir la

contaminación bacteriana (Hagens y Loessner, 2010). El potencial de los fagos para inhibir patógenos transmitidos por alimentos se refleja en diferentes estudios en los que se evitó la contaminación por *Salmonella* (Toro y col., 2005; Whichard y col., 2003), *S. aureus* (Bueno y col., 2012), *Campylobacter* (Atterbury y col., 2003) y *L. monocytogenes* (Murray et al., 2015). Varias compañías ya han comenzado a preparar y comercializar productos a base de fagos como PhageGuard Listex (Micreos) y Ecoshield™ (Intralytix), entre otros.

Los fagos también se pueden usar en medicina veterinaria para tratar infecciones bacterianas (Barrow, 2001). Por ejemplo, Johnson y col. (2008) utilizaron la terapia con bacteriófagos en distintos animales (terneros, pollos y cerdos) infectados con *Salmonella* y *E. coli*. Al igual que ocurre en la medicina humana, la evaluación significativa de la terapia con fagos requerirá la realización de estudios en animales que reflejen el uso previsto, así como una investigación exhaustiva de la aparición y las características de las bacterias resistentes a los fagos.

Algunos estudios recientes han llevado a cabo la caracterización de fagos que han sido aislados a partir de productos disponibles comercialmente que se usan para el tratamiento de estafilococos. En la Tabla 2, resumimos varios informes que describen las características de fagos aislado de varios productos comerciales.

Todos los productos descritos hasta ahora contienen fagos virulentos pertenecientes a la familia *Myoviridae* (Azam y Tanji, 2019). Pyophage de Microgen (Moscú, Rusia) es el único producto que contiene un fago virulento (SCH1) que pertenece a la familia *Podoviridae* (McCallin y col., 2018). Ninguno de los fagos presentes en los productos estudiados poseía genes de virulencia o resistencia a antibióticos. Los fagos purificados podían infectar una amplia gama de cepas, tanto sensibles como resistentes a la meticilina, e incluso eran efectivos para destruir células que formaban parte de un biofilm (Dvořáčková y col., 2019).

Tabla 2. Características de los fagos presentes en los preparados comerciales disponibles frente a *S. aureus.*

Producto	Fabricante	Fago	Características	Referencia
Fersisi	Instituto Eliava, República de Georgia	B1 y JA1	B1 y JA1 infectaron al 73.9% y 78.2% de 23 aislados de *S. aureus*, respectivamente.	Ajuebor y col.,2018
PhagoBioDerm		Team 1	Team 1 infectó a 51 de 57 cepas distintas de *S. aureus*.	El Haddad y col., 2014
Pyophage		Sb-1 y ISP	Sb-1 mostró un amplio rango de huésped, infectando 50 cepas SARM y 43 MSSA productoras de toxinas. Ninguna de las cepas era resistente al fago usado a título alto (1×10^{11} PFU/ml). ISP mostró un amplio rango de huésped, infectando al 86% de los 86 aislamientos de *S. aureus*. Este fago mostró estabilidad en condiciones relevantes *in vivo* y la administración de ISP subcutánea, nasal y oral a conejos no pareció causar efectos adversos.	Kvachadze y col., 2011; Vandersteegen y col., 2011
Stafal®	Bohemia Pharmaceuticals, República Checa	Stafal® fago	El fago infectó al 83% de SARM (108/120) y al 99% de SASM (169/170). Puede destruir a las células planctónicas de manera muy efectiva.	Dvořáčková y col, 2019
Pyophage	Microgen, Rusia	vB_SauM-fRuSau02 y SCH1	El cóctel de fagos de Pyophage infectó el 97% de 31 SARM y el 85% de 20 aislados de SASM.	Leskinen y col., 2017; McCallin y col., 2018

Adaptada de Azam, A. H., & Tanji, Y. (2019).

En este contexto, resulta evidente que los fagos ofrecen una alternativa prometedora para tratar enfermedades infecciosas o eliminar patógenos asociados a distintas actividades humanas (agricultura, veterinaria, alimentación y tratamiento de aguas residuales) (García y col., 2010; Jassim y col., 2016; Carvalho y col., 2017). Además, tienen una serie de ventajas tales como su especificidad para atacar la bacteria diana,

capacidad de autoamplificación, habilidad para la degradación de biofilms y baja toxicidad para los humanos. No obstante, también presentan desventajas entre las que destaca el hecho de que las bacterias pueden adquirir resistencia a los fagos, si bien esta desventaja se puede minimizar mediante la utilización simultánea de varios fagos diferentes (cócteles de fagos) (Reina y Reina, 2018).

Por su parte, las proteínas líticas de origen fágico (endolisinas y peptidoglicano hidrolasas asociadas al virión) comparten muchas de las ventajas de los bacteriófagos pero no parecen seleccionar células resistentes (Barbosa y col., 2013; Fernández et al., 2018). Además, las endolisinas han demostrado su eficacia en varios modelos animales de infección bacteriana, así como en la descolonización de las membranas mucosas (Tabla 3). Así, la primera endolisina frente a *S. aureus* probada en modelos animales fue la MV-L, codificada por el fago ΦMR11, y que es capaz de lisar células pertenecientes a varias cepas, incluidas las variantes SARM, VISA, y VRSA. Por el contrario, esta proteína es inocua para otras especies comensales, tales como *S. epidermidis*, que es un habitante de la piel y las membranas mucosas que puede inhibir competitivamente la colonización de *S. aureus*.

Tabla 3. Selección de aplicaciones antimicrobianas de endolisinas y proteínas derivadas.

Patógeno diana	Endolisina (s) y / o derivado (s)	Modelo animal	Vía de administración	Descripción y / o resultado	Referencia
S. aureus	$CHAP_K$	*In vivo* (ratón)	Intranasal	Elimina *S. aureus* de las narinas de los ratones.	Fenton y col., 2010
S. aureus	ClyS	In vivo (ratón)	Tópica	Reducción de 3 unidades log UFC en la piel. Mejor rendimiento que el antibiótico mupirocina.	Pastagia y col., 2011
S. aureus	λ SA2-E-Lyso-SH3b, λ SA2-E-LysK-SH3b	In vivo (ratón)	Intramamaria	Reducción de 3.36 unidades log UFC con tratamiento combinado con lisostafina.	Schmelcher y col., 2012
S. aureus	SAL-2	In vitro		Actividad contra bacterias planctónicas y biofilm.	Son y col., 2010

S. aureus	Varias proteínas quiméricas	In vivo (ratón, rata)	Intranasal, intramamaria, intramuscular	Mejor actividad que la de la proteína parental en modelos de infección nasal, mastitis y osteomielitis.	Becker y col., 2016)
S. aureus	PlyGRCS	In vivo (ratón)	Intravenosa	Fue eficaz para rescatar al 30% de los ratones de la muerte inducida por bacteriemia por *S. aureus* después de 3,5 días.	Linden y col., 2015
SARM	SAL200 (SAL-1)	In vivo (humano)	Intravenosa	Estudio clínico de fase I que evalúa la farmacocinética, la farmacodinámica y la tolerancia de SAL200 en humanos; no se observaron efectos adversos graves.	Jun y col., 2017
SASM, SARM	SA.100	In vivo (humano)	Tópica	Caso clínico que describe el tratamiento exitoso de 3 dermatosis diferentes relacionadas con *S. aureus* mediante la aplicación tópica de Staphefekt SA.100, agente terapéutico basado en una endolisina.	Totté y col., 2017
SARM	MR-10	In vitro		Reducción significativa de biofilms después del tratamiento secuencial con minociclina durante 3 h seguido de tratamiento con endolisina MR-10 durante 16 h.	Chopra y col., 2015
S. aureus	LysSA97	In vitro		En carne y leche, se produjo una reduccion de 0.8 ± 0.2-log en el n° de UFC/ml; también una reducción de 4.5 ± 0.2-log UFC/ml cuando se combinó con carvacrol.	Chang y col., 2017
S. aureus	HydH5, HydH5Lyso, HydH5SH3b, CHAPSH3b	In vitro		En la leche, las bacterias eran indetectables (10^4 UFC/ml) después de 6 h de incubación a 37°C.	Rodriguez-Rubio y col., 2013

S. aureus , *S. epidermidis*	LysH5	In vitro		Se eliminó el biofilm después del tratamiento durante 6 h, seguido de un segundo tratamiento durante 12 h; en la leche pasteurizada, las bacterias fueron indetectables (10^6 UFC/ml) después del tratamiento durante 4 h; hubo un efecto sinérgico con nisina.	Gutiérrez y col., 2014; Garcia y col., 2010; Obeso y col., 2008,
S. aureus , *S. epidermidis*	LysRODI	*In vivo* (ratón)	Intramamario	Los ratones tratados mostraron una reducción de 3-4 unidades log de la carga bacteriana, en comparación con los controles.	Gutierrez y col., 2020

Antecedentes y objetivos

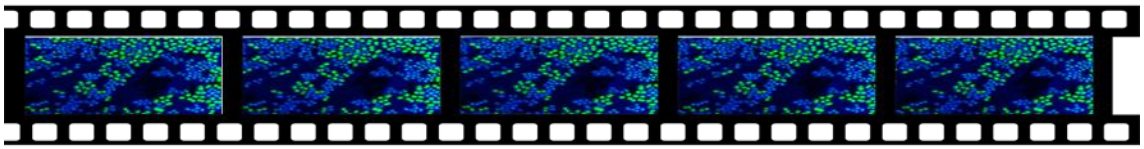

ANTECEDENTES Y OBJETIVOS

Estudios previos realizados en nuestro grupo (DairySafe) han permitido determinar que *S. aureus* se encuentra con frecuencia en superficies de la industria alimentaria formando biofilms mixtos con otras especies tales como *Bacillus cereus, Lactobacillus plantarum* o *Enterococcus faecium* (Gutiérrez y col., 2012).

En nuestro laboratorio se han aislado y caracterizado cuatro bacteriófagos (vB_SauS-phiIPLA35, vB_SauSphi-IPLA88, vB_SauM-phiIPLA-RODI y vB_SepM-phiIPLA-C1C) que infectan específicamente cepas de *S. aureus* aisladas del entorno alimentario (García y col., 2009; Gutiérrez y col., 2015a). Ensayos realizados con los fagos de la familia *Myoviridae* phiIPLA-RODI y phiIPLA-C1C frente a diversas cepas de estafilococos en fase planctónica confirmaron su capacidad lítica. Además, la exposición de biofilms de esas cepas a estos dos fagos tambien redujo la cantidad de bacterias adheridas, siendo el fago phiIPLA-RODI por sí mismo tan eficaz como la mezcla de ambos fagos (Gutiérrez y col., 2015b).

Además, en nuestro laboratorio tambien se han caracterizado cinco proteínas fágicas con capacidad para lisar *S. aureus* (LysH5, HydH5, HydH5SH3, HydH5Lyso, CHAPSH3) y una capaz de degradar la matriz extracelular de los biofilms (Dpo7) (Obeso y col., 2008; Rodríguez-Rubio y col., 2011; Rodríguez-Rubio y col., 2013; Gutiérrez y col., 2015a).

Por otra parte, la endolisina LysH5 mostró una gran eficacia en la eliminación de *S. aureus* en leche, siendo este efecto más notable cuando se usó combinada con nisina (García y col., 2010). LysH5 tambien mostó una notable actividad contra los biofilms estafilocócicos, siendo además lítica frente a células persistentes o “persisters”, las cuales son la causa de las infecciones recalcitrantes (Gutiérrez y col., 2014).

El grupo también caracterizó la peptidoglicano hidrolasa asociada a virión, HydH5, que además de tener buena capacidad antimicrobiana frente a *S. aureus*, fue utilizada para la generación de proteínas quimera, en combinación con dominios de la lisostafina, una bacteriolisina producida por *Staphylococcus simulans* (Rodríguez-Rubio y col., 2012a). Dichas proteínas quimera tambien tienen potencial como bioconservantes de leche por su actividad frente a *S. aureus* (Rodríguez-Rubio y col., 2013b).

Con respecto a la eliminación de biofilms, esta puede ser favorecida a través de la degradación de la matriz en la que están inmersas las células bacterianas. Gutiérrez y col. (2017) mostraron que la proteína Dpo7, codificada en el genoma del fago phiIPLA-C1C, tiene actividad exopolisacárido despolimerasa. Como ocurre con otras proteínas de este tipo, este enzima puede prevenir y dispersar los biofilms, lo que potencialmente permite un mejor acceso de los antimicrobianos al interior de los mismos (Abedon, 2017).

El amplio conocimiento sobre los fagos de *S. aureus* y las proteínas fágicas como agentes antimicrobianos ha permitido a nuestro grupo extender el estudio de la eficacia de los mismos en la eliminación de biofilms mixtos, con vistas a su futura aplicación como desinfectantes en distintos sectores.

El trabajo realizado en esta Tesis Doctoral abordó los siguientes objetivos:

1. Desarrollo de un modelo de estudio para biofilms mixtos formados por *S. aureus* y otras especies bacterianas, acompañantes habituales de la misma en la industria alimentaria.
2. Optimización de las condiciones de eliminación de biofilms mixtos de *S. aureus* con bacteriófagos y proteínas líticas de origen fágico.
3. Estudio del papel de los bacteriófagos (virulentos y atemperados) en el equilibrio ecológico de biofilms de *S. aureus*. Posible participación en la formación de biofilms.
4. Análisis de la respuesta adaptativa de los biofilms de *S. aureus* frente a dosis subinhibitorias de fagos y proteínas fágicas.

Trabajo Experimental

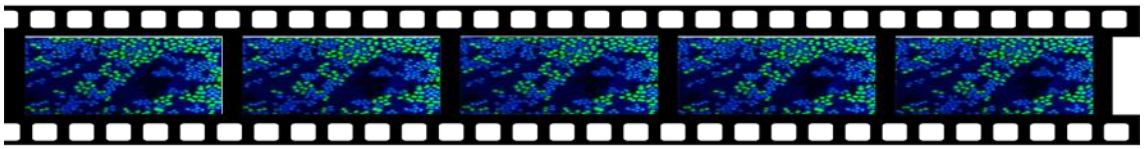

Capítulo 1

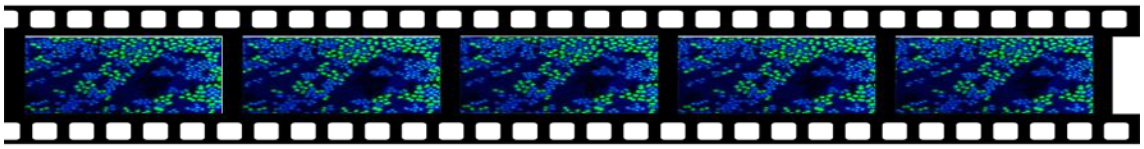

TRABAJO EXPERIMENTAL

Capítulo 1: Tratamiento de biofilms mixtos de *S. aureus* con bacteriófagos

El uso de los bacteriófagos como antimicrobianos puede ayudar a eliminar los biofilms de la industria alimentaria, ya que estos son resistentes a gran parte de los métodos de erradicación comúnmente utilizados. El desarrollo de una estrategia exitosa basada en fagos requiere un análisis en profundidad, y debe tener en cuenta que los biofilms que se forman en ambientes naturales generalmente consisten en poblaciones mixtas. Por ello, el primer objetivo del proyecto de esta Tesis Doctoral consistió en desarrollar un modelo de estudio para biofilms mixtos formados por *S. aureus* y otras especies bacterianas (*L. plantarum, E. faecium* o *Lactobacillus pentosus*), acompañantes habituales de la misma en la industria alimentaria. Posteriormente, se procedió a evaluar la utilización de bacteriófagos para su eliminación. Además, una vez optimizado el modelo, se analizó la capacidad de los fagos vB_SauM-phiIPLA-RODI (phiIPLA-RODI) y vB_SepM-phiIPLA-C1C (phiIPLA-C1C) para difundir, propagarse y permanecer viables dentro de la compleja estructura del biofilm.

1. González, S., Fernández, L., Campelo, A. B., Gutiérrez, D., Martínez, B., Rodríguez, A., & García, P. (2017). The Behavior of *Staphylococcus aureus* Dual-Species Biofilms Treated with Bacteriophage phiIPLA-RODI Depends on the Accompanying Microorganism. *Applied and environmental microbiology*, 83(3), e02821-16. https://doi.org/10.1128/AEM.02821-16
2. González, S., Fernández, L., Gutiérrez, D., Campelo, A. B., Rodríguez, A., & García, P. (2018). Analysis of Different Parameters Affecting Diffusion, Propagation and Survival of Staphylophages in Bacterial Biofilms. *Frontiers in microbiology*, 9, 2348. https://doi.org/10.3389/fmicb.2018.02348

The behavior of *Staphylococcus aureus* dual-species biofilms treated with bacteriophage phiIPLA-RODI depends on the accompanying microorganism

Silvia González, Lucía Fernández, Ana Belén Campelo, Diana Gutiérrez, Beatriz Martínez, Ana Rodríguez, Pilar García[#]

Instituto de Productos Lácteos de Asturias (IPLA-CSIC). Paseo Río Linares s/n 33300 - Villaviciosa, Asturias, Spain.

Running Head: Phage infection of dual-species biofilms

[#]Address correspondence to Dr. Pilar García, pgarcia@ipla.csic.es

SG and LF contributed equally to this work

Abstract

The use of bacteriophages as antimicrobials against pathogenic bacteria offers a promising alternative to traditional antibiotics and disinfectants. Significantly, phages may help to remove biofilms, which are notoriously resistant to commonly used eradication methods. However, the successful development of novel antibiofilm strategies must take into account that real-life biofilms usually consist of mixed-species populations. Within this context, this study aimed to explore the effectiveness of bacteriophage-based sanitation procedures for removing polymicrobial biofilms from food industry surfaces. To do that, dual-species biofilms formed by the food pathogenic bacterium *Staphylococcus aureus* in combination with *Lactobacillus plantarum*, *Enterococcus faecium* or *Lactobacillus pentosus* were treated with the staphylococcal phage phiIPLA-RODI. Our results suggest that the impact of bacteriophage treatment on *S. aureus* mixed-species biofilms varies depending on the accompanying species and the infection conditions. For instance, short treatments (4 h) with a phage suspension under nutrient-limiting conditions reduced the number of *S. aureus* cells in 5 h biofilms by ~1 log unit without releasing the non-susceptible species. In contrast, longer infection periods (18 h) with no nutrient limitation resulted in increased killing of *S. aureus* cells by the phage (decrease of up to 2.9 log units). However, in some cases, these conditions promoted growth of the accompanying species. For example, *L. plantarum* cell counts were up to 2.3 log units higher in the treated sample compared to the untreated control. Furthermore, phage propagation inside dual-species biofilms was also highly dependent on the accompanying species, with the highest rate detected in biofilms formed by *S. aureus*-*L. pentosus*. Scanning electron microscopy (SEM) and confocal laser scanning microscopy (CLSM) also showed changes in the three-dimensional structure of mixed-species biofilms after phage treatment. Altogether, the results presented here highlight

41 the need to study the impact of phage therapy on microbial communities that reflect a
42 more realistic setting.
43
44

Importance

Biofilms represent a major source of contamination in industrial and hospital settings. Therefore, the development of efficient strategies to combat bacterial biofilms is of the utmost importance from a medical as well as an economic perspective. Bacteriophages have shown potential as novel antibiofilm agents, but further research is still required to fully understand the interactions between phages and biofilm-embedded bacteria. The results presented in this manuscript contribute to achieving a better understanding of such interactions in a more realistic context, considering that most biofilms in the environment consist of mixed-species populations.

INTRODUCTION

Biofilms are microbial communities attached to biotic or abiotic surfaces (1), whose structure is maintained by an extracellular matrix (2). Biofilms can be composed of single or multiple species, the latter scenario being the most common in both natural and man-made environments. The presence of different microorganisms renders the structure of the biofilm very complex, which has important implications for biofilm eradication and removal. Indeed, multispecies interactions in mixed biofilms are known to affect resistance to disinfectants (3). For instance, the presence of a curli-producing *Escherichia coli* strain was found to protect *Salmonella* Typhimurium biofilm cells from chlorine (4). Additionally, the matrix of mixed-species biofilms often presents greater biochemical complexity compared to the matrix of single species communities (5). The presence of several microorganisms may also alter the spatial structure of the biofilm, as the different species tend to be distributed according to their particular requirements along gradients of nutrients, oxygen and metabolites (6). Finally, quorum-sensing signals from one microorganism may interfere with the signaling of other species, thereby altering their gene expression and physiology (7).

In the food industry, biofilms are an important source of food contamination (8), posing a serious risk for the health of consumers. Indeed, biofilm-related contamination of equipment has been estimated to cause 59% of food-borne disease outbreaks (9). For this reason, efforts to find new biofilm control strategies have increased considerably over the last decade. Recently developed methods include the use of antibacterial surfaces (10), biofilm detachment procedures (11) and matrix degradation techniques (12). Within this context, numerous studies have explored the potential use of bacteriophages and phage-encoded proteins as anti-biofilm agents. Phages, due to their antimicrobial activity, have been proposed as natural weapons for the control of pathogenic bacteria (“phage

therapy") in clinical, veterinary, food safety and environmental settings (13, 14). Moreover, numerous studies have already shown the ability of phages to remove biofilms formed by a variety of bacteria, including staphylococcal species (15-18). Additionally, phage-encoded proteins, such as endolysins and exopolysaccharide depolymerases, can also be used for biofilm removal (19-21). Nevertheless, most studies available to date have focused on single-species communities, while only limited work has tackled the elimination of polymicrobial biofilms with phage-based products (22-26).

The Gram-positive bacterium *Staphylococcus aureus* is a major cause of foodborne illness due to its ability to synthesize enterotoxins. Indeed, staphylococcal food poisoning represented 7.5% of all outbreaks reported in the EU in 2014 (27). Some studies have described a high incidence of *S. aureus* on food industry surfaces (28, 29), where this bacterium often forms complex communities with other pathogenic and spoilage bacteria (30). In a previous work, we described the isolation and characterization of the myophage phiIPLA-RODI. Notably, this lytic phage has a wide host range among staphylococcal species including *S. aureus* and *S. epidermidis*. Thus, exposure of 24 h biofilms to phage phiIPLA-RODI resulted in a 2 log decrease in the number of *S. aureus* cells in single-species biofilms and 4 log-units in *S. aureus-S. epidermidis* dual-species biofilms (15).

The aim of this study was to assess the efficacy of bacteriophage phiIPLA-RODI against dual-species biofilms formed by *S. aureus* with strains of *Lactobacillus plantarum*, *Enterococcus faecium* and *Lactobacillus pentosus*. All these accompanying bacteria have been isolated from food processing surfaces and are not sensitive to this phage. In this framework, we investigated the impact of different phage concentrations and incubation conditions on the behavior of *S. aureus* and the accompanying species. Additionally, we analyzed the ability of phiIPLA-RODI to propagate inside the dual-

105 species biofilms. These data should help towards the design of improved phage-based
106 disinfection products for the food industry.

107 **MATERIALS AND METHODS**

108 **Bacterial strains, bacteriophage and growth conditions.** All bacterial strains used in
109 this study are listed in Table 1. The staphylococcal strains and *E. faecium* MMRA were
110 routinely grown in TSB (Tryptic Soy Broth, Scharlau, Barcelona, Spain) at 37°C with
111 shaking or on TSB plates containing 2% (w/v) bacteriological agar (TSA). *L. plantarum*
112 55-1 (kindly supplied by Dr R. Jiménez-Díaz, IG_CSIC, Sevilla, Spain), and the
113 exopolysaccharide producers *L. pentosus* A1 (EPS A and EPS B) and *L. pentosus* B1
114 (EPS B) were grown in MRS (Scharlab S.L., Spain) broth or agar at 32°C (31). For
115 selective growth of the different species, the following media were used: Baird-Parker
116 agar (BP) for *S. aureus*, Kenner Fecal (KF) agar for *E. faecium* and MRS agar plates for
117 the other three strains. Bacteriophage phiIPLA-RODI was propagated on *S. aureus*
118 IPLA1 as previously described (15).

119 **Biofilm formation.** Overnight cultures of the different strains were diluted to 10^6 CFU/ml
120 into fresh TSB supplemented with 0.25% glucose (TSBG). 100 µl aliquots of each single
121 culture diluted into 100 µl of TSBG or a mixture of two strains (100 µl of each strain)
122 were poured into each well of a 96-well microtiter plate (Thermo Scientific, NUNC,
123 Madrid, Spain). These plates were incubated for 5 or 24 h at 37°C for *S. aureus*/*E. faecium*
124 biofilms or at 32°C for *S. aureus*/*L. plantarum* and *S. aureus*/*L. pentosus* biofilms.
125 Following biofilm formation, the planktonic phase was removed and wells were washed
126 twice with PBS buffer (137 mM NaCl, 2.7 mM KCl, 10 mM Na_2HPO_4 and 2 mM
127 KH_2PO_4, pH 7.4). The adhered cells were collected by scratching the bottom of the well
128 with a sterile swab and subsequently suspended in 9 ml of PBS buffer by vigorously
129 vortexing the sample for 1 min. Serial dilutions of these suspensions were plated on

selective medium for bacterial counting. Alternatively, the total biomass adhered to the well was determined by crystal violet (0.1% w/v) staining as described previously (20). Each experiment was repeated at least three times.

Infection of established biofilms with phage phiIPLA-RODI. To perform short infection period experiments, biofilms were grown for 5 h or 24 h and washed with PBS. Then, 100 µl of SM buffer and 100 µl of phiIPLA-RODI were added to each well (10^7, 10^8, 10^9 PFU/well). 200 µl of SM buffer were added to the control wells. The plates were incubated for 4 h at 32°C or at 37ºC depending on the accompanying species. To test the effect of long infection periods under nutrient-rich conditions, biofilms were established for 5 h, washed with TSBG, and incubated with phage diluted in TSBG (10^9 PFU/well or 10^6 PFU/well). TSBG was added to the control wells. Biofilms were treated for 18 h at 32°C or at 37ºC depending on the species. Afterwards, the planktonic phase was collected and the wells were washed twice with PBS. The number of cells attached to the well surface and the total adhered biomass were determined as described above.

Titration of "free" and "cell-associated" phages (or infective centers) in the planktonic phase and the biofilm was performed as follows. First, the planktonic phase was taken directly from the wells and adhered cells were collected, after washing, by scratching the wells as indicated above. Then, all samples were centrifuged at 16,100 x g for 5 min to separate the supernatant containing the "free" viral particles from the pellets containing the "cell-associated" phages. Both supernatants and pellets were stored at 4ºC until further processing. In order to determine the titer of "free" phages, the supernatants were filtered (0.45 µm, VWR, Spain), diluted in SM buffer and plated on the reference strain *S. aureus* IPLA1 by the double layer technique (32). Prior to the titration of infective centers, the pellets from planktonic and biofilm samples were resuspended in PBS. Then, 50 µl of chloroform were added to each sample in order to lyse the bacterial

cells and, as a result, release the viral particles. After vortexing, cell debris was separated by further centrifugation. The resulting supernatants were then titrated by the double layer technique.

Microscopy techniques. For microscopy analyses, biofilms were formed on borosilicate glass coverslips (18 mm diameter, VWR International, UK) previously placed into the wells of a 12-well microtiter plate (Thermo Scientific, NUNC, Madrid, Spain). To prepare the inoculum for each biofilms, overnight cultures of the different strains were diluted to 10^6 CFU/ml into fresh TSB supplemented with 0.25% glucose (TSBG). 1 ml aliquots of each single culture diluted into 1 ml of TSBG or a mixture of two strains (1 ml of each strain) were poured into each coverslip-containing well. These plates were incubated for 5 h at 37°C for *S. aureus*/*E. faecium* biofilms or at 32°C for *S. aureus*/*L. plantarum* and *S. aureus*/*L. pentosus* biofilms. Then, the planktonic phase was removed and the established biofilms were treated with phage phiIPLA-RODI (10^9 PFU/ml) or SM buffer for 4 h. After treatment, the coverslips were washed twice with PBS and dried for 20 h at 25°C.

For scanning electron microscopy (SEM), the samples were subsequently covered in gold (Gold Sputter Coating) and examined using a scanning electron microscope (JSM-6610LV, JEOL, Tokyo, Japan).

For confocal laser scanning microscopy (CLSM), samples were washed twice with PBS and stained with SYTO® 9 from the Live/Dead® BacLight™ kit (Invitrogen AG, Basel, Switzerland) and Wheat Germ Agglutinin (WGA) Alexa Fluor® 647 conjugate (Life Technologies, Oregon, USA) following the manufacturer´s instructions. SYTO® 9 and the WGA Alexa Fluor® 647 conjugate respectively stained bacterial cells of all species and the exopolysaccharide PNAG (poly-N-acetylglucosamine). Images were acquired

with a confocal scanning laser microscope (DMi8, Leica Microsystems) using a 100x oil objective.

Statistical analysis. All experiments were performed with at least three biological replicates and the means ± standard deviations were represented and further analyzed to establish significant differences. Statistical analyses were performed by a two-tailed Student´s t-test and significance was considered at $P<0.05$.

RESULTS

***S. aureus* forms biofilms with strains of *L. plantarum*, *L. pentosus* and *E. faecium*.** Before performing the phage-infection experiments, we examined the ability of *S. aureus* IPLA 16 to establish biofilms in the presence of other microorganisms. To do that, four strains belonging to three different species (*L. plantarum* 55-1, *L. pentosus* A1, *L. pentosus* B1 and *E. faecium* MMRA) were selected based on previous data demonstrating their presence in biofilm samples from food industry surfaces (16). These strains were grown in mono- and dual-species biofilms and, after 5 h of incubation, the total biomass and viable cell counts were determined (Fig. 1). The data obtained confirmed the formation of dual-species biofilms in all four cases. However, there were some differences in the behavior of *S. aureus* IPLA16 depending on the accompanying species. For instance, dual-species biofilms formed by *S. aureus* IPLA16 and *L. plantarum* 55-1 exhibited a 58% decrease in total biomass compared with *L. plantarum* 55-1 mono-species biofilms and a 100% increase compared with *S. aureus* mono-species biofilms (Fig. 1A). In contrast, dual-species biofilms formed by *S. aureus* with *L. pentosus* A1 or *L. pentosus* B1 displayed slightly smaller biomass values compared to *S. aureus* IPLA 16 mono-species biofilms (Fig. 1A). It must also be noted that while *L. pentosus* B1 formed biofilms even in the absence of *S. aureus*, *L. pentosus* A1 showed negligible attached biomass levels in monocultures (Fig. 1A). Despite not exhibiting

biofilm-forming capacity, *L. pentosus* A1 cells did adhere to the well surface, as determined by viable cell counts of mono-species and dual-species biofilms involving this strain (Fig. 1B). Nonetheless, the number of *L. pentosus* A1 cells in dual biofilms was approximately 1.6 log units smaller than that of *S. aureus* IPLA16 cells (Fig. 1B). Finally, dual biofilms formed by *S. aureus* IPLA16 and *E. faecium* MMRA showed no significant differences in biomass compared with *S. aureus* IPLA16 mono-species biofilms (Fig. 1A). In contrast, the biomass of the *E. faecium* MMRA single-culture biofilm was significantly smaller than that of the mixed biofilm (Fig. 1A). Both species, *S. aureus* and *E. faecium*, showed a small (< 1 log unit) but significant decrease in cell counts in the mixed-species biofilm compared to the respective single cultures (Fig. 1B).

Treatment of *S. aureus* dual-species biofilms with phage phiIPLA-RODI under nutrient-limiting conditions. Once characterized the dual-species biofilm models, we investigated the ability of bacteriophage phiIPLA-RODI to attack these structures. To do that, 5 h- and 24 h dual biofilms formed by *S. aureus* IPLA16 with *L. plantarum* 55-1 or *E. faecium* MMRA were established and then treated for 4 hours with increasing concentrations of phage phiIPLA-RODI diluted in SM buffer (10^7, 10^8, 10^9 PFU/well). These phage concentrations correspond, respectively, to MOIs of 10, 100 and 1000 in 5 h biofilms and to MOIs of 1, 10 and 100 in 24 h biofilms. MOIs were calculated considering the number of cells present in the biofilms at the time of treatment.

Exposure of the mixed-species biofilms to phage concentrations of 10^7 and 10^8 PFU/well did not significantly affect bacterial cell counts or biomass (data not shown). In contrast, treatment of 5 h biofilms with 10^9 PFU/well led to respective decreases in biomass of 31% and 67% for *S. aureus* IPLA16-*L. plantarum* 55-1 and *S. aureus* IPLA16-*E. faecium* MMRA biofilms (data not shown). In addition, *S. aureus* IPLA16 cell counts were respectively reduced by 0.8 and 0.7 log units (Fig. 2A). Similar results were obtained

after treatment of 24 h biofilms. Thus, exposure to the phage led to biomass reductions of 18% and 63% (data not shown) along with decreases in *S. aureus* viable cell counts of 0.4 and 0.6 log units in *S. aureus* IPLA16-*L. plantarum* 55-1 and *S. aureus* IPLA16-*E. faecium* MMRA biofilms, respectively (Fig. 2B).

Regarding the accompanying species, phage treatment of 5 h biofilms caused a slight but significant increase in *E. faecium* MMRA and *L. plantarum* 55-1 viable cell counts (Fig. 2A). In 24 h biofilms, however, only a slight decrease of *L. plantarum* 55-1 cell counts was observed, while *E. faecium* MMRA cell counts were not affected by phage treatment (Fig. 2B).

Analysis of dual-species biofilms by scanning and confocal microscopy. The effect of phage phiIPLA-RODI on dual-species biofilms was also evaluated by microscopy (Fig. 3, 4 and S1). Images obtained by scanning electron microscopy of control biofilms treated with SM buffer showed well-organized cells belonging to both species attached to the coverslip surface (Fig. 3). Extracellular material was observed in all dual biofilms, although it was more evident in the sample corresponding to *S. aureus* IPLA16-*L. plantarum* 55-1 (Fig. 3C). The biofilm formed by *S. aureus* IPLA16 and *L. pentosus* A1 (Fig. 3E) contained fewer apparent cells of the accompanying species than the other three dual biofilms (Fig. 3A, 3C and 3G). This was consistent with the results obtained in viable cell-counting experiments (Fig. 1B). Additionally, the biofilms formed by *S. aureus* IPLA16-*L. pentosus* A1 (Fig. 3E) and *S. aureus* IPLA16-*L. pentosus* B1 (Fig. 3G) were less dense than the other two (Fig. 3A and 3C). Similarly, the dual biofilms involving the two *L. pentosus* strains also displayed the lowest biomass values in polystyrene (Fig. 1A). All four dual-species biofilms treated with phiIPLA-RODI contained a lower number of cells than their respective control samples (Fig. 3B, 3D, 3F

and 3H). Also, the remaining cells appeared embedded in amorphous material, which is probably the result of *S. aureus* cell lysis (Fig. 3B, 3D, 3F and 3H).

Similar results were observed by confocal microscopy (CLSM). In this case, biofilms were dyed with SYTO 9, which stains cells from all species, and WGA Alexa Fluor® 647 to detect the presence of the extracellular polysaccharide PIA/PNAG (poly-beta-1,6-N-acetyl glucosamine). Observation of all untreated biofilm samples showed the presence of microcolony-like groups of bacteria (Fig. 4A, 4C, 4E and 4G), although these structures were organized differently depending on the accompanying species. Moreover, staining of PIA/PNAG revealed the presence of extracellular material in all mixed-species biofilms, particularly surrounding the *S. aureus* cells (Fig. 4A, 4C, 4E and 4G). Phage treatment led to the disaggregation of the biofilm structure along with a decrease in *S. aureus* intact cells (Fig. 4 and S1). Regarding the accompanying species, the number of cells did not appear to change in the case of the two *L. pentosus* strains (Fig. 4F and 4H). In contrast, there were fewer *E. faecium* and more *L. plantarum* cells evident in the treated biofilms (Fig. 4B and 4D). Treatment with phage phiIPLA-RODI also altered the three-dimensional structure of the mixed biofilms (Fig. S1). Biofilms formed by *S. aureus* IPLA16-*E. faecium* MMRA, *S. aureus* IPLA16-*L. pentosus* A1 and *S. aureus* IPLA16-*L. pentosus* B1 displayed a flatter and less organized biofilm compared to the untreated samples (Fig. S1B, S1F and S1H). Phage treatment also reduced the thickness of *S. aureus* IPLA16-*L. plantarum* 55-1 biofilms (Fig. S1D).

Infection of *S. aureus* dual-species biofilms by phiIPLA-RODI can have an impact on the accompanying species. In addition to infection experiments using SM buffer as a diluting agent, we also assessed the efficacy of the phage when applied in a rich growth medium. Our rationale was that efficient phage propagation, which relies on the availability of nutrients to sustain active growth of the host, may improve biofilm

278 removal. To test this hypothesis, dual-species biofilms formed by *S. aureus* IPLA16 and
279 the different accompanying species were infected with phiIPLA-RODI (10^9 and 10^6
280 PFU/well, corresponding to MOIs of 1000 and 1) diluted in TSBG. After incubating the
281 biofilms with the phage for 18 h at 37°C or 32ºC, total adhered biomass and viable cell
282 counts were determined. Treatment of *S. aureus* IPLA16-*E. faecium* MMRA biofilms
283 with 10^9 PFU/well or 10^6 PFU/well led to a biomass decrease of 61% or 21%, respectively
284 (Fig. S2). Similarly, viable cell counts of *S. aureus* decreased by 1.3 and 0.4 log units
285 after treatment with high and low phage concentrations, respectively. However, the
286 number of *E. faecium* MMRA viable cells was not affected by phage treatment (Fig. 5A).
287 Unexpectedly, the total biomass of biofilms formed by *S. aureus* IPLA16 and *L.*
288 *plantarum* 55-1 was 120% higher after treatment with 10^9 PFU/well compared with the
289 untreated control (Fig. S2). Regarding viable counts, there was a reduction for *S. aureus*
290 IPLA16 (about 2 log units) and an increase for *L. plantarum* 55-1 (about 2.3 log units)
291 following treatment with both phage concentrations (Fig. 5B).
292 Finally, phiIPLA-RODI infection of 5 h biofilms formed by *S. aureus* IPLA16
293 and *L. pentosus* A1 led to a biomass decrease of 86%, while no significant differences
294 were observed for *S. aureus* IPLA16-*L. pentosus* B1 biofilms (Fig. S2). Regarding *S.*
295 *aureus* IPLA16 viable counts, decreases of 2.9 and 1.8 log units were detected in *S. aureus*
296 IPLA16-*L. pentosus* A1 biofilms treated with 10^9 or 10^6 PFU/well, respectively (Fig. 5C).
297 A lesser impact was observed in *S. aureus* IPLA16-*L. pentosus* B1 biofilms, in which cell
298 counts were reduced by 1.7 and 0.7 log units following treatment with 10^9 or 10^6
299 PFU/well, respectively (Fig. 5D). A slight increase in the *L. pentosus* A1 population
300 (approximately 0.5 log units) was detected after treatment with 10^6 PFU/well (Fig. 5C).
301 In the case of *L. pentosus* B1, treatment with 10^6 PFU/well did not change the cell number
302 whereas a slightly lower count was observed for the samples treated with 10^9 PFU/well.

Propagation of phiIPLA-RODI in *S. aureus* mixed biofilms depends on the accompanying species. In order to maximize the efficacy of phages as antibiofilm agents, it is important to determine if the viral particles can reach the target bacteria and propagate inside the biofilms. Here, propagation was estimated by titrating the number of phages in the planktonic phase and the biofilm, differentiating between viral particles associated to cells (infectious centers) and those present as free virions.

Titration of phiIPLA-RODI isolated from dual-species biofilms challenged with 10^9 PFU/well showed the same trends for all species combinations. Thus, the highest number of viral particles was in the planktonic phase, being the number of free virions 0.5-1 log unit higher than that of infective centers. Biofilms contained a smaller viral load and most phage particles were free in the extracellular matrix. Consequently, the lowest phage titers were found in the cell-associated fraction corresponding to the biofilm. The total phage titer per well was approximately 10^9 PFU/well for all dual biofilms, which is equal to the starting inoculum. There were, however, differences in the ability of phiIPLA-RODI to multiply inside the biofilm depending on the accompanying species. Indeed, the number of both free and cell-associated viral particles in the biofilm was approximately 1 log unit higher in dual biofilms formed by *S. aureus* IPLA16 with *E. faecium* MMRA and *L. pentosus* A1 than in those formed by *S. aureus* IPLA16 with *L. plantarum* 55-1 or *L. pentosus* B1 (Fig. 6 A-D).

Propagation of phiIPLA-RODI in *S. aureus* dual biofilms treated with 10^6 PFU/well showed different patterns depending on the accompanying strain. In the case of biofilms involving the three lactobacilli strains, the trend was fairly similar to the one described for samples treated with 10^9 PFU/well. Indeed, phage titers obtained in samples from the planktonic phase were higher than those from biofilms (Fig. 6 B-D). Also, both phases (planktonic and biofilm) contained a higher number of free phage particles than

cell-associated virions (Fig. 6 B-D). All three dual biofilms formed by *S. aureus* with lactobacilli and treated with 10^6 PFU/well showed a significant increase in phage particles compared to the starting inoculum. Thus, the calculated P-values were 0.001, $3.15x10^{-5}$ and 0.001 for biofilms formed by *S. aureus* with *L. plantarum*, *L. pentosus* A1 and *L. pentosus* B1, respectively. Interestingly, the total phage titer (biofilm and planktonic phase) corresponding to *S. aureus-L. plantarum* biofilms (7.1 log PFU/well) was significantly lower than that estimated for sessile communities formed by *S. aureus-L. pentosus* A1 and *S. aureus-L. pentosus* B1 (8.5 and 8.4 log PFU/well). The respective P-values were $3.97x10^{-4}$ and $4.40x10^{-4}$ for comparison of *S. aureus-L. plantarum* with *S. aureus-L. pentosus* A1 and *S. aureus-L. pentosus* B1 biofilms treated with 10^6 PFU/well. Unexpectedly, a similar number of phages was obtained in the planktonic and biofilm phases of communities formed by *S. aureus* and *E. faecium* that had been treated with 10^6 PFU/well. Moreover, the number of infective centers and free particles in the planktonic phase were similar. Inside the biofilm structure, however, the phage titer was slightly higher than in the planktonic phase and more phage particles (about 10^6 log units) were free in the extracellular matrix than associated to host cells (Fig. 6A). Interestingly, there was no significant increase in phage titer compared with the starting inoculum in *S. aureus-E. faecium* biofilms treated with 10^6 PFU/well (P-value= 0.93).

DISCUSSION

Recently, a number of articles have reported the potential of bacteriophages for the control of bacterial biofilms. However, most of these studies have focused on monospecies cultures, which do not reflect the majority of biofilms found in nature. This study addressed the use of phage phiIPLA-RODI to control dual-species biofilms composed of *S. aureus* together with other species from food-related environments (*L.*

353 *plantarum*, *L. pentosus* and *E. faecium*). None of the selected microorganisms was
354 susceptible to phiIPLA-RODI infection and, importantly, all four strains were able to
355 form stable dual biofilms with *S. aureus*. In most cases, the number of cells of *S. aureus*
356 and the accompanying species was fairly similar, except for *L. pentosus* A1. This might
357 be due to the poor adhesion to polystyrene and glass displayed by strain A1, which was
358 observed even in the absence of *S. aureus*. Interestingly, there were fewer cells of *L.*
359 *plantarum* in dual-species biofilms compared to monocultures. In this case, it appears that
360 *S. aureus* might be exerting a negative impact on the presence of this bacterium.

361 A previous study performed in our laboratory had described that treatment with
362 phiIPLA-RODI led to reductions in *S. aureus* IPLA16 cells of 2.4 log units in mono-
363 species biofilms and 4.2 log units in dual-species biofilms formed with the phage-
364 sensitive strain *S. epidermidis* LO5081 (15). Thus, the presence of a second species, also
365 susceptible to the phage, seemed to enhance the efficacy of phage treatment. In contrast,
366 the results presented here show lower efficacy rates for short phage treatment of mixed-
367 species biofilms performed under nutrient-limiting conditions. Indeed, reductions in *S.*
368 *aureus* IPLA16 cell counts remained below 1 log unit for dual-biofilms formed with non-
369 sensitive bacteria such as *L. plantarum* and *E. faecium*, regardless of the biofilm
370 maturation stage and the phage concentration used. Therefore, it appears that the presence
371 of cells from a non-sensitive species in the biofilm may hinder the ability of the phage to
372 reach and lyse the target cells. It is well known that mixed-species biofilms frequently
373 display higher resistance to antibiotics than mono-species biofilms (33, 34). This
374 phenomenon may involve multiple mechanisms, including interspecies signaling, spatial
375 distribution of physiologically different bacteria, and interference exerted by the matrix
376 (3). Similarly, the low efficacy of phages to infect dual-species biofilms might be due to
377 the protection of the sensitive host by the non-sensitive species (35, 36), coaggregation

of biofilm communities (37), limited penetration of phages (38, 39) or changes in the availability of phage receptors on the cell surface of the host species (40).

Despite the low efficacy of applying short phage treatments to dual-species cultures, microscopy analysis revealed structural changes in the treated biofilms compared to their respective controls. Indeed, all mixed-species biofilms displayed a decrease in the number of intact *S. aureus* cells and disaggregation of the biofilm three-dimensional structure. It is possible, however, that the use of a different substrate for these experiments (glass instead of polystyrene) also has an influence in the final results. Therefore, application of the phage suspension to the biofilms formed on glass coverslips may be more effective than on polystyrene wells.

Regarding treatment duration, previous studies had reported that biofilm removal with phage-based products does not require incubation times longer than 5 hours (25, 41). However, our results indicate that the control of biofilms consisting of several species might benefit from longer incubation times. Additionally, treatment appears to be more effective under conditions that allow active growth of the host. Nonetheless, it must be considered that incubation under nutrient-rich conditions may also affect the proliferation of the accompanying species. This effect would be undesirable when the accompanying species are pathogenic or spoilage bacteria, especially if they are good biofilm producers. Conversely, interspecies competition during active growth may have a synergistic effect between the phage and the non-sensitive bacteria, thereby favoring the elimination of the target pathogen. This may also limit phage-resistance acquisition, which generally confers a loss in the competitive ability of bacteria (30). This seemed to be the case, for example, of dual-species biofilms formed by *E. coli* and *Pseudomonas aeruginosa* (22). Here, there were differences in the behavior of the four accompanying strains studied following antistaphylococcal phage treatment. Thus, reduction of *S. aureus* IPLA16 cells

403 due to phage infection led to an increase in the number of *L. plantarum* cells. Also, *S.*
404 *aureus-L. plantarum* biofilms displayed increased biomass following phage treatment.
405 These results were not surprising given the inhibitory effect of *S. aureus* over *L.*
406 *plantarum* observed in the preliminary experiments. As mentioned previously, the
407 number of *L. plantarum* 55-1 viable cell counts in dual-species biofilms formed with *S.*
408 *aureus* was significantly lower than in the *L. plantarum* single-species community. In
409 contrast, partial elimination of the *S. aureus* population by phage treatment seems to allow
410 the *L. plantarum* population to develop more similarly to the single-species biofilm. This
411 is reflected in the higher *L. plantarum* cell number and increase in adhered biomass.
412 Additionally, growth of *L. plantarum* may be facilitated by the greater availability of
413 nutrients resulting from phage-induced bacterial lysis or the reduced growth of *S. aureus*
414 IPLA16. Nevertheless, the interactions between bacterial species in a biofilm are very
415 complex and not always easy to explain. Although phage predation has been shown to
416 promote biofilm formation in certain bacteria growing in mono-species biofilms (43), our
417 results suggest that the increase in biomass in *S. aureus-L. plantarum* co-cultures is due
418 to an increase in the accompanying species rather than induction of the biofilm formation
419 ability of the surviving *S. aureus* cells.

420 With regards to the other three strains studied, namely *L. pentosus* A1, *L. pentosus*
421 B1 and *E. faecium* MMRA, no major increase in cell counts was observed after treatment
422 with phiIPLA-RODI. Nevertheless, comparison of the cell counts obtained here with
423 previous results regarding biofilm formation growth curves (unpublished data) indicate
424 that the population in both treated and control samples reached the maximum cell number
425 for the aforementioned strains. However, interestingly, phage treatment did not result in
426 significant release of cells from the accompanying species to the planktonic phase.
427 Similar results had been previously described for biofilms formed by *Pseudomonas*

fluorescens and *Staphylococcus lentus* under static conditions. However, under dynamic conditions, phage ΦIBB-PF7A did cause the release of the non-susceptible *S. lentus* cells (25).

Even though it is widely recognized that bacteriophages can replicate inside biofilms, data concerning phage propagation in multiple species communities are scarce. The phage life cycle inside the biofilm requires attachment to bacterial cells embedded in an extracellular matrix and, after production of the phage progeny, the diffusion of new phages to other areas of the biofilm to reach new susceptible cells (44). Depending on the bacterial species, the metabolic and physicochemical conditions of the biofilm (matrix density, number of cells, metabolic state) can be quite different. Phage propagation in the four dual-species biofilms studied here was evaluated by using two different phage concentrations. Not surprisingly, the phage titer in the planktonic phase was considerably higher than the number of phages inside the adhered phase for all dual-species biofilms. Moreover, our results showed that dual-species biofilms support phage multiplication since a significant percentage of phage particles was isolated as cell-associated infectious centers. Overall, it seems that the adsorption rate of phages to host cells is favored under planktonic conditions compared to a biofilm environment. One explanation for this phenomenon is that the production and migration of phage particles in biofilms is considerably limited by the presence of extracellular material (45). Interestingly, phage propagation in the biofilm phase was lower in *S. aureus-L. plantarum* biofilms than in the dual species biofilms involving either of the two *L. pentosus* strains. As mentioned previously, *L. plantarum* is a better biofilm former than the *L. pentosus* strains and is known to produce extracellular material. It is, therefore, possible that the greater complexity of the extracellular matrix in the *S. aureus-L. plantarum* biofilms hinders phage propagation in the biofilm. Nonetheless, some studies seem to indicate that phage

453 penetration into biofilms is not completely blocked by the extracellular matrix. For
454 instance, it has been shown that c2 phage can diffuse into biofilms through water-filled
455 channels, although some phage particles may interact with their specific binding sites on
456 bacteria and be immobilized there (39). However, the interaction of phages with
457 extracellular components cannot be completely discarded (22, 46). In addition to the role
458 played by the matrix, the lower infectivity detected in biofilms may also be due to the
459 heterogeneity of these communities regarding structure and metabolic state of the host
460 cells. Thus, phage infection may be more prevalent in metabolically active cells located
461 on the biofilm surface rather than the slow-growing cells located in the inner layers of the
462 biofilm (1, 44). Overall, we can conclude that successful propagation of phages in mixed-
463 species biofilms depends on the accompanying non-susceptible species. This is likely due
464 to the differences in the composition of the extracellular matrix, which can affect the
465 ability of the viral particles to reach susceptible cells.

466 In conclusion, this study provides evidence that phage infection in dual-biofilms
467 is a complex process likely subject to population dynamics. Hence, phage treatment may
468 require the use of phage cocktails or phages combined with other antimicrobials to target
469 the accompanying species. Overall, our results contribute to the understanding of
470 interspecies interactions in the context of the development of phage-based strategies for
471 the control of mixed-species biofilms.

472 **ACKNOWLEDGMENTS**

473 This study was supported by grants AGL2012-40194-C02-01 (Ministry of
474 Science and Innovation, Spain), AGL2015-65673-R (Program of Science, Technology
475 and Innovation 2013-2017), GRUPIN14-139 (FEDER EU funds, Principado de Asturias,
476 Spain). L.F. was awarded a “Marie Curie Clarin-Cofund” grant. PG, BM and AR are
477 members of the FWO Vlaanderen funded “Phagebiotics” research community

(WO.016.14) and the bacteriophage network FAGOMA. We thank Sonia Simón Vinagre and Rosana Calvo for their collaboration in this work. A. Rehaiem and R. Jiménez are acknowledged for sharing *E. faecium* and *Lactobacilli* strains, respectively.

We thank Dr. David M. Donovan (Animal and Natural Resources Institute, BARC, ARS, U.S. Department of Agriculture, Beltsville, Maryland, USA) for revising the English and making helpful suggestions for improving the manuscript.

REFERENCES

1. **Stoodley P, Sauer K, Davies DG, Costerton JW.** 2002. Biofilms as complex differentiated communities. Annu Rev Microbiol **56:**187-209.
2. **Flemming HC, Wingender J.** 2010. The biofilm matrix. Nat Rev Microbiol **8:**623-633.
3. **Sanchez-Vizuete P, Orgaz B, Aymerich S, Le Coq D, Briandet R.** 2015. Pathogens protection against the action of disinfectants in multispecies biofilms. Front Microbiol **6:**705.
4. **Wang R, Kalchayanand N, Schmidt JW, Harhay DM.** 2013. Mixed biofilm formation by Shiga toxin-producing *Escherichia coli* and *Salmonella enterica* serovar Typhimurium enhanced bacterial resistance to sanitization due to extracellular polymeric substances. J Food Prot **76:**1513-1522.
5. **Andersson S, Dalhammar G, Kuttuva Rajarao G.** 2011. Influence of microbial interactions and EPS/polysaccharide composition on nutrient removal activity in biofilms formed by strains found in wastewater treatment systems. Microbiol Res **166:**449-457.
6. **Stewart PS, Franklin MJ.** 2008. Physiological heterogeneity in biofilms. Nat Rev Microbiol **6:**199-210.

7. **Zhang LH, Dong YH.** 2004. Quorum sensing and signal interference: diverse implications. Mol Microbiol **53:**1563-1571.

8. **DeVita MD, Whadhera RK, Theis ML, Ingham SC.** 2007. Assessing the potential of *Streptococcus pyogenes* and *Staphylococcus aureus* transfer to foods and customers via a survey of hands, hand-contact surfaces and food-contact surfaces at foodservice facilities. Journal of Foodservice **18:**76-79.

9. **Midelet G, Carpentier B.** 2004. Impact of cleaning and disinfection agents on biofilm structure and on microbial transfer to a solid model food. J Appl Microbiol **97:**262-270.

10. **Pang LQ, Zhong LJ, Zhou HF, Wu XE, Chen XD.** 2015. Grafting of ionic liquids on stainless steel surface for antibacterial application. Colloids Surf B Biointerfaces **126:**162-168.

11. **Cerca N, Gomes F, Bento JC, Franca A, Rolo J, Miragaia M, Teixeira P, Oliveira R.** 2013. Farnesol induces cell detachment from established *S. epidermidis* biofilms. J Antibiot (Tokyo) **66:**255-258.

12. **Ramasubbu N, Thomas LM, Ragunath C, Kaplan JB.** 2005. Structural analysis of dispersin B, a biofilm-releasing glycoside hydrolase from the periodontopathogen *Actinobacillus actinomycetemcomitans*. J Mol Biol **349:**475-486.

13. **O'Flaherty S, Ross RP, Coffey A.** 2009. Bacteriophage and their lysins for elimination of infectious bacteria. FEMS Microbiol Rev **33:**801-819.

14. **García P, Rodríguez L, Rodríguez A, Martínez B.** 2010. Food biopreservation: promising strategies using bacteriocins, bacteriophages and endolysins. Trends in Food Science and Technology **21:**373-382.

15. **Gutiérrez D, Vandenheuvel D, Martínez B, Rodríguez A, Lavigne R, García P.** 2015. Two phages, phiIPLA-RODI and phiIPLA-C1C, lyse mono- and dual-species staphylococcal biofilms. Appl Environ Microbiol **81:**3336-3348.

16. **Gutiérrez D, Martínez B, Rodríguez A, García P.** 2012. Genomic characterization of two *Staphylococcus epidermidis* bacteriophages with anti-biofilm potential. BMC Genomics **13:**228.

17. **Kelly D, McAuliffe O, Ross RP, Coffey A.** 2012. Prevention of *Staphylococcus aureus* biofilm formation and reduction in established biofilm density using a combination of phage K and modified derivatives. Lett Appl Microbiol **54:**286-291.

18. **Cerca N, Oliveira R, Azeredo J.** 2007. Susceptibility of *Staphylococcus epidermidis* planktonic cells and biofilms to the lytic action of *Staphylococcus* bacteriophage K. Lett Appl Microbiol **45:**313-317.

19. **Cornelissen A, Ceyssens PJ, T'Syen J, Van Praet H, Noben JP, Shaburova OV, Krylov VN, Volckaert G, Lavigne R.** 2011. The T7-related *Pseudomonas putida* phage phi15 displays virion-associated biofilm degradation properties. PLoS One **6:**e18597.

20. **Gutiérrez D, Ruas-Madiedo P, Martínez B, Rodríguez A, García P.** 2014. Effective removal of staphylococcal biofilms by the endolysin LysH5. PLoS One **9:**e107307.

21. **Gutiérrez D, Briers Y, Rodríguez-Rubio L, Martínez B, Rodríguez A, Lavigne R, García P.** 2015. Role of the pre-neck appendage protein (Dpo7) from phage vB_SepiS-phiIPLA7 as an anti-biofilm agent in staphylococcal species. Frontiers in Microbiology **6:**1315.

551 22. **Kay MK, Erwin TC, McLean RJ, Aron GM.** 2011. Bacteriophage ecology in
552 *Escherichia coli* and *Pseudomonas aeruginosa* mixed-biofilm communities. Appl
553 Environ Microbiol **77:**821-829.
554 23. **Carson L, Gorman SP, Gilmore BF.** 2010. The use of lytic bacteriophages in
555 the prevention and eradication of biofilms of *Proteus mirabilis* and *Escherichia*
556 *coli*. FEMS Immunol Med Microbiol **59:**447-455.
557 24. **Coulter LB, McLean RJ, Rohde RE, Aron GM.** 2014. Effect of bacteriophage
558 infection in combination with tobramycin on the emergence of resistance in
559 *Escherichia coli* and *Pseudomonas aeruginosa* biofilms. Viruses **6:**3778-3786.
560 25. **Sillankorva S, Neubauer P, Azeredo J.** 2010. Phage control of dual species
561 biofilms of *Pseudomonas fluorescens* and *Staphylococcus lentus*. Biofouling
562 **26:**567-575.
563 26. **Harcombe WR, Bull JJ.** 2005. Impact of phages on two-species bacterial
564 communities. Appl Environ Microbiol **71:**5254-5259.
565 27. **EFSA, ECDC.** 2016. The European Union summary report on trends and sources
566 of zoonoses, zoonotic agents and food-borne outbreaks in 2014. EFSA Journal
567 **13:**4329.
568 28. **Gounadaki AS, Skandamis PN, Drosinos EH, Nychas GJ.** 2008. Microbial
569 ecology of food contact surfaces and products of small-scale facilities producing
570 traditional sausages. Food Microbiol **25:**313-323.
571 29. **Pala TR, Sevilla A.** 2004. Microbial contamination of carcasses, meat, and
572 equipment from an Iberian pork cutting plant. J Food Prot **67:**1624-1629.
573 30. **Gutiérrez D, Delgado S, Vázquez-Sánchez D, Martínez B, Cabo ML,**
574 **Rodríguez A, Herrera JJ, García P.** 2012. Incidence of *Staphylococcus aureus*

575 and analysis of associated bacterial communities on food industry surfaces. Appl
576 Environ Microbiol **78:**8547-8554.
577 31. **Sanchez JI, Martinez B, Guillen R, Jimenez-Diaz R, Rodriguez A.** 2006.
578 Culture conditions determine the balance between two different
579 exopolysaccharides produced by *Lactobacillus pentosus* LPS26. Appl Environ
580 Microbiol **72:**7495-7502.
581 32. **Gutiérrez D, Martínez B, Rodríguez A, García P.** 2010. Isolation and
582 characterization of bacteriophages infecting *Staphylococcus epidermidis*. Curr
583 Microbiol **61:**601-608.
584 33. **Leriche V, Briandet R, Carpentier B.** 2003. Ecology of mixed biofilms
585 subjected daily to a chlorinated alkaline solution: spatial distribution of bacterial
586 species suggests a protective effect of one species to another. Environ Microbiol
587 **5:**64-71.
588 34. **Burmolle M, Webb JS, Rao D, Hansen LH, Sorensen SJ, Kjelleberg S.** 2006.
589 Enhanced biofilm formation and increased resistance to antimicrobial agents and
590 bacterial invasion are caused by synergistic interactions in multispecies biofilms.
591 Appl Environ Microbiol **72:**3916-3923.
592 35. **Tait K, Sutherland IW.** 2002. Antagonistic interactions amongst bacteriocin-
593 producing enteric bacteria in dual species biofilms. J Appl Microbiol **93:**345-352.
594 36. **Bridier A, Sanchez-Vizuete Mdel P, Le Coq D, Aymerich S, Meylheuc T,**
595 **Maillard JY, Thomas V, Dubois-Brissonnet F, Briandet R.** 2012. Biofilms of
596 a *Bacillus subtilis* hospital isolate protect *Staphylococcus aureus* from biocide
597 action. PLoS One **7:**e44506.

37. **Rickard AH, McBain AJ, Ledder RG, Handley PS, Gilbert P.** 2003. Coaggregation between freshwater bacteria within biofilm and planktonic communities. FEMS Microbiol Lett **220:**133-140.

38. **Sutherland IW, Hughes KA, Skillman LC, Tait K.** 2004. The interaction of phage and biofilms. FEMS Microbiol Lett **232:**1-6.

39. **Briandet R, Lacroix-Gueu P, Renault M, Lecart S, Meylheuc T, Bidnenko E, Steenkeste K, Bellon-Fontaine MN, Fontaine-Aupart MP.** 2008. Fluorescence correlation spectroscopy to study diffusion and reaction of bacteriophages inside biofilms. Appl Environ Microbiol **74:**2135-2143.

40. **Hoyland-Kroghsbo NM, Maerkedahl RB, Svenningsen SL.** 2013. A quorum-sensing-induced bacteriophage defense mechanism. MBio **4:**e00362-00312.

41. **Hughes KA, Sutherland IW, Jones MV.** 1998. Biofilm susceptibility to bacteriophage attack: the role of phage-borne polysaccharide depolymerase. Microbiology **144:**3039-3047.

42. **Elias S, Banin E.** 2012. Multi-species biofilms: living with friendly neighbors. FEMS Microbiol Rev **36:**990-1004.

43. **Hosseinidoust Z, Tufenkji N, van de Ven TG.** 2013. Formation of biofilms under phage predation: considerations concerning a biofilm increase. Biofouling **29:**457-468.

44. **Abedon ST.** 2016. Bacteriophage exploitation of bacterial biofilms: phage preference for less mature targets? FEMS Microbiol Lett **363**. doi: 10.1093/femsle/fnv246.

45. **Gallet R, Shao Y, Wang IN.** 2009. High adsorption rate is detrimental to bacteriophage fitness in a biofilm-like environment. BMC Evol Biol **9:**241.

622 46. **Forde A, Fitzgerald GF.** 2003. Molecular organization of exopolysaccharide
623 (EPS) encoding genes on the lactococcal bacteriophage adsorption blocking
624 plasmid, pCI658. Plasmid **49:**130-142.
625 47. **Rodriguez-Carvajal MA, Sanchez JI, Campelo AB, Martinez B, Rodriguez**
626 **A, Gil-Serrano AM.** 2008. Structure of the high-molecular weight
627 exopolysaccharide isolated from *Lactobacillus pentosus* LPS26. Carbohydr Res
628 **343:**3066-3070.
629 48. **Rehaiem A, Martinez B, Manai M, Rodriguez A.** 2010. Production of enterocin
630 A by *Enterococcus faecium* MMRA isolated from 'Rayeb', a traditional Tunisian
631 dairy beverage. J Appl Microbiol **108:**1685-1693.
632 49. **Ruiz-Barba JL, Cathcart DP, Warner PJ, Jimenez-Diaz R.** 1994. Use of
633 *Lactobacillus plantarum* LPCO10, a bacteriocin producer, as a starter culture in
634 Spanish-style green olive fermentations. Appl Environ Microbiol **60:**2059-2064.

635 **FIGURE LEGENDS**

636 **FIG 1** Biofilms formed by *S. aureus* IPLA16 with *L. plantarum* 55-1, *E. faecium* MMRA,
637 *L. pentosus* A1 and *L. pentosus* B1 after 5 h of incubation at 32°C or 37°C. A) Biomass
638 of mono-species biofilms formed by *S. aureus* IPLA16 (white), accompanying species
639 (black) and dual-species biofilms (grey). B) Number of viable cells in mono-species
640 biofilms (white: *S. aureus* IPLA16; black: accompanying species) and dual-species
641 biofilms (light grey: *S. aureus* IPLA16; dark grey: accompanying species). Means and
642 standard deviations were calculated for three biological replicates. Data from dual-species
643 biofilms were compared to those from single-species biofilms with a two-tailed Student´s
644 t-test. $P<0.05$ (*) were considered significant.

FIG 2 Effect of phage phiIPLA-RODI on 5 h (A) and 24 h (B) biofilms formed by *S. aureus* IPLA16-*L.plantarum* 55-1 and *S. aureus* IPLA16-*E. faecium* MMRA after 4 h of treatment with 10^9 PFU/well in SM buffer. Values represent the means ± standard deviations of bacterial counts performed in triplicate. Light grey and dark grey bars correspond to control and treated samples, respectively. *, P-value<0.05.

FIG 3 Scanning electron micrographs of *S. aureus* dual-species biofilms. Images correspond to 5 h biofilms formed by *S. aureus* IPLA16 with *E. faecium* MMRA (A and B), *L. plantarum* 55-1 (C and D), *L. pentosus* A1 (E and F) or *L. pentosus* B1 (G and H) following a 4 h treatment with SM buffer (left) or phiIPLA-RODI (right). White arrows indicate cells from the accompanying species.

FIG 4 CLSM images of *S. aureus* IPLA16 and *E. faecium* MMRA (A and B), *L. plantarum* 55-1 (C and D), *L. pentosus* A1 (E and F) or *L. pentosus* B1 (G and H) dual-species biofilms. Images correspond to 5 h biofilms untreated (A, C, E and G) or treated with phiIPLA-RODI for 4 h (B, D, F and H). All samples were stained with SYTO® 9 (green), which dyes cells of all species, and WGA Alexa Fluor® 647 (blue), which stains the extracellular polysaccharide in the biofilm matrix. White arrows indicate cells from the accompanying species.

FIG 5 Bacterial counts of 5 h biofilms formed by *S. aureus* IPLA16 with other species under proliferation conditions and treated with phage phiIPLA-RODI. Values represent the means ± standard deviations of two independent biological replicates. The accompanying species were *E. faecium* MMRA (A), *L. plantarum* (B), *L. pentosus* A1 (C) and *L. pentosus* B1 (D). Error bars indicate standard deviation. White bars correspond to the untreated control, while black and grey bars represent samples treated with 10^9 or 10^6 PFU/well, respectively. *, P-value<0.05.

669 **FIG 6** Propagation of phage phiIPLA-RODI on 5 h dual-species biofilms of *S. aureus*
670 IPLA16 with other bacteria treated for 18 h with 10^9 PFU/well or 10^6 PFU/well. The
671 accompanying species tested were *E. faecium* MMRA (A), *L. plantarum* 55-1 (B), *L.*
672 *pentosus* A1 (C) and *L. pentosus* B1 (D). White and black bars correspond to the phages
673 present in the planktonic phase associated to cells or as free virions, respectively. Light
674 grey and dark grey bars represent infectious centers and free phages present in the adhered
675 (biofilm) phase. These results represent the means ± standard deviations of three
676 replicates. The following datasets were compared by statistical analysis (biofilm free vs
677 biofilm cell associated phages, planktonic free vs planktonic cell associated phages,
678 biofilm free vs planktonic free and biofilm cell associated vs planktonic cell associated
679 phages. *, P-value<0.05.
680

681 **SUPPLEMENTAL MATERIAL**

682 **FIG S1.** Three-dimensional structure of *S. aureus* IPLA16 and *E. faecium* MMRA (A
683 and B), *L. plantarum* 55-1 (C and D), *L. pentosus* A1 (E and F) or *L. pentosus* B1 (G and
684 H) dual-species biofilms. Images correspond to 5 h biofilms treated with SM buffer (A,
685 C, E and G) or phage phiIPLA-RODI for 4 h (B, D, F and H). Biofilms were stained with
686 SYTO® 9, which dyes cells from all species green.
687 **FIG S2.** Biomass quantification of 5 h biofilms formed by *S. aureus* IPLA16 with other
688 species under proliferation conditions and treated with phage phiIPLA-RODI. Values
689 represent the means ± standard deviations of 4 technical replicates corresponding to one
690 representative experiment out of three with the same trends. White bars correspond to the
691 untreated control, while black and grey bars represent samples treated with 10^9 or 10^6
692 PFU/well, respectively. Phage-infected samples were compared to their respective
693 untreated controls. *, P-value<0.05.

694 **TABLE LEGENDS**

695 **Table 1.** Bacterial strains used in this study.

Species	Strain	Origin	Reference
Staphylococcus aureus	IPLA1	Dairy industry surface	(30)
S. aureus	IPLA16	Meat industry surface	(30)
Enterococcus faecium	MMRA	Dairy product	(48)
Lactobacillus plantarum	55-1	Natural fermentation of olives	(49)
Lactobacillus pentosus	LPS26	Natural fermentation of olives	(31)
L. pentosus	A1	Derivative from LPS26	(31)
L. pentosus	B1	Derivative from LPS26	(31)

696

697

698

699

700

701

702

703

704

705

706

707

708

709

710

711

712

713

714

715

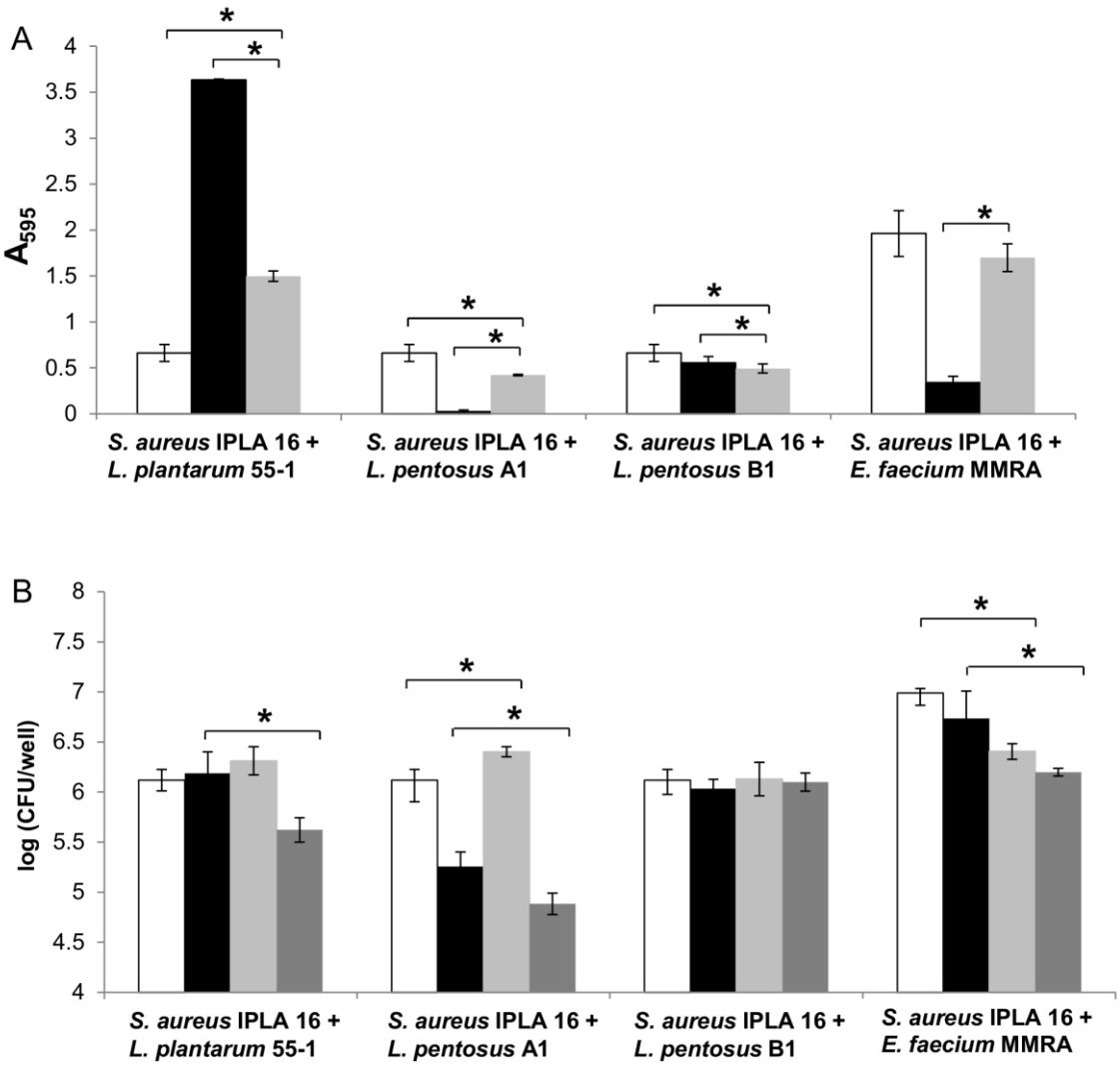

716

717

718

719

720

721

722

723

724

725

726

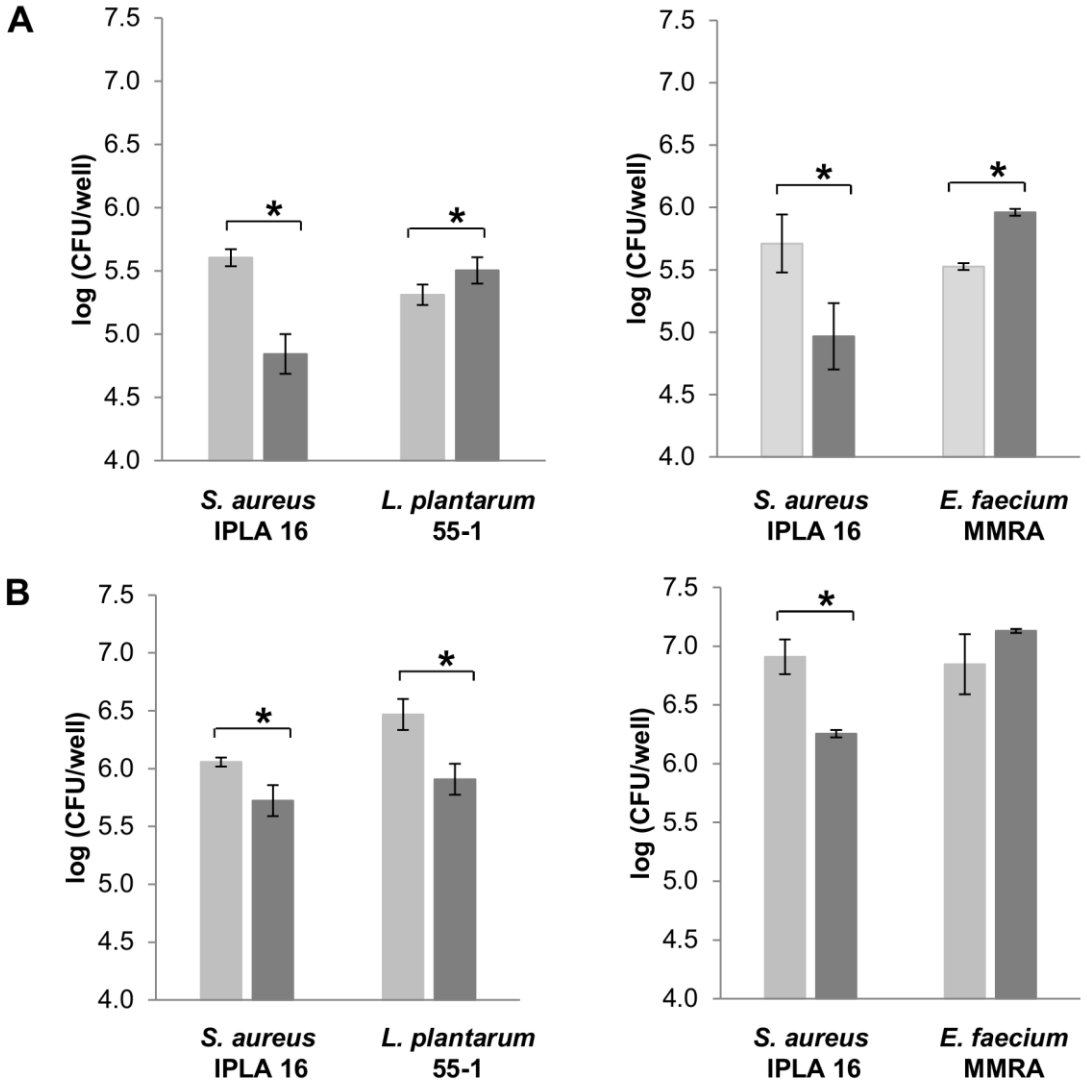

727

728

729

730

731

732

733

734

735

736

737

738

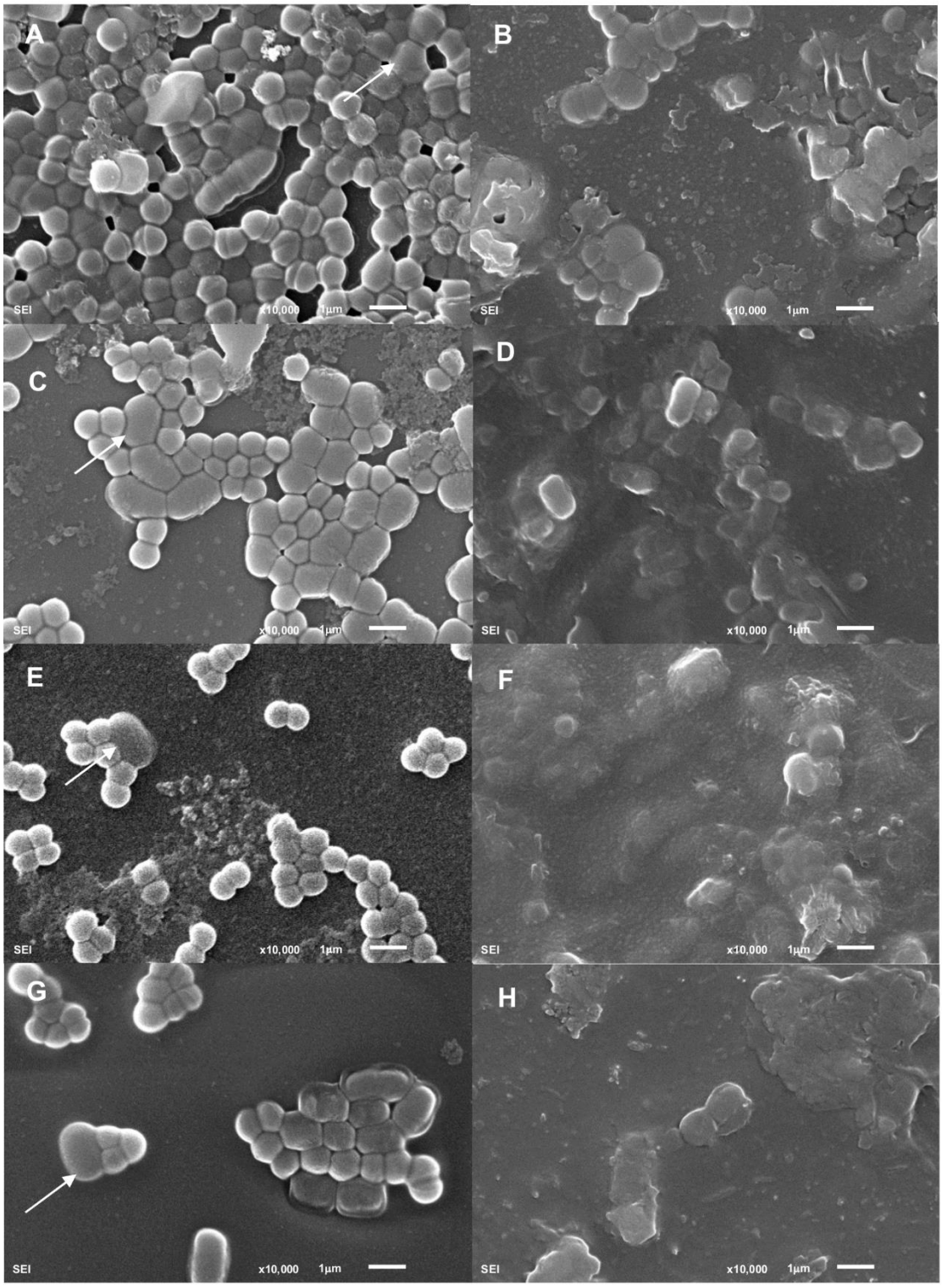

739

740

741

742

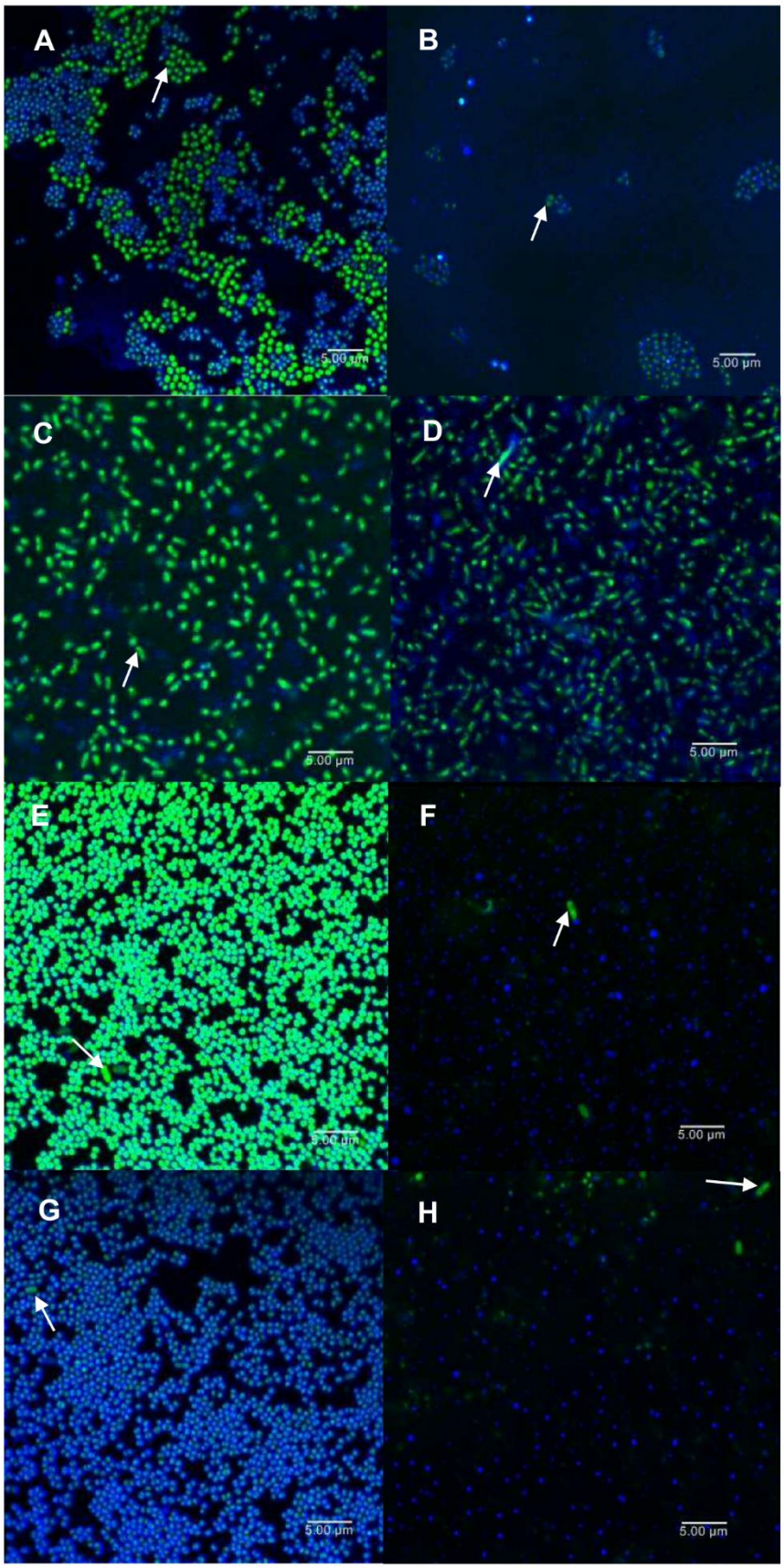

743

744

745

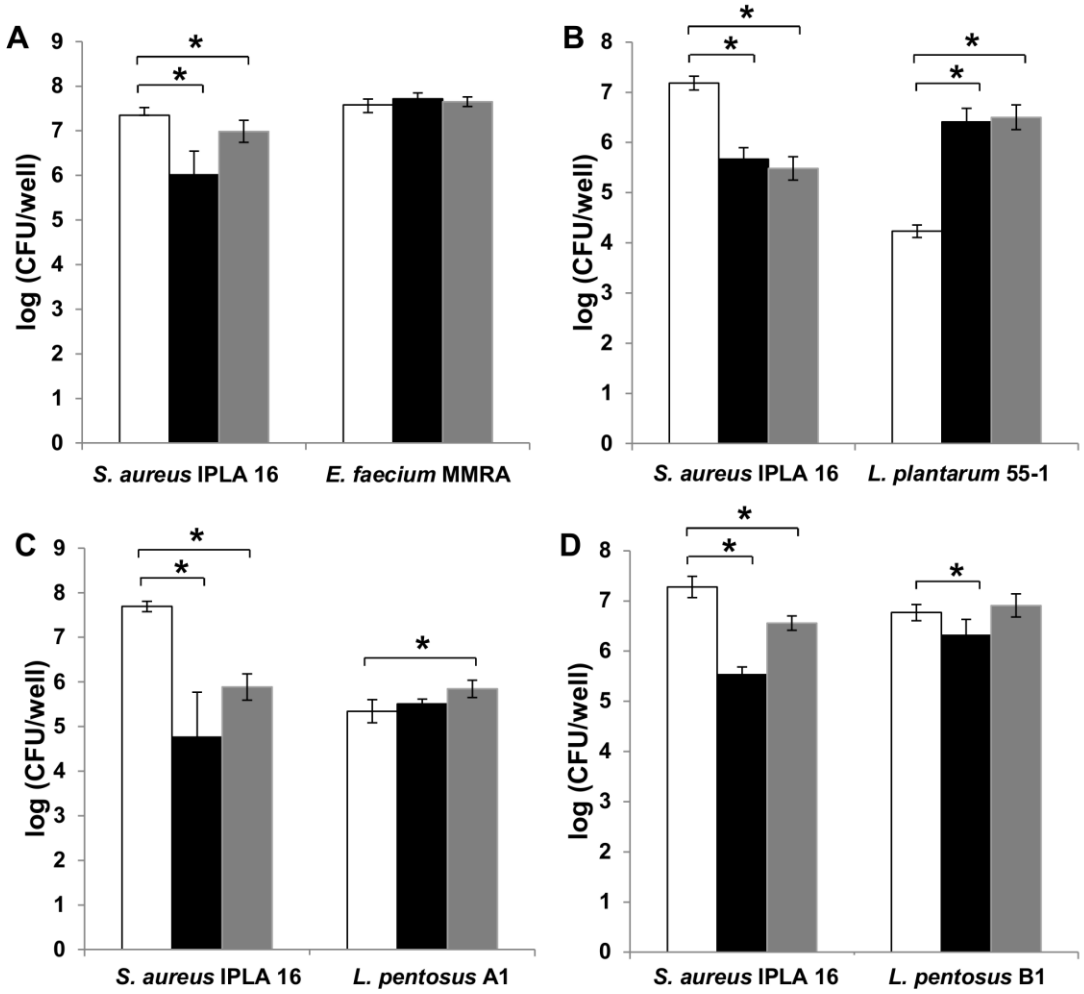

746

747

748

749

750

751

752

753

754

755

756

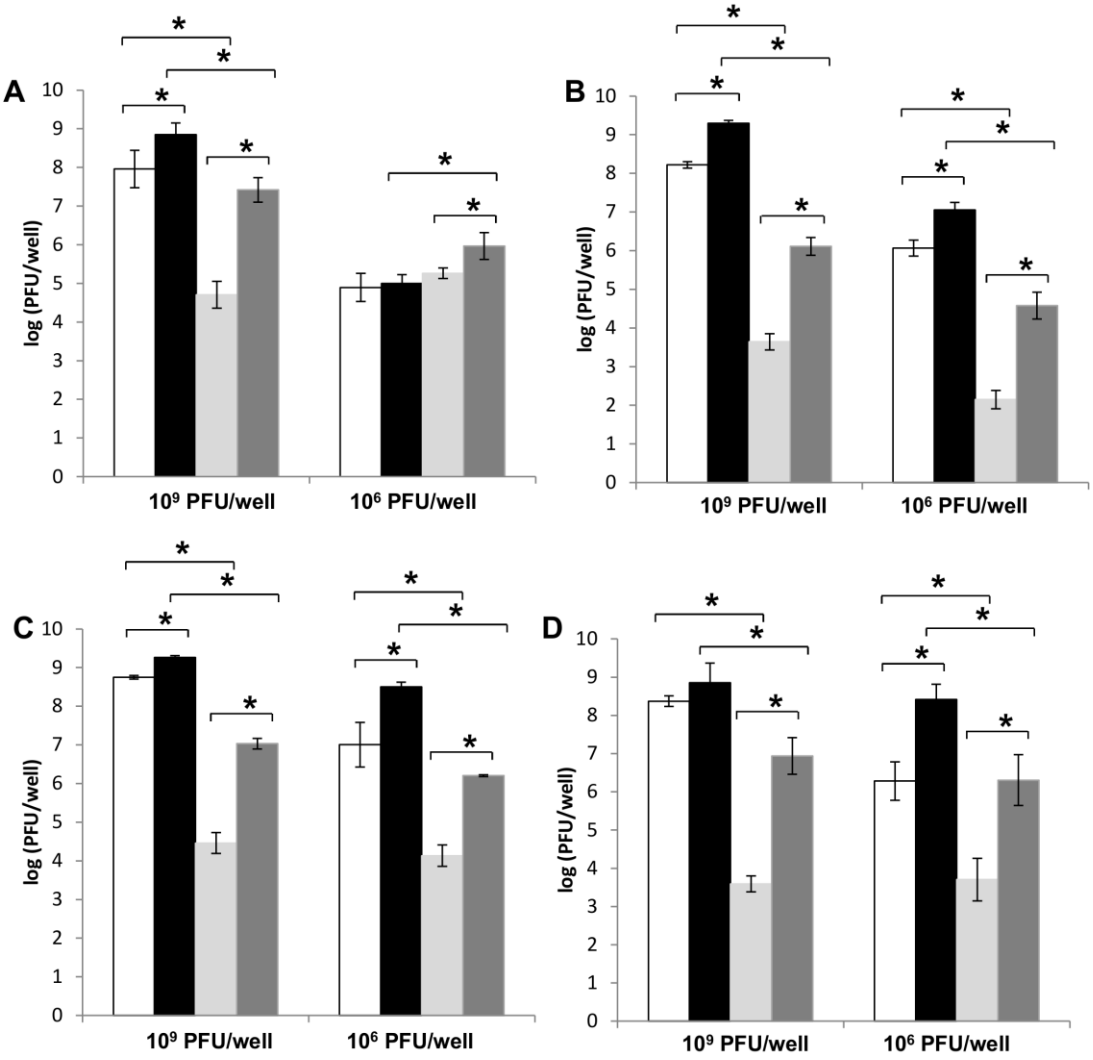
A
B
C
D
log (PFU/well)
10⁹ PFU/well
10⁶ PFU/well
*

769

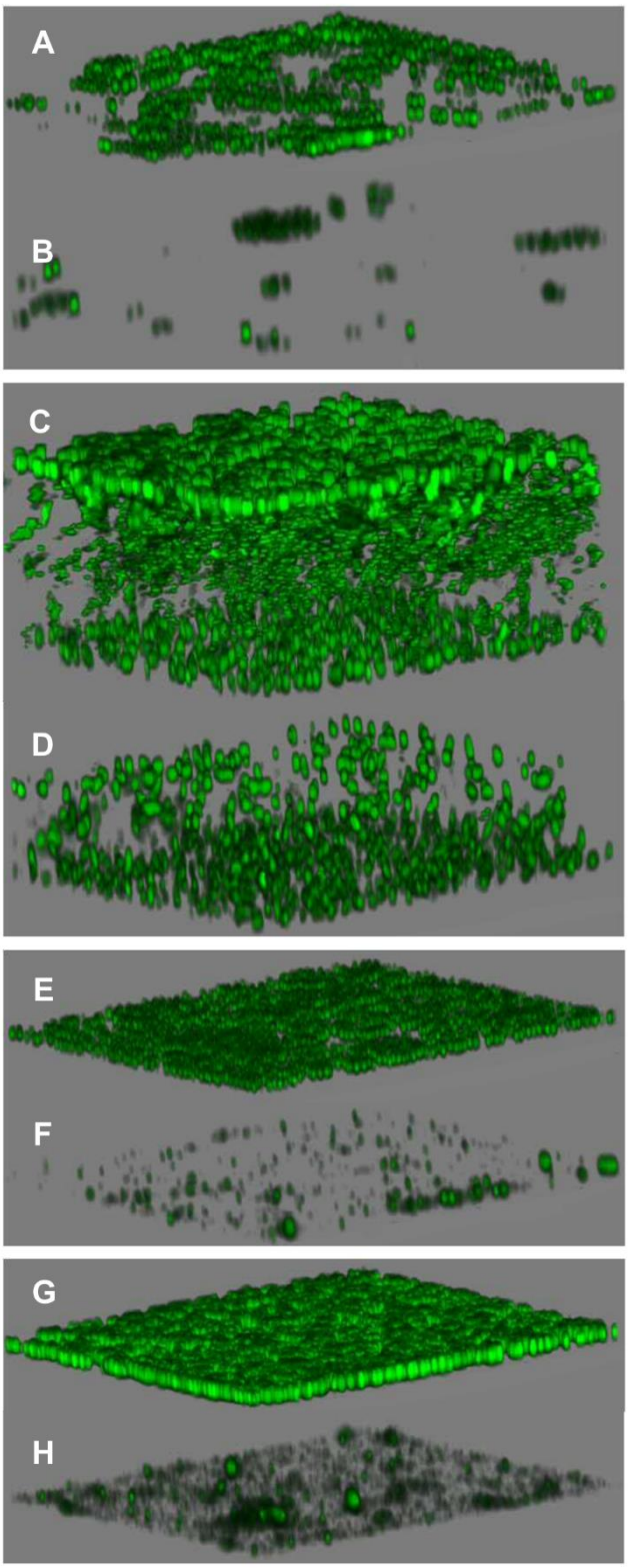

770

771

772

773

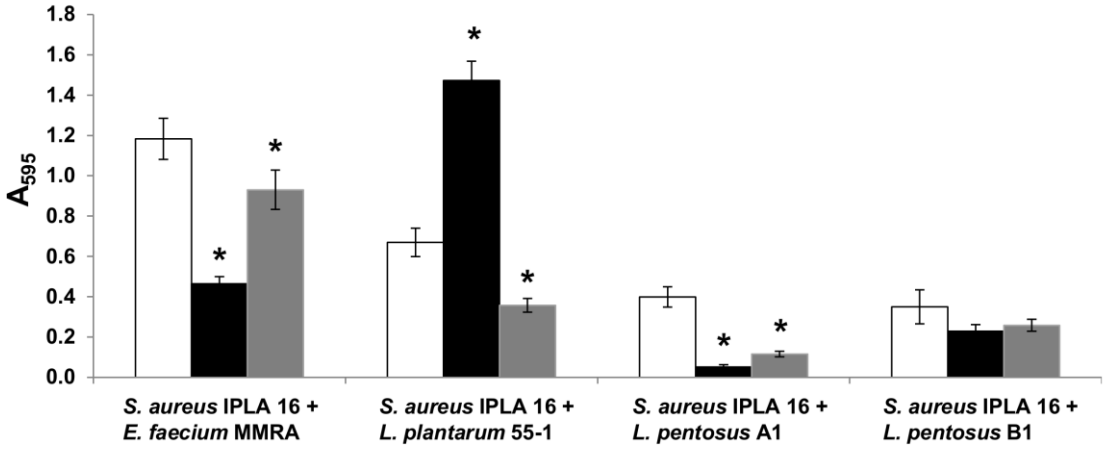
1.8
1.6
1.4
1.2
1.0
0.8
0.6
0.4
0.2
0.0
A595
*
*
*
*
*
*
S. aureus IPLA 16 + E. faecium MMRA
S. aureus IPLA 16 + L. plantarum 55-1
S. aureus IPLA 16 + L. pentosus A1
S. aureus IPLA 16 + L. pentosus B1

774

775

frontiers in Microbiology

ORIGINAL RESEARCH
published: 28 September 2018
doi: 10.3389/fmicb.2018.02348

Analysis of Different Parameters Affecting Diffusion, Propagation and Survival of Staphylophages in Bacterial Biofilms

Silvia González, Lucía Fernández, Diana Gutiérrez, Ana Belén Campelo, Ana Rodríguez and Pilar García*

Instituto de Productos Lácteos de Asturias (IPLA-CSIC), Villaviciosa, Spain

The elimination of bacterial biofilms remains a major challenge due to their recalcitrant nature. Bacteriophages, viruses that infect bacteria, have been gaining increasing attention as biofilm control agents. However, the development of a successful phage-based strategy requires in-depth analysis of different parameters. It is particularly important to determine the ability of a given phage to diffuse, propagate and remain viable within the complex biofilm structure. Here, we examine some of these properties for two staphylophages, vB_SauM_phiIPLA-RODI and vB_SepM_phiIPLA-C1C. Both *Staphylococcus aureus* and *Staphylococcus epidermidis* are important opportunistic pathogens that readily form biofilms on a wide array of biotic and abiotic surfaces. Our results confirmed that both phages could penetrate through biofilms formed by several bacterial strains with varying degrees of susceptibility to the viruses and biofilm-forming abilities. However, phage penetration differed depending on the specific bacterium or combination of bacteria. The data presented here suggest that the factors determining the diffusion rate of phages in biofilms include the amount of attached biomass, susceptibility of the strain, initial phage titer, phage entrapment in the extracellular matrix, and phage inactivation. This information will help to further characterize phage-bacteria interactions within biofilm communities and will be valuable for the development of antistaphylococcal products based on these phages.

Keywords: *Staphylococcus aureus*, biofilms, bacteriophages, phage diffusion, phage propagation

OPEN ACCESS

Edited by:
William Michael McShan, University of Oklahoma Health Sciences Center, United States

Reviewed by:
Bettina Buttaro, Temple University, United States
Eric Altermann, AgResearch, New Zealand

****Correspondence:***
Lucía Fernández
lucia.fernandez@ipla.csic.es

Specialty section:
This article was submitted to Virology, a section of the journal Frontiers in Microbiology

Received: *12 June 2018*
Accepted: *12 September 2018*
Published: *28 September 2018*

Citation:
González S, Fernández L, Gutiérrez D, Campelo AB, Rodríguez A and García P (2018) Analysis of Different Parameters Affecting Diffusion, Propagation and Survival of Staphylophages in Bacterial Biofilms. Front. Microbiol. 9:2348. doi: 10.3389/fmicb.2018.02348

INTRODUCTION

The relentless rise in antibiotic resistance has paved the way for the introduction of alternative antimicrobial strategies. An interesting approach is the use of bacteriophages (phages), viruses that can infect and kill bacterial cells (O'Flaherty et al., 2009; Nobrega et al., 2015; Abedon et al., 2017). Phage therapy offers some compelling advantages over conventional antibacterial strategies. Most remarkably, phages can be very target-specific, sometimes infecting only some strains of a given species, they are innocuous for humans and the environment and, last but not least, nature provides a huge reservoir of potential new variants so that new products can be under continuous development. All these interesting characteristics have led to a resurgence of bacteriophages as potential antimicrobials to be used in human and veterinary medicine or industrial settings, amongst other applications. However, there are still regulatory constraints

that prevent or delay the approval and commercialization of phage-based products. In order to overcome such difficulties, the scientific community must convince the authorities about the safety and efficacy of bacteriophages (EFSA, 2012). It must be noted, however, that several phage-based products are currently on the market despite the regulatory hurdles (Fernández et al., 2018a). For example, the FDA has approved the use in food environments of products containing bacteriophages against different pathogenic bacteria such as *Listeria monocytogenes* (ListShield™, developed by Intralytix, Inc., and PhageGuard Listex, developed by Micreos BV), *Salmonella enterica* (PhageGuard S, developed by Micreos BV, and SalmoFresh™, developed by Intralytix, Inc.) or *Escherichia coli* (EcoShield™, developed by Intralytix, Inc.).

Perhaps, one of the biggest challenges for controlling microbial pathogens is biofilm removal. Biofilms represent the most widespread lifestyle in natural and artificial environments alike. Indeed, estimates indicate that biofilms are involved in at least 65% of all bacterial infections (Potera, 1999). As a result, a good antibacterial strategy needs to be effective against biofilms. In biofilms, bacterial cells are embedded in a matrix that consists of polysaccharides, eDNA and proteins. Worryingly, microorganisms forming these structures are remarkably resistant to antibiotics and disinfectants. The resistance mechanisms inherent to the biofilm lifestyle are very diverse and include the interference of the extracellular matrix with antimicrobial agents (de la Fuente-Núñez et al., 2013). On the one hand, the matrix poses a physical barrier to the diffusion of compounds. On top of that, chemical interactions between the matrix polymers and the antimicrobials can also hinder antibacterial activity. Therefore, it is very important to demonstrate the ability of a given antimicrobial to penetrate the biofilm and reach target bacteria. Some studies have demonstrated that penetration across biofilms depends on the compound as well as the biofilm thickness and composition. For example, Anderl et al. (2000) designed an elegant protocol to quantify the penetration of antimicrobials across bacterial biofilms. In this study, biofilms of *Klebsiella pneumoniae* were formed on polycarbonate membranes placed on top of culture medium agar plates inoculated with a bacterial lawn. Subsequently, disks containing different antibiotics were placed on top of the membranes and the diameter of the inhibition zones was measured. The results demonstrated that, while ciprofloxacin could readily penetrate the biofilm, ampicillin was prevented from doing so by the accumulation of beta-lactamases in the biofilm matrix. This technique was later used to test the penetration of antibiotics through biofilms formed by *Staphylococcus aureus* and *Staphylococcus epidermidis* (Singh et al., 2010). In the case of bacteriophages, Briandet et al. (2008) showed that bacteriophage c2 could diffuse within biofilms formed by both a sensitive strain and an insensitive strain of *Lactococcus lactis* by using a fluorescent marker and further microscopic observation. On the basis of this study, it appears that the biofilm matrix does not pose a significant barrier to the diffusion of bacteriophages through the biofilm. However, while this highlights that phages can be potential antibiofilm antimicrobials, it also suggests that phages can find protection from environmental challenges within the biofilm structure. Nonetheless, further studies are still necessary to fully quantify and characterize the process of biofilm penetration by phages.

There has been a substantial amount of research aimed at the development of phage-based strategies against biofilms formed by different pathogenic bacteria, including the dangerous opportunistic pathogen *S. aureus* (Gutiérrez et al., 2016; Pires et al., 2017). This bacterium can develop biofilms on implant devices, human tissues or inert surfaces, such as those in hospital or food-industry environments (Otto, 2013). Organization into these microbial communities protects *Staphylococcus* cells from antibiotics and disinfectants, thereby hampering control of staphylococcal contamination. In that sense, bacteriophages represent an interesting antibacterial strategy. Indeed, several studies have shown that staphylophages alone or in combination with other compounds can be effective for biofilm removal (Son et al., 2010; Kelly et al., 2012). Quite recently, Gutiérrez et al. (2015) isolated two virulent staphylophages, vB_SauM_ phiIPLA-RODI (phiIPLA-RODI) and vB_SepM_ phiIPLA-C1C (phiIPLA-C1C) that exhibited antibiofilm activity against both single-species and mixed-species biofilms formed by *S. aureus* (Gutiérrez et al., 2015; González et al., 2017). Here, we set out to determine the ability of the aforementioned phages to penetrate biofilms formed by different species and strains, both sensitive and insensitive to the viruses. Additionally, we assessed whether phage diffusion was affected by formation of mixed-species biofilms. Another objective was to test the ability of the phage to remain active in the biofilm matrix of different bacteria. In order to carry out these analyses, we developed a method based on plates with transwell inserts, generally used for forming eukaryotic cells monolayers, to pre-form a bacterial biofilm and then test the behavior of phage particles following their diffusion across this structure. Overall, our findings show that staphylococcal phages can indeed penetrate and propagate in biofilms. However, the success of these processes depends on the phage dose, biofilm composition and thickness, susceptibility of the strains forming the biofilm, and phage inactivation. These results will be helpful for the development of novel phage-based antibiofilm products, and provide further insight into phage-bacteria interactions within attached microbial communities.

MATERIALS AND METHODS

Bacterial Strains, Bacteriophages and Culture Conditions

The bacterial strains used in this study are listed in **Table 1**. Routine growth of *S. aureus* and *S. epidermidis* cultures was performed at 37°C on Baird-Parker agar plates (AppliChem, Germany) or in TSB (Tryptic Soy Broth, Scharlau, Barcelona, Spain) with shaking in an orbital incubator at 250 rpm. When necessary, TSB was supplemented with glucose at a final concentration of 0.25% (TSBG) or with agar at a final concentration of 0.7% (soft-TSA) or 2% (TSA). *L. plantarum*

TABLE 1 | Bacterial strains and bacteriophages used in this study.

Bacterial strains/bacteriophages	Source*	Reference
Bacterial strains		
Staphylococcus aureus		
IPLA1	Dairy industry surface	Gutiérrez et al. (2012)
IPLA15 (Sa IPLA15)	Meat industry surface	Gutiérrez et al. (2012)
IPLA16 (Sa IPLA16)	Meat industry surface	Gutiérrez et al. (2012)
RN450 (Sa RN450)	Derivative of strain NCTC8325	Novick (1967)
ISP479r (Sa ISP479r)	Derivative of strain NCTC8325	Toledo-Arana et al. (2005)
V329 (Sa V329)	Bovine subclinical mastitis	Cucarella et al. (2001)
Staphylococcus epidermidis		
F12 (Se F12)	Milk from woman with mastitis	Delgado et al. (2009)
Z2LDC14 (Se Z2LDC14)	Milk from woman with mastitis	Delgado et al. (2009)
DG2ñ (Se DG2ñ)	Milk from woman with mastitis	Delgado et al. (2009)
Lactobacillus plantarum		
55-1 (Lp 55-1)	Natural fermentation of olives	Ruiz-Barba et al. (1994)
Bacteriophages		
vB_SauM_ philPLA-RODI	Isolated from STP*	Gutiérrez et al. (2015)
vB_SepM_ philPLA-C1C	Isolated from STP*	Gutiérrez et al. (2015)

STP, sewage treatment plant.

55-1 was grown on MRS (Scharlab S.L., Spain) broth or agar at 32°C. Bacteriophages phiIPLA-RODI and phiIPLA-C1C were, respectively, propagated on *S. aureus* IPLA 1 and *S. epidermidis* F12 as previously described (Gutiérrez et al., 2010).

Biofilm Formation Assays

To assess the biofilm-forming ability of the different strains used in the study, 450 μl from cell suspensions containing 10^6 CFU/ml in TSBG were inoculated into the inserts of 24-well Transwell® plates containing polycarbonate membranes (Corning, NY, United States). In the case of biofilms formed by two strains, we mixed the corresponding cells suspensions 1:1 prior to inoculating the inserts. Biofilms were allowed to develop for 24 h at 37°C and, following incubation, the attached biomass was stained with 0.1% crystal violet according to the protocol described previously (Gutiérrez et al., 2014). However, the volume used for washing, staining and distaining steps was 400 μl instead of 200 μl. Absorbance at 595 nm (A_{595}) was then quantified by using a Bio-Rad Benchmark Plus Microplate Spectrophotometer (Bio-Rad Laboratories, Hercules, CA, United States). The obtained values represent the crystal violet retained in the samples after the washing steps, which is, in turn, an indirect measurement of total attached biomass (cells and matrix). According to their A_{595} values, strains were categorized as strong ($A_{595} \geq 2$), intermediate ($1 < A_{595} < 2$), and weak ($A_{595} \leq 1$) biofilm formers.

Confocal Laser Scanning Microscopy (CLSM)

Each well of a 2-well μ-slide with a glass bottom (ibidi, United States) was inoculated with 1 ml of a cell suspension containing 10^6 cfu/ml in TSBG. Biofilms were then allowed to form for 24 h at 37°C. After biofilm development, the planktonic phase was removed and wells were washed with PBS prior to staining all cells (live and dead) with SYTO 9 from the LIVE/DEAD® BacLight™ Kit (Invitrogen AG, Basel, Switzerland) as indicated by the manufacturer. The biofilm samples were then observed under a DMi8 confocal laser scanning microscope (Leica Microsystems) using a 63× oil objective.

Determination of the Minimum Inhibitory Multiplicity of Infection (MIMOI)

The susceptibility of the different strains to phages phiIPLA-RODI and phiIPLA-C1C was assessed by a modification of the broth microdilution assay as described elsewhere (Fernández et al., 2017). The MIMOI was considered to be the lowest multiplicity of infection or MOI (number of phage particles per bacterial cell) at which no bacterial growth was observed with the naked eye, as indicated in the Clinical Laboratory Standards Institute (2015), following 24 h of incubation at 37°C.

Bacteriophage Diffusion Assays

A schematic representation of the protocol used to assess phage penetration across bacterial biofilms is depicted in **Figure 1**. In a first step, biofilms were pre-formed on polycarbonate membranes with 0.4 μm pore size placed inside the inserts of 24-well Transwell® plates (Corning, NY, United States). To do that, 450 μl from a cell suspension containing 10^6 CFU/ml in fresh TSBG were inoculated into each insert and incubated for 24 h at 37°C. Control wells were inoculated with 450 μl of TSBG medium. After incubation, the inserts were placed into new sterile wells containing a 100-μl drop of TSB, as this was found to facilitate movement of the liquid across the membrane. Next, 450 μl of phage suspensions containing 10^6 or 10^9 PFU/ml in TSB were carefully poured on top of the pre-formed biofilms. The plates were then further incubated for 24 h at 37°C, during which time the liquid moved across the polycarbonate membrane from the insert to the bottom chamber. The following day, the phage titer in the flow-through and the biofilm were determined by the double-layer assay (Gutiérrez et al., 2010). The biofilm was washed with PBS and then gently scraped from the membrane with a sterile cotton swab and then resuspended in 5 ml of SM buffer (20 mg/liter Tris–HCl, 10 mg/liter $MgSO_4$, 10 mg/liter $CaCl_2$, 100 mg/liter NaCl, pH 7.5) by vortexing the sample for 1 min. This suspension was then titrated to determine the number of phage particles trapped in the extracellular matrix. Then, the insert was removed and the flow-through was collected from the bottom chamber. Serial dilutions of these suspensions were used for phage titration.

Analysis of the correlation between biofilm formation or susceptibility and phage titer in the flow-through was performed by calculating indicators of these two properties. The indicator

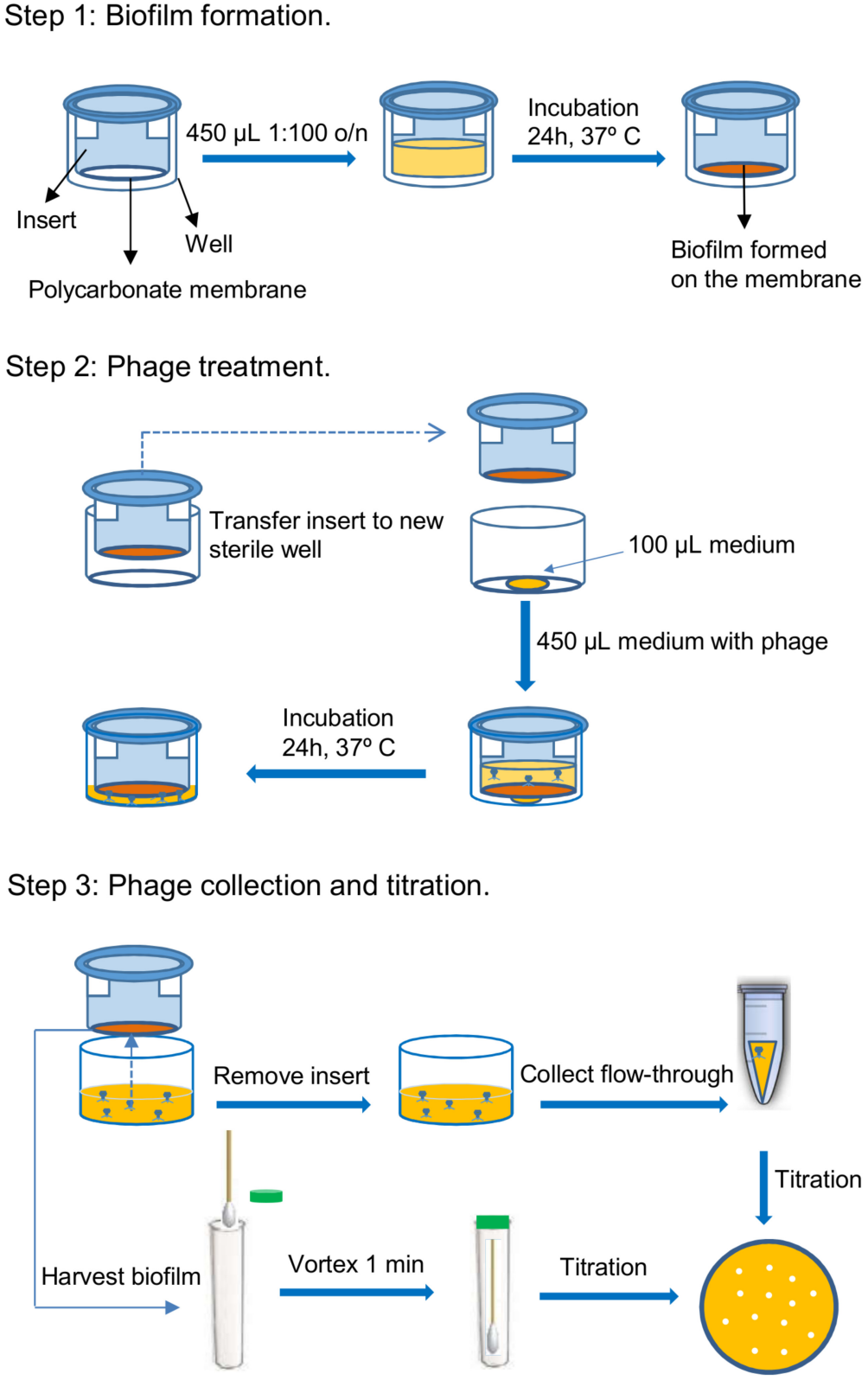

FIGURE 1 | Schematic representation of the steps involved in the protocol for testing the penetration of bacteriophages through bacterial biofilms. These steps are the following: 1. Biofilm formation, 2. Phage treatment, and 3. Phage collection and titration.

of biofilm formation ability was the average A_{595} resulting from crystal violet staining of biofilms for a given strain. Calculation of the susceptibility values was based on the results obtained in the MIMOI determination assays. The minimum susceptibility, with a value of 0, was assigned to the non-susceptible strains. In turn, the most susceptible strains for each phage were assigned a susceptibility value of 5. Susceptibility of the other strains was calculated by subtracting the change in logarithmic units between their MIMOIs and that of the most susceptible strain (strain MS):

$$\text{Susceptibility of strain A} = 5 - \log\left[\text{MIMOI (strain A)}/\text{MIMOI (strain MS)}\right]$$

Finally, a third indicator combining the two previous properties was calculated as the quotient susceptibility/biofilm formation. The results obtained in these three calculations for the different strains were then plotted against $\log_{10}$ (PFU/ml) in which PFU/ml corresponds to the phage titer in the flow-through. Subsequently, the values in the resulting chart were fitted to a trend line and the coefficient of determination (R^2) was calculated to determine the goodness of fit.

Phage Inactivation Assay

Different bacterial strains were grown overnight at 37°C in TSB or TSBG without shaking. Control samples with medium alone were also included. The following day, supernatants were collected and filtered after centrifugation at 13,200 rpm for 3 min. 900 µl aliquots from each sample were taken and mixed with 100 µl of a phage suspension to obtain a final concentration of 10^6 PFU/ml. All samples were subsequently incubated at 37°C for 3 h. After incubation, the phage titer was determined as described above. The pH of the different supernatants was determined by using pH-indicator strips (Merck, Darmstadt, Germany).

Statistical Analyses

All phage penetration experiments were performed with at least four technical repeats corresponding to two independent biological replicates. Biofilm formation, MIMOI determination and phage inactivation assays were performed with three independent biological replicates. Data was then analyzed with a two-tailed Student's *t*-test and significance was set at a *P*-value threshold of 0.05.

RESULTS

Biofilm Formation on Polycarbonate Membranes and Phage Susceptibility of Different Bacterial Strains

The aim of this study was to determine the impact of certain factors on the success of bacteriophage diffusion across bacterial biofilms. Amongst other factors, we wanted to examine the effect of biofilm-forming ability and phage susceptibility. To do that, it was necessary to ensure that the strains selected for the study represent varying degrees of these two characteristics prior to performing the biofilm penetration experiments. First, several strains of *S. aureus* and *S. epidermidis* were chosen based on previous data (Gutiérrez et al., 2014, 2015), as well as *Lactobacillus plantarum* 55-1. This bacterium can form mixed biofilms with *S. aureus* and is not susceptible to phage phiIPLA-RODI (González et al., 2017).

TABLE 2 | MIMOI values for phages phiIPLA-RODI and phiIPLA-C1C and biofilm-forming ability of the different bacterial strains used in this study.

Bacterial strain	phiIPLA-RODI	phiIPLA-C1C	Biofilm formation[1]
Sa IPLA15	100	NS	1.18 ± 0.24 (intermediate)
Sa IPLA16	0.01	1	1.48 ± 0.39 (intermediate)
Sa RN450	100	NS	0.72 ± 0.04 (weak)
Sa ISP479r	0.1	NS	2.04 ± 0.15 (strong)
Sa V329	10	NS	3.37 ± 0.82 (strong)
Se F12	NS	1	1.36 ± 0.38 (intermediate)
Se Z2LDC14	NS	0.1	1.86 ± 0.07 (intermediate)
Se DG2ñ	NS	100	1.66 ± 0.48 (intermediate)
Lp 55-1	NS	NS	0.64 ± 0.15 (weak)

**NS, not susceptible; [1]A_{595} was determined after crystal violet staining of 24-h biofilms formed on polycarbonate membranes at 37°C. Based on these values, strains were classified into strong ($A_{595} > 2$), intermediate ($1 < A_{595} < 2$) and weak ($A_{595} < 1$) biofilm formers.*

The assessment of biofilm formation was carried out on the polycarbonate membranes of transwell plates that would be subsequently used for phage penetration tests. Total biomass (cells plus matrix) attached to the membranes following 24 h of incubation at 37°C was quantified by crystal violet staining and subsequent measurement of absorbance at 595 nm (A_{595}). The results of these assays revealed that these bacterial strains display a wide range of biofilm-forming abilities. For the sake of this study, strains were classified as weak ($A_{595} \leq 1$), intermediate ($1 < A_{595} < 2$) and strong ($A_{595} \geq 2$) biofilm formers (**Table 2** and **Supplementary Figure S1A**). According to this criterion, strains *S. aureus* V329 (Sa V329) and *S. aureus* ISP479r (Sa ISP479r) were considered strong biofilm formers, whereas *L. plantarum* 55-1 (Lp 55-1) and *S. aureus* RN450 (Sa RN450) were weak biofilm formers (**Table 2** and **Supplementary Figure S1A**). All other strains displayed an intermediate ability to develop biofilms on polycarbonate membranes (**Table 2** and **Supplementary Figure S1A**). These strains included *S. aureus* IPLA15 (Sa IPLA15), *S. aureus* IPLA16 (Sa IPLA16), *S. epidermidis* F12 (Se F12), *S. epidermidis* Z2LDC14 (Se Z2LDC14) and *S. epidermidis* DG2ñ (Se DG2ñ). Besides being a strong biofilm former, strain Sa V329 is also interesting as it is the only *S. aureus* strain included here whose biofilm matrix is principally composed of proteins instead of polysaccharide (Gutiérrez et al., 2014).

Visual inspection of the polycarbonate membranes after incubation of the bacterial cultures showed the development of biofilm all over the membrane, from edge to edge. However, this does not necessarily mean that biofilm coverage and architecture is homogeneous at the microscopic level. For this reason, we examined the structure of biofilms formed by the different strains on glass-bottomed slides by CLSM. The thickness of the observed biofilms showed a relatively good correlation (0.6105)

with the crystal violet data from biofilms grown on polycarbonate membranes (**Supplementary Figure S1B**). Regarding surface coverage, most strains seem to have developed biofilms that covered the slide bottom rather homogeneously, with the exception of Sa IPLA15 and Se F12 (**Supplementary Figures S2**, **S3**). There were also differences between strains regarding the complexity of biofilm architecture (**Supplementary Figures S2**, **S3**). For instance, the two strong biofilm-forming strains, namely ISP479r and V329, showed notable differences, with the latter (V329) exhibiting a much more complex 3D structure (**Supplementary Figure S2**).

Besides biofilm-forming ability, susceptibility of the different strains to phages phiIPLA-RODI and phiIPLA-C1C was also assessed by determining their MIMOI values (**Table 2**). As is the case with the minimum inhibitory concentrations (MICs) of antibiotics, a higher MIMOI represents a lesser susceptibility to the phage. Based on this criterion, the most susceptible strains to phiIPLA-RODI were Sa IPLA 16, Sa ISP479r and Sa V329, while the other two *S. aureus* strains, Sa IPLA15 and Sa RN450, required a higher MOI to inhibit visible growth (**Table 2**). Finally, all the *S. epidermidis* strains and Lp 55-1 were insensitive to phiIPLA-RODI. Regarding phage phiIPLA-C1C, susceptible strains included Se Z2LDC14, Se F12, Sa IPLA16 and Se DG2ñ, while *L. plantarum* and most *S. aureus* strains (Sa IPLA15, Sa ISP479r, Sa RN450, and Sa V329) were insensitive to this phage (**Table 2**).

Diffusion of phiIPLA-RODI and phiIPLA-C1C Through Bacterial Biofilms

Once established that the selected strains displayed different degrees of biofilm-forming ability and susceptibility to the phages, penetration of phiIPLA-RODI and phiIPLA-C1C across bacterial biofilms was examined following the protocol depicted in **Figure 1**. To do that, 24-h biofilms were formed on the polycarbonate membranes of transwell plates and subsequently treated with different phage suspensions (**Figure 1**). Following incubation for another 24 h at 37°C, the liquid from the insert had moved across the biofilm and the membrane to the bottom chamber, and phage titer in the flow-through was determined to assess phage penetration. The results of biofilm-containing wells were compared to those of control wells (without biofilm) to correct for the possibility of bacteriophage particles being retained in the polycarbonate membrane.

In a first experiment, penetration was tested by treating pre-formed 24-h-old biofilms with phage suspensions containing a high titer ($\sim 10^9$ PFU/ml) of phages phiIPLA-RODI or phiIPLA-C1C. Phage titer in the flow-through was determined and compared to that of control non-inoculated wells. In the bacteria-inoculated membranes, phage penetration occurred in all samples but the titer in the flow-through varied depending on the specific strain. Thus, the titer of phiIPLA-RODI in the flow-through was significantly lower for strains Sa ISP479r, Lp 55-1, Se F12, and Sa V329. In contrast, the phage titer obtained for biofilms formed by Sa RN450, Sa IPLA 15, and Sa IPLA 16 was not significantly different from that of the control (**Figure 2A**). These three *S. aureus* strains were poor or intermediate biofilm formers (**Table 2**). However, even though Se F12 and Lp 55-1 did not form robust biofilms either, the phage titer in the flow-through was approximately 2 log units lower than that of the control. Interestingly, Se F12 and Lp 55-1 share their lack of susceptibility to phiIPLA-RODI. In the case of phiIPLA-C1C, a decrease in phage titer was observed for the biofilms formed by Se F12, Sa IPLA16, Se Z2LDC14, Se DG2ñ, and Lp 55-1. Indeed, the latter three strains showed reductions in the phage titer of up to 2 log units, despite the fact that none of them are strong biofilm formers and that two of them (Se Z2LDC14 and DG2ñ) are susceptible to the phage. Conversely, no decrease was observed for Sa V329 or Sa ISP479r (**Figure 2B**).

The assays performed with a high phage titer revealed different penetration rates for the phages depending on the bacterial strain forming the biofilm. However, they did not give any indication of whether propagation was taking place during this process. Perhaps this was due to the fact that the phage concentrations used were near the maximum propagation rates observed for these phages, thereby masking this phenomenon. Taking this into consideration, the assay was repeated by treating the biofilms with a lower phage titer ($\sim 10^6$ PFU/ml). The results obtained here were quite different from those in the previous experiment (**Figures 2C,D**). Thus, while the phage titer remained unchanged or decreased for some strains, there were examples in which a significant increase in phage titer in the flow-through was detected. This was the case, for instance, of strains Sa ISP479r and Sa IPLA 16 for phage phiIPLA-RODI (**Figure 2C**) or Se F12, Se Z2LDC14, and Sa IPLA 16 for phiIPLA-C1C (**Figure 2D**). As would be expected, these were the most susceptible strains to each phage. Instead of phage propagation, a decrease in phage titer was observed for the other strains. Notably, the phage titer of the insensitive bacterium Lp 55-1 exhibited a decrease of almost 2 log units for both viruses. Additionally, there were significant reductions for biofilms formed by Sa IPLA15 and Se F12 in the case of phiIPLA-RODI. This is interesting because neither of these two strains is a very good biofilm former and Sa IPLA15 shows susceptibility, albeit not very high, to this phage. Finally, no significant changes in phage titer were observed for strains Sa RN450 and Sa V329 in the case of phiIPLA-RODI, or strains Se DG2ñ, Sa ISP479r, and Sa V329 for phage phiIPLA-C1C.

In an attempt to examine the influence of biofilm-forming ability and phage susceptibility on phage diffusion across biofilms, these values were plotted against the phage titers quantified in the flow-through to detect potential trends (**Supplementary Figures S4**, **S5**). The indicators of biofilm-forming capacity and susceptibility were estimated as previously described (see Materials and Methods). The results of linear regression analysis obtained for a high concentration (10^9 PFU/ml) of phage phiIPLA-RODI indicated that the most acceptable model for predicting the phage titer in the flow-through of different biofilms was the one that considered both susceptibility and biofilm formation ($R^2 = 0.554$), whereas susceptibility and biofilm formation alone showed fairly low fitting coefficients ($R^2 < 0.5$) (**Supplementary Figure S4**). We observed that there was a positive correlation between both susceptibility and susceptibility/biofilm formation and phage titer in the flow-through as indicated by the fact that both

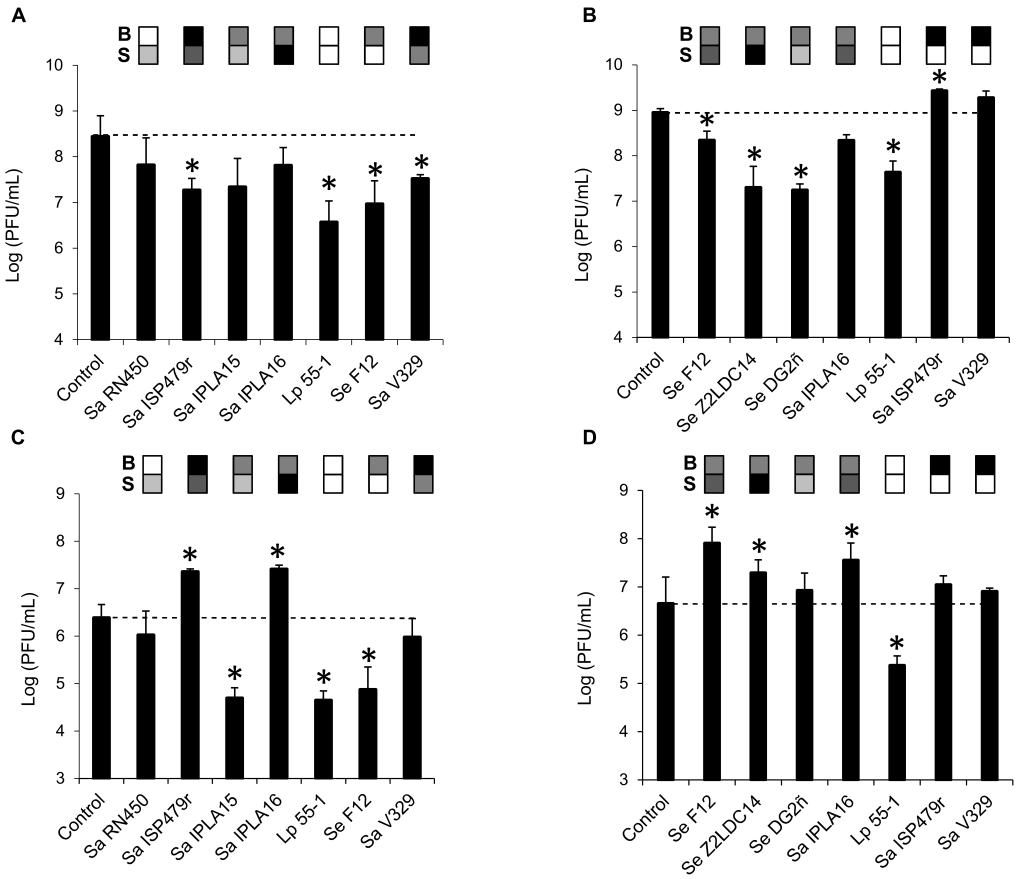

FIGURE 2 | Diffusion of bacteriophages philPLA-RODI and philPLA-C1C through bacterial biofilms formed by different strains. Biofilms were pre-formed on the membranes of transwell plates for 24 h at 37°C and subsequently treated with 10^9 **(A,B)** or 10^6 **(C,D)** PFU/ml of bacteriophages philPLA-RODI **(A,C)** or philPLA-C1C **(B,D)**. Phage particles in the flow-through were titrated after incubation at 37°C for 24 h. The values represent the average and standard deviation of at least three replicates. Differences compared to the control (membrane without biofilm) with *P*-values < 0.05 were considered significant (*). Sa, *S. aureus*; Se, *S. epidermidis*; and Lp, *L. plantarum*. The grid on top of each bar represents the biofilm strength (B) and susceptibility (S) of each strain in a color-coded manner. For biofilm strength, black, gray, and white represent strong, intermediate and weak biofilm formation. Susceptibility is represented in a scale that goes from white (non-susceptible strains) to black (most susceptible strain for a given phage).

trend lines had a positive slope (**Supplementary Figure S4**). When treatment was carried out with a low phage concentration (10^6 PFU/ml) of philPLA-RODI, the best predictive model was obtained when plotting phage titer in the flow-through against susceptibility (R^2 = 0. 872) (**Supplementary Figure S4**), which indicated that there was a positive correlation between the two variables. Analysis of the data obtained for phage philPLA-C1C, however, gave very different results. Thus, when treatment of bacterial biofilms was performed with a high phage concentration (10^9 PFU/ml) the most acceptable model was obtained by plotting phage titer against biofilm-forming ability (R^2 = 0.3417), although fitting was still very low ($R^2 < 0.5$) (**Supplementary Figure S3**). In the case of samples treated with a low concentration (10^6 PFU/ml) of philPLA-C1C, the best-fitting model was obtained for phage susceptibility/biofilm formation ($R^2 = 0.5225$), which was slightly better than the model that represented phage titer against susceptibility ($R^2 = 0.4566$). The correlation between susceptibility or susceptibility/biofilm formation and phage titer in the flow-through was positive. Overall, it seems that penetration of phage philPLA-RODI through biofilms is positively correlated with susceptibility of the bacterial strain after treatment with both high and low phage concentrations (**Supplementary Figure S4**). Moreover, at high phage concentrations the effect of susceptibility is further modulated by the biofilm-forming ability of the strain (**Supplementary Figure S4**). In contrast, penetration of philPLA-C1C does not appear to be highly correlated to biofilm formation or susceptibility of the strains involved, with perhaps additional undetermined factors playing a role in phage diffusion (**Supplementary Figure S5**).

Penetration of philPLA-RODI Through Mixed-Species Biofilms

Further experiments were performed to analyze more in-depth the properties that affect phage penetration through bacterial biofilms. In particular, we evaluated the ability of phage philPLA-RODI applied at a low phage titer ($\sim 10^6$ PFU/ml) to diffuse

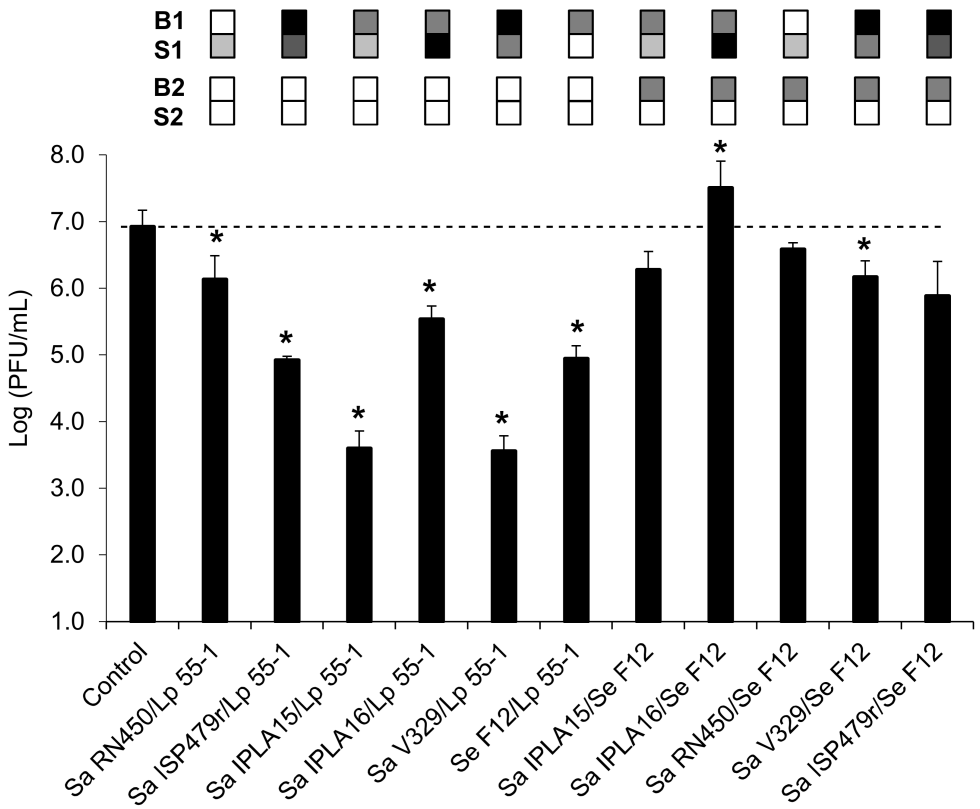

FIGURE 3 | Diffusion of phage philPLA-RODI through mixed-species biofilms. The ability of phage suspensions containing 10^6 PFU/ml to diffuse across biofilms formed by a combination of two strains (strain 1/strain 2) was examined. The changes observed in mixed-strain biofilms were compared to those observed when the same bacteria were forming single-strain biofilms. Differences compared to the control (membrane without biofilm) with *P*-values < 0.05 were considered significant (*). Sa, *S. aureus*; Se, *S. epidermidis*; and Lp, *L. plantarum*. The grid on top of each bar represents the biofilm strength (B) and susceptibility (S) of each strain in a color-coded manner. For biofilm strength, black, gray, and white represent strong, intermediate and weak biofilm formation. Susceptibility is represented in a scale that goes from white (non-susceptible strains) to black (most susceptible strain for a given phage). For each pair forming a mixed biofilm, B1 and S1 correspond to the first strain while B2 and S2 correspond to the second strain (*L. plantarum* or *S. epidermidis*).

across mixed-species biofilms. A previous study had shown that the propagation success of phiIPLA-RODI in multispecies biofilms formed by Sa IPLA16 differed depending on the accompanying species (González et al., 2017). Precisely one of the species used in the cited study was *L. plantarum*, which showed a good ability to form mixed-species biofilms with *S. aureus*. Indeed, the difference in viable cell counts in mixed biofilms of the two bacteria were less than one logarithmic unit and microscopy analysis indicated that cells of both species were mixed throughout the biofilm. The ability of *S. epidermidis* to form mixed biofilms with *S. aureus* with similar viable cell counts of the two species had been previously shown by Gutiérrez et al. (2015). In the present study, mixed-species biofilms were formed by inoculating different combinations of *S. aureus* strains with Se F12 or Lp 55-1, as well as a mixed biofilm formed by Se F12 and Lp 55-1. The results obtained were then compared to data from control wells (without biofilms). In general, the presence of Lp 55-1 led to a decrease in the phage titer of the flow-through compared to the non-inoculated control well, regardless of the accompanying strain (**Figure 3**). However, in some cases, this reduction was significantly smaller than that observed for the Lp 55-1 monospecies biofilms (2 log units, **Figure 2C**), as was the case of *L. plantarum* combined with Sa RN450 (1 log unit, **Figure 3**). Conversely, there was an increased reduction in phage titer compared to *L. plantarum* alone (2 log units, **Figure 2C**) when Lp 55-1 formed a biofilm with Sa IPLA15 or Sa V329 (3 log units, **Figure 3**). Perhaps, the mechanisms by which there is a decrease in the phage titer in these *S. aureus* strains and that of *L. plantarum* cultures have a cumulative effect. Mixed species biofilms of Lp 55-1 with Sa IPLA16 or Se F12 showed no significant difference compared to Lp 55-1 alone (2 log units decrease compared to the control wells, **Figure 3**). Overall, it seems quite clear that Lp 55-1 has a negative impact on the viability of phage phiIPLA-RODI.

Despite the fact that Lp 55-1 and Se F12 monospecies biofilms behaved similarly, the results obtained for mixed biofilms formed by Se F12 with different *S. aureus* strains were quite different from those displayed by mixed biofilms of the same strains with *L. plantarum* (**Figure 3**). Indeed, most combinations of Se F12 with *S. aureus* led to a lesser decrease in phage titer in the flow-through than that observed for Se F12 monospecies biofilms (2 log units, **Figure 2C**). This was, for instance, the case for

multispecies biofilms of Se F12 with Sa IPLA15 (no change, **Figure 3**), Sa RN450 (no change, **Figure 3**), Sa ISP479r (no change, **Figure 3**) and Sa V329 (1 log unit decrease, **Figure 3**). Moreover, development of mixed biofilms of Se F12 and Sa IPLA 16 allowed for phage propagation to occur (1 log unit increase compared to control wells, **Figure 3**). Interestingly, the combination of Sa IPLA15 with Se F12 led to a significantly lower decrease in phage titer than either bacterium alone, which is exactly the opposite to the results obtained when Sa IPLA15 was grown with Lp 55-1. Therefore, it seems that the mechanisms involved in Se F12 and Sa IPLA15 reduction in phage titer somehow counteract each other. Also, the phage titer in the flow-through obtained when treating mixed-strain biofilms formed by Sa IPLA15 and Sa ISP479r exhibited an intermediate result between those observed for the two monospecies biofilms. Overall, combination of Se F12 with any of the *S. aureus* strains seems to prevent the decrease in the phage titer observed for the *S. epidermidis* strain alone, which is in stark contrast to the results displayed by mixed biofilms involving Lp 55-1. This suggests that phage inactivation mechanisms differ between the two microorganisms.

Titration of Phage Particles Retained in the Biofilm Matrix

One possible explanation for the reduced phage titer observed in the flow-through for some strains is the entrapment of the virus in the extracellular matrix of the biofilm. To study this possibility, we analyzed the amount of viable phage phiIPLA-RODI particles trapped in the biofilms formed by the different strains after treatment with a low phage concentration ($\sim 10^6$ PFU/ml). These values were then compared to the number of phage particles present in the inoculum. Interestingly, the results of this experiment did not completely mirror those obtained in the analysis of the flow-through. Here, most strains showed a significant change in phage titer compared to the inoculum, with the only exception of Sa RN450 (**Figure 4**). In some cases, there was a one log unit increase in phage titer in the biofilm compared to the inoculum. More specifically, this occurred for strains Sa ISP479r, Sa IPLA15, Sa IPLA16, and Sa V329, all of which showed susceptibility to this phage. It is worth noting the fact that Sa IPLA15, which displayed a significant decrease in phage titer in the flow-through (**Figure 2C**), and Sa V329, which did not show any change in the flow-through (**Figure 2C**), exhibited evidence of phage propagation in the biofilm. Therefore, it appears that part of the phage population may be trapped within the extracellular matrix and does not diffuse easily through the biofilm. Alternatively, there may be phage inactivation during diffusion of the phage suspension across the biofilm and subsequent phage propagation in the biofilm. Regarding Sa RN450, whose susceptibility to phiIPLA-RODI is similar to that of Sa IPLA15, the results were more variable than for the other strains and, when taken together, did not give indication of a significant propagation in the biofilm. Conversely, the insensitive strains Lp 55-1 and Se F12 displayed a lower phage titer (1-2 log units) in the biofilm than in the inoculum. Therefore, phage phiIPLA-RODI titers for

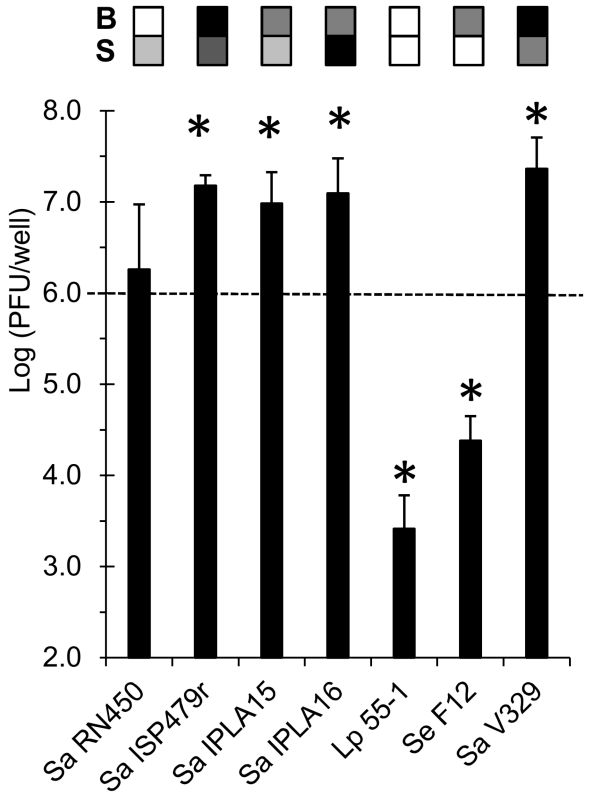

FIGURE 4 | Phage titer in the extracellular matrix of biofilms formed by the different bacterial strains treated with 10^6 PFU/ml of phage phiIPLA-RODI after incubation for 24 h at 37°C. The values represent the average and standard deviation of the PFUs per well obtained for at least three replicates. These values were compared to the inoculum (PFU/well) and *P*-values < 0.05 were considered significant (*). The grid on top of each bar represents the biofilm strength (B) and susceptibility (S) of each strain in a color-coded manner. For biofilm strength, black, gray, and white represent strong, intermediate and weak biofilm formation. Susceptibility is represented in a scale that goes from white (non-susceptible strains) to black (most susceptible strain for a given phage).

these two strains are low in both the biofilm matrix and the flow-through. This result suggests inactivation of a significant part of the initial phage population, although the specific mechanisms involved remain to be elucidated. Interestingly, regression analysis of the values obtained for phage entrapped in the biofilm matrix compared to the phage titer in the flow-through for the same samples did not show a high correlation unless the data point corresponding to strain Sa IPLA 15 was taken out (**Supplementary Figure S6**). Indeed, R^2 was 0.445 when all strains were considered, but increased up to $R^2 = 0.7966$ if Sa IPLA15 was taken out of the analysis.

Inactivation of Phage phiIPLA-RODI by Bacterial Supernatants

The significant depletion in active viral particles in most biofilms formed by *L. plantarum* 55-1, either alone or as part of mixed cultures, suggested that this bacterium might somehow inactivate the phage. On the other hand, data obtained thus far suggests that

TABLE 3 | Survival of phiIPLA-RODI after incubation with bacterial supernatants.

Bacterial strain	TSBG*	TSB*
Control	$1.27 \times 10^6 \pm 6.11 \times 10^4$ (pH = 7)	$1.46 \times 10^6 \pm 4.91 \times 10^5$ (pH = 7)
Lp 55-1	<10 (#) (pH = 4)	$1.31 \times 10^6 \pm 2.08 \times 10^4$ (pH = 5)
Se F12	$1.75 \times 10^5 \pm 7.63 \times 10^4$ (#) (pH = 5)	$1.91 \times 10^6 \pm 3.87 \times 10^5$ (pH = 6)

**Phage titer (PFU/ml) following incubation for 3 h at 37°C of a phage suspension in medium (control) or in supernatants of overnight liquid cultures of different bacterial strains. Values represent the average and standard deviation of three replicates. Values obtained with treated samples were compared to the control and P-values < 0.05 were considered significant (#). The pH of the different supernatants prior to the experiment is indicated in brackets.*

strain Se F12 also inactivates phiIPLA-RODI, although perhaps through a different mechanism. To explore these hypotheses, phage inactivation by supernatants of these two strains was examined. The experiment was performed with supernatants from overnight cultures of the two bacteria grown in TSBG (medium used for biofilm formation) and TSB (medium used for phage treatment step). Our results were different depending on the culture medium used. Thus, when bacteria were grown in TSB there were no significant changes in phage survival compared to the medium control (**Table 3**). In contrast, supernatants from cultures grown in TSB supplemented with 0.25% glucose (TSBG) led to a significant loss in phage viability after incubation at 37°C for 3 h (**Table 3**). Indeed, following incubation with the supernatant from strain Lp 55-1, the phage titer of the phage suspension was below the detection level (<10). In contrast, a significant but lesser degree of inactivation (about 1 log unit) was observed for strain Se F12.

Besides phage inactivation, we examined the pH of the different supernatants. When grown in TSBG, *L. plantarum* and *S. epidermidis* acidified the medium to pH values of 4 and 5, respectively. These values were exactly the same as those observed in the flow-through for Lp 55-1 and Se F12 when performing the phage-penetration experiments after the biofilm-formation step in TSBG. In contrast, the pH of cultures grown in TSB was 5 and 6 for *L. plantarum* and *S. epidermidis*, respectively. These values were exactly the same as those observed in the flow-through for Lp 55-1 and Se F12 when performing the phage-penetration experiments after the phage treatment step in TSB. Taking these results into consideration, it does not appear that lowering of the pH during phage treatment is fully responsible for the decrease in phage titer observed for biofilms of Lp 55-1 and Se F12. Perhaps, additional factors such as production of extracellular enzymes also play a role in phage inactivation.

DISCUSSION

Bacterial cells are most frequently organized in structured multicellular communities, biofilms, in which they can withstand environmental sources of stress that would easily kill them in the planktonic state. Indeed, one of the most challenging problems in bacterial contamination control is precisely biofilm eradication. Virulent bacteriophages are currently being considered as promising antibiofilm agents thanks to their ability to infect and lyse bacterial cells (Pires et al., 2017). However, the development of phage-based antimicrobial products aimed for biofilm removal requires careful consideration of several aspects of phage-host interactions within biofilms (Fernández et al., 2018a,b). One of the properties that must be explored is the ability of the phage to penetrate the tight-knit network of bacterial cells and matrix polymers that form these complex communities. This study describes the development of a new method that facilitates the analysis of phage diffusion as well as the potential factors affecting the ability of the virus to move across the biofilm. This technique is based on the use of transwell plates, which allow separating two chambers by a polycarbonate membrane. Coincidentally, a recent article used these plates to demonstrate that bacteriophages can move across human cell layers by transcytosis (Nguyen et al., 2017). So far, studies on the diffusion of bacteriophages through bacterial biofilms are scarce. For example, Briandet et al. (2008) analyzed diffusion of lactococcal phage c2 across biofilms formed by susceptible and non-susceptible strains by fluorescence correlation spectroscopy. This study found that the phage could diffuse across biofilms formed by the insensitive strain, *Stenotrophomonas maltophilia*, as well as a sensitive and a resistant strain of *Lactococcus lactis*. In both lactococcal strains, however, phage particles appeared to be immobile, suggesting binding to cell surface receptors. More recently, a computer simulation framework indicated that phage mobility may have an impact on phage-host interactions within the biofilm structure (Simmons et al., 2017).

One of the main target microorganisms of phage therapy research is the human pathogen *S. aureus*. Some strains of this bacterium have become resistant to a wide range of antimicrobials, including some of the last resort drugs currently used in the clinic. To make matters worse, this microbe can form biofilms on inert surfaces or human tissues and persist, thereby increasing danger of contamination as well as hindering infection treatment. Several studies have demonstrated that phages can be an option for treating staphylococcal infections, including those involving biofilms (Son et al., 2010; Kelly et al., 2012; Chhibber et al., 2013; Mendes et al., 2013; Seth et al., 2013; Drilling et al., 2014; Gutiérrez et al., 2015). The two bacteriophages selected for this analysis, phiIPLA-RODI and phiIPLA-C1C, have been isolated from sewage treatment plant samples and exhibit antibiofilm potential (Gutiérrez et al., 2015). In order to evaluate the factors affecting penetration into and propagation inside the biofilm, several strains were selected to represent varying biofilm-forming abilities and phage susceptibility profiles. Once established the bacterial strains and phages used to set up the model, penetration of phage suspensions through different monospecies biofilms was tested. These phage suspensions were prepared to represent a high ($\sim 10^9$ PFU/ml) or low ($\sim 10^6$ PFU/ml) viral concentration. The results from these experiments confirmed that the phage could effectively diffuse through all the different biofilms tested at both concentrations, although the phage titer determined in the flow-through varied for different bacterial strains. Analysis of these changes suggests that the phenotype that has a greater effect on the net phage

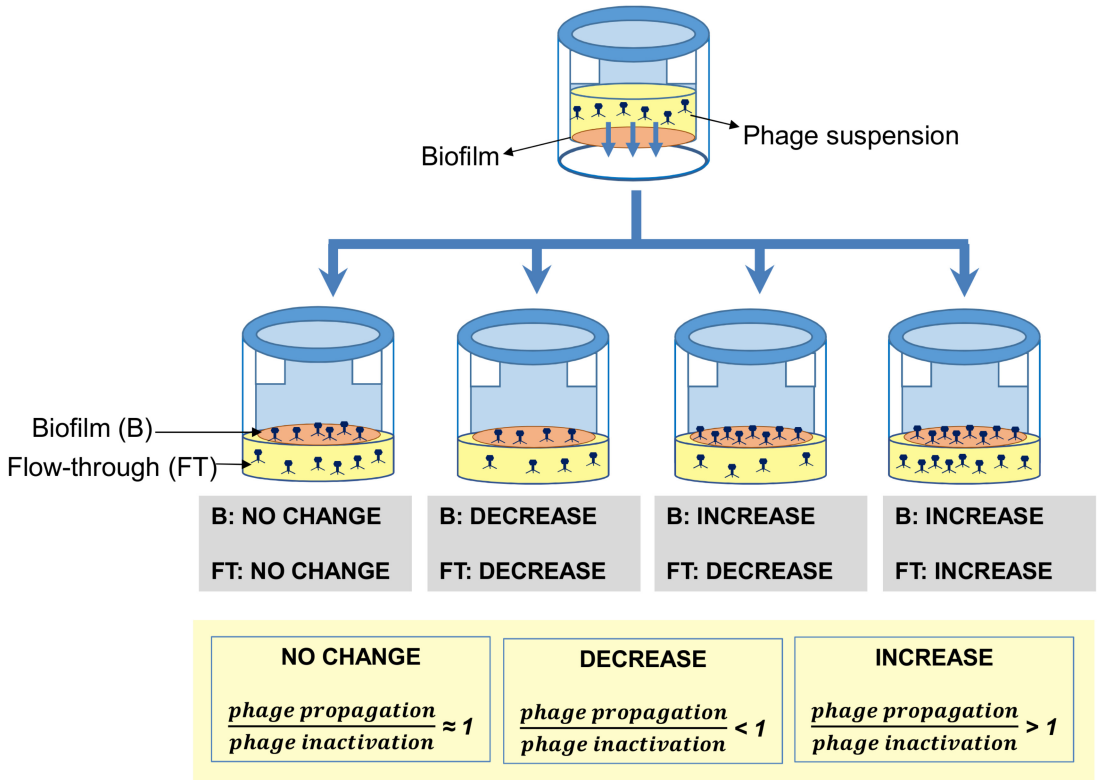

FIGURE 5 | Schematic representation of the different outcomes observed when preformed biofilms formed by different strains were treated with phage phiIPLA-RODI. In the biofilm, these results represent the overall balance between phage propagation and phage inactivation due to enzymatic activity or irreversible binding to the extracellular matrix or cell debris. In the flow-through, besides the aforementioned factors, net diffusion across the biofilm also contributes to the final outcome.

titer after diffusion through the biofilm is phage susceptibility of the strain forming the biofilm. Indeed, a correlation between susceptibility and phage titer was observed for phiIPLA-RODI at both concentrations tested and low concentrations of phiIPLA-C1C. Perhaps, this is partly due to the ability of the phage, especially at high doses, to kill susceptible cells and potentially disrupt the biofilm structure or its ability to cross the biofilm by propagating "from cell to cell" instead of having to move through the extracellular matrix. However, in some cases, the best correlation was obtained when both susceptibility and biofilm formation were taken into account, which indicates that the strength of the biofilm may also affect phage penetration across the structure. Nonetheless, the complex and varied architecture of bacterial biofilms, as observed in this study, are also likely to play a role in the ability of the bacteriophages to move across the biofilm, with the virus potentially taking advantage of thinner areas, especially in thick highly structured biofilms. Indeed, this would be an interesting topic to examine further in subsequent studies.

The subsequent studies performed with phage phiIPLA-RODI provided a closer look at the interaction between this phage and different bacterial biofilms. Thus, when mixed-strain biofilms were challenged with a low concentration of phiIPLA-RODI, the results were quite varied and, sometimes, unexpected. For example, *L. plantarum* 55-1 and *S. epidermidis* F12 exhibited a similar behavior when forming monospecies biofilms, reducing the phage titer by approximately 2 log units. However, biofilms formed by different *S. aureus* strains with *L. plantarum* 55-1 always led to a lower phage titer in the flow-through than in the control. In contrast, mixed biofilms of *S. aureus* strains with *S. epidermidis* F12 did not decrease phage titer. This suggested that the mechanisms by which these two species decrease the number of phage particles in the flow-through may be different and display different interactions with the phage propagation/phage inactivation dynamics of *S. aureus* strains. This hypothesis seems even more likely in view of the fact that filtered supernatants of *L. plantarum* appear to inactivate phiIPLA-RODI, whereas those of *S. epidermidis* F12 reduced but did not eliminate the phage below the detection level. More research is, nevertheless, necessary to explore the mechanism that leads to a decrease in the number of viable phage particles in the latter strain. Interestingly, a previous study had shown that phiIPLA-RODI propagation in biofilms formed by *S. aureus* IPLA16 with *L. plantarum* 55-1 was lower than in biofilms formed with *Lactobacillus pentosus* (González et al., 2017). This may also be a consequence of phage inactivation in the presence of *L. plantarum* but not *L. pentosus*. Additionally, analysis of the viable phage particles trapped in the extracellular matrix of

different biofilms showed interesting results. For instance, strains *S. epidermidis* F12 and *L. plantarum* 55-1 did not appear to have retained a high proportion of the viral particles within the matrix. This suggests that the low titer in the flow-through may be due to inactivation of the phage in the biofilms formed by these two strains. However, further research is necessary to establish the specific mechanism involved in this inactivation, which may involve enzymatic degradation or irreversible binding of the phage to cell debris or matrix components. Another interesting detail is the fact that the biofilm matrix of *S. aureus* IPLA 15 and *S. aureus* V329 exhibit a higher phage titer than that expected from the levels observed in the flow-through. As mentioned above, this may be related to differences in biofilm architecture or composition of the extracellular matrix. Of note, *S. aureus* V329 is the only strain analyzed that has a protein-based extracellular matrix. With regard to *S. aureus* IPLA15, a previous study suggested that exposure to subinhibitory levels of phage phiIPLA-RODI led to accumulation of extracellular DNA in the biofilm (Fernández et al., 2017).

Taking into account all these results, it can be concluded that the outcome of phage penetration across biofilms is the result of the net balance between phage propagation and phage inactivation in the biofilm, as well as phage penetration and diffusion into the biofilm (**Figure 5**). These processes will largely depend on the bacterial strains forming the biofilm on the basis of different properties. For instance, phage susceptibility of the strains in the biofilm will determine the propagation rate of the phage inside the biofilm. Conversely, entrapment of the phage particles may depend on the composition of the biofilm matrix or the bacterial cell surface. Finally, production of phage-inactivating enzymes and/or lowering of the pH by a bacterial strain in the community may have a deleterious effect on the phage population that cannot be overcome by phage propagation.

In conclusion, this study describes a new technique for the analysis of phage-bacteria interactions within biofilms and shows an example of its potential. Indeed, application of this protocol to staphylophages has revealed interesting aspects of phage-host interplay in biofilms that will be useful for the development of phage-based products aimed at the elimination of staphylococcal biofilms. In general, it seems that the two phages tested here can diffuse through biofilms formed by strains with different degrees of susceptibility and biofilm-forming abilities. This highlights the viability of phage-based biocontrol of bacterial biofilms. However, net diffusion depends on several factors, including phage concentration, biofilm-forming capability, susceptibility to the phage, phage inactivation and, potentially, changes in biofilm structure as a response to phage predation. As a result, all these conditions need to be evaluated to design the adequate composition of a phage-based product, especially in terms of phage concentration and addition of compounds that can inhibit undesired effects like phage inactivation in the biofilms. Furthermore, this technique provides a new tool for decrypting the complex dynamics of phage infection inside sessile microbial communities. Given that biofilms are the most widespread mode of bacterial growth in nature and that bacteriophages are very numerous, these interactions are bound to have an impact on the structure and physiology of microbial communities in natural environments.

AUTHOR CONTRIBUTIONS

SG, LF, AR, and PG conceived and designed the experiments and analyzed the data. SG, LF, and AC performed the experiments. SG, LF, DG, AR, and PG wrote the paper.

FUNDING

This study was funded by grants AGL2015-65673-R (Ministry of Science and Innovation, Spain), EU ANIWHA ERA-NET (BLAAT ID: 67)/PCIN-2017-001 (Ministry of Economy, Industry and Competitiveness, Spain), Proyecto Intramural CSIC 201770E016, GRUPIN14-139 (Program of Science, Technology and Innovation 2013–2017 and FEDER EU funds, Principado de Asturias, Spain). PG and AR are members of the bacteriophage network FAGOMA II and The FWO Vlaanderen funded "Phagebiotics" research community (WO.016.14). The funders had no role in study design, data collection and interpretation, or the decision to submit the work for publication.

SUPPLEMENTARY MATERIAL

The Supplementary Material for this article can be found online at: https://www.frontiersin.org/articles/10.3389/fmicb.2018.02348/full#supplementary-material

REFERENCES

Abedon, S. T., García, P., Mullany, P., and Aminov, R. (2017). Editorial: phage therapy: past, present and future. *Front. Microbiol.* 8:981. doi: 10.3389/fmicb.2017.00981

Anderl, J. N., Franklin, M. J., and Stewart, P. S. (2000). Role of antibiotic penetration limitation in *Klebsiella pneumoniae* biofilm resistance to ampicillin and ciprofloxacin. *Antimicrob. Agents Chemother.* 44, 1818–1824.

Briandet, R., Lacroix-Gueu, P., Renault, M., Lecart, S., Meylheuc, T., Bidnenko, E., et al. (2008). Fluorescence correlation spectroscopy to study diffusion and reaction of bacteriophages inside biofilms. *Appl. Environ. Microbiol.* 74, 2135–2143. doi: 10.1128/AEM.02304-07

Chhibber, S., Kaur, T., and Sandeep, K. (2013). Co-therapy using lytic bacteriophage and linezolid: effective treatment in eliminating methicillin resistant *Staphylococcus aureus* (MRSA) from diabetic foot infections. *PLoS One* 8:e56022. doi: 10.1371/journal.pone.0056022

Clinical Laboratory Standards Institute (2015). *Methods for Dilution Antimicrobial Susceptibility tests for Bacteria that Grow Aerobically. CLSI Approved Standard M07-A10*. Wayne, PA: Clinical and Laboratory Standards Institute.

Cucarella, C., Solano, C., Valle, J., Amorena, B., Lasa, Í, and Penadés, J. R. (2001). Bap, a *Staphylococcus aureus* surface protein involved in biofilm formation. *J. Bacteriol.* 183, 2888–2896.

de la Fuente-Núñez, C., Reffuveille, F., Fernández, L., and Hancock, R. E. (2013). Bacterial biofilm development as a multicellular adaptation: antibiotic

resistance and new therapeutic strategies. *Curr. Opin. Microbiol.* 16, 580–589. doi: 10.1016/j.mib.2013.06.013

Delgado, S., Arroyo, R., Jiménez, E., Marín, M. L., del Campo, R., Fernández, L., et al. (2009). *Staphylococcus epidermidis* strains isolated from breast milk of women suffering infectious mastitis: potential virulence traits and resistance to antibiotics. *BMC Microbiol.* 9:82. doi: 10.1186/1471-2180-9-82

Drilling, A., Morales, S., Jardeleza, C., Vreugde, S., Speck, P., and Wormald, P. J. (2014). Bacteriophage reduces biofilm of *Staphylococcus aureus* ex vivo isolates from chronic rhinosinusitis patients. *Am. J. Rhinol. Allergy* 28, 3–11. doi: 10.2500/ajra.2014.28.4001

EFSA. (2012). Scientific opinion on the evaluation of the safety and efficacy of ListexTM P100 for the removal of *Listeria monocytogenes* surface contamination of raw fish. *EFSA J.* 10:2615.

Fernández, L., González, S., Campelo, A. B., Martínez, B., Rodríguez, A., and García, P. (2017). Low-level predation by lytic phage phiIPLA-RODI promotes biofilm formation and triggers the stringent response in *Staphylococcus aureus*. *Sci. Rep.* 7:40965. doi: 10.1038/srep40965

Fernández, L., Gutiérrez, D., Rodríguez, A., and García, P. (2018a). Application of bacteriophages in the agro-food sector: a long way toward approval. *Front. Cell. Infect. Microbiol.* 8:296. doi: 10.3389/fcimb.2018.00296

Fernández, L., Rodríguez, A., and García, P. (2018b). Phage or foe: an insight into the impact of viral predation on microbial communities. *ISME J.* 12, 1171–1179. doi: 10.1038/s41396-018-0049-5

González, S., Fernández, L., Campelo, A. B., Gutiérrez, D., Martínez, B., Rodríguez, A., et al. (2017). The behavior of *Staphylococcus aureus* dual-species biofilms treated with bacteriophage phiIPLA-RODI depends on the accompanying microorganism. *Appl. Environ. Microbiol.* 8:e02821-16. doi: 10.1128/AEM.02821-16

Gutiérrez, D., Delgado, S., Vázquez-Sánchez, D., Martínez, B., Cabo, M. L., Rodríguez, A., et al. (2012). Incidence of *Staphylococcus aureus* and analysis of associated bacterial communities on food industry surfaces. *Appl. Environ. Microbiol.* 78, 8547–8554. doi: 10.1128/AEM.02045-12

Gutiérrez, D., Martinez, B., Rodriguez, A., and Garcia, P. (2010). Isolation and characterization of bacteriophages infecting *Staphylococcus epidermidis*. *Curr. Microbiol.* 61, 601–608. doi: 10.1007/s00284-010-9659-5

Gutiérrez, D., Rodríguez-Rubio, L., Martínez, B., Rodríguez, A., and García, P. (2016). Bacteriophages as weapons against bacterial biofilms in the food industry. *Front. Microbiol.* 7:825. doi: 10.3389/fmicb.2016.00825

Gutiérrez, D., Ruas-Madiedo, P., Martínez, B., Rodríguez, A., and García, P. (2014). Effective removal of staphylococcal biofilms by the endolysin LysH5. *PLoS One* 9:e107307. doi: 10.1371/journal.pone.0107307

Gutiérrez, D., Vandenheuvel, D., Martínez, B., Rodríguez, A., Lavigne, R., and García, P. (2015). Two phages, phiIPLA-RODI and phiIPLA-C1C, lyse mono- and dual-species staphylococcal biofilms. *Appl. Environ. Microbiol.* 81, 3336–3348. doi: 10.1128/AEM.03560-14

Kelly, D., McAuliffe, O., Ross, R. P., and Coffey, A. (2012). Prevention of *Staphylococcus aureus* biofilm formation and reduction in established biofilm density using a combination of phage K and modified derivatives. *Lett. Appl. Microbiol.* 54, 286–291. doi: 10.1111/j.1472-765X.2012.03205.x

Mendes, J. J., Leandro, C., Corte-Real, S., Barbosa, R., Cavaco-Silva, P., Melo-Cristino, J., et al. (2013). Wound healing potential of topical bacteriophage therapy on diabetic cutaneous wounds. *Wound Repair Regen.* 21, 595–603. doi: 10.1111/wrr.12056

Nguyen, S., Baker, K., Padman, B. S., Patwa, R., Dunstan, R. A., Weston, T. A., et al. (2017). Bacteriophage transcytosis provides a mechanism to cross epithelial cell layers. *mBio* 8:e1874-17. doi: 10.1128/mBio.01874-17

Nobrega, F. L., Costa, A. R., Kluskens, L. D., and Azeredo, J. (2015). Revisiting phage therapy: new applications for old resources. *Trends Microbiol.* 23, 185–191. doi: 10.1016/j.tim.2015.01.006

Novick, R. (1967). Properties of a cryptic high-frequency transducing phage in *Staphylococcus aureus*. *Virology* 33, 155–166.

O'Flaherty, S., Ross, R. P., and Coffey, A. (2009). Bacteriophage and their lysins for elimination of infectious bacteria. *FEMS Microbiol. Rev.* 33, 801–819. doi: 10.1111/j.1574-6976.2009.00176.x

Otto, M. (2013). Staphylococcal infections: mechanisms of biofilm maturation and detachment as critical determinants of pathogenicity. *Annu. Rev. Med.* 64, 175–188. doi: 10.1146/annurev-med-042711-140023

Pires, D. P., Melo, L., Vilas Boas, D., Sillankorva, S., and Azeredo, J. (2017). Phage therapy as an alternative or complementary strategy to prevent and control biofilm-related infections. *Curr. Opin. Microbiol.* 39, 48–56. doi: 10.1016/j.mib.2017.09.004

Potera, C. (1999). Forging a link between biofilms and disease. *Science* 283, 1837–1839.

Ruiz-Barba, J. L., Cathcart, D. P., Warner, P. J., and Jimenez-Diaz, R. (1994). Use of Lactobacillus plantarum LPCO10, a bacteriocin producer, as a starter culture in Spanish-style green olive fermentations. *Appl. Environ. Microbiol.* 60, 2059–2064.

Seth, A. K., Geringer, M. R., Nguyen, K. T., Agnew, S. P., Dumanian, Z., Galiano, R. D., et al. (2013). Bacteriophage therapy for *Staphylococcus aureus* biofilm-infected wounds: a new approach to chronic wound care. *Plast. Reconstr. Surg.* 131, 225–234. doi: 10.1097/PRS.0b013e31827e47cd

Simmons, M., Drescher, K., Nadell, C. D., and Bucci, V. (2017). Phage mobility is a core determinant of phage-bacteria coexistence in biofilms. *ISME J.* 12, 531–543. doi: 10.1038/ismej.2017.190

Singh, R., Ray, P., Das, A., and Sharma, M. (2010). Penetration of antibiotics through *Staphylococcus aureus* and *Staphylococcus epidermidis* biofilms. *J. Antimicrob. Chemother.* 65, 1955–1958. doi: 10.1093/jac/dkq257

Son, J. S., Lee, S. J., Jun, S. Y., Yoon, S. J., Kang, S. H., Paik, H. R., et al. (2010). Antibacterial and biofilm removal activity of a podoviridae *Staphylococcus aureus* bacteriophage SAP-2 and a derived recombinant cell-wall-degrading enzyme. *Appl. Microbiol. Biotechnol.* 86, 1439–1449. doi: 10.1007/s00253-009-2386-9

Toledo-Arana, A., Merino, N., Vergara-Irigaray, M., Debarbouille, M., Penades, J. R., and Lasa, I. (2005). *Staphylococcus aureus* develops an alternative, ica-independent biofilm in the absence of the arlRS two-component system. *J. Bacteriol.* 187, 5318–5329.

Conflict of Interest Statement: The authors declare that the research was conducted in the absence of any commercial or financial relationships that could be construed as a potential conflict of interest.

Capítulo 2

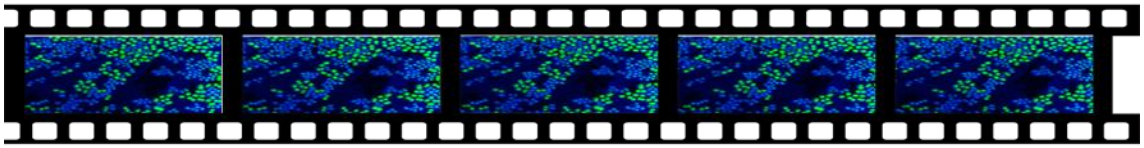

Capitulo 2: Influencia de los bacteriófagos en la formación de biofilms

Generalmente, las poblaciones bacterianas en el medio ambiente están formando biofilms sujetos a un cierto nivel de depredación por fagos, lo que permite a ambos tipos de microorganismos convivir en un equilibrio estable. Cuando ese equilibrio se desplaza como consecuencia del uso de fagos como antimicrobianos, la mayoría de las bacterias son eliminadas, pero se conoce muy poco del efecto que ese hecho puede tener en el resto de la población bacteriana. Por ello, en esta Tesis se ha querido mostrar la respuesta de los biofilms de *S. aureus* formados en presencia de una dosis no letal del fago phiIPLA-RODI. Además, se ha estudiado el impacto que tiene la presencia de profagos, insertados en el genoma bacteriano, en la fisiología de las células sésiles de *S. aureus.*

1. Fernández, L., González, S., Campelo, A. B., Martínez, B., Rodríguez, A., & García, P. (2017). Low-level predation by lytic phage phiIPLA-RODI promotes biofilm formation and triggers the stringent response in *Staphylococcus aureus*. *Scientific reports*, 7, 40965. https://doi.org/10.1038/srep40965

2. Fernández, L., González, S., Quiles-Puchalt, N., Gutiérrez, D., Penadés, JR., García, P and Rodríguez, A. (2018). Lysogenization of *Staphylococcus aureus* RN450 by phages φ11 and φ80α leads to the activation of the SigB regulon. Scientific Reports. 8:12662. https://doi.org/10.1038/s41598-018-31107-z

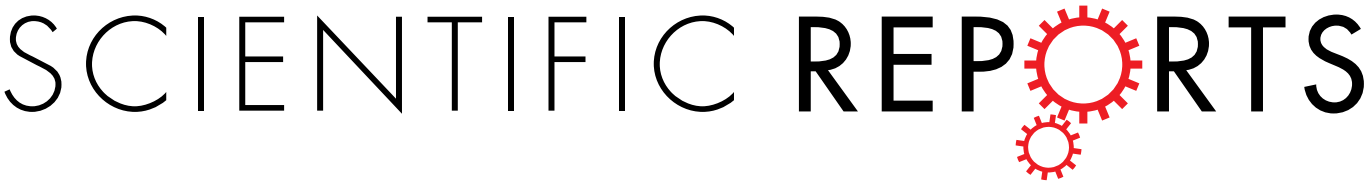

OPEN

Received: 23 August 2016
Accepted: 13 December 2016
Published: 19 January 2017

Low-level predation by lytic phage phiIPLA-RODI promotes biofilm formation and triggers the stringent response in *Staphylococcus aureus*

Lucía Fernández, Silvia González, Ana Belén Campelo, Beatriz Martínez, Ana Rodríguez & Pilar García

An important lesson from the war on pathogenic bacteria has been the need to understand the physiological responses and evolution of natural microbial communities. Bacterial populations in the environment are generally forming biofilms subject to some level of phage predation. These multicellular communities are notoriously resistant to antimicrobials and, consequently, very difficult to eradicate. This has sparked the search for new therapeutic alternatives, including phage therapy. This study demonstrates that *S. aureus* biofilms formed in the presence of a non-lethal dose of phage phiIPLA-RODI exhibit a unique physiological state that could potentially benefit both the host and the predator. Thus, biofilms formed under phage pressure are thicker and have a greater DNA content. Also, the virus-infected biofilm displayed major transcriptional differences compared to an untreated control. Significantly, RNA-seq data revealed activation of the stringent response, which could slow down the advance of the bacteriophage within the biofilm. The end result would be an equilibrium that would help bacterial cells to withstand environmental challenges, while maintaining a reservoir of sensitive bacterial cells available to the phage upon reactivation of the dormant carrier population.

The arms race between bacteriophages and their bacterial hosts is a major evolutionary driving force in the microbial world[1,2]. It is now widely recognized that phage predation contributes significantly to shaping bacterial communities[3,4]. For instance, bacteriophages can favor growth of certain species or strains in a given ecosystem, as well as facilitate DNA exchange between bacterial cells. Also, exposure to phages may lead to transcriptional changes in the prey population[5–9]. As a result, attaining a better understanding of the dynamics between bacteria and phages is of the utmost importance from an ecological perspective. Furthermore, this information would be valuable to design improved strategies for the control of undesired microorganisms. However, the currently available information regarding bacteria-phage interactions is still somewhat limited[2]. In addition to their environmental significance, bacteriophages are also promising therapeutics. Indeed, phage therapy has recently regained attention given the relentless rise in the resistance of pathogenic bacteria to more conventional antimicrobials[10]. Bacteriophages have been used in some Eastern European countries like Russia and Georgia for decades[11], but the costs necessary to comply with regulatory burdens have probably hindered their use in Western medicine. Interestingly, numerous studies indicate that phages can help to eliminate biofilms[12–14], which are an important challenge for antibacterial strategies due to their high resistance. Moreover, some authors indicate that phages are able to lyse biofilm-embedded bacteria even when they have become resistant to antibiotics[15].

Biofilms represent the most ubiquitous mode of bacterial growth in natural and artificial environments[16,17]. In the clinic, biofilms can develop on surfaces and implant devices as well as on living tissues, being a major problem in chronic recalcitrant infections. The opportunistic Gram-positive pathogen *Staphylococcus aureus* is a good example of an adept biofilm former[18]. Indeed, this bacterium does not only form biofilms in hospital settings, but also in the food industry. As a result, elimination of this pathogen by routine disinfection procedures can

Instituto de Productos Lácteos de Asturias (IPLA-CSIC), Paseo Río Linares s/n 33300, Villaviciosa, Asturias, Spain. Correspondence and requests for materials should be addressed to L.F. (email: lucia.fernandez@ipla.csic.es)

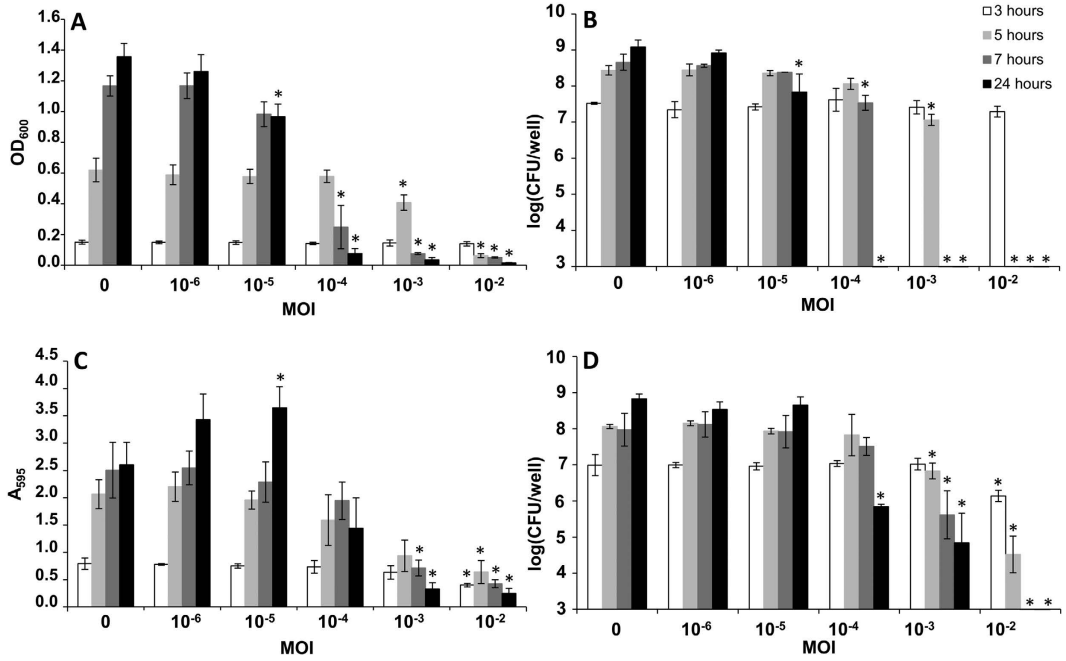

Figure 1. Biofilm formation and planktonic growth of *S. aureus* IPLA 1 in the presence of different MOIs of bacteriophage phiIPLA-RODI. (**A**) Planktonic growth measured as OD_{600}. (**B**) Viable cell numbers per well present in the planktonic phase. (**C**) Adhered biomass determined as absorbance at 595 nm (A_{595}) following crystal violet staining. (**D**) Viable cell numbers per well in the adhered phase (biofilm). All values represent the average and standard deviation of three independent biological repeats. Data obtained in the presence of different phage concentrations were compared to the control samples taken at the same time point. *P*-values < 0.05 were considered significant (*). Bars missing correspond to bacterial counts below the detection limit (10 CFU/well).

be quite difficult. In food environments, this further allows for the accumulation of enterotoxins produced by *S. aureus* and subsequent contamination of foodstuffs. In *S. aureus* biofilms, the cells are embedded in an extracellular matrix consisting of polysaccharides, proteins and extracellular DNA (eDNA), although the proportion of these components depends on the specific strain and growth conditions[18]. Besides their biofilm-forming capacity, some *S. aureus* strains are resistant to most antibiotics available today. Of particular relevance are the so-called methicillin-resistant *S. aureus* (MRSA) and vancomycin-resistant *S. aureus* (VRSA) strains[19]. There are several studies demonstrating the successful utilization of bacteriophages against *S. aureus*[20–22]. For example, the lytic phage vB_SauM_phiIPLA-RODI (phiIPLA-RODI), belonging to the *Myoviridae* family, has been recently isolated from sewage samples and has shown promising results for the disruption of staphylococcal biofilms[21].

The aim of this study was to characterize the physiological properties and transcriptional profile of *S. aureus* biofilm cells exposed to phage phiIPLA-RODI. The results presented here show that low-level exposure to phages can create a biofilm-enhancing environment that protects *S. aureus* cells from complete eradication. Furthermore, cells within phage-containing biofilms show a distinct expression pattern that indicates activation of the stringent response. To our knowledge, this is the first transcriptomic analysis of phage-infected biofilm cells. Bacteriophage pressure in sessile communities is common place not only in nature, but also in man-made environments, including surfaces in hospitals and the food industry. Also very importantly, the information provided here can help to predict possible scenarios that may occur following the application of phage therapy if the viral dose does not completely eradicate the biofilm.

Results

Biofilm formation is enhanced by infection with sub-inhibitory doses of phiIPLA-RODI. In order to study the effect of phage exposure on biofilm formation, we first followed bacterial growth in both the planktonic and the adhered phase in the presence of increasing multiplicities of infection (MOIs, 10^{-6} to 10^{-2}) of the lytic bacteriophage phiIPLA-RODI. *S. aureus* IPLA 1, a strain of dairy origin, was chosen for these experiments due to its sensitivity to this phage and because it exhibits a medium-level biofilm forming capacity. This facilitated the observation of changes in adhered biomass by crystal violet staining.

At all the MOIs tested, bacterial growth in the planktonic phase was equal to the non-infected control until three hours post-infection, reaching OD_{600} values of approximately 0.16 (Fig. 1A). Two hours later, the samples infected with an MOI of 10^{-2} showed a considerable reduction in OD_{600} (Fig. 1A) and there were no remaining viable cells (Fig. 1B). This indicates the occurrence of cell lysis due to the phage. The same occurred at MOIs 10^{-3} and 10^{-4} at 7 and 24 hours post-infection, respectively. In contrast, viable cells could be detected at all time points for the lower MOIs tested, namely 10^{-5} and 10^{-6}. However, a one-log reduction was observed in the planktonic phase of the 24-hour biofilm grown with an MOI of 10^{-5} compared to the control without phage. Regarding the adhered phase (biofilm), there were some major differences compared to the results observed for the planktonic

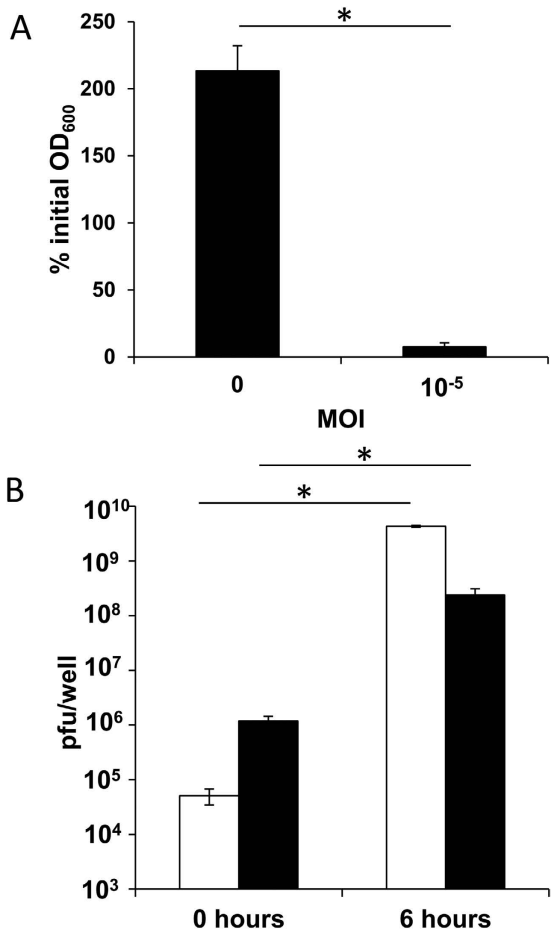

Figure 2. Evolution of cell density and phage titer after disaggregation of 24-hour biofilms of *S. aureus* IPLA 1 formed in the absence or presence of phiIPLA-RODI. (**A**) Percentage of the initial OD_{600} after 6 hours of incubation for biofilms grown without phage or in the presence of phage at an MOI of 10^{-5}. (**B**) Phage titer determined before and after 6 hours of incubation at 37 °C in biofilms formed in the presence of phiIPLA-RODI at an MOI of 10^{-5}. White and black bars correspond to phage titer of the matrix and the adhered cells, respectively. Values represent the average and standard deviation of 3 independent biological repeats. *P-values < 0.05.

phase. Interestingly, biomass quantification by crystal violet staining revealed a significant (P-value = 0.003) increase in biofilm formation after 24 hours of incubation in the sample inoculated with an MOI of 10^{-5} (Fig. 1C). Additionally, at the 24-hour time point, viable cells could be observed even at an MOI of 10^{-3} and there was no significant (P-value = 0.107) decrease in cell counts at an MOI of 10^{-5} (Fig. 1D). Biofilm formation in the presence of an MOI of 10^{-3} was also monitored by confocal laser scanning microscopy. Timing of bacterial growth and cell lysis by phiIPLA-RODI confirmed the observations described above (Supplementary video S1).

Considering the data gathered at the 24-hour time point, the minimum inhibitory MOI was determined to be 10^{-3} (10^3 PFU/well), whereas the minimum bactericidal MOI was 10^{-2} (10^4 PFU/well).

All subsequent experiments aimed at characterizing biofilms grown under phage predation were performed at an MOI of 10^{-5} (10 PFU/well). These conditions were selected because there was no major reduction in viable cell numbers, which would alter the expression of the quorum sensing regulon. This would, in turn, mask transcriptional changes specifically due to attack by the phage. Moreover, we intended on studying more in depth the characteristics of the enhanced biofilm formed in the presence of this low viral dose.

Disaggregation of phage-containing biofilms leads to generalized cell lysis. Before continuing the analysis of phage-treated biofilms, it was necessary to confirm that cells remained sensitive to phiIPLA-RODI. To do that, adhered cells were taken from the control and the infected biofilms and subsequently resuspended in fresh TSB-g medium. Cell density was measured as OD_{600} before and after incubation for 6 hours at 37 °C. At the end of the experiment, OD_{600} values had doubled in the control sample, whereas cell density was drastically reduced, by more than 90%, in the sample corresponding to the phage-infected biofilm (Fig. 2A). This demonstrated that the cells in the treated biofilm were susceptible to phage infection, resulting in cell lysis. Consequently, differences between the treated and the control samples would not be due to the selection of phage resistant mutants.

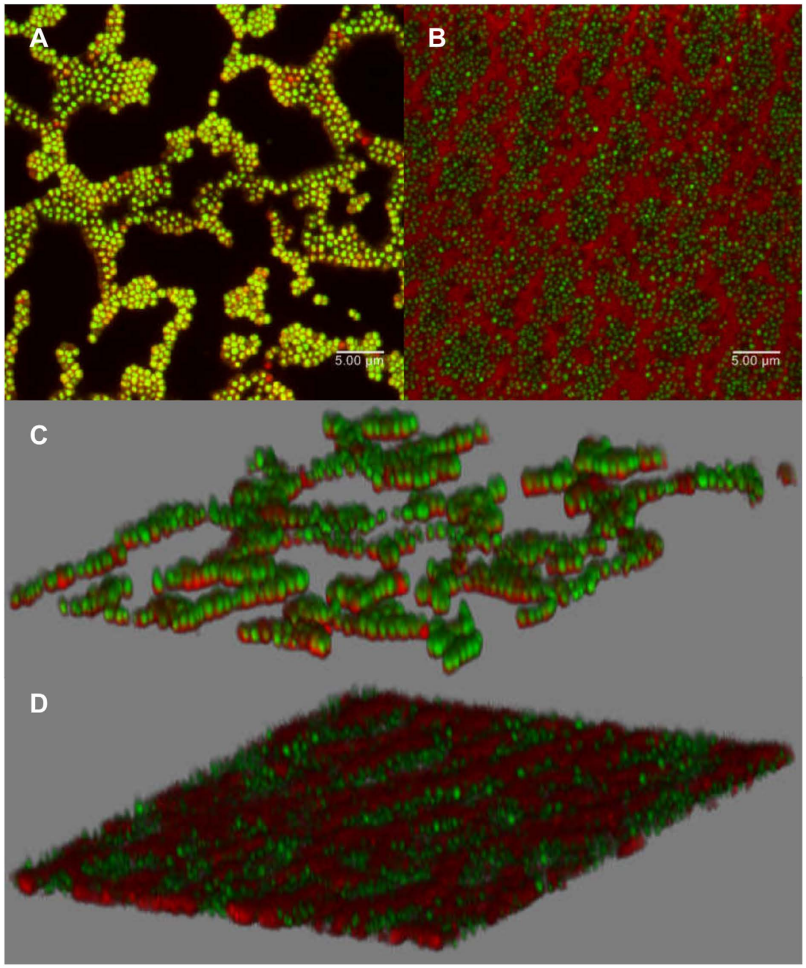

Figure 3. Confocal laser scanning microscopy images showing 24-hour biofilms formed in the presence or not of phiIPLA-RODI at an MOI of 10^{-5}. (**A** and **C**) untreated IPLA 1 biofilm. (**B** and **D**) IPLA1 biofilm formed with phage. Samples were stained with SYTO® 9 and PI. Green represents live cells and red represents dead cells or eDNA.

Additionally, the number of plaque-forming units (PFU) associated to cells or free in the extracellular matrix was determined before and after the 6-hour incubation of the infected sample. The total phage count at time point 0 was 10^6 PFU/well, which is a considerable increase from the starting inoculum of 10 PFU/well (Fig. 2B). It is noteworthy that the majority of the viral particles were associated to cells and not free in the extracellular matrix. In the postincubation sample, most infecting particles were free in the supernatant while only about 1% was cell-associated. This result is to be expected given the high level of lysis observed. Also, the total phage titer at the end of the experiment was 4×10^9 PFU/well, which demonstrates that there was propagation and not just lysis of the already infected cells (Fig. 2B). These results suggest that the viable cell counts corresponding to the treated biofilms may actually represent the number of cells not infected by the phage. In addition to these, the biofilm community would consist of a small but significant subset of viral carrier cells that would restart the lytic cycle upon reactivation.

Biofilms formed in the presence of subinhibitory MOIs of phiIPLA-RODI exhibit structural changes. Confocal laser scanning microscopy (CLSM) was used to further study the differences between 24-hour biofilms grown without phage predation and in the presence of a subinhibitory MOI of 10^{-5}. After incubation, the adhered cells were stained with SYTO® 9 and propidium iodide (PI) to distinguish between live cells (green), and damaged cells or eDNA (red). The control sample showed a typical "island-like" structure composed of different layers, in which most damaged cells (red) were located near the bottom (Fig. 3A and C). In contrast, the sample developed in the presence of phiIPLA-RODI exhibited a remarkably different architecture. Thus, cells covered a greater surface of the glass well, but seemed to be organized in a flatter structure (Fig. 3B and D). Also, a red net-like pattern surrounding the cells could be observed, which would very likely correspond to eDNA. Nevertheless, the increased abundance of eDNA in the treated versus the control biofilms remained to be confirmed.

Based on the observations made by microscopy, the next step was to demonstrate that bacteriophage-infected biofilms were richer in eDNA. First, the DNA present in the extracellular matrix was obtained from biofilms

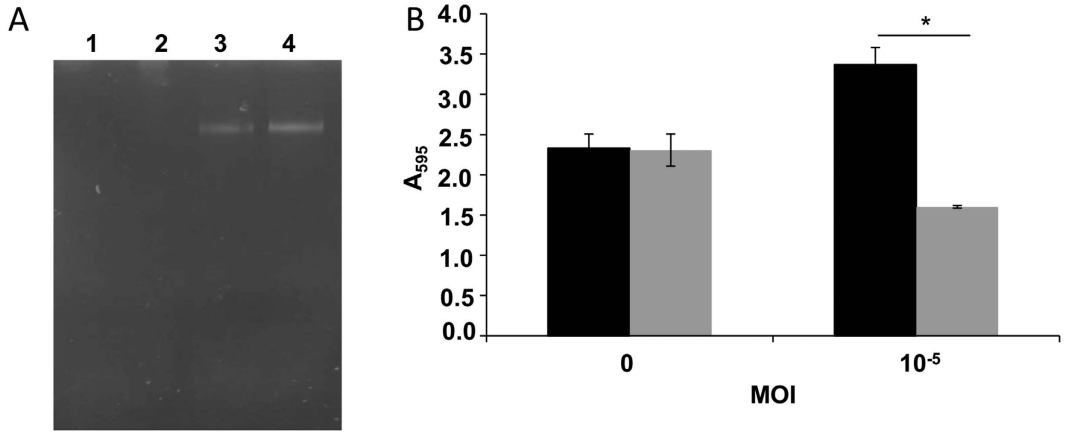

Figure 4. Comparison of eDNA content between untreated biofilms and those formed in the presence of low phage concentrations. (**A**) Agarose gel visualization of eDNA prepared from untreated biofilms (lanes 1 and 2) and biofilms formed in the presence of phiIPLA-RODI (MOI of 10^{-5}) (lanes 3 and 4). (**B**) DNAse treatment of 24 hour-biofilms developed without phage or with an MOI of 10^{-5}. Black and grey bars represent biofilms incubated without or with 200 μg/ml DNAse I for one hour at 37 °C. Values represent the average and standard deviation of four independent biological replicates. *P-values < 0.05.

subject to low phage predation and non-treated controls. Agarose gel electrophoresis of these samples showed that those biofilms developed in the presence of phiIPLA-RODI contained more DNA than control biofilms of *S. aureus* IPLA 1 (Fig. 4A). Additionally, biofilms formed under phage predation were more sensitive to DNAse treatment than their non-infected counterparts (Fig. 4B). Indeed, the biomass of control biofilms hardly changed during a 2-hour DNAse treatment. In contrast, the biomass of the phage-containing biofilm was reduced to approximately 47%. These results demonstrate that the biofilms formed under low-phage predation have a different extracellular matrix, containing a greater proportion of eDNA. These biofilms seem to be more stable and better withstand the washing steps of crystal violet staining, resulting in increased attached biomass.

The *S. aureus* IPLA 1 biofilm population exhibits a distinct transcriptional profile under low-level phage predation. Given the phenotypical differences observed between the infected and uninfected biofilms, it appeared important to discern if they also displayed distinct transcriptional profiles. To determine if that was the case, the transcriptome of 24-hour biofilms formed in the presence or absence of a low dose of phiIPLA-RODI (10 PFU/well, corresponding to an MOI of 10^{-5}) was analysed through RNA-seq. Transcripts were then aligned with the *S. aureus* NCTC 8325 and phage phiIPLA-RODI genomes. In the control sample, 99% of sequences aligned with *S. aureus* NCTC8325 (Fig. 5A). However, only 51% aligned with the *S. aureus* reference genome in the bacteriophage-treated samples, with an additional 47% mapping to phiIPLA-RODI sequences (Fig. 5A).

Regarding bacteriophage gene expression, further analysis revealed that the genes showing the highest expression were located within the morphogenesis module (Fig. 5B, Table S1). Nonetheless, significant transcription was also observed for genes involved in lysis and replication/transcription (Fig. 5B, Table S1). These results were not surprising as the biofilm is not reflective of a synchronized infection. Therefore, it would be expected to harvest the infected cells at different stages of phage development. Also, in a previous study performed on *Lactococcus lactis*, a similar transcriptional profile was observed for phages Tuc2009 and c2 at late stages of the lytic cycle[5].

Regarding *S. aureus* genes, a total of 1063 transcripts showed significant changes (adjusted P-values < 0.01) between the two samples, of which 548 were downregulated and 515 were upregulated in the infected biofilms (Table S2). Interestingly, a subset of these genes indicated activation of the stringent response. Indeed, 76 genes (Table 1) showed the same regulation pattern observed in microarray analyses of the stringent response regulon performed by Anderson *et al.*[23] and Reiß *et al.*[24]. For instance, the bifunctional (p)ppGpp synthase and hydrolase RSH-encoding gene, a homolog of *relA*/*spoT*, is upregulated 4.9-fold. Another (p)ppGpp synthase gene, *relP*, was also upregulated by 2.21-fold in the phage-treated sample. This synthase, however, is not usually part of the stringent response and is induced by cell wall targeting antimicrobials[25]. The stringent response is typically triggered by amino acid starvation and tends to inhibit protein synthesis and promote amino acid biosynthesis. Other known triggers of this response are osmotic stress, carbon source starvation and depletion of fatty acids. The alarmone (p)ppGpp has been shown to participate in diverse processes such as biofilm development, sporulation, entry in the stationary phase and persistence, as well as virulence, particularly during chronic infections, and tolerance to antimicrobials[26–29].

Amongst the genes typically regulated by (p)ppGpp also worth mentioning are those encoding ribosomal proteins, which were downregulated (between 2- and 3-fold) in the phage-treated sample. Many genes encoding other proteins involved in the translation machinery were also downregulated, including several tRNA synthase-encoding genes (*lysS*, *metG*, *pheS*, *aspS*, *valS*) and the translation initiation factor-encoding gene *infB*. However, other genes coding for tRNA synthases were upregulated, namely *argS*, *trpS* and *tyrS*. Regarding

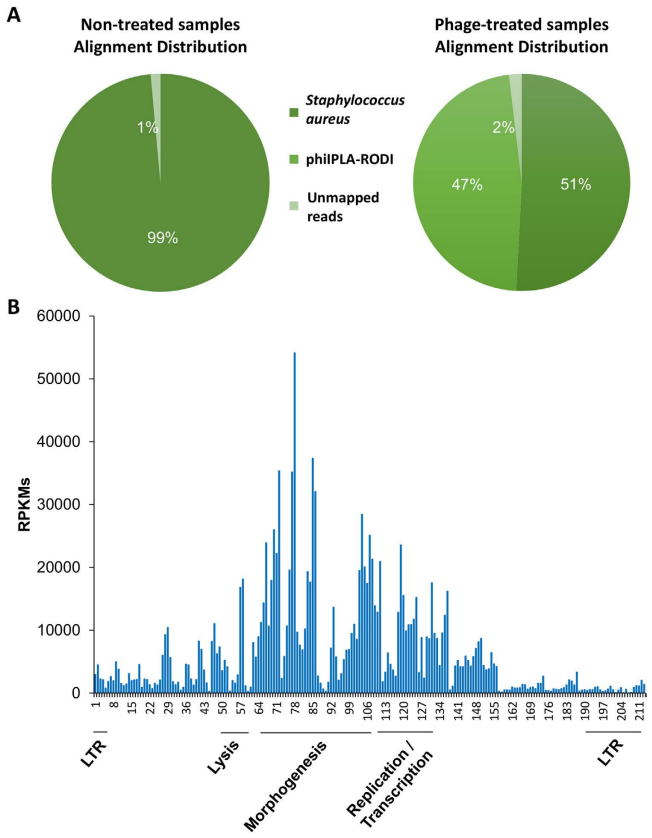

Figure 5. Transcriptomic analysis by RNA-seq of biofilms exposed to phiIPLA-RODI compared to untreated controls. (**A**) Average alignment distribution of three biological repeats of samples untreated or treated with phage phiIPLA-RODI. (**B**) normalized mean reads per kilobase million (RPKM) values corresponding to the different open reading frames (ORFs) of phiIPLA-RODI genome in the treated samples.

aminoacid metabolism genes, most showed increased expression (*dapB*, *hom*, *hisC*, *asd*, *hisZ*), while others were repressed (*arcC2*, *argF*, *arcA*). For instance, *asd*, the gene encoding the aspartate-semialdehyde dehydrogenase was upregulated by 4.3-fold. This enzyme participates in the biosynthesis of lysine, methionine, leucine and isoleucine from aspartate. Another product of this pathway is diaminopimelate, which is essential for bacterial cell wall formation. Further overlaps with the stringent response regulon included genes coding for proteins involved in energy metabolism such as ATP synthetase (*atpB*, *atpC*, *atpD*, *atpE*, *atpG*) and quinol oxidase (*qoxA-D*) subunits.

Interestingly, the gene encoding the major autolysin AtlA was upregulated by 5.42-fold. Also sortase A-encoding gene *srtA* was induced 2.95-fold. These two genes overlapped with the stringent response microarrays, confirming that they are part of the (p)ppGpp regulon in *S. aureus* IPLA 1. AtlA participates in cell wall metabolism, while SrtA participates in the processing of surface proteins. There were other changes in genes affecting cell wall synthesis and metabolism. For instance, several genes related to biosynthesis of peptidoglycan were downregulated (*glmM*, *glmU* and *glmS*). In contrast, some capsule-related genes were slightly upregulated, as were genes involved in D-alanylation of teichoic acids (*dltA*, *dltB* and *dltC*). In *S. aureus*, D-alanylation of teichoic acids plays an important role in adherence and, as a result, contributes to the initial stages of biofilm formation. Indeed, strains harboring mutations in the *dlt* operon cannot attach to surfaces or form biofilms[30]. The *dlt* operon can be induced by cations or cationic antimicrobial peptides, vancomycin and clindamycin[31,32]. D-alanylation also increases the net positive charge of the cell surface, thereby reducing the inhibition of autolysins (positively charged) by binding to the negatively charged teichoic acids[33]. Moreover, D-alanylation of teichoic acids has been related to phage resistance[34]. Interestingly, genes involved in restriction-modification, another known antiphage system, were also upregulated. The upregulation of mechanisms that give protection from bacteriophage infection may be a response of bacterial cells to the attack by the virus. In turn, it may be a competition strategy of the invading phage to prevent further infection by other viruses.

Regarding genes involved in nucleotide metabolism, most of the upregulated genes participate in purine biosynthesis (*purC*, *purl*, *purB*, *purH*, *purM*, *purQ*), while most of the downregulated genes are involved in the synthesis of pyrimidines (*pyrR*, *pyrC*, *pyrE*, *pyrF*). Interestingly, a similar trend was observed by Corrigan *et al.*[35] in the transcriptomic analysis of *S. aureus gdpD* mutants. This mutation leads to the accumulation of c-di-AMP, whose signaling pathway exhibits cross talk with (p)ppGpp. Indeed, *gdpP* mutants show increased (p)ppGpp levels and, in turn, (p)ppGpp is known to inhibit GdpP in a dose-dependent manner[35]. Several genes involved in DNA repair were downregulated (*recU*, *recF*, *recO*) except *mutS* and *mutL*, which were induced. A similar trend

Gene ID	Gene name	Gene product	FC
SAOUHSC_00005	*gyrB*	DNA gyrase subunit B	−2.89
SAOUHSC_00006	*gyrA*	DNA gyrase subunit A	−3.92
SAOUHSC_00121		Capsular polysaccharide synthesis enzyme O-acetyl transferase Cap5H, putative	2.03
SAOUHSC_00187	*pflB*	Formate acetyltransferase	−4.57
SAOUHSC_00188	*pflA*	Pyruvate formate-lyase-activating enzyme	−5.52
SAOUHSC_00350	*rpsR*	30 S ribosomal protein S18	−2.69
SAOUHSC_00471	*glmU*	Bifunctional protein GlmU	−2.73
SAOUHSC_00474	*rplY*	50 S ribosomal protein L25	−2.06
SAOUHSC_00528	*rpsG*	30 S ribosomal protein S7	−2.07
SAOUHSC_00733	*hisC*	Histidinol-phosphate aminotransferase	3.53
SAOUHSC_00780	*uvrA*	UvrABC system protein A	−2.07
SAOUHSC_00796	*pgk*	Phosphoglycerate kinase	−2.90
SAOUHSC_00797	*tpiA*	Triosephosphate isomerase	−3.32
SAOUHSC_00799	*eno*	Enolase	−4.31
SAOUHSC_00802		Carboxylesterase, putative	−2.11
SAOUHSC_00818	*nuc*	Thermonuclease	5.72
SAOUHSC_00933	*trpS*	Tryptophan–tRNA ligase	2.25
SAOUHSC_00994	*atl*	Bifunctional autolysin	5.42
SAOUHSC_01002	*qoxA*	Probable quinol oxidase subunit 2	−2.54
SAOUHSC_01092	*pheS*	Phenylalanine–tRNA ligase alpha subunit	−2.04
SAOUHSC_01093	*pheT*	Phenylalanine–tRNA ligase beta subunit	−3.45
SAOUHSC_01164	*pyrR*	Bifunctional protein PyrR	−2.25
SAOUHSC_01168	*pyrC*	Dihydroorotase	−4.79
SAOUHSC_01207	*ffh*	Signal recognition particle protein	−2.50
SAOUHSC_01216	*sucC*	Succinyl-CoA ligase [ADP-forming] subunit beta	−2.80
SAOUHSC_01247	*rbfA*	Ribosome-binding factor A	−4.19
SAOUHSC_01276	*glpK*	Glycerol kinase	−2.56
SAOUHSC_01320	*hom*	Homoserine dehydrogenase	3.25
SAOUHSC_01395	*asd*	Aspartate-semialdehyde dehydrogenase	4.35
SAOUHSC_01396	*dapA*	4-hydroxy-tetrahydrodipicolinate synthase	4.40
SAOUHSC_01397	*dapB*	4-hydroxy-tetrahydrodipicolinate reductase	2.81
SAOUHSC_01466	*recU*	Holliday junction resolvase RecU	−3.02
SAOUHSC_01504		Ferredoxin, putative	−3.37
SAOUHSC_01585	*srrB*	Sensor protein SrrB	−3.29
SAOUHSC_01586	*srrA*	Transcriptional regulatory protein SrrA	−5.06
SAOUHSC_01601		Alpha-glucosidase, putative	−2.76
SAOUHSC_01668	*era*	GTPase Era	−2.96
SAOUHSC_01681	*prmA*	Ribosomal protein L11 methyltransferase	−13.21
SAOUHSC_01715	*udk*	Uridine kinase	−2.38
SAOUHSC_01737	*aspS*	Aspartate–tRNA ligase	−2.95
SAOUHSC_01742	*rsh*	GTP pyrophosphokinase	4.91
SAOUHSC_01755	*rpmA*	50 S ribosomal protein L27	−3.58
SAOUHSC_01767	*valS*	Valine–tRNA ligase	−3.46
SAOUHSC_01771	*hemL1*	Glutamate-1-semialdehyde 2,1-aminomutase 1	−2.90
SAOUHSC_01772	*hemB*	Delta-aminolevulinic acid dehydratase	−2.71
SAOUHSC_01776	*hemA*	Glutamyl-tRNA reductase	−2.06
SAOUHSC_01784	*rplT*	50 S ribosomal protein L20	−2.31
SAOUHSC_01818	*ald2*	Alanine dehydrogenase 2	−2.89
SAOUHSC_01886	*ribH*	6,7-dimethyl-8-ribityllumazine synthase	−10.04
SAOUHSC_01887	*ribBA*	Riboflavin biosynthesis protein	−7.35
SAOUHSC_01889	*ribD*	Riboflavin biosynthesis protein	−4.03
SAOUHSC_01961	*hemH*	Ferrochelatase	−2.32
SAOUHSC_01972	*prsA*	Foldase protein PrsA	−3.26
SAOUHSC_02254	*groEL*	60 kDa chaperonin	−4.48
SAOUHSC_02340	*atpC*	ATP synthase epsilon chain	−2.87

Continued

Gene ID	Gene name	Gene product	FC
SAOUHSC_02341	*atpD*	ATP synthase subunit beta	−2.87
SAOUHSC_02349	*atpE*	ATP synthase subunit c	−2.38
SAOUHSC_02350	*atpB*	ATP synthase subunit a	−2.31
SAOUHSC_02477	*rpsI*	30 S ribosomal protein S9	−2.08
SAOUHSC_02505	*rplP*	50 S ribosomal protein L16	−2.02
SAOUHSC_02506	*rpsC*	30 S ribosomal protein S3	−2.11
SAOUHSC_02509	*rplB*	50 S ribosomal protein L2	−2.72
SAOUHSC_02510	*rplW*	50 S ribosomal protein L23	−2.71
SAOUHSC_02511	*rplD*	50 S ribosomal protein L4	−2.65
SAOUHSC_02536	*moaA*	Cyclic pyranopterin monophosphate synthase	−2.81
SAOUHSC_02537	*mobA*	Probable molybdenum cofactor guanylyltransferase	−3.16
SAOUHSC_02635	*tcaA*	Membrane-associated protein TcaA	−2.32
SAOUHSC_02669	*sarZ*	HTH-type transcriptional regulator SarZ	4.75
SAOUHSC_02696	*fmhA*	FmhA protein	2.68
SAOUHSC_02834	*srtA*	Sortase	2.95
SAOUHSC_02850	*cidB*	Holin-like protein CidB	−2.28
SAOUHSC_02965	*arcC2*	Carbamate kinase 2	−6.75
SAOUHSC_02969	*arcA*	Arginine deiminase	−5.89
SAOUHSC_03002	*zwf*	Poly-beta-1,6-N-acetyl-D-glucosamine synthase	3.16
SAOUHSC_03002	*icaA*	Poly-beta-1,6-N-acetyl-D-glucosamine synthase	3.16
SAOUHSC_03055	*rpmH*	50 S ribosomal protein L34	−3.07

Table 1. List of genes related to the stringent response that are dysregulated in biofilms treated with subinhibitory doses of phiIPLA-RODI compared to untreated biofilms according to RNA-seq.

was observed for genes involved in cell division and DNA replication, which were largely downregulated (*gyrA*, *gyrB*, *dinB*), although *parE*, which encodes DNA topoisomerase 4 subunit B was upregulated.

Also remarkable was the downregulation of genes encoding intracellular proteases (including *clpB*, *clpC*, *clpL* and *clpX*) and chaperones (*dnaK*, *dnaJ*, *groEL*, *grpE* and foldase *prsA*). In fact, *clpB* displayed the most pronounced change in gene expression, being downregulated by 112-fold. Many of these proteins are part of the heat shock response regulon and participate in refolding or degradation of misfolded or defective proteins. In contrast to *S. aureus*, infection of *E. coli* by phage PRD1 activates the heat shock regulon[6]. Nonetheless, it seems clear that stress responses are generally affected by bacteriophage infection.

Genes related to virulence and adhesion were also dysregulated. For instance, *icaA* was upregulated by 3-fold, whereas genes coding for lipase, gamma hemolysin, aureolysin, and delta hemolysin (*hld*) were downregulated. In contrast, *nuc*, encoding a thermonuclease, was induced by nearly 6-fold. In addition to *hld*, genes *agrA* and *agrC* were also downregulated. The staphyloxanthin biosynthesis operon (*crtNMQPO*) was upregulated between 2- and 5-fold. This carotenoid pigment gives certain *S. aureus* strains their characteristic golden color, and protects the microbe from the reactive oxygen species produced by the immune system. There were also changes in the expression of many genes involved in transport. In particular, a large number of genes encoding small molecule transporters were upregulated, although others were downregulated.

Exposure to phage phiIPLA-RODI had a dramatic impact on the expression of transcriptional regulators, some of which were induced (*sarZ*, *lytR*) and some were repressed (*ctsR*, *vraR*, *rot*, *sarV*). It is worth noting that *sigA* was downregulated while the stress sigma factor *sigB* was upregulated.

Dysregulation of selected genes identified in the RNA-seq analysis was confirmed by RT-qPCR (Table 2).

Subinhibitory mupirocin increases resistance of *S. aureus* IPLA 1 to phage phiIPLA-RODI but not biofilm formation. As mentioned above, the phage-infected biofilm displayed an upregulation of the stringent response. Indeed, at least 7% of the genes identified by RNA-seq analysis belong to this regulon. For that reason, it seemed interesting to study whether this subset of genes played a role in phage resistance or increased biofilm formation. A common method to induce this response *in vitro* is exposure to the antibiotic mupirocin. To determine if the stringent response could be a defense mechanism against phage infection, we investigated the existence of synergism or antagonism between exposure to mupirocin and phage phiIPLA-RODI by the checkerboard assay. The presence of the phage at subinhibitory concentrations did not alter the mupirocin MIC (0.06 μg/ml). In contrast, low mupirocin concentrations led to a higher phage MIC. Thus, mupirocin concentrations corresponding to 1/16 × MIC led to a 10-fold increase in the MIC to phiIPLA-RODI that went from 5×10^4 PFU/ml to 5×10^5 PFU/ml. With higher concentrations of mupirocin (1/8, 1/4 and 1/2 of the MIC) sensitivity to the phage was reduced by 100-fold (MIC = 5×10^6 PFU/ml). These results can give us some hints about the possible role of the stringent response induced by phage infection. On the one hand, it could mean that phage proliferation inside the bacterial cell triggers a response that would prevent superinfection or infection by other phages. It could also be due to the bacterium responding to prevent the virus from killing the cell. Within the context of bacteriophage therapy, it seems that treatment under conditions that minimize the activation of the stringent response may also lead to more effective biofilm elimination.

Gene	Gene product	FC (RT-qPCR)	FC (RNA-seq)
atl	Bifunctional autolysin	31.92 ± 18.84	5.42
rsh	GTP pyrophosphokinase	33.90 ± 17.22	4.91
relP	GTP pyrophosphokinase	23.54 ± 8.95	2.21
clpC	ATP-dependent Clp protease, ATP-binding subunit	−4.96 ± 0.99	−22.97
clpB	ATP-dependent Clp protease, ATP-binding subunit	−28.03 ± 9.39	−112.83
crtP	Diapolycopene oxygenase	25.59 ± 14.78	3.34
dltA	D-alanine—poly(phosphoribitol) ligase subunit 1	20.21 ± 11.85	3.69
sigB	RNA polymerase sigma factor	16.13 ± 5.73	2.56
nuc	Thermonuclease	19.20 ± 11.24	5.72
icaA	Poly-beta-1,6-N-acetyl-D-glucosamine synthase	4.06 ± 0.76	3.16

Table 2. Confirmation by RT-qPCR of the dysregulation for selected genes identified by RNA-seq analysis.

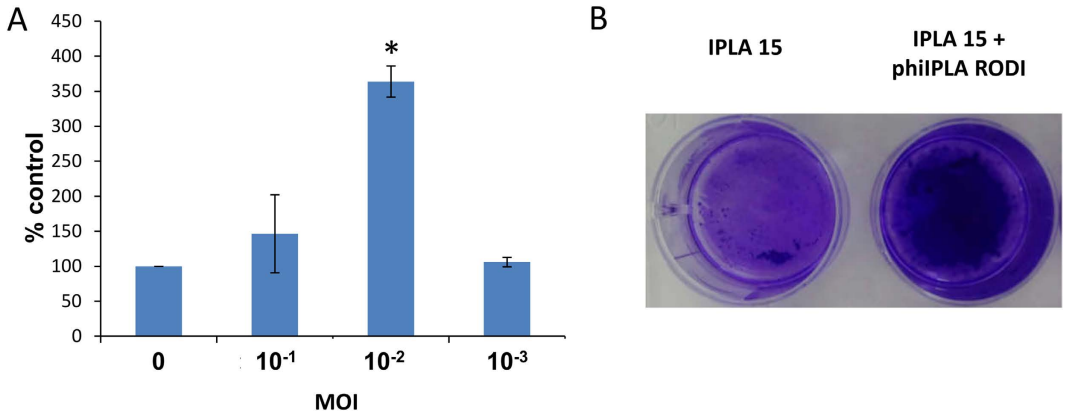

Figure 6. Effect of subinhibitory phage concentration on biofilm formation of strain *S. aureus* IPLA 15. (**A**) Adhered biomass of *S. aureus* IPLA 15 in the presence of different MOIs of phage phiIPLA-RODI after 24 hours of incubation at 37 °C determined by crystal violet staining and shown as percentage of the untreated control. Data correspond to the average and standard deviation of four independent biological replicates. The values obtained for each phage concentration were compared to the control grown without phage and *P*-values < 0.05 (*) were considered significant. (**B**) Photograph showing the crystal violet-stained biofilm formed by IPLA 15 in the absence (left) or presence (right) of phiIPLA-RODI at an MOI of 10^{-2}.

Interestingly, exposure to subinhibitory concentrations of mupirocin did not promote biofilm formation (data not shown). This suggests that upregulation of the stringent response is not the major cause of the increased adhered biomass observed in the presence of phiIPLA-RODI. Nevertheless, it cannot be ruled out that the greater expression of the major autolysin AtlA due to activation of the stringent response can have an additive effect with phage lysis and potentiate the accumulation of eDNA in the extracellular matrix. Indeed, previous reports have demonstrated the importance of autolysins in *S. epidermidis* and *S. aureus* for attachment and formation of DNA-rich biofilms[36,37].

Higher MOIs of phiIPLA-RODI can also enhance biofilm formation in more resistant strains. The study of biofilms formed by *S. aureus* IPLA 1 cells exposed to a lytic phage revealed notable changes in the bacterial population. Nevertheless, it would be very interesting to test whether this phenomenon can occur in other *S. aureus* strains, in particular strains with a lesser sensitivity to phiIPLA-RODI infection. Strain *S. aureus* IPLA 15 was isolated from the meat industry and is, like IPLA 1, a medium-level biofilm former. However, this strain is 1000 times more resistant to phiIPLA-RODI, as observed by minimum inhibitory concentration (MIC) determination (MIC was 10^6 PFU/well, which corresponds to an MOI of 1). The effect of subinhibitory phage MOIs on biofilm formation by IPLA 15 was analyzed. These experiments showed a 3.6-fold increase in biofilm formation at an MOI of 10^{-2}, which is 1000× higher than the MOI leading to the maximum increase in strain IPLA1 (Fig. 6). This seems to indicate that the biofilm-promoting effect by the phage requires a certain degree of infection of the host strain.

Discussion

It is becoming increasingly evident that understanding the dynamics of natural bacterial populations might hold the key to controlling them for our benefit. A good example is the need to overcome the growing problem of antimicrobial resistance. To do that, it is first essential to attain a greater knowledge about the physiological state of bacterial cells when they are exposed to antibiotics or disinfectants[38,39]. In this study, we have attempted the

characterization of *S. aureus* cells in a biofilm exposed to a lytic phage. Biofilms are known to be the most common mode of bacterial growth not only in nature, but also in many man-made environments[16,17]. In the case of this pathogen, there are two main relevant settings, namely the clinic and the food industry, and in both biofilm formation contributes to the persistence and antimicrobial resistance of *S. aureus*[40]. The consequence of this is a greater risk for human health. Another characteristic of natural populations is their interplay with bacteriophages[3]. These viruses can infect and sometimes kill bacterial cells and constitute the most abundant "organisms" on the planet. Additionally, the utilization of phages as antimicrobial weapons is gaining attention in recent years[10]. Experience with antibiotic therapy has shown that the more we understand the effects of antimicrobials at low doses, the more we can prevent undesirable consequences or maximize their efficacy[41]. Phage therapy should be no exception. Within this context, our results could be taken both as a dissection of a real-life microbial population subject to phage predation, as much as a potential result of treatment with bacteriophages at doses that do not lead to complete eradication of the target cells. In both situations, transcriptional and physiological changes resulting from exposure to phages might affect sensitivity of the bacterial cells to antibiotics or disinfectants.

Overall, our results confirm the link between enhanced biofilm formation and lysogeny[42–44] or exposure to lytic phages at concentrations that do not eradicate the population[45,46]. In the case of lytic phages, a study by Hosseinidoust *et al.*[45] showed that phage predation induced biofilm formation in *P. aeruginosa*, *S. aureus* and *Salmonella enterica* serotype Typhimurium through undetermined non-evolutionary mechanisms. Regarding lysogenic phages, some authors have hypothesized that release of prophages could be important for the process of biofilm development in bacteria[47]. Indeed, there are many examples in which lysogeny leads to a greater biofilm formation[42,43]. Phage-promoted biofilms are also slightly different in composition, exhibiting a greater content in eDNA[43,44]. This DNA is likely a consequence of lysis by the phage, although the participation of increased autolytic activity cannot be ruled out. In that sense, the fact that phage infected biofilms of *S. aureus* showed increased expression of the gene encoding the major autolysin AtlA is very interesting. Further work should determine if this upregulation has an influence on the distinct biofilm structure displayed under low-level phage predation.

Thanks to the use of transcriptomic analyses, we have begun to understand the changes in the expression profile of cells subject to phage predation at different stages. Indeed, several recent studies have provided us with valuable information regarding gene expression of bacterial cells infected with lytic or lysogenic phages. Some examples are the articles about *P. aeruginosa*[8,9], *Yersinia enterocolitica*[48], *E. coli*[6] or *L. lactis*[5,7]. However, we still had no information on *S. aureus* and, also importantly, none of these studies had attempted transcriptional profiling of surface-attached populations. Biofilm communities are notoriously complex, which makes interpretation of transcriptional or proteomic analysis more difficult. It is particularly challenging to determine which subset of the population is responsible for the observed expression changes. Albeit not a perfect system, global transcriptomic analyses of biofilm communities still provide information about general population trends in gene expression, thereby providing a good starting point to comprehend the interplay between phages and bacteria inside a biofilm. Thus, once established gene expression trends in our *in vitro* model, it would be interesting to determine if the same genes are dysregulated during phage infection of other biofilm models. For instance, subsequent experiments should study models mimicking a catheter or animal infection or models resembling the biofilms formed on food industrial surfaces.

Some of the transcriptional changes observed here are similar to those found in other phage-host models. For example, infection of *L. lactis* with the lytic phage c2 resulted in the upregulation of genes involved in D-Ala modification of teichoic acids, as well as downregulation of genes involved in metabolism, DNA replication, transcription and translation[7]. Overall, this response seemed to lead to preservation of cellular energy. D-alanylation of teichoic acids alters the structure of the cell surface and affects multiple phenotypes, including increased phage resistance and adherence to surfaces. Ainsworth *et al.*[5] also studied transcriptional changes in *L. lactis* in response to lytic infection by phages Tuc2009 and c2. In that study, most host transcriptional changes were observed at late infection stages and were phage specific. Interestingly, infection with phage Tuc2009 induced transcription of genes involved in translation at 25 to 45 minutes post-infection, which might be linked to the high production of viral proteins at that stage. During c2 infection, there is an upregulation of amino acid biosynthesis genes and nitrogen metabolism. It does not seem that this change is due to nutrient depletion and the authors explain this phenomenon as a consequence of the intense bacteriophage protein synthesis, which may result in a temporary depletion of intracellular amino acids. Interestingly, host protein shut-off is known to occur in plant and animal cells upon viral infections[49,50]. In general, the responses observed in *L. lactis* as well as other species, like *E. coli*[6] and *P. aeruginosa*[8], involve very limited changes in gene expression, which affected mostly stress responses and occurred in late stages of the infection. In the study by Zhao *et al.*[8] there was downregulation of ribosomal protein genes and many transcriptional regulators. Amongst the few genes upregulated several were related to cell wall metabolism. Very interestingly, the article by Poranen *et al.*[6] on *E. coli* describes the upregulation of *spoT* at 30 minutes post infection with phage PRD1. Additionally, a recent study using a metabolomics approach detected that changes in the levels of (p)ppGpp were fairly common in the infection of *P. aeruginosa* with different phages[51]. This clearly suggests that albeit the stringent response is not always present upon phage infection, it is fairly widespread in different microbe-phage systems. In that sense, it is noteworthy that, in our model, induction of the stringent response by subinhibitory mupirocin increases resistance to phage infection. It would be very interesting to perform studies on other bacteria to assess if this is a more widespread phenomenon. Despite these similarities between the abovementioned studies and the model presented here, it must be noted that there are also notable differences. First, we have studied a biofilm model, whereas previous transcriptional analyses had been performed using liquid cultures, generally in the exponential phase. Also, we have used low-level phage pressure and allowed the host-phage system to reach equilibrium, whereas liquid culture assays were performed for relatively short incubation times and synchronized infection of the bacterial population was preferred.

Our results suggest that, under low phage predation, the *S. aureus* biofilm community can reach a certain level of infection then slow down the advance of the phage. Thus, the bacterial population can obtain the benefits

of a more stable thicker biofilm, which is protective against other external sources of stress. At the same time, activation of the stringent response would keep the proliferation of the phage under control to avoid complete eradication of the bacteria. Although this may seem counterintuitive, this situation would also have benefits for the bacteriophage as the biofilm would be a continuous reservoir of new virions and sensitive host cells. Indeed, extermination of the host would ultimately lead to disappearance of the predator. Therefore, under the conditions of the experiment, interactions between prey and predator would reach an equilibrium that is advantageous to both. Nevertheless, the specific details of this equilibrium still need to be determined in subsequent studies. For instance, it will be imperative to discern which of the observed changes correspond to non-infected cells and which are displayed by cells infected by the bacteriophage. Also, it is necessary to dissect which of the identified genes bear relevance towards the biofilm increase observed, as well as towards phage sensitivity. To do that, subsequent studies should analyse the effects of lack or overexpression of selected genes whose expression changed in response to phage predation. Here, we have identified a potential link between the stringent response and phage resistance. Nonetheless, this phenomenon requires further attention to determine the molecular mechanisms involved.

The information presented in this study can be very useful to develop new products that minimize the occurrence of undesired effects upon application of phage-containing antimicrobials against *S. aureus*. For instance, our results identified the main responses of *S. aureus* biofilm cells exposed to phage predation. Subsequent studies should aim to determine whether inhibition of these responses may enhance the use of phages as antimicrobials. Furthermore, antibiotics and disinfectants may be improved by taking into consideration the effect of bacteriophages in the target populations. As mentioned previously, natural populations might exhibit some similarities to our *in vitro* biofilm model. More specifically, biofilm communities in nature are likely subject to phage predation but not generally at a level that would lead to complete eradication of the bacterial population. Therefore, the trascriptome of such communities might share some trends with the ones observed here. With this in mind, it would be interesting to determine if biofilms developed under low-level phage predation exhibit different sensitivity to commonly used antibiotics or disinfectants. Ultimately, when it comes to fighting bacteria, knowledge is our best weapon.

Methods

Bacterial strains, bacteriophages and culture conditions. Two different *S. aureus* strains were used for this study, namely IPLA 1 and IPLA 15, which had been respectively isolated from samples taken in the dairy and meat industry[52]. *S. aureus* cultures were routinely grown in TSB (Tryptic Soy Broth, Scharlau, Barcelona, Spain) at 37 °C with shaking or on Baird-Parker agar plates (AppliChem, Germany). The lytic bacteriophage phiIPLA-RODI[21] was propagated on *S. aureus* IPLA 1 as previously described[21]. Mupirocin was purchased from Panreac Quimica SLU (Spain).

Biofilm formation assays. Biofilms were grown in 12-well microtiter plates (Thermo Scientific, NUNC, Madrid, Spain) according to the method described by Herrera *et al.*[53] with some modifications. Briefly, overnight cultures of *S. aureus* were diluted in TSBg (TSB supplemented with 0.25% w/v D-(+)-glucose) to obtain a cell suspension of 10^6 cfu/ml. 1 ml aliquots of this suspension were used to inoculate each well and then 1 ml of phage suspensions at different titers were added. 1 ml of TSBg was added to the control well. These microtiter plates were then incubated for 3, 5, 7 or 24 hours at 37 °C.

Following incubation during the desired time, the planktonic phase was removed and analyzed for OD_{600} and viable cell counts. The adhered phase was washed twice with phosphate-buffered saline (PBS) buffer (137 mM NaCl, 2.7 mM KCl, 10 mM Na_2HPO_4 and 2 mM KH_2PO_4; pH 7.4) and subsequently stained with crystal violet or scraped to determine viable cell counts.

Crystal violet staining was performed by adding 2 ml of 0.1% (w/v) crystal violet to each well. Following 15 minutes of incubation, the excess dye was removed by washing twice with water. The crystal violet attached to the well was distained with 2 ml of a 33% (v/v) solution of acetic acid and absorbance at 595 nm was quantified with a Bio-Rad Benchmark plus microplate spectrophotometer (Bio-Rad Laboratories, Hercules, CA, USA).

In order to count the adhered cells, each well was washed with PBS and subsequently scraped twice with sterile cotton swabs. Then these cells were resuspended by vigorously vortexing for 1 min as described previously[54]. Serial dilutions of the resulting suspension were then plated on TSA and incubated at 37 °C.

The minimum inhibitory MOI was considered to be the one in which no visible growth could be observed in the well after 24 hours of incubation at 37 °C. The minimum bactericidal MOI was determined to be the one in which no viable cells could be recovered following incubation for 24 hours.

Confocal microscopy. 24 hour-old biofilms were formed on 2-well μ-slides with a glass bottom (ibidi, USA) in the presence of phage phiIPLA-RODI or SM (negative control). After removing the planktonic phase, wells were washed with PBS and stained with Live/Dead® BacLight™ kit (Invitrogen AG, Basel, Switzerland). Samples were observed with a confocal scanning laser microscope (DMi8, Leica Microsystems) using a 100 × oil objective.

Anaysis of eDNA composition of biofilms. Recovery and visualization of eDNA from *S. aureus* biofilms was performed as described by Kaplan *et al.*[55]. Briefly, biofilms were formed in 12-well microtiter plates. After 24 hours, the planktonic phase was removed and the biofilm was washed once with PBS. 1 ml of TE buffer (10 mM Tris, 1 mM EDTA [pH 8]) was added and the adhered cells were scraped from the bottom of the well with a pipette tip. The cell suspension was transferred to a 1.5-ml tube and centrifuged at 13,000 rpm for 30 s. The supernatant was discarded and the pellets were resuspended in 200 μl of TE. After a second centrifugation step, 20 μl of the supernatant were loaded into a 1% agarose gel and subsequently stained with ethidium bromide.

Additionally, to compare the eDNA content of different biofilms, DNAse treatment was performed as previously described with some modifications[54]. Briefly, biofilms were preformed for 24 hours in 12-well microtiter plates. The planktonic phase was removed and the adhered cells were washed once with PBS. Then, 1 ml of 200 μg/ml DNAse in activity buffer (150 mM NaCl and 1 mM $CaCl_2$) or buffer alone were added to the wells. The microtiter plate was incubated for 1 hour at 37 °C. After that, the liquid was removed and biofilms were stained with crystal violet.

RNA purification. In order to perform the transcriptomic analysis, total RNA was isolated from *S. aureus* IPLA 1 biofilms grown with or without addition of bacteriophage at an MOI of 10^{-5}. Following 24 hours of incubation at 37 °C, the supernatant was removed and the adhered cells were washed with PBS and subsequently scraped with a 1-ml pipette tip in a solution containing 1 ml RNA protect (Qiagen) and 0.5 ml PBS. Cells were then incubated at room temperature for 5 minutes, pelleted at 5,000 × g for 10 min and stored at −80 °C until further processing. Samples were thawed and cells were lysed by mechanical disruption with a FastPrep®-24 in a solution of phenol-chloroform 1:1, glass beads (Sigma) and 80 mM DTT. RNA was isolated using the Illustra RNA spin Mini kit (GE Healthcare) and treated with Turbo DNAse (Ambion) to remove traces of genomic DNA. For storage, 1 μl Superase inhibitor (Ambion) was added to 50 μl of sample. RNA concentration was measured by using a microplate spectrophotometer Epoch (Biotek). RNA quality was checked by agarose gel electrophoresis of the samples.

RNA-seq and RT-qPCR. A total of 8 μg of RNA from each sample were sent to Macrogen Inc. (South Korea) for sequencing using the Illumina HiSeq2000 platform (Illumina, San Diego, CA, USA). Bioinformatic analysis was performed at Dreamgenics (Dreamgenics, Oviedo, Spain). Quality control of the reads was performed with FastQC. RNA-seq reads were mapped to the *S. aureus* NCTC 8325 and phage phiIPLA-RODI genomes by using BowTie2. Only the uniquely mapped reads were kept for the subsequent analyses. Differential gene expression analysis was performed using EDGE-pro software. Quantitative reverse transcription-PCR (RT-qPCR) was performed to verify transcriptional changes for selected differentially-expressed genes identified in the RNA-seq analysis. Briefly, 0.5 μg of purified RNA were converted into cDNA with iScript™ Reverse Transcription Supermix for RT-qPCR (BioRad). The resulting cDNA was then diluted 1:25 and 2.5 μl were added to each well together with Power SYBR Green PCR Master Mix (Applied BioSystems) for qPCR analysis.

RNA-Seq data have been deposited in NCBI's Gene Expression Omnibus (GEO) and can be accessed through GEO series accession number GSE87706.

Assessment of interactions between mupirocin and phiIPLA-RODI. The technique used to test whether there were synergistic or antagonistic interactions between the phage phiIPLA-RODI and the antibiotic mupirocin was the checkerboard assay[56]. This method is based on the broth microdilution technique, in which two different antimicrobials are diluted in a two-dimensional fashion. Thus, each well of a 96-well microtiter plate contained a unique combination of mupirocin concentration and MOI. Broth microdilution was performed following the CLSI guidelines[57,58] but using TSBg as a growth medium. The minimum inhibitory concentration (MIC) for each antimicrobial was determined as the lowest concentration inhibiting visible bacterial growth after 24 hours of incubation at 37 °C. The experiment was performed with four independent biological repeats.

Statistical analyses. All experiments were performed with at least three independent biological replicates and on a minimum of two different days. Data were analyzed with a two-tailed Student's t-test by using IBM SPSS Statistics for Windows, Version 22.0 (IBN Corp. Armonk, NY). *P*-values < 0.05 were considered significant.

References

1. Koskella, B. & Brockhurst, M. A. Bacteria–phage coevolution as a driver of ecological and evolutionary processes in microbial communities. *FEMS Microbiology Reviews* **38,** 916–931 (2014).
2. Díaz-Muñoz, S. L. & Koskella, B. Bacteria-phage interactions in natural environments. *Adv Appl Microbiol* **89,** 135–183 (2014).
3. Chaturongakul, S. & Ounjai, P. Phage–host interplay: examples from tailed phages and Gram-negative bacterial pathogens. *Front Microbiol* **5,** 442 (2014).
4. Obeng, N., Pratama, A. A. & Elsas, J. D. The significance of mutualistic phages for bacterial ecology and evolution. *Trends Microbiol* **24,** 440–449 (2016).
5. Ainsworth, S., Zomer, A., Mahony, J. & van Sinderen, D. Lytic infection of *Lactococcus lactis* by bacteriophages Tuc2009 and c2 triggers alternative transcriptional host responses. *Appl Environ Microbiol* **79,** 4786–4798 (2013).
6. Poranen, M. M. *et al.* Global changes in cellular gene expression during bacteriophage PRD1 infection. *J Virol* **80,** 8081–8088 (2006).
7. Fallico, V., Ross, R. P., Fitzgerald, G. F. & McAuliffe, O. Genetic response to bacteriophage infection in *Lactococcus lactis* reveals a four-strand approach involving induction of membrane stress proteins, D-alanylation of the cell wall, maintenance of proton motive force, and energy conservation. *J Virol* **85,** 12032–12042 (2011).
8. Zhao, X. *et al.* Global transcriptomic analysis of interactions between *Pseudomonas aeruginosa* and bacteriophage PaP3. *Sci Rep* **6,** 19237 (2016).
9. Lavigne, R. *et al.* A multifaceted study of *Pseudomonas aeruginosa* shutdown by virulent podovirus LUZ19. *MBio* **4,** e00061–13 (2013).
10. Kutateladze, M. & Adamia, R. Bacteriophages as potential new therapeutics to replace or supplement antibiotics. *Trends Biotechnol* **28,** 591–595 (2010).
11. Kutter, E. *et al.* Phage therapy in clinical practice: treatment of human infections. *Curr Pharm Biotechnol* **11,** 69–86 (2010).
12. Chan, B. K. & Abedon, S. T. Bacteriophages and their enzymes in biofilm control. *Curr Pharm Des* **21,** 85–99 (2015).
13. Gutiérrez, D., Martínez, B., Rodríguez, A. & García, P. Genomic characterization of two *Staphylococcus epidermidis* bacteriophages with anti-biofilm potential. *BMC Genomics* **13,** 228 (2012).
14. Parasion, S., Kwiatek, M., Gryko, R., Mizak, L. & Malm, A. Bacteriophages as an alternative strategy for fighting biofilm development. *Pol J Microbiol* **63,** 137–145 (2014).
15. Gupta, K., Marques, C. N., Petrova, O. E. & Sauer, K. Antimicrobial tolerance of *Pseudomonas aeruginosa* biofilms is activated during an early developmental stage and requires the two-component hybrid SagS. *J Bacteriol* **195,** 4975–4987 (2013).
16. Costerton, J. W. *et al.* Bacterial biofilms in nature and disease. *Annu Rev Microbiol* **41,** 435–464 (1987).

17. de la Fuente-Núñez, C., Reffuveille, F., Fernández, L. & Hancock, R. E. W. Bacterial biofilm development as a multicellular adaptation: antibiotic resistance and new therapeutic strategies. *Curr Opin Microbiol* **16,** 580–589 (2013).
18. Otto, M. Staphylococcal infections: mechanisms of biofilm maturation and detachment as critical determinants of pathogenicity. *Annu Rev Med* **64,** 175–188 (2013).
19. Lowy, F. D. Antimicrobial resistance: the example of *Staphylococcus aureus*. *J Clin Invest* **111,** 1265–1273 (2003).
20. Alves, D. R. *et al.* Combined use of bacteriophage K and a novel bacteriophage to reduce *Staphylococcus aureus* biofilm formation. *Appl Environ Microbiol* **80,** 6694–6703 (2014).
21. Gutiérrez, D. *et al.* Two Phages, phiIPLA-RODI and phiIPLA-C1C, Lyse Mono- and Dual-Species Staphylococcal Biofilms. *Appl Environ Microbiol* **81,** 3336–3348 (2015).
22. Kelly, D., McAuliffe, O., Ross, R. P. & Coffey, A. Prevention of *Staphylococcus aureus* biofilm formation and reduction in established biofilm density using a combination of phage K and modified derivatives. *Lett Appl Microbiol* **54,** 286–291 (2012).
23. Anderson, K. L. *et al.* Characterization of the *Staphylococcus aureus* heat shock, cold shock, stringent, and SOS responses and their effects on log-phase mRNA turnover. *J Bacteriol* **188,** 6739–6756 (2006).
24. Reiß, S. *et al.* Global analysis of the *Staphylococcus aureus* response to mupirocin. *Antimicrob Agents Chemother* **56,** 787–804 (2012).
25. Geiger, T., Kästle, B., Gratani, F. L., Goerke, C. & Wolz, C. Two small (p)ppGpp synthases in *Staphylococcus aureus* mediate tolerance against cell envelope stress conditions. *J Bacteriol* **196,** 894–902 (2014).
26. Dalebroux, Z. D., Svensson, S. L., Gaynor, E. C. & Swanson, M. S. ppGpp conjures bacterial virulence. *Microbiol Mol Biol Rev* **74,** 171–199 (2010).
27. Maisonneuve, E., Castro-Camargo, M. & Gerdes, K. (p)ppGpp controls bacterial persistence by stochastic induction of toxin-antitoxin activity. *Cell* **154,** 1140–1150 (2013).
28. Nguyen, D. *et al.* Active starvation responses mediate antibiotic tolerance in biofilms and nutrient-limited bacteria. *Science* **334,** 982–986 (2011).
29. Ochi, K., Kandala, J. C. & Freese, E. Initiation of *Bacillus subtilis* sporulation by the stringent response to partial amino acid deprivation. *J Biol Chem* **256,** 6866–6875 (1981).
30. Gross, M., Cramton, S. E., Götz, F. & Peschel, A. Key role of teichoic acid net charge in *Staphylococcus aureus* colonization of artificial surfaces. *Infect Immun* **69,** 3423–3426 (2001).
31. Huang, Q., Fei, J., Yu, H. J., Gou, Y. B. & Huang, X. K. Effects of human β-defensin-3 on biofilm formation-regulating genes *dltB* and *icaA* in *Staphylococcus aureus*. *Mol Med Rep* **10,** 825–831 (2014).
32. Koprivnjak, T. *et al.* Cation-induced transcriptional regulation of the *dlt* operon of *Staphylococcus aureus*. *J Bacteriol* **188,** 3622–3630 (2006).
33. Steen, A. *et al.* Autolysis of *Lactococcus lactis* is increased upon d-alanine depletion of peptidoglycan and lipoteichoic acids. *J Bacteriol* **187,** 114–124 (2005).
34. Räisänen, L. *et al.* Molecular interaction between lipoteichoic acids and *Lactobacillus delbrueckii* phages depends on d-alanyl and alpha-glucose substitution of poly(glycerophosphate) backbones. *J Bacteriol* **189,** 4135–4140 (2007).
35. Corrigan, R. M., Bowman, L., Willis, A. R., Kaever, V. & Gründling, A. Cross-talk between two nucleotide-signaling pathways in *Staphylococcus aureus*. *J Biol Chem* **290,** 5826–5839 (2015).
36. Qin, Z. *et al.* Role of autolysin-mediated DNA release in biofilm formation of *Staphylococcus epidermidis*. *Microbiology* **153,** 2083–2092 (2007).
37. Houston, P., Rowe, S. E., Pozzi, C., Waters, E. M. & O'Gara, J. P. Essential role for the major autolysin in the fibronectin-binding protein-mediated *Staphylococcus aureus* biofilm phenotype. *Infect Immun* **79,** 1153–1165 (2011).
38. Brazas, M. D. & Hancock, R. E. W. Using microarray gene signatures to elucidate mechanisms of antibiotic action and resistance. *Drug Discov Today* **10,** 1245–1252 (2005).
39. Wecke, T. & Mascher, T. Antibiotic research in the age of omics: from expression profiles to interspecies communication. *J Antimicrob Chemother* **66,** 2689–2704 (2011).
40. Otto, M. Staphylococcal biofilms. *Curr Top Microbiol Immunol* **322,** 207–228 (2008).
41. Fernández, L., Breidenstein, E. B. & Hancock, R. E. W. Creeping baselines and adaptive resistance to antibiotics. *Drug Resist Updat* **14,** 1–21 (2011).
42. Fortier, L. C. & Sekulovic, O. Importance of prophages to evolution and virulence of bacterial pathogens. *Virulence* **4,** 354–365 (2013).
43. Gödeke, J., Paul, K., Lassak, J. & Thormann, K. M. Phage-induced lysis enhances biofilm formation in *Shewanella oneidensis* MR-1. *ISME J* **5,** 613–626 (2011).
44. Carrolo, M., Frias, M. J., Pinto, F. R., Melo-Cristino, J. & Ramirez, M. Prophage spontaneous activation promotes DNA release enhancing biofilm formation in *Streptococcus pneumoniae*. *PLoS One* **5,** e15678 (2010).
45. Hosseinidoust, Z., Tufenkji, N. & van de Ven, T. G. Formation of biofilms under phage predation: considerations concerning a biofilm increase. *Biofouling* **29,** 457–468 (2013).
46. Tan, D., Dahl, A. & Middelboe, M. Vibriophages differentially influence biofilm formation by *Vibrio anguillarum* strains. *Appl Environ Microbiol* **81,** 4489–4497 (2015).
47. Webb, J. S. *et al.* Cell death in *Pseudomonas aeruginosa* biofilm development. *J Bacteriol.* **185,** 4585–4592 (2003).
48. Leskinen, K., Blasdel, B. G., Lavigne, R. & Skurnik, M. RNA-sequencing reveals the progression of phage-host interactions between φR1-37 and *Yersinia enterocolitica*. *Freed EO, ed. Viruses*. **8,** 111 (2016).
49. Aranda, M. & Maule, A. Virus-induced host gene shutoff in animals and plants. *Virology* **243,** 261–267 (1998).
50. Ehrenfeld, E. Poliovirus-induced inhibition of host-cell protein synthesis. *Cell* **28,** 435–436 (1982).
51. de Smet, J. *et al.* High coverage metabolomics analysis reveals phage-specific alterations to *Pseudomonas aeruginosa* physiology during infection. *ISME J*. doi: 10.1038/ismej.2016.3 (2016).
52. Gutiérrez, D. *et al.* Incidence of *Staphylococcus aureus* and analysis of associated bacterial communities on food industry surfaces. *Appl Environ Microbiol* **78,** 8547–8554 (2012).
53. Herrera, J. J., Cabo, M. L., González, A., Pazos, I. & Pastoriza, L. Adhesion and detachment kinetics of several strains of *Staphylococcus aureus* subsp. *aureus* under three different experimental conditions. *Food Microbiol* **24,** 585–591 (2007).
54. Gutiérrez, D., Ruas-Madiedo, P., Martínez, B., Rodríguez, A. & García, P. Effective removal of staphylococcal biofilms by the endolysin LysH5. *PLoS One* **9,** e107307 (2014).
55. Kaplan, J. B. *et al.* Low levels of β-lactam antibiotics induce extracellular DNA release and biofilm formation in *Staphylococcus aureus*. *MBio* **3,** e00198–12 (2012).
56. Dougherty, P. F., Yotter, D. W. & Matthews, T. R. Microdilution transfer plate technique for determining *in vitro* synergy of antimicrobial agents. *Antimicrob Agents Chemother* **11,** 225–228 (1977).
57. Clinical and Laboratory Standards Institute. *M7-A7. Methods for dilution antimicrobial susceptibility tests for bacteria that grow aerobically; Approved Standard–7th ed.* (Clinical and Laboratory Standards Institute, 2006).
58. Clinical and Laboratory Standards Institute. *M100-S17. Performance standards for antimicrobial susceptibility testing; Approved Standard–17th ed.* (Clinical and Laboratory Standards Institute, 2007).

Acknowledgements

This study was supported by grants AGL2012-40194-C02-01 (Ministry of Science and Innovation, Spain), AGL2015-65673-R (Program of Science, Technology and Innovation 2013-2017), GRUPIN14-139 (FEDER EU funds, Principado de Asturias, Spain). L.F. was awarded a "Marie Curie Clarin-Cofund" grant (ACB14-01). PG, BM and AR are members of the FWO Vlaanderen funded "Phagebiotics" research community (WO.016.14) and the bacteriophage network FAGOMA.

Author Contributions

L.F., P.G. and A.R. wrote the manuscript. L.F., S.G. and A.C. performed the experiments. L.F., P.G., B.M. and A.R. conceived the experiments. All authors reviewed the manuscript.

Additional Information

Supplementary information accompanies this paper at http://www.nature.com/srep

Competing financial interests: The authors declare no competing financial interests.

How to cite this article: Fernández, L. *et al.* Low-level predation by lytic phage phiIPLA-RODI promotes biofilm formation and triggers the stringent response in *Staphylococcus aureus*. *Sci. Rep.* **7**, 40965; doi: 10.1038/srep40965 (2017).

Publisher's note: Springer Nature remains neutral with regard to jurisdictional claims in published maps and institutional affiliations.

SCIENTIFIC REPORTS

OPEN

Lysogenization of *Staphylococcus aureus* RN450 by phages ϕ11 and ϕ80α leads to the activation of the SigB regulon

Received: 1 May 2018
Accepted: 10 August 2018
Published online: 23 August 2018

Lucía Fernández[1], Silvia González[1], Nuria Quiles-Puchalt[2], Diana Gutiérrez[1], José R. Penadés[2], Pilar García[1] & Ana Rodríguez[1]

Staphylococcus aureus **is a major opportunistic pathogen that commonly forms biofilms on various biotic and abiotic surfaces. Also, most isolates are known to carry prophages in their genomes. With this in mind, it seems that acquiring a better knowledge of the impact of prophages on the physiology of *S. aureus* biofilm cells would be useful for developing strategies to eliminate this pathogen. Here, we performed RNA-seq analysis of biofilm cells formed by *S. aureus* RN450 and two derived strains carrying prophages ϕ11 and ϕ80α. The lysogenic strains displayed increased biofilm formation and production of the carotenoid pigment staphyloxanthin. These phenotypes could be partly explained by the differences in gene expression displayed by prophage-harboring strains, namely an activation of the alternative sigma factor (SigB) regulon and downregulation of genes controlled by the Agr quorum-sensing system, especially the decreased transcription of genes encoding dispersion factors like proteases. Nonetheless, spontaneous lysis of part of the population could also contribute to the increased attached biomass. Interestingly, it appears that the phage CI protein plays a role in orchestrating these phage-host interactions, although more research is needed to confirm this possibility. Likewise, future studies should examine the impact of these two prophages during the infection.**

Over the last 100 years, we have been gradually discovering the impact of bacteriophages, viruses that infect bacteria, on the fate of microbial communities[1,2]. In the case of prophages and prophage-like elements, for instance, advances in genome sequencing have revealed that phage-like sequences are present in almost all bacterial genomes and that they can amount to as much as 20% of the genetic material in some bacteria[3]. This fact indicates that phages have successfully spread within bacterial populations, and hints that carrying phage-related DNA in the bacterial chromosome might confer evolutionary advantages to the host. One of the most widely accepted beneficial roles of functional prophages is that they make the host bacterial population more competitive against phage-sensitive strains[4]. Thus, spontaneous prophage activation and subsequent lysis of individual cells within the population will release viral particles that can infect and lyse cells of the susceptible strain. Furthermore, the intracellular cell contents of the lysed cells can then be used by other cells as nutrients[5]. Conversely, other studies have pointed out that lysogeny may be detrimental under certain conditions. A clear example is the inhibition exerted by *Streptococcus pneumoniae* against *Staphylococcus aureus* in the nasal cavity. An elegant study by Selva *et al.*[6] demonstrated that this lesser competitive ability was due to the induction of the lytic cycle in *S. aureus* lysogenic strains by subinhibitory concentrations of H_2O_2 released by *Streptococcus*, a trigger of the SOS response. Nonetheless, the effect of prophage carriage on bacteria goes well beyond competition and can have a profound impact on the exchange of genetic information as well as diverse physiological traits. Regarding horizontal gene transfer, phages are known to participate in the dissemination of virulence and/or antibiotic resistance markers[7]. For instance, the Shiga toxin in *Escherichia coli* and many *S. aureus* toxins are harbored by prophages[8]. Additionally, bacteriophages help mobilize the superantigen-encoding pathogenicity islands (SaPIs) of *S. aureus*[9].

[1]Instituto de Productos Lácteos de Asturias (IPLA-CSIC), Paseo Río Linares s/n 33300 -, Villaviciosa, Asturias, Spain. [2]Institute of Infection, Immunity and Inflammation, College of Medical, Veterinary and Life Sciences, University of Glasgow, G12 8TA, Glasgow, UK. Lucía Fernández and Silvia González contributed equally. Correspondence and requests for materials should be addressed to L.F. (email: lucia.fernandez@ipla.csic.es)

Prophages can also affect the fitness of their bacterial host. Thus, some cryptic prophages can increase the growth rate in *E. coli*[10], whereas *Bacillus thuringiensis* strains lysogenized by tectiviruses GIL01 and GIL16 showed a lower growth rate than their non-lysogenic counterparts. *In B. thuringiensis*, lysogenic strains also displayed greater swarming motility and reduced sporulation rate[11]. Another widely studied phenotype in lysogenized strains is biofilm formation. The results obtained so far indicate that there is no general rule in this regard, with some phages promoting dispersal, as is the case of prophage-harboring *Enterococcus faecalis* V583ΔABC[12], while others enhance the development of sessile communities. An example of the latter is the environmental bacterium *Shewanella oneidensis*, in which bacteriophage-mediated lysis contributes to the release of eDNA to the extracellular matrix and, consequently, promotes biofilm development[13]. In *Pseudomonas aeruginosa*, the filamentous prophage Pf4 plays a fairly complex role in biofilm development and is essential for microcolony architecture[14,15].

The human and animal pathogen *S. aureus* is a highly clonal species[16], in which intraspecific variation is due to a large extent to the presence of mobile genetic elements like pathogenicity islands and prophages[17]. Indeed, most strains of this pathogen carry one to four prophages in their chromosome[18]. In some cases, these prophages carry accessory genes involved in virulence, such as the Panton-Valentine leukocidin, exfoliative toxin, enterotoxin A or staphylokinase, a phenomenon known as lysogenic conversion[8]. However, most prophages do not harbor virulence-related genes in their chromosome, which suggests that they may have other physiological roles that benefit their host. All staphylococcal phages known to date belong to the order Caudovirales and are included in families Podoviridae, Siphoviridae, and Myoviridae[17]. In addition to their role in the pathogenicity and evolution of their host, staphylophages have been widely used for the genetic manipulation of *Staphylococcus*, such as the well-studied siphoviruses ϕ11 and ϕ80α[17]. *S. aureus* can form biofilms on different environments, including food industry surfaces, implanted devices and biotic surfaces like human tissues[19]. This ability makes this pathogen able to withstand harsh conditions such as antimicrobial pressure. Since natural communities of *S. aureus* are expected to carry prophages, it would be interesting to determine whether their presence has an effect on the development of staphylococcal biofilms. However, the impact of phages on *S. aureus* biofilm formation has not been studied in depth. Thus far, two articles assessed the impact of virulent phages on the development of biofilms by this microbe[20,21], while the influence of temperate phages remains to be elucidated. Also, there is no information available regarding the influence of lysogeny on the transcriptome of biofilm-forming cells. With this in mind, this study aimed to determine the impact of temperate phages ϕ11 and ϕ80α on the physiology of *S. aureus* cells during biofilm development. This knowledge will shed light on the interplay between prophages and their bacterial hosts in natural sessile communities; an information that is particularly relevant given the prevalence of lysogenic strains in this pathogen. Moreover, a better understanding of these interactions will be useful for designing strategies to eradicate biofilms in industrial and hospital settings.

Results

Effect of lysogenization with phages ϕ11 and ϕ80α on biofilm formation of *S. aureus* RN450. Previous studies have shown that the presence of prophages in the bacterial chromosome may have an impact on biofilm formation. Here, we sought to determine if lysogenization with the well-characterized phages ϕ11 and ϕ80α affects the development of biofilms by *S. aureus*. To make sure that all strains used for this study had the same genetic background, the two phages were isolated and used to lysogenize strain RN450 to obtain strains RN450-ϕ11 and RN450-ϕ80α. Then, biofilms of the three strains (lysogens and non-lysogenic strain) were allowed to develop for 5 and 24 hours. At the earlier time point, both lysogenic strains showed an increase in adhered biomass of 78% and 68% for strains carrying phages ϕ11 and ϕ80α, respectively (Fig. 1A). However, the results obtained for 24-hour biofilms were different. Thus, the strain carrying ϕ11 prophage still displayed 39% greater biofilm formation than the non-lysogenic strain, whereas the ϕ80α lysogen showed no significant (P-value = 0.48) difference compared to strain RN450 (Fig. 1B).

Spontaneous release of phage particles in *S. aureus* RN450 biofilms. Once established that the presence of the two prophages affects biofilm formation in *S. aureus* RN450, we assessed whether there was spontaneous induction of the lytic cycle in the biofilm after 5 hours of development. It must be noted that preliminary data had shown that the maximum phage titer in the biofilm of these two lysogenic strains is precisely at 5 hours of development, later decreasing slightly at 8 h and even further at 24 h (Fig. S1). For both lysogenic strains, RN450-ϕ11 and RN450-ϕ80α, phage particles were found in both the planktonic phase and the surface-attached biomass of 5-hour biofilms (Fig. 1C). The total titer for both phages was approximately 10^5 PFUs per well. Also, virions were isolated not only free in the supernatant or the extracellular matrix, but also inside *S. aureus* cells (infectious centers) (Fig. 1C). The distribution of phage particles in the different fractions was the same for both prophages. Thus, the number of PFUs in the planktonic phase (both free and cell-associated) and in the extracellular matrix of the biofilm was very similar (~10^5 PFU/well), and higher than those found inside biofilm cells (~10^4 PFU/well).

Transcriptional analysis of bacterial genes in the presence of prophages. With the aim of studying more in-depth the impact of prophages ϕ11 and ϕ80α on bacterial physiology, we performed genome-wide transcriptional analysis of biofilms formed by RN450, RN450-ϕ11 and RN450-ϕ80α by RNA-seq. In samples corresponding to strains RN450 and RN450-ϕ11, 100% of sequences aligned with *S. aureus* NCTC8325. In the case of strain RN450-ϕ80α, 99% of sequences aligned with the reference *S. aureus* strain and 1% aligned with the phage ϕ80α genome. These results are consistent with the fact that bacteriophage ϕ11 is part of the NCTC8325 reference genome, whereas ϕ80α is not. Differential gene expression between samples from the lysogenic strains and the phage-free strain RN450 was also determined. The data obtained from this analysis revealed significant changes in the bacterial transcriptome as a result of lysogenization. It must be noted that prophage genes were excluded from this analysis and that only genes displaying changes in expression ≥ 2 with an adjusted P-value ≤ 0.05 were

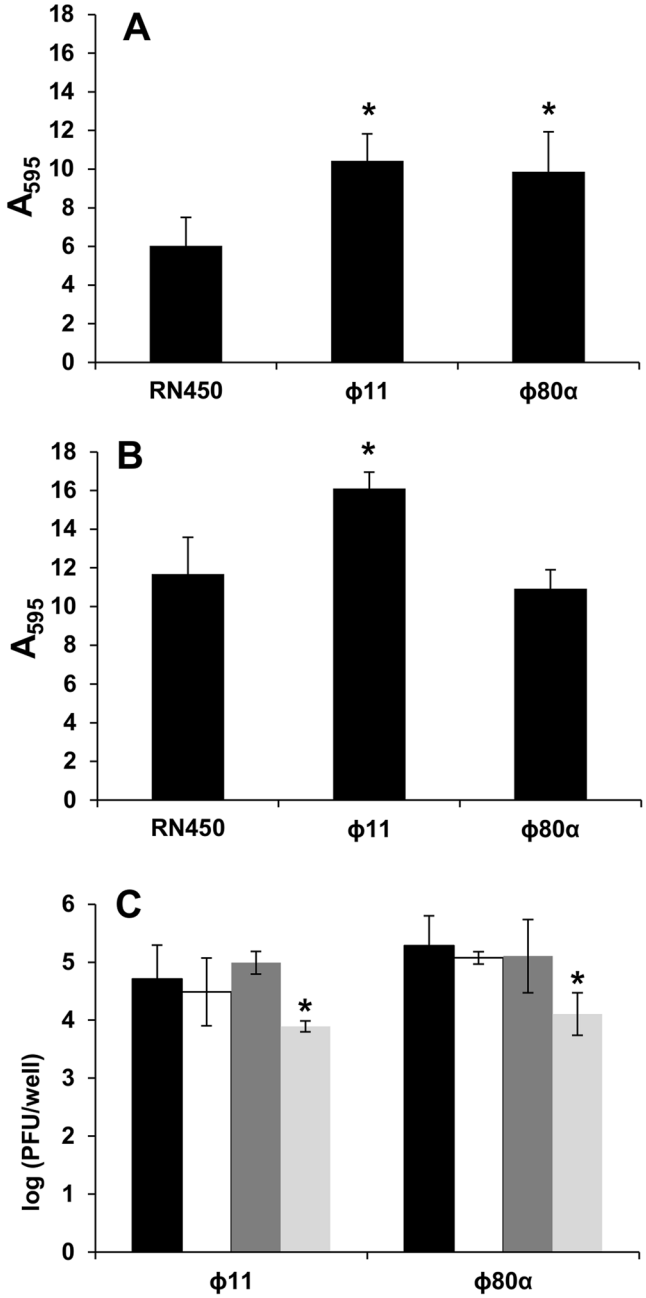

Figure 1. Analysis of biofilms formed by the non-lysogenic strain RN450 and the lysogenic strains RN450-ϕ11 and RN450-ϕ80α. Biofilms were formed for 5 hours (**A**) or 24 hours (**B**) and then analyzed by crystal violet staining and subsequent measurement of A_{595}. (**C**) Titration of phage particles released by spontaneous induction in 5 h biofilms formed by the lysogenic strains RN450-ϕ11 and RN450-ϕ80α. Black bars, phages present as free virions in the planktonic phase; white bars, phages associated with cells present in the planktonic phase; dark gray bars, free phages present in the adhered (biofilm) phase; light gray bars, infectious centers in the adhered (biofilm) phase. The results correspond to the means and standard deviation of 3 independent biological replicates. *P-value < 0.05.

selected. Considering these parameters, the lysogenic strain RN450-ϕ11 showed upregulation of 68 genes and downregulation of 38 genes compared to the non-lysogenic strain (Table S1). Similarly, RN450-ϕ80α exhibited increased expression of 176 genes and decreased expression of 111 genes compared to strain RN450 (Table S2). There was a considerable overlap between the transcriptional changes observed in both lysogenic strains, with the results obtained for RN450-ϕ80α practically including all genes dysregulated in RN450-ϕ11 (Table 1). The only exceptions included a gene encoding a hypothetical phage protein, as well as genes *lacA* and *lacB*, all of which were slightly downregulated in the ϕ11 lysogen but not in the ϕ80α lysogen (Table S1). On the other hand, there were many genes dysregulated in the ϕ80α–harboring strain that did not change in the ϕ11 lysogen (Table S2). The genes dysregulated in both lysogenic strains were assigned to different pathways according to the KEGG

Gene[a]	Gene name	ϕ11[b]	ϕ80α[b]	SigB regulon[c]	CcpA regulon[c]
SAOUHSC_00061		2.35	4.97	Up	
SAOUHSC_00069*	*spa*	3.70	5.40		Up
SAOUHSC_00070	*sarS*	3.26	4.73	Up	
SAOUHSC_00156		2.47	3.18		Up
SAOUHSC_00157	*murQ*	3.13	4.18		Up
SAOUHSC_00158		3.39	4.35		Up
SAOUHSC_00160		2.31	3.46		Up
SAOUHSC_00183	*uhpT*	3.72	7.31		Up
SAOUHSC_00196	*fadB*	2.82	4.12		Up
SAOUHSC_00257		0.48	0.28		
SAOUHSC_00291		2.32	2.18		Up
SAOUHSC_00317		2.81	3.78		Up
SAOUHSC_00356		3.96	11.49	Up	
SAOUHSC_00358		4.67	12.22	Up	
SAOUHSC_00401		0.33	0.16		
SAOUHSC_00619		5.66	21.10	Up	
SAOUHSC_00624		2.72	7.23	Up	
SAOUHSC_00625	*mnhA2*	2.10	4.29	Up	
SAOUHSC_00626	*mnhB2*	2.14	3.70	Up	
SAOUHSC_00627	*mnhC2*	2.13	3.97	Up	
SAOUHSC_00628	*mnhD2*	2.14	3.75	Up	
SAOUHSC_00629	*mnhE2*	2.08	3.58	Up	
SAOUHSC_00630		2.05	3.51		
SAOUHSC_00632	*mnhG2*	2.04	3.42	Up	
SAOUHSC_00655		2.07	2.76		Up
SAOUHSC_00831		3.48	9.45	Up	
SAOUHSC_00845		8.90	31.38	Up	
SAOUHSC_00846		2.97	8.59		
SAOUHSC_00988*	*sspA*	0.49	0.32	Down	
SAOUHSC_01017	*purH*	2.17	2.57		
SAOUHSC_01018	*purD*	2.00	2.43		
SAOUHSC_01135		0.40	0.06		
SAOUHSC_01136		0.44	0.06		
SAOUHSC_01318		2.18	2.48		Up
SAOUHSC_01513		0.49	0.26		
SAOUHSC_01601		2.70	4.10		
SAOUHSC_01602		2.67	3.98		
SAOUHSC_01603		2.21	2.89		
SAOUHSC_01729		7.55	18.24	Up	
SAOUHSC_01730		6.31	19.71	Up	
SAOUHSC_01794		3.77	5.80		
SAOUHSC_01910	*pckA*	3.14	4.92		Up
SAOUHSC_01918		2.01	2.89		
SAOUHSC_01920		2.35	3.23		
SAOUHSC_01921		2.21	2.74		
SAOUHSC_01935	*splF*	0.46	0.47		
SAOUHSC_01939	*splC*	0.47	0.47	Down	
SAOUHSC_01941	*splB*	0.40	0.32	Down	
SAOUHSC_01942	*splA*	0.36	0.26	Down	
SAOUHSC_01945		0.46	0.41		
SAOUHSC_01949		0.48	0.36		
SAOUHSC_01950		0.46	0.32		
SAOUHSC_01951		0.48	0.31		
SAOUHSC_01952		0.48	0.30		
SAOUHSC_02137	*sdcS*	2.15	3.17		Up
SAOUHSC_02163		0.19	0.08		
SAOUHSC_02240		0.31	0.11		
Continued					

Gene[a]	Gene name	ϕ11[b]	ϕ80α[b]	SigB regulon[c]	CcpA regulon[c]
SAOUHSC_02260*	*hld*	0.40	0.04		
SAOUHSC_02261*	*agrB*	0.50	0.17		
SAOUHSC_02265		0.50	0.20		
SAOUHSC_02266		0.45	0.24		
SAOUHSC_02387		3.30	11.15	Up	
SAOUHSC_02400		3.31	8.23		
SAOUHSC_02401		3.63	9.77	Up	
SAOUHSC_02402		4.08	11.06	Up	
SAOUHSC_02403	*mtlD*	3.27	8.74	Up	
SAOUHSC_02425		2.39	3.26		Up
SAOUHSC_02441	*asp23*	9.56	28.18	Up	
SAOUHSC_02442		7.60	27.27	Up	
SAOUHSC_02443		8.17	29.88	Up	
SAOUHSC_02444		4.99	19.92	Up	
SAOUHSC_02451		0.44	0.49		
SAOUHSC_02452	*lacD*	0.38	0.45		
SAOUHSC_02453	*lacC*	0.39	0.49		
SAOUHSC_02597		2.12	2.90		Up
SAOUHSC_02620		0.45	0.24	Down	
SAOUHSC_02729		2.20	3.14		Up
SAOUHSC_02771		2.96	5.46	Up	
SAOUHSC_02772		2.32	6.49	Up	
SAOUHSC_02812		3.00	7.98	Up	
SAOUHSC_02815		2.63	4.38		Up
SAOUHSC_02822	*fbp*	2.31	3.17		Up
SAOUHSC_02848	*glcB*	2.07	2.90		
SAOUHSC_02862	*clpL*	5.24	16.79	Up	
SAOUHSC_02877	*crtN*	2.14	5.93	Up	
SAOUHSC_02879	*crtM*	3.46	10.17	Up	
SAOUHSC_02880	*crtQ*	3.88	13.11	Up	
SAOUHSC_02881*	*crtP*	3.08	10.10	Up	
SAOUHSC_02882	*crtO*	2.93	8.93	Up	
SAOUHSC_02905		0.35	0.15		
SAOUHSC_02906		0.31	0.14		
SAOUHSC_02907		0.35	0.14		
SAOUHSC_02908		2.49	5.89	Up	
SAOUHSC_02964	*arcR*	0.42	0.24		Down
SAOUHSC_02965	*arcC2*	0.34	0.24		Down
SAOUHSC_02967		0.33	0.22		Down
SAOUHSC_02968	*argF*	0.38	0.22		Down
SAOUHSC_02969	*arcA*	0.34	0.22		Down
SAOUHSC_02970		0.48	0.19		
SAOUHSC_02971		0.45	0.30	Down	
SAOUHSC_03028		2.34	6.42	Up	
SAOUHSC_03032		2.09	4.46	Up	
SAOUHSC_A00354		5.17	13.93		

Table 1. Genes identified by RNA-seq analysis that were dysregulated in both lysogenic strains (RN450-ϕ11 and RN450-ϕ80α) compared to prophage-free strain RN450 and overlaps with sigma B- and CcpA-regulated genes. [a]Genes marked with an asterisk (*) were confirmed by RT-qPCR; the reference gene used to calculate the fold-change was *rplD*. [b]Changes in gene expression below 1 (<1) indicate downregulation in the lysogen, whereas changes above 1 (>1) indicate upregulation in the lysogenic strain. [c]Genes under SigB and CcpA control.

database (Fig. 2A). Amongst the upregulated genes, there were a significant number of genes related to different metabolic pathways. Notably, many genes were involved in pathways related to carbohydrate metabolism, phosphotransferase systems, energy metabolism and carotenoid biosynthesis. Most of the genes that showed lower expression in the lysogenic strains were related to quorum-sensing signaling pathways and two-component regulatory systems.

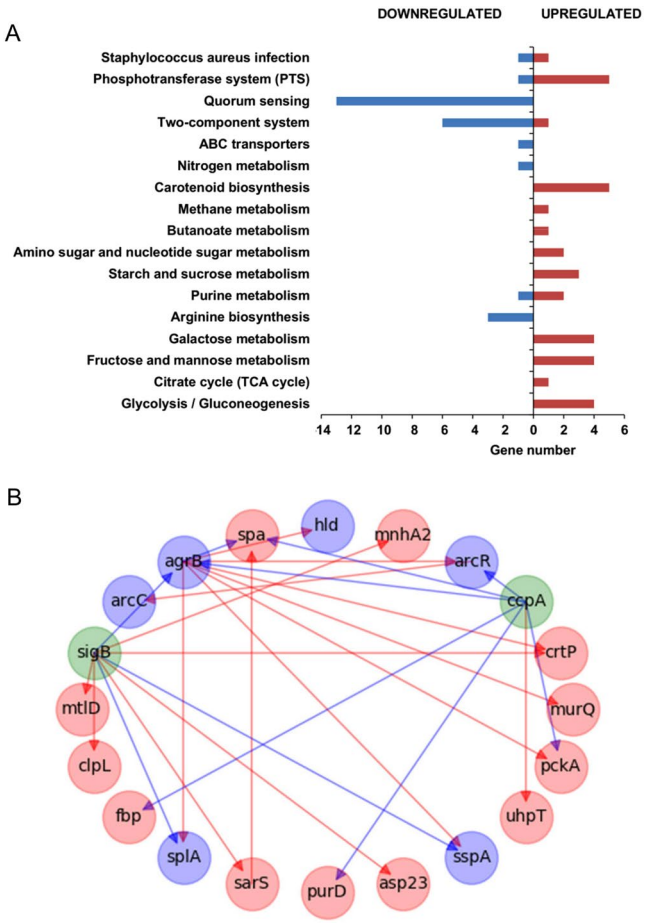

Figure 2. Effects of lysogenization on the transcriptome of *S. aureus* RN450. (**A**) KEGG pathway analysis of genes up- (red) and down-regulated (blue) in both lysogenic strains compared to the non-lysogenic strain. Bars indicate the number of genes belonging to those pathways that changed in both lysogenic strains. (**B**) Overlap of genes dysregulated in both lysogens with the SigB and CcpA regulons. Green nodes represent regulators SigB and CcpA, which did not show changes in gene expression in the RNA-seq analysis. Red and blue nodes represent up- and down-regulated genes identified by RNA-seq analysis, respectively. Red and blue arrows represent a positive and negative effect on the expression of another gene, respectively.

Interestingly, several genes that exhibited expression changes in the presence of the two prophages are potentially involved in biofilm formation (Table 1). For instance, the gene coding for the adhesion protein A (*spa*) was upregulated in both lysogens, which is consistent with the literature[22]. In contrast, several genes encoding dispersion factors, such as proteases (*sspA*, *splF*, *splC*, *splB*, *splA*) or surfactants (*hld*), were downregulated in both strains. Additionally, upregulation of other proteins involved in adhesion was observed in RN450-ϕ80α, such as *fnbA* and *clfA*. However, in strain RN450-ϕ80α there was also a slight downregulation of *icaB* and *icaD* (Table S2). These two genes are involved in the production of polysaccharide intercellular adhesin (PIA), which is a major component in the extracellular matrix of *S. aureus* biofilms.

Some genes that encode proteins with a regulatory function, such as *agrB*, *arcR*, *sarS* or *clpL*, were dysregulated in both lysogenic strains. For instance, *agrB*, which encodes a protein that participates in quorum-sensing signaling, was downregulated. This would explain, at least to some extent, the general downregulation of genes under quorum-sensing control, including proteases and *hld*. In RN450-ϕ80α there was also a lesser expression of hemolysin-encoding genes *hlgB*, *hlgC* and *hly* (Table S2), which are also under the control of Agr. ArcR is a regulator of the *arcABDC* operon, which is necessary for using arginine as a source of energy under anaerobic conditions[23], and was found to be downregulated in both lysogens. In contrast to *agrB* and *arcR*, the SarS-encoding gene was upregulated in both lysogenic strains. In strain RN450-ϕ80α, another SarA homolog, SarT, was also induced. Finally, *clpL*, encoding an Hsp100/Clp ATPase belonging to a family of chaperones that can form a proteolytic complex with the intracellular protease ClpP, was also upregulated in both lysogenic strains[24].

As mentioned previously, both prophages led to changes in the expression of multiple genes that participate in different metabolic pathways. For example, genes involved in nucleotide metabolism (*purH* and *purD*) and fatty acids metabolism (*fadB*) were upregulated in both lysogenic strains. Notably, there were a considerable number of genes related to carbohydrate metabolism with altered expression in the presence of the prophages. For instance, there were genes involved in glycolysis/gluconeogenesis, such as *fbp* (fructose-1,6-bisphosphatase) and *pckA*

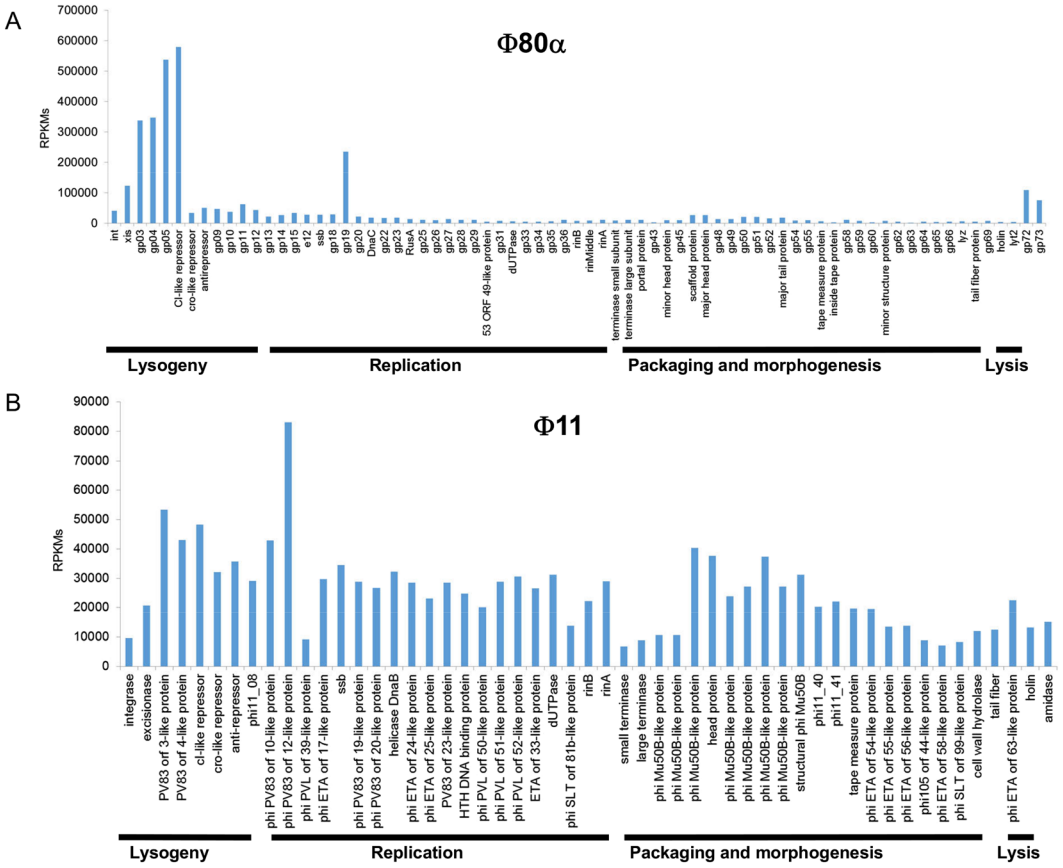

Figure 3. Transcriptome of prophages ϕ80α and ϕ11. Normalized mean reads per kilobase million (RPKM) values corresponding to the different open reading frames (ORFs) from the genome of phages ϕ80α (**A**) and ϕ11 (**B**).

(phosphoenolpyruvate carboxykinase), as well as genes *lacC* and *lacD*, which belong to the tagatose-6-phosphate pathway. Other genes related to carbohydrate metabolism were *mtlD* (mannitol-1-phosphate 5-dehydrogenase) and *glcB* (a glucoside-specific PTS system). Additionally, several genes involved in transport were upregulated in both lysogenic strains. These genes included *mnhG2*, *mnhA2*, *mnhE2*, *mnhB2*, *mnhD2* and *sdcS* (sodium dependent dicarboxylate transporter) and the gene coding for the membrane hexose phosphate transporter protein UhpT.

Some of the genes mentioned above are known to be under the control of the catabolite control protein A (CcpA), even though the gene coding for this regulator was not identified in the transcriptional analysis (fold changes for RN450-ϕ80α and RN450-ϕ11 were $1.45 \pm 0.11$and 1.21 ± 0.08, respectively). Indeed, comparison of the genes dysregulated in both lysogenic strains with the information available on the CcpA regulon in the RegPrecise database (http://regprecise.lbl.gov/RegPrecise/regulog.jsp?regulog_id=662) led to the identification of 23 genes (Table 1).

Further examination of the genes that changed in both lysogenic strains revealed a significant overlap (42 genes) with the SigB regulon (Table 1), indicating a potential activation of the alternative sigma factor in the presence of the two prophages[25]. It must be noted that genes *rsbV*, *rsbW*, *sigB* and *rsbX* were not dysregulated, with respective fold-changes in RN450-ϕ11 of 1.04 ± 0.09, 0.97 ± 0.07, 0.85 ± 0.14 and 1.04 ± 0.02. Similar results were observed in RN450-ϕ80α, with fold-change values of 1.21 ± 0.02, 1.14 ± 0.02, 1.09 ± 0.06 and $1.03 \pm 0.01$for genes *rsbV*, *rsbW*, *sigB* and *rsbX*, respectively. Some of the most characteristic genes in the SigB regulon include *asp23*, encoding the alkaline shock protein, and the operon responsible for the biosynthesis of staphyloxanthin, the characteristic yellow pigment of *S. aureus*[25]. All of these genes were upregulated in the two lysogenic strains, although this increase was more pronounced in RN450-ϕ80α than in RN450-ϕ11.

Transcriptional analysis of bacteriophage gene expression. In addition to studying transcriptional changes in bacterial genes, RNAseq data also provided information regarding the expression of phage genes in the samples corresponding to the lysogenic strains. In the case of RN450-ϕ80α, although there was some level of expression of all genes throughout the genome, the highest transcription levels were found in genes of the lysogeny module (Fig. 3A). Thus, the highest expression was displayed by genes gp05 and the gene encoding the CI protein, with RPKM values between 500,000 and 600,000. Next in expression levels were gp03 and gp04, with RPKM values of 300,000. Unexpectedly, a gene in the replication module, gp19, exhibited a high expression, with RPKM values of approximately 200,000. The excisionase-encoding gene *xis* and hypothetical proteins gp72 and

S. aureus strains	Description	Reference
RN450	NCTC8325 strain curated of prophages ϕ11, ϕ12 and ϕ13	[55]
RN451	RN450 lysogenized with prophage ϕ11	[55]
RN10359	RN450 lysogenized with prophage ϕ80α	[56]
RN450-ϕ11	RN450 lysogenized with prophage ϕ11	This study
RN450-ϕ80α	RN450 lysogenized with prophage ϕ80α	This study
RN450-ϕ53	RN450 lysogenized with prophage ϕ53	This study
RN450-ϕ85	RN450 lysogenized with prophage ϕ85	This study
JP6001	ϕ80α Δ *int* (*gp01*)	This study
JP6002	ϕ80α Δ *xis* (*gp02*)	This study
JP6003	ϕ80α Δ *gp03*	This study
JP6004	ϕ80α Δ *gp04*	This study
JP6005	ϕ80α Δ *gp05*	This study
JP6020	ϕ80α Δ *gp20*	This study
JP6021	ϕ80α Δ *gp21*	This study
JP3592	ϕ80α *cI* G130E (phage mutant non-responsive to SOS activation)	[6]

Table 2. Bacterial strains used in this study.

gp73 had RPKM values of about 100,000. All other ORFs showed RPKM values below 100,000. In the case of *xis*, it must be noted that the transcription levels quantified here may reflect reads of the transcriptional unit encoding gp03 which is encoded in the complementary strand. In order to determine if this is the case, strand specific RNA-seq would have to be performed. The transcriptional profile of phage ϕ11 was quite different. At first glance, it can be observed that expression was more evenly distributed along the genome and no specific region was overrepresented (Fig. 3B). The gene with the highest level of expression, with RPKM values of 80,000, was phi11_10, which belongs to the replication module.

Effect of mutations in different phage ϕ80α genes on biofilm formation, phage release and staphyloxanthin production. In an attempt to characterize the mechanisms involved in the phenotypic and physiological changes observed in the lysogenic strains, several mutant strains derived from RN450-ϕ80α were analyzed (Table 2). Some of these strains had deletions affecting genes involved in prophage integration into or excision from the bacterial chromosome (JP6001 and JP6002), genes involved in phage DNA replication (JP6020 and JP6021) or genes of unknown function located in the lysogeny module (JP6003, JP6004 and JP6005). Also, there was one strain with a point mutation in the CI protein that made it insensitive to the SOS response (JP3592), thereby abrogating induction of the lytic cycle. First, prophage release upon mitomycin C induction was examined. We observed that strains RN450-ϕ80α, JP6003, JP6004 and JP6005 exhibited similar levels of phage release, with respective phage titers of 7.62 ± 0.60, 8.08 ± 0.45, 7.7 ± 0.74 and 7.85 ± 0.73 log (PFU/ml). In contrast, the mutant strains JP6001, JP6002, JP6020, JP6021 and JP3592 did not exhibit detectable levels of released phage particles (Fig. 4A).

Next, we assessed whether these mutations had an impact on the biofilm formation ability of the lysogenic strain. The results of these assays showed that deletion of genes *xis*, gp20 or gp21 or a point mutation in the *cI* gene led to a lesser biofilm formation compared to the parent lysogenic strain RN450-ϕ80α (Fig. 4A). Indeed, the mutant in gp21 exhibited an even lower biofilm-forming ability than the nonlysogen RN450. In contrast, strains with deletion mutations in gp04 and gp05 showed greater biofilm development than RN450; in fact, JP6004 formed even more biofilm than RN450-ϕ80α (Fig. 4A). Strain JP6003 showed no significant difference in biofilm formation compared to RN450 or RN450-ϕ80α (Fig. 4A).

Another phenotype of interest was staphyloxanthin production, which was visualized after growth of bacterial colonies for 48 hours on TSA plates. As mentioned above, strains carrying ϕ11 and ϕ80α as prophages showed an increased expression of genes involved in the biosynthesis of the carotenoid pigment staphyloxanthin. As predicted by transcriptional analysis, colonies of the lysogenic strain RN450-ϕ80α displayed a more intense yellow/orange color than those of RN450 (Fig. 4A). Regarding the effect of mutations in phage genes, results showed that deletion of genes gp04 and gp05 as well as a point mutation in the adjacent gp06, encoding protein CI, resulted in a lesser carotenoid production. In contrast, genes involved in integration/excision of the prophage from the chromosome (*int* and *xis*) or genes involved in phage replication (gp20 and gp21) had no impact whatsoever on staphyloxanthin production (Fig. 4A). We also compared staphyloxanthin production in lysogenic strains harboring prophages ϕ80α, ϕ11, ϕ53 and ϕ85 and observed that the most intense color was displayed by the ϕ80α lysogenic strain, followed by ϕ11 and ϕ53, which were quite similar to each other, and ϕ85, which exhibited a color akin to that of the non-lysogen RN450 (Fig. 4B). These results were interesting considering the similarity amongst the CI proteins of the four phages analyzed with the BLASTP program[26]. Thus, the identity between CI proteins of ϕ11 and ϕ53 was about 99%, whereas identity between ϕ11 or ϕ53 with ϕ80α CI protein was 76 and 77%, respectively. The CI protein from phage ϕ85 was the least similar to any of the other three proteins with 23, 30 and 21% identity with CI proteins from phages ϕ11, ϕ80α and ϕ53, respectively.

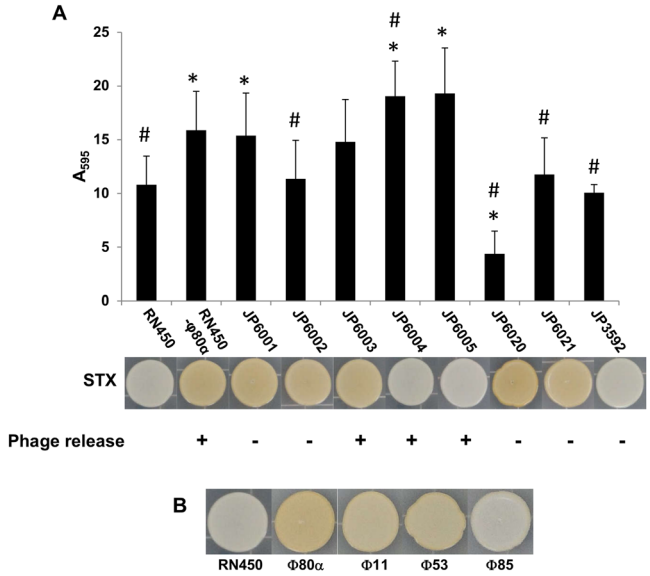

Figure 4. Involvement of phage genes in biofilm formation and staphyloxanthin production in lysogenic strains. (**A**) Biofilm formation (black bars), staphyloxanthin production and spontaneous release of virions of mutants derived from the lysogenic strain RN450-ϕ80α after 5 hours of incubation at 37 °C. Values represent the average and standard deviation of 4 independent experiments. *Differences compared to RN450 were statistically significant (p-values < 0.05); #Differences compared to RN450-ϕ80α were statistically significant (p-values < 0.05). (**B**) Staphyloxanthin (STX) production of *S. aureus* RN450 and its derived lysogenic strains.

Discussion

Prophages play an important role in the evolution and fate of microbial communities[1,2,7]. Embedded in bacterial genomes, these viral entities can enhance fitness of their host bacteria or, conversely, make them more vulnerable to certain environmental challenges. Examples of the former include lysogenic conversion, in which the phage genetic material encodes virulence factors, or enhanced biofilm development as a result of lysogenization. However, there are instances in which carrying a prophage may be lethal in the presence of a triggering factor of the lytic cycle. This has been observed in *E. faecalis* biofilm dispersion of lysogenic strains, and the heightened susceptibility of *S. aureus* lysogens to the hydrogen peroxide produced by *S. pneumoniae*[6,12]. Until now, the impact of prophages during biofilm development had not been examined in depth in *S. aureus*. Within this context, this study aimed to determine how two well-known temperate phages, ϕ80α and ϕ11, altered the transcriptome of their host during biofilm formation.

The preliminary studies performed prior to the transcriptional analysis showed that both lysogenic strains exhibited greater biomass accumulation in earlier stages of biofilm development. However, biomass of mature biofilms only increased in the ϕ11 lysogen. This would suggest that the mechanism(s) responsible for biofilm increase in the two lysogenic strains may be different, at least in late biofilm developmental stages. Indeed, it appears that for the ϕ80α lysogen, biofilm formation occurs at a faster rate but ultimately leads to a similar amount of total adhered biomass. Spontaneous release of phage particles was observed for both lysogens in the planktonic phase and the biofilm. Interestingly, there were fewer virions inside biofilm cells than free in the extracellular matrix. This suggests that spontaneous induction of the lytic cycle has slowed down in sessile cells at this stage of biofilm formation. Indeed, such hypothesis was re-inforced by an additional experiment showing that the maximum phage titer in the biofilm was found at 5 hours of development (Fig. S1). Similarly, Resch *et al.*[27] observed that maximum spontaneous phage release in the lysogenic strains *S. aureus* Sa113 and *S. aureus* Newman peaked before 8 hours of growth both in biofilms and in planktonic cultures. Also, these results hint that, upon lysis of the bacterial cells, the phage particles may accumulate in the matrix and, together with the released cell contents, contribute to the total biomass of the biofilm. In fact, spontaneous induction of the lytic cycle had been previously linked to increased biofilm formation in some bacteria[13]. Moreover, this "phage network" may act as a defense mechanism against competing susceptible strains as well as enhance genetic transfer within the biofilm. Indeed, Haaber *et al.*[28] already demonstrated that prophages can promote transfer of antibiotic resistance markers from neighboring cells into prophage-carrying bacteria. Taken together, all these data indicate that prophages may contribute to the increase in horizontal gene transfer observed in biofilms[29,30].

Transcriptional analysis of prophage ϕ80α genes showed a higher level of expression of genes in the lysogeny module. Interestingly, phage Tuc2009 exhibited a similar expression pattern during lysogeny of *Lactococcus lactis* UC509.9[31]. Indeed, the genes displaying the highest level of expression were those in the lysogeny module, especially the lytic cycle repressor, and one gene in the early replication module. In contrast to the results presented here, previous transcriptomic analysis of phage ϕ80α in *S. aureus* had shown expression distributed more evenly across the genome during lysogeny[32]. It is very likely that the discrepancies in the expression profile between the two studies are due to the fact that the lysogen cells were in two different growth states. Thus, while Quiles-Puchalt *et al.*[32] examined transcription in a liquid culture during early exponential phase, the analysis

described here corresponds to biofilm cells after 5 hours of development, which corresponds more accurately to late exponential phase. The results obtained for ϕ11, however, revealed a more homogeneous expression of genes throughout the phage genome, a profile that seems to correspond to a population in different stages of the lysogenic/lytic cycle. Interestingly, the gene displaying the highest level of transcription was located in the replication module. A higher gene expression in the gene replication and gene regulation module was also found in the transcriptomic analysis of a *Clostridium difficile* lysogenic strain carrying prophage phi-027[33].

Transcriptional profiling of biofilms formed by the two lysogenic strains and the prophage-free strain revealed major changes associated with the presence of the prophages. A closer look at the results from these analyses indicates that strains harboring temperate phages exhibit differences in genes affecting metabolism, virulence, biofilm formation or production of the protective pigment staphyloxanthin. From a regulatory perspective, many of the genes with differential expression in lysogenic strains belong to the SigB, CcpA and Agr regulons (Table 1 and Fig. 2B). However, the exact regulatory cascade between these systems in response to the phages remains unknown. Similarly, it is difficult to find a direct connection between the changes in gene expression and the biofilm phenotypes of the two strains. Thus, some of the genes dysregulated in both lysogens could explain an increased biofilm formation, although no hint was found regarding the lack of biofilm increase at 24 hours of development in RN450-ϕ80α. For example, extracellular proteases, which are known to reduce biofilm formation in *S. aureus*[34], were downregulated in the lysogens. This may be related to the lesser expression of genes belonging to the Agr quorum sensing system, which is known to participate in biofilm dispersion in *S. aureus*[35,36]. Also, there is increased expression of genes coding for proteins involved in adhesion and in production of extracellular polysaccharide. Other genes that may alter biofilm formation in the presence of the prophages are those encoding regulatory proteins SarS, SarT or ClpL. SarS is one of several SarA-like regulators that participate in the complex network controlling virulence-gene expression in *S. aureus*[37]. In particular, SarS is a positive regulator of *spa*, the gene that codes for staphylococcal protein A, which is involved in virulence-related traits as well as adherence[22]. Interestingly, SarT was previously found to induce expression of SarS[38]. ClpP, on the other hand, is one of the ATPases that form the ClpP proteolytic complex, which is known to have a pleiotropic effect on *S. aureus*, participating in processes like biofilm formation, virulence, antibiotic resistance and survival under stressful conditions[24,39]. However, the specific role of ClpL in *S. aureus* has not been well defined yet, although a study by Frees *et al.*[24] revealed its involvement in the multiplication of the pathogen inside bovine mammary epithelial cells.

As mentioned previously, there are several dysregulated genes in prophage-carrying strains that are known to be under the control of CcpA. However, some of the identified genes exhibited changes indicating that CcpA was activated in the lysogens, whereas other dysregulated genes appeared to indicate the opposite. For example, CcpA activation could explain the higher expression of *uhpT* and the lower expression of *arcR* and *arcABDC*[40]. In contrast, the upregulation of *spa*, *purD*, *pckA* and *fbp* would suggest inhibition of CcpA activity[40]. Interestingly, deletion of CcpA in *S. aureus* SA113 inhibited biofilm formation as it decreased production of PIA and accumulation of eDNA[41]. In a previous work, Seidl *et al.*[42] had also demonstrated that gene regulation by CcpA modulated expression of antibiotic and virulence determinants in *S. aureus* by studying the transcriptional changes displayed by *ccpA* deletion mutants derived from strains COLn and Newman.

The sigma B regulon is typically induced under stress conditions, including heat, oxidative and antibiotic stress. One of the genes upregulated by SigB is *asp23*, which codes for the alkaline shock protein Asp23, a membrane-anchored protein thought to participate in homeostasis of the cell envelope[43]. Another effect of this response is the increased production of staphyloxanthin. This carotenoid pigment embeds itself into the cytoplasmic membrane and has been shown to promote virulence, hamper killing by neutrophils and decrease susceptibility to cationic antimicrobial peptides[44,45]. The alternative sigma factor also participates in the regulation of biofilm formation in *S. aureus* by leading to decreased expression of extracellular dispersion factors, like proteases[25]. Thus, activation of the SigB regulon may be to some extent related to the increased attached biomass displayed by the lysogenic strains. Moreover, biofilm formation is a recognized persistence strategy of bacterial pathogens that marks the transition from an acute infection to a chronic infection[46]. In that sense, it has been recently shown that activation of the SigB regulon and inactivation of the Agr regulon are necessary for adaptation of *Staphylococcus* during chronic infections[46]. All this information suggests that prophage carriage may be beneficial for the microbe during the infection process, a possibility that should be the focus of subsequent studies. In that sense, it must be highlighted that strain RN450 is a good model for studying this phenomenon precisely because of its inherent SigB-negative phenotype. Indeed, this strain is known to carry a mutation in the *rsbUVW-sigB* operon that leads to reduced activation of SigB[47]. Therefore, the phenomenon observed here could be regarded as if lysogenization of this strain compensates for the aforementioned mutation[47]. Conversely, staphyloxanthin production in SigB-positive strains may mask the potential impact of prophages on the regulation of the SigB regulon. Interestingly, the alternative sigma factor in *E. coli*, RpoS, was upregulated in a lysogenic strain carrying prophage ϕ24B[48]. A consequence of this was increased acid resistance due to upregulation of the glutamic acid decarboxylase (GAD) operon. Another interesting observation is that RpoS was found to modulate phage induction in *E. coli*[49]. There are also examples of prophages encoding alternative sigma factors in their genomes, as is the case of *Bacillus anthracis* phages, which have an effect on important processes like biofilm formation and sporulation[50]. A further connection between phages and sigma factors is that the RepR repressor from *C. difficile* temperate phage CD119 repressed the expression of the alternative sigma factor TcdR[51]. Altogether, these results reflect the existence of complex interactions between the CcpA and SigB regulons, and their respective connections to the agr quorum-sensing system (Fig. 2B). Further studies should decipher more in detail the physiological and molecular processes involved in this regulatory network.

Experiments carried out with mutant strains of prophage ϕ80α indicated that the mechanisms behind biofilm induction and greater staphyloxanthin production were different. Indeed, the biofilm phenotype seemed to correlate with spontaneous activation of the lytic cycle. This suggests that release of cellular components and phage particles due to cell lysis may be responsible for the enhanced accumulation of adhered biomass. By contrast,

there was no apparent connection between staphyloxanthin production and phage particle release. It is worth noting, however, that an intact CI protein is necessary for both properties. This suggests that the CI protein may play a role within the bacterial regulatory networks. Interestingly, the regulator CI from phage ϕ11 was shown to inhibit aureocin A79 production in synergy with the bacterial regulatory protein AurR[52]. Nonetheless, further research is still necessary to determine how these interactions take place. Likewise, staphyloxanthin production varied in different lysogenic strains, carrying prophages ϕ80α, ϕ11, ϕ53 and ϕ85, which exhibit differences in the sequence of their respective CI proteins. However, no conclusions can be drawn without performing further experiments, such as studies involving heterologous complementation of the CI protein. Moreover, differences in the lysogeny module between these lysogenic strains are not limited to the CI protein. Therefore, the effect of other phage proteins on this phenotype should also be examined.

In conclusion, the results of this study show that lysogenization of *S. aureus* with two phages leads to increased biofilm formation and staphyloxanthin production, as well as transcriptional changes involving some of the major regulatory networks in this pathogen. Indeed, as discussed above, the interconnection between the SigB regulon and the Agr quorum-sensing signaling cascade plays a paramount role in modulating the alternation between the lifestyles associated to acute and chronic infections, as well as the development of sessile communities. In that sense, carrying a prophage may contribute to these bacterial adaptions, thereby exerting a positive impact on the host population. Moreover, it appears that mutations in certain phage genes abrogate this effect, being especially interesting the potential participation of the CI protein in regulating the expression of host genes. Nonetheless, further work is still needed to ascertain if this is really the case. Altogether, our data emphasizes again the dramatic effect of bacteriophages on microbial communities. Evidently, more studies are still required to understand how interactions between staphylophages and their host develop. However, what is becoming increasingly clear is that studying phage-host interactions will be paramount to gain more knowledge of bacterial population dynamics. In turn, this information will provide a more realistic view of the role that microbes play in natural environments as well as help to design new strategies to fight unwanted microorganisms.

Methods

Bacterial strains and growth conditions. All bacterial strains used in this study are listed in Table 2. Routine growth of *S. aureus* cultures was performed at 37 °C on Baird-Parker agar plates (AppliChem, Germany) or in TSB (Tryptic Soy Broth, Scharlau, Barcelona, Spain) with shaking. Staphyloxanthin production was monitored by inoculating 5 µl drops from overnight cultures on TSA plates containing 1.5% agar and 0.25% glucose. These plates were subsequently incubated for 48 hours at 37 °C.

Biofilm formation assays. Biofilm assays were performed as previously described but with some modifications[53]. Thus, *S. aureus* strains were grown overnight and subsequently diluted to a cell count of 10^6 cfu/ml in TSB supplemented with 0.25% w/v D-(+)-glucose (TSBG). 200 µl aliquots from these cell suspensions were poured into the wells of a 96-well microtiter plate (Thermo Scientific, NUNC, Madrid, Spain). Biofilms were allowed to develop for 24 hours at 37 °C, after which adhered biomass was quantified by crystal violet staining. Briefly, the supernatant was removed and the wells were washed twice with PBS (137 mM NaCl, 2.7 mM KCl, 10 mM Na_2HPO_4 and 2 mM KH_2PO_4; pH 7.4). Then, 200 µl of 0.1% (w/v) crystal violet were added to the wells and subsequently removed after 15 minutes of incubation. Excess crystal violet was washed with water and 33% (v/v) acetic acid was added to solubilize the dye attached to the well prior to quantification by measuring absorbance at 595 nm (A_{595}) with a Bio-Rad Benchmark plus microplate spectrophotometer (Bio-Rad Laboratories, Hercules, CA, USA).

Titration of plaque forming units present in the planktonic phase and the biofilm was carried out according to the protocol described by González *et al.*[54], in which phages were identified as being "free" or "cell-associated" (infectious centers) for each phase. The resulting samples were filtered (0.45 µm, VWR, Spain) to remove bacterial cells and titrated according to the double layer technique using strain *S. aureus* RN4220 as a host.

RNA purification and analysis. Samples of 5 h biofilms grown at 37 °C were collected from two independent biological replicates for each strain (RN450, RN450-ϕ11 and RN450-ϕ80α) and total RNA was prepared as described elsewhere[21]. Purity and concentration of the RNA samples were checked by agarose gel electrophoresis and quantification with an Epoch microplate spectrophotometer (Biotek). 10 µg of RNA from each sample were sent to Macrogen Inc. (South Korea) for sequencing with the Illumina HiSeq2000 platform (Illumina, San Diego, CA, USA). Bioinformatic analysis was carried out at Dreamgenics (Dreamgenics, Oviedo, Spain). Quality of the RNA-seq reads was checked with FastQC. RNA-seq reads were then mapped to the *S. aureus* NCTC 8325, phage ϕ11 and phage ϕ80α genomes by using BowTie2. Uniquely mapped reads were kept for subsequent analysis of differential gene expression using EDGE-pro software. RNA-Seq data have been deposited in NCBI's Gene Expression Omnibus (GEO) and can be accessed through GEO series accession number GSE111012.

Transcriptional changes for selected differentially-expressed genes identified in the RNA-seq analyses were confirmed by quantitative reverse transcription-PCR (RT-qPCR). Briefly, following RNA preparation, cDNA was obtained from 0.5 µg aliquots of the RNA samples by using iScript™ Reverse Transcription Supermix for RT-qPCR (BioRad). The resulting cDNA samples were then used as templates for RT-qPCR analysis using Power SYBR Green PCR Master Mix (Applied BioSystems). Three independent biological replicates were analyzed for each strain. Fold-changes were calculated following the Ct method and the reference gene was *rplD*.

Statistical analyses. Data from independent biological replicates was analyzed with a two-tailed Student's t-test. Significance was set at a P-value threshold of 0.05.

References

1. Howard-Varona, C., Hargreaves, K. R., Abedon, S. T. & Sullivan, M. B. Lysogeny in nature: mechanisms, impact and ecology of temperate phages. *ISME J.* **11**, 1511–1520 (2017).
2. Fernández, L., Rodríguez, A. & García, P. Phage or foe: an insight into the impact of viral predation on microbial communities. *ISME J*. (2018).
3. Casjens, S. Prophages and bacterial genomics: what have we learned so far? *Mol. Microbiol.* **49**, 277–300 (2003).
4. Duerkop, B. A., Clements, C. V., Rollins, D., Rodrigues, J. L. & Hooper, L. V. A composite bacteriophage alters colonization by an intestinal commensal bacterium. *Proc. Natl. Acad. Sci. USA* **109**, 17621–17626 (2012).
5. Nanda, A. M., Thormann, K. & Frunzke, J. Impact of spontaneous prophage induction on the fitness of bacterial populations and host-microbe interactions. *J. Bacteriol.* **197**, 410–419 (2015).
6. Selva, L. *et al*. Killing niche competitors by remote control bacteriophage induction. *Proc. Natl. Acad. Sci. USA* **106**, 1234–1238 (2009).
7. Fortier, L. C. & Sekulovic, O. Importance of prophages to evolution and virulence of bacterial pathogens. *Virulence* **4**, 354–365 (2013).
8. Brüssow, H., Canchaya, C. & Hardt, W.-D. Phages and the evolution of bacterial pathogens: from genomic rearrangements to lysogenic conversion. *Microbiol. Mol. Biol. Rev.* **68**, 560–602 (2004).
9. Novick, R. P., Christie, G. E. & Penadés, J. R. The phage-related chromosomal islands of Gram-positive bacteria. *Nat. Rev. Microbiol.* **8**, 541–551 (2010).
10. Wang, X. *et al*. Cryptic prophages help bacteria cope with adverse environments. *Nat. Commun.* **1**, 147 (2010).
11. Gillis, A. & Mahillon, J. Influence of lysogeny of Tectiviruses GIL01 and GIL16 on *Bacillus thuringiensis* growth, biofilm formation, and swarming motility. *Appl. Environ. Microbiol.* **80**, 7620–7630 (2014).
12. Rossmann, F. S. *et al*. Phage-mediated dispersal of biofilm and distribution of bacterial virulence genes is induced by quorum sensing. *PLoS Pathog.* **11**, e1004653 (2015).
13. Gödeke, J., Paul, K., Lassak, J. & Thormann, K. M. Phage-induced lysis enhances biofilm formation in *Shewanella oneidensis* MR-1. *ISME J* **5**, 613–626 (2011).
14. Rice, S. A. *et al*. The biofilm life cycle and virulence of *Pseudomonas aeruginosa* are dependent on a filamentous prophage. *ISME J.* **3**, 271–282 (2009).
15. Webb, J. S., Lau, M. & Kjelleberg, S. Bacteriophage and phenotypic variation in *Pseudomonas aeruginosa* biofilm development. *J. Bacteriol.* **186**, 8066–8073 (2004).
16. Feil, E. J. *et al*. How clonal is *Staphylococcus aureus*? *J. Bacteriol.* **185**, 3307–3316 (2003).
17. Xia, G. & Wolz, C. Phages of *Staphylococcus aureus* and their impact on host evolution. *Infect. Genet. Evol.* **21**, 593–601 (2014).
18. Lindsay, J. A. & Holden, M. T. *Staphylococcus aureus*: superbug, super genome? *Trends Microbiol.* **12**, 378–385 (2004).
19. Otto, M. Staphylococcal infections: mechanisms of biofilm maturation and detachment as critical determinants of pathogenicity. *Annu. Rev. Med.* **64**, 175–188 (2013).
20. Hosseinidoust, Z., Tufenkji, N. & van de Ven, T. G. Formation of biofilms under phage predation: considerations concerning a biofilm increase. *Biofouling* **29**, 457–468 (2013).
21. Fernández, L. *et al*. Low-level predation by lytic phage phiIPLA-RODI promotes biofilm formation and triggers the stringent response in *Staphylococcus aureus*. *Sci. Rep*. **7**, 40965 (2017).
22. Merino, N. *et al*. Protein A-mediated multicellular behavior in *Staphylococcus aureus*. *J. Bacteriol.* **191**, 832–843 (2009).
23. Makhlin, J. *et al*. *Staphylococcus aureus* ArcR controls expression of the arginine deiminase operon. *J. Bacteriol.* **189**, 5976–5986 (2007).
24. Frees, D. *et al*. Clp ATPases are required for stress tolerance, intracellular replication and biofilm formation in *Staphylococcus aureus*. *Mol. Microbiol.* **54**, 1445–1462 (2004).
25. Bischoff, M. *et al*. Microarray-based analysis of the *Staphylococcus aureus* sigmaB regulon. *J. Bacteriol.* **186**, 4085–4099 (2004).
26. Altshul, S. F., Gish, W., Miller, W., Myers, E. W. & Lipman, D. J. Basic local alignment search tool. *J. Mol. Biol.* **215**, 403–410 (1990).
27. Resch, A., Fehrenbacher, B., Eisele, K., Schaller, M. & Götz, F. Phage release from biofilm and planktonic *Staphylococcus aureus* cells. *FEMS Microbiol. Lett.* **52**, 89–96 (2005).
28. Haaber, J. *et al*. Bacterial viruses enable their host to acquire antibiotic resistance genes from neighbouring cells. *Nat. Commun.* **7**, 13333 (2016).
29. Cook, L. *et al*. Biofilm growth alters regulation of conjugation by a bacterial pheromone. *Mol. Microbiol.* **81**, 1499–1510 (2011).
30. Savage, V. J., Chopra, I. & O'Neill, A. J. *Staphylococcus aureus* biofilms promote horizontal transfer of antibiotic resistance. *Antimicrob. Agents Chemother.* **57**, 1968–1970 (2013).
31. Ainsworth, S., Zomer, A., Mahony, J. & van Sinderen, D. Lytic infection of *Lactococcus lactis* by bacteriophages Tuc2009 and c2 triggers alternative transcriptional host responses. *Appl. Environ. Microbiol.* **79**, 4786-4798 (2013).
32. Quiles-Puchalt, N. *et al*. A super-family of transcriptional activators regulates bacteriophage packaging and lysis in Gram-positive bacteria. *Nucleic Acids Res.* **41**, 7260–7275 (2013).
33. Sekulovic, O. & Fortier, L. C. Global transcriptional response of *Clostridium difficile* carrying the CD38 prophage. *Appl. Environ. Microbiol.* **81**, 1364–1374 (2015).
34. Martí, M. *et al*. Extracellular proteases inhibit protein-dependent biofilm formation in *Staphylococcus aureus*. *Microbes Infect.* **12**, 55–64 (2010).
35. Vuong, C., Saenz, H. L., Götz, F. & Otto, M. Impact of the agr quorum-sensing system on adherence to polystyrene in *Staphylococcus aureus*. *J. Infect. Dis.* **182**, 1688–93 (2000).
36. Boles, B. R. & Horswill, A. R. Agr-mediated dispersal of *Staphylococcus aureus* biofilms. *PLoS Pathog.* **4**, e1000052 (2008).
37. Cheung, A. L., Nishina, K. A., Trotonda, M. P. & Tamber, S. The SarA protein family of *Staphylococcus aureus*. *Int. J. Biochem. Cell Biol.* **40**, 355–361 (2008).
38. Schmidt, K. A., Manna, A. C. & Cheung, A. L. SarT influences *sarS* expression in *Staphylococcus aureus*. *Infect. Immun.* **71**, 5139–5148 (2003).
39. Frees, D., Gerth, U. & Ingmer, H. Clp chaperones and proteases are central in stress survival, virulence and antibiotic resistance of *Staphylococcus aureus*. *Int. J. Med. Microbiol.* **304**, 142–149 (2014).
40. Seidl, K. *et al*. Effect of a glucose impulse on the CcpA regulon in *Staphylococcus aureus*. *BMC Microbiol.* **9**, 95 (2009).
41. Seidl, K. *et al*. *Staphylococcus aureus* CcpA affects biofilm formation. *Infect. Immun.* **76**, 2044–2050 (2008).
42. Seidl, K. *et al*. *Staphylococcus aureus* CcpA affects virulence determinant production and antibiotic resistance. *Antimicrob. Agents Chemother.* **50**, 1183–1194 (2006).
43. Müller, M. *et al*. Deletion of membrane-associated Asp23 leads to upregulation of cell wall stress genes in *Staphylococcus aureus*. *Mol Microbiol* **93**, 1259–1268 (2014).
44. Liu, G. Y. *et al*. *Staphylococcus aureus* golden pigment impairs neutrophil killing and promotes virulence through its antioxidant activity. *J. Exp. Med.* **202**, 209–215 (2005).
45. Mishra, N. N. *et al*. Carotenoid-related alteration of cell membrane fluidity impacts *Staphylococcus aureus* susceptibility to host defense peptides. *Antimicrob. Agents Chemother.* **55**, 526–531 (2011).
46. Tuchscherr, L. *et al*. Sigma factor SigB is crucial to mediate *Staphylococcus aureus* adaptation during chronic infections. *PLoS Pathog.* **11**, e1004870 (2015).

47. Kullik, I., Giachino, P. & Fuchs, T. Deletion of the alternative sigma factor sigmaB in *Staphylococcus aureus* reveals its function as a global regulator of virulence genes. *J. Bacteriol.* **180**, 4814–4820 (1998).
48. Veses-García, M. *et al*. Transcriptomic analysis of Shiga-toxigenic bacteriophage carriage reveals a profound regulatory effect on acid resistance in *Escherichia coli*. *Appl. Environ. Microbiol.* **81**, 8118–8125 (2015).
49. Imamovic, L., Ballesté, E., Martínez-Castillo, A., García-Aljaro, C. & Muniesa, M. Heterogeneity in phage induction enables the survival of the lysogenic population. *Environ Microbiol.* **18**, 957–969 (2016).
50. Schuch, R. & Fischetti, V. A. The secret life of the anthrax agent *Bacillus anthracis*: bacteriophage-mediated ecological adaptations. *PLoS One* **4**, e6532 (2009).
51. Govind, R., Vediyappan, G., Rolfe, R. D., Dupuy, B. & Fralick, J. A. Bacteriophage-mediated toxin gene regulation in *Clostridium difficile*. *J. Virol.* **83**, 12037–12045 (2009).
52. Coelho, M. L., Fleming, L. R. & Bastos, M. C. Insights into aureocin A70 regulation: participation of regulator AurR, alternative transcription factor σ(B) and phage ϕ11 regulator cI. *Res. Microbiol.* **167**, 90–102 (2016).
53. Herrera, J. J., Cabo, M. L., González, A., Pazos, I. & Pastoriza, L. Adhesion and detachment kinetics of several strains of *Staphylococcus aureus* subsp. *aureus* under three different experimental conditions. *Food Microbiol.* **24**, 585–591 (2007).
54. González, S. *et al*. The behavior of *Staphylococcus aureus* dual-species biofilms treated with bacteriophage phiIPLA-RODI depends on the accompanying microorganism. *Appl. Environ. Microbiol.* **83**, e02821–16 (2017).
55. Novick, R. Properties of a cryptic high-frequency transducing phage in *Staphylococcus aureus*. *Virology* **33**, 155–166 (1967).
56. Úbeda, C., Barry, P., Penadés, J. R. & Novick, R. P. A pathogenicity island replicon in *Staphylococcus aureus* replicates as an unstable plasmid. *Proc Natl Acad Sci USA* **104**, 14182–14188 (2007).

Acknowledgements

Special thanks to Roxana Calvo and Ana Belén Campelo for technical assistance. This work was funded by grants AGL2015-65673-R (Program of Science, Technology and Innovation 2013–2017), Proyecto Intramural CSIC 201770E016, and GRUPIN14-139 (FEDER EU funds, Principado de Asturias, Spain). L.F. was awarded a "Marie Curie Clarin-Cofund" grant. PG, BM and AR are members of the bacteriophage network FAGOMA and the FWO Vlaanderen funded "Phagebiotics" research community (WO.016.14).

Author Contributions

L.F., S.G., N.Q.-P., J.R.P., P.G., D.G. and A.R. wrote the manuscript. L.F., S.G. and N.Q.-P. performed the experiments. L.F., P.G. and A.R. conceived the experiments. All authors reviewed the manuscript.

Additional Information

Supplementary information accompanies this paper at https://doi.org/10.1038/s41598-018-31107-z.

Competing Interests: The authors declare no competing interests.

Publisher's note: Springer Nature remains neutral with regard to jurisdictional claims in published maps and institutional affiliations.

Capítulo 3

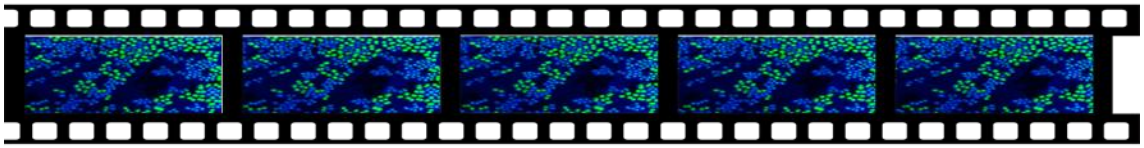

Capítulo 3: Influencia de las proteínas líticas en la formación de biofilms

Las proteínas líticas derivadas de fagos son una alternativa prometedora a los antimicrobianos convencionales. Una de sus propiedades más interesantes es que no seleccionan cepas resistentes con una frecuencia alta. Este fenómeno se debe probablemente al hecho de que el sustrato de su actividad enzimática, el peptidoglicano, es esencial para la viabilidad de la célula bacteriana y, por lo tanto, no puede modificarse con tanta facilidad como otras estructuras. Además, la ingeniería genética permite el diseño de nuevas proteínas "a medida" que pueden exhibir propiedades antibacterianas mejoradas. Un ejemplo de esto es la proteína quimérica CHAPSH3b, que está formada por un dominio catalítico de la peptidoglicano hidrolasa asociada al virión del fago vB_SauS-phiIPLA88 (HydH5) y el dominio de unión a la pared celular de la lisostafina. En esta Tesis se ha estudiado el efecto de dosis subinhibitorias de dos proteínas líticas derivadas de fagos, la proteína quimérica CHAPSH3b y la endolisina LysH5, sobre la capacidad de distintas cepas de *S. aureus* para formar biofilms.

1. Fernández, L., González, S., Campelo, A. B., Martínez, B., Rodríguez, A., & García, P. (2017). Downregulation of Autolysin-Encoding Genes by Phage-Derived Lytic Proteins Inhibits Biofilm Formation in *Staphylococcus aureus*. *Antimicrobial agents and chemotherapy*, 61(5), e02724-16. https://doi.org/10.1128/AAC.02724-16

2. Fernández, L., González, S., Gutiérrez, D., Campelo, AB, Martínez, B., Rodríguez, A. and García, P. (2018). Characterizing the Transcriptional Effects of Endolysin Treatment on Established Biofilms of *Staphylococcus aureus*. *Bio-protocol* 8(12): e2891. https://doi.org/10.21769/BioProtoc.2891

Downregulation of autolysin-encoding genes by phage-derived lytic proteins inhibits biofilm formation in *Staphylococcus aureus*

Running title: Transcriptional responses to phage-derived lysins

Lucía Fernández*, Silvia González, Ana Belén Campelo, Beatriz Martínez, Ana Rodríguez, Pilar García

Address: Instituto de Productos Lácteos de Asturias (IPLA-CSIC). Paseo Río Linares s/n 33300- Villaviciosa, Asturias, Spain.

*Corresponding author: Lucía Fernández

IPLA-CSIC, 33300-Villaviciosa, Asturias, Spain.

e-mail: lucia.fernandez@ipla.csic.es

Phone: +34 985 89 21 31

Fax: +34 985 89 22 33

Abstract

Phage-derived lytic proteins are a promising alternative to conventional antimicrobials. One of their most interesting properties is that they do not readily select for resistant strains, which is likely due to the fact that their targets are essential for the viability of the bacterial cell. Moreover, genetic engineering allows the design of new "tailor-made" proteins that may exhibit improved antibacterial properties. One example of this is the chimeric protein CHAPSH3b, which consists of a catalytic domain from the virion-associated peptidoglycan (PG) hydrolase of phage vB_SauS-phiIPLA88 (HydH5) and the cell wall binding domain of lysostaphin. CHAPSH3b had previously shown the ability to kill *S. aureus* cells. Here, we demonstrate that this lytic protein also has potential for the control of biofilm-embedded *S. aureus* cells. Additionally, subinhibitory doses of CHAPSH3b can decrease biofilm formation by some *S. aureus* strains. Trancriptional analysis revealed that exposure of *S. aureus* cells to this enzyme leads to the downregulation of several genes coding for bacterial autolysins. One of these proteins, namely the major autolysin AtlA, is known to participate in staphylococcal biofilm development. Interestingly, an *atl* mutant strain did not display inhibition of biofilm development when grown at subinhibitory concentrations of CHAPSH3b, contrary to the observations made for the parental and complemented strains. Also, deletion of *atl* led to low-level resistance to CHAPSH3b and endolysin LysH5. Overall, our results reveal new aspects that should be considered when designing new phage-derived lytic proteins aimed for antimicrobial applications.

INTRODUCTION

Over the last few decades, there has been a dramatic rise in the resistance of bacterial pathogens to conventional antimicrobials. In response to this phenomenon, scientists have stepped up their efforts to develop new agents for the control of pathogenic microbes. This research has involved careful reconsideration of some previously dismissed strategies, sometimes giving a new twist to old therapeutics. One such example is phage therapy, which has recently attracted considerable attention in the field of antimicrobial development (1, 2). Moreover, advances in molecular biology allow a more sophisticated design of phage-derived therapeutics. Thus, we can now dissect the specific mechanisms employed by phages to attack bacteria and use them to our advantage. For instance, phage lytic proteins, such as endolysins and virion-associated peptidoglycan (PG) hydrolases, have been proposed as promising antibacterial agents, the so-called enzybiotics (3). These enzymes play a very important role in the lytic cycle, as their muralytic activity enables the phage to enter the bacterial cell (virion-associated PG hydrolases) and ultimately lyse the host cell to release the viral progeny (endolysins). However, both types of proteins can potentially cause exolysis or "lysis from without" when used as antimicrobials (4, 5). Indeed, several studies have proven their ability to lyse planktonic and biofilm-embedded cells from different species (3).

There is evidence that phage lytic proteins can be effective for the control of the notorious human pathogen *Staphylococcus aureus* (6). This bacterium is particularly problematic due to its ability to form biofilms on a wide range of surfaces, which facilitates survival of bacterial cells even in hostile environments (7). Additionally, there is a high prevalence of *S. aureus* strains resistant to most antibiotics available on the market. This is why the term "superbug" has been often used in connection with this

71 microorganism (8). Some antistaphylococcal phage endolysins have shown antibiofilm
72 activity, including phage 11 endolysin (9), lysin CF-301 (10) and SAL-2, an endolysin
73 derived from phage SAP-2 (11), amongst others (12, 13). Other two promising phage
74 lytic proteins used against *S. aureus* are endolysin LysH5 and PG hydrolase HydH5,
75 both derived from phage vB_SauS-phiIPLA88 (14, 15). In the case of LysH5, Gutiérrez
76 et al. (13) showed not only that this protein is effective for biofilm removal but also that
77 subinhibitory concentrations resulted in decreased biofilm formation. However, the
78 molecular mechanisms mediating this effect remained unknown. Indeed, there is no
79 available information regarding the responses of bacterial cells to phage-derived lytic
80 proteins as of now. The virion-associated PG hydrolase HydH5 consists of two lytic
81 domains: an N-terminal cysteine, histidine-dependent amidohydrolase/peptidase
82 (CHAP) domain and a C-terminal LYZ2 (lysozyme subfamily 2) domain. However, no
83 cell wall binding (CWB) domain could be identified in the amino acid sequence of
84 HydH5. In a subsequent study, Rodríguez-Rubio et al. (16) demonstrated that the
85 activity of protein HydH5 could be improved upon by fusing its CHAP domain to the
86 CWB domain SH3b of lysostaphin. The resulting chimeric protein was designated
87 CHAPSH3b and exhibited specific activity against staphylococci. Moreover,
88 CHAPSH3b displayed the ability to eliminate *S. aureus* cells in milk and could
89 withstand pasteurization treatment as well as storage at 4 ºC for 3 days (17).
90 Nonetheless, the potential of CHAPSH3b for biofilm removal remained to be explored.

91 Initially, our main goal was to evaluate the antibiofilm ability of protein CHAPSH3b.
92 However, our preliminary data led us to investigate the transcriptional responses of *S.*
93 *aureus* cells to subinhibitory concentrations of this enzybiotic. The results of this
94 analysis suggest that the biofilm inhibitory effect of these proteins may be due to
95 downregulation of endogenous cell wall hydrolases, which are known to participate in

biofilm development in staphylococci. Furthermore, we show here that deletion of the gene encoding the major autolysin of *S. aureus*, AtlA, confers low-level resistance to phage lytic proteins on *S. aureus* cells. Thus, this work reports for the first time gene expression changes associated with exposure to phage lytic proteins and reveals that these changes may be linked to adaptive resistance and antibiofilm properties.

MATERIALS AND METHODS

Bacterial strains, culture conditions and purification of phage-derived lytic proteins. The *S. aureus* strains used in this study are listed in Table 1. *S. aureus* cultures were routinely grown at 37 ºC on Baird-Parker agar plates (AppliChem, Germany) or in TSB (Tryptic Soy Broth, Scharlau, Barcelona, Spain) with shaking. When necessary, the antibiotics spectinomycin and chloramphenicol, both purchased from Sigma (Sigma, Missouri, USA), were added to the growth media at concentrations of 150 μg/ml and 20 μg/ml, respectively.

PG hydrolases CHAPSH3b and LysH5 were purified as described previously (18). The purified proteins were then checked by SDS-PAGE analysis and quantified by using the Quick Start™ Bradford Protein Assay kit (Bio-Rad).

Treatment of preformed biofilms. Biofilms were grown according to the protocol described by Herrera et al. (19) with some modifications. Briefly, overnight cultures of the different *S. aureus* strains were diluted in fresh TSBg (TSB supplemented with 0.25% w/v D-(+)-glucose) medium down to a final concentration of 10^6 cfu/ml. 200 μl of these suspensions were poured into each well of a 96-well microtiter plate (Thermo Scientific, NUNC, Madrid, Spain). These microtiter plates were then incubated for 24 hours at 25 ºC or 37 ºC to allow biofilm formation. The planktonic phase was then removed and the adhered cells were washed twice with phosphate-buffered saline (PBS)

120 (137 mM NaCl, 2.7 mM KCl, 10 mM Na_2HPO_4 and 2 mM KH_2PO_4; pH 7.4). These
121 preformed biofilms were subsequently treated with sodium phosphate (NaPi) buffer (50
122 mM pH 7.4) alone or containing 4× MIC of protein CHAPSH3b (15.64 μg/ml or 250.24
123 μg/ml for samples incubated at 25 ºC or 37 ºC, respectively) for 6 hours at the same
124 temperature of biofilm formation. After treatment, the adhered phase was washed again
125 with PBS and stained with 200 μl of 0.1% (w/v) crystal violet for biomass
126 quantification as described previously (13). After 15 minutes, the excess crystal violet
127 was washed with water and the dye attached to the well was solubilized with 33% (v/v)
128 acetic acid. Finally, absorbance at 595 nm (A_{595}) was measured with a Bio-Rad
129 Benchmark plus microplate spectrophotometer (Bio-Rad Laboratories, Hercules, CA,
130 USA). Alternatively, the adhered viable cells were counted by scratching the wells
131 twice with sterile cotton swabs as previously described (13). The cells were then
132 resuspended into 9 ml of PBS by vigorous vortexing and serial dilutions were plated
133 onto TSA plates and incubated at 37 ºC.

134 **Minimal inhibitory concentration (MIC) determination and biofilm formation in**
135 **the presence of subinhibitory concentrations of PG hydrolases.** Determination of
136 MIC values was performed according to the broth microdilution technique following the
137 CLSI guidelines (20, 21) but using TSBg as a growth medium. The MIC was
138 determined as the lowest concentration of the protein that inhibited visible bacterial
139 growth after 24 hours of incubation at 37 ºC or 25 ºC. At the end of the incubation, the
140 attached biomass was quantified by crystal violet staining as described above. All MIC
141 assays were repeated 5 to 8 times.

142 **Analysis by confocal laser scanning microscopy (CLSM) and time-lapse**
143 **microscopy.** For microscopy analyses, biofilms were grown on 2-well μ-slides with a

glass bottom (ibidi, USA). Each well was inoculated with 1 ml of a cell suspension containing 10^6 cfu/ml in TSBg and 1 ml of TSBg alone or 1 ml of TSBg containing a subinhibitory concentration of CHAPSH3b. Biofilms were then allowed to grow for 24 hours at 37 ºC or 25 ºC. To test the effect of subinhibitory concentrations of the protein, the planktonic phase was removed after biofilm development and wells were washed with PBS prior to staining with Live/Dead® BacLight™ kit (Invitrogen AG, Basel, Switzerland). To analize the impact of CHAPSH3B treatment on preformed biofilms, the planktonic phase was replaced by NaPi buffer (negative control) or buffer containing 4x MIC of CHAPSH3b and then incubated for an additional 6 hours at the same temperature. After treatment, biofilms were stained with Live/Dead® BacLight™ kit (Invitrogen AG, Basel, Switzerland). All samples were then observed under a confocal scanning laser microscope (DMi8, Leica Microsystems) using a 63× oil objective.

For time-lapse microscopy, 24-hour biofilms grown at 37 ºC were washed with PBS and then placed in an incubation chamber set at 37 ºC connected to an inverted microscope (DMi8, Leica Microsystems) equipped with a Leica DFC365FX digital camera. Then, the biofilm was treated with NaPi buffer containing CHAPSH3b at 250.24 µg/ml (4× MIC) and monitored for 6 hours. Images were acquired every 15 minutes with software LasX (Leica Microsystems).

Transcriptional analysis. Samples from liquid cultures were grown to an OD_{600} of 0.5 at 25 ºC and then exposed to a subinhibitory concentration of CHAPSH3b (0.98 µg/ml) or LysH5 (10.94 µg/ml) for 10 minutes. Cells were then centrifuged and the pellets were frozen at -80 ºC until further processing. Biofilms were grown for 24 hours at 25 ºC, supernatant was then removed and replaced by NaPi buffer alone or containing

168 10.94 μg/ml of protein LysH5. Biofilms were then incubated for 30 minutes before
169 scraping the adhered cells as previously described (22). Following treatment with RNA
170 protect (Qiagen), the samples were stored at -80 ºC prior to RNA purification. Total
171 RNA from *S. aureus* samples was isolated as previously described (22). Briefly, cell
172 lysis was performed by mechanical disruption with a FastPrep®-24 in a solution of
173 phenol-chloroform 1:1, glass beads (Sigma) and 80 mM DTT. RNA isolation was
174 performed with the Illustra RNA spin Mini kit (GE Healthcare). Afterwards, RNA
175 samples were treated with Turbo DNAse (Ambion) to remove traces of genomic DNA
176 and 1 μl Superase inhibitor (Ambion) was added to each 50 μl sample for storage at -80
177 ºC. RNA quality was checked by agarose gel electrophoresis and RNA concentration
178 was determined with a microplate spectrophotometer Epoch (Biotek).

179 For RNA-seq analysis, 8 μg of RNA from each sample were sent to Macrogen Inc.
180 (South Korea). Sequencing was performed by using the Illumina HiSeq2000 platform
181 (Illumina, San Diego, CA, USA) and quality control of the reads was carried out by
182 using FastQC. Mapping of the RNA-seq reads to the *S. aureus* NCTC 8325 genome was
183 carried out with BowTie2 and uniquely mapped reads were used for subsequent
184 analyses. The differential gene expression analysis was carried out with EDGE-pro
185 software. Bioinformatic analysis was performed at Dreamgenics (Dreamgenics, Oviedo,
186 Spain). RNA-Seq data have been deposited in NCBI's Gene Expression Omnibus
187 (GEO) and can be accessed through GEO series accession number GSE94512.

188 To perform quantitative reverse transcription-PCR (RT-qPCR), 0.5 μg of each RNA
189 sample were converted into cDNA by using iScript™ Reverse Transcription Supermix
190 for RT-qPCR (BioRad). Then, 2.5 μl of a 1:25 dilution of cDNA were added to each
191 well together with Power SYBR Green PCR Master Mix (Applied BioSystems). Three

192 independent cultures, each repeated in duplicate, were tested for each condition.
193 Calculation of the fold-changes was carried out according to the Ct method using the
194 *rplD* gene as a control.

195 **Statistical analyses.** Data corresponding to three independent biological replicates was
196 analyzed with a two-tailed Student´s t-test. P-values < 0.05 were considered significant.

197 **RESULTS**

198 **Treatment of preformed biofilms with protein CHAPSH3b.** Previous studies had
199 demonstrated the antistaphylococcal activity of the fusion protein CHAPSH3b at room
200 temperature and at 37 ºC (16, 17). In this study, we sought to investigate whether this
201 protein can also be used for the control of biofilms formed by *S. aureus*, which
202 generally exhibit resistance to many conventional antimicrobial agents. Two strains
203 were chosen for these experiments on the basis of their different origin and ability to
204 form sessile communities. One of them, *S. aureus* IPLA 1, was isolated from a dairy
205 industry sample and is a poor biofilm former, while the other, *S .aureus* ISP479r, is a
206 strain derived from the clinical isolate NCTC 8325 and can form strong biofilms.
207 Interestingly, both *S. aureus* strains showed identical susceptibility to CHAPSH3b, with
208 MIC values of 3.91 μg/ml and 62.48 μg/ml at 25 ºC and 37 ºC, respectively.

209 To evaluate the antibiofilm activity of this protein, biofilms of the two strains were
210 grown for 24 hours at 25 ºC or 37 ºC and then treated with 4× MIC of CHAPSH3b
211 (15.64 and 250.24 μg/ml at 25 ºC and 37 ºC, respectively) for 6 hours. The results
212 showed a significant decrease in the adhered biomass for both strains at both
213 temperatures (Fig. 1A and 1C). Thus, treatment of biofilms formed by *S .aureus* IPLA 1
214 led to reductions of 70% and 53% at 25 ºC and 37 ºC, respectively (Fig. 1A). In the case
215 of *S .aureus* ISP479r, biofilm formation decreased by 30% and 61% at 25 ºC and 37 ºC,

respectively, compared to the untreated controls (Fig. 1C). A significant reduction in bacterial cell counts was also observed in all biofilms treated with CHAPSH3b (Fig. 1B and 1D). Nevertheless, the results showed that treatment with this protein was more effective at 37 ºC than at 25 ºC. Thus, viable cells counts of both strains only decreased by less than one logarithmic unit in biofilms treated at 25 ºC (Fig. 1B). In contrast, treatment at 37 ºC led to respective reductions of 1 and 2 logarithmic units for strains ISP479r and IPLA 1 (Fig. 1D).

After confirming the ability of CHAPSH3b to kill *S. aureus* cells forming biofilms, microscopy analyses were performed to observe the effects of the lytic protein in greater detail. To do that, biofilms of strain ISP479r were grown for 24 hours at 37 ºC and subsequently treated for 6 hours with 250.24 μg/ml of CHAPSH3b (4× MIC) or with buffer alone at the same temperature. These samples were then stained with SYTO 9, which dyes live cells, and propidium iodide, which dyes dead cells and eDNA, and observed by confocal scanning laser microscopy. The control samples showed well-organized biofilms that completely covered the glass surface (Fig. 2A), whereas the treated biofilm contained fewer bacterial cells and displayed a general loss of structure together with accumulation of eDNA, probably the result of widespread cell lysis (Fig. 2B). Additionally, time-lapse microscopy allowed us to monitor the changes in the *S. aureus* ISP479r biofilm throughout the 6-hour treatment (Video S1). This experiment confirmed the data described above, as areas of lysis appeared in the biofilm and gradually increased in size during the incubation period.

Subinhibitory concentrations of CHAPSH3b decrease biofilm formation in *S. aureus*. Gutiérrez et al. (13) had previously shown that exposure to endolysin LysH5 at the beginning of biofilm formation inhibited this process in some *S. aureus* strains. Here, we wanted to determine if this phenomenon also occurred as a result of exposure

241 to the fusion protein CHAPSH3b. To do that, biofilms of strains IPLA 1 and ISP479r
242 were grown for 24 hours at 25 ºC or 37 ºC in the presence of increasing concentrations
243 of CHAPSH3b and the adhered biomass was then compared to a control grown without
244 protein. Interestingly, the protein showed the ability to significantly reduce the adhered
245 biomass at both growth temperatures, even at concentrations well below the MIC (Fig.
246 3). Indeed, biofilm formation of strain IPLA 1 was reduced by about 50% at
247 concentrations corresponding to 0.125× MIC at both 25 ºC (Fig. 3A) and 37 ºC (Fig.
248 3C). In the case of strain ISP479r, 0.125× MIC led to respective reductions of 34% and
249 52% at 25 ºC (Fig. 3B) and 37 ºC (Fig. 3D). In contrast, growth of IPLA 1 and ISP479r
250 at subinhibitory concentrations of the antibiotic vancomycin did not significantly inhibit
251 biofilm formation (Fig. S2).

252 The data described above showed that very low doses of CHAPSH3b are necessary to
253 exert a significant inhibition of the biofilm formation process at room temperature (25
254 ºC). This would be very interesting to reduce biofilm formation on surfaces of the food
255 industry or the hospital environment, as well as for the use of this protein in human
256 therapy. For this reason, the effects of subinhibitory CHAPSH3b on biofilm structure at
257 25 ºC were studied in greater detail by confocal laser microscopy. After 24 hours of
258 development without protein, strain ISP479r could form thick biofilms that contained a
259 well-defined network of eDNA surrounding the bacterial cells, with visible areas of
260 accumulation (Fig. 4A and 4B). In contrast, when biofilm formation took place in the
261 presence of 0.25× MIC (0.98 μg/ml) of CHAPSH3b the resulting structure was
262 different. On the one hand, thickness of the biofilm was overall reduced and cells tended
263 to accumulate in specific areas (Fig. 4C and 4D). Also, eDNA accumulation appeared to
264 be reduced, whereas the number of dead cells had increased (Fig. 4C and 4D). Thus,
265 propidium iodide was predominantly bound to small cell-size dots instead of forming a

266 network around the cells (Fig. 4C and 4D). Furthermore, differences in the structure of
267 biofilms formed by strain ISP479r with and without subinhibitory lytic protein could
268 even be observed macroscopically in biofilms stained with crystal violet (Fig. 4E). It is
269 of particular note the observation of intensely stained areas located on a seemingly thin
270 biofilm layer. In the case of strain IPLA 1 the changes displayed by biofilms developed
271 in the presence of the fusion protein were not as obvious as in strain ISP479r.
272 Nevertheless, a greater coverage of the glass surface could be observed in the untreated
273 control (Fig. 5A and 5C) compared to the sample grown in the presence of CHAPSH3b
274 (Fig. 5B and 5D). This would be consistent with the lower biomass values determined
275 by crystal violet staining.

276 **Transcriptional responses to phage-derived lytic proteins.** Previous data had shown
277 the biofilm-inhibiting effect of endolysin LysH5 for some *S. aureus* strains. However,
278 we still had no information concerning the underlying molecular mechanisms behind
279 this phenomenon. In an attempt to understand how phage-derived lytic proteins exert
280 their antibiofilm activity, we explored the transcriptional responses of *S. aureus* cells
281 exposed to these antimicrobials. A preliminary study performed with 24-h biofilms of
282 strain *S. aureus* IPLA 1 exposed to 0.25× MIC of LysH5 (10.94 μg/ml) had provided
283 some hints about transcriptional responses to lytic proteins. In that experiment,
284 preformed biofilms were incubated for 30 minutes with the buffer containing the protein
285 or buffer alone. After treatment, RNA was purified from all samples and analyzed by
286 RNA-seq to assess the effect of LysH5 exposure on the transcriptome of the biofilm
287 cells. The results revealed that 61 genes were significantly dysregulated (adjusted P-
288 values <0.05) between the two conditions (Table S3). However, in most cases, these
289 expression changes were less than twofold. Interestingly, several genes encoding
290 proteins with PG hydrolase activity were identified amongst the differentially-expressed

transcripts. These genes included *lytM*, *sceD*, *sle1* and *atl*, which were downregulated by 1.43, 1.76, 1.35 and 1.31, respectively. Transcriptional analysis of biofilms presents a significant problem as it is difficult to ensure that all cells are exposed to the protein. In order to obtain a more homogenous response of the bacterial culture, transcriptional analysis of liquid cultures was also performed. For this purpose, *S. aureus* IPLA 1 cultures grown to mid logarithmic phase at 25 ºC were exposed for 10 minutes to the same concentration of LysH5 used for the biofilm samples (10.94 μg/ml) and RNA was isolated and subsequently analyzed. RT-qPCR analysis of these samples confirmed that exposure to the endolysin resulted in decreased expression of endogenous PG hydrolases (Table 2). Dysregulation of other genes identified by RNA-seq in the biofilm samples could not be confirmed in the liquid cultures exposed to LysH5 (data not shown). As a result, we did not further study the role of these genes in the response to phage lytic proteins.

With these results in mind, we examined whether exposure to subinhibitory CHAPSH3b also resulted in downregulation of genes encoding bacterial PG hydrolases in strains IPLA 1 and ISP479r. To do that, mid logarithmic cultures of the two strains grown at 25 ºC were challenged with 0.25× MIC of CHAPSH3b (0.98 μg/ml) and RNA was isolated for transcriptional analysis. RT-qPCR data confirmed that autolysin-encoding genes *atl*, *sle1*, *lytM* and *sceD* were indeed repressed following exposure to the lytic protein in both strains (Table 3).

Mutation of the major autolysin AtlA in *S. aureus* SA113 prevents biofilm inhibition by CHAPSH3b but leads to low-level resistance to phage lytic proteins. Transcriptional analysis revealed a direct link between exposure to phage lytic proteins and downregulation of autolysins in *S. aureus* strains. For instance, the gene coding for *S. aureus* major autolysin AtlA showed a 3-fold and 13-fold downregulation in strains

316 IPLA 1 and ISP479r, respectively. Sometimes, bacterial responses to antimicrobial
317 challenge provide us with hints about resistance mechanisms (23). For this reason, we
318 studied the participation of the major autolysin *atl* in resistance to phage lytic proteins.
319 To do that, MICs of lytic proteins for strain SA113 and its isogenic *atl* mutant were
320 determined. These assays indicated that the *atl* mutant was slightly more resistant to
321 CHAPSH3b. Thus, the MIC of the mutant was 7.81 μg/ml, while the MIC of the
322 parental strain was 3.91 μg/ml. Notably, the mutant was also more resistant to the
323 endolysin LysH5, with an MIC > 43.75 μg/ml, compared to the MIC of the parental
324 strain (21.88 μg/ml). This resistant phenotype was reverted in the complemented strain.
325 It must be noted that no statistically significant difference was found between the
326 growth rate of the *atl* mutant and that of the wild-type strain, which had respective
327 generation times of 41.27±1.04 min and 38.30±0.15 min (p-value = 0.14).

328 It is well established that the major autolysin AtlA plays a key role in *S. aureus* biofilm
329 formation (24). Therefore, we sought to investigate the possible participation of this
330 gene in biofilm inhibition by phage-derived lytic proteins. This was achieved by
331 comparing biofilm formation of strain SA113 and its isogenic *atl* mutant strain in the
332 presence of increasing concentrations of CHAPSH3b. The attached biomass was then
333 quantified by crystal violet staining and the resulting values were compared to those of
334 a control biofilm of each strain grown without the protein (Fig. 6). Strain SA113
335 showed a similar trend to that observed for strain ISP479r, with decreases in biofilm
336 formation of 26% and 51% at 0.125× MIC (0.49 μg/ml) and 0.25× MIC (0.98 μg/ml),
337 respectively. Conversely, no significant change in biofilm formation was observed at
338 either 0.125× MIC (0.98 μg/ml) or 0.25× MIC (1.96 μg/ml) for the *atl* mutant (P-values
339 > 0.05). The complemented strain showed the same behavior as the parental SA113
340 strain, with respective reductions in biomass of 37% and 63% at 0.125× MIC (0.49

μg/ml) and 0.25× MIC (0.98 μg/ml). As a negative control for the effect of CHAPSH3b on biofilm formation, strains SA113 and the *atl* mutant were also grown in the presence of subinhibitory concentrations of vancomycin, but no significant biofilm inhibition was observed for either strain (Fig. S2).

DISCUSSION

The "honeymoon" period of antibiotic therapy is over. By now, we have encountered microbes resistant to practically all antibiotics available on the market, including superbug strains of *S. aureus*. This situation is only worsened by the ability of this bacterium to form attached multicellular communities with inherent resistance to external challenges. Indeed, biofilms are known to withstand very high concentrations of antibacterial agents that would be lethal to cells in the planktonic state. As a response to this threat, researchers have been steadily working on the development of novel antimicrobials. An interesting possibility is the use of bacteriophages, one of bacteria's natural predators, or phage-derived proteins as therapeutics. For instance, phage PG hydrolases have shown promising results for the control of *S. aureus*, even when they are part of a biofilm (9, 10, 11, 13). Moreover, some phage lytic proteins, like LysH5, display biofilm-inhibiting activity (13). Also importantly, lysin CF-301 has been shown to be effective for the treatment of systemic *S. aureus* infections in a mouse model (10).

Here, we set out to study the ability of the fusion protein CHAPSH3b to kill *S. aureus* biofilm cells and/or to prevent biofilm development. Regarding treatment of preformed biofilms, we have demonstrated that this protein can reduce viable cell counts as well as total adhered biomass at both 25 ºC (room temperature) and at 37 ºC (infection temperature). Microscopy analysis also confirmed that treatment of *S. aureus* biofilms with CHAPSH3b could lyse part of the population and reduce the number of bacterial

365 cells in the biofilm. However, it must be noted that the activity of the protein was higher
366 at 37 ºC than at 25 ºC, even though MIC determination assays indicated that bacteria
367 were actually more sensitive at room temperature. To explain this phenomenon, it must
368 be considered that biofilm treatment was performed under conditions that did not allow
369 bacterial growth. Consequently, the results may reflect the activity of the enzyme,
370 which is higher at 37 ºC compared to 25 ºC (15). In contrast, MIC determination assays
371 are affected by differences in the bacterial growth rate, which is higher at 37 ºC than at
372 25 ºC. Similarly, CHAPSH3b was more effective in killing *S. aureus* cells in raw and
373 pasteurized milk at room temperature than at 37 ºC. It is very likely that, at the latter
374 temperature, the bacterial cell population can increase too rapidly, making it necessary
375 to use a higher enzyme concentration to control the whole population.

376 Addition of CHAPSH3b at the beginning of the biofilm-forming process also proved to
377 exert an inhibitory effect on biofilm development at both 25 ºC and 37 ºC. This is a very
378 interesting property, as some antimicrobials like vancomycin have precisely the
379 opposite effect, that is, they promote biofilm formation (25, 26). Other compounds that
380 exert a negative effect on biofilm development by *S. aureus* include the lantibiotic
381 gallidermin (27) and the synthetic cationic peptide IDR-1018 (28). Gallidermin was
382 shown to decrease expression of the genes encoding autolysin AtlA and the *ica* operon,
383 involved in synthesis of polysaccharide intercellular adhesin (27). In contrast, IDR-1018
384 prevents biofilm formation in different bacterial species by interfering with the stringent
385 response (28). As mentioned above, Gutiérrez et al. (13) had already demonstrated that
386 endolysin LysH5 inhibited biofilm formation in different *S. aureus* strains. In the case
387 of CHAPSH3b, we also investigated the effect on the biofilm structure by confocal
388 microscopy. The structure of the biofilm formed by the food industry strain IPLA 1 did
389 not exhibit major structural alterations, although surface coverage was diminished in the

samples grown in the presence of the protein. In contrast, the strong biofilm former ISP479r displayed more noticeable changes in the lysin-exposed biofilm compared to the control. Indeed, the control biofilms of this strain were thicker and contained more eDNA surrounding the bacterial cells, whereas treated biofilms were overall thinner with areas of cell accumulation. This phenotype could even be observed macroscopically in crystal violet stained biofilms, where the surface of the well appeared covered by a thin layer with scattered intensely-stained spots.

In many cases, the phenotypic effects associated with exposure to subinhibitory antimicrobials can be understood by studying the transcriptional responses of bacterial cells under these conditions (23, 29). Until now, there was no information on the gene expression changes triggered by exposure to phage lytic proteins. In this work, we show that *S. aureus* cells challenged with two different lytic proteins, namely LysH5 and CHAPSH3b, display downregulation of several genes coding for endogenous PG hydrolases, including gene *atl*, encoding the major autolysin. The *atl* gene had been previously shown to be downregulated upon exposure to other cell-wall active antimicrobials, namely bacitracin, D-cycloserine and oxacillin (30). The *S. aureus* autolysin, AtlA, and its homolog in *S. epidermidis*, AtlE, participate in the biofilm formation process of these microbes. In fact, autolysins are thought to be especially important during the initial attachment phase (31). Taking this into account, we thought that there might be a link between lysin-induced downregulation of *atl* expression and biofilm inhibition. Study of an *atl* mutant strain derived from SA113 indicated that this was indeed a possibility. Thus, strain SA113 displayed a phenotypic response similar to that of strains IPLA 1 and ISP479r, with decreased biofilm formation in the presence of subinhibitory concentrations of CHAPSH3b. In contrast, its isogenic *atl* mutant strain did not show a significant reduction in biofilm-forming ability at low doses of the

protein, a phenotype that could be complemented by expressing the gene in trans. Interestingly, while performing these experiments, we also realized that *atl* mutation leads to low-level resistance to both CHAPSH3b and LysH5. To our knowledge, this would make *atlA* the first known phage-lysin resistance determinant. Moreover, the downregulation of *atl* triggered by lytic proteins suggests that this may be a defense mechanism against these antimicrobials, thereby constituting an example of adaptive resistance. The phenomenon of adaptive resistance had been originally dismissed, but it is now gaining attention in the field of antibiotic development (32). It is particularly interesting because there seems to be a connection between mechanisms of adaptive resistance and mechanisms of mutational resistance (23). For example, a given gene may be downregulated upon exposure to subinhibitory antimicrobial concentrations or be mutated in a particular strain, leading in both cases to reduced susceptibility to an antimicrobial compound. Therefore, attaining a better understanding of bacterial responses to non-lethal antimicrobial concentrations may provide hints about mutations that lead to resistance. In the case of phage-derived lytic proteins, our results show that mutational resistance is possible, but that the increase may be so small that these mutants would be difficult to identify in routine screenings. This would explain why no resistant strains have been generally isolated after rounds of exposure to phage lytic proteins (3, 33). Additionally, autolysins are very important for cell wall turnover and cell division amongst other functions, which probably makes these mutants less competitive in a real-life situation. Of note, Becker et al. (12) recently reported the selection of increased resistance in *S. aureus* Newman following 10 rounds of exposure to sublethal concentrations of LysK and chimeric endolysins, although they did not identify the genetic mechanisms responsible for this phenotype.

In *S. aureus*, decreased expression of autolysins may help bacterial cells cope with the deleterious effect of phage lytic proteins. However, it also results in a lesser ability to form biofilms, at least in some strains. This would, in turn, make the population more sensitive to treatment with other antimicrobials as cells would not be able to attach so readily to surfaces and would remain in the planktonic phase. Taking all of these factors into consideration, it may be a good compromise to change low-level resistance by biofilm inhibition. Nonetheless, this would still be an important aspect to consider for the design of phage-derived lytic proteins. For instance, our results show that the *atl* mutant displays a greater increase in resistance to LysH5 than to CHAPSH3b when compared to the parental and complemented strains. Thus, depending on their specific targets in the PG or their binding sites, some lytic proteins may be more affected by lower expression or mutation of autolysin genes.

To sum up, the main achievement of this work lies in the identification of transcriptional responses to phage lytic proteins and their potential role in biofilm inhibition and adaptive resistance to enzybiotics. These are factors that definitely need to be considered for the improvement of products based on these novel antimicrobials and, especially so, for the design of new lytic enzymes. It will also be interesting to find out if this phenomenon is specific to *S. aureus* or if similar transcriptional trends exist in other microorganisms. Despite the negative connotations generally associated with the identification of novel resistance mechanisms, the overall conclusion of this study is, in our opinion, a positive one. On the one hand, our results seem to confirm that mutational resistance to phage lytic proteins would involve loss of important cell functions. Moreover, we demonstrate that this same resistance mechanism plays in our favor by decreasing the ability of *S. aureus* to form the dreaded biofilms. Therefore, enzybiotics remain a promising therapeutic alternative to conventional antimicrobials.

ACKNOWLEDGMENTS

This study was funded by grants AGL2012-40194-C02-01 (Ministry of Science and Innovation, Spain), AGL2015-65673-R (Program of Science, Technology and Innovation 2013-2017) and GRUPIN14-139 (FEDER EU funds, Principado de Asturias, Spain). L.F. was awarded a "Marie Curie Clarin-Cofund" postdoctoral fellowship. PG, BM and AR are members of the bacteriophage network FAGOMA and the FWO Vlaanderen funded "Phagebiotics" research community (WO.016.14). We would also like to thank Professor F. Götz and M. Nega (U. of Tübingen) for providing us with strain SA113 and its derived *atl* mutant and complemented strains, as well as Dr. A. Toledo-Arana (Instituto de Agrobiotecnología, CSIC, Universidad Pública de Navarra, Spain) for sending strain ISP479r.

475 **REFERENCES**

476 1. **Knoll BM, Mylonakis E.** 2014. Antibacterial bioagents based on principles of
477 bacteriophage biology: an overview. Clin Infect Dis **58:**528–534.

478 2. **Kutateladze M, Adamia R.** 2010. Bacteriophages as potential new therapeutics to
479 replace or supplement antibiotics. Trends Biotechnol **28:**591–595.

480 3. **Nelson DC, Schmelcher M, Rodriguez-Rubio L, Klumpp J, Pritchard DG, Dong**
481 **S, Donovan DM.** 2012. Endolysins as antimicrobials. Adv Virus Res **83:**299–365.

482 4. **Rodríguez-Rubio L, Gutiérrez D, Donovan DM, Martínez B, Rodríguez A,**
483 **García P.** 2016. Phage lytic proteins: biotechnological applications beyond clinical
484 antimicrobials. Crit Rev Biotechnol **36:**542–552.

485 5. **Schmelcher M, Donovan DM, Loessner MJ.** 2012. Bacteriophage endolysins as
486 novel antimicrobials. Future Microbiol **7:**1147–1171.

487 6. **Szweda P, Schielmann M, Kotlowski R, Gorczyca G, Zalewska M, Milewski S.**
488 2012. Peptidoglycan hydrolases-potential weapons against *Staphylococcus aureus*. Appl
489 Microbiol Biotechnol **96:**1157–1174.

490 7. **Brooks JL, Jefferson KK.** 2012. Staphylococcal biofilms: quest for the magic bullet.
491 Adv Appl Microbiol **81:**63–87.

492 8. **Ippolito G, Leone S, Lauria FN, Nicastri E, Wenzel RP.** 2010. Methicillin-
493 resistant *Staphylococcus aureus*: the superbug. Int J Infect Dis 14 Suppl **4:**S7–11.

494 9. **Sass P, Bierbaum G.** 2007. Lytic activity of recombinant bacteriophage phi11 and
495 phi12 endolysins on whole cells and biofilms of *Staphylococcus aureus*. Appl Environ
496 Microbiol **73:**347–352.

10. **Schuch R, Lee HM, Schneider BC, Sauve KL, Law C, Khan BK, Rotolo JA, Horiuchi Y, Couto DE, Raz A, Fischetti VA, Huang DB, Nowinski RC, Wittekind M.** 2014. Combination therapy with lysin CF-301 and antibiotic is superior to antibiotic alone for treating methicillin-resistant *Staphylococcus aureus*-induced murine bacteremia. J Infect Dis **209:**1469-1478.

11. **Son JS, Lee SJ, Jun SY, Yoon SJ, Kang SH, Paik HR, Kang JO, Choi YJ.** 2010. Antibacterial and biofilm removal activity of a podoviridae *Staphylococcus aureus* bacteriophage SAP-2 and a derived recombinant cell-wall-degrading enzyme. Appl Microbiol Biotechnol **86:**1439–1449.

12. **Becker SC, Roach DR, Chauhan VS, Shen Y, Foster-Frey J, Powell AM, Bauchan G, Lease RA, Mohammadi H, Harty WJ, Simmons C, Schmelcher M, Camp M, Dong S, Baker JR, Sheen TR, Doran KS, Pritchard DG, Almeida RA, Nelson DC, Marriott I, Lee JC, Donovan DM.** 2016. Triple-acting lytic enzyme treatment of drug-resistant and intracellular *Staphylococcus aureus*. Sci Rep **6:**25063.

13. **Gutiérrez D, Ruas-Madiedo P, Martínez B, Rodríguez A, García P.** 2014. Effective removal of staphylococcal biofilms by the endolysin LysH5. PLoS One **9:**e107307.

14. **Obeso JM, Martínez B, Rodríguez A, García P.** 2008. Lytic activity of the recombinant staphylococcal bacteriophage PhiH5 endolysin active against *Staphylococcus aureus* in milk. Int J Food Microbiol **128:**212–218.

15. **Rodríguez L, Martínez B, Zhou Y, Rodríguez A, Donovan DM, García P.** 2011. Lytic activity of the virion-associated peptidoglycan hydrolase HydH5 of *Staphylococcus aureus* bacteriophage vB_SauS-phiIPLA88. BMC Microbiol **11:**138.

16. **Rodríguez-Rubio L, Martínez B, Rodríguez A, Donovan DM, García P.** 2012. Enhanced staphylolytic activity of the *Staphylococcus aureus* bacteriophage vB_SauS-phiIPLA88 HydH5 virion-associated peptidoglycan hydrolase: fusions, deletions, and synergy with LysH5. Appl Environ Microbiol **78:**2241–2248.

17. **Rodríguez-Rubio L, Martínez B, Donovan DM, García P, Rodríguez A.** 2013. Potential of the virion-associated peptidoglycan hydrolase HydH5 and its derivative fusion proteins in milk biopreservation. PLoS One **8:**e54828.

18. **García P, Martínez B, Rodríguez L, Rodríguez A.** 2010. Synergy between the phage endolysin LysH5 and nisin to kill *Staphylococcus aureus* in pasteurized milk. Int J Food Microbiol **141:**151–155.

19. **Herrera JJ, Cabo ML, González A, Pazos I, Pastoriza L.** 2007. Adhesion and detachment kinetics of several strains of *Staphylococcus aureus* subsp. aureus under three different experimental conditions. Food Microbiol **24:**585–591.

20. **Clinical and Laboratory Standards Institute.** 2006. Methods for dilution antimicrobial susceptibility tests for bacteria that grow aerobically, 7th ed. Approved standard M7-A7. Clinical and Laboratory Standards Institute, Wayne, PA.

21. **Clinical and Laboratory Standards Institute.** 2007. Performance standards for antimicrobial susceptibility testing. CLSI approved standard M100-S17. Clinical and Laboratory Standards Institute, Wayne, PA.

22. **Fernández L, González S, Campelo AB, Martínez B, Rodríguez A, García P.** Low-level predation by lytic phage phiIPLA-RODI promotes biofilm formation and triggers the stringent response in *Staphylococcus aureus*. Sci Rep. In press.

23. **Fernández L, Breidenstein EBM, Hancock REW.** 2011. Importance of adaptive and stepwise changes in the rise and spread of antimicrobial resistance, p 43-72. In Keen PL, Montforts MHMM (ed), Antimicrobial resistance in the environment, John Wiley & Sons, Inc., Hoboken, NJ, USA.

24. **Houston P, Rowe SE, Pozzi C, Waters EM, O'Gara JP.** 2011. Essential role for the major autolysin in the fibronectin-binding protein-mediated *Staphylococcus aureus* biofilm phenotype. Infect Immun **79:**1153–1165.

25. **Hsu CY, Lin MH, Chen CC, Chien SC, Cheng YH, Su IN, et al.** 2011. Vancomycin promotes the bacterial autolysis, release of extracellular DNA, and biofilm formation in vancomycin-non-susceptible *Staphylococcus aureus*. FEMS Immunol Med Microbiol **63:**236–247.

26. **Kaplan JB, Izano EA, Gopal P, Karwacki MT, Kim S, Bose JL, Bayles KW, Horswill AR.** 2012. Low levels of β-lactam antibiotics induce extracellular DNA release and biofilm formation in *Staphylococcus aureus*. MBio **3:**e00198–12.

27. **Saising J, Dube L, Ziebandt AK, Voravuthikunchai SP, Nega M, Götz F.** 2012. Activity of gallidermin on *Staphylococcus aureus* and *Staphylococcus epidermidis* biofilms. Antimicrob Agents Chemother **56:**5804–5810.

28. **de la Fuente-Núñez C, Reffuveille F, Haney EF, Straus SK, Hancock REW.** 2014. Broad-spectrum anti-biofilm peptide that targets a cellular stress response. PLoS Pathog **10:**e1004152.

29. **Linares JF, Gustafsson I, Baquero F, Martinez JL.** 2006. Antibiotics as intermicrobial signaling agents instead of weapons. Proc Natl Acad Sci USA **103:**19484–19489.

30. **Utaida S, Dunman PM, Macapagal D, Murphy E, Projan SJ, Singh VK, Jayaswal RK, Wilkinson BJ.** 2003. Genome-wide transcriptional profiling of the response of *Staphylococcus aureus* to cell-wall-active antibiotics reveals a cell-wall-stress stimulon. Microbiology **149:**2719–2732.

31. **Heilmann C, Hussain M, Peters G, Götz F.** 1997. Evidence for autolysin-mediated primary attachment of *Staphylococcus epidermidis* to a polystyrene surface. Mol Microbiol **24:**1013–1024.

32. **Fernández L, Breidenstein EB, Hancock REW.** 2011. Creeping baselines and adaptive resistance to antibiotics. Drug Resist Updat **14:**1–21.

33. **Rodríguez-Rubio L, Martínez B, Rodríguez A, Donovan DM, Götz F, García P.** 2013. The phage lytic proteins from the *Staphylococcus aureus* bacteriophage vB_SauS-phiIPLA88 display multiple active catalytic domains and do not trigger staphylococcal resistance. PLoS One **8:**e64671.

34. **Gutiérrez D, Delgado S, Vázquez-Sánchez D, Martínez B, Cabo ML, Rodríguez A, Herrera JJ, García P.** 2012. Incidence of *Staphylococcus aureus* and analysis of associated bacterial communities on food industry surfaces. Appl Environ Microbiol **78:**8547–8554.

35. **Toledo-Arana A, Merino N, Vergara-Irigaray M, Débarbouillé M, Penadés JR, Lasa I.** 2005. *Staphylococcus aureus* develops an alternative, *ica*-independent biofilm in the absence of the *arlRS* two-component system. J Bacteriol **187:**5318–5329.

36. **Iordanescu S, Surdeanu M.** 1976. Two restriction and modification systems in *Staphylococcus aureus* NCTC8325. J Gen Microbiol **96:**277–281.

587 37. **Biswas R, Voggu L, Simon UK, Hentschel P, Thumm G, Götz F.** 2006. Activity
588 of the major staphylococcal autolysin Atl. FEMS Microbiol Lett **259:**260–268.

589 38. **Heilmann C, Schweitzer O, Gerke C, Vanittanakom N, Mack D, Götz F.** 1996.
590 Molecular basis of intercellular adhesion in the biofilm-forming *Staphylococcus*
591 *epidermidis*. Mol Microbiol **20:**1083–1091.

592 Table 1. Bacterial strains used in this study.

Strain	Description	Reference
S. aureus IPLA1	Isolate from dairy industry sample	34
S. aureus ISP479r	NCTC 8325-4 derivative with *rsbU* restored	35
S. aureus SA113	NCTC8325 derivative, *agr*–, 11-bp deletion in *rsbU*	36
S. aureus SA113 Δ*atl::spc*	Δ*atl::spc*, Spc^r	37
S. aureus SA113 Δ*atl::spc* (pRB*atlE*)	Δ*atl::spc* complemented with pRC14, Spc^r, Cm^r	38

593

594

595

596

597 Table 2. Transcriptional analysis of *S. aureus* IPLA 1 cells exposed to 0.25× MIC of
598 endolysin LysH5. Total RNA was purified from biofilms or a liquid culture grown at 25
599 ºC and then exposed to the lytic protein. Gene expression in these samples was then
600 compared to an untreated control by RNA-seq or RT-qPCR. Results show the average
601 of three independent biological replicates (BRs).

602

603

Gene	**Fold change in biofilms**	**Fold change in liquid culture**
atl	-1.31	-3.08± 0.86
sle1	-1.35	-5.14± 0.82
lytM	-1.42	-4.30± 1.90
sceD	-1.76	-14.40±6.17

Table 3. Effect of CHAPSH3b on the transcription of autolysin-encoding genes in *S. aureus* strains IPLA 1 and ISP479r. RNA was isolated from liquid cultures grown at 25 ºC to mid logarithmic phase and then exposed to 0.98 μg/ml of CHAPSH3b (0.25× MIC) for 10 minutes. Values represent the means and standard deviations of three independent biological replicates.

Gene	**Fold-change in strain IPLA 1**	**Fold-change in strain ISP479r**
atl	-3.15±0.28	-13.35±3.25
sle1	-9.19±2.06	-29.70±6.27
lytM	-2.31±0.38	-14.07±1.38
sceD	-5.24±1.84	-12.96±3.45

Fig. 1. Treatment of preformed biofilms of *S. aureus* IPLA 1 and ISP479r with the fusion protein CHAPSH3b. Biofilms were formed for 24 hours and then treated with 4× MIC of CHAPSH3b for 6 hours at 25 ºC (A and B) or 37 ºC (C and D). Control wells were incubated with NaPi buffer alone. After incubation, adhered biomass was quantified by reading absorbance at 595 nm after crystal violet staining (A and C). Alternatively, viable cell counts of bacteria adhered to the well were determined (B and D). Black and grey bars correspond to control and treated samples, respectively. The represented values correspond to the means and standard deviations of three independent biological repeats (BRs). *, P-value<0.05

Fig. 2. Confocal laser scanning micrographs of *S. aureus* biofilms treated or not with CHAPSH3b. Biofilms of strain ISP479r were grown for 24 hours at 37 ºC and then treated with NaPi buffer alone (A) or containing 4× MIC of CHAPSH3b (250.24 μg/ml). After incubation, the planktonic phase was removed and samples were stained with Live/Dead staining kit. Intact cells appear green, whereas dead cells and eDNA are stained red.

Fig. 3. Biofilm formation of *S. aureus* strains in the presence of subinhibitory concentrations of CHAPSH3b. Biofilms of strains IPLA 1 (A and C) and ISP479r (B and D) were grown for 24 hours at 25 ºC (A and B) or 37 ºC (C and D). Then, the planktonic phase was removed and the adhered biomass was quantified by crystal violet staining and subsequent A_{595} determination. The percentage biomass production compared to the untreated controls was then calculated and represented. Values correspond to the mean and standard deviation of three independent BRs. *, P<0.05. The MICs of both strains were 3.91 μg/ml and 62.48 μg/ml at 25 and 37 ºC, respectively.

644 Fig. 4. Effect of subinhibitory concentrations of CHAPSH3b on *S. aureus* ISP479r
645 biofilm formation. A-D, micrographs obtained by CLSM of biofilms grown in the
646 absence (A and B) or presence (C and D) of 0.98 μg/ml of CHAPSH3b at 25 ºC. The
647 samples were stained with the Live/Dead kit. B and D show the 3D structure of the
648 biofilms. E, Photograph of biofilms formed by *S. aureus* ISP479r in the presence of
649 increasing concentrations of CHAPSH3b ranging from 0 to 3.91 μg /ml at 25 ºC and
650 subsequently stained with crystal violet.

651 Fig. 5. Effect of subinhibitory concentrations of CHAPSH3b on *S. aureus* IPLA 1
652 biofilm formation. A-D, micrographs obtained by CLSM of biofilms grown in the
653 absence (A and B) or presence (C and D) of 0.98 μg/ml of CHAPSH3b at 25 ºC. The
654 samples were stained with the Live/Dead kit. B and D show the 3D structure of the
655 biofilms.

656 Fig. 6. Effect of *atl* mutation on the antibiofilm effect of CHAPSH3b. Biofilms of
657 strains *S. aureus* SA113 (black), its isogenic *atl* mutant (white) and the complemented
658 strain (grey) were formed at 25 ºC in the presence of increasing concentrations of the
659 lysin (0 to 7.81 μg/ml). Attached biomass was quantified by crystal violet staining and
660 subsequent A_{595} determination. The data corresponding to the treated wells were
661 compared to their respective controls. The values represent the average and standard
662 deviation of three independent BRs. *, P-value<0.05. The MIC of the parental and
663 complemented strains was 3.91 μg/ml, whereas the MIC of the mutant was 7.81 μg/ml.

664

665 Figure 1

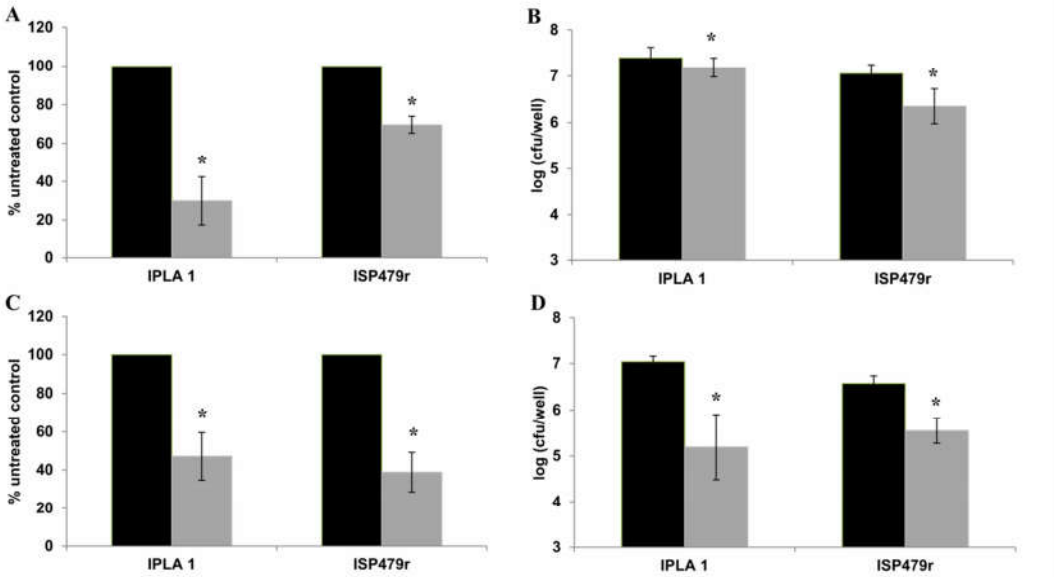

666

667

668 Figure 2

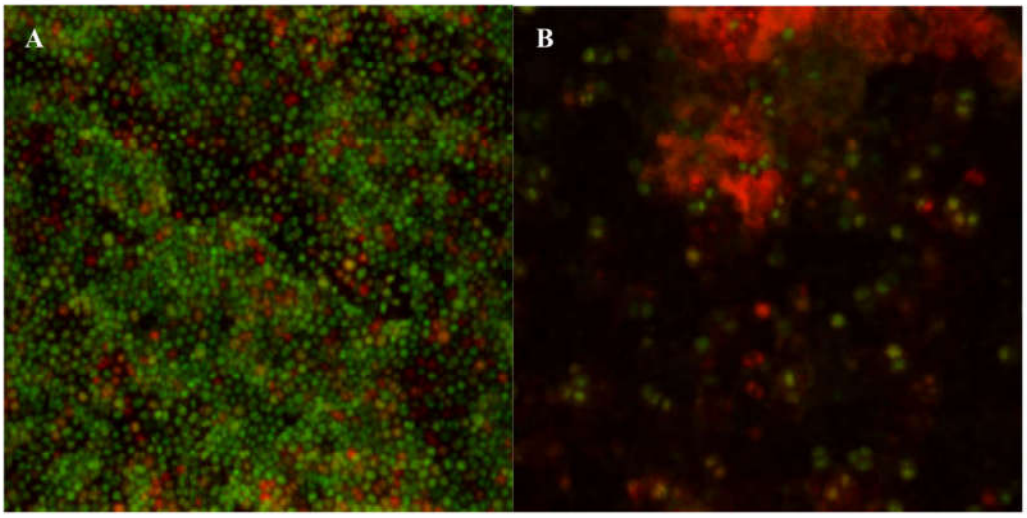

669

670

671 Figure 3

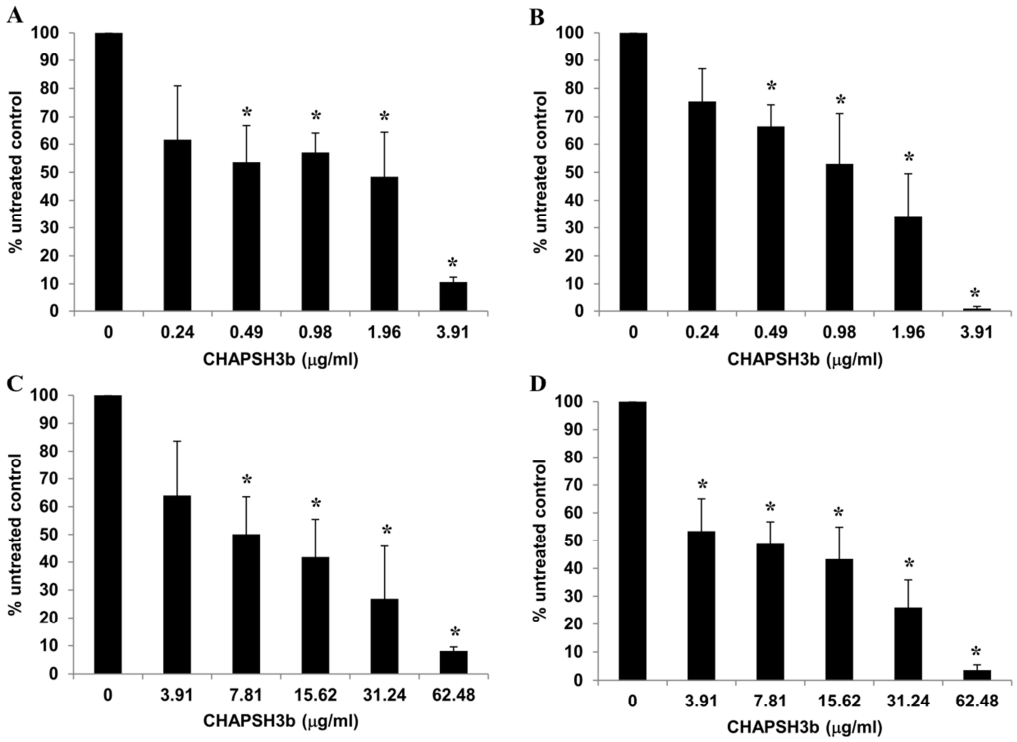

672

673

674 Figure 4

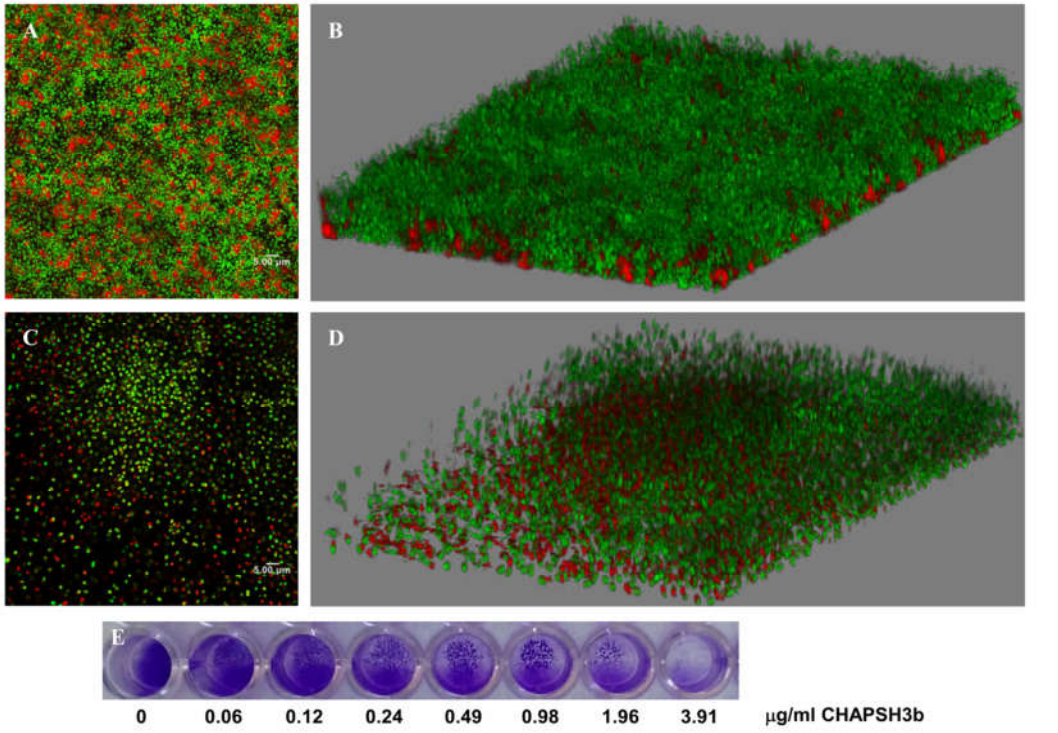

675

676

677 Figure 5

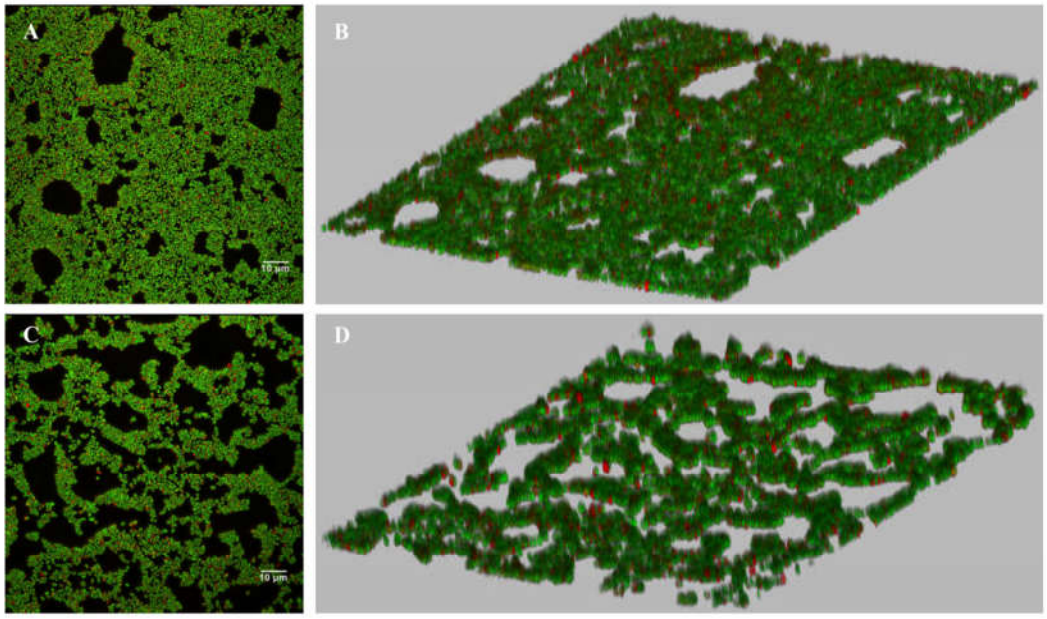

678

679

680 Figure 6

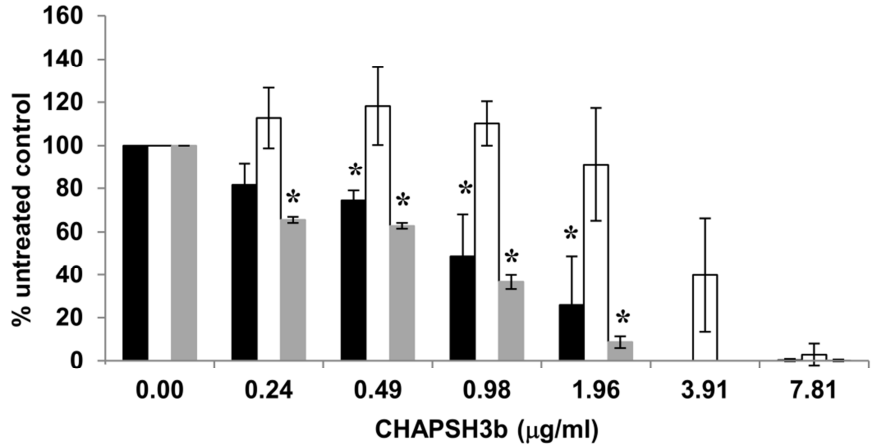

681

Bio-Protocol Vol 8, Iss 12, Jun 20, 2018; doi: 10.21769/BioProtoc.2891

Characterizing the Transcriptional Effects of Endolysin Treatment on Established Biofilms of *Staphylococcus aureus*

Lucía Fernández*, Silvia González, Diana Gutiérrez, Ana Belén Campelo, Beatriz Martínez, Ana Rodríguez and Pilar García

Instituto de Productos Lácteos de Asturias (IPLA-CSIC), Villaviciosa, Asturias, Spain
*For correspondence: lucia.fernandez@ipla.csic.es

[Abstract] Biofilms are the most common lifestyle of bacteria in both natural and human environments. The organized structure of these multicellular communities generally protects bacterial cells from external challenges, thereby enhancing their ability to survive treatment with antibiotics or disinfectants. For this reason, the search for new antibiofilm strategies is an active field of study. In this context, bacteriophages (viruses that infect bacteria) and their derived proteins have been proposed as promising alternatives for eliminating biofilms. For instance, endolysins can degrade peptidoglycan and, ultimately, lyse the target bacterial cells. However, it is important to characterize the responses of bacterial cells exposed to these compounds in order to improve the design of phage-based antimicrobial strategies.

This protocol was developed to examine the transcriptional responses of *Staphylococcus aureus* biofilm cells exposed to endolysin treatment, as previously described in Fernández *et al.* (2017). However, it may be subsequently adapted to analyze the response of other microorganisms to different antimicrobials.

Keywords: Biofilms, Endolysins, *Staphylococcus aureus*, RNA-seq, Responses to antimicrobials

[Background] It is becoming increasingly clear that subinhibitory doses of antimicrobials may have a regulatory effect on different phenotypes of the target microbes, including biofilm formation, metabolism or virulence. Therefore, studying the potential impact of a novel compound on the target cells at low-level concentrations should be a part of the development process. Indeed, a very effective antibacterial agent that triggers production of virulence factors or antibiotic resistance determinants may not be a good candidate for therapeutic application. On the other hand, considering the physiological differences between biofilm and planktonic cells, it seems logical that the effect of new antibiofilm agents should be analyzed on biofilm-forming cells. Here, we describe a protocol for the analysis of transcriptional responses of biofilm cells upon exposure to subinhibitory concentrations of

endolysins, phage-derived proteins that show great promise as biofilm removal agents. Thus, the transcriptome of endolysin-treated cells was compared to control cells by RNA-seq and differential expression of selected genes was later confirmed by RT-qPCR.

Materials and Reagents

1. Standard Petri dishes (Labbox, catalog number: PDIP-09N-500)
2. Sterile 10 ml polystyrene culture tubes (Deltalab, catalog number: 300903)
3. Cuvettes for OD_{600} reading (Deltalab, catalog number: 303103)
4. 1.5 ml microcentrifuge tubes (SARSTEDT, catalog number: 72.690.001)
5. 12-well microtiter plates with Nunclon Delta surface (Thermo Fisher Scientific, Nunc, catalog number: 150628)
6. Sterile plastic loops (1 µl) (VWR, catalog number: 612-9351)
7. MicroAmp® Fast optical 96-well reaction plate with barcode (Thermo Fisher Scientific, Applied Biosystems, catalog number: 4346906)
8. MicroAmp® optical adhesive film (Thermo Fisher Scientific, Applied Biosystems, catalog number: 4311971)
9. Frozen stock of *Staphylococcus aureus* (for example, *S. aureus* IPLA1 from our laboratory collection) stored in glycerol at -80 °C
10. Filtered LysH5 endolysin stock stored in NaPi buffer with 30% glycerol at -80 °C (~350 µg/ml = 5.8 µM) purified as described previously (Gutiérrez *et al.*, 2014)
11. Agarose for electrophoresis (Conda, catalog number: 8008)
12. Glass beads, acid washed (≤ 106 µm, sterile) (Sigma-Aldrich, catalog number: G4649)
13. RNA protect® Bacteria Reagent (QIAGEN, catalog number:-76560)
14. Illustra™ RNAspin Mini Kit (GE Healthcare, catalog number: 25050071)
15. Chloroform (Merck, catalog number: 1024451000)
16. Ethanol (Fisher Scientific, catalog number: BP28184)
17. SUPERase-In™ RNase Inhibitor (Thermo Fisher Scientific, Invitrogen™, catalog number: AM2694)
18. Turbo DNA-free kit™ (Thermo Fisher Scientific, Invitrogen™, catalog number: AM1907)
19. DL-Dithiothreitol (Sigma-Aldrich, catalog number: D0632-5G)
20. Phenol, Molecular Biology Grade (Merck, Calbiochem, catalog number: 516724-100GM)
21. iScript™ Reverse Transcription Supermix for RT-qPCR (Bio-Rad Laboratories, catalog number: 1708841)
22. Power SYBR® Green PCR Master Mix (Thermo Fisher Scientific, Applied Biosystems™, catalog number: 4367659)

23. Bacteriological agar (ROKO S.A.)
24. D(+)-Glucose (Merck, catalog number: 1.08337.1000)
25. Sodium chloride (NaCl) (Merck, catalog number: 1.06404.1000)
26. Potassium chloride (KCl) (VWR, BDH, catalog number: 437025H)
27. Sodium phosphate dibasic (Na_2HPO_4) (VWR, AnalaR NORMAPUR, catalog number: 102495D)
28. Potassium phosphate monobasic (KH_2PO_4) (Merck, catalog number: 1048731000)
29. Sodium dihydrogen phosphate monohydrate ($NaH_2PO_4 \cdot H_2O$) (ITW Reagents Division, AppliChem, catalog number: 131965.1211)
30. UltraPure™ Tris Buffer (Thermo Fisher Scientific, catalog number: 15504020)
31. Glacial acetic acid (Merck, catalog number: 1.00063.2500)
32. 0.5 M EDTA (pH 8.0) (Alfa Aesar, USB, catalog number: J15701)
33. TSB medium (tryptic soy broth, Scharlab, catalog number: 02-200-500) (see Recipes)
34. TSA agar plates (see Recipes)
35. TSB medium supplemented with glucose (TSBG) (see Recipes)
36. Phosphate buffered saline (PBS) solution (see Recipes)
37. Sodium phosphate (NaPi) buffer (see Recipes)
38. Tris-acetate-EDTA (TAE) buffer (see Recipes)

Equipment

1. Pipettes (volume ranges: 1 µl-10 µl, 2 µl-20 µl, 20 µl-200 µl, 200 µl-1,000 µl)
2. Shaking (250 rpm) and static incubators at 25 °C and 37 °C
3. Spectrophotometer
   Note: It is used to measure optical density (OD_{600}) of cell culture.
4. Epoch microplate spectrophotometer (BioTek Instruments, model: Epoch)
5. Refrigerated centrifuge (Eppendorf, model: 5415 R)
6. FastPrep®-24 (MP Biomedicals, catalog number: 116004500)
7. Gel electrophoresis apparatus (Bio-Rad Laboratories, Mini-Sub® Cell GT Cell)
8. Vortex
9. 7500 Fast Real-Time PCR System (Thermo Fisher Scientific, Applied Biosystems, catalog number: 4351107)
10. Illumina HiSeq2000 platform
11. Computer equipped with four Intel Xeon E5-4650 v2 2.4GHz 25M 8GT/s 10-core processors, 256 GB RAM, and running CentOS Linux release 7.3.1611
    Note: The computer is for carrying out computation.

Software

1. FastQC (http://www.bioinformatics.babraham.ac.uk/projects/download.html#fastqc)
2. BowTie2 (http://bowtie-bio.sourceforge.net/bowtie2/index.shtml) (Langmead and Salzberg, 2012)
3. EDGE-Pro (http://ccb.jhu.edu/software/EDGE-pro/) (Magoc *et al.*, 2013)
4. DEseq2 (http://bioconductor.org/packages/release/bioc/html/DESeq2.html) (Love *et al.*, 2014)

Procedure

A. Biofilm formation and treatment (Figure 1)

1. Streak out *S. aureus* strain (IPLA1) from the frozen stock onto a TSB agar plate and incubate statically overnight at 37 °C.
2. To obtain three biological replicates, pick 3 isolated colonies of *S. aureus* from the agar plate with a sterile plastic loop and inoculate into three 10-ml polystyrene tubes containing 2 ml of TSB medium.
3. Grow bacterial cultures overnight at 37 °C, with shaking at 250 rpm.
4. Dilute the overnight cultures to an OD_{600} of 0.1 in TSBG medium (TSB supplemented with glucose), containing approximately 10^7 CFU/ml, and then make a 1:20 dilution in the same medium to prepare the inoculum for the biofilm assays.
5. Inoculate 2 ml from this cell suspension (approximately 5 x 10^5 CFU/ml) into each well of a 12-well microtiter plate (four wells per biological replicate).
6. Incubate the microtiter plate in static for 24 h at 25 °C.
   Note: In this case, the temperature used for biofilm formation and treatment was 25 °C, which represents treatment/disinfection at "room temperature". Nonetheless, the experiment could have also been performed at different temperatures; for instance, at 37 °C to represent treatment of human infection.
7. Remove the planktonic phase from the wells and wash the biofilms twice each with 2 ml of PBS.
8. For each replicate, add 1 ml of NaPi buffer alone to two wells and 1 ml of NaPi containing 10.94 μg/ml (0.18 μM) of LysH5 to the other two wells.
9. Incubate in static for 30 min at 25 °C.
10. Remove supernatant.
11. Wash twice with PBS.
12. Harvest cells corresponding to the same biological replicate and treatment in 1 ml of RNA protect® and 500 μl PBS by scraping with a pipette tip and transfer to a clean Eppendorf tube.

13. Process the samples according to the RNA protect® manufacturer's instructions.
14. Store at -80 °C or proceed to RNA purification.

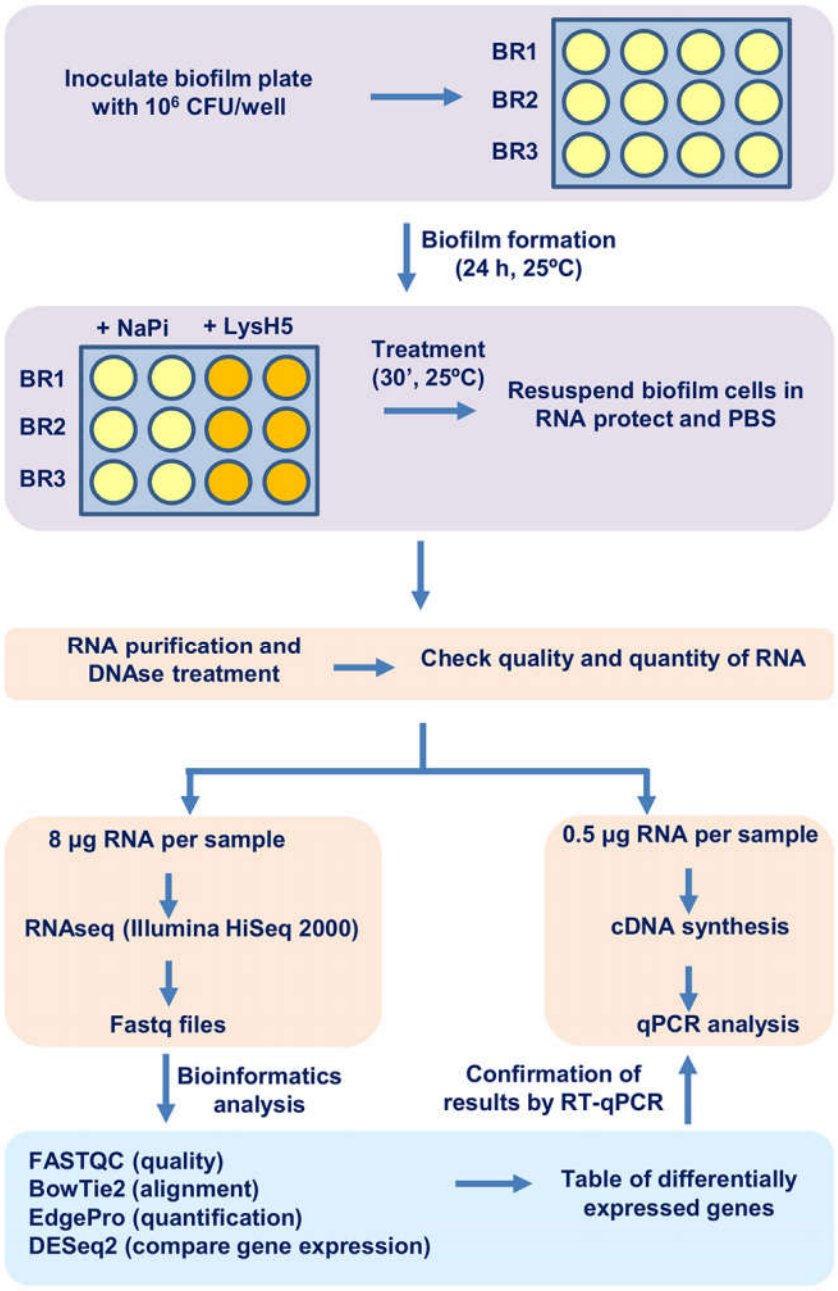

Figure 1. Schematic representation of the protocol. The different steps of this method include biofilm formation and treatment (purple), subsequent RNA purification and RNA-sequencing (pink) and, finally, computer analysis of the generated data (light green).

B. RNA purification and sequencing (Figure 1)

1. To achieve cell lysis, perform mechanical disruption of the cells with glass beads and phenol using FastPrep equipment.
2. After lysis, samples were centrifuged at 9,000 *x g* for 10 min at 4 °C.
3. Transfer the upper phase to a clean tube and add 500 µl chloroform and then centrifuge for 5 min at 9,000 *x g* and 4 °C.
4. Transfer the upper phase to a clean tube and mix with 250 µl of ethanol by pipetting.
5. Transfer the samples mixed with ethanol to the columns provided with the illustra™ RNAspin Mini kit and perform the rest of RNA purification steps following the instructions provided by the manufacturer.
6. Elute in 50 µl of nuclease-free water and add 1 µl of SUPERase-In™.
7. Add 5 µl of Turbo DNase buffer and 1 µl of Turbo DNase per 50 µl sample and incubate for 30 min at 37 °C.
8. Add 1 µl of Turbo DNase per sample and incubate for another 30 min at 37 °C.
9. Remove DNase from sample with inactivation reagent as indicated by the manufacturer.
10. Add 1 µl of SUPERase inhibitor per 50 µl sample.
11. Check RNA quality and concentration by agarose gel electrophoresis (1% agarose) in TAE buffer and the Epoch microplate spectrophotometer (Figure 2). RNA concentrations obtained with this protocol usually range between 200 and 700 ng/µl.
12. Samples with A_{260}/A_{280} ratios $\geq$ 1.8 can be considered adequate for RNA-seq analysis. Otherwise, clean up the samples with the illustra™ RNAspin Mini kit following the protocol recommended by the manufacturer.
13. Take 8 µg of RNA from each sample and proceed with sequencing steps according to the protocols recommended by the manufacturer of the selected platform. For example, in this study samples were sent to an external service provider (Macrogen Inc., South Korea) for sequencing with an Illumina HiSeq2000 platform according to the protocols recommended by Illumina, generating 100-bp paired-end reads.

C. Computer analysis of the generated data (Figure 1)

1. Check the quality of the reads in FASTQ format with FastQC.
2. Download the reference genome in FASTA format (.fa or .fna), the protein table file (.ptt) and the RNA table (.rnt) from the NCBI archive (ftp://ftp.ncbi.nlm.nih.gov/genomes/archive/old_genbank/Bacteria/).
3. Run script "edge.pl" with arguments indicating the FASTQ files containing paired-end reads for each sample (-u and –v) as well as the three files mentioned above (-g, -p and –r) and the prefix for the output files names (-o). In a first step, EDGE-Pro will map the reads to the reference genome using program BowTie2 and create an alignment file as output (this file will be in

sequence alignment map or SAM format). BowTie2 also indicates the percentage of alignment to the reference genome. Once completed this step, EDGE-Pro performs transcript quantification into Reads Per Kilobase of transcript per Million mapped reads (RPKMs). The output files containing the RPKM counts will end in ".rpkm_0".

Example:

/edge.pl -g SAreference.fna -p SAreference.ptt -r SAreference.rnt -u Lys_1-1.fastq -o Lys1 -v Lys_1-2.fastq

4. Run script "edgeToDeseq.perl" indicating the .rpkm_0 files to be analyzed in order to generate a table gathering the raw counts for each gene and each sample. This table will be saved in the output "deseqFile".

   Example:

   /edgeToDeseq.perl NaPi1.rpkm_0 NaPi2.rpkm_0 NaPi3.rpkm_0 Lys1.rpkm_0 Lys2.rpkm_0 Lys3.rpkm_0

   Note: This step is necessary because DESeq2 requires information on raw counts and not RPKMs.

5. Perform differential expression analysis between treated and untreated samples with DESeq2 by using the "deseqFile" from the previous step as an input. Select genes with an adjusted *P*-value < 0.05 for further analysis and save the table of differentially-expressed genes in .csv format.

D. Confirmation of RNA-seq results by RT-qPCR (Figure 1)

1. Convert 0.5 µg RNA from each sample into cDNA with iScript™ Reverse Transcription Supermix for RT-qPCR as indicated by the manufacturer.
2. Dilute cDNA samples 1:25 in nuclease-free water and use them as a template for qPCR.
3. To perform qPCR, add 2.5 µl aliquots from the different samples to each well of a MicroAmp® Fast optical 96-well reaction plate together with 3.25 µl of nuclease-free water, 0.25 µl of each primer from a 10 µM stock, and 6.25 µl of Power SYBR® Green PCR Master Mix.
4. Analyze each biological replicate in duplicate.
5. Determine changes in gene expression by using a reference gene (in this case *rplD*) according to the $2^{-\Delta\Delta CT}$ method (Livak and Schmittgen, 2001), in which ΔCT = CT(target gene) - CT(reference gene) and $\Delta\Delta CT = \Delta CT$(target sample) - ΔCT(reference sample).

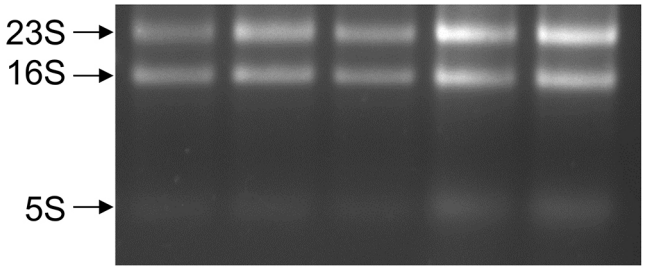

Figure 2. Agarose gel electrophoresis of total RNA from *S. aureus* biofilm samples. Aliquots (1-2 µl) from different RNA samples were run in a 1% agarose gel. Two bands corresponding to the 23S and 16S rRNAs should be visible and preferably in a proportion of 2:1 (23S:16S) indicating RNA integrity. Sometimes a lower band corresponding to 5S rRNA can also be observed.

Please cite Figure 2 in the text.

Data analysis

For reproducibility, it is recommended to analyze three independent biological replicates (BR). Statistical analysis of RNAseq data was performed as part of the differential gene expression analysis with the DESeq2 package, and only those genes with adjusted *P*-values < 0.05 were selected for further analysis. Regarding fold-change, we normally set the cut-off at 2-fold change ($\log_2$ fold-change = 1). However, in this case all genes displaying significant changes based on the adjusted *P*-values were analyzed further. The small changes are probably due to the fact that only part of the biofilm population was exposed to the antimicrobial. In addition to confirming the genes under the conditions described here, changes were further evaluated in a liquid culture exposed to endolysin LysH5. This analysis showed more evident changes in some of the genes identified by RNA-seq, which reinforced the idea that the transcriptional changes observed in the biofilm were indeed a result of endolysin exposure.

Recipes

1. Tryptic soy broth (TSB)
   30 g TSB medium
   Dissolve in 1 L ddH_2O and autoclave
2. TSA agar plates
   TSB medium with 2% agar
   Dissolve in ddH_2O and autoclave
3. TSBG medium
   TSB medium with 0.25% glucose

Dissolve in ddH_2O and autoclave

4. Phosphate buffered saline (PBS) solution
   137 mM NaCl
   2.7 mM KCl
   10 mM Na_2HPO_4
   2 mM KH_2PO_4
   Adjust pH to 7.4
   Dissolve in ddH_2O and autoclave
5. NaPi buffer
   50 mM sodium phosphate
   Adjust pH to 7.4
   Dissolve in ddH_2O and autoclave
6. TAE buffer (50x stock solution)
   242 g of Tris
   57.1 ml of glacial acetic acid
   100 ml of 0.5 M EDTA (pH 8.0)
   Add deionized water to 1 L

Acknowledgments

The development of this protocol was funded by grant AGL2012-40194-C02-01 (Ministry of Science and Innovation, Spain), AGL2015-65673-R (Program of Science, Technology and Innovation 2013-2017), Proyecto Intramural CSIC 201770E016, EU ANIWHA ERA-NET (BLAAT ID: 67), and GRUPIN14-139 (FEDER EU funds, Principado de Asturias, Spain). L.F. was awarded a Marie Curie Clarin-Cofund postdoctoral fellowship. P.G. and A.R. are members of the FWO Vlaanderen-funded PhageBiotics Research community (WO.016.14) and the bacteriophage network FAGOMA. This protocol was adapted from the previously published article Fernández *et al.* (2017).
The authors declare that they have no conflict of interest.

References

1. Fernández, L., González, S., Campelo, A. B., Martínez, B., Rodríguez, A. and García, P. (2017). Downregulation of autolysin-encoding genes by phage-derived lytic proteins inhibits biofilm formation in *Staphylococcus aureus*. *Antimicrob Agents Chemother* 61(5).

2. Gutiérrez, D., Ruas-Madiedo, P., Martínez, B., Rodríguez, A. and García, P. (2014). Effective removal of staphylococcal biofilms by the endolysin LysH5. *PLoS One* 9(9): e107307.
3. Langmead, B. and Salzberg, S. L. (2012). Fast gapped-read alignment with Bowtie 2. *Nat Methods* 9(4): 357-359.
4. Livak, K. J. and Schmittgen, T. D. (2001). Analysis of relative gene expression data using real-time quantitative PCR and the $2^{-\Delta\Delta CT}$ method. *Methods* 25(4): 402-408.
5. Love, M. I., Huber, W. and Anders, S. (2014). Moderated estimation of fold change and dispersion for RNA-seq data with DESeq2. *Genome Biol* 15(12): 550.
6. Magoc, T., Wood, D. and Salzberg, S. L. (2013). EDGE-pro: Estimated degree of gene expression in prokaryotic genomes. *Evol Bioinform Online* 9: 127-136.

Discusión

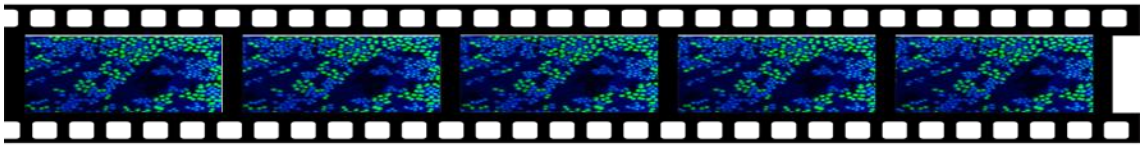

DISCUSIÓN

Utilización de los bacteriófagos phiIPLA-RODI y phiIPLA-C1C para el tratamiento de biofilms mixtos de *S. aureus*

Nuestro conocimiento acerca de la naturaleza y el proceso de desarrollo de los biofilms microbianos ha aumentado significativamente desde que Antonie Van Leeuwenhoek los describió por primera vez a fines del siglo XVII. Hasta el momento, la mayoría de los estudios realizados se han centrado en los biofilms monoespecie, es decir, aquellos que están formados por una única especie microbiana. Sin embargo, estas condiciones no reflejan la realidad, ya que los biofilms que se encuentran tanto en ambientes naturales como industriales suelen componerse de células de microorganismos diferentes. De hecho, las especies que constituyen un biofilm mixto y las interacciones entre las mismas influyen de manera crítica en el desarrollo de estas estructuras y, por tanto, en el tratamiento más adecuado para su eliminación. Esto debe ser tenido especialmente en cuenta cuando se van a utilizar antimicrobianos tan específicos como los bacteriófagos y las proteínas líticas.

Al igual que ocurre en otros ambientes, los biofilms formados en el contexto de la industria alimentaria no suelen estar formados por simples agrupaciones tridimensionales de microorganismos idénticos, sino por subpoblaciones heterogéneas con comportamientos distintos. En un trabajo anterior llevado a cabo por nuestro grupo se observó que *S. aureus* aparecía acompañado de otras especies en biofilms procedentes de las industrias láctea, cárnica y pesquera (Gutiérrez y col., 2012). Basándonos en estos datos, nos propusimos desarrollar un modelo de estudio de biofilms de dos especies compuesto de *S. aureus* junto con otras especies de ambientes relacionados con los alimentos (*L. plantarum, L. pentosus y E. faecium*), y evaluar la utilización del bacteriófago phiIPLA-RODI para su eliminación. Previamente, ya se había demostrado la eficacia de este fago para eliminar biofilms formados por cepas susceptibles de *S. aureus* y *S. epidermidis*, tanto monoespecie como mixtos (Gutiérrez y col., 2015). Sin embargo, ninguna de las cepas acompañantes utilizadas en este estudio (*L. plantarum* 55-1*, L. pentosus* A1*, L. pentosus* B1*,* y *E. faecium* MMRA) son susceptibles al fago phiIPLA-RODI.

En primer lugar, se comprobó que todas estas cepas forman biofilms estables con *S. aureus*. Además, en la mayoría de los casos, el número de bacterias de *S. aureus* y de la especie acompañante era bastante similar. La única excepción fue *L. pentosus* A1, lo que podría deberse a la baja capacidad de adhesión al poliestireno de esta cepa, fenómeno observado incluso en ausencia de *S. aureus*. Es preciso señalar también que el número de bacterias de *L. plantarum* era menor en los biofilms mixtos que en los monoespecie. En este caso, la explicación más plausible de este fenómeno es que *S. aureus* ejerce un efecto inhibitorio sobre el crecimiento de *L. plantarum*.

Una vez caracterizada la composición bacteriana de estos biofilms mixtos, se procedió a explorar la capacidad del bacteriófago phiIPLA-RODI para eliminarlos. En el estudio llevado a cabo por Gutiérrez y col. (2015) se observó que el fago era más efectivo en el tratamiento de los biofilms mixtos formados por *S. aureus* IPLA16 y *S. epidermidis* LO5081 que los respectivos biofilms monoespecie. Así, parecía que la presencia de una segunda especie, también susceptible al fago, tenía un efecto potenciador del tratamiento. Sin embargo, los resultados obtenidos en esta Tesis indican que un tratamiento de corta duración con el fago en condiciones de escasez de nutrientes es menos efectivo en los biofilms mixtos que en el biofilm formado solo por *S. aureus*. De hecho, la disminución en los recuentos celulares de *S. aureus* IPLA16 fue inferior a 1 unidad logarítmica en los biofilms mixtos formados por bacterias no sensibles, como *L. plantarum* y *E. faecium*, independientemente de la etapa de maduración del biofilm o de la concentración de fago utilizada. Por lo tanto, parece que la presencia de bacterias de una especie no sensible en el biofilm puede dificultar la capacidad del fago para alcanzar y lisar las células diana. Es bien sabido que los biofilms mixtos muestran con frecuencia una mayor resistencia a los antibióticos que los biofilms formados por una única especie (Burmølle y col., 2012). Este fenómeno puede deberse a mecanismos diversos, incluida la señalización molecular entre especies, la distribución espacial de bacterias fisiológicamente diferentes y la interferencia de la matriz (Sanchez-Vizuete y col., 2015). Del mismo modo, la baja eficacia de los fagos para infectar biofilms formados por dos especies podría deberse a la protección del hospedador sensible por parte de las especies no sensibles (Oxaran y col., 2018), coagregación de comunidades microbianas (Rickard y col., 2003), la penetración limitada de los fagos (Briandet y col.,

2008) o cambios en la presencia de receptores de fagos en la superficie celular de la especie diana (Hoyland-Kroghsbo y col., 2013).

A pesar de la baja eficacia del tratamiento de corta duración con el fago en las comunidades multiespecie, la microscopía reveló la existencia de cambios estructurales en los biofilms tratados en comparación con sus respectivos controles. De hecho, todos los biofilms mixtos mostraron una reducción visible en el número de bacterias de *S. aureus* intactas, así como una disgregación de la estructura tridimensional del biofilm. Sin embargo, es posible que el uso de un sustrato diferente para estos experimentos (vidrio en lugar de poliestireno) influyera en el resultado final. Así, parece que la aplicación de la suspensión de fagos a los biofilms formados en cubreobjetos de vidrio resultó ser más efectiva que el tratamiento de aquellos formados en placas de poliestireno.

Con respecto a la duración del tratamiento, hay estudios previos que indican que la eliminación de biofilms con productos basados en fagos no requiere tiempos de incubación de más de 5 h (Sillankorva y col., 2010). Sin embargo, nuestros resultados sugieren que el control de biofilms multiespecie podría requerir la utilización de tiempos de incubación más largos. Además, parece que el tratamiento es más efectivo en condiciones que permiten el crecimiento activo del hospedador. No obstante, es importante tener en cuenta que la incubación en condiciones de abundancia de nutrientes también puede afectar a la proliferación de las especies acompañantes. Este efecto sería indeseable cuando las especies acompañantes son microorganismos patógenos o alterantes de los alimentos, especialmente si son buenos formadores de biofilms. Por el contrario, también es posible que haya un efecto sinérgico como resultado de la acción del fago y de la competencia entre especies ejercida por las bacterias no sensibles durante el crecimiento activo. Esta situación facilitaría la eliminación del patógeno diana, pudiendo además limitar la adquisición de resistencia a los fagos, ya que esta generalmente disminuye la capacidad competitiva de la bacteria (Gutiérrez y col., 2012). Por ejemplo, este parece ser el caso en biofilms mixtos de *E. coli* y *P. aeruginosa* (Coulter y col., 2014). En nuestro estudio hubo diferencias en el comportamiento de las cuatro cepas acompañantes estudiadas después del tratamiento con el fago phiIPLA-RODI. Así, los biofilms de *S. aureus* - *L. plantarum* mostraron una

mayor cantidad de biomasa después del tratamiento con el fago. Esto se debe probablemente a que, si bien el número de células de *S. aureus* IPLA16 se redujo debido a la infección por el fago, el número de células de *L. plantarum* aumentó. Como ya se había visto en los experimentos preliminares, *L. plantarum* 55-1 es capaz por sí solo de formar biofilms robustos. Por otro lado, estos resultados no fueron sorprendentes dado el efecto inhibitorio de *S. aureus* sobre *L. plantarum* del que ya se habló anteriormente. Por el contrario, la eliminación parcial de la población de *S. aureus*, a consecuencia del tratamiento con phiIPLA-RODI, parece permitir que la población de *L. plantarum* se desarrolle de manera similar al biofilm monoespecie formado por este microorganismo. Esto se refleja tanto en el mayor número de bacterias de *L. plantarum* como en el aumento de la biomasa adherida. Además, el crecimiento de *L. plantarum* puede verse facilitado por la mayor disponibilidad de nutrientes resultantes de la lisis bacteriana inducida por el fago o por el crecimiento reducido de *S. aureus* IPLA16. No obstante, las interacciones entre especies bacterianas en un biofilm son muy complejas y no siempre fáciles de explicar. Aunque se ha demostrado que la depredación por fagos promueve la formación de biofilms en ciertas bacterias (Hosseinidoust y col., 2013b), nuestros resultados sugieren que el aumento de la biomasa en los cultivos de *S. aureus* - *L. plantarum* se debe al aumento de la especie acompañante y no a una inducción de la formación de biofilm por las células de *S. aureus* que sobrevivieron a la infección. Con respecto a las otras tres cepas estudiadas (*L. pentosus* A1*, L. pentosus* B1 *y E. faecium* MMRA), no se observó un aumento significativo en el número de bacterias viables después del tratamiento con phiIPLA-RODI. Sin embargo, la comparación de los recuentos celulares obtenidos aquí con resultados previos obtenidos en curvas de formación de biofilm (datos no publicados) indica que las poblaciones tanto en las muestras tratadas como en las muestras control alcanzaron el número máximo de células para las cepas mencionadas anteriormente. Curiosamente, el tratamiento con el fago tampoco pareció favorecer la dispersión de bacterias de las especies acompañantes a la fase planctónica. Sillankorva y col. (2010) describieron resultados similares para los biofilms formados por *Pseudomonas fluorescens* y *Staphylococcus lentu*s en condiciones estáticas. Por el contrario, en condiciones dinámicas, el fago ΦIBB-PF7A, que infecta *P. fluorescens*, provocó la liberación de las bacterias no susceptibles de *S. lentus* a la fase planctónica.

Aunque está ampliamente aceptado que los bacteriófagos pueden replicarse dentro de los biofilms, los datos sobre la propagación de fagos en comunidades formadas por múltiples especies son escasos. El ciclo de vida del fago dentro de un biofilm requiere la unión a células bacterianas embebidas en una matriz extracelular y, después de la producción de la progenie del fago, la difusión de los nuevos fagos a otras áreas del biofilm para encontrar nuevas células susceptibles (Abedon, 2016). Dependiendo de la especie bacteriana, las condiciones metabólicas y fisicoquímicas del biofilm (densidad de la matriz, número de células y estado metabólico de las mismas) pueden ser bastante diferentes. En esta Tesis Doctoral se evaluó la propagación de fagos en los cuatro biofilms de doble especie estudiados utilizando dos concentraciones diferentes de fago. No es sorprendente que el título del fago en la fase planctónica fuera considerablemente mayor que el número de partículas fágicas en la fase adherida para todos los biofilms de doble especie. Así, se espera que parte de los fagos liberados por la lisis de células situadas en la capa superior del biofilm pasen directamente a la fase planctónica. Además, nuestros resultados mostraron que los biofilms de dos especies permiten la multiplicación del fago, ya que un porcentaje significativo de las partículas fágicas se aisló como centros infecciosos asociados a células. En general, parece que la tasa de adsorción de los fagos a las células del hospedador se ve favorecida en condiciones planctónicas en comparación con las de un biofilm (Gallet y col., 2009). Curiosamente, la propagación de fagos en la fase adherida fue menor en los biofilms de *S. aureus* - *L. plantarum* que en los biofilms de dos especies que involucran a cualquiera de las dos cepas de *L. pentosus*. Como se mencionó anteriormente, *L. plantarum* forma biofilms mejor que las cepas de *L. pentosus* y se sabe que produce material extracelular. Por lo tanto, es posible que la mayor complejidad de la matriz extracelular de *S. aureus* - *L. plantarum* dificulte la movilidad y posterior propagación del fago en el biofilm. No obstante, algunos estudios parecen indicar que la matriz extracelular no bloquea completamente la penetración del fago en el biofilm (Briandet y col., 2008). Sin embargo, no puede descartarse por completo la interacción de algunos fagos con componentes extracelulares (Kay y col., 2011). Además del papel desempeñado por la matriz, la menor infectividad detectada en los biofilms también puede deberse a la heterogeneidad de estas comunidades con respecto a la estructura y el estado metabólico de las células del hospedador. Por lo tanto, la infección por fagos puede ser

más frecuente en las células metabólicamente activas, ubicadas en la superficie del biofilm, que en las células de crecimiento lento ubicadas en las capas internas (Abedon, 2016). En general, se puede decir que la propagación exitosa de un fago en un biofilm mixto depende de cuáles son las especies no susceptibles que acompañan al hospedador. Esto probablemente se deba a las diferencias en la composición de la matriz extracelular, que puede afectar la capacidad de las partículas virales para llegar a las células susceptibles.

Este estudio proporciona evidencia de que la infección por fagos en biopelículas de doble especie es un proceso complejo, que probablemente esté sujeto a la dinámica de las poblaciones implicadas. Por lo tanto, el tratamiento de fagos podría requerir el uso de cócteles de fagos o fagos combinados con otros antimicrobianos para eliminar a las especies acompañantes.

Una vez estudiado y optimizado el modelo de biofilms mixtos de *S. aureus*, se analizó la capacidad de los fagos phiIPLA-RODI y phiIPLA-C1C para difundir, propagarse y permanecer viables dentro de la compleja estructura del biofilm. Hasta ahora, los estudios sobre la difusión de bacteriófagos a través de biofilms bacterianos son escasos (Nguyen y col., 2017). Por ejemplo, Briandet y col. (2008) analizaron la difusión del fago de *Lactococcus* c2 a través de biofilms formados por cepas susceptibles y no susceptibles mediante espectroscopía de correlación de fluorescencia. En este estudio se observó que el fago podía difundirse a través de biofilms formados por la cepa no susceptible, *Stenotrophomonas maltophilia*, así como por una cepa susceptible y una resistente de *Lactococcus lactis*. Sin embargo, en el caso de las cepas de *Lactococcus*, las partículas del fago parecían inmóviles, lo que sugiere la unión a los receptores de la superficie celular. Más recientemente, un marco de simulación por ordenador indicó que la movilidad de las partículas fágicas dentro de la estructura de un biofilm podría tener un impacto en las interacciones fago-hospedador (Simmons y col., 2018).

En el trabajo desarrollado en esta Tesis Doctoral se describe el desarrollo de un nuevo método para facilitar el análisis de la difusión de fagos, así como los posibles factores que afectan la capacidad del virus para moverse a través del biofilm. Esta técnica se basa en el uso de placas “transwell”, que permiten dividir un pocillo en dos cámaras (una superior y una inferior) separadas por una membrana de policarbonato.

La aplicación de este protocolo a los fagos phiIPLA-RODI y phiIPLA-C1C nos ha permitido evaluar los factores que afectan a su penetración y propagación dentro del biofilm. Para ello, se seleccionaron varias cepas que representan diferentes capacidades de formación de biofilm y distintos perfiles de susceptibilidad a los fagos utilizados. Una vez establecidas las cepas bacterianas a ensayar, se probó la penetración de suspensiones de fagos con una concentración viral alta ($\sim 10^9$ PFU/ml) o baja ($\sim 10^6$ PFU/ml) a través de diferentes biofilms monoespecie. Los resultados de estos experimentos confirmaron que el fago puede difundir a través de todos los biofilms analizados y a las dos concentraciones estudiadas, si bien el título del fago presente en el filtrado (es decir, que había difundido a través del biofilm) variaba para diferentes cepas bacterianas.

El análisis de estos cambios sugiere que el fenotipo que tiene un mayor efecto sobre el título neto de los fagos después de la difusión a través del biofilm es la susceptibilidad de la cepa que lo forma. De hecho, se observó una correlación entre la susceptibilidad de la cepa y el título de fago presente en el filtrado para phiIPLA-RODI a concentraciones bajas y altas, y para phiIPLA-C1C cuando este era aplicado a una concentración baja. Tal vez, esto se debe en parte a la capacidad del fago, especialmente a dosis altas, de matar a las células susceptibles y potencialmente alterar la estructura del biofilm, o bien a su capacidad de atravesar dicha estructura al propagarse "de célula a célula", en lugar de tener que moverse a través de la matriz extracelular. Sin embargo, en algunos casos, la mejor correlación se obtuvo cuando se tuvieron en cuenta tanto la susceptibilidad como la capacidad de formar biofilms de la cepa hospedadora. No obstante, también es probable que la arquitectura compleja y diversa de los biofilms bacterianos desempeñe un papel en la capacidad de los bacteriófagos para moverse a través de ellos, aprovechando potencialmente áreas más finas, especialmente en biofilms gruesos bien estructurados. Hasta el momento, hay muy poco trabajo experimental sobre la localización espacial y la difusión de fagos dentro de los biofilms, pero la literatura disponible es consistente con la idea de que la matriz puede alterar el movimiento de los fagos (Simmons y col., 2018).

Los experimentos posteriores realizados con el fago phiIPLA-RODI proporcionaron datos adicionales sobre la interacción entre el fago y las células presentes en los diferentes biofilms. Cuando se llevó a cabo un tratamiento de los biofilms mixtos con una

concentración baja de phiIPLA-RODI, los resultados fueron bastante variados y, a veces, inesperados. Por ejemplo, la combinación de *L. plantarum* 55-1 y *S. epidermidis* F12 muestra un comportamiento similar al que tiene lugar cuando estos microorganismos forman biofilms monoespecie, es decir, el título de fago se reduce aproximadamente 2 unidades logarítmicas. Sin embargo, los biofilms formados por diferentes cepas de *S. aureus* con *L. plantarum* 55-1 siempre condujeron a un título de fago más bajo en el filtrado que el control sin biofilm. Por el contrario, en los biofilms mixtos de cepas de *S. aureus* con *S. epidermidis* F12 no se observó una disminución del título de los fagos. Esto sugiere que los mecanismos por los cuales estas dos especies disminuyen el número de partículas de fago en el filtrado pueden ser diferentes, representando diferentes efectos sobre la dinámica de propagación o inactivación del mismo. Esta hipótesis parece aún más probable en vista de que sobrenadantes filtrados de *L. plantarum* inactivaban al fago phiIPLA-RODI por debajo del nivel de detección, mientras que los de *S. epidermidis* F12 redujeron, pero no eliminaron el fago. Sin embargo, se necesitaría llevar a cabo nuevos estudios para explorar el mecanismo que conduce a una disminución en el número de partículas de fago viables en esta última cepa. Curiosamente, un estudio anterior había demostrado que la propagación de phiIPLA-RODI en biofilms formados por *S. aureus* IPLA16 con *L. plantarum* 55-1 fue menor que en los formados con *L. pentosus* (González y col., 2017). Esto también puede ser una consecuencia de la inactivación del fago en presencia de *L. plantarum* pero no de *L. pentosus*. Además, el análisis de las partículas fágicas viables atrapadas en la matriz extracelular de diferentes biofilms mostró resultados interesantes. Por ejemplo, las cepas *S. epidermidis F12* y *L. plantarum* 55-1 no parecían haber retenido una alta proporción de partículas fágicas dentro de la matriz. Esto sugiere que el título bajo en el filtrado puede deberse a la inactivación del fago en los biofilms formados por estas dos cepas. Sin embargo, se necesita más investigación para establecer el mecanismo específico implicado en esta inactivación, que puede involucrar degradación enzimática, inactivación por el pH o unión irreversible del fago a desechos celulares o componentes de la matriz. Otro detalle interesante es el hecho de que la matriz de los biofilms de *S. aureus* IPLA 15 y *S. aureus* V329 exhiben un título de fago mayor que el esperado de acuerdo a los niveles observados en el filtrado. Como ya se mencionó anteriormente, esto puede estar relacionado con diferencias en la arquitectura de los biofilms o con la composición de la

matriz extracelular, puesto que *S. aureus* V329 es la única cepa analizada que tiene una matriz extracelular basada en proteínas. Con respecto a *S. aureus* IPLA15, un estudio anterior sugirió que la exposición a niveles subinhibitorios del fago phiIPLA-RODI conducía a la acumulación de ADN extracelular en el biofilm (Fernández y col., 2017).

Teniendo en cuenta todos estos resultados, se puede concluir que la penetración del fago a través de los biofilms es el resultado del equilibrio neto entre la propagación del fago y la inactivación del mismo, así como su penetración y difusión en el biofilm. Estos procesos dependerán en gran medida de las cepas bacterianas que forman la estructura en función de diferentes propiedades. Por ejemplo, la susceptibilidad al fago de las cepas que forman el biofilm determinará la velocidad de propagación del virus dentro de esta estructura. Por el contrario, la retención de las partículas fágicas puede depender de la composición de la matriz extracelular o de la superficie celular bacteriana. Finalmente, la producción de enzimas que inactiven el fago y/o la disminución del pH por una cepa bacteriana presente en la comunidad pueden tener un efecto tan perjudicial sobre la población de fagos que no pueda compensarse mediante la propagación del fago en la cepa susceptible.

La aplicación de este protocolo a dos fagos de *Staphylococcus* ha revelado aspectos interesantes de la interacción entre el fago y el hospedador en biofilms que serán útiles para el desarrollo de productos basados en fagos destinados a la eliminación de los biofilms estafilocócicos. Además, esta técnica proporciona una nueva herramienta para descifrar la dinámica compleja de la infección por fagos dentro de las comunidades microbianas sésiles.

Influencia de los bacteriófagos phiIPLA-RODI, Φ11 y Φ80α en la formación de biofilms de *S. aureus*.

Los fagos, tanto líticos como atemperados, juegan un papel importante en la evolución y el destino de las comunidades microbianas (Fernández y col., 2018). En el caso de los biofilms, cada vez hay más datos que indican que la depredación por fagos juega un papel modulador, en algunas ocasiones favoreciendo su formación y en otras desencadenando su dispersión. No obstante, la mayor parte de estos estudios se centran en el impacto de los fagos atemperados. Por el contrario, en el caso de los fagos virulentos hay pocos datos acerca de su posible efecto en el desarrollo de los biofilms. Así, se sabe que cuando están presentes a dosis suficientemente elevadas, como las que se aplicarían, por ejemplo, buscando un efecto terapéutico, pueden disminuir el número de bacterias adheridas e incluso la cantidad de biomasa. Recordemos que este es el caso del fago phiIPLA-RODI, el cual como ya hemos visto anteriormente, puede reducir los biofilms de cepas susceptibles al mismo. Sin embargo, al igual que ocurre con otros antimicrobianos, durante la aplicación de los bacteriófagos con fines de desinfección o de terapia fágica, podría ocurrir que la dosis que llegue a las células diana no sea lo suficientemente alta para llevar a cabo su acción antibacteriana con la eficacia necesaria. En estos casos, es posible que el impacto del fago sobre la población tenga un efecto no deseado; por ejemplo, que potencie la formación de biofilms. Esto contribuiría a proteger a las células bacterianas de agentes deletéreos externos, incluyendo los antibióticos y desinfectantes. A su vez, esto dificultaría la posterior eliminación del microorganismo patógeno. Teniendo en cuenta estas premisas, en este trabajo se abordó el estudio de la formación de biofilms de *S. aureus* IPLA1 en presencia de dosis del fago virulento phiIPLA-RODI que no consiguen eliminar la población de bacterias susceptibles al mismo. A dosis iniciales altas, se observa un claro descenso en el número de bacterias viables en el biofilm y en la cantidad de biomasa adherida (MOI inicial de 10^{-4} y 10^{-3}). Sin embargo, si la dosis inicial del fago desciende aún más (MOI inicial de 10^{-5}), se observa no solo que el número de células adheridas no baja significativamente, sino que hay una mayor cantidad de biomasa total. Un estudio anterior llevado a cabo por Hosseinidoust y col. (2013a) ya había mostrado que el tratamiento con ciertos fagos virulentos daba lugar a una mayor formación de biofilms en *P. aeruginosa*, *Salmonella* Typhimurium y una cepa de *S. aureus* diferente a la

utilizada con phiIPLA-RODI. En dicho trabajo, se observó que, en el caso de *P. aeruginosa*, este efecto se debía a la selección de células resistentes a la infección fágica que poseían una mejor capacidad para formar biofilms. Por el contrario, en el caso de *S.* Typhimurium y *S. aureus*, los autores indican que el incremento de biomasa se debe a mecanismos no evolutivos, es decir, no basados en mutación, aún por determinar. Los indicios obtenidos para *S. aureus* IPLA1 mostraron que el aumento de biomasa en biofilms infectados por phiIPLA-RODI se debe a un incremento notable en su contenido en ADN extracelular. Este fenómeno se debe probablemente a la lisis parcial de parte de la población por el fago, con la consiguiente liberación de ADN cromosómico bacteriano a la matriz extracelular. Este es el caso de *Shewanella oneidensis* MR1, un microorganismo que requiere la inducción de tres profagos para poder formar biofilms estables con un elevado contenido de ADN extracelular (Gödeke y col., 2011). Sin embargo, no es esperable que esto ocurra con todos los fagos ya que algunos de ellos producen endonucleasas que degradan el cromosoma bacteriano y utilizan los nucleótidos para llevar a cabo la replicación del genoma fágico (Miller y col., 2003). Sería interesante determinar si este es el caso de phiIPLA-RODI. Por otro lado, con los datos disponibles, no se puede descartar la participación de las autolisinas producidas por la propia célula bacteriana. Estos enzimas participan en el proceso de biosíntesis y reciclado de la pared celular, pero se sabe que en algunos casos también participan en la formación de biofilms. Por ejemplo, hasta el momento se ha determinado que la autolisina principal de *S. aureus* (AtlA) es importante en la liberación de ADN extracelular que participa en la etapa de adherencia inicial al sustrato (Bose y col., 2012). Además, la sobreexpresión del enzima autolítico Sle1 conduce a la acumulación de ADN en la matriz del biofilm y, por tanto, a un incremento en la biomasa total (Schilcher y col., 2016). En este sentido, cabe destacar que los biofilms infectados por phiIPLA-RODI muestran una mayor expresión de los genes que codifican distintas autolisinas del microorganismo, incluyendo AtlA y Sle1. Las diferencias a nivel de transcriptoma entre los biofilms infectados por el fago y los biofilms control no solo afectan a la expresión de autolisinas. De hecho, se encontraron cambios significativos en la expresión de 1063 genes, de los cuales aproximadamente la mitad mostraban mayor nivel de transcripción en presencia del fago. En cambio, la otra mitad tenía una menor expresión en biofilms infectados con phiIPLA-RODI. Dentro de esta lista, cabe destacar la presencia de al menos 71 genes que

están implicados en la respuesta estricta en este microorganismo. Entre estos genes se incluye además el gen *rsh* que codifica una proteína que participa en la síntesis e hidrólisis de la alarmona (p)ppGpp, responsable de modular la aparición de esta respuesta. Hasta el momento, todos los estudios transcripcionales realizados durante la infección por fagos virulentos se habían centrado en los cambios que tienen lugar a lo largo del desarrollo del ciclo lítico llevando a cabo infecciones sincronizadas de la población. Esta información es muy importante a la hora de entender cómo afecta la toma de control de la célula bacteriana por parte del fago. Sin embargo, en una situación real las condiciones no van a reflejar necesariamente una infección sincronizada de la población bacteriana. De hecho, es más probable que solo una fracción de las células estén infectadas por el fago. Por lo tanto, nos propusimos estudiar las diferencias a nivel de transcriptoma en una población de este tipo. No obstante, es necesario indicar que los datos obtenidos en este trabajo solo nos informan de los valores medios del cambio a nivel poblacional entre el biofilm infectado por phiIPLA-RODI y el biofilm control. Por lo tanto, no revelan si estas diferencias se deben a las células infectadas por el fago, estando asociadas al desarrollo del ciclo lítico en las mismas, o son cambios que aparecen en la población no infectada. Más recientemente, Fernández y col. (artículo en revisión) han comprobado que los cambios observados durante una infección sincronizada en cultivo líquido no se corresponden con los mostrados por los biofilms infectados con un título inicial del fago bajo. Por lo tanto, es probable que las diferencias a nivel transcripcional de los biofilms infectados se deban a las células no infectadas. Sin embargo, aún está por determinar cuál es el agente inductor de dichos cambios. Se puede especular que, tal vez, la lisis parcial de la población libere al medio distintas moléculas (incluyendo ADN, proteínas, etc.) que puedan ejercer un efecto sobre las células vecinas. En este sentido, cabe señalar que Fernández y col. (artículo en revisión) han demostrado que el pH juega un papel fundamental en el control del desarrollo de biofilms a dosis bajas del fago phiIPLA-RODI. Por un lado, la bajada del pH a 5 o menos lleva a la inactivación de parte de la población de fagos, lo que permite limitar el avance de la infección en la población bacteriana. Por otra parte, un pH ligeramente ácido es necesario para que tenga lugar el cambio en la estructura del biofilm. Esto coincide con los resultados publicados por Foulston y col. (2014) en los que mostraban que la

acumulación de ADN extracelular en los biofilms de *S. aureus* requería la acidificación del medio de cultivo.

Como ya se ha comentado anteriormente, hay varios estudios que muestran la influencia de la presencia de profagos en el cromosoma bacteriano sobre la formación de biofilms. Por ejemplo, en el caso de *S. oneidensis* (Gödeke y col., 2011), *Bacillus anthracis* (Schuch y Fischetti, 2009) y *S. pneumoniae* (Carrolo y col., 2010) se observó una mayor formación de biofilms en cepas portadoras de ciertos profagos. Por el contrario, la inducción de profagos en *Enterococcus faecalis* (Rossman y col., 2015) o *E. coli* (Liu y col., 2015) provocó una mayor dispersión del biofilm. Sin embargo, hasta ahora, el impacto de los profagos durante el desarrollo de biofilms de *S. aureus* no había sido examinado en profundidad. En este contexto, nuestro estudio tuvo como objetivo determinar cómo dos fagos atemperados ya descritos, φ80α y φ11, afectan a la capacidad de formar biofilms de la cepa *S. aureus* RN450 y si alteran el transcriptoma de su hospedador.

Los estudios preliminares realizados antes del análisis transcripcional mostraron que ambas cepas lisogénicas exhibían una mayor acumulación de biomasa en las primeras etapas del desarrollo del biofilm. Sin embargo, la biomasa de los biofilms maduros solo aumentó en el lisógeno φ11. Esto sugiere que los mecanismos responsables del aumento del biofilm en las dos cepas lisogénicas pueden ser diferentes, al menos en las últimas etapas de desarrollo del mismo. De hecho, parece que para el lisógeno φ80α, la formación de biofilm se produce a un ritmo más rápido, pero finalmente conduce a una cantidad similar de biomasa adherida total. Se observó liberación espontánea de partículas de fago para ambos lisógenos, tanto en la fase planctónica como en el biofilm. Curiosamente, había menos viriones dentro de las células del biofilm que libres en la matriz extracelular. Esto sugiere que la inducción espontánea del ciclo lítico se ha ralentizado en las células sésiles en esta etapa de la formación del biofilm. De hecho, dicha hipótesis se ve reforzada por los resultados obtenidos en un experimento adicional que muestra que el título máximo de fagos en el biofilm se encuentra a las 5 horas de desarrollo, disminuyendo posteriormente. Del mismo modo, Resch y col. (2005) observaron que la liberación espontánea de fago en las cepas lisogénicas *S. aureus* SA113 y *S. aureus* Newman alcanzaba su punto máximo

antes de las 8 horas de crecimiento, tanto en biopelículas como en cultivos planctónicos. Además, estos resultados sugieren que, tras la lisis de las células bacterianas, las partículas fágicas pueden acumularse en la matriz y, junto con el contenido celular liberado, contribuir a la biomasa total del biofilm. De este modo, esta "red de fagos" podría actuar como un mecanismo de defensa contra las cepas competidoras que sean susceptibles al mismo, así como contribuir a incrementar la transferencia genética dentro del biofilm. De hecho, Haaber y col. (2013) ya demostraron que los profagos pueden promover la transferencia de marcadores de resistencia a los antibióticos entre las células que forman parte de un biofilm.

El perfil transcripcional de los biofilms formados por las dos cepas lisogénicas y la cepa libre de profagos reveló cambios importantes asociados con la presencia de los mismos en el genoma bacteriano. Por ejemplo, se encontró que ambos lisógenos mostraban signos de activación del factor de transcripción alternativo SigB (Bischoff y col., 2004). Un análisis más detallado de los resultados de estos datos indica que las cepas que albergan fagos atemperados exhiben diferencias en genes que afectan el metabolismo, la virulencia, la formación de biofilms o la producción del pigmento protector estafiloxantina. Entre los genes identificados en el análisis transcriptómico se encontraron algunos que podrían explicar la mayor formación de biofilms en comparación con la cepa libre de profagos. Por ejemplo, los lisógenos exhiben una menor expresión de proteasas, enzimas que participan en la dispersión de biofilms en este microorganismo. Además, las cepas lisógenas muestran una mayor expresión de proteínas que participan en el proceso de adherencia y en la producción de polisacárido extracelular. Schuch y Fischetti (2009) también habían observado que una cepa de *B. anthracis* portadora de profagos producía una mayor cantidad de polisacárido extracelular que la cepa libre de ellos.

En conclusión, los resultados de este estudio muestran que la lisogenización de *S . aureus* con estos dos fagos conduce a una mayor formación de biofilm y producción de estafiloxantina, así como a cambios transcripcionales que afectan a algunas de las principales cascadas de regulación transcripcional de este patógeno. En ese sentido, llevar un profago puede contribuir a estas adaptaciones bacterianas, ejerciendo así un impacto positivo en la población de la bacteria hospedadora. En conjunto, nuestros

datos apoyan la idea de que los bacteriófagos juegan un papel importante en las comunidades microbianas. Evidentemente, aún se requieren más estudios para comprender cómo se desarrollan las interacciones entre los fagos de *S. aureus* y su hospedador. Sin embargo, lo que está cada vez más claro es que estudiar las interacciones fago-hospedador será primordial para obtener un mayor conocimiento de la dinámica de la población bacteriana. A su vez, esta información proporcionará una visión más realista del papel que juegan los microbios en los entornos naturales, y ayudará a diseñar nuevas estrategias para combatir los microorganismos no deseados.

Utilización de proteínas líticas de origen fágico para la prevención y eliminación de biofilms de *S. aureus*.

Las proteínas líticas procedentes de fagos (endolisinas y peptidoglicano hidrolasas asociadas al virión, VAPGH) son una alternativa prometedora a los antimicrobianos convencionales, debido a que muestran actividad antimicrobiana de espectro reducido y no seleccionan cepas resistentes. Por este motivo, existen en la actualidad numerosos estudios acerca de la utilización de dichas proteínas en modelos animales de infección y frente a biofilms desarrollados *in vitro* (Gutierrez y col., 2018). Por ejemplo, el uso terapéutico de proteínas líticas en animales infectados por *S. aureus* está proporcionando resultados prometedores, ya que estas proteínas están mostrando una buena eficacia sin efectos secundarios aparentes (Gutiérrez y col., 2018). Los ensayos clínicos en humanos aún están en desarrollo, aunque cabe destacar el realizado por la empresa ContraFect Corp, se trata de CF-301 (Exebacase), primera lisina derivada de bacteriófagos con gran actividad contra *Staphylococcus aureus*, puesto que ha superado la fase 2 en mayo de 2019, y se encuentra en estos momentos en ensayo clínico de fase 3, para el tratamiento de pacientes con bacteriemia por *Staphylococcus aureus*, incluida la endocarditis.

Otra ventaja de las proteínas líticas es que, gracias a su estructura modular, se puede utilizar la ingeniería genética para el diseño de nuevas proteínas "a medida" que pueden exhibir mejores propiedades antibacterianas. Un ejemplo de esto es la proteína quimérica CHAPSH3b, que consiste en un dominio catalítico de la

peptidoglicano hidrolasa asociada al virión del fago vB_SauS-phiIPLA88 (HydH5) y el dominio de unión a la pared celular de la lisostafina (Rodriguez-Rubio y col, 2013). Esta proteína quimérica, CHAPSH3b, tiene una actividad muy superior a la proteína lítica de la que se deriva, HydH5. En este trabajo, se trató de analizar si CHAPSH3b tiene también potencial frente a biofilms de *S. aureus*, tanto para facilitar su eliminación como para prevenir su formación. En cuanto al tratamiento de biofilms preformados, hemos demostrado que la proteína reduce el número de bacterias viables y la cantidad de biomasa adherida tanto a 25°C (temperatura ambiente) como a 37°C (temperatura de la infección). El análisis mediante microscopía confocal confirmó que el tratamiento lisa parte de la población y reduce el número de bacterias en el biofilm. Sin embargo, es necesario señalar que la actividad de la proteína en estas condiciones era superior a 37°C que a 25°C, a pesar de que los ensayos de determinación de la CMI de CHAPSH3b indicaban que las células eran más susceptibles a temperatura ambiente. Este fenómeno podría deberse a que, a diferencia de los ensayos de CMI, el tratamiento del biofilm se llevó a cabo en condiciones que no permiten el crecimiento bacteriano. Por lo tanto, los resultados obtenidos podrían reflejar la actividad enzimática, que es más alta a 37°C que a 25°C (Rodriguez-Rubio y col., 2013). Por el contrario, los ensayos de determinación de la CMI se ven afectados por diferencias en la tasa de crecimiento bacteriano, que es más elevada a 37°C que a 25°C. Es muy probable que la población bacteriana aumente demasiado rápido a 37°C, haciendo necesaria la utilización de una concentración más alta del enzima para eliminar la población completa.

En cuanto a la utilización de CHAPSH3b para la prevención de la formación de biofilms, se observó un efecto inhibitorio sobre este proceso tanto a 25°C como a 37°C. Esta es una propiedad muy interesante ya que algunos antimicrobianos como la vancomicina tienen precisamente el efecto contrario, es decir, favorecen la formación de biofilms (Cargill y Upton, 2009; Kaplan y col., 2012). Otros compuestos que, como CHAPSH3b, ejercen un efecto inhibitorio sobre el desarrollo de biofilms en *S. aureus* son el lantibiótico gallidermina (Saising y col, 2012) y el péptido catiónico sintético IDR-1018 (de la Fuente Nuñez y col., 2014). En el caso de la gallidermina, se demostró que disminuye la expresión del gen que codifica la autolisina AtlA y el operón *ica*, implicado en la síntesis del polisacárido extracelular

(Saising y col., 2012). Por el contrario, IDR-1018 previene la formación de biofilms en distintas especies bacterianas interfiriendo con la respuesta estricta (de la Fuente-Nuñez y col., 2014). Como se mencionó anteriormente, Gutiérrez y col. (2014) ya habían demostrado que la endolisina LysH5 inhibe la formación de biofilms en algunas cepas de *S. aureus*. En el caso de CHAPSH3b, se investigó además el efecto de esta proteína sobre la estructura del biofilm mediante microscopía confocal. En el caso de la cepa *S. aureus* IPLA1, que proviene de la industria alimentaria, no se encontraron diferencias notables en cuanto a la arquitectura del biofilm, si bien la cobertura de la superficie de adhesión se veía muy reducida en las muestras tratadas con la proteína. Sin embargo, en la cepa *S. aureus* ISP479r, que es buena formadora de biofilms, se encontraron cambios notables en los biofilms expuestos a la proteína lítica. Así, los biofilms no tratados eran más gruesos y contenían mayor cantidad de ADN extracelular rodeando las células, mientras que los tratados eran más finos y tenían zonas donde se acumulaban más células mientras otras mostraban una menor densidad. Este fenotipo podía observarse incluso macroscópicamente en biofilms teñidos con cristal violeta, en los que la superficie del pocillo parecía estar cubierta por una fina capa con puntos teñidos intensamente.

En muchos casos, se pueden comprender los efectos fenotípicos asociados con la exposición a concentraciones subinhibitorias de antibióticos mediante el estudio de las respuestas transcripcionales de las células bacterianas en estas condiciones (Fernández y col., 2012; Linares y col., 2006). Hasta ahora, no había ninguna información acerca de los cambios en la expresión génica que se dan como respuesta a la exposición a proteínas líticas de origen fágico. En este trabajo, se muestra que las células de *S. aureus* expuestas a dos proteínas líticas diferentes, LysH5 y CHAPSH3b, exhiben una menor expresión de genes que codifican proteínas con actividad autolítica, incluyendo la autolisina principal de *S. aureus* AtlA. En estudios anteriores ya se había demostrado que el gen *atl* muestra una menor expresión tras la exposición a otros compuestos antimicrobianos que afectan a la pared celular, como la bacitracina, la D-cicloserina y la oxacilina (Utaida y col., 2003). La autolisina AtlA de *S. aureus* y su homóloga AtlE en *S. epidermidis* participan

en el proceso de formación de biofilms de estos microorganismos. De hecho, se considera que las autolisinas son especialmente importantes durante la fase inicial de adhesión (Fernandez y col., 2017). Por tanto, en *S. aureus*, la disminución en la expresión de autolisinas en respuesta a las proteínas fágicas podría resultar en una menor habilidad para formar biofilms, al menos en algunas cepas. A su vez, esto podría facilitar que la población sea más susceptible a su eliminación mediante otros compuestos antimicrobianos ya que las células en los biofilms son menos accesibles y más tolerantes a los mismos. Parece, por tanto, que la capacidad de inhibir la formación de biofilms debería ser una propiedad deseable a la hora de diseñar nuevos enzimas líticos.

Consideraciones finales

La necesidad de desarrollar nuevos métodos para combatir los biofilms bacterianos en distintos ambientes es actualmente uno de los problemas mas releventes a nivel mundial. En este contexto, los bacteriófagos y las proteínas líticas derivadas de los mismos poseen propiedades únicas que los hacen unos candidatos prometedores como agentes antibiofilm. Sin embargo, aún hay aspectos sobre su utilización con esta finalidad que necesitan ser estudiados en mayor profundidad.

Por un lado, si bien ya existen numerosos estudios que muestran cómo los fagos pueden infectar bacterias y causar la lisis bacteriana en biofilms de una sola especie, su eficacia en el tratamiento de biofilms mixtos ha sido menos estudiada. En los biofilms multiespecie, las interacciones fago-biofilm pueden ser mucho más complejas. En los estudios incluidos en esta memoria se demuestra que los bacteriófagos de *S. aureus*, especialmente phiIPLA-RODI, tienen potencial como agentes de eliminación de biofilms tanto monoespecie como mixtos. De hecho, este fago puede penetrar en el biofilm y matar a sus células diana incluso cuando la especie acompañante en el biofilm no es susceptible al mismo. No obstante, nuestros resultados indican que la eficacia del tratamiento sí varía en función de qué especie o especies estén formando el biofilm con *S. aureus*. Por un lado, esto se debe a las interacciones entre las especies bacterianas. Sin embargo, también observamos que en muchos casos estas variaciones se deben a un efecto directo

sobre el fago. De hecho, la presencia de determinadas cepas bacterianas parece llevar a una inactivación parcial de la población del mismo.

Otro aspecto importante es la posibilidad de que el tratamiento con antimicrobianos de origen fágico afecte a la formación de biofilms u a otros aspectos de la biología de la bacteria diana. Nuestros datos muestran que tratamientos con dosis bajas de phiIPLA-RODI pueden llevar a una mayor acumulación de biomasa, especialmente de ADN extracelular. Sin embargo, resultados más recientes muestran que este efecto solo se observa cuando el pH ambiental es ligeramente ácido. Además, la suplementación de este tratamiento con desoxirribonucleasa previene la acumulación de biomasa y lleva a una clara reducción del biofilm por el fago. Por lo tanto, conocer la existencia de problemas potenciales antes de aplicar un compuesto antimicrobiano nos ha permitido diseñar nuevas estrategias para evitar su aparición. Además, hay que tener en cuenta que los bacteriófagos también forman parte de las comunidades microbianas en la naturaleza. Por lo tanto, es posible que en algunos casos puedan también ejercer un papel modulador sobre la formación de las mismas. A su vez, esto dificultaría la elimininación de la contaminación bacteriana dada la elevada resistencia de estas estructuras multicelulares a distintos compuestos antimicrobianos. Nuestro trabajo indica que, en *S. aureus*, este fenómeno puede estar mediado tanto por fagos virulentos (phiIPLA-RODI) como por fagos atemperados (Φ11 y Φ80α). En cuanto a las proteínas líticas LysH5 y CHAP-SH3b, nuestros resultados demuestran que además de su acción bactericida, también tienen la capacidad de inhibir la formación de biofilms cuando están presentes en dosis subinhibitorias. Esta es evidentemente una propiedad muy deseable a la hora de llevar a cabo tratamientos de eliminación de biofilms, ya sea en el ámbito industrial o en el clínico.

En conjunto, todos estos datos aportan información valiosa acerca de la aplicación de los bacteriófagos y sus proteínas líticas como antimicrobianos. Así, se ponen de manifiesto algunas de sus propiedades positivas pero también algunos posibles efectos no deseados. Esto último es imprescindible para poder diseñar estrategias de utilización inteligentes que saquen el máximo partido posible a las

ventajas de estos compuestos y, al mismo tiempo, minimicen o impidan la aparición de los efectos negativos de los mismos.

Conclusiones

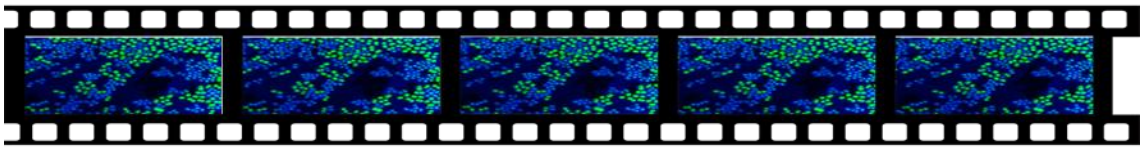

CONCLUSIONES

1. El estudio de biofilms mixtos compuestos por *S. aureus* y cuatro cepas de las especies *L. plantarum, L. pentosus y E. faecium* permitió confirmar que estas especies forman estructuras sésiles estables.
2. El tratamiento de estos biofilms mixtos con el bacteriófago phiIPLA-RODI da lugar a una reducción en el número de células viables de *S. aureus*, sobre todo cuando se realiza en condiciones de crecimiento activo del hospedador. A su vez, esto provoca un aumento en el número de células de la especie acompañante *L. plantarum*, pero no afecta a los recuentos de *L. pentosus* o *E. faecium*.
3. El fago phiIPLA-RODI puede difundir a través de biofilms formados por diferentes cepas bacterianas. Esta difusión depende de la susceptibilidad de la cepa, el título inicial del fago, las interacciones del fago con la matriz extracelular y la inactivación del fago, pero no de la cantidad de biomasa adherida.
4. Los biofilms formados por algunas cepas de *S. aureus* en presencia de dosis bajas del fago phiIPLA-RODI tienen más biomasa total y la matriz extracelular contiene una mayor cantidad de ADN que los biofilms no infectados.
5. La presencia de los profagos φ11 y φ80α en *S. aureus* RN450 da lugar a cambios fenotípicos tales como un incremento en la capacidad para formar biofilms y una mayor producción del pigmento carotenoide estafiloxantina.
6. A nivel transcripcional, las cepas lisogénicas RN450-φ11 y RN450-φ80α mostraron una activación del regulón del factor sigma alternativo (SigB) y una inhibición de los genes controlados por el sistema de quórum sensing Agr.
7. Dosis subinhibitorias de la proteína lítica CHAPSH3b pueden inhibir la formación de biofilms por algunas cepas de *S. aureus*. El análisis transcripcional reveló que la exposición de las células de *S. aureus* a este enzima inhibe la expresión de varios genes que codifican autolisinas bacterianas, lo que podría explicar la menor formación de biofilms en presencia de CHAPSH3b.

Bibliografía

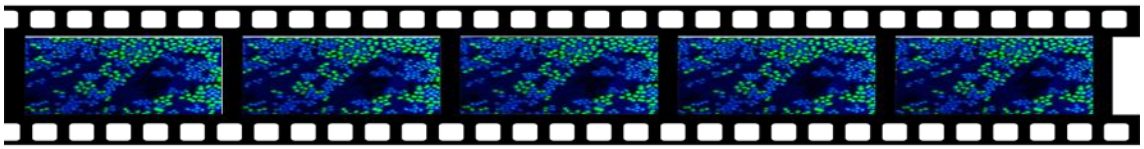

BIBLIOGRAFÍA

Abedon S. T. (2016). Phage therapy dosing: The problem(s) with multiplicity of infection (MOI). *Bacteriophage*, 6(3), e1220348. https://doi.org/10.1080/21597081.2016.1220348

Abedon S. T. (2017). Information Phage Therapy Research Should Report. *Pharmaceuticals (Basel, Switzerland)*, 10(2), 43. https://doi.org/10.3390/ph10020043

Abedon, S. T., García, P., Mullany, P., & Aminov, R. (2017). Editorial: Phage Therapy: Past, Present and Future. *Frontiers in microbiology*, 8, 981. https://doi.org/10.3389/fmicb.2017.00981

Ackermann H. W. (2007). 5500 Phages examined in the electron microscope. *Archives of virology*, 152(2), 227–243. https://doi.org/10.1007/s00705-006-0849-1

Ackermann, H. W., & Kropinski, A. M. (2007). Curated list of prokaryote viruses with fully sequenced genomes. *Research in microbiology*, 158(7), 555–566. https://doi.org/10.1016/j.resmic.2007.07.006

Ajuebor, J., Buttimer, C., Arroyo-Moreno, S., Chanishvili, N., Gabriel, E. M., O'Mahony, J., McAuliffe, O., Neve, H., Franz, C., & Coffey, A. (2018). Comparison of *Staphylococcus* Phage K with Close Phage Relatives Commonly Employed in Phage Therapeutics. *Antibiotics (Basel, Switzerland)*, 7(2), 37. https://doi.org/10.3390/antibiotics7020037

Amorena, B., Gracia, E., Monzón, M., Leiva, J., Oteiza, C., Pérez, M., Alabart, J. L., & Hernández-Yago, J. (1999). Antibiotic susceptibility assay for *Staphylococcus aureus* in biofilms developed in vitro. *The Journal of antimicrobial chemotherapy*, 44(1), 43–55. https://doi.org/10.1093/jac/44.1.43

Anderl, J. N., Franklin, M. J., & Stewart, P. S. (2000). Role of antibiotic penetration limitation in Klebsiella pneumoniae biofilm resistance to ampicillin and ciprofloxacin. *Antimicrobial agents and chemotherapy*, 44(7), 1818–1824. https://doi.org/10.1128/aac.44.7.1818-1824.2000

Archer, N. K., Mazaitis, M. J., Costerton, J. W., Leid, J. G., Powers, M. E., & Shirtliff, M. E. (2011). *Staphylococcus aureus* biofilms: properties, regulation, and roles in human disease. *Virulence*, 2(5), 445–459. https://doi.org/10.4161/viru.2.5.17724

Arias, C. A., Rincon, S., Chowdhury, S., Martínez, E., Coronell, W., Reyes, J., Nallapareddy, S. R., & Murray, B. E. (2008). MRSA USA300 clone and VREF--a U.S.-Colombian connection?. *The New England journal of medicine*, 359(20), 2177–2179. https://doi.org/10.1056/NEJMc0804021

Armand-Lefevre, L., Ruimy, R., & Andremont, A. (2005). Clonal comparison of *Staphylococcus aureus* isolates from healthy pig farmers, human controls, and pigs. *Emerging infectious diseases*, 11(5), 711–714. https://doi.org/10.3201/eid1105.04086

Atterbury, R. J., Connerton, P. L., Dodd, C. E., Rees, C. E., & Connerton, I. F. (2003). Isolation and characterization of Campylobacter bacteriophages from retail poultry. *Applied and environmental microbiology*, 69(8), 4511–4518. https://doi.org/10.1128/aem.69.8.4511-4518.2003

Azam, A. H., & Tanji, Y. (2019). Peculiarities of *Staphylococcus aureus* phages and their possible application in phage therapy. *Applied microbiology and biotechnology*, 103(11), 4279–4289. https://doi.org/10.1007/s00253-019-09810-2

Azeredo, J., & Sutherland, I. W. (2008). The use of phages for the removal of infectious biofilms. *Current pharmaceutical biotechnology*, 9(4), 261–266. https://doi.org/10.2174/138920108785161604

Baird-Parker. A. C. (1965). The classification of staphylococci and micrococci from world-wide sources. *Journal of general microbiology*, 38, 363–387. https://doi.org/10.1099/00221287-38-3-363

Barbosa, C., Venail, P., Holguin, A. V., & Vives, M. J. (2013). Co-evolutionary dynamics of the bacteria Vibrio sp. CV1 and phages V1G, V1P1, and V1P2: implications for phage therapy. *Microbial ecology*, 66(4), 897–905. https://doi.org/10.1007/s00248-013-0284-2

Barrio, B., Vangroenweghe, F., Dosogne, H., & Burvenich, C. (2000). Decreased neutrophil bactericidal activity during phagocytosis of a slime-producing *Staphylococcus aureus* strain. *Veterinary research*, 31(6), 603–609. https://doi.org/10.1051/vetres:2000143

Barrow, PA (2001). The use of bacteriophages for treatment and prevention of bacterial disease in animals and animal models of human infection. *J Chem Technol Biotechnol,* 76 (7):677–682. https://doi.org/10.1002/jctb.436

Barylski, J., Enault, F., Dutilh, B. E., Schuller, M. B., Edwards, R. A., Gillis, A., Klumpp, J., Knezevic, P., Krupovic, M., Kuhn, J. H., Lavigne, R., Oksanen, H. M., Sullivan, M. B., Jang, H. B., Simmonds, P., Aiewsakun, P., Wittmann, J., Tolstoy, I., Brister, J. R., Kropinski, A. M., … Adriaenssens, E. M. (2020). Analysis of Spounaviruses as a Case Study for the Overdue Reclassification of Tailed Phages. *Systematic biology*, 69(1), 110–123. https://doi.org/10.1093/sysbio/syz036

Baugh, S., Ekanayaka, A. S., Piddock, L. J., & Webber, M. A. (2012). Loss of or inhibition of all multidrug resistance efflux pumps of Salmonella enterica serovar Typhimurium results in impaired ability to form a biofilm. *The Journal of antimicrobial chemotherapy*, 67(10), 2409–2417. https://doi.org/10.1093/jac/dks228

Becker, S. C., Roach, D. R., Chauhan, V. S., Shen, Y., Foster-Frey, J., Powell, A. M., Bauchan, G., Lease, R. A., Mohammadi, H., Harty, W. J., Simmons, C., Schmelcher, M., Camp, M., Dong, S., Baker, J. R., Sheen, T. R., Doran, K. S., Pritchard, D. G., Almeida, R. A., Nelson, D. C., … Donovan, D. M. (2016). Triple-acting Lytic Enzyme Treatment of Drug-Resistant and Intracellular *Staphylococcus aureus*. *Scientific reports*, 6, 25063. https://doi.org/10.1038/srep25063

Bischoff, M., Dunman, P., Kormanec, J., Macapagal, D., Murphy, E., Mounts, W., Berger-Bächi, B., & Projan, S. (2004). Microarray-based analysis of the *Staphylococcus aureus* sigmaB regulon. *Journal of bacteriology*, 186(13), 4085–4099. https://doi.org/10.1128/JB.186.13.4085-4099.2004

Bose, J. L., Lehman, M. K., Fey, P. D., & Bayles, K. W. (2012). Contribution of the *Staphylococcus aureus* Atl AM and GL murein hydrolase activities in cell division, autolysis, and biofilm formation. *PloS one*, 7(7), e42244. https://doi.org/10.1371/journal.pone.0042244

Bradley D. E. (1967). Ultrastructure of bacteriophage and bacteriocins. *Bacteriological reviews*, 31(4), 230–314.

Briandet, R., Lacroix-Gueu, P., Renault, M., Lecart, S., Meylheuc, T., Bidnenko, E., Steenkeste, K., Bellon-Fontaine, M. N., & Fontaine-Aupart, M. P. (2008). Fluorescence correlation spectroscopy to study diffusion and reaction of bacteriophages inside biofilms. *Applied and environmental microbiology*, 74(7), 2135–2143. https://doi.org/10.1128/AEM.02304-07

Brooks, S. E., Walczak, M. A., Hameed, R., & Coonan, P. (2002). Chlorhexidine resistance in antibiotic-resistant bacteria isolated from the surfaces of dispensers of soap containing chlorhexidine. *Infection control and hospital epidemiology*, 23(11), 692–695. https://doi.org/10.1086/501996

Brown-Jaque, M., Calero-Cáceres, W., & Muniesa, M. (2015). Transfer of antibiotic-resistance genes via phage-related mobile elements. *Plasmid*, 79, 1–7. https://doi.org/10.1016/j.plasmid.2015.01.001

Brüssow H. (2001). Phages of dairy bacteria. *Annual review of microbiology*, 55, 283–303. https://doi.org/10.1146/annurev.micro.55.1.283

Brüssow H. (2007). Bacteria between protists and phages: from antipredation strategies to the evolution of pathogenicity. *Molecular microbiology*, 65(3), 583–589. https://doi.org/10.1111/j.1365-2958.2007.05826.x

Brüssow H. (2017). Phage therapy for the treatment of human intestinal bacterial infections: soon to be a reality?. *Expert review of gastroenterology & hepatology*, 11(9), 785–788. https://doi.org/10.1080/17474124.2017.1342534

Bruttin, A., & Brüssow, H. (2005). Human volunteers receiving *Escherichia coli* phage T4 orally: a safety test of phage therapy. *Antimicrobial agents and chemotherapy*, 49(7), 2874–2878. https://doi.org/10.1128/AAC.49.7.2874-2878.2005

Bueno E., García P., Martínez B. y, Rodríguez A. (2012). Phage inactivation of *Staphylococcus aureus* in fresh and hard-type. *International Journal of Food Microbiology*,En t. J. Food Microbiol. 2012; 158 (1), : 23–27. doi: 10.1016 / j.ijfoodmicro.2012.06.012.

Burmølle, M., Norman, A., Sørensen, S. J., & Hansen, L. H. (2012). Sequencing of IncX-plasmids suggests ubiquity of mobile forms of a biofilm-promoting gene cassette recruited from *Klebsiella pneumoniae*. *PloS one*, 7(7), e41259. https://doi.org/10.1371/journal.pone.0041259

Cargill, J. S., & Upton, M. (2009). Low concentrations of vancomycin stimulate biofilm formation in some clinical isolates of *Staphylococcus epidermidis*. *Journal of clinical pathology*, 62(12), 1112–1116. https://doi.org/10.1136/jcp.2009.069021

Carrolo, M., Frias, M. J., Pinto, F. R., Melo-Cristino, J., & Ramirez, M. (2010). Prophage spontaneous activation promotes DNA release enhancing biofilm formation in *Streptococcus pneumoniae*. *PloS one*, 5(12), e15678. https://doi.org/10.1371/journal.pone.0015678

Carvalho, C., Costa, A. R., Silva, F., & Oliveira, A. (2017). Bacteriophages and their derivatives for the treatment and control of food-producing animal infections. *Critical reviews in microbiology*, 43(5), 583–601. https://doi.org/10.1080/1040841X.2016.1271309

Casjens S. (2003). Prophages and bacterial genomics: what have we learned so far?. *Molecular microbiology*, 49(2), 277–300. https://doi.org/10.1046/j.1365-2958.2003.03580.x

Chang, V. S., Dhaliwal, D. K., Raju, L., & Kowalski, R. P. (2015). Antibiotic Resistance in the Treatment of *Staphylococcus aureus* Keratitis: a 20-Year Review. *Cornea*, 34(6), 698–703. https://doi.org/10.1097/ICO.0000000000000431

Chang, Y., Yoon, H., Kang, D. H., Chang, P. S., & Ryu, S. (2017). Endolysin LysSA97 is synergistic with carvacrol in controlling *Staphylococcus aureus* in foods. *International journal of food microbiology*, 244, 19–26. https://doi.org/10.1016/j.ijfoodmicro.2016.12.007

Chen, S., Wang, Y., Chen, F., Yang, H., Gan, M., & Zheng, S. J. (2007). A highly pathogenic strain of *Staphylococcus sciuri* caused fatal exudative epidermitis in piglets. *PloS one*, 2(1), e147. https://doi.org/10.1371/journal.pone.0000147

Cheung, G. Y., Kretschmer, D., Queck, S. Y., Joo, H. S., Wang, R., Duong, A. C., Nguyen, T. H., Bach, T. H., Porter, A. R., DeLeo, F. R., Peschel, A., & Otto, M. (2014). Insight into structure-function relationship in phenol-soluble modulins using an alanine screen of the phenol-soluble modulin (PSM) α3 peptide. *FASEB journal*

: official publication of the Federation of American Societies for Experimental Biology, 28(1), 153–161. https://doi.org/10.1096/fj.13-23204

Chmielewski RAN, Frank JF (2003) Biofilm formation and control in food processing facilities. *Compr Rev Food Sci Food Saf* 2:22–32. https://doi.org/10.1111/j.1541-4337.2003.tb00012.x

Chopra, S., Harjai, K., & Chhibber, S. (2015). Potential of sequential treatment with minocycline and S. aureus specific phage lysin in eradication of MRSA biofilms: an in vitro study. *Applied microbiology and biotechnology*, 99(7), 3201–3210. https://doi.org/10.1007/s00253-015-6460-1

Cisek, A. A., Dąbrowska, I., Gregorczyk, K. P., & Wyżewski, Z. (2017). Phage Therapy in Bacterial Infections Treatment: One Hundred Years After the Discovery of Bacteriophages. *Current microbiology*, 74(2), 277–283. https://doi.org/10.1007/s00284-016-1166-x

Clark, J. R., & March, J. B. (2006). Bacteriophages and biotechnology: vaccines, gene therapy and antibacterials. *Trends in biotechnology*, 24(5), 212–218. https://doi.org/10.1016/j.tibtech.2006.03.003

Cook, L., Chatterjee, A., Barnes, A., Yarwood, J., Hu, W. S., & Dunny, G. (2011). Biofilm growth alters regulation of conjugation by a bacterial pheromone. *Molecular microbiology*, 81(6), 1499–1510. https://doi.org/10.1111/j.1365-2958.2011.07786.x

Costerton, J. W., Cheng, K. J., Geesey, G. G., Ladd, T. I., Nickel, J. C., Dasgupta, M., & Marrie, T. J. (1987). Bacterial biofilms in nature and disease. *Annual review of microbiology*, 41, 435–464. https://doi.org/10.1146/annurev.mi.41.100187.002251

Coulter, L. B., McLean, R. J., Rohde, R. E., & Aron, G. M. (2014). Effect of bacteriophage infection in combination with tobramycin on the emergence of resistance in Escherichia coli and Pseudomonas aeruginosa biofilms. *Viruses*, 6(10), 3778–3786. https://doi.org/10.3390/v6103778

Culotti, A., & Packman, A. I. (2015). Pseudomonas aeruginosa facilitates Campylobacter jejuni growth in biofilms under oxic flow conditions. *FEMS microbiology ecology*, 91(12), fiv136. https://doi.org/10.1093/femsec/fiv136

Davies, E. V., Winstanley, C., Fothergill, J. L., & James, C. E. (2016). The role of temperate bacteriophages in bacterial infection. *FEMS microbiology letters*, 363(5), fnw015. https://doi.org/10.1093/femsle/fnw015

de la Fuente-Núñez C, Reffuveille F, Haney EF, Straus SK, Hancock REW (2014) Broad-Spectrum Anti-biofilm Peptide That Targets a Cellular Stress Response. *PLoS Pathog* 10(5): e1004152. https://doi.org/10.1371/journal.ppat.1004152

de la Fuente-Núñez, C., Reffuveille, F., Fernández, L., & Hancock, R. E. (2013). Bacterial biofilm development as a multicellular adaptation: antibiotic resistance and new therapeutic strategies. *Current opinion in microbiology*, 16(5), 580–589. https://doi.org/10.1016/j.mib.2013.06.013

Deghorain, M., y Van Melderen, L. (2012). La familia de los fagos estafilococos: una visión general. Virus , 4 (12), 3316–3335. doi: 10.3390 / v4123316

DeLeo, F. R., Otto, M., Kreiswirth, B. N., & Chambers, H. F. (2010). Community-associated meticillin-resistant *Staphylococcus aureus*. *Lancet* (London, England), 375(9725), 1557–1568. https://doi.org/10.1016/S0140-6736(09)61999-1

Dengler, V., Foulston, L., DeFrancesco, A. S., & Losick, R. (2015). An Electrostatic Net Model for the Role of Extracellular DNA in Biofilm Formation by *Staphylococcus aureus*. *Journal of bacteriology*, 197(24), 3779–3787. https://doi.org/10.1128/JB.00726-15

Devriese LA y Casas J. (1975) Epidemiology of methicillin-resistant *Staphylococcus aureus* in dairy herds. Research in Veterinary Science 9; 23-7. https://doi.org/10.1016/S0034-5288(18)33549-5

D'Herelle F. (2007). On an invisible microbe antagonistic toward dysenteric bacilli: brief note by Mr. F. D'Herelle, presented by Mr. Roux. 1917. *Research in microbiology*, 158(7), 553–554. https://doi.org/10.1016/j.resmic.2007.07.005

Donlan R. M. (2002). Biofilms: microbial life on surfaces. *Emerging infectious diseases*, 8(9), 881–890. https://doi.org/10.3201/eid0809.020063

Driffield, K., Miller, K., Bostock, J. M., O'Neill, A. J., & Chopra, I. (2008). Increased mutability of *Pseudomonas aeruginosa* in biofilms. *The Journal of antimicrobial chemotherapy*, 61(5), 1053–1056. https://doi.org/10.1093/jac/dkn044

Dvořáčková, M., Růžička, F., Benešík, M., Pantůček, R., & Dvořáková-Heroldová, M. (2019). Antimicrobial effect of commercial phage preparation Stafal® on biofilm and planktonic forms of methicillin-resistant *Staphylococcus aureus*. *Folia microbiologica*, 64(1), 121–126. https://doi.org/10.1007/s12223-018-0622-3

EFSA & ECDC. (2018). The European Union summary report on trends and sources of zoonoses, zoonotic agents and food-borne outbreaks in 2017. *EFSA Journal* 2018;16(12):5500, 262 pp. https://doi.org/10.2903/j.efsa.2018.5500

EFSA, 2006. The Community summary reports on trends and sources of zoonoses, zoonotic agents, antimicrobial resistance and foodborne outbreaks in the European Union in 2005. EFSA J. 94, 1–288.

EFSA, 2007. The Community summary report on trends and sources of zoonoses, zoonotic agents, antimicrobial resistance and foodborne outbreaks in the European Union in 2006. EFSA J. 130, 1–352.

EFSA, 2009a. The Community summary report on food-borne outbreaks in the European Union in 2007. EFSA J. 271, 1–102.

EFSA, 2009b. Joint scientific report of ECDC, EFSA and EMEA on meticillin resistant Staphylococcus aureus (MRSA) in livestock, companion animals and food. EFSA Sci. Rep. 301, 1–10.

EFSA, 2010. The Community summary report on trends and sources of zoonoses and zoonotic agents and food-borne outbreaks in the European Union in 2008. EFSA J. 8, 1–368.

EFSA, 2011. The European Union summary report on trends and sources of zoonoses and zoonotic agents and food-borne outbreaks in 2009. EFSA J. 9, 1–378.

EFSA, 2012. The European Union summary report on trends and sources of zoonoses, zoonotic agents and food-borne outbreaks in 2010. EFSA J. 10, 1–442.

El Haddad, L., Ben Abdallah, N., Plante, P. L., Dumaresq, J., Katsarava, R., Labrie, S., Corbeil, J., St-Gelais, D., & Moineau, S. (2014). Improving the safety of *Staphylococcus aureus* polyvalent phages by their production on a *Staphylococcus xylosus* strain. *PloS one*, 9(7), e102600. https://doi.org/10.1371/journal.pone.0102600

Elias, S., & Banin, E. (2012). Multi-species biofilms: living with friendly neighbors. *FEMS microbiology reviews*, 36(5), 990–1004. https://doi.org/10.1111/j.1574-6976.2012.00325.x

Erez Z, Steinberger-Levy I, Shamir M, Doron S, Stokar-Avihail A, Peleg Y et al. (2017). Communication between viruses guides lysis-lysogeny decisions. *Nature* 541: 488–493.

European Centre for Disease Prevention and Control (ECDC). 2018. Antimicrobial resistance surveillance in Europe 2017.

Evans, J.B., Bradford, W. L. y Niven, C. F. Jr. (1955). Comments concerning the taxonomy of the genera *Micrococcus* and *Staphylococcus*. Int. Bull. bact. Nomen. 5, 61.

Exebacase. (2019). Recuperado 6 de mayo de 2020 de: https://www.contrafect.com/pipeline/exebacase

Federle M. J. (2009). Autoinducer-2-based chemical communication in bacteria: complexities of interspecies signaling. *Contributions to microbiology*, 16, 18–32. https://doi.org/10.1159/000219371

Feiner, R., Argov, T., Rabinovich, L., Sigal, N., Borovok, I., & Herskovits, A. A. (2015). A new perspective on lysogeny: prophages as active regulatory switches of bacteria. *Nature reviews. Microbiology*, 13(10), 641–650. https://doi.org/10.1038/nrmicro3527

Feiss, M., & Rao, V. B. (2012). The bacteriophage DNA packaging machine. *Advances in experimental medicine and biology*, 726, 489–509. https://doi.org/10.1007/978-1-4614-0980-9_22

Fenton, M., Casey, P. G., Hill, C., Gahan, C. G., Ross, R. P., McAuliffe, O., O'Mahony, J., Maher, F., & Coffey, A. (2010). The truncated phage lysin CHAP(k) eliminates *Staphylococcus aureus* in the nares of mice. *Bioengineered bugs*, 1(6), 404–407. https://doi.org/10.4161/bbug.1.6.13422

Fernández, L., González, S., Campelo, A. B., Martínez, B., Rodríguez, A., & García, P. (2017). Downregulation of Autolysin-Encoding Genes by Phage-Derived Lytic Proteins Inhibits Biofilm Formation in *Staphylococcus aureus*. *Antimicrobial agents and chemotherapy*, 61(5), e02724-16. https://doi.org/10.1128/AAC.02724-16

Fernández, L., González, S., Campelo, A. B., Martínez, B., Rodríguez, A., & García, P. (2017). Low-level predation by lytic phage phiIPLA-RODI promotes biofilm formation and triggers the stringent response in *Staphylococcus aureus*. *Scientific reports*, 7, 40965. https://doi.org/10.1038/srep40965

Fernández, L., González, S., Quiles-Puchalt, N., Gutiérrez, D., Penadés, J. R., García, P., & Rodríguez, A. (2018). Lysogenization of *Staphylococcus aureus* RN450 by phages φ11 and φ80α leads to the activation of the SigB regulon. *Scientific reports*, 8(1), 12662. https://doi.org/10.1038/s41598-018-31107-z

Fernández, L., Gutiérrez, D., García, P., & Rodríguez, A. (2020). Environmental pH is a key modulator of *Staphylococcus aureus* biofilm development under predation by the virulent phage phiIPLA-RODI. Articulo en revisión.

Fernández, L., Rodríguez, A., & García, P. (2018). Phage or foe: an insight into the impact of viral predation on microbial communities. *The ISME journal*, 12(5), 1171–1179. https://doi.org/10.1038/s41396-018-0049-5

Ferry, T., Boucher, F., Fevre, C., Perpoint, T., Chateau, J., Petitjean, C., Josse, J., Chidiac, C., L'hostis, G., Leboucher, G., Laurent, F., & Lyon Bone and Joint Infection Study Group (2018). Innovations for the treatment of a complex bone and joint infection due to XDR Pseudomonas aeruginosa including local application of a selected cocktail of bacteriophages. *The Journal of antimicrobial chemotherapy*, 73(10), 2901–2903. https://doi.org/10.1093/jac/dky263

Ferry, T., Leboucher, G., Fevre, C., Herry, Y., Conrad, A., Josse, J., Batailler, C., Chidiac, C., Medina, M., Lustig, S., Laurent, F., & Lyon BJI Study Group (2018). Salvage Debridement, Antibiotics and Implant Retention ("DAIR") With Local Injection of a Selected Cocktail of Bacteriophages: Is It an Option for an Elderly Patient With Relapsing *Staphylococcus aureus* Prosthetic-Joint Infection?. *Open forum infectious diseases*, 5(11), ofy269. https://doi.org/10.1093/ofid/ofy269

Figueiredo, A. M., & Ferreira, F. A. (2014). The multifaceted resources and microevolution of the successful human and animal pathogen methicillin-resistant *Staphylococcus aureus*. *Memorias do Instituto Oswaldo Cruz*, 109(3), 265–278. https://doi.org/10.1590/0074-0276140016

Figueroa G, Guillermo, Navarrete W, Paola, Caro C, Maricela, Troncoso H, Miriam, & Faúndez Z, Gustavo. (2002). Portación de *Staphylococcus aureus* enterotoxigénicos en manipuladores de alimentos. *Revista médica de Chile*, 130(8), 859-864. https://dx.doi.org/10.4067/S0034-98872002000800003

Filippov, A. A., Sergueev, K. V., He, Y., Huang, X. Z., Gnade, B. T., Mueller, A. J., Fernandez-Prada, C. M., & Nikolich, M. P. (2011). Bacteriophage-resistant mutants in Yersinia pestis: identification of phage receptors and attenuation for mice. *PloS one*, 6(9), e25486. https://doi.org/10.1371/journal.pone.0025486

Fischetti V. A. (2008). Bacteriophage lysins as effective antibacterials. *Current opinion in microbiology*, 11(5), 393–400. https://doi.org/10.1016/j.mib.2008.09.012

Fish, R., Kutter, E., Bryan, D., Wheat, G., & Kuhl, S. (2018). Resolving Digital Staphylococcal Osteomyelitis Using Bacteriophage-A Case Report. *Antibiotics (Basel, Switzerland)*, 7(4), 87. https://doi.org/10.3390/antibiotics7040087

Flemming, H. C., & Wingender, J. (2010). The biofilm matrix. Nature reviews. *Microbiology*, 8(9), 623–633. https://doi.org/10.1038/nrmicro2415

Fortier, L. C., & Sekulovic, O. (2013). Importance of prophages to evolution and virulence of bacterial pathogens. *Virulence*, 4(5), 354–365. https://doi.org/10.4161/viru.24498

Foster A. P. (2012). Staphylococcal skin disease in livestock. *Veterinary dermatology*, 23(4), 342–e63. https://doi.org/10.1111/j.1365-3164.2012.01093.x

Foster, T. J., & Höök, M. (1998). Surface protein adhesins of *Staphylococcus aureus*. *Trends in microbiology*, 6(12), 484–488. https://doi.org/10.1016/s0966-842x(98)01400-0

Foulston, L., Elsholz, A. K., DeFrancesco, A. S., & Losick, R. (2014). The extracellular matrix of *Staphylococcus aureus* biofilms comprises cytoplasmic proteins that associate with the cell surface in response to decreasing pH. *mBio*, 5(5), e01667-14. https://doi.org/10.1128/mBio.01667-14

Fux, C. A., Costerton, J. W., Stewart, P. S., & Stoodley, P. (2005). Survival strategies of infectious biofilms. *Trends in microbiology*, 13(1), 34–40. https://doi.org/10.1016/j.tim.2004.11.010

Galkin, V. E., Yu, X., Bielnicki, J., Ndjonka, D., Bell, C. E., & Egelman, E. H. (2009). Cleavage of bacteriophage lambda cI repressor involves the RecA C-terminal domain. *Journal of molecular biology*, 385(3), 779–787. https://doi.org/10.1016/j.jmb.2008.10.081

Gallet, R., Shao, Y., & Wang, I. N. (2009). High adsorption rate is detrimental to bacteriophage fitness in a biofilm-like environment. *BMC evolutionary biology*, 9, 241. https://doi.org/10.1186/1471-2148-9-241

Gao, R., Krysciak, D., Petersen, K., Utpatel, C., Knapp, A., Schmeisser, C., Daniel, R., Voget, S., Jaeger, K. E., & Streit, W. R. (2015). Genome-wide RNA sequencing analysis of quorum sensing-controlled regulons in the plant-associated Burkholderia glumae PG1 strain. *Applied and environmental microbiology*, 81(23), 7993–8007. https://doi.org/10.1128/AEM.01043-15

García, P., Martínez, B., Obeso, J. M., Lavigne, R., Lurz, R., & Rodríguez, A. (2009). Functional genomic analysis of two *Staphylococcus aureus* phages isolated from the dairy environment. *Applied and environmental microbiology*, 75(24), 7663–7673. https://doi.org/10.1128/AEM.01864-09

García, P., Martínez, B., Rodríguez, L., & Rodríguez, A. (2010). Synergy between the phage endolysin LysH5 and nisin to kill *Staphylococcus aureus* in pasteurized milk. *International journal of food microbiology*, 141(3), 151–155. https://doi.org/10.1016/j.ijfoodmicro.2010.04.029

Gödeke, J., Paul, K., Lassak, J., & Thormann, K. M. (2011). Phage-induced lysis enhances biofilm formation in *Shewanella oneidensis* MR-1. *The ISME journal*, 5(4), 613–626. https://doi.org/10.1038/ismej.2010.153

González-Menéndez, E., Arroyo-López, F. N., Martínez, B., García, P., Garrido-Fernández, A., & Rodríguez, A. (2018). Optimizing Propagation of *Staphylococcus aureus* Infecting Bacteriophage vB_SauM-phiIPLA-RODI on *Staphylococcus xylosus* Using Response Surface Methodology. *Viruses*, 10(4), 153. https://doi.org/10.3390/v10040153

Gordon JR y Lowy FD (2008) Pathogenesis of Methicillin-Resistant *Staphylococcus aureus* Infection. *Clinical Infectious Diseases* 46 (5) S350–S359. https://doi.org/10.1086/533591

Gorski L. A. (2017). The 2016 Infusion Therapy Standards of Practice. *Home healthcare now*, 35(1), 10–18. https://doi.org/10.1097/NHH.0000000000000481

Götz F. (2002). *Staphylococcus* and biofilms. *Molecular microbiology*, 43(6), 1367–1378. https://doi.org/10.1046/j.1365-2958.2002.02827.x

Gross, M., Cramton, S. E., Götz, F., & Peschel, A. (2001). Key role of teichoic acid net charge in *Staphylococcus aureus* colonization of artificial surfaces. *Infection and immunity*, 69(5), 3423–3426. https://doi.org/10.1128/IAI.69.5.3423-3426.2001

Grundmann, D., Markwart, F., Scheller, A., Kirchhoff, F., & Schäfer, K. H. (2016). Phenotype and distribution pattern of nestin-GFP-expressing cells in murine myenteric plexus. *Cell and tissue research*, 366(3), 573–586. https://doi.org/10.1007/s00441-016-2476-9

Guinto, C. H., Bottone, E. J., Raffalli, J. T., Montecalvo, M. A., & Wormser, G. P. (2002). Evaluation of dedicated stethoscopes as a potential source of nosocomial pathogens. *American journal of infection control*, 30(8), 499–502. https://doi.org/10.1067/mic.2002.126427

Gutiérrez, D., Briers, Y., Rodríguez-Rubio, L., Martínez, B., Rodríguez, A., Lavigne, R., & García, P. (2015a). Role of the Pre-neck Appendage Protein (Dpo7) from Phage vB_SepiS-phiIPLA7 as an Anti-biofilm Agent in Staphylococcal Species. *Frontiers in microbiology*, 6, 1315. https://doi.org/10.3389/fmicb.2015.01315

Gutiérrez, D., Delgado, S., Vázquez-Sánchez, D., Martínez, B., Cabo, M. L., Rodríguez, A., Herrera, J. J., & García, P. (2012). Incidence of *Staphylococcus aureus* and analysis of associated bacterial communities on food industry surfaces. *Applied and environmental microbiology*, 78(24), 8547–8554. https://doi.org/10.1128/AEM.02045-12

Gutiérrez, D., Fernández, L., Martínez, B., Ruas-Madiedo, P., García, P., & Rodríguez, A. (2017). Real-Time Assessment of *Staphylococcus aureus* Biofilm Disruption by Phage-Derived Proteins. *Frontiers in microbiology*, 8, 1632. https://doi.org/10.3389/fmicb.2017.01632

Gutiérrez, D., Fernández, L., Rodríguez, A., & García, P. (2018). Are Phage Lytic Proteins the Secret Weapon To Kill *Staphylococcus aureus*?. *mBio*, 9(1), e01923-17. https://doi.org/10.1128/mBio.01923-17

Gutiérrez, D., Garrido, V., Fernández, L., Portilla, S., Rodríguez, A., Grilló, M. J., & García, P. (2020). Phage Lytic Protein LysRODI Prevents Staphylococcal Mastitis in Mice. *Frontiers in microbiology*, 11, 7. https://doi.org/10.3389/fmicb.2020.00007

Gutiérrez, D., Martínez, B., Rodríguez, A., & García, P. (2010). Isolation and characterization of bacteriophages infecting *Staphylococcus epidermidis*. *Current microbiology*, 61(6), 601–608. https://doi.org/10.1007/s00284-010-9659-5

Gutiérrez, D., Ruas-Madiedo, P., Martínez, B., Rodríguez, A., & García, P. (2014). Effective removal of staphylococcal biofilms by the endolysin LysH5. *PloS one*, 9(9), e107307. https://doi.org/10.1371/journal.pone.0107307

Gutiérrez, D., Vandenheuvel, D., Martínez, B., Rodríguez, A., Lavigne, R., & García, P. (2015b). Two Phages, phiIPLA-RODI and phiIPLA-C1C, Lyse Mono- and Dual-Species Staphylococcal Biofilms. *Applied and environmental microbiology*, 81(10), 3336–3348. https://doi.org/10.1128/AEM.03560-14

Haaber, J., Leisner, J. J., Cohn, M. T., Catalan-Moreno, A., Nielsen, J. B., Westh, H., Penadés, J. R., & Ingmer, H. (2016). Bacterial viruses enable their host to acquire antibiotic resistance genes from neighbouring cells. *Nature communications*, 7, 13333. https://doi.org/10.1038/ncomms13333

Haaber, J., Penadés, J. R., & Ingmer, H. (2017). Transfer of Antibiotic Resistance in *Staphylococcus aureus*. *Trends in microbiology*, 25(11), 893–905. https://doi.org/10.1016/j.tim.2017.05.011

Hagens, S., & Loessner, M. J. (2010). Bacteriophage for biocontrol of foodborne pathogens: calculations and considerations. *Current pharmaceutical biotechnology*, 11(1), 58–68. https://doi.org/10.2174/138920110790725429

Hall-Stoodley, L., Costerton, J. W., & Stoodley, P. (2004). Bacterial biofilms: from the natural environment to infectious diseases. *Nature reviews. Microbiology*, 2(2), 95–108. https://doi.org/10.1038/nrmicro821

Hargreaves KR, Kropinski AM, Clokie MRJ. (2014). What does the talking? Quorum sensing signalling genes discovered in a bacteriophage genome. PLoS ONE 9: e85131.

Harris, L. G., & Richards, R. G. (2006). Staphylococci and implant surfaces: a review. *Injury*, 37 Suppl 2, S3–S14. https://doi.org/10.1016/j.injury.2006.04.003

Harris, L. G., Foster, S. J., & Richards, R. G. (2002). An introduction to *Staphylococcus aureus*, and techniques for identifying and quantifying S. aureus adhesins in relation to adhesion to biomaterials: review. *European cells & materials*, 4, 39–60. https://doi.org/10.22203/ecm.v004a04

Hatcher, S. M., Rhodes, S. M., Stewart, J. R., Silbergeld, E., Pisanic, N., Larsen, J., Jiang, S., Krosche, A., Hall, D., Carroll, K. C., & Heaney, C. D. (2017). The Prevalence of Antibiotic-Resistant *Staphylococcus aureus* Nasal Carriage among Industrial Hog Operation Workers, Community Residents, and Children Living in Their Households: North Carolina, USA. *Environmental health perspectives*, 125(4), 560–569. https://doi.org/10.1289/EHP35

Hatcher, SM, Rhodes, SM, Stewart, JR, Silbergeld, E., Pisanic, N., Larsen, J., Jiang, S., Krosche, A., Hall, D., Carroll, KC, and Heaney, CD (2017). Prevalence of nasal transport of antibiotic-resistant *Staphylococcus aureus* among industrial pig workers, community residents and children living in their homes: North Carolina, USA. UU. *Environmental health perspectives*, 125 (4), 560-569. https://doi.org/10.1289/EHP35

Heilmann, C., Hussain, M., Peters, G., & Götz, F. (1997). Evidence for autolysin-mediated primary attachment of *Staphylococcus epidermidis* to a polystyrene surface. Molecular microbiology, 24(5), 1013–1024. https://doi.org/10.1046/j.1365-2958.1997.4101774.x

Heydari, H., Mutha, N. V., Mahmud, M. I., Siow, C. C., Wee, W. Y., Wong, G. J., Yazdi, A. H., Ang, M. Y., & Choo, S. W. (2014). StaphyloBase: a specialized genomic resource for the staphylococcal research community.

Database : the journal of biological databases and curation, 2014, bau010. https://doi.org/10.1093/database/bau010

Hoque, M. M., Naser, I. B., Bari, S. M., Zhu, J., Mekalanos, J. J., & Faruque, S. M. (2016). Quorum Regulated Resistance of Vibrio cholerae against Environmental Bacteriophages. *Scientific reports*, 6, 37956. https://doi.org/10.1038/srep37956

Hosseinidoust, Z., Tufenkji, N., & van de Ven, T. G. (2013b). Formation of biofilms under phage predation: considerations concerning a biofilm increase. *Biofouling*, 29(4), 457–468. https://doi.org/10.1080/08927014.2013.779370

Hosseinidoust, Z., van de Ven, T. G., & Tufenkji, N. (2013a). Evolution of Pseudomonas aeruginosa virulence as a result of phage predation. *Applied and environmental microbiology*, 79(19), 6110–6116. https://doi.org/10.1128/AEM.01421-13

Høyland-Kroghsbo, N. M., Maerkedahl, R. B., & Svenningsen, S. L. (2013). A quorum-sensing-induced bacteriophage defense mechanism. *mBio*, 4(1), e00362-12. https://doi.org/10.1128/mBio.00362-12

Høyland-Kroghsbo, N. M., Paczkowski, J., Mukherjee, S., Broniewski, J., Westra, E., Bondy-Denomy, J., & Bassler, B. L. (2017). Quorum sensing controls the Pseudomonas aeruginosa CRISPR-Cas adaptive immune system. *Proceedings of the National Academy of Sciences of the United States of America*, 114(1), 131–135. https://doi.org/10.1073/pnas.1617415113

Hu, D. L., & Nakane, A. (2014). Mechanisms of staphylococcal enterotoxin-induced emesis. *European journal of pharmacology*, 722, 95–107. https://doi.org/10.1016/j.ejphar.2013.08.050

Hughes, K. A., Sutherland, I. W., & Jones, M. V. (1998). Biofilm susceptibility to bacteriophage attack: the role of phage-borne polysaccharide depolymerase. *Microbiology (Reading, England)*, 144 (Pt 11), 3039–3047. https://doi.org/10.1099/00221287-144-11-3039

Ivanovska, I. L., de Pablo, P. J., Ibarra, B., Sgalari, G., MacKintosh, F. C., Carrascosa, J. L., Schmidt, C. F., & Wuite, G. J. (2004). Bacteriophage capsids: tough nanoshells with complex elastic properties. *Proceedings of the National Academy of Sciences of the United States of America*, 101(20), 7600–7605. https://doi.org/10.1073/pnas.0308198101

Jaśkiewicz, M., Janczura, A., Nowicka, J., & Kamysz, W. (2019). Methods Used for the Eradication of Staphylococcal Biofilms. *Antibiotics (Basel, Switzerland),* 8(4), 174. https://doi.org/10.3390/antibiotics8040174

Jassim, S. A., Limoges, R. G., & El-Cheikh, H. (2016). Bacteriophage biocontrol in wastewater treatment. *World journal of microbiology & biotechnology*, 32(4), 70. https://doi.org/10.1007/s11274-016-2028-1

Jault, P., Leclerc, T., Jennes, S., Pirnay, J. P., Que, Y. A., Resch, G., Rousseau, A. F., Ravat, F., Carsin, H., Le Floch, R., Schaal, J. V., Soler, C., Fevre, C., Arnaud, I., Bretaudeau, L., & Gabard, J. (2019). Efficacy and tolerability of a cocktail of bacteriophages to treat burn wounds infected by Pseudomonas aeruginosa (PhagoBurn): a randomised, controlled, double-blind phase 1/2 trial. *The Lancet*. Infectious diseases, 19(1), 35–45. https://doi.org/10.1016/S1473-3099(18)30482-1

Johnson, R. P., Gyles, C. L., Huff, W. E., Ojha, S., Huff, G. R., Rath, N. C., & Donoghue, A. M. (2008). Bacteriophages for prophylaxis and therapy in cattle, poultry and pigs. *Animal health research reviews*, 9(2), 201–215. https://doi.org/10.1017/S1466252308001576

Johnson, R. P., Gyles, C. L., Huff, W. E., Ojha, S., Huff, G. R., Rath, N. C., & Donoghue, A. M. (2008). Bacteriophages for prophylaxis and therapy in cattle, poultry and pigs. *Animal health research reviews*, 9(2), 201–215. https://doi.org/10.1017/S1466252308001576

Jun, S. Y., Jang, I. J., Yoon, S., Jang, K., Yu, K. S., Cho, J. Y., Seong, M. W., Jung, G. M., Yoon, S. J., & Kang, S. H. (2017). Pharmacokinetics and Tolerance of the Phage Endolysin-Based Candidate Drug SAL200 after a Single Intravenous Administration among Healthy Volunteers. *Antimicrobial agents and chemotherapy*, 61(6), e02629-16. https://doi.org/10.1128/AAC.02629-16

Kaneko, J., & Kamio, Y. (2004). Bacterial two-component and hetero-heptameric pore-forming cytolytic toxins: structures, pore-forming mechanism, and organization of the genes. *Bioscience, biotechnology, and biochemistry*, 68(5), 981–1003. https://doi.org/10.1271/bbb.68.981

Kania, S. A., Williamson, N. L., Frank, L. A., Wilkes, R. P., Jones, R. D., & Bemis, D. A. (2004). Methicillin resistance of staphylococci isolated from the skin of dogs with pyoderma. *American journal of veterinary research*, 65(9), 1265–1268. https://doi.org/10.2460/ajvr.2004.65.1265

Kaplan, J. B., Izano, E. A., Gopal, P., Karwacki, M. T., Kim, S., Bose, J. L., Bayles, K. W., & Horswill, A. R. (2012). Low levels of β-lactam antibiotics induce extracellular DNA release and biofilm formation in *Staphylococcus aureus*. *mBio*, 3(4), e00198-12. https://doi.org/10.1128/mBio.00198-12

Kay, M. K., Erwin, T. C., McLean, R. J., & Aron, G. M. (2011). Bacteriophage ecology in *Escherichia coli* and *Pseudomonas aeruginosa* mixed-biofilm communities. *Applied and environmental microbiology*, 77(3), 821–829. https://doi.org/10.1128/AEM.01797-10

Keen, E. C., Bliskovsky, V. V., Malagon, F., Baker, J. D., Prince, J. S., Klaus, J. S., & Adhya, S. L. (2017). Novel "Superspreader" Bacteriophages Promote Horizontal Gene Transfer by Transformation. *mBio*, 8(1), e02115-16. https://doi.org/10.1128/mBio.02115-16

King, A.M., Adams, M.J., Carstens, E.B. & Lefkowitz, E.J. (2012). Virus taxonomy. *Ninth report of the International Committee on Taxonomy of Viruses*, 1,3-20. https://doi.org/10.1016/B978-0-12-384684-6.00114-2

Kropec, A., Maira-Litran, T., Jefferson, K. K., Grout, M., Cramton, S. E., Götz, F., Goldmann, D. A., & Pier, G. B. (2005). Poly-N-acetylglucosamine production in *Staphylococcus aureus* is essential for virulence in murine models of systemic infection. *Infection and immunity*, 73(10), 6868–6876. https://doi.org/10.1128/IAI.73.10.6868-6876.2005

Kvachadze, L., Balarjishvili, N., Meskhi, T., Tevdoradze, E., Skhirtladze, N., Pataridze, T., Adamia, R., Topuria, T., Kutter, E., Rohde, C., & Kutateladze, M. (2011). Evaluation of lytic activity of staphylococcal bacteriophage Sb-1 against freshly isolated clinical pathogens. *Microbial biotechnology*, 4(5), 643–650. https://doi.org/10.1111/j.1751-7915.2011.00259.x

Kwan, T., Liu, J., DuBow, M., Gros, P., & Pelletier, J. (2005). The complete genomes and proteomes of 27 *Staphylococcus aureus* bacteriophages. *Proceedings of the National Academy of Sciences of the United States of America*, 102(14), 5174–5179. https://doi.org/10.1073/pnas.0501140102

Lakhundi, S., & Zhang, K. (2018). Methicillin-Resistant *Staphylococcus aureus*: Molecular Characterization, Evolution, and Epidemiology. *Clinical microbiology reviews*, 31(4), e00020-18. https://doi.org/10.1128/CMR.00020-18

Lamers, R. P., Muthukrishnan, G., Castoe, T. A., Tafur, S., Cole, A. M., & Parkinson, C. L. (2012). Phylogenetic relationships among *Staphylococcus* species and refinement of cluster groups based on multilocus data. *BMC evolutionary biology*, 12, 171. https://doi.org/10.1186/1471-2148-12-171

Latasa, C., Solano, C., Penadés, J. R., & Lasa, I. (2006). Biofilm-associated proteins. *Comptes rendus biologies*, 329(11), 849–857. https://doi.org/10.1016/j.crvi.2006.07.008

Laverty A, Jennifer S. Mindell, Elizabeth A. y Christopher Millett. (2013) Active Travel to Work and Cardiovascular Risk Factors in the United Kingdom. *American Journal of Preventive Medicine*, 45(3):282-288. DOI: https://doi.org/10.1016/j.amepre.2013.04.012

Leskinen, K., Tuomala, H., Wicklund, A., Horsma-Heikkinen, J., Kuusela, P., Skurnik, M., & Kiljunen, S. (2017). Characterization of vB_SauM-fRuSau02, a Twort-Like Bacteriophage Isolated from a Therapeutic Phage Cocktail. *Viruses*, 9(9), 258. https://doi.org/10.3390/v9090258

Lewis K. (2008). Multidrug tolerance of biofilms and persister cells. *Current topics in microbiology and immunology*, 322, 107–131. https://doi.org/10.1007/978-3-540-75418-3_6

Lina, G., Bohach, G. A., Nair, S. P., Hiramatsu, K., Jouvin-Marche, E., Mariuzza, R., & International Nomenclature Committee for Staphylococcal Superantigens (2004). Standard nomenclature for the superantigens expressed by *Staphylococcus*. *The Journal of infectious diseases*, 189(12), 2334–2336. https://doi.org/10.1086/420852

Linares, J. F., Gustafsson, I., Baquero, F., & Martinez, J. L. (2006). Antibiotics as intermicrobial signaling agents instead of weapons. *Proceedings of the National Academy of Sciences of the United States of America*, 103(51), 19484–19489. https://doi.org/10.1073/pnas.0608949103

Linden, S. B., Zhang, H., Heselpoth, R. D., Shen, Y., Schmelcher, M., Eichenseher, F., & Nelson, D. C. (2015). Biochemical and biophysical characterization of PlyGRCS, a bacteriophage endolysin active against methicillin-resistant *Staphylococcus aureus*. *Applied microbiology and biotechnology*, 99(2), 741–752. https://doi.org/10.1007/s00253-014-5930-1

Lister, J. L., & Horswill, A. R. (2014). *Staphylococcus aureus* biofilms: recent developments in biofilm dispersal. *Frontiers in cellular and infection microbiology*, 4, 178. https://doi.org/10.3389/fcimb.2014.00178

Liu, Q., Yeo, W. S., & Bae, T. (2016). The SaeRS Two-Component System of *Staphylococcus aureus. Genes*, 7(10), 81. https://doi.org/10.3390/genes7100081

Liu, X., Li, Y., Guo, Y., Zeng, Z., Li, B., Wood, T. K., Cai, X., & Wang, X. (2015). Physiological Function of Rac Prophage During Biofilm Formation and Regulation of Rac Excision in *Escherichia coli* K-12. *Scientific reports*, 5, 16074. https://doi.org/10.1038/srep16074

Lowy F. D. (1998). *Staphylococcus aureus* infections. *The New England journal of medicine*, 339(8), 520–532. https://doi.org/10.1056/NEJM199808203390806

Mack, D., Fischer, W., Krokotsch, A., Leopold, K., Hartmann, R., Egge, H., & Laufs, R. (1996). The intercellular adhesin involved in biofilm accumulation of *Staphylococcus epidermidis* is a linear beta-1,6-linked glucosaminoglycan: purification and structural analysis. *Journal of bacteriology*, 178(1), 175–183. https://doi.org/10.1128/jb.178.1.175-183.1996

Mah, T. F., Pitts, B., Pellock, B., Walker, G. C., Stewart, P. S., & O'Toole, G. A. (2003). A genetic basis for *Pseudomonas aeruginosa* biofilm antibiotic resistance. *Nature*, 426(6964), 306–310. https://doi.org/10.1038/nature02122

Manandhar, S., Singh, A., Varma, A., Pandey, S., & Shrivastava, N. (2018). Biofilm Producing Clinical *Staphylococcus aureus* Isolates Augmented Prevalence of Antibiotic Resistant Cases in Tertiary Care Hospitals of Nepal. *Frontiers in microbiology*, 9, 2749. https://doi.org/10.3389/fmicb.2018.02749

McCallin, S., Sacher, J. C., Zheng, J., & Chan, B. K. (2019). Current State of Compassionate Phage Therapy. *Viruses*, 11(4), 343. https://doi.org/10.3390/v11040343

McCallin, S., Sarker, S. A., Sultana, S., Oechslin, F., & Brüssow, H. (2018). Metagenome analysis of Russian and Georgian Pyophage cocktails and a placebo-controlled safety trial of single phage versus phage cocktail in healthy *Staphylococcus aureus* carriers. *Environmental microbiology*, 20(9), 3278–3293. https://doi.org/10.1111/1462-2920.14310

McCarthy, B., Casey, D., Devane, D., Murphy, K., Murphy, E., & Lacasse, Y. (2015). Pulmonary rehabilitation for chronic obstructive pulmonary disease. *The Cochrane database of systematic reviews*, (2), CD003793. https://doi.org/10.1002/14651858.CD003793.pub3

Miller, E. S., Kutter, E., Mosig, G., Arisaka, F., Kunisawa, T., & Rüger, W. (2003). Bacteriophage T4 genome. Microbiology and molecular biology reviews : MMBR, 67(1), 86–156. https://doi.org/10.1128/mmbr.67.1.86-156.2003

Miller, E. S., Kutter, E., Mosig, G., Arisaka, F., Kunisawa, T., & Rüger, W. (2003). Bacteriophage T4 genome. *Microbiology and molecular biology reviews : MMBR*, 67(1), 86–156. https://doi.org/10.1128/mmbr.67.1.86-156.2003

Modi, R., Hirvi, Y., Hill, A., & Griffiths, M. W. (2001). Effect of phage on survival of Salmonella enteritidis during manufacture and storage of cheddar cheese made from raw and pasteurized milk. *Journal of food protection*, 64(7), 927–933. https://doi.org/10.4315/0362-028x-64.7.927

Modi, S. R., Lee, H. H., Spina, C. S., & Collins, J. J. (2013). Antibiotic treatment expands the resistance reservoir and ecological network of the phage metagenome. *Nature*, 499(7457), 219–222. https://doi.org/10.1038/nature12212

Monzón, M., Oteiza, C., Leiva, J., & Amorena, B. (2001). Synergy of different antibiotic combinations in biofilms of *Staphylococcus epidermidis*. *The Journal of antimicrobial chemotherapy*, 48(6), 793–801. https://doi.org/10.1093/jac/48.6.793

Monzón, M., Oteiza, C., Leiva, J., Lamata, M., & Amorena, B. (2002). Biofilm testing of *Staphylococcus epidermidis* clinical isolates: low performance of vancomycin in relation to other antibiotics. *Diagnostic microbiology and infectious disease*, 44(4), 319–324. https://doi.org/10.1016/s0732-8893(02)00464-9

Moormeier, D. E., & Bayles, K. W. (2017). *Staphylococcus aureus* biofilm: a complex developmental organism. *Molecular microbiology*, 104(3), 365–376. https://doi.org/10.1111/mmi.13634

Murray, K., Wu, F., Aktar, R., Amvar, A., & Warriner, K. (2015). Comparative Study on the Efficacy of Bacteriophages, Sanitizers, and UV Light Treatments To Control *Listeria monocytogenes* on Sliced Mushrooms (*Agaricus bisporus*). *Journal of Food Protection*, 78 (6): 1147–1153. https://doi.org/10.4315/0362-028X.JFP-14-389

Nelson D. (2004). Phage taxonomy: we agree to disagree. *Journal of bacteriology,* 186(21), 7029–7031. https://doi.org/10.1128/JB.186.21.7029-7031.2004

Neve, H., Kemper, U., Geis, A., & Heller, K. J. (1994). Monitoring and characterization of lactococcal bacteriophages in a dairy plant. *Kieler Milchwirtschaftliche Forschungsberichte*, 46(2), 167-178.

Nguyen, S., Baker, K., Padman, B. S., Patwa, R., Dunstan, R. A., Weston, T. A., Schlosser, K., Bailey, B., Lithgow, T., Lazarou, M., Luque, A., Rohwer, F., Blumberg, R. S., & Barr, J. J. (2017). Bacteriophage Transcytosis

Provides a Mechanism To Cross Epithelial Cell Layers. *mBio*, 8(6), e01874-17. https://doi.org/10.1128/mBio.01874-17

Novick R. P. (2003). Autoinduction and signal transduction in the regulation of staphylococcal virulence. *Molecular microbiology*, 48(6), 1429–1449. https://doi.org/10.1046/j.1365-2958.2003.03526.x

Novick, R. P., Christie, G. E., & Penadés, J. R. (2010). The phage-related chromosomal islands of Gram-positive bacteria. *Nature reviews. Microbiology*, 8(8), 541–551. https://doi.org/10.1038/nrmicro2393

Obeso, J. M., Martínez, B., Rodríguez, A., & García, P. (2008). Lytic activity of the recombinant staphylococcal bacteriophage PhiH5 endolysin active against *Staphylococcus aureus* in milk. *International journal of food microbiology*, 128(2), 212–218. https://doi.org/10.1016/j.ijfoodmicro.2008.08.010

Ogston A. (1882). Micrococcus Poisoning. *Journal of anatomy and physiology*, 17(Pt 1), 24–58.

OMS. (2017). La OMS publica la lista de las bacterias para las que se necesitan urgentemente nuevos antibióticos. Recuperado de https://www.who.int/es/news-room/detail/27-02-2017-who-publishes-list-of-bacteria-for-which-new-antibiotics-are-urgently-needed

OMS. (2018). Datos recientes revelan los altos niveles de resistencia a los antibióticos en todo el mundo. Recuperado de https://www.who.int/es/news-room/detail/29-01-2018-high-levels-of-antibiotic-resistance-found-worldwide-new-data-shows

OMS. (2019). Resistencia a los antimicrobianos. Recuperado de https://www.who.int/es/news-room/fact-sheets/detail/resistencia-a-los-antimicrobianos

Oppenheim, A. B., Kobiler, O., Stavans, J., Court, D. L., & Adhya, S. (2005). Switches in bacteriophage lambda development. *Annual review of genetics*, 39, 409–429. https://doi.org/10.1146/annurev.genet.39.073003.113656

Otto M. (2009). *Staphylococcus epidermidis*--the 'accidental' pathogen. *Nature reviews. Microbiology*, 7(8), 555–567. https://doi.org/10.1038/nrmicro2182

Otto M. (2013a). Staphylococcal infections: mechanisms of biofilm maturation and detachment as critical determinants of pathogenicity. *Annual review of medicine*, 64, 175–188. https://doi.org/10.1146/annurev-med-042711-140023

Otto M. (2014). *Staphylococcus aureus* toxins. *Current opinion in microbiology*, 17, 32–37. https://doi.org/10.1016/j.mib.2013.11.004

Oxaran, V., Dittmann, K. K., Lee, S., Chaul, L. T., Fernandes de Oliveira, C. A., Corassin, C. H., Alves, V. F., De Martinis, E., & Gram, L. (2018). Behavior of Foodborne Pathogens *Listeria monocytogenes* and *Staphylococcus aureus* in Mixed-Species Biofilms Exposed to Biocides. *Applied and environmental microbiology*, 84(24), e02038-18. https://doi.org/10.1128/AEM.02038-18

Parisi J. T. (1985). Coagulase-negative staphylococci and the epidemiological typing of *Staphylococcus epidermidis*. *Microbiological reviews*, 49(2), 126–139.

Parte A. C. (2018). LPSN - List of Prokaryotic names with Standing in Nomenclature (bacterio.net), 20 years on. *International journal of systematic and evolutionary microbiology*, 68(6), 1825–1829. https://doi.org/10.1099/ijsem.0.002786

Pastagia, M., Euler, C., Chahales, P., Fuentes-Duculan, J., Krueger, J. G., & Fischetti, V. A. (2011). A novel chimeric lysin shows superiority to mupirocin for skin decolonization of methicillin-resistant and -sensitive

Staphylococcus aureus strains. *Antimicrobial agents and chemotherapy*, 55(2), 738–744. https://doi.org/10.1128/AAC.00890-10

Pastar, I., Nusbaum, A. G., Gil, J., Patel, S. B., Chen, J., Valdes, J., Stojadinovic, O., Plano, L. R., Tomic-Canic, M., & Davis, S. C. (2013). Interactions of methicillin resistant *Staphylococcus aureus* USA300 and *Pseudomonas aeruginosa* in polymicrobial wound infection. *PloS one*, 8(2), e56846. https://doi.org/10.1371/journal.pone.0056846

Patterson, A. G., Jackson, S. A., Taylor, C., Evans, G. B., Salmond, G., Przybilski, R., Staals, R., & Fineran, P. C. (2016). Quorum Sensing Controls Adaptive Immunity through the Regulation of Multiple CRISPR-Cas Systems. *Molecular cell*, 64(6), 1102–1108. https://doi.org/10.1016/j.molcel.2016.11.012

Pelz, A., Wieland, K. P., Putzbach, K., Hentschel, P., Albert, K., & Götz, F. (2005). Structure and biosynthesis of staphyloxanthin from *Staphylococcus aureus*. *The Journal of biological chemistry*, 280(37), 32493–32498. https://doi.org/10.1074/jbc.M505070200

Peterson LR. (2009) Bad Bugs, No Drugs: No ESCAPE Revisited. *Clinical Infectious Diseases* 49(96) 992-993, https://doi.org/10.1086/605539

Prescott, L., Harley, J., Klein, D., Gamazo de la Rasilla, C. and Uzcudum, I. (2004). Microbiología. 5th ed. Madrid: MCGRAW-HILL / INTERAMERICANA DE ESPAÑA.

Prevost, G. P., Brezak, M. C., Goubin, F., Mondesert, O., Galcera, M. O., Quaranta, M., Alby, F., Lavergne, O., & Ducommun, B. (2003). Inhibitors of the CDC25 phosphatases. *Progress in cell cycle research*, 5, 225–234.

Qu, Y., Daley, A. J., Istivan, T. S., Rouch, D. A., & Deighton, M. A. (2010). Densely adherent growth mode, rather than extracellular polymer substance matrix build-up ability, contributes to high resistance of *Staphylococcus epidermidis* biofilms to antibiotics. *The Journal of antimicrobial chemotherapy*, 65(7), 1405–1411. https://doi.org/10.1093/jac/dkq119

Reina, J., & Reina, N. (2018). Phage therapy, an alternative to antibiotic therapy?. *Revista espanola de quimioterapia: publicacion oficial de la Sociedad Espanola de Quimioterapia*, 31(2), 101-104.

Rendueles, O., & Ghigo, J. M. (2012). Multi-species biofilms: how to avoid unfriendly neighbors. *FEMS microbiology reviews*, 36(5), 972–989. https://doi.org/10.1111/j.1574-6976.2012.00328.x

Resch, A., Fehrenbacher, B., Eisele, K., Schaller, M., & Götz, F. (2005). Phage release from biofilm and planktonic *Staphylococcus aureus* cells. *FEMS microbiology letters*, 252(1), 89–96. https://doi.org/10.1016/j.femsle.2005.08.048

Rhoads, D. D., Wolcott, R. D., Kuskowski, M. A., Wolcott, B. M., Ward, L. S., & Sulakvelidze, A. (2009). Bacteriophage therapy of venous leg ulcers in humans: results of a phase I safety trial. *Journal of wound care*, 18(6), 237–243. https://doi.org/10.12968/jowc.2009.18.6.42801

Rice SA, Tan CH, Mikkelsen PJ, Kung V, Woo J, Tay M et al. (2009). The biofilm life cycle and virulence of Pseudomonas aeruginosa are dependent on a filamentous prophage. *ISME J* 3: 271–282. https://doi.org/10.1038/ismej.2008.109

Rickard, A. H., Gilbert, P., High, N. J., Kolenbrander, P. E., & Handley, P. S. (2003). Bacterial coaggregation: an integral process in the development of multi-species biofilms. *Trends in microbiology*, 11(2), 94–100. https://doi.org/10.1016/s0966-842x(02)00034-3

Roach, D. R., & Donovan, D. M. (2015). Antimicrobial bacteriophage-derived proteins and therapeutic applications. *Bacteriophage*, 5(3), e1062590. https://doi.org/10.1080/21597081.2015.1062590

Rodríguez-Rubio, L., Gutiérrez, D., Martínez, B., Rodríguez, A., Götz, F., & García, P. (2012b). The tape measure protein of the *Staphylococcus aureus* bacteriophage vB_SauS-phiIPLA35 has an active muramidase domain. *Applied and environmental microbiology*, 78(17), 6369–6371. https://doi.org/10.1128/AEM.01236-12

Rodríguez-Rubio, L., Martínez, B., Donovan, D. M., García, P., & Rodríguez, A. (2013). Potential of the virion-associated peptidoglycan hydrolase HydH5 and its derivative fusion proteins in milk biopreservation. *PloS one*, 8(1), e54828. https://doi.org/10.1371/journal.pone.0054828

Rodríguez-Rubio, L., Martínez, B., Donovan, D. M., Rodríguez, A., & García, P. (2013). Bacteriophage virion-associated peptidoglycan hydrolases: potential new enzybiotics. *Critical reviews in microbiology*, 39(4), 427–434. https://doi.org/10.3109/1040841X.2012.723675

Rodríguez-Rubio, L., Martínez, B., Rodríguez, A., Donovan, D. M., & García, P. (2012a). Enhanced staphylolytic activity of the *Staphylococcus aureus* bacteriophage vB_SauS-phiIPLA88 HydH5 virion-associated peptidoglycan hydrolase: fusions, deletions, and synergy with LysH5. *Applied and environmental microbiology*, 78(7), 2241–2248. https://doi.org/10.1128/AEM.07621-11

Rodríguez-Rubio, L., Martínez, B., Rodríguez, A., Donovan, D. M., Götz, F., & García, P. (2013). The phage lytic proteins from the *Staphylococcus aureus* bacteriophage vB_SauS-phiIPLA88 display multiple active catalytic domains and do not trigger staphylococcal resistance. *PloS one*, 8(5), e64671. https://doi.org/10.1371/journal.pone.0064671

Rossmann, F. S., Racek, T., Wobser, D., Puchalka, J., Rabener, E. M., Reiger, M., Hendrickx, A. P., Diederich, A. K., Jung, K., Klein, C., & Huebner, J. (2015). Phage-mediated dispersal of biofilm and distribution of bacterial virulence genes is induced by quorum sensing. *PLoS pathogens*, 11(2), e1004653. https://doi.org/10.1371/journal.ppat.1004653

Ryder, V. J., Chopra, I., & O'Neill, A. J. (2012). Increased mutability of Staphylococci in biofilms as a consequence of oxidative stress. *PloS one*, 7(10), e47695. https://doi.org/10.1371/journal.pone.0047695

Sadovskaya, I., Chaignon, P., Kogan, G., Chokr, A., Vinogradov, E., & Jabbouri, S. (2006). Carbohydrate-containing components of biofilms produced in vitro by some staphylococcal strains related to orthopaedic prosthesis infections. *FEMS immunology and medical* microbiology, 47(1), 75–82. https://doi.org/10.1111/j.1574-695X.2006.00068.x

Saising, J., Dube, L., Ziebandt, A. K., Voravuthikunchai, S. P., Nega, M., & Götz, F. (2012). Activity of gallidermin on Staphylococcus aureus and Staphylococcus epidermidis biofilms. *Antimicrobial agents and chemotherapy*, 56(11), 5804–5810. https://doi.org/10.1128/AAC.01296-12

Sanchez-Vizuete, P., Orgaz, B., Aymerich, S., Le Coq, D., & Briandet, R. (2015). Pathogens protection against the action of disinfectants in multispecies biofilms. *Frontiers in microbiology*, 6, 705. https://doi.org/10.3389/fmicb.2015.00705

Savage, V. J., Chopra, I., & O'Neill, A. J. (2013). *Staphylococcus aureus* biofilms promote horizontal transfer of antibiotic resistance. *Antimicrobial agents and chemotherapy*, 57(4), 1968–1970. https://doi.org/10.1128/AAC.02008-12

Schilcher, K., Andreoni, F., Dengler Haunreiter, V., Seidl, K., Hasse, B., & Zinkernagel, A. S. (2016). Modulation of *Staphylococcus aureus* Biofilm Matrix by Subinhibitory Concentrations of Clindamycin. *Antimicrobial agents and chemotherapy*, 60(10), 5957–5967. https://doi.org/10.1128/AAC.00463-16

Schmelcher, M., Powell, A. M., Becker, S. C., Camp, M. J., & Donovan, D. M. (2012). Chimeric phage lysins act synergistically with lysostaphin to kill mastitis-causing *Staphylococcus aureus* in murine mammary glands. *Applied and environmental microbiology*, 78(7), 2297–2305. https://doi.org/10.1128/AEM.07050-11

Schuch, R., & Fischetti, V. A. (2006). Detailed genomic analysis of the Wbeta and gamma phages infecting Bacillus anthracis: implications for evolution of environmental fitness and antibiotic resistance. *Journal of bacteriology*, 188(8), 3037–3051. https://doi.org/10.1128/JB.188.8.3037-3051.2006

Schuch, R., & Fischetti, V. A. (2009). The secret life of the anthrax agent Bacillus anthracis: bacteriophage-mediated ecological adaptations. *PloS one*, 4(8), e6532. https://doi.org/10.1371/journal.pone.000653

Scott, A. E., Timms, A. R., Connerton, P. L., Loc Carrillo, C., Adzfa Radzum, K., & Connerton, I. F. (2007). Genome dynamics of *Campylobacter jejuni* in response to bacteriophage predation. *PLoS pathogens*, 3(8), e119. https://doi.org/10.1371/journal.ppat.0030119

Séchaud, L., Rousseau, M., Fayard, B., Callegari, M. L., Quénée, P., & Accolas, J. P. (1992). Comparative Study of 35 Bacteriophages of *Lactobacillus helveticus*: Morphology and Host Range. *Applied and environmental microbiology*, 58(3), 1011–1018.

Silva, N. C., Guimarães, F. F., de P Manzi, M., Gómez-Sanz, E., Gómez, P., Araújo-Júnior, J. P., Langoni, H., Rall, V. L., & Torres, C. (2014). Characterization of methicillin-resistant coagulase-negative staphylococci in milk from cows with mastitis in Brazil. *Antonie van Leeuwenhoek*, 106(2), 227–233. https://doi.org/10.1007/s10482-014-0185-5

Simmons, M., Drescher, K., Nadell, C. D., & Bucci, V. (2018). Phage mobility is a core determinant of phage-bacteria coexistence in biofilms. *The ISME journal*, 12(2), 531–543. https://doi.org/10.1038/ismej.2017.190

Smith T.C. (2015). Livestock-associated *Staphylococcus aureus*: the United States experience. *PLoS pathogens*, 11(2), e1004564. https://doi.org/10.1371/journal.ppat.1004564

Son, J. S., Lee, S. J., Jun, S. Y., Yoon, S. J., Kang, S. H., Paik, H. R., Kang, J. O., & Choi, Y. J. (2010). Antibacterial and biofilm removal activity of a podoviridae *Staphylococcus aureus* bacteriophage SAP-2 and a derived recombinant cell-wall-degrading enzyme. *Applied microbiology and biotechnology*, 86(5), 1439–1449. https://doi.org/10.1007/s00253-009-2386-9

Spoering, A. L., & Lewis, K. (2001). Biofilms and planktonic cells of *Pseudomonas aeruginosa* have similar resistance to killing by antimicrobials. *Journal of bacteriology*, 183(23), 6746–6751. https://doi.org/10.1128/JB.183.23.6746-6751.2001

Stefani, S., Chung, D. R., Lindsay, J. A., Friedrich, A. W., Kearns, A. M., Westh, H., & Mackenzie, F. M. (2012). Meticillin-resistant *Staphylococcus aureus* (MRSA): global epidemiology and harmonisation of typing methods. *International journal of antimicrobial agents*, 39(4), 273–282. https://doi.org/10.1016/j.ijantimicag.2011.09.030

Stewart P. S. (1996). Theoretical aspects of antibiotic diffusion into microbial biofilms. *Antimicrobial agents and chemotherapy*, 40(11), 2517–2522.

Stewart P. S. (2015). Antimicrobial Tolerance in Biofilms. *Microbiology spectrum*, 3(3), 10.1128/microbiolspec.MB-0010-2014. https://doi.org/10.1128/microbiolspec.MB-0010-2014

Stickler D. J. (2002). Susceptibility of antibiotic-resistant Gram-negative bacteria to biocides: a perspective from the study of catheter biofilms. *Journal of applied microbiology*, 92 Suppl, 163S–70S.

Summers W. C. (2001). Bacteriophage therapy. *Annual review of microbiology*, 55, 437–451. https://doi.org/10.1146/annurev.micro.55.1.437

Tan, D., Svenningsen, S. L., & Middelboe, M. (2015). Quorum Sensing Determines the Choice of Antiphage Defense Strategy in *Vibrio anguillarum*. *mBio*, 6(3), e00627. https://doi.org/10.1128/mBio.00627-15

Taylor, T. A., & Unakal, C. G. (2020). *Staphylococcus Aureus*. In *StatPearls*. StatPearls Publishing. Recuperado de: https://www.ncbi.nlm.nih.gov/books/NBK441868/

Thammavongsa, V., Kim, H. K., Missiakas, D., & Schneewind, O. (2015). Staphylococcal manipulation of host immune responses. *Nature reviews. Microbiology*, 13(9), 529–543. https://doi.org/10.1038/nrmicro3521

Toro, H., Price, S. B., McKee, A. S., Hoerr, F. J., Krehling, J., Perdue, M., & Bauermeister, L. (2005). Use of bacteriophages in combination with competitive exclusion to reduce *Salmonella* from infected chickens. *Avian diseases*, 49(1), 118–124. https://doi.org/10.1637/7286-100404R

Totté, J., van Doorn, M. B., & Pasmans, S. (2017). Successful Treatment of Chronic *Staphylococcus aureus*-Related Dermatoses with the Topical Endolysin Staphefekt SA.100: A Report of 3 Cases. *Case reports in dermatology*, 9(2), 19–25. https://doi.org/10.1159/000473872

Utaida, S., Dunman, P. M., Macapagal, D., Murphy, E., Projan, S. J., Singh, V. K., Jayaswal, R. K., & Wilkinson, B. J. (2003). Genome-wide transcriptional profiling of the response of *Staphylococcus aureus* to cell-wall-active antibiotics reveals a cell-wall-stress stimulon. *Microbiology (Reading, England)*, 149(Pt 10), 2719–2732. https://doi.org/10.1099/mic.0.26426-0

van Hal, S. J., & Fowler, V. G., Jr (2013). Is it time to replace vancomycin in the treatment of methicillin-resistant *Staphylococcus aureus* infections?. *Clinical infectious diseases : an official publication of the Infectious Diseases Society of America*, 56(12), 1779–1788. https://doi.org/10.1093/cid/cit178

van Loo, I., Huijsdens, X., Tiemersma, E., de Neeling, A. J., van de Sande-Bruinsma, N., Beaujean, D....Kluytmans, J. (2007). Emergence of Methicillin-Resistant *Staphylococcus aureus* of Animal Origin in Humans. *Emerging Infectious Diseases*, 13(12), 1834-1839. https://dx.doi.org/10.3201/eid1312.070384.

van Loo, I., Huijsdens, X., Tiemersma, E., de Neeling, A., van de Sande-Bruinsma, N., Beaujean, D., Voss, A., & Kluytmans, J. (2007). Emergence of methicillin-resistant *Staphylococcus aureus* of animal origin in humans. *Emerging infectious diseases*, 13(12), 1834–1839. https://doi.org/10.3201/eid1312.070384

Vandenheuvel, D., Lavigne, R., & Brüssow, H. (2015). Bacteriophage Therapy: Advances in Formulation Strategies and Human Clinical Trials. *Annual review of virology*, 2(1), 599–618. https://doi.org/10.1146/annurev-virology-100114-054915

Vandersteegen, K., Mattheus, W., Ceyssens, P. J., Bilocq, F., De Vos, D., Pirnay, J. P., Noben, J. P., Merabishvili, M., Lipinska, U., Hermans, K., & Lavigne, R. (2011). Microbiological and molecular assessment of bacteriophage ISP for the control of *Staphylococcus aureus*. *PloS one*, 6(9), e24418. https://doi.org/10.1371/journal.pone.0024418

Veses-Garcia, M., Liu, X., Rigden, D. J., Kenny, J. G., McCarthy, A. J., & Allison, H. E. (2015). Transcriptomic analysis of Shiga-toxigenic bacteriophage carriage reveals a profound regulatory effect on acid resistance in *Escherichia coli*. *Applied and environmental microbiology*, 81(23), 8118–8125. https://doi.org/10.1128/AEM.02034-15

Viertel, T. M., Ritter, K., & Horz, H. P. (2014). Viruses versus bacteria-novel approaches to phage therapy as a tool against multidrug-resistant pathogens. *The Journal of antimicrobial chemotherapy*, 69(9), 2326–2336. https://doi.org/10.1093/jac/dku173

Vispo, N., & Puchades, Y. (2001). Bacteriophages: from phage therapy to combinatorial biology. *Biotecnologia Aplicada*, 18(3), 135-147.

Wang, R., Braughton, K. R., Kretschmer, D., Bach, T. H., Queck, S. Y., Li, M., Kennedy, A. D., Dorward, D. W., Klebanoff, S. J., Peschel, A., DeLeo, F. R., & Otto, M. (2007). Identification of novel cytolytic peptides as key virulence determinants for community-associated MRSA. *Nature medicine*, 13(12), 1510–1514. https://doi.org/10.1038/nm1656

Wang, X., Kim, Y., Ma, Q., Hong, S. H., Pokusaeva, K., Sturino, J. M., & Wood, T. K. (2010). Cryptic prophages help bacteria cope with adverse environments. *Nature communications*, 1, 147. https://doi.org/10.1038/ncomms1146

Waters, C. M., & Bassler, B. L. (2005). Quorum sensing: cell-to-cell communication in bacteria. *Annual review of cell and developmental biology*, 21, 319–346. https://doi.org/10.1146/annurev.cellbio.21.012704.131001

Wertheim, H. F., Melles, D. C., Vos, M. C., van Leeuwen, W., van Belkum, A., Verbrugh, H. A., & Nouwen, J. L. (2005). The role of nasal carriage in *Staphylococcus aureus* infections. *The Lancet. Infectious diseases*, 5(12), 751–762. https://doi.org/10.1016/S1473-3099(05)70295-4

Whichard, J. M., Sriranganathan, N., & Pierson, F. W. (2003). Suppression of *Salmonella* growth by wild-type and large-plaque variants of bacteriophage Felix O1 in liquid culture and on chicken frankfurters. *Journal of food protection*, 66(2), 220–225. https://doi.org/10.4315/0362-028x-66.2.220

Wood, T. K., Knabel, S. J., & Kwan, B. W. (2013). Bacterial persister cell formation and dormancy. *Applied and environmental microbiology*, 79(23), 7116–7121. https://doi.org/10.1128/AEM.02636-13

World Health Organization. (2019). Antimicrobial resistance. [online] Recuperado de https://www.who.int/antimicrobial-resistance [7 de Marzo de 2019].

Wright, A., Hawkins, C. H., Anggård, E. E., & Harper, D. R. (2009). A controlled clinical trial of a therapeutic bacteriophage preparation in chronic otitis due to antibiotic-resistant *Pseudomonas aeruginosa*; a preliminary report of efficacy. *Clinical otolaryngology : official journal of ENT-UK ; official journal of Netherlands Society for Oto-Rhino-Laryngology & Cervico-Facial Surgery*, 34(4), 349–357. https://doi.org/10.1111/j.1749-4486.2009.01973.x

Xia, G., & Wolz, C. (2014). Phages of *Staphylococcus aureus* and their impact on host evolution. *Infection, genetics and evolution : journal of molecular epidemiology and evolutionary genetics in infectious diseases*, 21, 593–601. https://doi.org/10.1016/j.meegid.2013.04.022

Anexos

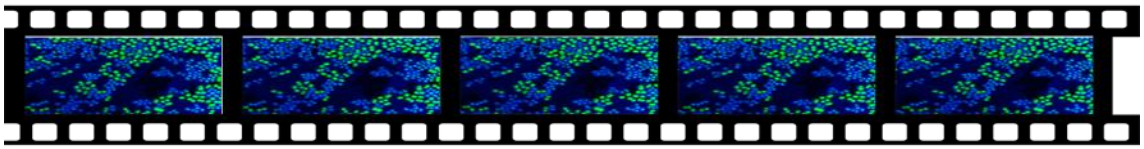

ANEXOS

Material suplementario del CAPÍTULO 1, Artículo 1.

González, S., Fernández, L., Campelo, A. B., Gutiérrez, D., Martínez, B., Rodríguez, A., & García, P. (2017). The Behavior of *Staphylococcus aureus* Dual-Species Biofilms Treated with Bacteriophage phiIPLA-RODI Depends on the Accompanying Microorganism. *Applied and environmental microbiology*, 83(3), e02821-16. https://doi.org/10.1128/AEM.02821-16

Figure S1. Three-dimensional structure of *S. aureus* IPLA16 and *E. faecium* MMRA (A and B), *L. plantarum* 55-1 (C and D), *L. pentosus* A1 (E and F) or *L. pentosus* B1 (G and H) dual-species biofilms. Images correspond to 5 h biofilms treated with SM buffer (A, C, E and G) or phage phiIPLA-RODI for 4 h (B, D, F and H). Biofilms were stained with SYTO® 9, which dyes cells from all species green.

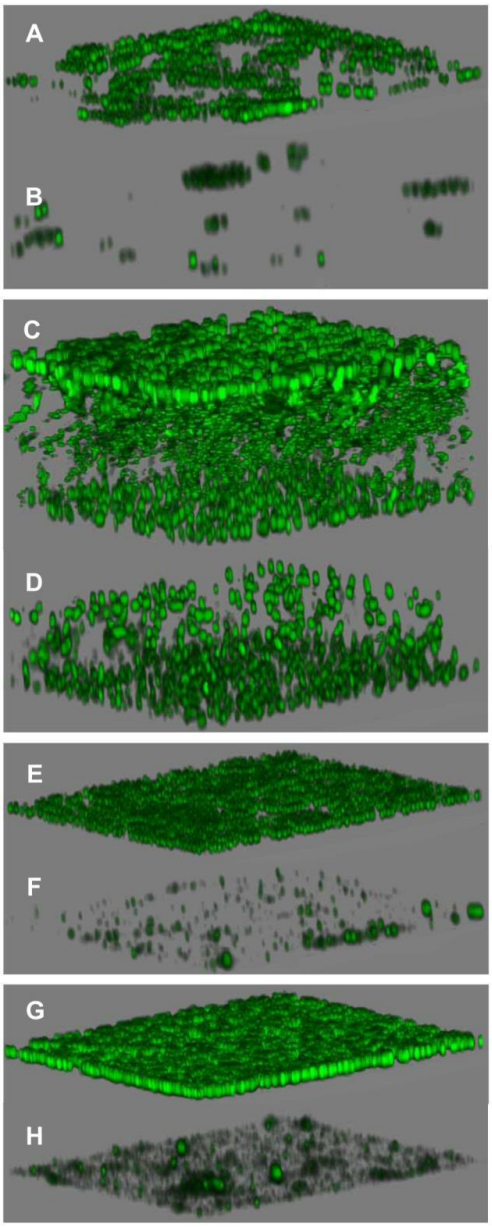

Figure S2. Biomass quantification of 5 h biofilms formed by *S. aureus* IPLA16 with other species under proliferation conditions and treated with phage phiIPLA-RODI. Values represent the means ± standard deviations of 4 technical replicates corresponding to one representative experiment out of three with the same trends. White bars correspond to the untreated control, while black and grey bars represent samples treated with 109 or 106 PFU/well, respectively. Phage-infected samples were compared to their respective untreated controls. *, P-value<0.05.

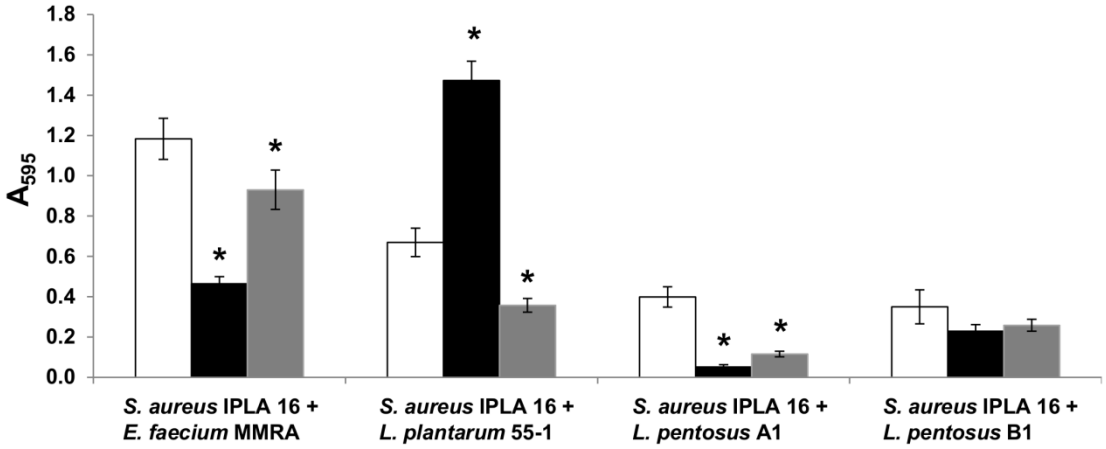

Material suplementario del CAPÍTULO 1, Artículo 2

González, S., Fernández, L., Gutiérrez, D., Campelo, A. B., Rodríguez, A., & García, P. (2018). Analysis of Different Parameters Affecting Diffusion, Propagation and Survival of Staphylophages in Bacterial Biofilms. *Frontiers in microbiology*, 9, 2348. https://doi.org/10.3389/fmicb.2018.02348

FIGURE S1. Biofilm formation of different bacterial strains on polycarbonate membranes after 24 hours of incubation at 37ºC. A) The depicted values correspond to the average and standard deviation of at least three independent repeats. Sa, *S. aureus*; Se, *S. epidermidis* and Lp, *L. plantarum*. Strong (A_{595}>2), intermediate (1<A_{595}<2) and weak (A_{595}<1) biofilm formers are represented in black, grey and white bars, respectively. The P-values shown in the table below the histogram were obtained comparing biofilm formation of the different strains. P-values < 0.05 were considered significant (light grey cells). B) Linear regression analysis between average values of biofilm formation on polycarbonate membranes (quantified as A_{595} of crystal violet stained biofilms) and biofilm thickness (in µm) as determined by confocal microscopy of biofilms formed in glass and stained with SYTO 9 are also shown.

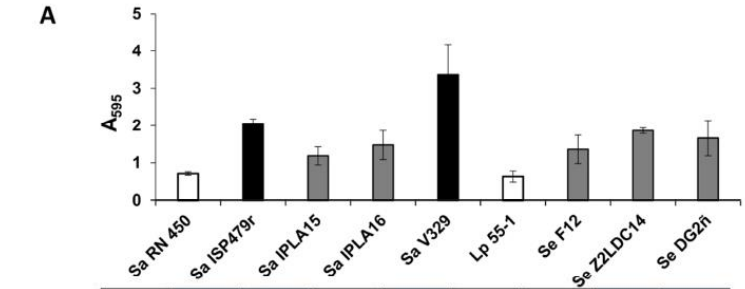

Sa RN450		**0.002**	**0.028**	0.076	**0.030**	0.447	0.098	**0.000**	**0.028**
Sa ISP479r	**0.002**		**0.002**	0.116	0.103	**0.000**	0.078	0.166	0.218
Sa IPLA15	**0.028**	**0.002**		0.167	**0.019**	**0.007**	0.267	**0.004**	0.071
Sa IPLA16	0.076	0.116	0.167		**0.040**	0.050	0.733	0.223	0.594
Sa V329	**0.030**	0.103	**0.019**	**0.040**		**0.029**	**0.035**	0.086	**0.049**
Lp 55-1	0.447	**0.000**	**0.007**	0.050	**0.029**		0.067	**0.001**	**0.018**
Se F12	0.098	0.078	0.267	0.733	**0.035**	0.067		0.073	0.198
Se Z2LDC14	**0.000**	0.166	**0.004**	0.223	0.086	**0.001**	0.073		0.231
Se DG2ñ	**0.028**	0.218	0.071	0.594	**0.049**	**0.018**	0.198	0.231	

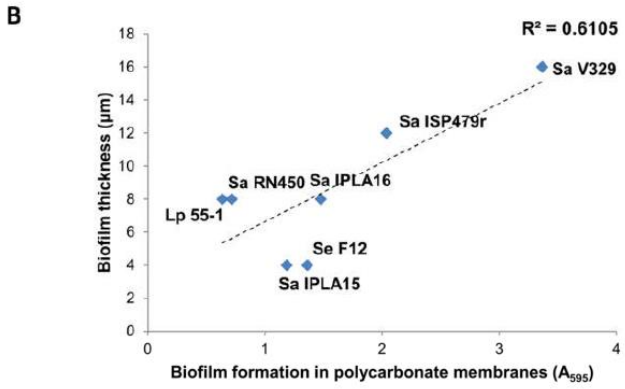

FIGURE S2. Confocal microscopy analysis of biofilms formed by different *S. aureus* strains. Biofilms were allowed to form on glass-bottomed slides for 24 h at 37º C and then washed with PBS and stained with SYTO 9 prior to observation with a confocal laser scanning microscope. The two images for each strain respectively show a 2D view of the biofilm surface (top) and a lateral view of the biofilm (bottom).

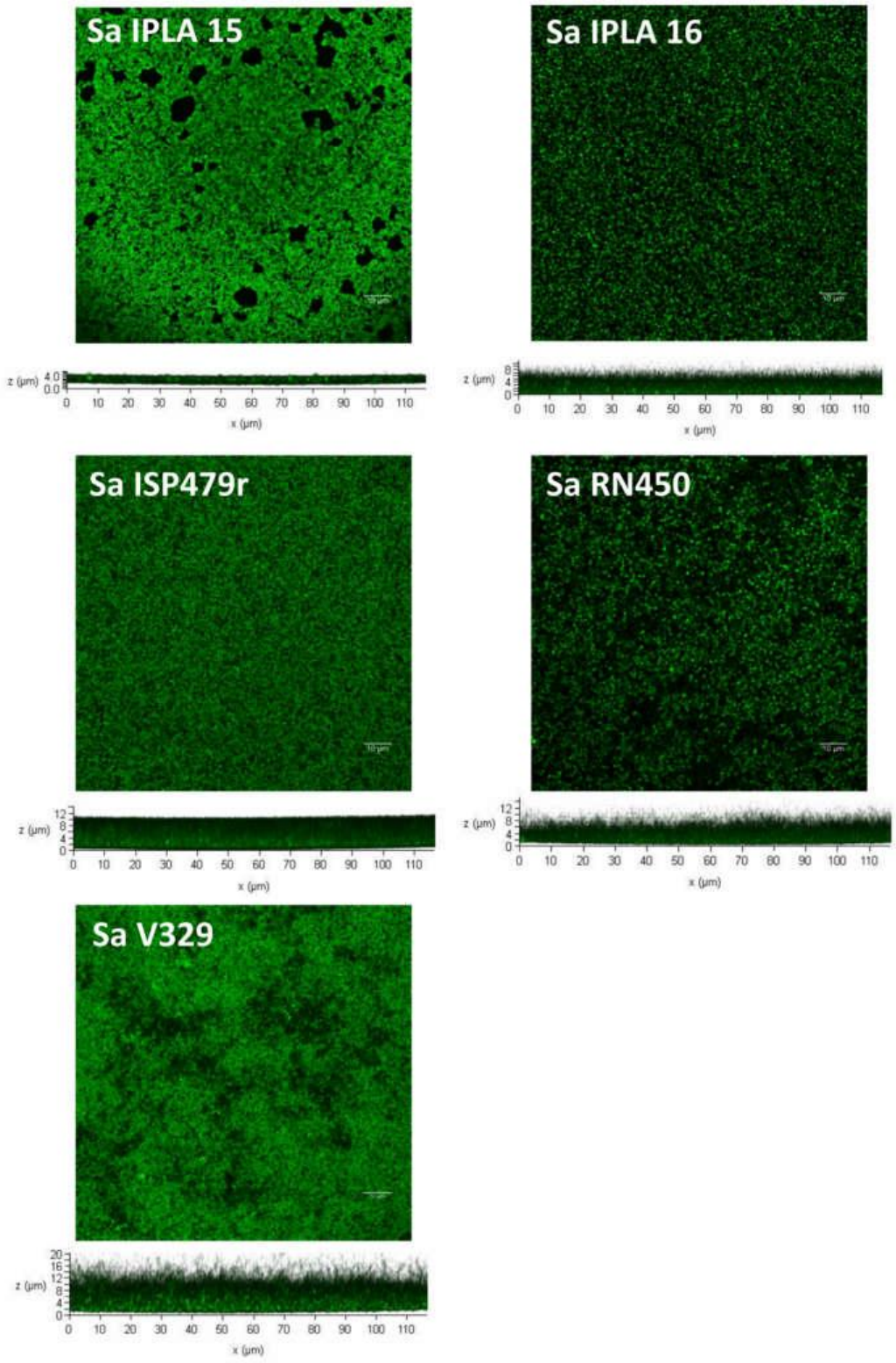

FIGURE S3. Confocal microscopy analysis of biofilms formed by different *S. epidermidis* and *L. plantarum* strains. Biofilms were allowed to form on glass-bottomed slides for 24 h at 37º C and then washed with PBS and stained with SYTO 9 prior to observation with a confocal laser scanning microscope. The two images for each strain respectively show a 2D view of the biofilm surface (top) and a lateral view of the biofilm (bottom).

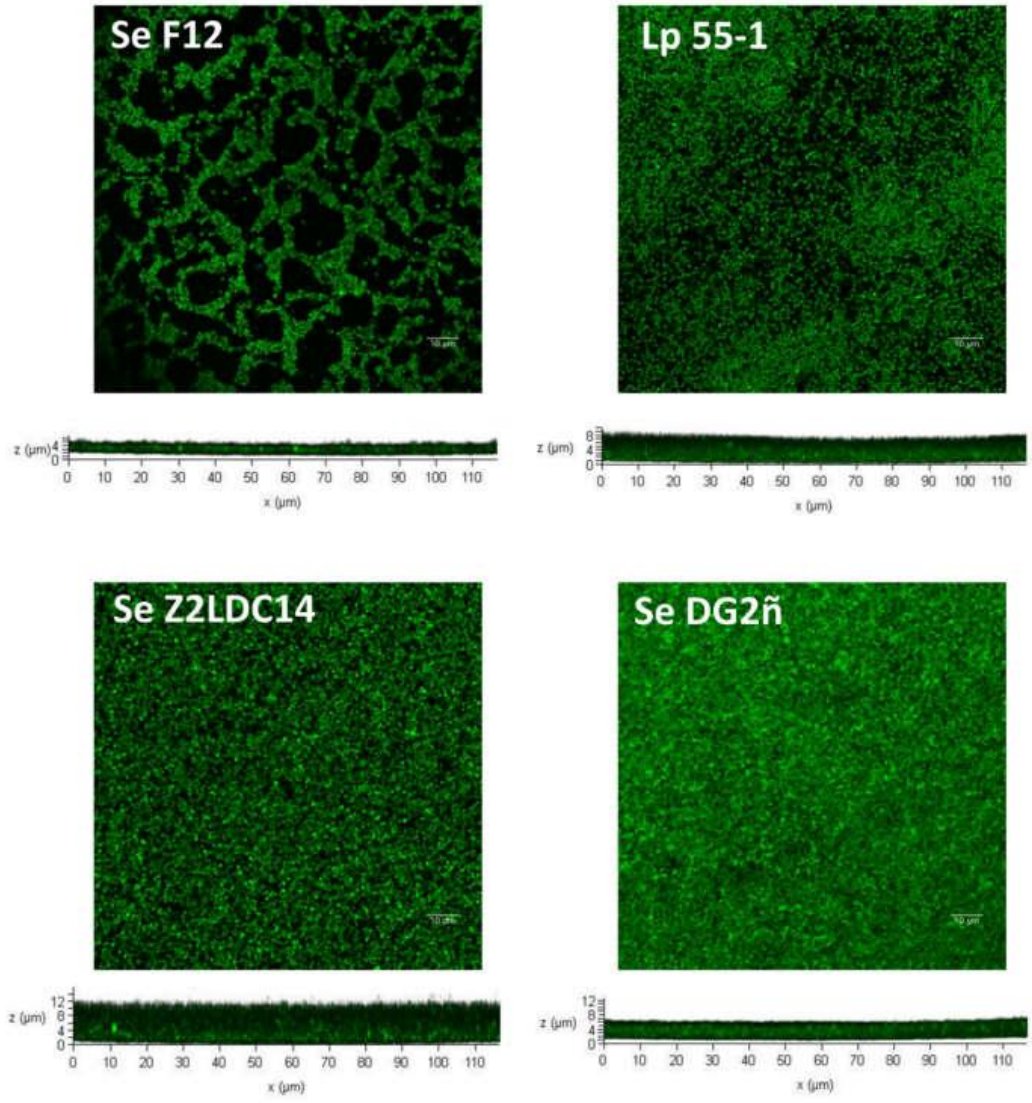

FIGURE S4. Linear regression analysis of the relationship between biofilm formation, phage susceptibility or a combination of both and phage titer in the flow-through of biofilms formed by different bacterial strains treated with phiIPLA-RODI. The graphs on the left and right correspond to treatment with a high (10^9 PFU/ml) and low (10^6 PFU/ml) phage concentration, respectively. The equation of the trend line is shown in the upper left corner of each chart. The goodness of fit of the trend line estimated as coefficient of determination (R^2) is shown in the upper right corner of each chart.

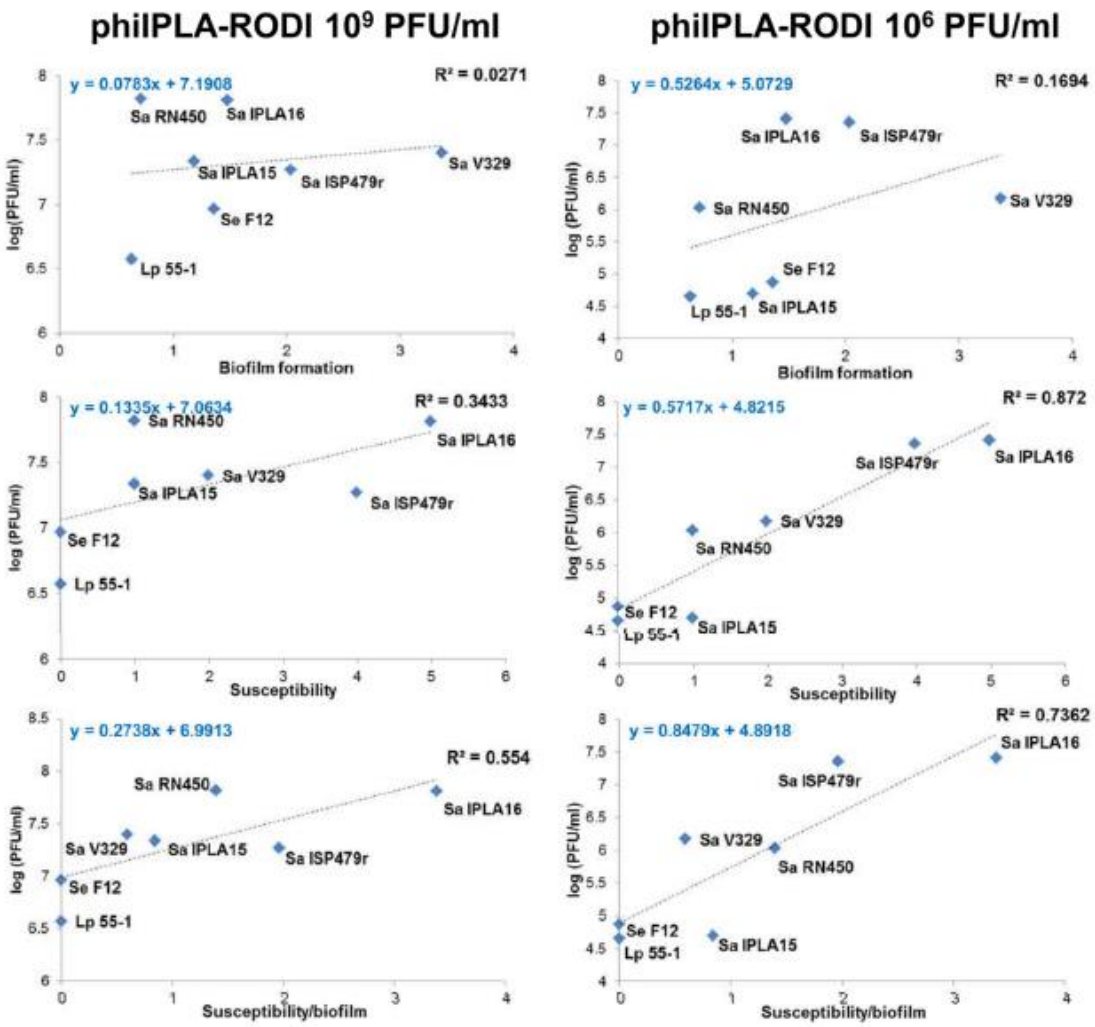

FIGURE S5. Linear regression analysis of the relationship between biofilm formation, phage susceptibility or a combination of both and phage titer in the flow-through of biofilms formed by different bacterial strains treated with phiIPLA-C1C. The graphs on the left and right correspond to treatment with a high (10^9 PFU/ml) and low (10^6 PFU/ml) phage concentration, respectively. The equation of the trend line is shown in the upper left corner of each chart. The goodness of fit of the trend line estimated as coefficient of determination (R^2) is shown in the upper right corner of each chart.

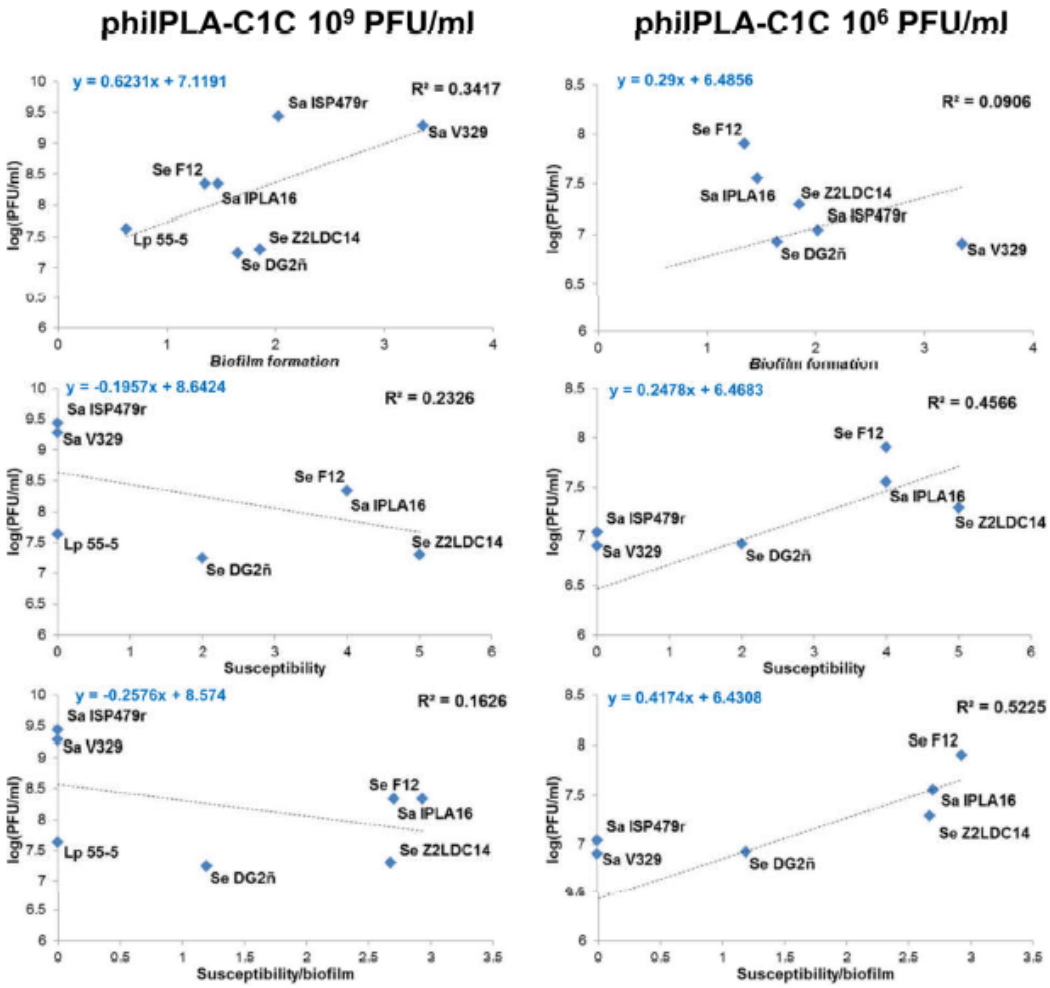

FIGURE S6. Linear regression analysis of the relationship between number of phage particles entrapped in the matrix and phage titer in the flow-through of biofilms formed by different bacterial strains treated with 10^6 PFU/ml of phiIPLA-RODI. The graph on the left corresponds to the analysis carried out including all strains, while the graph on the right represents the análisis performed excluding strain *S. aureus* IPLA 15. The equation of the trend line is shown in the upper left corner of each chart. The goodness of fit of the trend line estimated as coefficient of determination (R^2) is shown in the upper right corner of each chart.

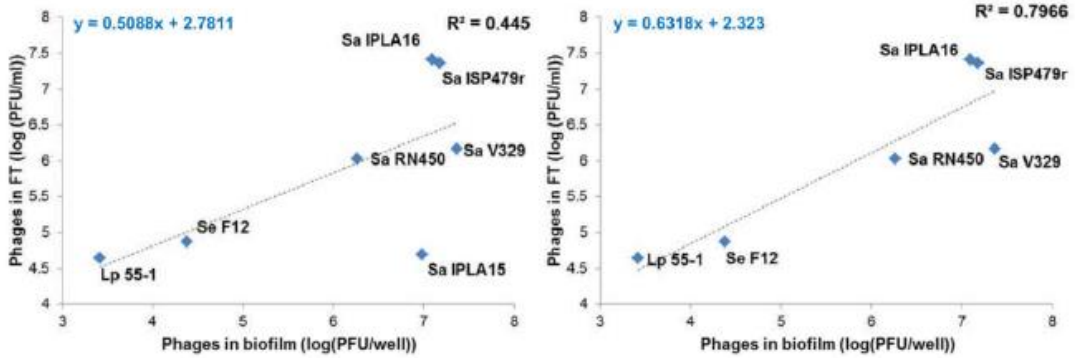

Material suplementario del CAPÍTULO 2, Artículo 1

Fernández, L., González, S., Campelo, A. B., Martínez, B., Rodríguez, A., & García, P. (2017). Low-level predation by lytic phage phiIPLA-RODI promotes biofilm formation and triggers the stringent response in *Staphylococcus aureus*. *Scientific reports*, 7, 40965. https://doi.org/10.1038/srep40965

Video S1. Biofilm formation of strain *S. aureus* IPLA 1 in the presence of phage phiIPLA-RODI at an MOI of 10^{-3} (10^3 <pFU/well) monitored in real time for 7 hours by confocal laser scanning microscopy. https://www.ncbi.nlm.nih.gov/pmc/articles/PMC5244418/bin/srep40965-s1.mov

Table S1. Normalized mean reads per kilobase million (RPKM) values corresponding to the different open reading frames (ORFs) of phiIPLA-RODI genome in the treated samples

gene_ID	start_coord	end_coord	RODI-1 Reads	RODI-2 Reads	RODI-3 Reads	RODI-1 RPKM	RODI-2 RPKM	RODI-3 RPKM	RPKM MEAN	RPKM STD	gene_product_acce	gene_name
AVU41_gp001	14	496	7265	4771	7648	3210	2128	3504	**2947.333333**	724.6304805	YP_009195837.1	terminal repeat-encoded protein
AVU41_gp002	575	739	3937	2829	3479	5092	3694	4665	**4483.666667**	716.423292	YP_009195838.1	terminal repeat-encoded protein
AVU41_gp003	739	1008	3190	2073	3133	2522	1654	2568	**2248**	514.9330054	YP_009195839.1	TreT
AVU41_gp004	1093	1314	2503	1646	2382	2406	1597	2374	**2125.666667**	458.1182526	YP_009195840.1	TreU
AVU41_gp005	1642	1932	1046	970	1200	767	718	912	**799**	100.8811182	YP_009195841.1	hypothetical protein
AVU41_gp006	2036	2272	1823	1778	2467	1642	1616	2303	**1853.666667**	389.3511697	YP_009195842.1	BofL
AVU41_gp007	2274	2759	5572	5262	6959	2447	2332	3168	**2649**	453.1302241	YP_009195843.1	hypothetical protein
AVU41_gp008	2772	3179	3516	3108	4572	1839	1641	2480	**1986.666667**	438.559384	YP_009195844.1	hypothetical protein
AVU41_gp009	3179	3610	9576	8941	11293	4731	4459	5784	**4991.333333**	699.8116413	YP_009195845.1	UboA
AVU41_gp010	3613	3804	3336	3022	3763	3708	3391	4337	**3812**	481.498702	YP_009195846.1	hypothetical protein
AVU41_gp011	3801	4286	3305	3091	4100	1451	1370	1867	**1562.666667**	266.653958	YP_009195847.1	membrane protein
AVU41_gp012	4279	4710	2428	2089	2732	1200	1042	1399	**1213.666667**	178.8919599	YP_009195848.1	hypothetical protein
AVU41_gp013	4724	5266	3328	3414	4129	1308	1354	1683	**1448.333333**	204.5246521	YP_009195849.1	nucleotidyl transferase
AVU41_gp014	5278	5766	6345	6231	8380	2769	2745	3792	**3102**	597.678007	YP_009195850.1	hypothetical protein
AVU41_gp015	5779	6177	3378	3210	4436	1807	1733	2460	**2000**	400.0862407	YP_009195851.1	hypothetical protein
AVU41_gp016	6174	6881	6144	6251	8004	1852	1902	2501	**2085**	361.1329395	YP_009195852.1	phosphatase
AVU41_gp017	6981	7535	6037	5482	5303	2322	2128	2114	**2188**	116.258333	YP_009195853.1	hypothetical protein
AVU41_gp018	7551	7868	7066	6899	6048	4742	4674	4208	**4541.333333**	290.6704893	YP_009195854.1	hypothetical protein
AVU41_gp019	8854	9402	2185	1898	2869	849	745	1156	**916.6666667**	213.6921462	YP_009195855.1	hypothetical protein
AVU41_gp020	9406	9624	2219	1802	2772	2163	1773	2801	**2245.666667**	518.9617841	YP_009195856.1	hypothetical protein
AVU41_gp021	9625	9819	1871	1570	2425	2048	1734	2752	**2178**	521.3022156	YP_009195857.1	hypothetical protein
AVU41_gp022	9809	10546	4348	3530	5848	1257	1030	1753	**1346.666667**	369.7463094	YP_009195858.1	hypothetical protein
AVU41_gp023	10609	10713	335	292	463	681	599	976	**752**	198.2750615	YP_009195859.1	hypothetical protein
AVU41_gp024	10735	10962	1610	1501	1905	1507	1418	1849	**1591.333333**	227.5397401	YP_009195860.1	aspartate aminotransferase
AVU41_gp025	10964	11350	2175	1928	2765	1199	1073	1581	**1284.333333**	264.5322917	YP_009195861.1	hypothetical protein
AVU41_gp026	11447	11620	1724	1641	1644	2115	2032	2091	**2079.333333**	42.71221527	YP_009195862.1	hypothetical protein
AVU41_gp027	11661	12143	13837	13526	12982	6114	6033	5947	**6031.333333**	83.51247412	YP_009195863.1	hypothetical protein
AVU41_gp028	12193	12735	21313	21377	27265	8377	8481	11110	**9322.666667**	1548.74928	YP_009195864.1	hypothetical protein
AVU41_gp029	12735	13265	23677	23393	29378	9516	9490	12242	**10416**	1581.415821	YP_009195865.1	hypothetical protein
AVU41_gp030	13268	13432	4071	4012	4881	5266	5238	6546	**5683.333333**	747.2224122	YP_009195866.1	membrane protein
AVU41_gp031	13435	13722	2278	1776	3181	1688	1328	2444	**1820**	569.5893257	YP_009195867.1	membrane protein
AVU41_gp032	13722	14567	4783	3788	6867	1207	965	1796	**1322.666667**	427.4041803	YP_009195868.1	hypothetical protein
AVU41_gp033	14580	15698	8045	6581	12094	1534	1267	2391	**1730.666667**	587.2412906	YP_009195869.1	AAA family ATPase
AVU41_gp034	15851	16177	614	656	765	401	432	518	**450.3333333**	60.61627944	YP_009195870.1	hypothetical protein
AVU41_gp035	16170	16586	1544	1932	1989	790	998	1055	**947.6666667**	139.4859611	YP_009195871.1	hypothetical protein
AVU41_gp036	16718	17020	5337	5998	7994	3759	4264	5838	**4620.333333**	1084.338662	YP_009195872.1	NTP-PPase
AVU41_gp037	17020	17208	3201	3761	4758	3615	4287	5570	**4490.666667**	993.2856253	YP_009195873.1	hypothetical protein
AVU41_gp038	17252	17413	1350	1629	2048	1779	2166	2797	**2247.333333**	513.8504971	YP_009195874.1	hypothetical protein
AVU41_gp039	17413	19464	9764	10668	15555	1016	1120	1677	**1271**	355.4307246	YP_009195875.1	hypothetical protein
AVU41_gp040	19543	19806	2595	2249	2986	2098	1835	2503	**2145.333333**	336.5060673	YP_009195876.1	hypothetical protein
AVU41_gp041	19823	19996	6780	6140	7010	8316	7602	8914	**8277.333333**	656.8541188	YP_009195877.1	peptidoglycan binding protein
AVU41_gp042	20003	20581	19312	17405	19132	7119	6476	7312	**6969**	437.7202303	YP_009195878.1	hypothetical protein
AVU41_gp043	20574	21173	9978	7850	12773	3549	2818	4711	**3692.666667**	954.642516	YP_009195879.1	nucleoside 2-deoxyribosyltransferase
AVU41_gp044	21166	22059	6664	5609	7706	1591	1352	1907	**1616.666667**	278.3888168	YP_009195880.1	RNA ligase
AVU41_gp045	22063	22287	253	255	304	240	244	299	**261**	32.96968304	YP_009195881.1	hypothetical protein
AVU41_gp046	22356	23096	25456	23540	34928	7332	6844	10430	**8202**	1944.871204	YP_009195882.1	PhoH-related protein
AVU41_gp047	23148	23762	27662	26138	40088	9600	9156	14423	**11059.66667**	2921.179956	YP_009195883.1	hypothetical protein
AVU41_gp048	23778	24203	10524	10653	15774	5272	5387	8193	**6284**	1654.242123	YP_009195884.1	ribonuclease
AVU41_gp049	24193	24384	5604	5524	8335	6229	6198	9606	**7344.333333**	1958.722117	YP_009195885.1	hypothetical protein
AVU41_gp050	24407	25048	8752	9321	13661	2909	3128	4708	**3581.666667**	981.5601527	YP_009195886.1	hypothetical protein
AVU41_gp051	25038	25268	4584	4822	7272	4235	4497	6966	**5232.666667**	1506.815959	YP_009195887.1	DNA binding protein
AVU41_gp052	25271	25498	3861	4178	5144	3614	3948	4992	**4184.666667**	718.8388786	YP_009195888.1	hypothetical protein

AVU41_gp053	25607	26299	1469	1155	635	452	359	203	**338**	125.8213019	YP_009195889.1	transglycosylase
AVU41_gp054	26497	27291	6536	5291	10391	1755	1434	2892	**2027**	766.112916	YP_009195890.1	membrane protein
AVU41_gp055	27291	27599	1943	1822	3039	1342	1270	2176	**1596**	503.583161	YP_009195891.1	hypothetical protein
AVU41_gp056	27712	28332	7312	8527	9061	2513	2958	3229	**2900**	361.5065698	YP_009195892.1	hypothetical protein
AVU41_gp057	28395	29885	133411	112691	101786	19097	16282	15106	**16828.33333**	2050.824306	YP_009195893.1	endolysin
AVU41_gp058	29885	30388	49610	42239	35054	21008	18054	15390	**18150.66667**	2810.247201	YP_009195894.1	holin
AVU41_gp059	30473	30658	1312	1003	761	1505	1162	905	**1190.666667**	301.0254696	YP_009195895.1	hypothetical protein
AVU41_gp060	32211	32429	280	292	223	273	287	225	**261.6666667**	32.5166624	YP_009195896.1	hypothetical protein
AVU41_gp061	32909	33118	1097	1000	727	1115	1026	766	**969**	181.3477323	YP_009195897.1	hypothetical protein
AVU41_gp062	33131	33463	14729	13806	8734	9440	8931	5804	**8058.333333**	1968.828162	YP_009195898.1	hypothetical protein
AVU41_gp063	33476	33802	10441	9343	6250	6815	6155	4229	**5733**	1343.656206	YP_009195899.1	membrane protein
AVU41_gp064	34243	34629	17048	19193	12013	9402	10684	6869	**8985**	1941.3843	YP_009195900.1	membrane protein
AVU41_gp065	34607	34885	15366	17116	10999	11754	13216	8723	**11231**	2291.704388	YP_009195901.1	hypothetical protein
AVU41_gp066	34882	35292	27305	31601	22802	14179	16564	12276	**14339.66667**	2148.510259	YP_009195902.1	hypothetical protein
AVU41_gp067	35307	35657	38490	43395	34365	23404	26634	21664	**23900.66667**	2521.950304	YP_009195903.1	terminase large subunit
AVU41_gp068	35897	36667	39613	42217	32044	10965	11796	9196	**10652.33333**	1327.900724	YP_009195904.1	VSR homing endonuclease
AVU41_gp069	36734	38194	117317	132310	113521	17138	19509	17193	**17946.66667**	1353.299794	YP_009195905.1	terminase large subunit
AVU41_gp070	38187	39008	94010	107990	93952	24409	28301	25291	**26000.33333**	2040.657084	YP_009195906.1	hypothetical protein
AVU41_gp071	39165	39644	47206	53379	47202	20989	23957	21759	**22235**	1540.190897	YP_009195907.1	hypothetical protein
AVU41_gp072	39686	40936	185309	209017	217667	31614	35993	38500	**35369**	3485.151503	YP_009195908.1	membrane protein
AVU41_gp073	41021	41362	3965	4162	3090	2474	2622	1999	**2365**	325.4888631	YP_009195909.1	membrane protein
AVU41_gp074	41372	41752	11515	11811	7605	6450	6678	4417	**5848.333333**	1244.802126	YP_009195910.1	hypothetical protein
AVU41_gp075	41756	43447	85790	90354	73991	10821	11504	9676	**10667**	923.6790568	YP_009195911.1	portal protein
AVU41_gp076	43641	44414	85103	75376	50044	23466	20979	14307	**19584**	4736.173455	YP_009195912.1	prohead protease
AVU41_gp077	44433	45383	179706	168734	116254	40330	38222	27049	**35200.33333**	7137.513036	YP_009195913.1	hypothetical protein
AVU41_gp078	45499	46890	400189	355493	289563	61358	55016	46029	**54134.33333**	7702.438726	YP_009195914.1	capsid protein
AVU41_gp079	46982	47278	15120	15188	9738	10865	11016	7255	**9712**	2129.163451	YP_009195915.1	hypothetical protein
AVU41_gp080	47291	48199	35073	33918	27137	8235	8038	6606	**7626.333333**	889.107605	YP_009195916.1	hypothetical protein
AVU41_gp081	48213	49091	29854	30190	24121	7249	7399	6072	**6906.666667**	726.72301	YP_009195917.1	hypothetical protein
AVU41_gp082	49091	49711	31388	31848	24688	10787	11048	8797	**10210.66667**	1231.20686	YP_009195918.1	hypothetical protein
AVU41_gp083	49730	50566	84852	82994	56840	21636	21361	15026	**19341**	3739.428432	YP_009195919.1	hypothetical protein
AVU41_gp084	50568	50783	20270	18872	13855	20028	18822	14193	**17681**	3080.294953	YP_009195920.1	hypothetical protein
AVU41_gp085	50810	52573	357465	306226	250417	43249	37397	31412	**37352.66667**	5918.624531	YP_009195921.1	major tail sheath protein
AVU41_gp086	52646	52984	59237	50340	41201	37294	31990	26893	**32059**	5200.843297	YP_009195922.1	tail tube
AVU41_gp087	53779	54783	12733	13501	11690	2704	2894	2574	**2724**	160.9347694	YP_009195923.1	Ioh
AVU41_gp088	54840	54980	990	1115	1015	1499	1704	1593	**1598.666667**	102.6174124	YP_009195924.1	hypothetical protein
AVU41_gp089	55023	55481	1450	1502	1196	674	705	577	**652**	66.7757441	YP_009195925.1	hypothetical protein
AVU41_gp090	55494	55688	238	241	296	260	266	336	**287.3333333**	42.25320501	YP_009195926.1	hypothetical protein
AVU41_gp091	55770	56081	2581	1886	3034	1766	1302	2152	**1740**	425.5960526	YP_009195927.1	hypothetical protein
AVU41_gp092	56213	56671	17573	17600	10456	8171	8260	5041	**7157.333333**	1833.338576	YP_009195928.1	hypothetical protein
AVU41_gp093	56715	57251	37759	36595	27545	15007	14681	11350	**13679.33333**	2023.836538	YP_009195929.1	tail morphogenetic protein
AVU41_gp094	57307	61362	115298	114435	93488	6067	6078	5100	**5748.333333**	561.5000742	YP_009195930.1	TMP protein
AVU41_gp095	61441	63867	23300	23989	21662	2049	2129	1975	**2051**	77.01947806	YP_009195931.1	CHAP domain protein
AVU41_gp096	63881	64768	11986	13188	12693	2881	3199	3163	**3081**	174.1378764	YP_009195932.1	protease
AVU41_gp097	64768	67314	59937	61044	66555	5022	5163	5782	**5322.333333**	404.2775449	YP_009195933.1	glycerophosphoryl diester phosphatase
AVU41_gp098	67421	68212	22376	25359	27205	6030	6898	7601	**6843**	786.9428188	YP_009195934.1	hypothetical protein
AVU41_gp099	68212	68736	14306	17270	18795	5816	7086	7922	**6941.333333**	1060.426958	YP_009195935.1	hypothetical protein
AVU41_gp100	68736	69440	27111	31742	33870	8207	9699	10630	**9512**	1222.276155	YP_009195936.1	baseplate protein
AVU41_gp101	69455	70501	47274	55072	56453	9636	11331	11931	**10966**	1190.241572	YP_009195937.1	baseplate protein
AVU41_gp102	70522	73587	108767	122687	131758	7571	8620	9509	**8566.666667**	970.1001666	YP_009195938.1	hypothetical protein
AVU41_gp103	73698	74219	43363	48259	49367	17729	19916	20926	**19523.66667**	1634.211227	YP_009195939.1	baseplate protein
AVU41_gp104	74240	77698	427519	413149	519699	26378	25731	33245	**28451.33333**	4164.022374	YP_009195940.1	adsorption-associated tail protein
AVU41_gp105	77747	77905	14311	14889	15019	19210	20173	20901	**20094.66667**	848.2171499	YP_009195941.1	hypothetical protein
AVU41_gp106	77906	79825	147215	146940	169589	16364	16487	19544	**17465**	1801.516861	YP_009195942.1	carbohydrate binding domain protein

AVU41_gp107	79847	80218	41204	41929	46099	23640	24281	27420	**25113.66667**	2022.894049	YP_009195943.1	hypothetical protein
AVU41_gp108	80225	81601	129068	118055	158599	20005	18469	25485	**21319.66667**	3688.133042	YP_009195944.1	hypothetical protein
AVU41_gp109	81691	83439	104968	126857	104460	12809	15625	13216	**13883.33333**	1521.993539	YP_009195945.1	DNA helicase
AVU41_gp110	83451	85064	88245	107746	91658	11669	14381	12566	**12872**	1381.652272	YP_009195946.1	Rep protein
AVU41_gp111	85057	86499	126228	154229	138061	18670	23025	21170	**20955**	2185.446179	YP_009195947.1	ATPase
AVU41_gp112	86578	86997	3541	3255	3802	1799	1670	2003	**1824**	167.901757	YP_009195948.1	hypothetical protein
AVU41_gp113	86997	88022	15407	11488	20011	3205	2412	4316	**3311**	956.4157046	YP_009195949.1	exonuclease
AVU41_gp114	88022	88399	11285	8773	13360	6372	5000	7821	**6397.666667**	1410.675134	YP_009195950.1	hypothetical protein
AVU41_gp115	88399	90318	40434	33423	47864	4495	3750	5516	**4587**	886.5872771	YP_009195951.1	ATPase
AVU41_gp116	90318	90914	10093	8169	12113	3608	2948	4490	**3682**	773.6588395	YP_009195952.1	hypothetical protein
AVU41_gp117	90929	91996	13291	10508	15639	2656	2120	3240	**2672**	560.1714023	YP_009195953.1	DNA primase
AVU41_gp118	92062	92400	20634	20095	19622	12991	12770	12808	**12856.33333**	118.1623177	YP_009195954.1	hypothetical protein
AVU41_gp119	92400	92852	49783	48713	49343	23455	23166	24102	**23574.33333**	479.2747994	YP_009195955.1	hypothetical protein
AVU41_gp120	92839	93447	42706	41351	46882	14966	14627	17034	**15542.33333**	1302.89383	YP_009195956.1	resolvase
AVU41_gp121	93437	93856	20775	20403	16505	10557	10465	8695	**9905.666667**	1049.476695	YP_009195957.1	ribonucleotide reductase flavodoxin
AVU41_gp122	93871	95985	113256	109276	96148	11429	11130	10059	**10872.66667**	720.3404288	YP_009195958.1	ribonucleotide reductase large subunit
AVU41_gp123	95999	97048	56205	55409	47206	11424	11368	9948	**10913.33333**	836.4719561	YP_009195959.1	ribonucleotide reductase small subunit
AVU41_gp124	97066	97395	19006	18752	16105	12292	12241	10799	**11777.33333**	847.6451695	YP_009195960.1	hypothetical protein
AVU41_gp125	97379	97699	23791	22298	21680	15818	14964	14944	**15242**	498.9308569	YP_009195961.1	thioredoxin-like protein
AVU41_gp126	97906	98502	8806	7651	10555	3148	2761	3912	**3273.666667**	585.6998663	YP_009195962.1	hypothetical protein
AVU41_gp127	98512	98817	12562	10494	14275	8762	7388	10322	**8824**	1467.982289	YP_009195963.1	integration host factor
AVU41_gp128	98893	102111	31013	33510	42341	2056	2243	2910	**2403**	448.9198147	YP_009195964.1	DNA polymerase
AVU41_gp129	102181	102423	8199	9380	12466	7201	8316	11351	**8956**	2147.748821	YP_009195965.1	hypothetical protein
AVU41_gp130	102440	102922	15910	18319	23451	7030	8171	10743	**8648**	1901.904046	YP_009195966.1	hypothetical protein
AVU41_gp131	103009	104280	91416	91552	125481	15338	15505	21828	**17557**	3699.736883	YP_009195967.1	hypothetical protein
AVU41_gp132	104340	105596	50955	53327	61353	8652	9139	10800	**9530.333333**	1126.202616	YP_009195968.1	DNA repair protein
AVU41_gp133	105600	105953	12959	14284	15460	7813	8692	9663	**8722.666667**	925.3811827	YP_009195969.1	hypothetical protein
AVU41_gp134	105940	106602	12067	12596	15643	3884	4093	5221	**4399.333333**	719.2164718	YP_009195970.1	sigma factor
AVU41_gp135	106730	107362	31878	29859	22414	10748	10162	7835	**9581.666667**	1540.773291	YP_009195971.1	putative Ig-like protein
AVU41_gp136	107385	107897	33697	30152	24383	14019	12662	10517	**12399.33333**	1765.714114	YP_009195972.1	major tail protein
AVU41_gp137	107912	108139	19923	18041	13344	18649	17046	12950	**16215**	2938.974481	YP_009195973.1	tail protein
AVU41_gp138	108235	108495	663	694	483	542	573	409	**508**	87.12634504	YP_009195974.1	hypothetical protein
AVU41_gp139	108499	109254	3949	4476	3081	1115	1275	902	**1097.333333**	187.1265169	YP_009195975.1	hypothetical protein
AVU41_gp140	109247	110497	23377	27880	23574	3988	4801	4170	**4319.666667**	426.6641927	YP_009195976.1	DNA polymerase
AVU41_gp141	110511	110879	7774	9969	8765	4496	5820	5256	**5190.666667**	664.4135259	YP_009195977.1	hypothetical protein
AVU41_gp142	110866	111177	5423	6820	5991	3710	4709	4249	**4222.666667**	500.0203329	YP_009195978.1	hypothetical protein
AVU41_gp143	111241	111777	9692	11338	10168	3852	4548	4190	**4196.666667**	348.0478894	YP_009195979.1	hypothetical protein
AVU41_gp144	111770	112537	19858	22730	20159	5518	6376	5808	**5900.666667**	436.4416723	YP_009195980.1	hypothetical protein
AVU41_gp145	112515	112961	10472	11957	9676	5000	5762	4790	**5184**	511.456743	YP_009195981.1	hypothetical protein
AVU41_gp146	112961	113824	16185	17832	17363	3998	4446	4447	**4297**	258.9420785	YP_009195982.1	hypothetical protein
AVU41_gp147	114196	114927	18281	20746	19738	5330	6105	5966	**5800.333333**	413.2073733	YP_009195983.1	hypothetical protein
AVU41_gp148	114945	115403	14287	15585	15329	6643	7315	7390	**7116**	411.3429226	YP_009195984.1	hypothetical protein
AVU41_gp149	115468	115911	14866	16965	18288	7146	8231	9114	**8163.666667**	985.7262974	YP_009195985.1	hypothetical protein
AVU41_gp150	115928	116632	26860	26753	31296	8131	8175	9823	**8709.666667**	964.4259087	YP_009195986.1	hypothetical protein
AVU41_gp151	116694	117092	8561	8582	7207	4579	4634	3997	**4403.333333**	352.9678928	YP_009195987.1	hypothetical protein
AVU41_gp152	117239	117481	4192	3925	4341	3682	3480	3953	**3705**	237.3373127	YP_009195988.1	hypothetical protein
AVU41_gp153	117486	118043	10184	9448	10176	3895	3648	4035	**3859.333333**	195.9498235	YP_009195989.1	membrane protein
AVU41_gp154	118079	118255	5309	5072	5458	6402	6173	6823	**6466**	329.6922808	YP_009195990.1	hypothetical protein
AVU41_gp155	118248	118496	5396	4815	5812	4625	4166	5165	**4652**	500.0469978	YP_009195991.1	membrane protein
AVU41_gp156	118489	118722	4678	4008	5022	4267	3690	4749	**4235.333333**	530.2097069	YP_009195992.1	hypothetical protein
AVU41_gp157	118804	119448	857	860	862	284	287	296	**289**	6.244997998	YP_009195993.1	ribulose carboxylase/oxygenase
AVU41_gp158	119464	119712	168	216	248	144	187	220	**183.6666667**	38.10949138	YP_009195994.1	hypothetical protein
AVU41_gp159	119724	119900	383	433	434	462	527	543	**510.6666667**	42.89910644	YP_009195995.1	hypothetical protein
AVU41_gp160	119893	120189	661	723	740	475	524	551	**516.6666667**	38.52704678	YP_009195996.1	hypothetical protein

AVU41_gp161	120237	120419	402	321	462	469	378	559	**468.6666667**	90.5004604	YP_009195997.1	membrane protein
AVU41_gp162	120432	120803	1719	1298	2006	986	752	1193	**977**	220.6377121	YP_009195998.1	hypothetical protein
AVU41_gp163	120816	121163	1336	1008	1562	819	624	993	**812**	184.5995666	YP_009195999.1	hypothetical protein
AVU41_gp164	121169	121441	1052	873	1142	822	689	926	**812.3333333**	118.7953422	YP_009196000.1	membrane protein
AVU41_gp165	121511	121816	1244	1049	1363	868	738	986	**864**	124.0483777	YP_009196001.1	hypothetical protein
AVU41_gp166	121831	122181	2273	1908	2611	1382	1171	1646	**1399.666667**	237.9922968	YP_009196002.1	hypothetical protein
AVU41_gp167	122215	122394	1125	974	1233	1334	1166	1516	**1338.666667**	175.0466604	YP_009196003.1	hypothetical protein
AVU41_gp168	122620	123030	1254	937	1416	651	491	762	**634.6666667**	136.2363143	YP_009196004.1	membrane protein
AVU41_gp169	123032	123256	889	733	1090	843	702	1072	**872.3333333**	186.735999	YP_009196005.1	hypothetical protein
AVU41_gp170	123269	123469	990	745	1013	1051	798	1115	**988**	167.6275634	YP_009196006.1	hypothetical protein
AVU41_gp171	123470	123760	1035	747	1120	759	553	852	**721.3333333**	153.0174282	YP_009196007.1	membrane protein
AVU41_gp172	123853	124146	2285	1561	2555	1659	1144	1923	**1575.333333**	396.1821971	YP_009196008.1	hypothetical protein
AVU41_gp173	124143	125051	6566	4684	8461	1542	1110	2060	**1570.666667**	475.6483295	YP_009196009.1	phosphoribosyl pyrophosphate synthetase
AVU41_gp174	125069	126538	18849	12563	23224	2737	1841	3496	**2691.333333**	828.4445264	YP_009196010.1	nicotinamide phosphoribosyltransferase
AVU41_gp175	126629	126940	655	416	748	448	287	530	**421.6666667**	123.6217349	YP_009196011.1	hypothetical protein
AVU41_gp176	126957	127190	522	273	547	476	251	517	**414.6666667**	143.2142917	YP_009196012.1	hypothetical protein
AVU41_gp177	127270	127464	372	193	305	407	213	346	**322**	99.2018145	YP_009196013.1	hypothetical protein
AVU41_gp178	127478	127801	1120	650	1217	738	432	831	**667**	208.7606285	YP_009196014.1	hypothetical protein
AVU41_gp179	127814	128176	1234	743	1066	726	441	650	**605.6666667**	147.5816158	YP_009196015.1	hypothetical protein
AVU41_gp180	128176	128415	755	451	676	671	405	623	**566.3333333**	141.7650639	YP_009196016.1	hypothetical protein
AVU41_gp181	128488	128898	1495	1004	1615	776	526	869	**723.6666667**	177.387523	YP_009196017.1	hypothetical protein
AVU41_gp182	128903	129157	1092	798	1169	914	674	1014	**867.3333333**	174.737899	YP_009196018.1	hypothetical protein
AVU41_gp183	129261	129659	2499	1612	2972	1337	870	1648	**1285**	391.5980082	YP_009196019.1	hypothetical protein
AVU41_gp184	129673	130101	4533	2591	5340	2255	1301	2754	**2103.333333**	738.2779513	YP_009196020.1	hypothetical protein
AVU41_gp185	130103	130378	2635	1528	3089	2038	1193	2476	**1902.333333**	652.1704787	YP_009196021.1	hypothetical protein
AVU41_gp186	130392	130781	2403	1367	3060	1315	755	1736	**1268.666667**	492.1385306	YP_009196022.1	hypothetical protein
AVU41_gp187	130897	131523	10770	5699	12327	3666	1958	4350	**3324.666667**	1231.989177	YP_009196023.1	hypothetical protein
AVU41_gp188	131604	131720	196	124	201	358	228	380	**322**	82.14621111	YP_009196024.1	hypothetical protein
AVU41_gp189	131734	132135	884	622	1151	469	333	634	**478.6666667**	150.7326552	YP_009196025.1	hypothetical protein
AVU41_gp190	132167	132376	535	400	660	544	410	695	**549.6666667**	142.5844779	YP_009196026.1	hypothetical protein
AVU41_gp191	132376	132732	677	588	853	405	355	529	**429.6666667**	89.5842248	YP_009196027.1	hypothetical protein
AVU41_gp192	133332	133631	814	659	960	579	473	708	**586.6666667**	117.6874391	YP_009196028.1	TreA
AVU41_gp193	133647	133832	505	389	549	579	451	653	**561**	102.1958903	YP_009196029.1	TreB
AVU41_gp194	133939	134226	1328	1065	1377	984	797	1058	**946.3333333**	134.5151788	YP_009196030.1	TreC
AVU41_gp195	134226	134552	1627	1199	1726	1062	790	1168	**1006.666667**	194.9803409	YP_009196031.1	TreE
AVU41_gp196	134567	134860	803	545	828	583	399	623	**535**	119.4654762	YP_009196032.1	TreE
AVU41_gp197	134864	135049	262	156	265	301	181	315	**265.6666667**	73.65686209	YP_009196033.1	TreF
AVU41_gp198	135186	135479	570	369	598	414	270	450	**378**	95.2470472	YP_009196034.1	TreE
AVU41_gp199	135483	135740	849	567	874	702	473	750	**641.6666667**	148.0281505	YP_009196035.1	TreF
AVU41_gp200	135828	136067	1265	932	1389	1125	837	1281	**1081**	225.2465316	YP_009196036.1	hypothetical protein
AVU41_gp201	136078	136425	961	695	967	589	430	615	**544.6666667**	100.1515518	YP_009196037.1	hypothetical protein
AVU41_gp202	136630	136968	124	90	129	78	57	84	**73**	14.17744688	YP_009196038.1	hypothetical protein
AVU41_gp203	137279	137587	723	608	635	499	424	455	**459.3333333**	37.68730998	YP_009196039.1	TreJ
AVU41_gp204	137793	138077	1200	1044	1143	899	789	887	**858.3333333**	60.3434614	YP_009196040.1	hypothetical protein
AVU41_gp205	138152	138343	55	43	33	61	48	38	**49**	11.53256259	YP_009196041.1	hypothetical protein
AVU41_gp206	138843	139325	1159	1344	1542	512	599	706	**605.6666667**	97.1716694	YP_009196042.1	HNH homing endonuclease
AVU41_gp207	139493	139651	27	23	23	36	31	32	**33**	2.645751311	YP_009196043.1	TreN
AVU41_gp208	139724	139870	94	84	83	136	123	125	**128**	7	YP_009196044.1	hypothetical protein
AVU41_gp209	140036	140359	1470	1070	1477	968	711	1009	**896**	161.5208965	YP_009196045.1	TreP
AVU41_gp210	140445	140840	2216	1589	2761	1194	864	1543	**1200.333333**	339.5443025	YP_009196046.1	hypothetical protein
AVU41_gp211	141309	141530	1455	708	1361	1399	687	1357	**1147.666667**	399.5013559	YP_009196047.1	hypothetical protein
AVU41_gp212	141789	141953	1891	1127	1640	2446	1471	2199	**2038.666667**	506.8888767	YP_009196048.1	hypothetical protein
AVU41_gp213	142033	142269	1734	1037	1848	1562	943	1725	**1410**	412.5639344	YP_009196049.1	hypothetical protein

Table S2. Full list of genes dysregulated in biofilms treated with subinhibitory doses of phiIPLA-RODI compared to untreated biofilms according to RNA-seq

Gene ID	Gene name	Gene product	Fold-change	padj
SAOUHSC_00003	SAOUHSC_00003	Putative uncharacterized protein	-2.66	1.04E-06
SAOUHSC_00004	recF	DNA replication and repair protein RecF	-2.47	1.08E-07
SAOUHSC_00005	gyrB	DNA gyrase subunit B	-2.89	1.77E-13
SAOUHSC_00006	gyrA	DNA gyrase subunit A	-3.92	6.47E-19
SAOUHSC_00008	hutH	Histidine ammonia-lyase	-2.23	9.86E-10
SAOUHSC_00010	SAOUHSC_00010	Putative uncharacterized protein	2.03	7.94E-04
SAOUHSC_00012	SAOUHSC_00012	Putative uncharacterized protein	2.10	2.57E-03
SAOUHSC_00021	walK	Sensor protein kinase WalK	-3.80	1.15E-28
SAOUHSC_00022	SAOUHSC_00022	Putative uncharacterized protein	-5.44	3.28E-37
SAOUHSC_00023	SAOUHSC_00023	Putative uncharacterized protein	-5.48	3.85E-40
SAOUHSC_00027	rlmH	Ribosomal RNA large subunit methyltransferase H	-2.15	3.76E-08
SAOUHSC_00036	SAOUHSC_00036	Putative uncharacterized protein	-2.19	3.48E-05
SAOUHSC_00057	SAOUHSC_00057	Putative uncharacterized protein	-4.02	3.53E-22
SAOUHSC_00058	SAOUHSC_00058	Putative uncharacterized protein	-4.03	7.96E-21
SAOUHSC_00060	SAOUHSC_00060	Putative uncharacterized protein	3.26	8.01E-10
SAOUHSC_00061	SAOUHSC_00061	Putative uncharacterized protein	-2.89	2.06E-16
SAOUHSC_00074	SAOUHSC_00074	Periplasmic binding protein, putative	4.80	5.34E-04
SAOUHSC_00081	SAOUHSC_00081	Putative uncharacterized protein	-3.00	2.33E-11
SAOUHSC_00082	SAOUHSC_00082	Putative uncharacterized protein	-2.69	2.69E-14
SAOUHSC_00083	SAOUHSC_00083	Putative uncharacterized protein	-2.29	5.67E-11
SAOUHSC_00085	SAOUHSC_00085	Putative uncharacterized protein	2.93	8.68E-10
SAOUHSC_00086	SAOUHSC_00086	3-ketoacyl-acyl carrier protein reductase, putative	-10.40	6.84E-35
SAOUHSC_00094	SAOUHSC_00094	Uncharacterized protein SAOUHSC_00094	-16.68	1.82E-33
SAOUHSC_00097			-2.62	1.40E-04
SAOUHSC_00100			-3.72	1.79E-19
SAOUHSC_00101	deoB	Phosphopentomutase	-8.81	3.25E-41
SAOUHSC_00102	SAOUHSC_00102	Phosphonates ABC transporter, permease protein CC0363, put	-2.08	1.39E-05
SAOUHSC_00103	SAOUHSC_00103	Phosphonates ABC transporter, permease protein CC0363, put	-2.00	6.68E-04
SAOUHSC_00104	phnC	Phosphonates import ATP-binding protein PhnC	-2.41	1.89E-05
SAOUHSC_00106	SAOUHSC_00106	Putative uncharacterized protein	4.17	8.38E-09
SAOUHSC_00114	SAOUHSC_00114	Capsular polysaccharide biosynthesis protein, putative	2.29	1.30E-03
SAOUHSC_00121	SAOUHSC_00121	Capsular polysaccharide synthesis enzyme O-acetyl transferase	2.03	2.43E-03
SAOUHSC_00129	SAOUHSC_00129	UDP-N-acetylglucosamine 2-epimerase	-2.34	1.34E-13
SAOUHSC_00134	SAOUHSC_00134	Putative uncharacterized protein	2.34	6.24E-03
SAOUHSC_00142	SAOUHSC_00142	Formate dehydrogenase, NAD-dependent, putative	-7.47	2.44E-21
SAOUHSC_00158	SAOUHSC_00158	PTS system EIIBC component SAOUHSC_00158	-2.34	2.87E-04
SAOUHSC_00160	SAOUHSC_00160	Putative uncharacterized protein	-2.11	2.50E-03
SAOUHSC_00162	SAOUHSC_00162	Type I site-specific deoxyribonuclease, HsdR family, putative	2.39	6.56E-13
SAOUHSC_00163	SAOUHSC_00163	Putative uncharacterized protein	-2.14	1.31E-05
SAOUHSC_00171	SAOUHSC_00171	Gamma-glutamyltranspeptidase, putative	-2.65	1.12E-11
SAOUHSC_00173	azoR	FMN-dependent NADH-azoreductase	-3.42	5.36E-16
SAOUHSC_00178	SAOUHSC_00178	Maltose ABC transporter, permease protein	-2.67	1.10E-05
SAOUHSC_00179	SAOUHSC_00179	Putative uncharacterized protein	-2.76	2.12E-07
SAOUHSC_00180	SAOUHSC_00180	Putative uncharacterized protein	-2.45	3.67E-09
SAOUHSC_00181	SAOUHSC_00181	Putative uncharacterized protein	-3.03	2.25E-10
SAOUHSC_00185	SAOUHSC_00185	Uncharacterized sensor-like histidine kinase SAOUHSC_00185	3.20	1.13E-07
SAOUHSC_00186	SAOUHSC_00186	Lipoprotein, putative	2.46	1.51E-06
SAOUHSC_00187	pflB	Formate acetyltransferase	-4.57	3.18E-26
SAOUHSC_00188	pflA	Pyruvate formate-lyase-activating enzyme	-5.52	2.45E-50
SAOUHSC_00189	SAOUHSC_00189	Putative uncharacterized protein	-3.08	9.56E-13
SAOUHSC_00195	SAOUHSC_00195	Acetyl-CoA acetyltransferase, putative	-2.72	7.58E-06
SAOUHSC_00201	SAOUHSC_00201	Putative uncharacterized protein	-2.14	1.78E-13
SAOUHSC_00202	SAOUHSC_00202	Putative uncharacterized protein	3.53	2.78E-22
SAOUHSC_00203	SAOUHSC_00203	Putative uncharacterized protein	2.20	1.15E-07
SAOUHSC_00204	SAOUHSC_00204	Globin domain protein	2.52	6.01E-28
SAOUHSC_00216	SAOUHSC_00216	PTS system component	-2.24	4.42E-07
SAOUHSC_00217	SAOUHSC_00217	Sorbitol dehydrogenase, putative	-2.62	2.75E-07
SAOUHSC_00218	SAOUHSC_00218	Putative uncharacterized protein	-3.02	1.23E-05
SAOUHSC_00219	SAOUHSC_00219	Putative uncharacterized protein	-3.44	5.04E-15
SAOUHSC_00220	SAOUHSC_00220	Putative uncharacterized protein	3.10	7.97E-10
SAOUHSC_00221	SAOUHSC_00221	Alcohol dehydrogenase, zinc-containing	2.09	8.18E-07
SAOUHSC_00222	SAOUHSC_00222	TagB protein, putative	3.48	1.14E-13
SAOUHSC_00231	lytR	Sensory transduction protein LytR	3.14	2.16E-14
SAOUHSC_00234	SAOUHSC_00234	Putative uncharacterized protein	-2.25	7.25E-17
SAOUHSC_00242	SAOUHSC_00242	Putative uncharacterized protein	-2.58	3.56E-11
SAOUHSC_00247	SAOUHSC_00247	Putative uncharacterized protein	-3.77	1.24E-22
SAOUHSC_00249	SAOUHSC_00249	Putative uncharacterized protein	2.15	3.65E-04
SAOUHSC_00250	SAOUHSC_00250	Putative uncharacterized protein	2.41	2.61E-05
SAOUHSC_00251	SAOUHSC_00251	Putative uncharacterized protein	3.86	1.74E-16
SAOUHSC_00253	SAOUHSC_00253	Putative uncharacterized protein	3.43	3.91E-26
SAOUHSC_00260	SAOUHSC_00260	Putative uncharacterized protein	3.35	4.32E-05
SAOUHSC_00261	SAOUHSC_00261	Putative uncharacterized protein	2.40	5.01E-06
SAOUHSC_00282	SAOUHSC_00282	Branched-chain amino acid transport system II carrier protein	6.01	4.13E-14
SAOUHSC_00284	SAOUHSC_00284	5'-nucleotidase, lipoprotein e(P4) family	4.72	2.26E-14
SAOUHSC_00289	SAOUHSC_00289	Putative uncharacterized protein	4.48	2.56E-04
SAOUHSC_00293	SAOUHSC_00293	Putative uncharacterized protein	-3.47	4.31E-05
SAOUHSC_00297	SAOUHSC_00297	Putative uncharacterized protein	3.34	4.75E-07
SAOUHSC_00302	SAOUHSC_00302	Putative uncharacterized protein	3.39	2.96E-07
SAOUHSC_00316	SAOUHSC_00316	Putative uncharacterized protein	4.09	7.04E-07
SAOUHSC_00319	SAOUHSC_00319	Putative uncharacterized protein	-2.87	7.08E-20
SAOUHSC_00320	SAOUHSC_00320	NADPH-dependent FMN reductase, putative	-4.02	1.51E-35
SAOUHSC_00325	SAOUHSC_00325	Efem/EfeO family lipoprotein	-2.43	1.18E-03
SAOUHSC_00326	SAOUHSC_00326	Putative uncharacterized protein	-2.54	1.51E-06
SAOUHSC_00327	SAOUHSC_00327	Putative uncharacterized protein	-2.35	1.08E-06

SAOUHSC_00328	tatC	Sec-independent protein translocase protein TatC	2.67	5.87E-08
SAOUHSC_00330	SAOUHSC_00330	Putative uncharacterized protein	8.48	1.17E-11
SAOUHSC_00331	SAOUHSC_00331	Putative uncharacterized protein	-3.01	7.86E-05
SAOUHSC_00332	SAOUHSC_00332	Putative uncharacterized protein	-6.06	1.29E-30
SAOUHSC_00333	SAOUHSC_00333	ABC transporter, ATP-binding protein, putative	-6.62	4.59E-47
SAOUHSC_00334	SAOUHSC_00334	Putative uncharacterized protein	-6.55	1.08E-44
SAOUHSC_00335	SAOUHSC_00335	Putative uncharacterized protein	7.83	8.67E-12
SAOUHSC_00336	SAOUHSC_00336	Probable acetyl-CoA acyltransferase	-2.77	5.35E-22
SAOUHSC_00344	SAOUHSC_00344	Putative uncharacterized protein	-2.07	9.41E-07
SAOUHSC_00346	ychF	Ribosome-binding ATPase YchF	-2.44	3.07E-11
SAOUHSC_00347	SAOUHSC_00347	Putative uncharacterized protein	-2.84	1.21E-10
SAOUHSC_00349	SAOUHSC_00349	Single-stranded DNA-binding protein	-2.67	2.49E-18
SAOUHSC_00350	rpsR	30S ribosomal protein S18	-2.69	2.34E-18
SAOUHSC_00357	SAOUHSC_00357	Putative uncharacterized protein	2.15	2.20E-04
SAOUHSC_00359	SAOUHSC_00359	Phosphoglycerate mutase family protein	2.18	5.63E-08
SAOUHSC_00360	SAOUHSC_00360	Putative uncharacterized protein	2.01	6.68E-06
SAOUHSC_00363	SAOUHSC_00363	Putative uncharacterized protein	2.62	6.15E-06
SAOUHSC_00364	ahpF	Alkyl hydroperoxide reductase subunit F	-3.86	4.38E-21
SAOUHSC_00371	SAOUHSC_00371	Putative uncharacterized protein	-3.04	1.70E-15
SAOUHSC_00372	xpt	Xanthine phosphoribosyltransferase	8.25	3.11E-34
SAOUHSC_00373	SAOUHSC_00373	Xanthine permease, putative	5.23	7.80E-31
SAOUHSC_00381	SAOUHSC_00381	Putative uncharacterized protein	-2.44	3.75E-10
SAOUHSC_00397	SAOUHSC_00397	Type I restriction-modification system, M subunit	2.58	2.15E-12
SAOUHSC_00398	SAOUHSC_00398	Restriction modification system specificity subunit, putative	4.07	2.14E-22
SAOUHSC_00406	SAOUHSC_00406	Putative uncharacterized protein	2.78	3.62E-05
SAOUHSC_00407	SAOUHSC_00407	Putative uncharacterized protein	4.20	1.31E-07
SAOUHSC_00409	SAOUHSC_00409	Putative uncharacterized protein	-4.81	8.51E-20
SAOUHSC_00410	SAOUHSC_00410	Putative uncharacterized protein	-2.04	1.67E-05
SAOUHSC_00411	SAOUHSC_00411	Putative uncharacterized protein	-23.42	6.39E-22
SAOUHSC_00413	SAOUHSC_00413	UPF0753 protein SAOUHSC_00413	-3.05	9.59E-09
SAOUHSC_00414	SAOUHSC_00414	Putative uncharacterized protein	-2.74	7.44E-08
SAOUHSC_00417	SAOUHSC_00417	Putative uncharacterized protein	-2.21	3.13E-14
SAOUHSC_00424	SAOUHSC_00424	ABC transporter, permease protein, putative	-3.15	2.47E-04
SAOUHSC_00426	SAOUHSC_00426	Lipoprotein	-2.71	3.36E-06
SAOUHSC_00427	sle1	N-acetylmuramoyl-L-alanine amidase sle1	10.27	1.78E-100
SAOUHSC_00429	SAOUHSC_00429	MutT/nudix family protein, putative	-2.01	2.00E-04
SAOUHSC_00430	SAOUHSC_00430	Putative uncharacterized protein	-3.25	4.39E-14
SAOUHSC_00431	SAOUHSC_00431	Putative uncharacterized protein	2.70	4.57E-07
SAOUHSC_00433	SAOUHSC_00433	Putative uncharacterized protein	4.34	3.53E-20
SAOUHSC_00434	SAOUHSC_00434	Transcriptional regulator, lysR family, putative	2.43	1.34E-05
SAOUHSC_00437	SAOUHSC_00437	Putative uncharacterized protein	-6.65	1.26E-20
SAOUHSC_00438	SAOUHSC_00438	Alpha amylase family protein, putative	-5.06	2.93E-14
SAOUHSC_00439	SAOUHSC_00439	Putative uncharacterized protein	-4.40	8.15E-16
SAOUHSC_00440	SAOUHSC_00440	Putative uncharacterized protein	-9.37	3.96E-36
SAOUHSC_00450	SAOUHSC_00450	Orn/Lys/Arg decarboxylase, putative	2.55	3.97E-11
SAOUHSC_00451	tmk	Thymidylate kinase	2.56	3.72E-13
SAOUHSC_00455	SAOUHSC_00455	Putative uncharacterized protein	-2.22	1.38E-14
SAOUHSC_00456	SAOUHSC_00456	Putative uncharacterized protein	-3.48	3.54E-23
SAOUHSC_00457	SAOUHSC_00457	Putative uncharacterized protein	-3.15	4.12E-24
SAOUHSC_00458	SAOUHSC_00458	UPF0213 protein SAOUHSC_00458	-2.59	8.31E-13
SAOUHSC_00459	rsmI	Ribosomal RNA small subunit methyltransferase I	-2.75	2.27E-10
SAOUHSC_00461	metG	Methionine--tRNA ligase	-3.00	2.86E-19
SAOUHSC_00462	SAOUHSC_00462	Putative uncharacterized protein	-3.96	1.34E-28
SAOUHSC_00468	SAOUHSC_00468	Putative uncharacterized protein	-2.97	3.81E-11
SAOUHSC_00469	spoVG	Putative septation protein SpoVG	-2.71	4.22E-12
SAOUHSC_00471	glmU	Bifunctional protein GlmU	-2.73	1.28E-10
SAOUHSC_00472	prs	Ribose-phosphate pyrophosphokinase	-2.22	1.20E-12
SAOUHSC_00473	SAOUHSC_00473	Putative uncharacterized protein	-2.18	7.81E-13
SAOUHSC_00474	rplY	50S ribosomal protein L25	-2.06	2.24E-12
SAOUHSC_00479	SAOUHSC_00479	Putative uncharacterized protein	-2.03	4.17E-11
SAOUHSC_00482	SAOUHSC_00482	Putative uncharacterized protein	-2.52	9.79E-11
SAOUHSC_00484	tilS	tRNA(Ile)-lysidine synthase	2.13	9.47E-10
SAOUHSC_00485	SAOUHSC_00485	Hypoxanthine phosphoribosyltransferase	2.00	5.39E-05
SAOUHSC_00489	SAOUHSC_00489	Dihydropteroate synthase	-2.52	1.03E-15
SAOUHSC_00490	SAOUHSC_00490	Dihydroneopterin aldolase	-2.82	5.54E-13
SAOUHSC_00491	SAOUHSC_00491	2-amino-4-hydroxy-6-hydroxymethyldihydropteridine pyrophos	-3.28	1.61E-23
SAOUHSC_00493	lysS	Lysine--tRNA ligase	-3.26	1.22E-20
SAOUHSC_00500	pdxT	Glutamine amidotransferase subunit PdxT	-2.03	2.66E-06
SAOUHSC_00502	ctsR	Transcriptional regulator CtsR	-7.24	7.02E-22
SAOUHSC_00503	SAOUHSC_00503	UvrB/uvrC motif domain protein	-9.09	4.61E-27
SAOUHSC_00504	SAOUHSC_00504	Putative ATP:guanido phosphotransferase SAOUHSC_00504	-10.59	7.91E-32
SAOUHSC_00505	clpC	ATP-dependent Clp protease ATP-binding subunit ClpC	-22.97	1.00E-52
SAOUHSC_00506	SAOUHSC_00506	Putative uncharacterized protein	-23.28	1.17E-58
SAOUHSC_00515	SAOUHSC_00515	Putative uncharacterized protein	2.51	4.36E-16
SAOUHSC_00516	secE	Protein translocase subunit SecE	2.42	2.06E-16
SAOUHSC_00517	nusG	Transcription termination/antitermination protein NusG	2.13	4.22E-15
SAOUHSC_00524	rpoB	DNA-directed RNA polymerase subunit beta	-2.92	2.05E-18
SAOUHSC_00525	rpoC	DNA-directed RNA polymerase subunit beta'	-5.03	2.50E-35
SAOUHSC_00528	rpsG	30S ribosomal protein S7	-2.07	1.17E-09
SAOUHSC_00529	fusA	Elongation factor G	-2.56	1.46E-16
SAOUHSC_00531	SAOUHSC_00531	Putative uncharacterized protein	2.27	6.05E-11
SAOUHSC_00533	hchA	Molecular chaperone Hsp31 and glyoxalase 3	3.07	1.39E-11
SAOUHSC_00538	SAOUHSC_00538	Haloacid dehalogenase-like hydrolase, putative	2.95	2.00E-18
SAOUHSC_00539	SAOUHSC_00539	Putative uncharacterized protein	3.58	3.34E-13
SAOUHSC_00540	SAOUHSC_00540	Putative uncharacterized protein	4.36	6.71E-06
SAOUHSC_00544	sdrC	Serine-aspartate repeat-containing protein C	-3.90	6.13E-21

SAOUHSC_00545	sdrD	Serine-aspartate repeat-containing protein D	-5.59	4.67E-22
SAOUHSC_00550	SAOUHSC_00550	Putative uncharacterized protein	2.86	1.77E-22
SAOUHSC_00551	SAOUHSC_00551	Putative uncharacterized protein	4.85	2.97E-31
SAOUHSC_00552	nagB	Glucosamine-6-phosphate deaminase	-2.15	1.58E-06
SAOUHSC_00556	SAOUHSC_00556	Proline/betaine transporter, putative	3.42	1.39E-15
SAOUHSC_00557	SAOUHSC_00557	Putative uncharacterized protein	3.61	9.95E-06
SAOUHSC_00559	SAOUHSC_00559	Putative uncharacterized protein	-2.91	7.70E-07
SAOUHSC_00560	SAOUHSC_00560	Putative uncharacterized protein	-4.22	4.90E-13
SAOUHSC_00561	SAOUHSC_00561	Putative uncharacterized protein	-8.57	1.14E-40
SAOUHSC_00562	SAOUHSC_00562	Phosphomethylpyrimidine kinase	2.37	4.59E-17
SAOUHSC_00564	ung	Uracil-DNA glycosylase	3.34	8.45E-15
SAOUHSC_00565	SAOUHSC_00565	Putative uncharacterized protein	3.18	5.18E-11
SAOUHSC_00569	SAOUHSC_00569	Putative uncharacterized protein	3.76	6.54E-07
SAOUHSC_00571	SAOUHSC_00571	Putative uncharacterized protein	2.12	3.96E-04
SAOUHSC_00572	SAOUHSC_00572	Putative uncharacterized protein	2.36	1.28E-05
SAOUHSC_00573	SAOUHSC_00573	Putative heme-dependent peroxidase SAOUHSC_00573	2.90	5.53E-19
SAOUHSC_00577	SAOUHSC_00577	Mevalonate kinase, putative	-2.47	1.18E-12
SAOUHSC_00578	SAOUHSC_00578	Diphosphomevalonate decarboxylase	-3.65	3.17E-20
SAOUHSC_00579	SAOUHSC_00579	Phosphomevalonate kinase	-4.77	7.94E-28
SAOUHSC_00580	SAOUHSC_00580	UPF0741 protein SAOUHSC_00580	-4.22	1.09E-33
SAOUHSC_00585	SAOUHSC_00585	Putative uncharacterized protein	2.69	3.17E-03
SAOUHSC_00586	SAOUHSC_00586	Putative uncharacterized protein	2.60	1.21E-05
SAOUHSC_00587	SAOUHSC_00587	Putative uncharacterized protein	2.02	6.94E-05
SAOUHSC_00588	SAOUHSC_00588	Putative uncharacterized protein	2.98	4.74E-05
SAOUHSC_00589	SAOUHSC_00589	Putative uncharacterized protein	3.86	9.61E-04
SAOUHSC_00591	SAOUHSC_00591	Putative uncharacterized protein	3.67	1.76E-05
SAOUHSC_00592	SAOUHSC_00592	Putative uncharacterized protein	3.43	1.95E-03
SAOUHSC_00596	SAOUHSC_00596	Putative uncharacterized protein	3.52	2.13E-03
SAOUHSC_00603	SAOUHSC_00603	Putative uncharacterized protein	-3.07	2.91E-28
SAOUHSC_00604	SAOUHSC_00604	Putative uncharacterized protein	-2.67	2.07E-23
SAOUHSC_00605	SAOUHSC_00605	Putative uncharacterized protein	3.13	5.29E-11
SAOUHSC_00608	adh	Alcohol dehydrogenase	-6.51	3.30E-40
SAOUHSC_00609	SAOUHSC_00609	Putative uncharacterized protein	-5.30	1.67E-22
SAOUHSC_00610	SAOUHSC_00610	Putative uncharacterized protein	2.65	2.89E-12
SAOUHSC_00611	argS	Arginine--tRNA ligase	2.00	5.76E-12
SAOUHSC_00613	SAOUHSC_00613	Iron compound ABC transporter, substrate-binding protein, put	3.14	4.44E-11
SAOUHSC_00617	SAOUHSC_00617	Putative uncharacterized protein	-5.04	4.56E-15
SAOUHSC_00619	SAOUHSC_00619	Putative uncharacterized protein	-8.10	1.26E-51
SAOUHSC_00624	SAOUHSC_00624	Integrase/recombinase, putative	5.92	1.84E-03
SAOUHSC_00625	mnhA2	Putative antiporter subunit mnhA2	3.98	4.62E-03
SAOUHSC_00626	mnhB2	Putative antiporter subunit mnhB2	4.40	1.18E-05
SAOUHSC_00627	mnhC2	Putative antiporter subunit mnhC2	2.99	8.80E-03
SAOUHSC_00640	SAOUHSC_00640	Putative uncharacterized protein	4.36	2.47E-22
SAOUHSC_00641	tagH	Teichoic acids export ATP-binding protein TagH	-2.09	8.94E-12
SAOUHSC_00646	SAOUHSC_00646	Penicillin-binding protein 4, putative	2.65	3.08E-06
SAOUHSC_00647	SAOUHSC_00647	Putative uncharacterized protein	-2.20	1.02E-09
SAOUHSC_00648	SAOUHSC_00648	Putative uncharacterized protein	-3.53	1.68E-27
SAOUHSC_00651	SAOUHSC_00651	Putative uncharacterized protein	-2.83	5.52E-09
SAOUHSC_00655	SAOUHSC_00655	Putative uncharacterized protein	-2.65	1.63E-12
SAOUHSC_00656	SAOUHSC_00656	Putative uncharacterized protein	-3.67	1.41E-18
SAOUHSC_00658	SAOUHSC_00658	Putative uncharacterized protein	-4.75	1.62E-29
SAOUHSC_00661	SAOUHSC_00661	Putative uncharacterized protein	4.71	1.88E-11
SAOUHSC_00663	SAOUHSC_00663	Putative uncharacterized protein	3.20	1.77E-25
SAOUHSC_00667	SAOUHSC_00667	ABC transporter ATP-binding protein, putative	2.57	1.04E-14
SAOUHSC_00668	SAOUHSC_00668	ABC transporter permease, putative	2.77	7.13E-11
SAOUHSC_00671	SAOUHSC_00671	Secretory antigen SsaA-like protein	9.36	5.45E-82
SAOUHSC_00672	SAOUHSC_00672	Putative uncharacterized protein	2.57	5.58E-07
SAOUHSC_00673	SAOUHSC_00673	Putative uncharacterized protein	3.79	5.96E-08
SAOUHSC_00683	SAOUHSC_00683	Putative uncharacterized protein	4.44	1.76E-11
SAOUHSC_00685	SAOUHSC_00685	Putative uncharacterized protein	4.50	3.70E-17
SAOUHSC_00686	SAOUHSC_00686	Putative uncharacterized protein	3.46	7.18E-10
SAOUHSC_00687	SAOUHSC_00687	Putative uncharacterized protein	3.60	7.11E-09
SAOUHSC_00690	SAOUHSC_00690	Putative uncharacterized protein	3.09	9.99E-09
SAOUHSC_00691	uppP	Undecaprenyl-diphosphatase	2.04	1.96E-07
SAOUHSC_00693	SAOUHSC_00693	Putative uncharacterized protein	-2.76	1.65E-11
SAOUHSC_00696	SAOUHSC_00696	Putative uncharacterized protein	2.75	8.49E-18
SAOUHSC_00697	SAOUHSC_00697	Putative uncharacterized protein	2.87	4.29E-10
SAOUHSC_00698	SAOUHSC_00698	Putative uncharacterized protein	-3.65	1.06E-32
SAOUHSC_00699	SAOUHSC_00699	Deoxyribodipyrimidine photolyase, putative	-3.27	9.51E-26
SAOUHSC_00701	SAOUHSC_00701	Putative uncharacterized protein	2.45	5.44E-06
SAOUHSC_00704	SAOUHSC_00704	Putative uncharacterized protein	12.44	2.70E-39
SAOUHSC_00706	SAOUHSC_00706	Putative uncharacterized protein	-4.52	9.66E-19
SAOUHSC_00707	SAOUHSC_00707	Tagatose-6-phosphate kinase	-5.98	1.50E-28
SAOUHSC_00708	SAOUHSC_00708	Fructose specific permease, putative	-6.17	1.15E-33
SAOUHSC_00709	SAOUHSC_00709	Putative uncharacterized protein	-6.11	2.25E-20
SAOUHSC_00710	SAOUHSC_00710	N-acetylglucosamine-6-phosphate deacetylase	3.32	3.82E-26
SAOUHSC_00711	SAOUHSC_00711	Putative uncharacterized protein	3.43	5.08E-30
SAOUHSC_00729	SAOUHSC_00729	ABC transporter, ATP-binding protein	3.17	1.41E-26
SAOUHSC_00731	SAOUHSC_00731	ABC transporter domain protein	3.08	8.41E-20
SAOUHSC_00732	SAOUHSC_00732	Amino acid ABC transporter, permease protein, putative	2.12	2.88E-13
SAOUHSC_00733	hisC	Histidinol-phosphate aminotransferase	3.53	8.89E-25
SAOUHSC_00738	SAOUHSC_00738	Putative uncharacterized protein	10.46	4.57E-42
SAOUHSC_00743	SAOUHSC_00743	Ribonucleotide-disphosphate reductase beta chain, putative	3.32	3.38E-23
SAOUHSC_00744	SAOUHSC_00744	Putative uncharacterized protein	3.78	1.74E-05
SAOUHSC_00746	SAOUHSC_00746	Putative uncharacterized protein	2.70	3.37E-04
SAOUHSC_00753	SAOUHSC_00753	Putative uncharacterized protein	3.03	7.42E-08

SAOUHSC_00756	SAOUHSC_00756	Putative uncharacterized protein	-3.27	4.03E-19
SAOUHSC_00762	SAOUHSC_00762	Putative uncharacterized protein	2.03	7.67E-07
SAOUHSC_00763	SAOUHSC_00763	Putative uncharacterized protein	2.36	9.62E-11
SAOUHSC_00767	SAOUHSC_00767	Uncharacterized protein SAOUHSC_00767	-4.04	2.17E-19
SAOUHSC_00770	SAOUHSC_00770	Putative uncharacterized protein	-2.09	7.94E-06
SAOUHSC_00774	SAOUHSC_00774	Putative uncharacterized protein	2.00	2.68E-03
SAOUHSC_00775	SAOUHSC_00775	Putative uncharacterized protein	2.94	1.21E-04
SAOUHSC_00780	uvrA	UvrABC system protein A	-2.07	3.89E-06
SAOUHSC_00781	hprK	HPr kinase/phosphorylase	2.37	9.76E-17
SAOUHSC_00782	lgt	Prolipoprotein diacylglyceryl transferase	2.53	3.43E-18
SAOUHSC_00784	SAOUHSC_00784	Putative uncharacterized protein	-2.30	9.20E-14
SAOUHSC_00786	SAOUHSC_00786	Putative uncharacterized protein	-2.47	7.61E-08
SAOUHSC_00789	whiA	Putative sporulation transcription regulator WhiA	-2.75	7.89E-21
SAOUHSC_00793	SAOUHSC_00793	Putative uncharacterized protein	2.50	1.93E-10
SAOUHSC_00795	SAOUHSC_00795	Glyceraldehyde-3-phosphate dehydrogenase, type I	-6.94	3.47E-38
SAOUHSC_00796	pgk	Phosphoglycerate kinase	-2.90	1.58E-19
SAOUHSC_00797	tpiA	Triosephosphate isomerase	-3.32	1.27E-19
SAOUHSC_00798	gpmI	2,3-bisphosphoglycerate-independent phosphoglycerate mutas	-3.49	1.16E-22
SAOUHSC_00799	eno	Enolase	-4.31	6.68E-30
SAOUHSC_00802	SAOUHSC_00802	Carboxylesterase, putative	-2.11	5.28E-09
SAOUHSC_00803	rnr	Ribonuclease R	-2.98	7.80E-15
SAOUHSC_00804	smpB	SsrA-binding protein	-3.12	3.94E-13
SAOUHSC_00818	SAOUHSC_00818	Thermonuclease	5.72	7.07E-08
SAOUHSC_00820	SAOUHSC_00820	Putative uncharacterized protein	3.91	1.17E-05
SAOUHSC_00821	SAOUHSC_00821	Putative uncharacterized protein	4.84	1.49E-06
SAOUHSC_00822	SAOUHSC_00822	Putative uncharacterized protein	3.67	7.88E-06
SAOUHSC_00823	SAOUHSC_00823	Putative uncharacterized protein	-5.53	1.14E-12
SAOUHSC_00824	SAOUHSC_00824	Putative uncharacterized protein	-2.54	5.48E-07
SAOUHSC_00828	SAOUHSC_00828	Putative uncharacterized protein	2.60	7.60E-04
SAOUHSC_00830	SAOUHSC_00830	Putative uncharacterized protein	-2.89	1.54E-18
SAOUHSC_00834	SAOUHSC_00834	Thioredoxin, putative	2.54	4.39E-09
SAOUHSC_00835	SAOUHSC_00835	Putative uncharacterized protein	2.01	2.18E-07
SAOUHSC_00843	SAOUHSC_00843	Putative uncharacterized protein	2.04	4.47E-10
SAOUHSC_00844	SAOUHSC_00844	Lipoprotein	2.15	2.02E-14
SAOUHSC_00848	SAOUHSC_00848	Putative uncharacterized protein	-2.20	2.40E-16
SAOUHSC_00849	SAOUHSC_00849	Aminotransferase, class V superfamily, putative	-2.63	8.02E-15
SAOUHSC_00850	SAOUHSC_00850	Putative uncharacterized protein	-2.54	1.30E-15
SAOUHSC_00851	SAOUHSC_00851	UPF0051 protein SAOUHSC_00851	-3.01	4.12E-25
SAOUHSC_00858	SAOUHSC_00858	Putative uncharacterized protein	2.27	2.57E-11
SAOUHSC_00862	SAOUHSC_00862	Putative uncharacterized protein	3.06	2.67E-13
SAOUHSC_00863	SAOUHSC_00863	Putative uncharacterized protein	3.36	5.42E-10
SAOUHSC_00864	SAOUHSC_00864	Putative uncharacterized protein	5.91	1.61E-38
SAOUHSC_00865	nagD	Protein NagD homolog	3.24	1.89E-29
SAOUHSC_00867	SAOUHSC_00867	Putative uncharacterized protein	5.04	3.53E-07
SAOUHSC_00868	SAOUHSC_00868	Putative uncharacterized protein	7.17	3.00E-39
SAOUHSC_00869	dltA	D-alanine--poly(phosphoribitol) ligase subunit 1	3.69	1.12E-28
SAOUHSC_00870	SAOUHSC_00870	DltB protein, putative	2.33	1.50E-08
SAOUHSC_00871	dltC	D-alanine--poly(phosphoribitol) ligase subunit 2	2.44	7.64E-07
SAOUHSC_00876	SAOUHSC_00876	UPF0349 protein SAOUHSC_00876	2.93	1.09E-15
SAOUHSC_00878	SAOUHSC_00878	NADH dehydrogenase-like protein SAOUHSC_00878	-6.42	1.68E-60
SAOUHSC_00882	SAOUHSC_00882	Putative uncharacterized protein	-2.20	1.20E-05
SAOUHSC_00888	mnhB1	Na(+)/H(+) antiporter subunit B1	2.68	6.94E-08
SAOUHSC_00889	mnhA1	Na(+)/H(+) antiporter subunit A1	2.92	8.79E-26
SAOUHSC_00890	SAOUHSC_00890	Putative uncharacterized protein	2.61	2.44E-08
SAOUHSC_00893	SAOUHSC_00893	FMN oxidoreductase, putative	4.48	2.68E-12
SAOUHSC_00895	SAOUHSC_00895	Glutamate dehydrogenase	-2.84	3.08E-22
SAOUHSC_00896	SAOUHSC_00896	Putative uncharacterized protein	-3.28	2.89E-09
SAOUHSC_00897	SAOUHSC_00897	Putative uncharacterized protein	2.05	2.17E-07
SAOUHSC_00901	SAOUHSC_00901	Putative uncharacterized protein	3.37	4.96E-11
SAOUHSC_00902	SAOUHSC_00902	Signal peptidase IA, putative	2.97	2.07E-10
SAOUHSC_00909	SAOUHSC_00909	Putative uncharacterized protein	2.60	9.76E-16
SAOUHSC_00912	SAOUHSC_00912	ATP-dependent Clp protease, ATP-binding subunit ClpB	-112.83	1.68E-85
SAOUHSC_00913	SAOUHSC_00913	Putative uncharacterized protein	-140.47	1.98E-118
SAOUHSC_00914	SAOUHSC_00914	2-isopropylmalate synthase, putative	-3.13	4.78E-04
SAOUHSC_00916	SAOUHSC_00916	Putative uncharacterized protein	2.83	7.31E-03
SAOUHSC_00923	SAOUHSC_00923	Putative uncharacterized protein	7.86	4.00E-12
SAOUHSC_00924	SAOUHSC_00924	Putative uncharacterized protein	7.06	3.95E-10
SAOUHSC_00925	SAOUHSC_00925	Putative uncharacterized protein	4.15	7.89E-09
SAOUHSC_00926	SAOUHSC_00926	Oligopeptide ABC transporter, ATP-binding protein, putative	2.69	1.54E-05
SAOUHSC_00927	SAOUHSC_00927	Oligopeptide ABC transporter, substrate-binding protein, putat	2.08	5.94E-04
SAOUHSC_00931	SAOUHSC_00931	Oligopeptide ABC transporter, permease protein, putative	2.28	8.44E-04
SAOUHSC_00933	trpS	Tryptophan--tRNA ligase	2.25	1.28E-11
SAOUHSC_00934	spxA	Regulatory protein Spx	-4.24	6.48E-17
SAOUHSC_00935	mecA	Adapter protein MecA	-4.15	4.84E-31
SAOUHSC_00936	SAOUHSC_00936	Putative uncharacterized protein	-2.63	6.77E-11
SAOUHSC_00937	SAOUHSC_00937	Oligoendopeptidase F	5.77	2.61E-35
SAOUHSC_00938	SAOUHSC_00938	UPF0413 protein SAOUHSC_00938	2.32	5.79E-10
SAOUHSC_00939	SAOUHSC_00939	Putative uncharacterized protein	2.98	1.83E-18
SAOUHSC_00943	ppnK	Probable inorganic polyphosphate/ATP-NAD kinase	-2.26	4.26E-06
SAOUHSC_00948	SAOUHSC_00948	Putative uncharacterized protein	3.07	5.42E-16
SAOUHSC_00949	SAOUHSC_00949	Putative uncharacterized protein	2.33	5.69E-04
SAOUHSC_00951	SAOUHSC_00951	UPF0477 protein SAOUHSC_00951	-5.42	4.75E-25
SAOUHSC_00957	SAOUHSC_00957	Putative uncharacterized protein	-2.44	2.45E-07
SAOUHSC_00958	SAOUHSC_00958	Serine protease HtrA-like	2.84	5.72E-10
SAOUHSC_00962	SAOUHSC_00962	Putative uncharacterized protein	-6.94	1.85E-22
SAOUHSC_00968	SAOUHSC_00968	Putative uncharacterized protein	3.37	5.41E-03

SAOUHSC_00975	SAOUHSC_00975	Putative uncharacterized protein	3.42	2.58E-03
SAOUHSC_00979	SAOUHSC_00979	Putative uncharacterized protein	4.80	1.37E-18
SAOUHSC_00980	SAOUHSC_00980	Putative uncharacterized protein	2.58	1.26E-09
SAOUHSC_00981	SAOUHSC_00981	Putative uncharacterized protein	2.35	3.30E-04
SAOUHSC_00985	SAOUHSC_00985	Enoyl-CoA hydratase/isomerase family protein, putative	-2.97	8.75E-19
SAOUHSC_00989	SAOUHSC_00989	Putative uncharacterized protein	4.77	7.03E-14
SAOUHSC_00991	SAOUHSC_00991	Putative uncharacterized protein	2.87	7.20E-05
SAOUHSC_00994	atl	Bifunctional autolysin	5.42	1.96E-54
SAOUHSC_00995	SAOUHSC_00995	UPF0039 protein SAOUHSC_00995	7.13	2.68E-13
SAOUHSC_00997	SAOUHSC_00997	Uncharacterized protein SAOUHSC_00997	2.33	5.51E-14
SAOUHSC_00999	qoxD	Probable quinol oxidase subunit 4	-4.64	1.09E-24
SAOUHSC_01000	qoxC	Probable quinol oxidase subunit 3	-3.86	1.51E-22
SAOUHSC_01001	qoxB	Probable quinol oxidase subunit 1	-3.05	1.04E-18
SAOUHSC_01002	qoxA	Probable quinol oxidase subunit 2	-2.54	1.51E-12
SAOUHSC_01007	folD	Bifunctional protein FolD	-3.11	1.97E-19
SAOUHSC_01008	SAOUHSC_01008	Phosphoribosylaminoimidazole carboxylase, catalytic subunit	18.54	2.93E-58
SAOUHSC_01009	SAOUHSC_01009	Phosphoribosylaminoimidazole carboxylase, ATPase subunit	28.76	5.45E-82
SAOUHSC_01010	purC	Phosphoribosylaminoimidazole-succinocarboxamide synthase	33.49	2.62E-58
SAOUHSC_01011	SAOUHSC_01011	Phosphoribosylformylglycinamidine synthase, PurS protein	28.82	3.67E-45
SAOUHSC_01012	purQ	Phosphoribosylformylglycinamidine synthase 1	22.50	2.27E-44
SAOUHSC_01013	purL	Phosphoribosylformylglycinamidine synthase 2	12.41	4.90E-33
SAOUHSC_01014	SAOUHSC_01014	Amidophosphoribosyltransferase	6.50	4.52E-22
SAOUHSC_01015	purM	Phosphoribosylformylglycinamidine cyclo-ligase	4.84	3.28E-17
SAOUHSC_01016	SAOUHSC_01016	Phosphoribosylglycinamide formyltransferase, putative	4.03	3.43E-15
SAOUHSC_01017	purH	Bifunctional purine biosynthesis protein PurH	2.23	6.92E-08
SAOUHSC_01019	SAOUHSC_01019	Putative uncharacterized protein	-2.79	2.08E-15
SAOUHSC_01021	SAOUHSC_01021	Putative uncharacterized protein	-2.17	3.89E-08
SAOUHSC_01037	SAOUHSC_01037	Putative uncharacterized protein	3.46	2.23E-25
SAOUHSC_01040	SAOUHSC_01040	Pyruvate dehydrogenase complex, E1 component, alpha subun	-3.78	4.59E-27
SAOUHSC_01041	SAOUHSC_01041	Pyruvate dehydrogenase complex, E1 component, pyruvate del	-5.18	4.83E-39
SAOUHSC_01042	SAOUHSC_01042	Dihydrolipoamide S-acetyltransferase component of pyruvate (	-6.50	3.94E-50
SAOUHSC_01043	SAOUHSC_01043	Dihydrolipoyl dehydrogenase	-10.69	1.02E-64
SAOUHSC_01044	SAOUHSC_01044	UPF0223 protein SAOUHSC_01044	-2.76	5.62E-12
SAOUHSC_01051	SAOUHSC_01051	Putative uncharacterized protein	2.20	3.99E-06
SAOUHSC_01054	SAOUHSC_01054	UPF0637 protein SAOUHSC_01054	3.85	2.16E-14
SAOUHSC_01055	SAOUHSC_01055	Inositol monophosphatase family protein, putative	-6.79	5.50E-46
SAOUHSC_01057	SAOUHSC_01057	Putative uncharacterized protein	-2.30	2.84E-08
SAOUHSC_01060	SAOUHSC_01060	Putative uncharacterized protein	2.32	7.70E-07
SAOUHSC_01061	SAOUHSC_01061	Putative uncharacterized protein	2.45	8.12E-13
SAOUHSC_01062	SAOUHSC_01062	UPF0358 protein SAOUHSC_01062	2.64	3.75E-20
SAOUHSC_01063	SAOUHSC_01063	Putative uncharacterized protein	3.35	9.64E-14
SAOUHSC_01064	SAOUHSC_01064	Pyruvate carboxylase	2.42	5.65E-10
SAOUHSC_01069	SAOUHSC_01069	Putative uncharacterized protein	2.19	3.70E-11
SAOUHSC_01072	SAOUHSC_01072	UPF0298 protein SAOUHSC_01072	2.50	8.92E-07
SAOUHSC_01077	SAOUHSC_01077	Putative uncharacterized protein	-2.08	3.90E-08
SAOUHSC_01081	isdA	Iron-regulated surface determinant protein A	5.87	3.66E-09
SAOUHSC_01084	SAOUHSC_01084	Putative uncharacterized protein	2.48	7.21E-03
SAOUHSC_01092	pheS	Phenylalanine--tRNA ligase alpha subunit	-2.04	1.50E-06
SAOUHSC_01093	pheT	Phenylalanine--tRNA ligase beta subunit	-3.45	5.11E-14
SAOUHSC_01095	rnhC	Ribonuclease HIII	3.05	5.62E-08
SAOUHSC_01101	SAOUHSC_01101	Putative uncharacterized protein	2.34	4.18E-09
SAOUHSC_01103	SAOUHSC_01103	Succinate dehydrogenase cytochrome b-558 subunit, putative	-4.65	5.31E-21
SAOUHSC_01104	SAOUHSC_01104	Succinate dehydrogenase, flavoprotein chain TC0881, putative	-6.52	1.80E-31
SAOUHSC_01105	SAOUHSC_01105	Iron-sulphur subunit of succinate dehydrogenase, putative	-7.62	7.09E-37
SAOUHSC_01110	SAOUHSC_01110	Fibrinogen-binding protein-related	-2.23	6.12E-06
SAOUHSC_01123	SAOUHSC_01123	Putative uncharacterized protein	-2.28	1.69E-05
SAOUHSC_01124	SAOUHSC_01124	Putative uncharacterized protein	3.63	1.11E-03
SAOUHSC_01125	SAOUHSC_01125	Putative uncharacterized protein	7.28	6.55E-09
SAOUHSC_01127	SAOUHSC_01127	Putative uncharacterized protein	6.04	5.46E-19
SAOUHSC_01133	SAOUHSC_01133	Putative uncharacterized protein	2.59	6.78E-13
SAOUHSC_01134	SAOUHSC_01134	Putative uncharacterized protein	4.23	1.90E-12
SAOUHSC_01135	SAOUHSC_01135	Putative uncharacterized protein	-3.05	1.77E-15
SAOUHSC_01136	SAOUHSC_01136	Putative uncharacterized protein	-3.54	1.06E-25
SAOUHSC_01138	SAOUHSC_01138	Uncharacterized N-acetyltransferase SAOUHSC_01138	-3.94	3.63E-22
SAOUHSC_01160	SAOUHSC_01160	Putative uncharacterized protein	2.36	8.57E-13
SAOUHSC_01161	SAOUHSC_01161	Truncated transposase	2.81	9.50E-08
SAOUHSC_01163	SAOUHSC_01163	Pseudouridine synthase	-2.07	1.36E-09
SAOUHSC_01164	pyrR	Bifunctional protein PyrR	-2.25	1.97E-08
SAOUHSC_01165	SAOUHSC_01165	Uracil permease, putative	-4.58	7.74E-04
SAOUHSC_01166	pyrB	Aspartate carbamoyltransferase	-6.22	1.68E-14
SAOUHSC_01168	pyrC	Dihydroorotase	-4.79	4.95E-14
SAOUHSC_01169	carA	Carbamoyl-phosphate synthase small chain	-4.56	7.27E-17
SAOUHSC_01170	carB	Carbamoyl-phosphate synthase large chain	-4.01	3.27E-20
SAOUHSC_01171	pyrF	Orotidine 5'-phosphate decarboxylase	-3.86	2.99E-15
SAOUHSC_01172	pyrE	Orotate phosphoribosyltransferase	-3.95	2.47E-21
SAOUHSC_01175	SAOUHSC_01175	Fibronectin-binding protein A-related	2.14	3.63E-07
SAOUHSC_01176	gmk	Guanylate kinase	2.99	5.70E-23
SAOUHSC_01180	SAOUHSC_01180	Putative uncharacterized protein	2.33	3.80E-08
SAOUHSC_01181	SAOUHSC_01181	Putative uncharacterized protein	-2.56	4.12E-15
SAOUHSC_01182			2.25	8.16E-11
SAOUHSC_01184	SAOUHSC_01184	Sun protein	2.09	5.24E-11
SAOUHSC_01186	SAOUHSC_01186	Putative uncharacterized protein	2.44	4.27E-14
SAOUHSC_01187	SAOUHSC_01187	Putative uncharacterized protein	2.00	9.99E-11
SAOUHSC_01189	SAOUHSC_01189	Ribulose-phosphate 3-epimerase	-2.70	6.25E-23
SAOUHSC_01190	SAOUHSC_01190	Putative uncharacterized protein	-2.92	1.59E-21
SAOUHSC_01191	rpmB	50S ribosomal protein L28	-6.40	3.61E-41

SAOUHSC_01198	SAOUHSC_01198	Malonyl CoA-acyl carrier protein transacylase	-2.21	1.11E-07
SAOUHSC_01199	SAOUHSC_01199	3-oxoacyl-(Acyl-carrier-protein) reductase, putative	-2.35	2.78E-09
SAOUHSC_01207	ffh	Signal recognition particle protein	-2.50	1.45E-24
SAOUHSC_01210	trmD	tRNA (guanine-N(1)-)-methyltransferase	-2.95	6.72E-09
SAOUHSC_01214	SAOUHSC_01214	Ribosome biogenesis GTPase A	-3.10	1.38E-15
SAOUHSC_01215	rnhB	Ribonuclease HII	-4.25	3.06E-24
SAOUHSC_01216	sucC	Succinyl-CoA ligase [ADP-forming] subunit beta	-2.80	9.38E-22
SAOUHSC_01218	SAOUHSC_01218	Succinyl-CoA ligase [ADP-forming] subunit alpha	-2.91	2.07E-19
SAOUHSC_01221	SAOUHSC_01221	Putative uncharacterized protein	2.28	1.06E-03
SAOUHSC_01242	rimP	Ribosome maturation factor RimP	-3.07	1.57E-17
SAOUHSC_01243	nusA	Transcription termination/antitermination protein NusA	-4.99	1.04E-30
SAOUHSC_01244	SAOUHSC_01244	Putative uncharacterized protein	-6.44	2.34E-40
SAOUHSC_01245	SAOUHSC_01245	Putative uncharacterized protein	-5.12	2.65E-36
SAOUHSC_01246	infB	Translation initiation factor IF-2	-11.77	1.67E-49
SAOUHSC_01247	rbfA	Ribosome-binding factor A	-4.19	1.31E-26
SAOUHSC_01248	truB	tRNA pseudouridine synthase B	3.19	1.53E-09
SAOUHSC_01249	SAOUHSC_01249	Riboflavin biosynthesis protein RibF	2.61	2.61E-20
SAOUHSC_01255	SAOUHSC_01255	Putative uncharacterized protein	3.13	1.05E-06
SAOUHSC_01257	SAOUHSC_01257	Putative uncharacterized protein	-2.23	1.72E-08
SAOUHSC_01263	rny	Ribonuclease Y	-3.47	5.86E-29
SAOUHSC_01264	SAOUHSC_01264	Putative uncharacterized protein	4.26	1.07E-23
SAOUHSC_01266	SAOUHSC_01266	Putative uncharacterized protein	-3.58	5.62E-19
SAOUHSC_01267	SAOUHSC_01267	Putative uncharacterized protein	-4.12	1.64E-24
SAOUHSC_01269	miaB	(Dimethylallyl)adenosine tRNA methylthiotransferase MiaB	2.99	2.32E-22
SAOUHSC_01270	SAOUHSC_01270	Putative uncharacterized protein	2.88	1.18E-21
SAOUHSC_01271	SAOUHSC_01271	Putative uncharacterized protein	2.31	1.34E-13
SAOUHSC_01272	mutS	DNA mismatch repair protein MutS	3.70	3.87E-40
SAOUHSC_01273	mutL	DNA mismatch repair protein MutL	3.81	3.28E-26
SAOUHSC_01274	SAOUHSC_01274	Glycerol uptake operon antiterminator regulatory protein, puta	2.67	1.50E-11
SAOUHSC_01276	glpK	Glycerol kinase	-2.56	1.48E-08
SAOUHSC_01282	SAOUHSC_01282	Glutathione peroxidase	2.14	1.08E-10
SAOUHSC_01285	SAOUHSC_01285	Putative uncharacterized protein	3.25	8.02E-15
SAOUHSC_01295	SAOUHSC_01295	Putative uncharacterized protein	-2.84	8.78E-03
SAOUHSC_01296	SAOUHSC_01296	Putative uncharacterized protein	-7.36	2.32E-04
SAOUHSC_01304	SAOUHSC_01304	Putative uncharacterized protein	-4.26	5.41E-27
SAOUHSC_01305	SAOUHSC_01305	Putative uncharacterized protein	-3.59	2.56E-07
SAOUHSC_01310			2.46	1.51E-12
SAOUHSC_01316	SAOUHSC_01316	Putative uncharacterized protein	2.29	7.01E-04
SAOUHSC_01320	SAOUHSC_01320	Homoserine dehydrogenase	3.25	1.43E-07
SAOUHSC_01323	SAOUHSC_01323	Putative uncharacterized protein	-2.90	1.40E-11
SAOUHSC_01324	SAOUHSC_01324	Putative uncharacterized protein	-5.51	1.46E-13
SAOUHSC_01325	SAOUHSC_01325	Putative uncharacterized protein	-4.98	5.47E-13
SAOUHSC_01326	SAOUHSC_01326	Putative uncharacterized protein	2.09	4.28E-06
SAOUHSC_01330	guaC	GMP reductase	3.59	5.25E-21
SAOUHSC_01331	SAOUHSC_01331	Putative uncharacterized protein	3.81	2.71E-05
SAOUHSC_01332	SAOUHSC_01332	Putative uncharacterized protein	2.61	7.95E-18
SAOUHSC_01333	lexA	LexA repressor	-2.31	4.41E-06
SAOUHSC_01336	SAOUHSC_01336	UPF0291 protein SAOUHSC_01336	4.18	8.82E-18
SAOUHSC_01340	SAOUHSC_01340	Putative uncharacterized protein	2.37	1.67E-09
SAOUHSC_01344	SAOUHSC_01344	Putative uncharacterized protein	3.09	1.02E-26
SAOUHSC_01347	SAOUHSC_01347	Aconitate hydratase 1	-3.42	1.60E-17
SAOUHSC_01351	parE	DNA topoisomerase 4 subunit B	2.77	4.04E-15
SAOUHSC_01353	SAOUHSC_01353	Putative uncharacterized protein	2.47	1.00E-04
SAOUHSC_01356	glcT	Protein GlcT	3.34	5.86E-20
SAOUHSC_01357	SAOUHSC_01357	Putative uncharacterized protein	4.12	1.69E-10
SAOUHSC_01358	SAOUHSC_01358	Putative uncharacterized protein	2.45	2.88E-18
SAOUHSC_01366	SAOUHSC_01366	Anthranilate synthase component I	4.73	4.30E-04
SAOUHSC_01370	trpF	N-(5'-phosphoribosyl)anthranilate isomerase	4.10	7.66E-03
SAOUHSC_01372	trpA	Tryptophan synthase alpha chain	-2.41	5.66E-08
SAOUHSC_01373	femA	Aminoacyltransferase FemA	3.86	2.44E-20
SAOUHSC_01374	femB	Aminoacyltransferase FemB	2.26	4.33E-11
SAOUHSC_01375	SAOUHSC_01375	Putative uncharacterized protein	7.03	6.91E-19
SAOUHSC_01376	SAOUHSC_01376	Putative uncharacterized protein	-2.19	5.93E-12
SAOUHSC_01377	oppF2	Putative oligopeptide transport ATP-binding protein oppF2	-3.08	1.03E-22
SAOUHSC_01378	oppD2	Putative oligopeptide transport ATP-binding protein oppD2	-2.49	6.62E-13
SAOUHSC_01379	oppC2	Putative oligopeptide transport system permease protein oppC	-3.27	2.10E-18
SAOUHSC_01380	oppB2	Putative oligopeptide transport system permease protein oppB	-3.15	1.34E-14
SAOUHSC_01381	SAOUHSC_01381	Putative uncharacterized protein	-2.53	5.37E-05
SAOUHSC_01383	SAOUHSC_01383	Putative uncharacterized protein	6.93	7.10E-37
SAOUHSC_01394	SAOUHSC_01394	Aspartokinase	3.77	4.69E-06
SAOUHSC_01395	asd	Aspartate-semialdehyde dehydrogenase	4.35	5.76E-07
SAOUHSC_01396	dapA	4-hydroxy-tetrahydrodipicolinate synthase	4.40	7.12E-07
SAOUHSC_01397	dapB	4-hydroxy-tetrahydrodipicolinate reductase	2.81	8.50E-06
SAOUHSC_01399	SAOUHSC_01399	Uncharacterized hydrolase SAOUHSC_01399	2.19	7.31E-06
SAOUHSC_01402	msa	Protein msa	-3.14	1.28E-03
SAOUHSC_01403	cspA	Cold shock protein CspA	-2.45	7.07E-16
SAOUHSC_01404	SAOUHSC_01404	Putative uncharacterized protein	-2.21	3.58E-14
SAOUHSC_01405	SAOUHSC_01405	Putative uncharacterized protein	2.48	6.86E-08
SAOUHSC_01408	SAOUHSC_01408	TelA-like protein SAOUHSC_01408	-2.02	8.12E-06
SAOUHSC_01412	SAOUHSC_01412	Putative uncharacterized protein	-2.47	5.39E-17
SAOUHSC_01414	SAOUHSC_01414	Putative uncharacterized protein	-5.12	4.10E-21
SAOUHSC_01415	SAOUHSC_01415	Putative uncharacterized protein	-4.24	1.24E-18
SAOUHSC_01416	odhB	Dihydrolipoyllysine-residue succinyltransferase component of 2	-4.55	3.89E-45
SAOUHSC_01418	odhA	2-oxoglutarate dehydrogenase E1 component	-3.67	1.25E-34
SAOUHSC_01427	SAOUHSC_01427	Putative uncharacterized protein	3.18	2.07E-19
SAOUHSC_01428	SAOUHSC_01428	Putative uncharacterized protein	5.34	2.76E-08

SAOUHSC_01429	SAOUHSC_01429	UPF0346 protein SAOUHSC_01429	-4.54	1.23E-25
SAOUHSC_01430	SAOUHSC_01430	Phosphotransferase system enzyme IIA, putative	-4.43	1.45E-22
SAOUHSC_01431	msrB	Peptide methionine sulfoxide reductase MsrB	-3.37	9.67E-20
SAOUHSC_01432	msrA2	Peptide methionine sulfoxide reductase MsrA 2	-3.04	4.16E-16
SAOUHSC_01435	thyA	Thymidylate synthase	2.84	2.45E-06
SAOUHSC_01438	SAOUHSC_01438	Putative uncharacterized protein	2.19	4.38E-08
SAOUHSC_01439	SAOUHSC_01439	Putative uncharacterized protein	3.53	3.60E-17
SAOUHSC_01440	SAOUHSC_01440	Putative uncharacterized protein	2.36	1.58E-05
SAOUHSC_01443	SAOUHSC_01443	Putative uncharacterized protein	3.89	2.63E-04
SAOUHSC_01447	ebh	Extracellular matrix-binding protein ebh	-5.16	9.29E-42
SAOUHSC_01448	norB	Quinolone resistance protein NorB	2.44	1.77E-03
SAOUHSC_01450	SAOUHSC_01450	Putative uncharacterized protein	3.20	3.51E-11
SAOUHSC_01451	tdcB	L-threonine dehydratase catabolic TdcB	2.62	9.20E-09
SAOUHSC_01452	ald1	Alanine dehydrogenase 1	10.65	1.77E-42
SAOUHSC_01455	SAOUHSC_01455	Putative uncharacterized protein	2.65	4.43E-23
SAOUHSC_01460	SAOUHSC_01460	Putative uncharacterized protein	2.22	8.53E-08
SAOUHSC_01464	SAOUHSC_01464	Putative uncharacterized protein	2.02	3.15E-13
SAOUHSC_01466	recU	Holliday junction resolvase RecU	-3.02	5.02E-15
SAOUHSC_01467	SAOUHSC_01467	Penicillin-binding protein 2	-3.23	1.50E-18
SAOUHSC_01468	SAOUHSC_01468	Putative uncharacterized protein	-2.86	9.33E-11
SAOUHSC_01469	nth	Endonuclease III	-2.81	2.39E-11
SAOUHSC_01477	SAOUHSC_01477	Putative uncharacterized protein	-2.90	3.49E-12
SAOUHSC_01479	SAOUHSC_01479	UPF0302 protein SAOUHSC_01479	2.12	2.06E-06
SAOUHSC_01485	ndk	Nucleoside diphosphate kinase	2.28	1.59E-05
SAOUHSC_01486	SAOUHSC_01486	Heptaprenyl diphosphate syntase component II, putative	3.95	2.03E-31
SAOUHSC_01487	SAOUHSC_01487	Menaquinone biosynthesis methyltransferase, putative	2.93	7.96E-21
SAOUHSC_01488	SAOUHSC_01488	Putative uncharacterized protein	3.62	3.73E-21
SAOUHSC_01489	SAOUHSC_01489	Putative uncharacterized protein	3.57	6.75E-13
SAOUHSC_01490	SAOUHSC_01490	DNA-binding protein HU, putative	2.11	4.75E-10
SAOUHSC_01492	der	GTPase Der	2.33	2.42E-11
SAOUHSC_01496	SAOUHSC_01496	Cytidylate kinase	3.68	1.16E-17
SAOUHSC_01502	SAOUHSC_01502	ATP-dependent DNA helicase RecQ, putative	3.47	2.47E-08
SAOUHSC_01503	SAOUHSC_01503	Putative uncharacterized protein	2.81	2.00E-11
SAOUHSC_01504	SAOUHSC_01504	Ferredoxin, putative	-3.37	1.08E-20
SAOUHSC_01513	SAOUHSC_01513	Putative uncharacterized protein	-3.24	1.08E-12
SAOUHSC_01575	SAOUHSC_01575	Helix-turn-helix domain protein	-2.28	1.36E-08
SAOUHSC_01585	srrB	Sensor protein SrrB	-3.29	5.11E-19
SAOUHSC_01586	srrA	Transcriptional regulatory protein SrrA	-5.06	4.42E-22
SAOUHSC_01590	SAOUHSC_01590	Putative uncharacterized protein	2.52	8.68E-07
SAOUHSC_01591	xerD	Tyrosine recombinase XerD	-2.44	1.34E-11
SAOUHSC_01593	SAOUHSC_01593	NUDIX domain protein	2.70	1.08E-09
SAOUHSC_01594	SAOUHSC_01594	Putative uncharacterized protein	3.98	1.77E-42
SAOUHSC_01595	SAOUHSC_01595	Putative uncharacterized protein	4.01	1.49E-10
SAOUHSC_01596	SAOUHSC_01596	Putative uncharacterized protein	3.31	7.56E-16
SAOUHSC_01597	SAOUHSC_01597	Pyrroline-5-carboxylate reductase	2.91	3.15E-20
SAOUHSC_01598	rnz	Ribonuclease Z	2.23	4.56E-10
SAOUHSC_01599	zwf	Glucose-6-phosphate 1-dehydrogenase	2.40	6.53E-16
SAOUHSC_01601	SAOUHSC_01601	Alpha-glucosidase, putative	-2.76	7.18E-19
SAOUHSC_01604	SAOUHSC_01604	Putative uncharacterized protein	3.83	4.17E-11
SAOUHSC_01610	SAOUHSC_01610	UPF0403 protein SAOUHSC_01610	2.53	5.36E-18
SAOUHSC_01611	SAOUHSC_01611	2-oxoisovalerate dehydrogenase, E2 component, dihydrolipoar	-3.18	2.20E-22
SAOUHSC_01612	SAOUHSC_01612	2-oxoisovalerate dehydrogenase, E1 component, beta subunit,	-3.14	8.61E-21
SAOUHSC_01613	SAOUHSC_01613	2-oxoisovalerate dehydrogenase, E1 component, alpha subunit	-2.90	4.47E-20
SAOUHSC_01618	SAOUHSC_01618	Geranyltranstransferase, putative	2.63	1.80E-13
SAOUHSC_01619	xseB	Exodeoxyribonuclease 7 small subunit	2.26	2.75E-08
SAOUHSC_01622	SAOUHSC_01622	Putative uncharacterized protein	2.43	5.19E-13
SAOUHSC_01623	SAOUHSC_01623	Acetyl-CoA carboxylase, biotin carboxylase	2.39	9.11E-22
SAOUHSC_01624	SAOUHSC_01624	Acetyl-CoA carboxylase, biotin carboxyl carrier protein	2.77	6.64E-24
SAOUHSC_01626	SAOUHSC_01626	Proline dipeptidase, putative	3.41	2.62E-20
SAOUHSC_01627	SAOUHSC_01627	Putative uncharacterized protein	2.39	1.03E-11
SAOUHSC_01628	SAOUHSC_01628	Putative uncharacterized protein	2.10	7.72E-04
SAOUHSC_01632	gcvPB	Probable glycine dehydrogenase (decarboxylating) subunit 2	-2.53	7.58E-15
SAOUHSC_01633	gcvPA	Probable glycine dehydrogenase (decarboxylating) subunit 1	-2.14	9.35E-13
SAOUHSC_01644	SAOUHSC_01644	Putative uncharacterized protein	-3.27	1.44E-23
SAOUHSC_01645	SAOUHSC_01645	Putative uncharacterized protein	-2.79	3.17E-24
SAOUHSC_01646	SAOUHSC_01646	Glucokinase, putative	-2.61	2.14E-19
SAOUHSC_01652	SAOUHSC_01652	Penicillin-binding protein 3	2.14	5.91E-12
SAOUHSC_01655	fur	Ferric uptake regulation protein	-2.75	3.27E-14
SAOUHSC_01656	SAOUHSC_01656	Putative uncharacterized protein	-2.47	3.75E-10
SAOUHSC_01660	SAOUHSC_01660	Putative GTP cyclohydrolase 1 type 2	-2.04	3.24E-10
SAOUHSC_01662	sigA	RNA polymerase sigma factor SigA	-2.42	2.64E-15
SAOUHSC_01664	SAOUHSC_01664	Putative pyruvate, phosphate dikinase regulatory protein	-2.05	7.81E-09
SAOUHSC_01667	recO	DNA repair protein RecO	-3.63	1.56E-20
SAOUHSC_01668	era	GTPase Era	-2.96	1.35E-21
SAOUHSC_01669	SAOUHSC_01669	Putative uncharacterized protein	-2.55	5.19E-15
SAOUHSC_01670	SAOUHSC_01670	Cytidine deaminase	-2.87	1.19E-15
SAOUHSC_01675	SAOUHSC_01675	Putative uncharacterized protein	-4.51	3.47E-26
SAOUHSC_01676	SAOUHSC_01676	UPF0365 protein SAOUHSC_01676	-3.57	1.73E-22
SAOUHSC_01677	SAOUHSC_01677	Putative uncharacterized protein	-2.28	9.56E-10
SAOUHSC_01681	prmA	Ribosomal protein L11 methyltransferase	-13.21	1.35E-51
SAOUHSC_01682	dnaJ	Chaperone protein DnaJ	-10.77	2.58E-54
SAOUHSC_01683	dnaK	Chaperone protein DnaK	-12.28	4.54E-49
SAOUHSC_01684	grpE	Protein GrpE	-3.99	3.55E-18
SAOUHSC_01685	hrcA	Heat-inducible transcription repressor HrcA	-4.30	1.01E-24
SAOUHSC_01691	SAOUHSC_01691	DNA internalization-related competence protein ComEC/Rec2	2.36	7.53E-06
SAOUHSC_01707	SAOUHSC_01707	Putative uncharacterized protein	-3.57	2.17E-16

SAOUHSC_01708	SAOUHSC_01708	UPF0271 protein SAOUHSC_01708	-3.07	1.98E-14
SAOUHSC_01709	SAOUHSC_01709	Acetyl-CoA carboxylase, biotin carboxylase, putative	-2.64	5.73E-12
SAOUHSC_01714	greA	Transcription elongation factor GreA	-2.36	1.47E-12
SAOUHSC_01715	udk	Uridine kinase	-2.38	3.77E-17
SAOUHSC_01716	SAOUHSC_01716	Putative uncharacterized protein	-2.69	2.33E-20
SAOUHSC_01725			-2.62	1.20E-14
SAOUHSC_01730	SAOUHSC_01730	UPF0337 protein SAOUHSC_01730	2.61	4.70E-05
SAOUHSC_01732	SAOUHSC_01732	Putative uncharacterized protein	4.06	2.25E-20
SAOUHSC_01733	SAOUHSC_01733	Putative uncharacterized protein	3.29	5.74E-09
SAOUHSC_01737	aspS	Aspartate--tRNA ligase	-2.95	1.54E-18
SAOUHSC_01739	lytH	Probable cell wall amidase LytH	5.61	1.18E-40
SAOUHSC_01741	dtd	D-tyrosyl-tRNA(Tyr) deacylase	4.93	7.33E-43
SAOUHSC_01742	SAOUHSC_01742	GTP pyrophosphokinase	4.91	1.40E-49
SAOUHSC_01746	SAOUHSC_01746	Protein-export membrane protein SecDF	2.49	2.12E-14
SAOUHSC_01755	rpmA	50S ribosomal protein L27	-3.58	8.26E-21
SAOUHSC_01756	SAOUHSC_01756	Putative uncharacterized protein	-2.34	6.41E-16
SAOUHSC_01760	SAOUHSC_01760	Putative uncharacterized protein	-4.93	1.19E-30
SAOUHSC_01761	SAOUHSC_01761	Putative uncharacterized protein	-3.83	5.00E-25
SAOUHSC_01766	SAOUHSC_01766	Folylpolyglutamate synthase/dihydrofolate synthase, putative	-5.21	3.88E-37
SAOUHSC_01767	valS	Valine--tRNA ligase	-3.46	3.21E-23
SAOUHSC_01771	hemL1	Glutamate-1-semialdehyde 2,1-aminomutase 1	-2.90	1.17E-22
SAOUHSC_01772	hemB	Delta-aminolevulinic acid dehydratase	-2.71	6.78E-21
SAOUHSC_01776	hemA	Glutamyl-tRNA reductase	-2.06	9.18E-07
SAOUHSC_01778	clpX	ATP-dependent Clp protease ATP-binding subunit ClpX	-2.72	4.06E-15
SAOUHSC_01781	SAOUHSC_01781	Putative uncharacterized protein	2.56	3.21E-12
SAOUHSC_01782	SAOUHSC_01782	Putative uncharacterized protein	2.95	1.51E-17
SAOUHSC_01784	rplT	50S ribosomal protein L20	-2.31	2.41E-11
SAOUHSC_01793	nrdR	Transcriptional repressor NrdR	2.28	3.03E-07
SAOUHSC_01801	SAOUHSC_01801	Isocitrate dehydrogenase [NADP]	-6.73	2.07E-44
SAOUHSC_01802	SAOUHSC_01802	Putative uncharacterized protein	-5.22	6.25E-42
SAOUHSC_01803	SAOUHSC_01803	Putative uncharacterized protein	4.77	1.37E-23
SAOUHSC_01804	SAOUHSC_01804	Transposase, putative	5.61	2.09E-04
SAOUHSC_01806	pyk	Pyruvate kinase	-4.16	1.95E-22
SAOUHSC_01807	pfkA	6-phosphofructokinase	-3.01	2.90E-10
SAOUHSC_01808	accA	Acetyl-coenzyme A carboxylase carboxyl transferase subunit al	-3.16	6.05E-17
SAOUHSC_01809	accD	Acetyl-coenzyme A carboxylase carboxyl transferase subunit be	-3.16	9.53E-17
SAOUHSC_01810	SAOUHSC_01810	NADP-dependent malic enzyme, putative	-2.28	2.26E-14
SAOUHSC_01814	SAOUHSC_01814	Putative uncharacterized protein	-3.30	2.44E-14
SAOUHSC_01816	SAOUHSC_01816	Uncharacterized peptidase SAOUHSC_01816	4.87	2.45E-41
SAOUHSC_01817	SAOUHSC_01817	Putative uncharacterized protein	4.67	2.44E-14
SAOUHSC_01818	ald2	Alanine dehydrogenase 2	-2.89	1.60E-25
SAOUHSC_01819	SAOUHSC_01819	Putative universal stress protein SAOUHSC_01819	-21.58	2.21E-47
SAOUHSC_01821	SAOUHSC_01821	Putative uncharacterized protein	2.69	1.56E-17
SAOUHSC_01827	ezrA	Septation ring formation regulator EzrA	-2.54	9.35E-09
SAOUHSC_01830	SAOUHSC_01830	Putative uncharacterized protein	2.10	3.40E-07
SAOUHSC_01832	SAOUHSC_01832	Putative uncharacterized protein	4.12	7.86E-10
SAOUHSC_01833	SAOUHSC_01833	D-3-phosphoglycerate dehydrogenase	2.99	1.29E-06
SAOUHSC_01837	SAOUHSC_01837	1-acyl-sn-glycerol-3-phosphate acyltransferases domain protei	2.26	4.50E-12
SAOUHSC_01838	SAOUHSC_01838	Putative uncharacterized protein	2.71	7.18E-24
SAOUHSC_01839	tyrS	Tyrosine--tRNA ligase	2.95	8.78E-10
SAOUHSC_01840	SAOUHSC_01840	Transglycosylase domain protein	3.38	3.96E-12
SAOUHSC_01841	SAOUHSC_01841	Putative uncharacterized protein	2.46	6.39E-03
SAOUHSC_01843	isdH	Iron-regulated surface determinant protein H	-2.29	4.63E-13
SAOUHSC_01846	SAOUHSC_01846	Acetyl-CoA synthetase, putative	-2.35	5.67E-09
SAOUHSC_01847	SAOUHSC_01847	Putative uncharacterized protein	3.34	2.43E-13
SAOUHSC_01849	SAOUHSC_01849	Putative uncharacterized protein	3.33	3.00E-18
SAOUHSC_01850	SAOUHSC_01850	Catabolite control protein A	-2.43	9.94E-23
SAOUHSC_01854	SAOUHSC_01854	Putative uncharacterized protein	-2.37	3.03E-12
SAOUHSC_01860	SAOUHSC_01860	Putative uncharacterized protein	-3.71	1.99E-28
SAOUHSC_01861	SAOUHSC_01861	Putative uncharacterized protein	-3.16	2.91E-16
SAOUHSC_01865	trmB	tRNA (guanine-N(7)-)-methyltransferase	-2.24	1.45E-07
SAOUHSC_01866	SAOUHSC_01866	Putative uncharacterized protein	-2.87	1.23E-10
SAOUHSC_01867	SAOUHSC_01867	D-alanine aminotransferase	2.07	2.13E-10
SAOUHSC_01868	SAOUHSC_01868	Putative dipeptidase SAOUHSC_01868	5.31	2.08E-52
SAOUHSC_01873	SAOUHSC_01873	Putative uncharacterized protein	-4.93	4.41E-31
SAOUHSC_01877	SAOUHSC_01877	Putative uncharacterized protein	2.40	7.64E-15
SAOUHSC_01879	rot	HTH-type transcriptional regulator rot	-5.48	8.27E-29
SAOUHSC_01884	SAOUHSC_01884	Putative uncharacterized protein	-2.73	9.99E-06
SAOUHSC_01886	ribH	6,7-dimethyl-8-ribityllumazine synthase	-10.04	4.00E-41
SAOUHSC_01887	ribBA	Riboflavin biosynthesis protein RibBA	-7.35	1.37E-28
SAOUHSC_01888	SAOUHSC_01888	Riboflavin synthase, alpha subunit	-5.78	7.98E-19
SAOUHSC_01889	SAOUHSC_01889	Riboflavin biosynthesis protein RibD	-4.03	2.93E-15
SAOUHSC_01890	SAOUHSC_01890	Putative uncharacterized protein	3.06	1.55E-08
SAOUHSC_01895	SAOUHSC_01895	Putative uncharacterized protein	4.00	1.82E-38
SAOUHSC_01896	SAOUHSC_01896	Putative uncharacterized protein	3.52	2.25E-20
SAOUHSC_01898	SAOUHSC_01898	Putative uncharacterized protein	4.07	3.95E-08
SAOUHSC_01899	SAOUHSC_01899	Putative uncharacterized protein	6.24	2.57E-11
SAOUHSC_01901	SAOUHSC_01901	Putative uncharacterized protein	2.03	7.50E-13
SAOUHSC_01902	SAOUHSC_01902	Putative uncharacterized protein	3.18	1.94E-03
SAOUHSC_01903	crcB1	Putative fluoride ion transporter CrcB 1	6.79	2.64E-10
SAOUHSC_01904	crcB2	Putative fluoride ion transporter CrcB 2	3.31	1.03E-05
SAOUHSC_01907	SAOUHSC_01907	Putative uncharacterized protein	2.20	3.48E-13
SAOUHSC_01915	SAOUHSC_01915	Putative uncharacterized protein	-2.89	2.41E-25
SAOUHSC_01917	SAOUHSC_01917	Putative uncharacterized protein	2.74	5.81E-04
SAOUHSC_01924	SAOUHSC_01924	Putative uncharacterized protein	-2.41	1.55E-06
SAOUHSC_01925	SAOUHSC_01925	Putative uncharacterized protein	-2.05	4.74E-05

SAOUHSC_01929	SAOUHSC_01929	Putative uncharacterized protein	-2.90	1.28E-05
SAOUHSC_01933	SAOUHSC_01933	Type I restriction-modification system, M subunit	2.36	1.24E-11
SAOUHSC_01945	SAOUHSC_01945	Membrane protein, putative	5.52	1.50E-05
SAOUHSC_01957	SAOUHSC_01957	Putative uncharacterized protein	-2.96	1.44E-06
SAOUHSC_01958	SAOUHSC_01958	Putative uncharacterized protein	3.60	7.49E-17
SAOUHSC_01959	SAOUHSC_01959	Putative uncharacterized protein	-3.10	1.19E-21
SAOUHSC_01960	SAOUHSC_01960	Protoporphyrinogen oxidase	-3.28	1.12E-21
SAOUHSC_01961	hemH	Ferrochelatase	-2.32	9.47E-15
SAOUHSC_01966	SAOUHSC_01966	Putative uncharacterized protein	2.54	3.57E-13
SAOUHSC_01967	SAOUHSC_01967	ABC transporter, ATP-binding protein, putative	4.13	3.50E-28
SAOUHSC_01971	SAOUHSC_01971	Putative uncharacterized protein	2.63	2.58E-03
SAOUHSC_01972	prsA	Foldase protein PrsA	-3.26	1.22E-15
SAOUHSC_01974	SAOUHSC_01974	Putative uncharacterized protein	2.49	3.64E-20
SAOUHSC_01975	SAOUHSC_01975	Putative uncharacterized protein	3.59	1.98E-20
SAOUHSC_01979	SAOUHSC_01979	Putative uncharacterized protein	5.20	3.59E-17
SAOUHSC_01980	SAOUHSC_01980	DNA-binding response regulator, putative	3.25	1.70E-12
SAOUHSC_01981	SAOUHSC_01981	Sensor histidine kinase, putative	2.05	3.58E-09
SAOUHSC_01983	fumC	Fumarate hydratase class II	-2.72	9.99E-14
SAOUHSC_01986	SAOUHSC_01986	Putative uncharacterized protein	-2.40	2.69E-08
SAOUHSC_01997	perR	Peroxide-responsive repressor PerR	-3.54	7.07E-13
SAOUHSC_01999	SAOUHSC_01999	Putative uncharacterized protein	2.28	9.62E-09
SAOUHSC_02002	SAOUHSC_02002	Putative uncharacterized protein	-2.03	1.49E-03
SAOUHSC_02003	SAOUHSC_02003	Putative multidrug export ATP-binding/permease protein SAOU	-2.61	2.19E-11
SAOUHSC_02004	SAOUHSC_02004	UPF0374 protein SAOUHSC_02004	-2.01	8.51E-05
SAOUHSC_02008	SAOUHSC_02008	Putative uncharacterized protein	2.58	2.99E-11
SAOUHSC_02009	SAOUHSC_02009	Putative uncharacterized protein	3.28	1.94E-26
SAOUHSC_02010	SAOUHSC_02010	Putative uncharacterized protein	3.56	1.26E-16
SAOUHSC_02011	recX	Regulatory protein RecX	3.92	7.45E-28
SAOUHSC_02090	SAOUHSC_02090	Conserved hypothetical phage protein	-2.25	1.30E-05
SAOUHSC_02093	SAOUHSC_02093	UPF0435 protein SAOUHSC_02093	3.04	1.41E-12
SAOUHSC_02098	SAOUHSC_02098	DNA-binding response regulator VraR, putative	-5.89	3.74E-32
SAOUHSC_02099	SAOUHSC_02099	Histidine kinase, putative	-4.76	1.78E-30
SAOUHSC_02100	SAOUHSC_02100	Putative uncharacterized protein	-4.36	1.16E-20
SAOUHSC_02101	SAOUHSC_02101	Putative uncharacterized protein	-3.44	9.38E-17
SAOUHSC_02108	ftnA	Ferritin	-7.44	5.99E-15
SAOUHSC_02109	SAOUHSC_02109	Putative uncharacterized protein	-6.43	1.18E-14
SAOUHSC_02110	SAOUHSC_02110	Putative uncharacterized protein	-2.83	7.53E-18
SAOUHSC_02111	dinB	DNA polymerase IV	-4.62	5.01E-28
SAOUHSC_02112	SAOUHSC_02112	Putative uncharacterized protein	-2.06	2.73E-04
SAOUHSC_02115	SAOUHSC_02115	Putative uncharacterized protein	3.17	2.26E-04
SAOUHSC_02116	gatB	Aspartyl/glutamyl-tRNA(Asn/Gln) amidotransferase subunit B	2.07	1.22E-09
SAOUHSC_02117	gatA	Glutamyl-tRNA(Gln) amidotransferase subunit A	2.69	9.64E-12
SAOUHSC_02118	gatC	Aspartyl/glutamyl-tRNA(Asn/Gln) amidotransferase subunit C	5.92	9.83E-21
SAOUHSC_02119	putP	Sodium/proline symporter	2.01	1.01E-04
SAOUHSC_02126	purB	Adenylosuccinate lyase	3.42	7.98E-19
SAOUHSC_02129	SAOUHSC_02129	Putative uncharacterized protein	2.91	2.18E-03
SAOUHSC_02133	SAOUHSC_02133	Nicotinate phosphoribosyltransferase	2.38	4.86E-19
SAOUHSC_02135	SAOUHSC_02135	Putative uncharacterized protein	2.02	3.48E-13
SAOUHSC_02139	SAOUHSC_02139	Pyrazinamidase/nicotinamidase, putative	4.03	4.87E-30
SAOUHSC_02140	ppaC	Probable manganese-dependent inorganic pyrophosphatase	-2.62	9.43E-14
SAOUHSC_02141	SAOUHSC_02141	Putative uncharacterized protein	6.63	6.37E-03
SAOUHSC_02142	SAOUHSC_02142	Aldehyde dehydrogenase	2.40	5.12E-13
SAOUHSC_02146	SAOUHSC_02146	Putative uncharacterized protein	3.80	6.22E-12
SAOUHSC_02147	SAOUHSC_02147	Putative uncharacterized protein	2.27	2.69E-10
SAOUHSC_02148	SAOUHSC_02148	Putative uncharacterized protein	2.63	2.81E-11
SAOUHSC_02149	SAOUHSC_02149	Putative uncharacterized protein	5.36	2.56E-28
SAOUHSC_02150	SAOUHSC_02150	Putative uncharacterized protein	2.26	1.19E-15
SAOUHSC_02157	SAOUHSC_02157	Putative uncharacterized protein	-3.37	7.70E-10
SAOUHSC_02170	SAOUHSC_02170	Peptidoglycan hydrolase, putative	-4.29	1.09E-33
SAOUHSC_02171	SAOUHSC_02171	Staphylokinase, putative	-2.15	3.63E-06
SAOUHSC_02175	SAOUHSC_02175	Hypothetical phage protein	-7.04	8.85E-41
SAOUHSC_02176	SAOUHSC_02176	Conserved hypothetical phage protein	-7.42	3.03E-43
SAOUHSC_02179	SAOUHSC_02179	Conserved hypothetical phage protein	-3.66	5.39E-05
SAOUHSC_02180	SAOUHSC_02180	Phage minor structural protein, N-terminal region domain prot	-4.19	1.13E-28
SAOUHSC_02181	SAOUHSC_02181	Phi PVL orfs 18-19-like protein	-2.26	1.72E-03
SAOUHSC_02182	SAOUHSC_02182	Tail length tape measure protein	-4.71	7.70E-23
SAOUHSC_02241	SAOUHSC_02241	Uncharacterized leukocidin-like protein 1	-2.54	2.20E-13
SAOUHSC_02243	SAOUHSC_02243	Uncharacterized leukocidin-like protein 2	-2.31	1.02E-06
SAOUHSC_02254	groL	60 kDa chaperonin	-4.48	1.68E-16
SAOUHSC_02257	SAOUHSC_02257	Putative uncharacterized protein	3.68	6.84E-20
SAOUHSC_02260	hld	Delta-hemolysin	-6.14	4.41E-37
SAOUHSC_02264	SAOUHSC_02264	Accessory gene regulator protein C	-4.13	6.84E-35
SAOUHSC_02265	SAOUHSC_02265	Accessory gene regulator protein A	-3.82	3.93E-28
SAOUHSC_02266	SAOUHSC_02266	Putative uncharacterized protein	-2.89	6.73E-15
SAOUHSC_02268	SAOUHSC_02268	Sucrose-6-phosphate dehydrogenase, putative	2.05	2.41E-10
SAOUHSC_02269	SAOUHSC_02269	Sucrose operon repressor, putative	2.23	1.91E-05
SAOUHSC_02274	SAOUHSC_02274	ABC transporter, ATP-binding protein, putative	3.95	2.07E-17
SAOUHSC_02278	SAOUHSC_02278	Ribosomal-protein-alanine acetyltransferase	2.80	6.27E-17
SAOUHSC_02279	SAOUHSC_02279	Putative uncharacterized protein	2.62	3.70E-17
SAOUHSC_02280	SAOUHSC_02280	Putative uncharacterized protein	2.68	3.40E-12
SAOUHSC_02294	SAOUHSC_02294	Putative uncharacterized protein	2.20	5.47E-05
SAOUHSC_02298	SAOUHSC_02298	RNA polymerase sigma factor	2.56	6.23E-16
SAOUHSC_02299	rsbW	Serine-protein kinase RsbW	2.82	1.94E-21
SAOUHSC_02300	rsbV	Anti-sigma-B factor antagonist	2.59	8.91E-19
SAOUHSC_02301	SAOUHSC_02301	SigmaB regulation protein RsbU, putative	2.08	3.54E-06
SAOUHSC_02306	acpS	Holo-[acyl-carrier-protein] synthase	2.52	1.88E-13

SAOUHSC_02307	SAOUHSC_02307	Putative uncharacterized protein	3.07	2.97E-24
SAOUHSC_02308	SAOUHSC_02308	Putative uncharacterized protein	3.11	1.33E-27
SAOUHSC_02309	SAOUHSC_02309	Putative uncharacterized protein	3.20	3.41E-15
SAOUHSC_02314	SAOUHSC_02314	Sensor protein KdpD, putative	3.57	3.70E-17
SAOUHSC_02315	SAOUHSC_02315	DNA-binding response regulator, putative	3.14	1.26E-08
SAOUHSC_02319	SAOUHSC_02319	Putative uncharacterized protein	2.75	1.48E-17
SAOUHSC_02320	SAOUHSC_02320	Putative uncharacterized protein	-2.60	1.96E-12
SAOUHSC_02323	cls	Cardiolipin synthase	3.10	1.19E-15
SAOUHSC_02333	sceD	Probable transglycosylase SceD	10.84	4.34E-17
SAOUHSC_02335	SAOUHSC_02335	Putative uncharacterized protein	3.60	8.19E-09
SAOUHSC_02338	SAOUHSC_02338	Putative uncharacterized protein	4.13	1.94E-15
SAOUHSC_02340	atpC	ATP synthase epsilon chain	-2.87	3.54E-18
SAOUHSC_02341	atpD	ATP synthase subunit beta	-2.87	4.16E-15
SAOUHSC_02343	atpG	ATP synthase gamma chain	-2.46	8.02E-17
SAOUHSC_02349	atpE	ATP synthase subunit c	-2.38	2.74E-10
SAOUHSC_02350	atpB	ATP synthase subunit a	-2.31	7.99E-14
SAOUHSC_02351	SAOUHSC_02351	Putative uncharacterized protein	-2.07	9.56E-13
SAOUHSC_02352	SAOUHSC_02352	UDP-N-acetylglucosamine 2-epimerase	-2.28	2.22E-14
SAOUHSC_02357	SAOUHSC_02357	Putative uncharacterized protein	2.27	2.64E-08
SAOUHSC_02360	tdk	Thymidine kinase	2.27	1.43E-06
SAOUHSC_02364	SAOUHSC_02364	Putative uncharacterized protein	-5.72	1.30E-22
SAOUHSC_02365			-2.53	7.39E-16
SAOUHSC_02367	SAOUHSC_02367	Putative uncharacterized protein	2.99	1.99E-09
SAOUHSC_02372	SAOUHSC_02372	Putative uncharacterized protein	2.73	1.60E-12
SAOUHSC_02376	SAOUHSC_02376	Putative uncharacterized protein	-5.57	5.75E-49
SAOUHSC_02377	pdp	Pyrimidine-nucleoside phosphorylase	-6.11	6.41E-62
SAOUHSC_02378	SAOUHSC_02378	Putative uncharacterized protein	-5.34	1.13E-46
SAOUHSC_02379	deoC	Deoxyribose-phosphate aldolase	-4.44	1.27E-28
SAOUHSC_02381	SAOUHSC_02381	Putative uncharacterized protein	-12.02	1.55E-22
SAOUHSC_02383	SAOUHSC_02383	Putative uncharacterized protein	3.58	5.68E-31
SAOUHSC_02384	SAOUHSC_02384	Putative uncharacterized protein	3.17	6.13E-08
SAOUHSC_02385	SAOUHSC_02385	Mannose-6-phosphate isomerase, class I	3.97	9.25E-25
SAOUHSC_02386	SAOUHSC_02386	Putative uncharacterized protein	3.94	2.90E-16
SAOUHSC_02388	SAOUHSC_02388	Putative uncharacterized protein	-2.00	6.34E-06
SAOUHSC_02389	SAOUHSC_02389	Cation efflux family protein, putative	-2.71	2.03E-12
SAOUHSC_02390	SAOUHSC_02390	Lytic regulatory protein, putative	2.26	1.60E-09
SAOUHSC_02396	SAOUHSC_02396	Putative uncharacterized protein	-2.29	4.97E-13
SAOUHSC_02397	SAOUHSC_02397	ABC transporter, ATP-binding protein, putative	-2.79	8.33E-14
SAOUHSC_02399	glmS	Glutamine--fructose-6-phosphate aminotransferase [isomerizir	-2.40	2.16E-10
SAOUHSC_02404	SAOUHSC_02404	Putative uncharacterized protein	-5.82	8.55E-50
SAOUHSC_02405	glmM	Phosphoglucosamine mutase	-3.83	4.87E-30
SAOUHSC_02419	sepA	Multidrug resistance efflux pump SepA	2.82	2.18E-07
SAOUHSC_02426	SAOUHSC_02426	Membrane protein, putative	-2.10	3.41E-11
SAOUHSC_02444	SAOUHSC_02444	Osmoprotectant transporter, BCCT family, opuD-like protein, p	5.53	2.42E-11
SAOUHSC_02445	SAOUHSC_02445	Putative uncharacterized protein	-2.81	1.04E-11
SAOUHSC_02447	SAOUHSC_02447	Putative uncharacterized protein	-4.21	6.38E-25
SAOUHSC_02457	cobB	NAD-dependent protein deacetylase	-2.34	1.03E-06
SAOUHSC_02458	SAOUHSC_02458	Putative uncharacterized protein	2.46	9.44E-03
SAOUHSC_02459	SAOUHSC_02459	Putative uncharacterized protein	5.71	5.24E-08
SAOUHSC_02466	SAOUHSC_02466	Truncated MHC class II analog protein	-2.61	4.67E-11
SAOUHSC_02467	SAOUHSC_02467	Alpha-acetolactate decarboxylase	-7.63	4.34E-39
SAOUHSC_02468	SAOUHSC_02468	Acetolactate synthase, putative	-3.95	1.86E-29
SAOUHSC_02477	rpsI	30S ribosomal protein S9	-2.08	2.53E-11
SAOUHSC_02484	rplQ	50S ribosomal protein L17	-2.91	3.32E-24
SAOUHSC_02485	rpoA	DNA-directed RNA polymerase subunit alpha	-2.65	1.79E-22
SAOUHSC_02486	rpsK	30S ribosomal protein S11	-2.89	4.98E-23
SAOUHSC_02487	rpsM	30S ribosomal protein S13	-2.21	3.13E-14
SAOUHSC_02492	rplO	50S ribosomal protein L15	-2.09	4.38E-11
SAOUHSC_02494	rpsE	30S ribosomal protein S5	-2.06	2.78E-08
SAOUHSC_02496	rplF	50S ribosomal protein L6	-2.41	8.59E-12
SAOUHSC_02505	rplP	50S ribosomal protein L16	-2.02	4.42E-07
SAOUHSC_02506	rpsC	30S ribosomal protein S3	-2.11	9.78E-07
SAOUHSC_02509	rplB	50S ribosomal protein L2	-2.72	1.13E-10
SAOUHSC_02510	rplW	50S ribosomal protein L23	-2.71	1.88E-12
SAOUHSC_02511	rplD	50S ribosomal protein L4	-2.65	8.22E-14
SAOUHSC_02518	SAOUHSC_02518	Putative uncharacterized protein	2.84	7.94E-04
SAOUHSC_02520	SAOUHSC_02520	Sugar transporter, putative	2.52	6.23E-06
SAOUHSC_02521	SAOUHSC_02521	Putative uncharacterized protein	3.02	1.34E-03
SAOUHSC_02523	SAOUHSC_02523	Putative uncharacterized protein	2.89	6.79E-04
SAOUHSC_02524	SAOUHSC_02524	Putative uncharacterized protein	3.39	2.01E-15
SAOUHSC_02529	SAOUHSC_02529	Putative uncharacterized protein	2.19	1.49E-07
SAOUHSC_02532	sarV	HTH-type transcriptional regulator SarV	-3.03	5.31E-17
SAOUHSC_02536	moaA	Cyclic pyranopterin monophosphate synthase	-2.81	1.57E-15
SAOUHSC_02537	mobA	Probable molybdenum cofactor guanylyltransferase	-3.16	6.31E-21
SAOUHSC_02538	SAOUHSC_02538	Molybdopterin converting factor, subunit 1	-2.58	5.96E-14
SAOUHSC_02540	SAOUHSC_02540	Molybdopterin converting factor moa, putative	-2.47	2.91E-13
SAOUHSC_02541	SAOUHSC_02541	Molybdopterin-guanine dinucleotide biosynthesis protein Mob	-2.44	2.92E-12
SAOUHSC_02542	SAOUHSC_02542	Molybdopterin biosynthesis protein moeA, putative	-2.89	6.27E-13
SAOUHSC_02543	moaC	Cyclic pyranopterin monophosphate synthase accessory protei	-2.62	8.12E-13
SAOUHSC_02544	SAOUHSC_02544	Molybdopterin biosynthesis moaB, putative	-3.10	8.63E-21
SAOUHSC_02549	SAOUHSC_02549	Molybdenum ABC transporter, periplasmic molybdate-binding	2.18	1.78E-14
SAOUHSC_02555	SAOUHSC_02555	Putative uncharacterized protein	-2.40	4.27E-05
SAOUHSC_02556	SAOUHSC_02556	Putative uncharacterized protein	-2.18	1.02E-03
SAOUHSC_02558	ureA	Urease subunit gamma	2.14	1.26E-09
SAOUHSC_02567	SAOUHSC_02567	Putative uncharacterized protein	-6.92	1.51E-17
SAOUHSC_02568	SAOUHSC_02568	Putative uncharacterized protein	-6.85	3.84E-22

SAOUHSC_02569	SAOUHSC_02569	Putative uncharacterized protein	-3.30	1.90E-12
SAOUHSC_02571	ssaA2	Staphylococcal secretory antigen ssaA2	4.76	9.26E-17
SAOUHSC_02575	SAOUHSC_02575	Putative uncharacterized protein	2.29	6.25E-05
SAOUHSC_02576	SAOUHSC_02576	Secretory antigen SsaA, putative	44.15	4.25E-65
SAOUHSC_02577	SAOUHSC_02577	Putative 2-hydroxyacid dehydrogenase SAOUHSC_02577	-4.27	1.86E-25
SAOUHSC_02583	SAOUHSC_02583	Transcriptional regulator, putative	-3.80	5.12E-24
SAOUHSC_02584	SAOUHSC_02584	Putative uncharacterized protein	-2.46	3.27E-17
SAOUHSC_02585	SAOUHSC_02585	Putative uncharacterized protein	3.36	2.06E-24
SAOUHSC_02586	SAOUHSC_02586	Putative uncharacterized protein	3.28	1.57E-05
SAOUHSC_02587	SAOUHSC_02587	Putative uncharacterized protein	5.70	1.63E-20
SAOUHSC_02588	SAOUHSC_02588	Putative uncharacterized protein	4.57	9.18E-11
SAOUHSC_02591	SAOUHSC_02591	Putative uncharacterized protein	2.30	6.83E-08
SAOUHSC_02592	SAOUHSC_02592	Putative uncharacterized protein	2.56	1.65E-08
SAOUHSC_02595	SAOUHSC_02595	Putative uncharacterized protein	2.14	2.64E-04
SAOUHSC_02599	SAOUHSC_02599	Hex regulon repressor, putative	3.39	1.32E-06
SAOUHSC_02600	SAOUHSC_02600	Putative uncharacterized protein	-3.52	2.99E-21
SAOUHSC_02602	SAOUHSC_02602	Putative uncharacterized protein	2.27	6.05E-04
SAOUHSC_02604	SAOUHSC_02604	Putative uncharacterized protein	-2.31	3.70E-16
SAOUHSC_02606	hutI	Imidazolonepropionase	-4.37	5.71E-31
SAOUHSC_02607	hutU	Urocanate hydratase	-4.94	3.68E-25
SAOUHSC_02608	SAOUHSC_02608	Putative uncharacterized protein	2.58	2.33E-05
SAOUHSC_02609	fosB	Metallothiol transferase FosB	4.29	1.16E-03
SAOUHSC_02610	hutG	Formimidoylglutamase	-2.04	2.89E-08
SAOUHSC_02611	lyrA	Lysostaphin resistance protein A	7.65	1.88E-40
SAOUHSC_02613	SAOUHSC_02613	Putative uncharacterized protein	2.11	1.88E-08
SAOUHSC_02614	SAOUHSC_02614	Aldose 1-epimerase, putative	-2.03	1.75E-04
SAOUHSC_02618	SAOUHSC_02618	Putative uncharacterized protein	2.31	1.36E-09
SAOUHSC_02619	SAOUHSC_02619	Putative uncharacterized protein	2.88	2.64E-11
SAOUHSC_02620	SAOUHSC_02620	Putative uncharacterized protein	-3.30	4.97E-19
SAOUHSC_02625	SAOUHSC_02625	Putative uncharacterized protein	2.64	2.87E-11
SAOUHSC_02628	SAOUHSC_02628	Putative uncharacterized protein	3.37	2.38E-20
SAOUHSC_02629	SAOUHSC_02629	Drug resistance transporter, EmrB/QacA subfamily, putative	-2.13	1.21E-10
SAOUHSC_02631	SAOUHSC_02631	Putative uncharacterized protein	3.50	3.70E-11
SAOUHSC_02635	tcaA	Membrane-associated protein TcaA	-2.32	1.91E-05
SAOUHSC_02636	SAOUHSC_02636	Putative uncharacterized protein	-37.53	1.02E-148
SAOUHSC_02637	SAOUHSC_02637	Putative uncharacterized protein	-29.03	1.88E-138
SAOUHSC_02638	SAOUHSC_02638	Putative uncharacterized protein	-55.07	5.14E-88
SAOUHSC_02640	hrtA	Putative hemin import ATP-binding protein HrtA	-101.71	3.86E-92
SAOUHSC_02641	hrtB	Putative hemin transport system permease protein HrtB	-69.11	2.38E-84
SAOUHSC_02644	hssS	Heme sensor protein HssS	-2.06	6.41E-11
SAOUHSC_02647			-4.61	4.97E-26
SAOUHSC_02649	SAOUHSC_02649	Putative uncharacterized protein	2.22	5.19E-11
SAOUHSC_02650	SAOUHSC_02650	Uncharacterized lipoprotein SAOUHSC_02650	-2.46	8.73E-12
SAOUHSC_02653	SAOUHSC_02653	Putative uncharacterized protein	2.01	1.03E-04
SAOUHSC_02661	SAOUHSC_02661	PTS system sucrose-specific IIBC component, putative	-2.41	2.46E-14
SAOUHSC_02662	SAOUHSC_02662	PTS system sucrose-specific IIBC component	-2.34	3.14E-07
SAOUHSC_02664	SAOUHSC_02664	Transcriptional regulator, putative	2.67	3.65E-07
SAOUHSC_02666	SAOUHSC_02666	Putative uncharacterized protein	6.09	1.38E-27
SAOUHSC_02667	SAOUHSC_02667	Putative uncharacterized protein	4.11	1.10E-41
SAOUHSC_02668	SAOUHSC_02668	Putative uncharacterized protein	3.40	3.49E-20
SAOUHSC_02669	sarZ	HTH-type transcriptional regulator SarZ	4.75	8.00E-19
SAOUHSC_02670	SAOUHSC_02670	Putative uncharacterized protein	2.73	8.81E-16
SAOUHSC_02671	narT	Probable nitrate transporter NarT	-2.58	2.46E-12
SAOUHSC_02682	SAOUHSC_02682	Uroporphyrin-III C-methyltransferase, putative	-3.39	2.45E-30
SAOUHSC_02683	SAOUHSC_02683	Assimilatory nitrite reductase [NAD(P)H], small subunit, putativ	-2.51	2.86E-19
SAOUHSC_02684	SAOUHSC_02684	Assimilatory nitrite reductase [NAD(P)H], large subunit, putativ	-2.17	5.90E-15
SAOUHSC_02686	SAOUHSC_02686	Putative uncharacterized protein	2.11	5.13E-03
SAOUHSC_02688	SAOUHSC_02688	Putative uncharacterized protein	4.09	7.25E-06
SAOUHSC_02689	SAOUHSC_02689	Putative uncharacterized protein	5.20	2.00E-11
SAOUHSC_02691	SAOUHSC_02691	Putative uncharacterized protein	-5.69	6.69E-18
SAOUHSC_02692	SAOUHSC_02692	Putative uncharacterized protein	-5.23	1.36E-15
SAOUHSC_02696	SAOUHSC_02696	FmhA protein, putative	2.68	2.18E-12
SAOUHSC_02700	SAOUHSC_02700	Putative uncharacterized protein	-2.00	2.34E-05
SAOUHSC_02702	SAOUHSC_02702	Putative uncharacterized protein	-2.13	7.11E-04
SAOUHSC_02709	hlgC	Gamma-hemolysin component C	-3.42	1.13E-08
SAOUHSC_02710	hlgB	Gamma-hemolysin component B	-3.31	7.74E-12
SAOUHSC_02721	SAOUHSC_02721	Putative uncharacterized protein	-8.30	8.83E-28
SAOUHSC_02723	SAOUHSC_02723	Glycerate kinase, putative	-3.06	4.38E-17
SAOUHSC_02724	SAOUHSC_02724	Putative uncharacterized protein	-3.90	4.24E-30
SAOUHSC_02725	SAOUHSC_02725	Putative uncharacterized protein	2.02	1.42E-03
SAOUHSC_02731	SAOUHSC_02731	Putative uncharacterized protein	2.73	7.23E-09
SAOUHSC_02736	flp	Protein flp	2.52	1.39E-09
SAOUHSC_02741	SAOUHSC_02741	Amino acid ABC transporter, permease protein, putative	-2.77	8.61E-28
SAOUHSC_02742	SAOUHSC_02742	Amino acid transporter, putative	-2.44	9.58E-20
SAOUHSC_02750	SAOUHSC_02750	Putative uncharacterized protein	3.26	3.54E-24
SAOUHSC_02753	SAOUHSC_02753	Membrane protein, putative	-2.02	1.40E-03
SAOUHSC_02759	SAOUHSC_02759	Putative uncharacterized protein	-7.30	2.67E-19
SAOUHSC_02761	SAOUHSC_02761	Putative uncharacterized protein	2.72	1.86E-07
SAOUHSC_02771	SAOUHSC_02771	Putative uncharacterized protein	-2.50	2.96E-03
SAOUHSC_02780	SAOUHSC_02780	Putative uncharacterized protein	-2.14	3.72E-07
SAOUHSC_02781	SAOUHSC_02781	Putative uncharacterized protein	-3.36	5.11E-17
SAOUHSC_02782	SAOUHSC_02782	Putative uncharacterized protein	-2.39	5.62E-07
SAOUHSC_02790	SAOUHSC_02790	Putative uncharacterized protein	-2.87	1.25E-11
SAOUHSC_02791	SAOUHSC_02791	Pyrophosphohydrolase, putative	-3.35	6.35E-13
SAOUHSC_02793	pgcA	Phosphoglucomutase	2.27	2.80E-07
SAOUHSC_02794	SAOUHSC_02794	Putative uncharacterized protein	3.45	7.98E-13

SAOUHSC_02795	SAOUHSC_02795	Putative uncharacterized protein	3.35	5.70E-06
SAOUHSC_02802	SAOUHSC_02802	Fibronectin binding protein B, putative	-2.78	5.98E-07
SAOUHSC_02803	fnbA	Fibronectin-binding protein A	-4.28	1.04E-18
SAOUHSC_02806	SAOUHSC_02806	Gluconate permease, putative	-2.69	1.69E-10
SAOUHSC_02809	SAOUHSC_02809	Gluconate operon transcriptional repressor, putative	2.26	9.54E-04
SAOUHSC_02811	SAOUHSC_02811	Putative uncharacterized protein	2.21	8.67E-16
SAOUHSC_02813	SAOUHSC_02813	Putative uncharacterized protein	2.65	6.93E-08
SAOUHSC_02814	SAOUHSC_02814	Putative uncharacterized protein	3.65	6.90E-11
SAOUHSC_02815	SAOUHSC_02815	Putative uncharacterized protein	-2.20	1.70E-05
SAOUHSC_02816	SAOUHSC_02816	Putative uncharacterized protein	4.35	5.37E-17
SAOUHSC_02821	SAOUHSC_02821	Membrane spanning protein, putative	3.44	4.07E-03
SAOUHSC_02823	SAOUHSC_02823	Putative uncharacterized protein	2.20	6.48E-07
SAOUHSC_02824	SAOUHSC_02824	Putative uncharacterized protein	-5.01	4.22E-33
SAOUHSC_02825	SAOUHSC_02825	Putative uncharacterized protein	-3.52	2.24E-20
SAOUHSC_02828	SAOUHSC_02828	Putative uncharacterized protein	2.09	2.29E-09
SAOUHSC_02829	SAOUHSC_02829	Putative NAD(P)H nitroreductase SAOUHSC_02829	-2.30	9.78E-06
SAOUHSC_02830	SAOUHSC_02830	D-lactate dehydrogenase, putative	-3.56	3.34E-27
SAOUHSC_02831	SAOUHSC_02831	Putative uncharacterized protein	-2.24	7.87E-09
SAOUHSC_02832	SAOUHSC_02832	Putative uncharacterized protein	3.81	4.98E-10
SAOUHSC_02833	SAOUHSC_02833	Putative uncharacterized protein	2.13	1.32E-05
SAOUHSC_02834	SAOUHSC_02834	Sortase, putative	2.95	3.33E-15
SAOUHSC_02839	SAOUHSC_02839	L-serine dehydratase, iron-sulfur-dependent, alpha subunit	-4.71	9.38E-22
SAOUHSC_02840	SAOUHSC_02840	L-serine dehydratase, iron-sulfur-dependent, beta subunit	-2.56	1.13E-13
SAOUHSC_02841	SAOUHSC_02841	Putative uncharacterized protein	-2.48	3.38E-15
SAOUHSC_02843	SAOUHSC_02843	Putative uncharacterized protein	3.26	7.98E-11
SAOUHSC_02844	SAOUHSC_02844	Putative uncharacterized protein	-3.59	5.09E-15
SAOUHSC_02845	SAOUHSC_02845	Putative uncharacterized protein	-2.18	2.80E-07
SAOUHSC_02849	SAOUHSC_02849	Pyruvate oxidase, putative	-3.77	1.88E-11
SAOUHSC_02850	cidB	Holin-like protein CidB	-2.28	1.11E-04
SAOUHSC_02851	cidA	Holin-like protein CidA	-3.32	2.22E-11
SAOUHSC_02852	SAOUHSC_02852	Putative uncharacterized protein	3.40	1.40E-12
SAOUHSC_02853	SAOUHSC_02853	Putative uncharacterized protein	-6.89	4.70E-53
SAOUHSC_02855	SAOUHSC_02855	LysM domain protein	7.20	3.14E-15
SAOUHSC_02862	clpL	ATP-dependent Clp protease ATP-binding subunit ClpL	-3.30	1.64E-22
SAOUHSC_02863	SAOUHSC_02863	Putative uncharacterized protein	-2.98	2.72E-13
SAOUHSC_02865	SAOUHSC_02865	Putative uncharacterized protein	3.43	2.06E-07
SAOUHSC_02872	SAOUHSC_02872	Putative uncharacterized protein	-22.01	4.63E-46
SAOUHSC_02873	copA	Copper-exporting P-type ATPase A	-3.03	1.24E-16
SAOUHSC_02874	copZ	Copper chaperone CopZ	-3.00	5.10E-19
SAOUHSC_02877	crtN	Dehydrosqualene desaturase	2.15	3.44E-04
SAOUHSC_02879	crtM	Dehydrosqualene synthase	3.04	1.06E-04
SAOUHSC_02880	crtQ	4,4'-diaponeurosporenoate glycosyltransferase	2.32	3.09E-04
SAOUHSC_02881	crtP	Diapolycopene oxygenase	3.34	6.81E-06
SAOUHSC_02882	crtO	Glycosyl-4,4'-diaponeurosporenoate acyltransferase	5.29	1.00E-03
SAOUHSC_02883	ssaA	Staphylococcal secretory antigen SsaA	14.02	1.22E-07
SAOUHSC_02886	SAOUHSC_02886	Putative uncharacterized protein	11.13	1.18E-40
SAOUHSC_02887	isaA	Probable transglycosylase IsaA	15.80	1.67E-49
SAOUHSC_02888	SAOUHSC_02888	Putative uncharacterized protein	3.79	5.42E-06
SAOUHSC_02889	SAOUHSC_02889	Putative uncharacterized protein	12.74	9.38E-05
SAOUHSC_02891	SAOUHSC_02891	Putative uncharacterized protein	2.49	2.29E-06
SAOUHSC_02892	SAOUHSC_02892	Putative uncharacterized protein	-3.92	2.20E-14
SAOUHSC_02900	SAOUHSC_02900	Uncharacterized hydrolase SAOUHSC_02900	-2.28	2.88E-18
SAOUHSC_02905	SAOUHSC_02905	Putative uncharacterized protein	-3.34	3.99E-23
SAOUHSC_02906	SAOUHSC_02906	Putative uncharacterized protein	-4.33	1.28E-28
SAOUHSC_02907	SAOUHSC_02907	Putative uncharacterized protein	-5.40	2.53E-37
SAOUHSC_02909	SAOUHSC_02909	Dihydroorotate dehydrogenase	5.41	3.65E-17
SAOUHSC_02910	SAOUHSC_02910	Putative uncharacterized protein	2.30	1.42E-06
SAOUHSC_02912	SAOUHSC_02912	Putative uncharacterized protein	-2.08	1.00E-08
SAOUHSC_02921	SAOUHSC_02921	Alpha-acetolactate decarboxylase	-4.76	2.15E-22
SAOUHSC_02922	ldh2	L-lactate dehydrogenase 2	2.08	4.79E-06
SAOUHSC_02923	SAOUHSC_02923	Putative uncharacterized protein	3.03	4.56E-06
SAOUHSC_02925	SAOUHSC_02925	Putative uncharacterized protein	3.79	6.80E-04
SAOUHSC_02926	fda	Fructose-bisphosphate aldolase class 1	3.60	8.17E-37
SAOUHSC_02930	SAOUHSC_02930	Putative uncharacterized protein	-2.61	4.64E-09
SAOUHSC_02932	betA	Oxygen-dependent choline dehydrogenase	5.43	2.97E-21
SAOUHSC_02933	SAOUHSC_02933	Betaine aldehyde dehydrogenase	3.60	2.91E-23
SAOUHSC_02934	SAOUHSC_02934	Putative uncharacterized protein	33.15	6.53E-15
SAOUHSC_02935	SAOUHSC_02935	Putative uncharacterized protein	3.04	3.53E-16
SAOUHSC_02941	SAOUHSC_02941	Anaerobic ribonucleoside-triphosphate reductase-activating pr	2.20	2.25E-10
SAOUHSC_02942	SAOUHSC_02942	Anaerobic ribonucleoside-triphosphate reductase, putative	2.73	2.22E-14
SAOUHSC_02943	SAOUHSC_02943	Citrate transporter, putative	3.18	3.66E-06
SAOUHSC_02944	SAOUHSC_02944	Putative uncharacterized protein	-2.04	8.77E-05
SAOUHSC_02945	SAOUHSC_02945	Siroheme synthase, putative	-2.23	9.60E-07
SAOUHSC_02950	SAOUHSC_02950	Putative uncharacterized protein	3.72	4.34E-03
SAOUHSC_02955	SAOUHSC_02955	Sensor histidine kinase, putative	-2.13	1.87E-08
SAOUHSC_02956	SAOUHSC_02956	DNA-binding response regulator, putative	-2.07	1.32E-08
SAOUHSC_02964	arcR	HTH-type transcriptional regulator ArcR	-6.65	4.60E-55
SAOUHSC_02965	arcC2	Carbamate kinase 2	-6.75	1.68E-85
SAOUHSC_02967	SAOUHSC_02967	Arginine/ornithine antiporter, putative	-7.48	2.91E-81
SAOUHSC_02968	argF	Ornithine carbamoyltransferase	-6.45	1.01E-76
SAOUHSC_02969	arcA	Arginine deiminase	-5.89	2.26E-58
SAOUHSC_02970			-2.83	6.52E-07
SAOUHSC_02971	SAOUHSC_02971	Aureolysin, putative	-2.07	9.32E-10
SAOUHSC_02972	isaB	Immunodominant staphylococcal antigen B	-2.91	1.59E-10
SAOUHSC_02991	SAOUHSC_02991	Putative uncharacterized protein	-2.02	1.21E-04
SAOUHSC_02994	SAOUHSC_02994	Putative uncharacterized protein	-2.58	4.18E-11

SAOUHSC_03002	icaA	Poly-beta-1,6-N-acetyl-D-glucosamine synthase	3.16	1.29E-03
SAOUHSC_03006	lipA	Lipase 1	-4.27	5.00E-15
SAOUHSC_03008	SAOUHSC_03008	Imidazole glycerol phosphate synthase subunit hisF	-4.17	7.18E-41
SAOUHSC_03009	hisA	1-(5-phosphoribosyl)-5-[(5-phosphoribosylamino)methylidenea	-2.63	6.67E-12
SAOUHSC_03015	hisZ	ATP phosphoribosyltransferase regulatory subunit	3.74	9.93E-05
SAOUHSC_03016	SAOUHSC_03016	Putative uncharacterized protein	2.20	1.67E-12
SAOUHSC_03017	SAOUHSC_03017	Putative uncharacterized protein	3.66	1.32E-04
SAOUHSC_03018	SAOUHSC_03018	Putative uncharacterized protein	2.12	3.80E-03
SAOUHSC_03023	drp35	Lactonase drp35	-2.33	3.13E-12
SAOUHSC_03024	SAOUHSC_03024	UPF0176 protein SAOUHSC_03024	-2.78	2.42E-20
SAOUHSC_03031	SAOUHSC_03031	Putative uncharacterized protein	3.79	8.52E-14
SAOUHSC_03032	SAOUHSC_03032	Putative uncharacterized protein	2.86	8.96E-04
SAOUHSC_03033	SAOUHSC_03033	High affinity nickel transporter, putative	2.44	3.88E-10
SAOUHSC_03035	SAOUHSC_03035	Putative uncharacterized protein	-4.64	5.26E-14
SAOUHSC_03049	SAOUHSC_03049	Putative uncharacterized protein	-2.12	1.19E-05
SAOUHSC_03051	rsmG	Ribosomal RNA small subunit methyltransferase G	-2.86	3.21E-09
SAOUHSC_03052	mnmG	tRNA uridine 5-carboxymethylaminomethyl modification enzyn	-2.66	1.28E-09
SAOUHSC_03053	mnmE	tRNA modification GTPase MnmE	-2.01	1.54E-07
SAOUHSC_03055	rpmH	50S ribosomal protein L34	-3.07	5.21E-19
SAOUHSC_A00084	SAOUHSC_00083.1	Putative uncharacterized protein	-2.08	2.13E-04
SAOUHSC_A00219	SAOUHSC_00221.1	Putative uncharacterized protein	4.06	1.39E-07
SAOUHSC_A00283	SAOUHSC_00284.1	Putative uncharacterized protein	2.95	3.51E-04
SAOUHSC_A00635	SAOUHSC_00661.1	Putative uncharacterized protein	2.69	6.57E-04
SAOUHSC_A01436	SAOUHSC_01493.1	Putative uncharacterized protein	2.64	8.08E-03
SAOUHSC_A02013	SAOUHSC_02102.1	Putative uncharacterized protein	2.04	1.04E-03
SAOUHSC_A02169	SAOUHSC_02280.1	Putative uncharacterized protein	3.41	1.90E-06
SAOUHSC_A02189	SAOUHSC_02302.1	Putative uncharacterized protein	2.51	3.92E-07
SAOUHSC_A02445	SAOUHSC_02576.1	Putative uncharacterized protein	16.35	1.39E-15
SAOUHSC_A02771	SAOUHSC_02922.1	Putative uncharacterized protein	8.72	5.12E-04
SAOUHSC_A02856	SAOUHSC_03006.1	Putative uncharacterized protein	-3.31	3.76E-06
SAOUHSC_R00011			-4.13	8.44E-04
SAOUHSC_R00012			-4.40	5.06E-04
SAOUHSC_T00012			2.40	4.90E-08
SAOUHSC_T00026			2.20	1.03E-06
SAOUHSC_T00038			2.69	1.18E-07
SAOUHSC_T00042			2.25	4.88E-07
SAOUHSC_T00055			-2.06	7.49E-04

Material suplementario del CAPÍTULO 2, Artículo 2

Fernández, L., González, S., Quiles-Puchalt, N., Gutiérrez, D., Penadés, J. R., García, P., & Rodríguez, A. (2018). Lysogenization of *Staphylococcus aureus* RN450 by phages φ11 and φ80α leads to the activation of the SigB regulon. *Scientific reports*, 8(1), 12662. https://doi.org/10.1038/s41598-018-31107-z

Figure S1. Analysis of phage release throughout biofilm development in lysogenic strains RN450-ϕ11 and RN450-ϕ80α. Biofilms were formed for 3, 5, 8 or 24 hours by strains RN450-f80a (A) or RN450-f11 (B). Then, free phage particles in the adhered phase (biofilm) were titrated using strain *S. aureus* RN4220 as a host.

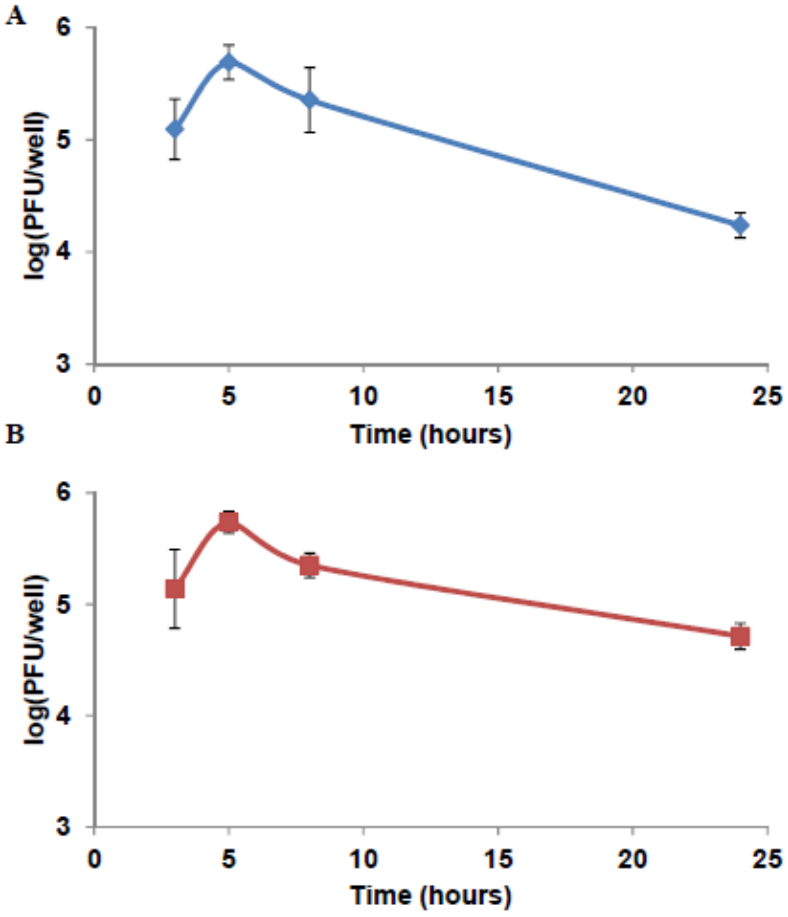

Table S1. Full list of genes dysregulated in biofilms formed by the lysogenic strain RN450-Φ11 compared to the non-lysogenic strain RN4

Gene ID*	Gene name	Gene product	Fold-change	padj
SAOUHSC_02163			-5.22	9.41E-10
SAOUHSC_02906	SAOUHSC_02906	Putative uncharacterized protein	-3.24	5.66E-08
SAOUHSC_02240			-3.21	8.61E-06
SAOUHSC_02967	SAOUHSC_02967	"Arginine/ornithine antiporter, putative"	-3.06	7.63E-09
SAOUHSC_00401	SAOUHSC_00401	Putative uncharacterized protein	-2.99	4.41E-04
SAOUHSC_02969	arcA	Arginine deiminase	-2.98	6.10E-07
SAOUHSC_02965	arcC2	Carbamate kinase 2	-2.94	9.53E-12
SAOUHSC_02907	SAOUHSC_02907	Putative uncharacterized protein	-2.89	1.29E-05
SAOUHSC_02905	SAOUHSC_02905	Putative uncharacterized protein	-2.83	5.78E-08
SAOUHSC_01942	splA	Serine protease SplA	-2.75	4.30E-04
SAOUHSC_02968	argF	Ornithine carbamoyltransferase	-2.66	2.81E-06
SAOUHSC_02452	lacD	"Tagatose 1,6-diphosphate aldolase"	-2.60	1.07E-05
SAOUHSC_02453	lacC	Tagatose-6-phosphate kinase	-2.56	2.50E-06
SAOUHSC_01941	splB	Serine protease SplB	-2.51	1.33E-02
SAOUHSC_02454	lacB	Galactose-6-phosphate isomerase subunit LacB	-2.49	4.14E-03
SAOUHSC_01135	SAOUHSC_01135	Putative uncharacterized protein	-2.49	1.91E-03
SAOUHSC_02260	hld	Delta-hemolysin	-2.48	1.54E-04
SAOUHSC_02090	SAOUHSC_02090	Conserved hypothetical phage protein	-2.45	1.21E-15
SAOUHSC_02964	arcR	HTH-type transcriptional regulator ArcR	-2.41	8.50E-06
SAOUHSC_01136	SAOUHSC_01136	Putative uncharacterized protein	-2.27	2.43E-03
SAOUHSC_02451	SAOUHSC_02451	"PTS system lactose-specific IIA component, putative"	-2.26	1.21E-02
SAOUHSC_02266	SAOUHSC_02266	Putative uncharacterized protein	-2.25	4.99E-06
SAOUHSC_02620	SAOUHSC_02620	Putative uncharacterized protein	-2.24	6.23E-06
SAOUHSC_02971	SAOUHSC_02971	"Aureolysin, putative"	-2.21	4.19E-11
SAOUHSC_01950	SAOUHSC_01950	"Flavoprotein, epiD, putative"	-2.20	1.19E-04
SAOUHSC_01945	SAOUHSC_01945	"Membrane protein, putative"	-2.17	7.81E-06
SAOUHSC_01935	splF	Serine protease SplF	-2.15	9.18E-04
SAOUHSC_01939	splC	Serine protease SplC	-2.14	1.53E-03
SAOUHSC_01949	SAOUHSC_01949	"Intracellular serine protease, putative"	-2.10	2.50E-05
SAOUHSC_00257	SAOUHSC_00257	Putative uncharacterized protein	-2.09	1.13E-05
SAOUHSC_01952	SAOUHSC_01952	"Lantibiotic epidermin biosynthesis protein EpiB, putative"	-2.07	2.41E-04
SAOUHSC_01951	SAOUHSC_01951	"Epidermin biosynthesis protein EpiC, authentic point mutatio	-2.07	1.21E-04
SAOUHSC_02970			-2.06	5.66E-04
SAOUHSC_01513	SAOUHSC_01513	Putative uncharacterized protein	-2.03	1.42E-05
SAOUHSC_00988	sspA	Glutamyl endopeptidase	-2.03	1.95E-04
SAOUHSC_02455	lacA	Galactose-6-phosphate isomerase subunit LacA	-2.01	1.42E-02
SAOUHSC_02261	agrB	Accessory gene regulator protein B	-2.00	1.08E-04
SAOUHSC_02265	SAOUHSC_02265	Accessory gene regulator protein A	-2.00	8.54E-06
SAOUHSC_01018	purD	Phosphoribosylamine--glycine ligase	2.00	1.69E-03
SAOUHSC_01918	SAOUHSC_01918	Putative uncharacterized protein	2.01	1.13E-02
SAOUHSC_00632	mnhG2	Putative antiporter subunit mnhG2	2.04	5.53E-05
SAOUHSC_00630	SAOUHSC_00630	Putative uncharacterized protein	2.05	6.38E-06
SAOUHSC_02848	glcB	PTS system glucoside-specific EIICBA component	2.07	1.21E-04
SAOUHSC_00655	SAOUHSC_00655	Putative uncharacterized protein	2.07	4.88E-02
SAOUHSC_00629	mnhE2	Putative antiporter subunit mnhE2	2.08	1.37E-05
SAOUHSC_03032	SAOUHSC_03032	Putative uncharacterized protein	2.09	4.16E-03
SAOUHSC_00625	mnhA2	Putative antiporter subunit mnhA2	2.10	2.46E-08
SAOUHSC_02597	SAOUHSC_02597	"PTS system component, putative"	2.12	1.07E-02
SAOUHSC_00627	mnhC2	Putative antiporter subunit mnhC2	2.13	2.68E-04
SAOUHSC_00626	mnhB2	Putative antiporter subunit mnhB2	2.14	7.06E-05
SAOUHSC_00628	mnhD2	Putative antiporter subunit mnhD2	2.14	5.08E-08
SAOUHSC_02877	crtN	Dehydrosqualene desaturase	2.14	2.28E-11
SAOUHSC_02137	sdcS	Sodium-dependent dicarboxylate transporter SdcS	2.15	7.79E-06
SAOUHSC_01017	purH	Bifunctional purine biosynthesis protein PurH	2.17	2.39E-02
SAOUHSC_01318	SAOUHSC_01318	Putative uncharacterized protein	2.18	1.61E-03
SAOUHSC_02729	SAOUHSC_02729	"Amino acid ABC transporter-like protein, putative"	2.20	2.19E-02
SAOUHSC_01603	SAOUHSC_01603	Putative uncharacterized protein	2.21	2.71E-02
SAOUHSC_01921	SAOUHSC_01921	Putative uncharacterized protein	2.21	1.54E-03
SAOUHSC_02822	fbp	"Fructose-1,6-bisphosphatase class 3"	2.31	4.20E-02
SAOUHSC_00160	SAOUHSC_00160	Putative uncharacterized protein	2.31	3.00E-02

SAOUHSC_00291	SAOUHSC_00291	"PfkB family carbohydrate kinase family, putative"	2.32	2.99E-02
SAOUHSC_02772	SAOUHSC_02772	Putative uncharacterized protein	2.32	6.38E-06
SAOUHSC_03028	SAOUHSC_03028	Putative uncharacterized protein	2.34	1.12E-04
SAOUHSC_01920	SAOUHSC_01920	Putative uncharacterized protein	2.35	1.72E-04
SAOUHSC_00061	SAOUHSC_00061	Putative uncharacterized protein	2.35	8.91E-11
SAOUHSC_02425	SAOUHSC_02425	UPF0457 protein SAOUHSC_02425	2.39	1.50E-02
SAOUHSC_00156	SAOUHSC_00156	Putative uncharacterized protein	2.47	5.99E-03
SAOUHSC_02908	SAOUHSC_02908	Putative uncharacterized protein	2.49	3.11E-13
SAOUHSC_02815	SAOUHSC_02815	Putative uncharacterized protein	2.63	1.37E-03
SAOUHSC_01602	SAOUHSC_01602	"Transcriptional regulator, putative"	2.67	2.41E-03
SAOUHSC_01601	SAOUHSC_01601	"Alpha-glucosidase, putative"	2.70	2.45E-03
SAOUHSC_00624	SAOUHSC_00624	"Integrase/recombinase, putative"	2.72	4.42E-10
SAOUHSC_00317	SAOUHSC_00317	Glycerol-3-phosphate transporter	2.81	2.54E-05
SAOUHSC_00196	SAOUHSC_00196	Putative uncharacterized protein	2.82	3.92E-02
SAOUHSC_02882	crtO	"Glycosyl-4,4'-diaponeurosporenoate acyltransferase"	2.93	3.13E-03
SAOUHSC_02771	SAOUHSC_02771	Putative uncharacterized protein	2.96	2.96E-06
SAOUHSC_00846	SAOUHSC_00846	Putative uncharacterized protein	2.97	4.87E-17
SAOUHSC_02812	SAOUHSC_02812	Putative uncharacterized protein	3.00	1.36E-16
SAOUHSC_02881	crtP	Diapolycopene oxygenase	3.08	1.46E-03
SAOUHSC_00157	murQ	N-acetylmuramic acid 6-phosphate etherase	3.13	2.71E-03
SAOUHSC_01910	pckA	Phosphoenolpyruvate carboxykinase [ATP]	3.14	2.47E-03
SAOUHSC_00070	sarS	HTH-type transcriptional regulator SarS	3.26	5.67E-06
SAOUHSC_02403	mtlD	Mannitol-1-phosphate 5-dehydrogenase	3.27	2.51E-06
SAOUHSC_02387	SAOUHSC_02387	Putative uncharacterized protein	3.30	1.70E-22
SAOUHSC_02400	SAOUHSC_02400	"PTS system, mannitol-specific component, putative"	3.31	6.11E-04
SAOUHSC_00158	SAOUHSC_00158	PTS system EIIBC component SAOUHSC_00158	3.39	1.23E-03
SAOUHSC_02879	crtM	Dehydrosqualene synthase	3.46	7.53E-23
SAOUHSC_00831	SAOUHSC_00831	Organic hydroperoxide resistance protein-like	3.48	4.53E-14
SAOUHSC_02401	SAOUHSC_02401	Putative uncharacterized protein	3.63	2.55E-04
SAOUHSC_00069	spa	Immunoglobulin G-binding protein A	3.70	3.06E-06
SAOUHSC_00183	SAOUHSC_00183	"Membrane protein, putative"	3.72	4.68E-05
SAOUHSC_01794	SAOUHSC_01794	"Glyceraldehyde-3-phosphate dehydrogenase, type I"	3.77	2.50E-06
SAOUHSC_02880	crtQ	"4,4'-diaponeurosporenoate glycosyltransferase"	3.88	2.54E-12
SAOUHSC_00356	SAOUHSC_00356	Putative uncharacterized protein	3.96	1.13E-25
SAOUHSC_02402	SAOUHSC_02402	"PTS system, mannitol-specific IIa component, putative"	4.08	7.79E-06
SAOUHSC_00358	SAOUHSC_00358	Putative uncharacterized protein	4.67	3.86E-41
SAOUHSC_02444	SAOUHSC_02444	"Osmoprotectant transporter, BCCT family, opuD-like protein,	4.99	1.19E-39
SAOUHSC_A00354	SAOUHSC_00358.1	Putative uncharacterized protein	5.17	3.74E-17
SAOUHSC_02862	clpL	ATP-dependent Clp protease ATP-binding subunit ClpL	5.24	1.68E-66
SAOUHSC_00619	SAOUHSC_00619	Putative uncharacterized protein	5.66	1.56E-60
SAOUHSC_01730	SAOUHSC_01730	UPF0337 protein SAOUHSC_01730	6.31	4.25E-33
SAOUHSC_01729	SAOUHSC_01729	Putative uncharacterized protein	7.55	3.12E-31
SAOUHSC_02442	SAOUHSC_02442	Putative uncharacterized protein	7.60	4.64E-86
SAOUHSC_02443	SAOUHSC_02443	Putative uncharacterized protein	8.17	7.15E-89
SAOUHSC_00845	SAOUHSC_00845	UPF0337 protein SAOUHSC_00845	8.90	8.31E-61
SAOUHSC_02441	asp23	Alkaline shock protein 23	9.56	2.20E-91

*** Genes highlighted in grey correspond to genes dysregulated in this lysogen but not in the phi80alpha lysogenic strain**

Table S2. Full list of genes dysregulated in biofilms formed by the lysogenic strain RN450-Φ80α compared to the non-lysogenic strain RN

Gene ID*	Gene name	Gene product	Fold-change	padj
SAOUHSC_02260	hld	Delta-hemolysin	-25.60	2.36E-92
SAOUHSC_01135	SAOUHSC_01135	Putative uncharacterized protein	-17.63	4.45E-106
SAOUHSC_01136	SAOUHSC_01136	Putative uncharacterized protein	-16.54	1.11E-100
SAOUHSC_02163			-11.84	5.09E-20
SAOUHSC_02240			-9.04	3.86E-18
SAOUHSC_02907	SAOUHSC_02907	Putative uncharacterized protein	-7.37	7.77E-32
SAOUHSC_02906	SAOUHSC_02906	Putative uncharacterized protein	-7.29	2.90E-26
SAOUHSC_02905	SAOUHSC_02905	Putative uncharacterized protein	-6.71	3.86E-32
SAOUHSC_00401	SAOUHSC_00401	Putative uncharacterized protein	-6.40	2.49E-10
SAOUHSC_02262	SAOUHSC_02262	Putative uncharacterized protein	-6.04	9.89E-47
SAOUHSC_02261	agrB	Accessory gene regulator protein B	-5.98	9.95E-55
SAOUHSC_02264	SAOUHSC_02264	Accessory gene regulator protein C	-5.60	2.13E-53
SAOUHSC_02970			-5.20	2.91E-18
SAOUHSC_02265	SAOUHSC_02265	Accessory gene regulator protein A	-5.03	5.09E-71
SAOUHSC_02969	arcA	Arginine deiminase	-4.59	4.43E-21
SAOUHSC_02967	SAOUHSC_02967	"Arginine/ornithine antiporter, putative"	-4.55	1.80E-36
SAOUHSC_02968	argF	Ornithine carbamoyltransferase	-4.51	1.91E-25
SAOUHSC_02965	arcC2	Carbamate kinase 2	-4.25	3.20E-25
SAOUHSC_02964	arcR	HTH-type transcriptional regulator ArcR	-4.19	3.74E-35
SAOUHSC_01953	SAOUHSC_01953	"Gallidermin superfamily epiA, putative"	-4.17	4.26E-23
SAOUHSC_02266	SAOUHSC_02266	Putative uncharacterized protein	-4.17	1.82E-40
SAOUHSC_02620	SAOUHSC_02620	Putative uncharacterized protein	-4.09	3.78E-31
SAOUHSC_01584	SAOUHSC_01584	Putative uncharacterized protein	-4.03	9.78E-44
SAOUHSC_01942	splA	Serine protease SplA	-3.91	1.68E-07
SAOUHSC_01583	SAOUHSC_01583	Conserved hypothetical phage protein	-3.89	8.70E-36
SAOUHSC_01513	SAOUHSC_01513	Putative uncharacterized protein	-3.80	5.79E-21
SAOUHSC_01512	SAOUHSC_01512	Putative uncharacterized protein	-3.77	3.14E-26
SAOUHSC_00256	SAOUHSC_00256	Putative uncharacterized protein	-3.74	7.77E-32
SAOUHSC_02462	SAOUHSC_02462	Putative uncharacterized protein	-3.69	3.21E-02
SAOUHSC_00257	SAOUHSC_00257	Putative uncharacterized protein	-3.59	1.73E-15
SAOUHSC_01511	SAOUHSC_01511	Putative uncharacterized protein	-3.43	5.25E-19
SAOUHSC_02241	SAOUHSC_02241	Uncharacterized leukocidin-like protein 1	-3.40	1.27E-25
SAOUHSC_02971	SAOUHSC_02971	"Aureolysin, putative"	-3.37	1.69E-32
SAOUHSC_01510	SAOUHSC_01510	Putative uncharacterized protein	-3.37	2.94E-29
SAOUHSC_00272	SAOUHSC_00272	Putative uncharacterized protein	-3.36	2.99E-09
SAOUHSC_01952	SAOUHSC_01952	"Lantibiotic epidermin biosynthesis protein EpiB, putative"	-3.31	2.37E-24
SAOUHSC_01951	SAOUHSC_01951	"Epidermin biosynthesis protein EpiC, authentic point mutatio	-3.24	6.66E-23
SAOUHSC_01508	SAOUHSC_01508	Putative uncharacterized protein	-3.24	1.09E-25
SAOUHSC_02243	SAOUHSC_02243	Uncharacterized leukocidin-like protein 2	-3.20	1.11E-28
SAOUHSC_01950	SAOUHSC_01950	"Flavoprotein, epiD, putative"	-3.15	1.70E-25
SAOUHSC_00988	sspA	Glutamyl endopeptidase	-3.11	8.34E-10
SAOUHSC_01941	splB	Serine protease SplB	-3.10	6.38E-05
SAOUHSC_00274	SAOUHSC_00274	Putative uncharacterized protein	-3.05	5.24E-13
SAOUHSC_00259	SAOUHSC_00259	Putative uncharacterized protein	-3.03	6.68E-12
SAOUHSC_00258	SAOUHSC_00258	Putative uncharacterized protein	-3.03	7.93E-16
SAOUHSC_00260	SAOUHSC_00260	Putative uncharacterized protein	-2.94	1.47E-12
SAOUHSC_00267	SAOUHSC_00267	Putative uncharacterized protein	-2.87	1.64E-19
SAOUHSC_00266	SAOUHSC_00266	Putative uncharacterized protein	-2.85	2.64E-22
SAOUHSC_02709	hlgC	Gamma-hemolysin component C	-2.85	1.58E-09
SAOUHSC_01949	SAOUHSC_01949	"Intracellular serine protease, putative"	-2.78	2.01E-15
SAOUHSC_00262	SAOUHSC_00262	Putative uncharacterized protein	-2.75	3.54E-09

SAOUHSC_00261	SAOUHSC_00261	Putative uncharacterized protein	-2.75	5.72E-11
SAOUHSC_02161	SAOUHSC_02161	MHC class II analog protein	-2.72	5.19E-03
SAOUHSC_00264	SAOUHSC_00264	Putative uncharacterized protein	-2.72	1.81E-08
SAOUHSC_02706	sbi	Immunoglobulin-binding protein sbi	-2.69	1.12E-03
SAOUHSC_01944	SAOUHSC_01944	Putative uncharacterized protein	-2.65	2.97E-04
SAOUHSC_00961	SAOUHSC_00961	Putative uncharacterized protein	-2.63	8.10E-08
SAOUHSC_00265	SAOUHSC_00265	Putative uncharacterized protein	-2.60	1.72E-09
SAOUHSC_00717	SAOUHSC_00717	Putative uncharacterized protein	-2.59	8.28E-03
SAOUHSC_00275	SAOUHSC_00275	Putative uncharacterized protein	-2.57	5.72E-09
SAOUHSC_00280	SAOUHSC_00280	Putative uncharacterized protein	-2.55	2.68E-14
SAOUHSC_T0003			-2.53	3.24E-03
SAOUHSC_00055	SAOUHSC_00055	Uncharacterized lipoprotein SAOUHSC_00055	-2.50	1.88E-16
SAOUHSC_A01912	SAOUHSC_01993.3	Putative uncharacterized protein	-2.46	8.49E-03
SAOUHSC_01945	SAOUHSC_01945	"Membrane protein, putative"	-2.46	1.27E-13
SAOUHSC_00561	SAOUHSC_00561	Putative uncharacterized protein	-2.46	1.88E-16
SAOUHSC_00054	SAOUHSC_00054	Uncharacterized lipoprotein SAOUHSC_00054	-2.45	3.30E-12
SAOUHSC_00053	SAOUHSC_00053	Uncharacterized lipoprotein SAOUHSC_00053	-2.43	1.11E-16
SAOUHSC_02707	SAOUHSC_02707	Putative uncharacterized protein	-2.40	3.17E-02
SAOUHSC_01121	hly	Alpha-hemolysin	-2.38	3.50E-05
SAOUHSC_02795	SAOUHSC_02795	Putative uncharacterized protein	-2.38	5.58E-10
SAOUHSC_02710	hlgB	Gamma-hemolysin component B	-2.37	4.00E-13
SAOUHSC_01948	SAOUHSC_01948	ABC transporter domain protein	-2.36	6.55E-17
SAOUHSC_02872	SAOUHSC_02872	Putative uncharacterized protein	-2.36	3.93E-04
SAOUHSC_02108	ftnA	Ferritin	-2.34	1.30E-02
SAOUHSC_01947	SAOUHSC_01947	"Membrane protein, putative"	-2.33	3.30E-18
SAOUHSC_00986	sspC	Staphostatin B	-2.29	8.68E-05
SAOUHSC_T00029			-2.29	5.69E-03
SAOUHSC_00279	SAOUHSC_00279	Putative uncharacterized protein	-2.27	2.33E-12
SAOUHSC_00987	sspB	Staphopain B	-2.26	5.87E-04
SAOUHSC_02312	kdpA	Potassium-transporting ATPase A chain	-2.25	1.06E-04
SAOUHSC_02452	lacD	"Tagatose 1,6-diphosphate aldolase"	-2.23	4.99E-04
SAOUHSC_00052	SAOUHSC_00052	Uncharacterized lipoprotein SAOUHSC_00052	-2.23	2.36E-12
SAOUHSC_02109	SAOUHSC_02109	Putative uncharacterized protein	-2.22	2.34E-02
SAOUHSC_01936	splE	Serine protease SplE	-2.21	2.89E-05
SAOUHSC_02692	SAOUHSC_02692	Putative uncharacterized protein	-2.21	6.50E-04
SAOUHSC_00807	SAOUHSC_00807	Putative uncharacterized protein	-2.21	2.93E-12
SAOUHSC_00975	SAOUHSC_00975	Putative uncharacterized protein	-2.20	3.16E-07
SAOUHSC_00047	SAOUHSC_00047	Putative uncharacterized protein	-2.19	2.06E-10
SAOUHSC_00818	SAOUHSC_00818	Thermonuclease	-2.17	4.60E-07
SAOUHSC_00277	SAOUHSC_00277	Putative uncharacterized protein	-2.16	4.87E-11
SAOUHSC_00918	SAOUHSC_00918	Truncated MHC class II analog protein	-2.14	3.54E-10
SAOUHSC_00276	SAOUHSC_00276	Putative uncharacterized protein	-2.14	1.16E-06
SAOUHSC_03003	icaD	"Poly-beta-1,6-N-acetyl-D-glucosamine synthesis protein IcaD'	-2.14	1.69E-03
SAOUHSC_02794	SAOUHSC_02794	Putative uncharacterized protein	-2.13	3.17E-07
SAOUHSC_00808	SAOUHSC_00808	Putative uncharacterized protein	-2.13	2.62E-12
SAOUHSC_01939	splC	Serine protease SplC	-2.12	3.12E-05
SAOUHSC_01935	splF	Serine protease SplF	-2.11	9.33E-05
SAOUHSC_02160	SAOUHSC_02160	Putative uncharacterized protein	-2.10	3.73E-02
SAOUHSC_02865	SAOUHSC_02865	Putative uncharacterized protein	-2.09	2.53E-09
SAOUHSC_01180	SAOUHSC_01180	Putative uncharacterized protein	-2.09	9.16E-12
SAOUHSC_02691	SAOUHSC_02691	Putative uncharacterized protein	-2.07	3.38E-03
SAOUHSC_00268	SAOUHSC_00268	Putative uncharacterized protein	-2.06	7.68E-12

SAOUHSC_02451	SAOUHSC_02451	"PTS system lactose-specific IIA component, putative"	-2.06	1.05E-02
SAOUHSC_03004	icaB	"Poly-beta-1,6-N-acetyl-D-glucosamine N-deacetylase"	-2.05	7.71E-05
SAOUHSC_02999	SAOUHSC_02999	Capsular polysaccharide biosynthesis protein Cap5B	-2.04	1.66E-05
SAOUHSC_00806	SAOUHSC_00806	Putative uncharacterized protein	-2.04	2.93E-11
SAOUHSC_02453	lacC	Tagatose-6-phosphate kinase	-2.03	4.34E-05
SAOUHSC_00191	SAOUHSC_00191	Putative uncharacterized protein	-2.02	2.09E-02
SAOUHSC_03000	SAOUHSC_03000	"Capsular polysaccharide biosynthesis, capA, putative"	-2.00	2.55E-03
SAOUHSC_00716	SAOUHSC_00716	Putative uncharacterized protein	-2.00	2.78E-02
SAOUHSC_03023	drp35	Lactonase drp35	2.01	9.53E-05
SAOUHSC_01014	SAOUHSC_01014	Amidophosphoribosyltransferase	2.01	3.90E-02
SAOUHSC_02763	SAOUHSC_02763	"Peptide ABC transporter, ATP-binding protein, putative"	2.01	6.83E-07
SAOUHSC_02820	SAOUHSC_02820	Putative uncharacterized protein	2.01	1.26E-08
SAOUHSC_02767	SAOUHSC_02767	"Peptide ABC transporter, peptide-binding protein, putative"	2.01	5.23E-05
SAOUHSC_01087	SAOUHSC_01087	"Iron compound ABC transporter, permease protein"	2.02	1.16E-03
SAOUHSC_02994	SAOUHSC_02994	Putative uncharacterized protein	2.02	1.06E-11
SAOUHSC_01088	SAOUHSC_01088	Putative uncharacterized protein	2.02	7.59E-04
SAOUHSC_00532	SAOUHSC_00532	Putative uncharacterized protein	2.03	4.41E-03
SAOUHSC_01082	isdC	Iron-regulated surface determinant protein C	2.03	1.17E-03
SAOUHSC_01079	isdB	Iron-regulated surface determinant protein B	2.03	2.93E-09
SAOUHSC_00155	ptsG	PTS system glucose-specific EIICBA component	2.04	9.04E-13
SAOUHSC_02830	SAOUHSC_02830	"D-lactate dehydrogenase, putative"	2.05	3.89E-08
SAOUHSC_02330	SAOUHSC_02330	Phosphomethylpyrimidine kinase	2.05	1.83E-13
SAOUHSC_00205	SAOUHSC_00205	Putative uncharacterized protein	2.06	3.77E-03
SAOUHSC_00604	SAOUHSC_00604	Putative uncharacterized protein	2.06	1.44E-03
SAOUHSC_00139	SAOUHSC_00139	Putative uncharacterized protein	2.07	2.46E-03
SAOUHSC_02466	SAOUHSC_02466	Truncated MHC class II analog protein	2.07	3.50E-07
SAOUHSC_00748	SAOUHSC_00748	Putative uncharacterized protein	2.08	1.67E-06
SAOUHSC_02331	tenA	Putative thiaminase-2	2.08	2.25E-14
SAOUHSC_00153	SAOUHSC_00153	"Indolepyruvate decarboxylase, putative"	2.09	1.35E-02
SAOUHSC_02936	SAOUHSC_02936	Putative uncharacterized protein	2.11	5.93E-06
SAOUHSC_00152	SAOUHSC_00152	Putative uncharacterized protein	2.12	1.10E-02
SAOUHSC_01854	SAOUHSC_01854	Putative uncharacterized protein	2.12	9.48E-15
SAOUHSC_02821	SAOUHSC_02821	"Membrane spanning protein, putative"	2.13	1.77E-10
SAOUHSC_00737	SAOUHSC_00737	Putative uncharacterized protein	2.13	3.54E-03
SAOUHSC_00848	SAOUHSC_00848	Putative uncharacterized protein	2.15	2.19E-09
SAOUHSC_02363	SAOUHSC_02363	Putative aldehyde dehydrogenase SAOUHSC_02363	2.17	8.45E-08
SAOUHSC_00371	SAOUHSC_00371	Putative uncharacterized protein	2.17	3.44E-04
SAOUHSC_02754	SAOUHSC_02754	"ABC transporter, ATP-binding protein, putative"	2.18	2.13E-03
SAOUHSC_00291	SAOUHSC_00291	"PfkB family carbohydrate kinase family, putative"	2.18	5.68E-03
SAOUHSC_00749	SAOUHSC_00749	Putative uncharacterized protein	2.19	3.21E-10
SAOUHSC_01855	SAOUHSC_01855	UPF0478 protein SAOUHSC_01855	2.22	1.02E-19
SAOUHSC_02975	SAOUHSC_02975	"PTS system, fructose-specific IIABC component, putative"	2.22	1.86E-03
SAOUHSC_02329	thiM	Hydroxyethylthiazole kinase	2.23	1.85E-13
SAOUHSC_00895	SAOUHSC_00895	Glutamate dehydrogenase	2.23	3.60E-04
SAOUHSC_01847	SAOUHSC_01847	Putative uncharacterized protein	2.24	4.98E-03
SAOUHSC_02663	SAOUHSC_02663	Putative uncharacterized protein	2.24	4.44E-04
SAOUHSC_02803	fnbA	Fibronectin-binding protein A	2.25	5.29E-09
SAOUHSC_00285	SAOUHSC_00285	Putative uncharacterized protein	2.26	3.68E-12
SAOUHSC_00690	SAOUHSC_00690	Putative uncharacterized protein	2.26	7.59E-18
SAOUHSC_01849	SAOUHSC_01849	Putative uncharacterized protein	2.26	9.57E-04
SAOUHSC_03006	lipA	Lipase 1	2.29	2.09E-03
SAOUHSC_01416	odhB	Dihydrolipoyllysine-residue succinyltransferase component of	2.29	3.42E-04

SAOUHSC_00180	SAOUHSC_00180	Putative uncharacterized protein	2.30	1.01E-02
SAOUHSC_02608	SAOUHSC_02608	Putative uncharacterized protein	2.31	1.24E-03
SAOUHSC_00847	SAOUHSC_00847	"ABC transporter, ATP-binding protein, putative"	2.31	1.95E-16
SAOUHSC_01844	SAOUHSC_01844	Putative uncharacterized protein	2.31	4.94E-02
SAOUHSC_02661	SAOUHSC_02661	"PTS system sucrose-specific IIBC component, putative"	2.33	7.38E-14
SAOUHSC_02409	SAOUHSC_02409	Arginase	2.34	2.42E-02
SAOUHSC_01015	purM	Phosphoribosylformylglycinamidine cyclo-ligase	2.34	3.00E-02
SAOUHSC_01027	SAOUHSC_01027	Putative uncharacterized protein	2.35	4.50E-14
SAOUHSC_01922	SAOUHSC_01922	Putative uncharacterized protein	2.36	9.54E-09
SAOUHSC_01018	purD	Phosphoribosylamine--glycine ligase	2.43	2.75E-06
SAOUHSC_02013	SAOUHSC_02013	Uncharacterized protein SAOUHSC_02013	2.43	1.98E-19
SAOUHSC_00747	SAOUHSC_00747	Putative uncharacterized protein	2.45	4.87E-12
SAOUHSC_02662	SAOUHSC_02662	PTS system sucrose-specific IIBC component	2.46	2.00E-19
SAOUHSC_01275	SAOUHSC_01275	Putative uncharacterized protein	2.48	1.73E-03
SAOUHSC_01318	SAOUHSC_01318	Putative uncharacterized protein	2.48	4.04E-05
SAOUHSC_01016	SAOUHSC_01016	"Phosphoribosylglycinamide formyltransferase, putative"	2.51	1.99E-02
SAOUHSC_00296	SAOUHSC_00296	ROK family protein	2.51	3.38E-02
SAOUHSC_00658	SAOUHSC_00658	Putative uncharacterized protein	2.53	1.40E-03
SAOUHSC_00294	SAOUHSC_00294	Putative uncharacterized protein	2.54	3.90E-02
SAOUHSC_01017	purH	Bifunctional purine biosynthesis protein PurH	2.57	7.82E-04
SAOUHSC_01418	odhA	2-oxoglutarate dehydrogenase E1 component	2.57	3.40E-05
SAOUHSC_02774	SAOUHSC_02774	Putative uncharacterized protein	2.60	1.24E-11
SAOUHSC_00746	SAOUHSC_00746	Putative uncharacterized protein	2.62	2.50E-08
SAOUHSC_00656	SAOUHSC_00656	Putative uncharacterized protein	2.64	4.91E-03
SAOUHSC_00310	SAOUHSC_00310	Putative uncharacterized protein	2.66	2.15E-03
SAOUHSC_00894	rocD	Ornithine aminotransferase	2.66	1.66E-04
SAOUHSC_02339	SAOUHSC_02339	Putative uncharacterized protein	2.67	3.51E-05
SAOUHSC_02899	SAOUHSC_02899	Putative uncharacterized protein	2.68	1.37E-23
SAOUHSC_02607	hutU	Urocanate hydratase	2.72	2.66E-03
SAOUHSC_00037	SAOUHSC_00037	Putative uncharacterized protein	2.72	1.19E-21
SAOUHSC_01921	SAOUHSC_01921	Putative uncharacterized protein	2.74	4.33E-09
SAOUHSC_00655	SAOUHSC_00655	Putative uncharacterized protein	2.76	9.29E-04
SAOUHSC_00199	SAOUHSC_00199	Acetate CoA-transferase YdiF	2.76	1.60E-03
SAOUHSC_01918	SAOUHSC_01918	Putative uncharacterized protein	2.89	1.22E-06
SAOUHSC_01603	SAOUHSC_01603	Putative uncharacterized protein	2.89	3.31E-04
SAOUHSC_02848	glcB	PTS system glucoside-specific EIICBA component	2.90	2.77E-13
SAOUHSC_02597	SAOUHSC_02597	"PTS system component, putative"	2.90	9.53E-06
SAOUHSC_00383	SAOUHSC_00383	Putative uncharacterized protein	2.90	1.03E-11
SAOUHSC_00309	SAOUHSC_00309	Putative uncharacterized protein	2.92	3.45E-32
SAOUHSC_00071	SAOUHSC_00071	"Lipoprotein, SirC, putative"	2.97	1.76E-21
SAOUHSC_03035	SAOUHSC_03035	Putative uncharacterized protein	3.01	1.98E-23
SAOUHSC_02610	hutG	Formimidoylglutamase	3.02	1.95E-23
SAOUHSC_02925	SAOUHSC_02925	Putative uncharacterized protein	3.06	2.90E-08
SAOUHSC_02097	SAOUHSC_02097	Putative uncharacterized protein	3.12	3.23E-21
SAOUHSC_02729	SAOUHSC_02729	"Amino acid ABC transporter-like protein, putative"	3.14	6.25E-05
SAOUHSC_02665	SAOUHSC_02665	Putative uncharacterized protein	3.14	1.54E-18
SAOUHSC_01919	SAOUHSC_01919	Putative uncharacterized protein	3.15	3.38E-08
SAOUHSC_02137	sdcS	Sodium-dependent dicarboxylate transporter SdcS	3.17	4.72E-17
SAOUHSC_02822	fbp	"Fructose-1,6-bisphosphatase class 3"	3.17	1.14E-03
SAOUHSC_00156	SAOUHSC_00156	Putative uncharacterized protein	3.18	4.41E-05
SAOUHSC_01920	SAOUHSC_01920	Putative uncharacterized protein	3.23	1.38E-15
SAOUHSC_02425	SAOUHSC_02425	UPF0457 protein SAOUHSC_02425	3.26	4.86E-05

SAOUHSC_02799	sarT	HTH-type transcriptional regulator SarT	3.35	5.41E-05
SAOUHSC_02753	SAOUHSC_02753	"Membrane protein, putative"	3.38	1.44E-13
SAOUHSC_00632	mnhG2	Putative antiporter subunit mnhG2	3.42	8.90E-17
SAOUHSC_00160	SAOUHSC_00160	Putative uncharacterized protein	3.46	2.96E-07
SAOUHSC_02930	SAOUHSC_02930	Putative uncharacterized protein	3.46	4.53E-16
SAOUHSC_00630	SAOUHSC_00630	Putative uncharacterized protein	3.51	1.99E-20
SAOUHSC_00629	mnhE2	Putative antiporter subunit mnhE2	3.58	2.47E-15
SAOUHSC_02869	rocA	1-pyrroline-5-carboxylate dehydrogenase	3.59	4.63E-04
SAOUHSC_00198	SAOUHSC_00198	Putative uncharacterized protein	3.66	6.96E-04
SAOUHSC_A02680	SAOUHSC_02822.1	Putative uncharacterized protein	3.69	7.84E-04
SAOUHSC_00626	mnhB2	Putative antiporter subunit mnhB2	3.70	2.15E-15
SAOUHSC_00628	mnhD2	Putative antiporter subunit mnhD2	3.75	2.23E-25
SAOUHSC_00317	SAOUHSC_00317	Glycerol-3-phosphate transporter	3.78	6.90E-10
SAOUHSC_00736	SAOUHSC_00736	Putative lipid kinase SAOUHSC_00736	3.78	3.09E-28
SAOUHSC_00812	clfA	Clumping factor A	3.82	4.54E-23
SAOUHSC_00627	mnhC2	Putative antiporter subunit mnhC2	3.97	1.02E-19
SAOUHSC_02863	SAOUHSC_02863	Putative uncharacterized protein	3.97	1.68E-30
SAOUHSC_01602	SAOUHSC_01602	"Transcriptional regulator, putative"	3.98	3.59E-06
SAOUHSC_01024	SAOUHSC_01024	Putative uncharacterized protein	4.03	5.53E-06
SAOUHSC_01601	SAOUHSC_01601	"Alpha-glucosidase, putative"	4.10	1.90E-07
SAOUHSC_00196	SAOUHSC_00196	Putative uncharacterized protein	4.12	4.20E-04
SAOUHSC_00157	murQ	N-acetylmuramic acid 6-phosphate etherase	4.18	1.77E-06
SAOUHSC_01846	SAOUHSC_01846	"Acetyl-CoA synthetase, putative"	4.19	4.25E-05
SAOUHSC_00625	mnhA2	Putative antiporter subunit mnhA2	4.29	4.23E-46
SAOUHSC_00569	SAOUHSC_00569	Putative uncharacterized protein	4.33	7.03E-40
SAOUHSC_00158	SAOUHSC_00158	PTS system EIIBC component SAOUHSC_00158	4.35	1.09E-07
SAOUHSC_01884	SAOUHSC_01884	Putative uncharacterized protein	4.36	1.36E-04
SAOUHSC_00179	SAOUHSC_00179	Putative uncharacterized protein	4.37	1.80E-04
SAOUHSC_00825	SAOUHSC_00825	Putative uncharacterized protein	4.37	2.78E-36
SAOUHSC_02815	SAOUHSC_02815	Putative uncharacterized protein	4.38	2.90E-08
SAOUHSC_02900	SAOUHSC_02900	Uncharacterized hydrolase SAOUHSC_02900	4.43	2.82E-60
SAOUHSC_03032	SAOUHSC_03032	Putative uncharacterized protein	4.46	6.47E-21
SAOUHSC_02604	SAOUHSC_02604	Putative uncharacterized protein	4.64	1.19E-64
SAOUHSC_00070	sarS	HTH-type transcriptional regulator SarS	4.73	7.12E-10
SAOUHSC_02809	SAOUHSC_02809	"Gluconate operon transcriptional repressor, putative"	4.82	2.57E-06
SAOUHSC_02440	SAOUHSC_02440	Putative uncharacterized protein	4.88	1.12E-04
SAOUHSC_01910	pckA	Phosphoenolpyruvate carboxykinase [ATP]	4.92	7.37E-07
SAOUHSC_00061	SAOUHSC_00061	Putative uncharacterized protein	4.97	3.31E-57
SAOUHSC_00175	SAOUHSC_00175	"Multiple sugar-binding transport ATP-binding protein, putativ	5.19	4.97E-06
SAOUHSC_00311	SAOUHSC_00311	Putative uncharacterized protein	5.24	1.73E-04
SAOUHSC_00069	spa	Immunoglobulin G-binding protein A	5.40	8.93E-13
SAOUHSC_02771	SAOUHSC_02771	Putative uncharacterized protein	5.46	2.23E-18
SAOUHSC_01794	SAOUHSC_01794	"Glyceraldehyde-3-phosphate dehydrogenase, type I"	5.80	6.92E-11
SAOUHSC_02908	SAOUHSC_02908	Putative uncharacterized protein	5.89	8.09E-49
SAOUHSC_00826	SAOUHSC_00826	Putative uncharacterized protein	5.92	5.39E-51
SAOUHSC_02877	crtN	Dehydrosqualene desaturase	5.93	2.91E-51
SAOUHSC_02808	SAOUHSC_02808	Gluconate kinase	6.39	6.98E-03
SAOUHSC_03028	SAOUHSC_03028	Putative uncharacterized protein	6.42	3.48E-34
SAOUHSC_02772	SAOUHSC_02772	Putative uncharacterized protein	6.49	7.77E-32
SAOUHSC_00312	SAOUHSC_00312	Putative uncharacterized protein	6.73	2.78E-02
SAOUHSC_02806	SAOUHSC_02806	"Gluconate permease, putative"	7.11	2.21E-08
SAOUHSC_00624	SAOUHSC_00624	"Integrase/recombinase, putative"	7.23	2.68E-57

SAOUHSC_00183	SAOUHSC_00183	"Membrane protein, putative"	7.31	1.18E-15
SAOUHSC_00176	SAOUHSC_00176	"Bacterial extracellular solute-binding protein, putative"	7.77	2.08E-02
SAOUHSC_02812	SAOUHSC_02812	Putative uncharacterized protein	7.98	1.32E-72
SAOUHSC_02400	SAOUHSC_02400	"PTS system, mannitol-specific component, putative"	8.23	1.50E-13
SAOUHSC_00177	SAOUHSC_00177	"Maltose ABC transporter, permease protein, putative"	8.41	7.15E-03
SAOUHSC_00846	SAOUHSC_00846	Putative uncharacterized protein	8.59	6.06E-82
SAOUHSC_00178	SAOUHSC_00178	"Maltose ABC transporter, permease protein"	8.60	3.24E-03
SAOUHSC_02403	mtlD	Mannitol-1-phosphate 5-dehydrogenase	8.74	2.87E-23
SAOUHSC_02882	crtO	"Glycosyl-4,4'-diaponeurosporenoate acyltransferase"	8.93	4.56E-14
SAOUHSC_00831	SAOUHSC_00831	Organic hydroperoxide resistance protein-like	9.45	2.42E-60
SAOUHSC_02401	SAOUHSC_02401	Putative uncharacterized protein	9.77	1.99E-14
SAOUHSC_02881	crtP	Diapolycopene oxygenase	10.10	1.13E-13
SAOUHSC_02879	crtM	Dehydrosqualene synthase	10.17	6.60E-88
SAOUHSC_02402	SAOUHSC_02402	"PTS system, mannitol-specific IIa component, putative"	11.06	3.94E-20
SAOUHSC_02387	SAOUHSC_02387	Putative uncharacterized protein	11.15	5.60E-97
SAOUHSC_00356	SAOUHSC_00356	Putative uncharacterized protein	11.49	2.50E-66
SAOUHSC_00358	SAOUHSC_00358	Putative uncharacterized protein	12.22	7.92E-85
SAOUHSC_02880	crtQ	"4,4'-diaponeurosporenoate glycosyltransferase"	13.11	1.33E-52
SAOUHSC_A00354	SAOUHSC_00358.1	Putative uncharacterized protein	13.93	9.78E-44
SAOUHSC_02862	clpL	ATP-dependent Clp protease ATP-binding subunit ClpL	16.79	1.28E-231
SAOUHSC_01729	SAOUHSC_01729	Putative uncharacterized protein	18.24	1.86E-105
SAOUHSC_01730	SAOUHSC_01730	UPF0337 protein SAOUHSC_01730	19.71	3.15E-197
SAOUHSC_02444	SAOUHSC_02444	"Osmoprotectant transporter, BCCT family, opuD-like protein,	19.92	1.15E-144
SAOUHSC_00619	SAOUHSC_00619	Putative uncharacterized protein	21.10	2.64E-196
SAOUHSC_02442	SAOUHSC_02442	Putative uncharacterized protein	27.27	1.58E-186
SAOUHSC_02441	asp23	Alkaline shock protein 23	28.18	2.18E-286
SAOUHSC_02443	SAOUHSC_02443	Putative uncharacterized protein	29.88	1.28E-231
SAOUHSC_00845	SAOUHSC_00845	UPF0337 protein SAOUHSC_00845	31.38	5.63E-205

*** Genes highlighted in grey correspond to genes dysregulated in this lysogen but not in the phi11 lysogenic strain**

Table S3. Normalized mean reads per kilobase million (RPKM) values corresponding to the different open reading frames (ORFs) of Φ11 genome in samples of strain RN450-Φ11

gene_ID	start_coord	end_coord	phi11-1 Reads	phi11-2 Reads	phi11-3 Reads	phi11-1 RPKM	phi11-2 RPKM	phi11-3 RPKM	RPKM MEAN	RPKM ESTAND.	gene_name
phi11_01	83	1129	2506	2033	1083	12992	9385	6630	**9669**	3190.494162	integrase
phi11_02	1241	1441	896	822	569	24196	19765	18144	**20701.66667**	3132.83966	excisionase
phi11_03	1378	2283	10055	9648	6842	60240	51468	48402	**53370**	6143.920898	PV83 orf 3-like protei
phi11_04	2319	2504	1764	1411	1186	51477	36664	40868	**43003**	7633.800561	PV83 orf 4-like protei
phi11_05	2901	3620	7063	6399	5458	53246	42954	48586	**48262**	5153.644148	cI-like repressor
phi11_06	3762	3980	1307	1493	1062	32394	32949	31081	**32141.33333**	959.289494	cro-like repressor
phi11_07	4427	5251	5420	5923	4727	35660	34699	36723	**35694**	1012.428269	anti-repressor
phi11_08	5252	5476	1262	1222	1082	30444	26249	30822	**29171.66667**	2538.150179	phi11_08
phi11_09	5518	5967	3391	4156	3029	40902	44637	43142	**42893.66667**	1879.842635	phi PV83 orf 10-like p
phi11_10	5981	6202	3158	4051	2895	77213	88194	83581	**82996**	5513.824353	phi PV83 orf 12-like p
phi11_11	6696	7016	473	657	482	7998	9892	9624	**9171.333333**	1024.933819	phi PVL orf 39-like pr
phi11_12	7566	8345	4210	4701	3756	29297	29129	30863	**29763**	956.3242128	phi ETA orf 17-like pr
phi11_13	8375	8929	3324	4191	2975	32509	36497	34356	**34454**	1995.805351	ssb
phi11_14	8942	9634	3489	4338	3094	27327	30254	28615	**28732**	1467.003408	phi PV83 orf 19-like p
phi11_15	9606	10412	3879	4462	3441	26090	26723	27329	**26714**	619.5490295	phi PV83 orf 20-like p
phi11_16	10765	12006	7167	8479	6286	31322	32995	32439	**32252**	852.0322764	helicase DnaB
phi11_17	12222	12443	1146	1316	999	28020	28650	28842	**28504**	430.0093022	phi ETA orf 24-like pr
phi11_18	12454	12858	1524	2095	1519	20425	25001	24039	**23155**	2412.682325	phi ETA orf 25-like pr
phi11_19	12863	13048	844	1122	917	24630	29155	31599	**28461.33333**	3535.904458	PV83 orf 23-like prote
phi11_20	13049	13318	1079	1421	1147	21691	25437	27228	**24785.33333**	2825.437016	HTH DNA binding pro
phi11_21	13319	13678	1168	1494	1276	17610	20058	22717	**20128.33333**	2554.226367	phi PVL orf 50-like pr
phi11_22	13679	13927	1276	1523	1120	27815	29562	28829	**28735.33333**	877.2584188	phi PVL orf 51-like pr
phi11_23	13933	14187	1365	1562	1325	29055	29605	33303	**30654.33333**	2310.238372	phi PVL orf 52-like pr
phi11_24	14184	14426	1082	1300	1120	24169	25856	29541	**26522**	2747.22824	ETA orf 33-like protei
phi11_25	14419	14928	2671	3217	2772	28427	30487	34836	**31250**	3271.917939	dUTPase
phi11_26	15037	15210	407	471	420	12696	13083	15471	**13750**	1502.938122	phi SLT orf 81b-like p
phi11_27	15558	15746	703	872	706	20189	22299	23942	**22143.33333**	1881.336316	rinB
phi11_28	15917	16339	1912	2743	2030	24535	31341	30759	**28878.33333**	3772.67668	rinA
phi11_29	16526	16966	385	686	552	4739	7518	8023	**6760**	1768.357147	small terminase
phi11_30	16887	18230	1581	2634	2267	6385	9472	10811	**8889.333333**	2269.800505	large terminase
phi11_31	18241	19776	2389	3576	2971	8442	11252	12397	**10697**	2035.073709	phi Mu50B-like prote
phi11_32	19894	20778	1302	1930	1840	7985	10540	13326	**10617**	2671.332439	phi Mu50B-like prote
phi11_33	21115	21750	3419	5277	5138	29179	40101	51778	**40352.66667**	11301.60176	phi Mu50B-like prote
phi11_34	21764	22738	4957	8108	6858	27596	40192	45082	**37623.33333**	9021.562245	head protein
phi11_35	22760	23047	874	1562	1304	16472	26213	29020	**23901.66667**	6585.573045	phi Mu50B-like prote
phi11_36	23056	23388	1095	2097	1726	17848	30436	33221	**27168.33333**	8190.880071	phi Mu50B-like prote
phi11_37	23687	24034	1713	2852	2472	26718	39609	45528	**37285**	9617.939332	phi Mu50B-like prote
phi11_38	24046	24429	1522	2280	1859	21514	28697	31028	**27079.66667**	4958.918666	phi Mu50B-like prote
phi11_39	24448	25029	2594	3798	3421	24192	31540	37674	**31135.33333**	6750.103505	structural phi Mu50B
phi11_40	25091	25456	991	1571	1443	14697	20746	25269	**20237.33333**	5304.323928	phi11_40
phi11_41	25486	25830	994	1641	1482	15639	22989	27532	**22053.33333**	6001.455351	phi11_41
phi11_42	26582	29314	8024	11459	9620	15936	20265	22560	**19587**	3363.644898	tape measure proteir
phi11_43	29327	30274	2796	3880	3386	16009	19781	22892	**19560.66667**	3446.785797	phi ETA orf 54-like pr
phi11_44	30283	32184	3977	5271	4712	11349	13394	15878	**13540.33333**	2268.043283	phi ETA orf 55-like pr
phi11_45	32199	34109	3926	5698	4762	11151	14411	15971	**13844.33333**	2459.457935	phi ETA orf 56-like pr
phi11_46	35932	36309	532	689	608	7639	8810	10309	**8919.333333**	1338.353591	phi105 orf 44-like prc

phi11_47	36313	36486	211	241	211	6582	6694	7772	**7016**	657.1057754	phi ETA orf 58-like pr
phi11_48	36526	36825	342	550	448	6188	8861	9571	**8206.666667**	1783.896391	phi SLT orf 99-like pro
phi11_49	36962	38860	3200	5130	4143	9147	13056	13983	**12062**	2566.66145	cell wall hydrolase
phi11_50	38873	40045	2234	3125	2565	10337	12876	14015	**12409.33333**	1882.884578	tail fiber
phi11_51	40051	40446	1378	1990	1505	18888	24288	24359	**22511.66667**	3138.388174	phi ETA orf 63-like pr
phi11_52	40502	40939	863	1228	1050	10695	13550	15365	**13203.33333**	2354.221386	holin
phi11_53	40920	42365	3572	4509	3873	13408	15071	17167	**15215.33333**	1883.651861	amidase

Table S4. Normalized mean reads per kilobase million (RPKM) values corresponding to the different open reading frames (ORFs) of Φ80α genome in samples of strain RN450-Φ80α

gene_ID	start_coord	end_coord	phi80-1 Reads	phi80-2 Reads	phi80-3 Reads	phi80-1 RPKM	phi80-2 RPKM	phi80-3 RPKM	RPKM MEAN	RPKM ESTAND	gene_name
SPV-80A_gp01	32	1417	17180	8997	6710	59202	34948	26071	**40073.66667**	17149.93103	int
SPV-80A_gp02	1525	1725	5870	4017	4490	139482	107594	120296	**122457.3333**	16053.49362	xis
SPV-80A_gp03	1662	2567	66096	55552	55700	348435	330107	331075	**336539**	10313.60112	hypothetical protein
SPV-80A_gp04	2603	2788	15034	12040	10498	386044	348495	303944	**346161**	41099.73439	hypothetical protein
SPV-80A_gp05	2948	3115	19816	17151	15551	563355	549621	498481	**537152.3333**	34187.12777	hypothetical protein
SPV-80A_gp06	3185	3901	85840	78565	76483	571802	589920	574441	**578721**	9787.966132	CI-like repressor
SPV-80A_gp07	4065	4307	2183	1450	1127	42906	32125	24976	**33335.66667**	9026.101613	cro-like repressor
SPV-80A_gp08	4323	5111	10593	6984	5787	64123	47655	39498	**50425.33333**	12544.07096	antirepressor
SPV-80A_gp09	5127	5321	2347	1680	1349	57485	46383	37254	**47040.66667**	10131.52182	hypothetical protein
SPV-80A_gp10	5374	5550	1400	1208	1193	37777	36743	36297	**36939**	759.2180188	hypothetical protein
SPV-80A_gp11	5525	5755	2510	2584	3177	51896	60223	74064	**62061**	11197.71133	hypothetical protein
SPV-80A_gp12	5814	5942	1286	993	976	47613	41442	40744	**43266.33333**	3780.467476	hypothetical protein
SPV-80A_gp13	5935	6096	983	655	464	28981	21768	15424	**22057.66667**	6783.1403	hypothetical protein
SPV-80A_gp14	6188	6448	1797	1154	1002	32884	23804	20674	**25787.33333**	6342.021234	hypothetical protein
SPV-80A_gp15	6458	6679	1879	1344	1110	40425	32593	26926	**33314.66667**	6778.373871	hypothetical protein
SPV-80A_gp16	6672	7295	4461	3097	2342	34145	26720	20212	**27025.66667**	6971.527547	e12
SPV-80A_gp17	7295	7723	3165	2049	1638	35236	25714	20562	**27170.66667**	7444.660995	ssb
SPV-80A_gp18	7737	8411	5083	3431	2738	35966	27365	21844	**28391.66667**	7116.758696	hypothetical protein
SPV-80A_gp19	8517	9374	33807	37725	44525	188189	236714	279458	**234787**	45665.00396	hypothetical protein
SPV-80A_gp20	9439	10209	3785	3010	2626	23447	21018	18342	**20935.66667**	2553.495709	hypothetical protein
SPV-80A_gp21	10219	10998	3490	2534	2149	21370	17490	14837	**17899**	3285.648033	DnaC
SPV-80A_gp22	10992	11150	703	496	415	21117	16795	14056	**17322.66667**	3559.951451	hypothetical protein
SPV-80A_gp23	11163	11384	996	696	579	21428	16879	14045	**17450.66667**	3724.550219	hypothetical protein
SPV-80A_gp24	11394	11801	1337	1016	890	15651	13407	11747	**13601.66667**	1959.266529	RusA
SPV-80A_gp25	11801	11986	511	375	348	13121	10854	10075	**11350**	1582.416191	hypothetical protein
SPV-80A_gp26	11987	12346	807	604	509	10706	9033	7614	**9117.666667**	1547.737812	hypothetical protein
SPV-80A_gp27	12347	12595	774	614	501	14846	13276	10835	**12985.66667**	2021.200221	hypothetical protein
SPV-80A_gp28	12610	13011	1061	749	648	12606	10031	8681	**10439.33333**	1994.105898	hypothetical protein
SPV-80A_gp29	13008	13355	880	679	672	12078	10504	10399	**10993.66667**	940.5266255	hypothetical protein
SPV-80A_gp30	13352	13660	388	304	261	5997	5297	4549	**5281**	724.1325845	53 ORF 49-like protei
SPV-80A_gp31	13653	13889	409	285	256	8242	6474	5817	**6844.333333**	1254.199479	hypothetical protein
SPV-80A_gp32	13894	14406	736	630	588	6852	6612	6172	**6545.333333**	344.8671242	dUTPase
SPV-80A_gp33	14443	14649	246	170	161	5676	4421	4188	**4761.666667**	800.3601273	hypothetical protein
SPV-80A_gp34	14646	14849	216	144	148	5057	3800	3907	**4254.666667**	696.8976491	hypothetical protein
SPV-80A_gp35	14842	15078	354	281	258	7134	6383	5862	**6459.666667**	639.4562795	hypothetical protein
SPV-80A_gp36	15071	15457	888	813	645	10959	11310	8975	**10414.66667**	1259.079161	hypothetical protein
SPV-80A_gp37	15454	15627	291	231	187	7988	7147	5788	**6974.333333**	1110.117261	rinB
SPV-80A_gp38	15628	15774	313	243	199	10170	8900	7290	**8786.666667**	1443.341032	rinMiddle
SPV-80A_gp39	15798	16220	1003	841	762	11325	10704	9701	**10576.66667**	819.4536798	rinA
SPV-80A_gp40	16407	16847	640	690	688	6931	8424	8401	**7918.666667**	855.4217284	terminase small subu
SPV-80A_gp41	16768	18111	2279	2895	3002	8099	11597	12028	**10574.66667**	2154.793339	terminase large subu
SPV-80A_gp42	18122	19657	2347	3147	3528	7298	11030	12369	**10232.33333**	2627.920154	portal protein
SPV-80A_gp43	19545	19730	63	66	77	1618	1910	2229	**1919**	305.599411	hypothetical protein
SPV-80A_gp44	19664	20659	1332	1968	2112	6387	10638	11419	**9481.333333**	2708.073916	minor head protein
SPV-80A_gp45	20732	20902	271	345	363	7569	10862	11432	**9954.333333**	2085.326433	hypothetical protein
SPV-80A_gp46	21011	21631	2539	3360	3645	19527	29129	31609	**26755**	6381.268526	scaffold protein

SPV-80A_gp47	21645	22619	3744	4966	5704	18340	27421	31505	**25755.33333**	6738.704648	major head protein
SPV-80A_gp48	22641	22928	568	739	876	9420	13814	16380	**13204.66667**	3519.782001	hypothetical protein
SPV-80A_gp49	22937	23269	796	867	964	11417	14017	15590	**13674.66667**	2107.457315	hypothetical protein
SPV-80A_gp50	23266	23568	1117	1185	1310	17607	21055	23282	**20648**	2859.308133	hypothetical protein
SPV-80A_gp51	23568	23915	1240	1342	1503	17018	20761	23258	**20345.66667**	3140.664951	hypothetical protein
SPV-80A_gp52	23927	24310	1014	1096	1294	12612	15366	18147	**15375**	2767.510976	hypothetical protein
SPV-80A_gp53	24329	24910	1825	1922	2127	14977	17779	19681	**17479**	2366.305982	major tail protein
SPV-80A_gp54	24972	25337	541	639	672	7060	9399	9888	**8782.333333**	1511.490765	hypothetical protein
SPV-80A_gp55	25367	25711	563	627	638	7794	9784	9959	**9179**	1202.632529	hypothetical protein
SPV-80A_gp56	25728	29192	3497	3833	4244	4820	5956	6596	**5790.666667**	899.4694733	tape measure protein
SPV-80A_gp57	27980	28372	188	213	248	2285	2918	3398	**2867**	558.249944	inside tape protein
SPV-80A_gp58	29205	30152	1872	1980	2049	9431	11244	11639	**10771.33333**	1177.444832	hypothetical protein
SPV-80A_gp59	30161	32062	2315	2447	2644	5813	6926	7486	**6741.666667**	851.5963441	hypothetical protein
SPV-80A_gp60	31875	32084	89	78	68	2024	2000	1744	**1922.666667**	155.1945016	hypothetical protein
SPV-80A_gp61	32077	33987	2476	2484	2654	6188	6998	7479	**6888.333333**	652.4494872	minor structure prote
SPV-80A_gp62	33987	35810	1827	1753	1975	4784	5174	5831	**5263**	529.1436478	hypothetical protein
SPV-80A_gp63	35284	35505	48	0	0	1033	0	0	**344.3333333**	596.4028281	hypothetical protein
SPV-80A_gp64	35810	36187	398	299	346	5029	4259	4929	**4739**	418.6884283	hypothetical protein
SPV-80A_gp65	36188	36370	131	109	116	3419	3207	3414	**3346.666667**	120.9807147	hypothetical protein
SPV-80A_gp66	36411	36710	237	241	272	3773	4325	4883	**4327**	555.0027027	hypothetical protein
SPV-80A_gp67	36847	38745	2046	2048	2160	5146	5806	6125	**5692.333333**	499.2998431	lyz
SPV-80A_gp68	38758	39930	1110	1160	1143	4520	5324	5247	**5030.333333**	443.6353608	tail fiber protein
SPV-80A_gp69	39936	40331	599	585	585	7224	7953	7955	**7710.666667**	421.4668828	hypothetical protein
SPV-80A_gp70	40387	40689	216	214	230	3405	3802	4088	**3765**	343	holin
SPV-80A_gp71	40701	42155	1095	1068	1043	3594	3952	3860	**3802**	185.9139586	lyt2
SPV-80A_gp72	42409	42636	3138	5168	5804	65734	122031	137086	**108283.6667**	37610.08982	hypothetical protein
SPV-80A_gp73	42770	43606	13354	12330	10659	76201	79309	68579	**74696.33333**	5520.981917	hypothetical protein

Material suplementario del CAPÍTULO 3, Artículo 1

Fernández, L., González, S., Campelo, A. B., Martínez, B., Rodríguez, A., & García, P. (2017). Downregulation of Autolysin-Encoding Genes by Phage-Derived Lytic Proteins Inhibits Biofilm Formation in *Staphylococcus aureus*. *Antimicrobial agents and chemotherapy*, 61(5), e02724-16. https://doi.org/10.1128/AAC.02724-16

Movie S1.
https://aac.asm.org/highwire/filestream/14320/field_highwire_adjunct_files/1/zac005176179sm1.avi

Fig. S2. Biofilm formation of *S. aureus* strains in the presence of subinhibitory concentrations of vancomycin. Biofilms of strains IPLA 1 (A), ISP479r (B), SA113 (C, black bars) and *atl* mutant (C, white bars) were grown for 24 hours at 37 ºC. Then, the planktonic phase was removed and the adhered biomass was quantified by crystal violet staining and subsequent A_{595} determination. The percentage biomass production compared to the untreated controls was then calculated and represented. Values correspond to the mean and standard deviation of four replicates. *, P<0.05. The MIC of all strains was 2 µg/ml.

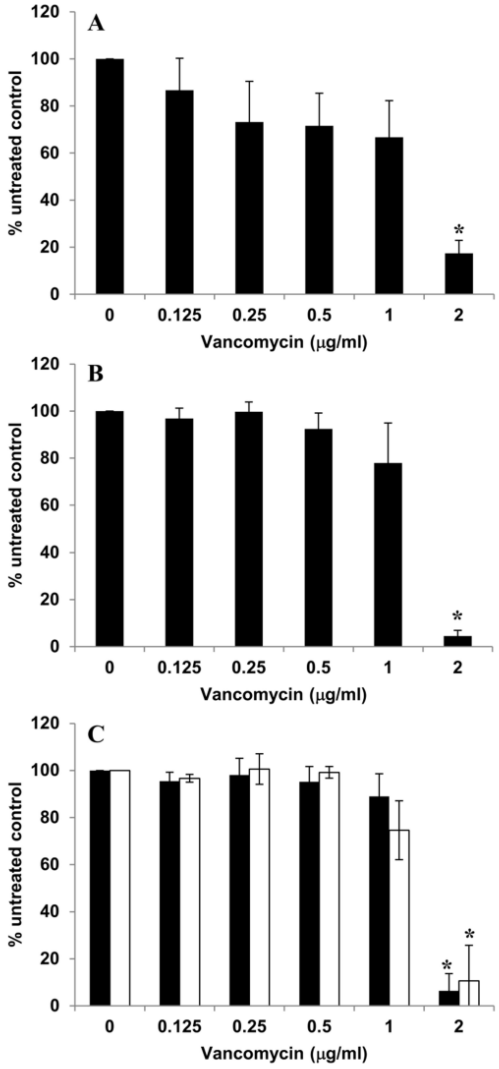

Table S3. Trancriptional analysis of *S. aureus* IPLA 1 cells exposed to 0.25x MIC of endolysin LysH5. Total RNA was purified from biofilms grown at 25ºC and then exposed to the lysin. Gene expression was then analyzed by RNA-seq. Results show the average of three independent BRs.

Gene ID	**Gene name**	**Gene product**	**Fold-change**	**padj**
SAOUHSC_00241		Putative uncharacterized protein	-2.29	3.29E-13
SAOUHSC_00239		Ribokinase, putative	-2.03	7.56E-11
SAOUHSC_00240	*rbsD*	D-ribose pyranase	-1.96	3.09E-08
SAOUHSC_02333	*sceD*	Probable transglycosylase SceD	-1.76	3.81E-08
SAOUHSC_02257		Putative uncharacterized protein	-1.51	0.0000369
SAOUHSC_02576		Secretory antigen SsaA, putative	-1.49	0.00347987
SAOUHSC_00365	*ahpC*	Alkyl hydroperoxide reductase subunit C	-1.45	0.00012275
SAOUHSC_01278	*glpD*	Aerobic glycerol-3-phosphate dehydrogenase	-1.43	0.00070914
SAOUHSC_00248	*lytM*	Glycyl-glycine endopeptidase LytM	-1.43	0.03599607
SAOUHSC_00364	*ahpF*	Alkyl hydroperoxide reductase subunit F	-1.42	0.0000421
SAOUHSC_A0244 5		Putative uncharacterized protein	-1.41	0.03722003
SAOUHSC_02934		Putative uncharacterized protein	-1.37	0.01247071
SAOUHSC_02109		Putative uncharacterized protein	-1.36	0.03519913
SAOUHSC_R00011			-1.36	0.04408635
SAOUHSC_00849		Aminotransferase, class V superfamily, putative	-1.35	0.00185408
SAOUHSC_00427	*sle1*	N-acetylmuramoyl-L-alanine amidase sle1	-1.35	0.0227978
SAOUHSC_00897		Putative uncharacterized protein	-1.33	0.03722003
SAOUHSC_00850		Putative uncharacterized protein	-1.33	0.00185408
SAOUHSC_02855		LysM domain protein	-1.32	0.04544626
SAOUHSC_00994	*atl*	Bifunctional autolysin	-1.31	0.00385901
SAOUHSC_02932	*betA*	Oxygen-dependent choline dehydrogenase	-1.28	0.03135986
SAOUHSC_00848		Putative uncharacterized protein	-1.27	0.0437064
SAOUHSC_00435		Glutamate synthase, large subunit, putative	-1.26	0.0223858
SAOUHSC_00964		Putative uncharacterized protein	1.25	0.03108964
SAOUHSC_01761		Putative uncharacterized protein	1.25	0.02719177
SAOUHSC_00901		Putative uncharacterized protein	1.26	0.03519913
SAOUHSC_02419	*sepA*	Multidrug resistance efflux pump SepA	1.28	0.03772162
SAOUHSC_02635	*tcaA*	Membrane-associated protein TcaA	1.29	0.03447569
SAOUHSC_00437		Putative uncharacterized protein	1.29	0.03135986
SAOUHSC_00618		Putative uncharacterized protein	1.35	0.01003792
SAOUHSC_00258		Putative uncharacterized protein	1.36	0.04408635
SAOUHSC_02872		Putative uncharacterized protein	1.37	0.01246251
SAOUHSC_03001	*icaR*	Biofilm operon icaADBC HTH-type negative transcriptional regulator IcaR	1.38	0.04408635
SAOUHSC_00674	*sarX*	HTH-type transcriptional regulator SarX	1.38	0.03736253
SAOUHSC_00259		Putative uncharacterized protein	1.39	0.0277283
SAOUHSC_02676	*nreB*	Oxygen sensor histidine kinase NreB	1.40	0.04131944
SAOUHSC_02675	*nreC*	Oxygen regulatory protein NreC	1.41	0.0223858
SAOUHSC_02167	*scn*	Staphylococcal complement inhibitor	1.42	0.03519913
SAOUHSC_00094		Uncharacterized protein SAOUHSC_00094	1.42	0.01632399
SAOUHSC_00400		Putative uncharacterized protein	1.42	0.00355077
SAOUHSC_01164	*pyrR*	Bifunctional protein PyrR	1.44	0.0223858
SAOUHSC_01113		Putative uncharacterized protein	1.45	0.03519913
SAOUHSC_02706	*sbi*	Immunoglobulin-binding protein sbi	1.45	0.01788934
SAOUHSC_02710	*hlgB*	Gamma-hemolysin component B	1.45	0.00948648
SAOUHSC_02677		Putative uncharacterized protein	1.49	0.00355077

SAOUHSC_01110		Fibrinogen-binding protein-related	1.50	0.00070914
SAOUHSC_02685		Putative uncharacterized protein	1.50	0.00691934
SAOUHSC_02709	*hlgC*	Gamma-hemolysin component C	1.51	0.00039987
SAOUHSC_01115		Putative uncharacterized protein	1.52	0.00691934
SAOUHSC_00191		Putative uncharacterized protein	1.52	0.00558099
SAOUHSC_02708		Gamma-hemolysin h-gamma-ii subunit, putative	1.52	0.00405368
SAOUHSC_00399		Putative uncharacterized protein	1.53	0.00070914
SAOUHSC_02707		Putative uncharacterized protein	1.53	0.00667332
SAOUHSC_02678		Respiratory nitrate reductase, gamma subunit	1.57	0.00185408
SAOUHSC_02683	*nirD*	Assimilatory nitrite reductase [NAD(P)H], small subunit, putative	1.58	0.00385901
SAOUHSC_02682		Uroporphyrin-III C-methyltransferase, putative	1.67	0.00045414
SAOUHSC_02684	*nirB*	Assimilatory nitrite reductase [NAD(P)H], large subunit, putative	1.74	0.0000282
SAOUHSC_02679		Respiratory nitrate reductase, delta subunit, putative	1.80	0.0000282
SAOUHSC_02671	*narT*	Probable nitrate transporter NarT	1.87	3.93E-07
SAOUHSC_02680	*narY*	Nitrate reductase, beta subunit	1.92	7.43E-07
SAOUHSC_02681	*narG*	Nitrate reductase, alpha subunit	1.98	2.36E-08

Factor de impacto de las publicaciones presentadas

El factor de impacto de cada publicación corresponde con el que figura en el "Journal Citation Report (JCR)" del año de publicación o, en el caso de las más recientes, con el último disponible.

1. González, S., Fernández, L., Campelo, A.B., Gutiérrez, D., Martínez, B., Rodríguez, A. and García, P. (2017). The Behavior of *Staphylococcus aureus* Dual-Species Biofilms Treated with Bacteriophage phiIPLA-RODI Depends on the Accompanying Microorganism. Applied and Environmental Microbiology. 83(3):e02821-16. doi:10.1128/AEM.02821-16.

   Factor de Impacto (JCR 2017): 3,633 (Microbiology, Q2)

2. Gonzalez, S., Fernandez, L., Gutierrez, D., Campelo, A.B., Rodriguez, A. and Garcia, P. (2018). Analysis of Different Parameters Affecting Diffusion, Propagation and Survival of Staphylophages in Bacterial Biofilms. Front. Microbiol. 2018, 9, 2348. https://doi.org/10.3390/v10120722

   Factor de Impacto (JCR 2018): 4,259 (Microbiology, Q1)

3. Fernández, L., González, S., Campelo, A.B., Martínez, B., Rodríguez, A., García, P. (2017). Low-level predation by lytic phage phiIPLA-RODI promotes biofilm formation and triggers the stringent response in *Staphylococcus aureus*. Scientific Reports. 7:40965. doi: 10.1038/srep40965

   Factor de Impacto (JCR 2017): 4,122 (Multidisciplinary sciences, Q1)

4. Fernández, L., González, S., Quiles-Puchalt, N., Gutiérrez, D., Penadés, JR., García, P and Rodríguez, A. (2018). Lysogenization of *Staphylococcus aureus* RN450 by phages φ11 and φ80α leads to the activation of the SigB regulon. Scientific Reports. 8:12662. doi: 10.1038/s41598-018-31107-z

   Factor de Impacto (JCR 2018): 4,011 (Multidisciplinary sciences, Q1)

5. Fernández, L., González, S., Campelo, A.B., Martínez, B., Rodríguez, A. and García, P. (2017). Downregulation of autolysin encoding genes by phage-derived lytic proteins inhibits biofilm formation in *Staphylococcus aureus*. Antimicrobial Agents and Chemotherapy. 24;61(5). pii: e02724-16. doi: 10.1128/AAC.02724-16

Factor de Impacto (JCR 2017): 4,256 (Microbiology, Q1)

6. Fernández, L., González, S., Gutiérrez, D., Campelo, AB, Martínez, B., Rodríguez, A. and García, P. (2018). Characterizing the Transcriptional Effects of Endolysin Treatment on Established Biofilms of *Staphylococcus aureus*. Bio-protocol 8(12): e2891. doi: 10.21769 / BioProtoc.2891 .

Universidad de Oviedo
Universidá d'Uviéu
University of Oviedo

FORMULARIO RESUMEN DE TESIS POR COMPENDIO

1.- Datos personales solicitante	
Apellidos: González Menéndez	Nombre: Silvia

Curso de inicio de los estudios de doctorado	2016/17

	SI	NO
Acompaña acreditación por el Director de la Tesis de la aportación significativa del doctorando	X	
Acompaña memoria que incluye		
Introducción justificativa de la unidad temática y objetivos	X	
Copia completa de los trabajos *	X	
Resultados/discusión y conclusiones	X	
Informe con el factor de impacto de las publicaciones	X	
Se acompaña aceptación de todos y cada uno de los coautores a presentar el trabajo como tesis por compendio	X	
Se acompaña renuncia de todos y cada uno de los coautores a presentar el trabajo como parte de otra tesis de compendio		

* Ha de constar el nombre y adscripción del autor y de todos los coautores asi como la referencia completa de la revista o editorial en la que los trabajos hayan sido publicados o aceptados en cuyo caso se aportará justificante de la aceptación por parte de la revista o editorial

FOR-MAT-VOA-033

Artículos, Capítulos, Trabajos

Trabajo, Artículo 1

Titulo (o título abreviado)	The Behavior of *Staphylococcus aureus* Dual-Species Biofilms Treated with Bacteriophage phiIPLA-RODI Depends on the Accompanying Microorganism
Fecha de publicación	17 de Enero de 2017
Fecha de aceptación	7 de Noviembre 2016
Inclusión en Science Citation Index o bases relacionadas por la CNEAI (indíquese)	Si
Factor de impacto	3,633

Coautor2	■ Doctor □ No doctor .	Indique nombre y apellidos	Lucía Fernández Llamas
Coautor3	■ Doctor □ No doctor .	Indique nombre y apellidos	Ana Belén Campelo Díez
Coautor4	■ Doctor □ No doctor .	Indique nombre y apellidos	Diana Gutiérrez Fernández
Coautor5	■ Doctor □ No doctor .	Indique nombre y apellidos	Beatriz Martínez Fernández
Coautor6	■ Doctor □ No doctor .	Indique nombre y apellidos	Ana Rodríguez González
Coautor7	■ Doctor □ No doctor .	Indique nombre y apellidos	Pilar García Suarez

Universidad de Oviedo
Universidá d'Uviéu
University of Oviedo

Trabajo, Artículo 2

Titulo (o título abreviado)	Analysis of Different Parameters Affecting Diffusion, Propagation and Survival of Staphylophages in Bacterial Biofilms
Fecha de publicación	18 septiembre de 2018
Fecha de aceptación	12 septiembre de 2018
Inclusión en Science Citation Index o bases relacionadas por la CNEAI (indíquese)	Si
Factor de impacto	4,259

Coautor2	■ Doctor □ No doctor .	Indique nombre y apellidos	Lucia Fernández Llamas
Coautor3	■ Doctor □ No doctor .	Indique nombre y apellidos	Diana Gutiérrez Fernández
Coautor4	■ Doctor □ No doctor .	Indique nombre y apellidos	Ana Belén Campelo Díez
Coautor5	■ Doctor □ No doctor .	Indique nombre y apellidos	Ana Rodríguez González
Coautor6	■ Doctor □ No doctor .	Indique nombre y apellidos	Pilar García Suarez

Trabajo, Artículo 3

Titulo (o título abreviado)	Low-level predation by lytic phage phiIPLA-RODI promotes biofilm formation and triggers the stringent response in Staphylococcus aureus.
Fecha de publicación	19 de enero de 2017
Fecha de aceptación	13 de diciembre de 2016
Inclusión en Science Citation Index o bases relacionadas por la CNEAI (indíquese)	Si
Factor de impacto	4,122

Coautor2	■ Doctor □ No doctor .	Indique nombre y apellidos	Lucia Fernández Llamas
Coautor3	■ Doctor □ No doctor .	Indique nombre y apellidos	Ana Belén Campelo Díez
Coautor4	■ Doctor □ No doctor .	Indique nombre y apellidos	Beatriz Martínez Fernández
Coautor5	■ Doctor □ No doctor .	Indique nombre y apellidos	Ana Rodríguez González
Coautor6	■ Doctor □ No doctor .	Indique nombre y apellidos	Pilar García Suarez

Trabajo, Artículo 4

Titulo (o título abreviado)	Lysogenization of Staphylococcus aureus RN450 by phages ϕ11 and ϕ80α leads to the activation of the SigB regulon.
Fecha de publicación	23 Agosto de 2018
Fecha de aceptación	10 Agosto de 2018
Inclusión en Science Citation Index o bases relacionadas por la CNEAI (indíquese)	Si
Factor de impacto	4,011

Coautor2	■ Doctor □ No doctor .	Indique nombre y apellidos	Lucia Fernández LLamas
Coautor3	■ Doctor □ No doctor .	Indique nombre y apellidos	Nuria Quiles-Puchalt
Coautor4	■ Doctor □ No doctor .	Indique nombre y apellidos	Diana Gutiérrez Fernández
Coautor5	■ Doctor □ No doctor .	Indique nombre y apellidos	José R. Penadés

Coautor6	■ Doctor	□ No doctor .	Indique nombre y apellidos
Coautor7	■ Doctor	□ No doctor .	Indique nombre y apellidos

Pilar Garcia Suarez
Ana Rodriguez González

Trabajo, Artículo 5

Titulo (o título abreviado)	Downregulation of autolysin-encoding genes by phage-derived lytic proteins inhibits biofilm formation in Staphylococcus aureus
Fecha de publicación	13 Marzo de 2017
Fecha de aceptación	6 Marzo de 2017
Inclusión en Science Citation Index o bases relacionadas por la CNEAI (indíquese)	Si
Factor de impacto	4,256

Coautor2	■ Doctor	□ No doctor .	Indique nombre y apellidos
Coautor3	■ Doctor	□ No doctor .	Indique nombre y apellidos
Coautor4	■ Doctor	□ No doctor .	Indique nombre y apellidos
Coautor5	■ Doctor	□ No doctor .	Indique nombre y apellidos
Coautor6	■ Doctor	□ No doctor .	Indique nombre y apellidos

Lucia Fernández Llamas
Ana Belén Campelo Díez
Beatriz Martínez Fernández
Ana Rodríguez González
Pilar García Suarez

Trabajo, Artículo 6

Titulo (o título abreviado)	Characterizing the Transcriptional Effects of Endolysin Treatment on Established Biofilms of Staphylococcus aureus.
Fecha de publicación	20 Junio de 2018
Fecha de aceptación	
Inclusión en Science Citation Index o bases relacionadas por la CNEAI (indíquese)	
Factor de impacto	

Coautor2	■ Doctor	□ No doctor .	Indique nombre y apellidos
Coautor3	■ Doctor	□ No doctor .	Indique nombre y apellidos
Coautor4	■ Doctor	□ No doctor .	Indique nombre y apellidos
Coautor5	■ Doctor	□ No doctor .	Indique nombre y apellidos
Coautor6	■ Doctor	□ No doctor .	Indique nombre y apellidos
Coautor7	■ Doctor	□ No doctor .	Indique nombre y apellidos

Lucia Fernández Llamas
Diana Gutiérrez Fernández
Ana Belén Campelo Díez
Beatriz Martínez Fernández
Ana Rodríguez González
Pilar García Suarez